CHEM 371: P-CHEM 2 TO FOLOW COMBINED BIOPHYSICAL AND P-CHEM 1



Jonathan Gutow
University of Wisconsin - Oshkosh

LibreTexts™

Chem 371: P-Chem 2 to Folow Combined Biophysical and P-Chem 1 (Gutow)

This text is disseminated via the Open Education Resource (OER) LibreTexts Project (https://LibreTexts.org) and like the thousands of other texts available within this powerful platform, it is freely available for reading, printing, and "consuming."

The LibreTexts mission is to bring together students, faculty, and scholars in a collaborative effort to provide an accessible, and comprehensive platform that empowers our community to develop, curate, adapt, and adopt openly licensed resources and technologies; through these efforts we can reduce the financial burden born from traditional educational resource costs, ensuring education is more accessible for students and communities worldwide.

Most, but not all, pages in the library have licenses that may allow individuals to make changes, save, and print this book. Carefully consult the applicable license(s) before pursuing such effects. Instructors can adopt existing LibreTexts texts or Remix them to quickly build course-specific resources to meet the needs of their students. Unlike traditional textbooks, LibreTexts' web based origins allow powerful integration of advanced features and new technologies to support learning.



LibreTexts is the adaptable, user-friendly non-profit open education resource platform that educators trust for creating, customizing, and sharing accessible, interactive textbooks, adaptive homework, and ancillary materials. We collaborate with individuals and organizations to champion open education initiatives, support institutional publishing programs, drive curriculum development projects, and more.

The LibreTexts libraries are Powered by NICE CXone Expert and was supported by the Department of Education Open Textbook Pilot Project, the California Education Learning Lab, the UC Davis Office of the Provost, the UC Davis Library, the California State University Affordable Learning Solutions Program, and Merlot. This material is based upon work supported by the National Science Foundation under Grant No. 1246120, 1525057, and 1413739.

Any opinions, findings, and conclusions or recommendations expressed in this material are those of the author(s) and do not necessarily reflect the views of the National Science Foundation nor the US Department of Education.

Have questions or comments? For information about adoptions or adaptions contact info@LibreTexts.org or visit our main website at https://LibreTexts.org.

This text was compiled on 04/28/2026

TABLE OF CONTENTS

Licensing

1: Thermodynamics

- 1.1: Review and Setting the Stage
- 1.2: Additional Measurable Quantities
- 1.3: Understanding Real Gases Using Measurable Quantities
- 1.4: Joule-Thompson Coefficient
- 1.5: Heat Engines
- 1.6: Multicomponent Phase Diagrams

2: Statistical Mechanics

- 2.1: Microcanonical and Canonical Ensembles
- 2.2: Statistical Thermodynamic Functions
- 2.3: Microconanonical (q molecular) Versus Canonical (Q) Partition Functions
- 2.4: From Quantum States to Partition Functions
- 2.5: Derivation of Ideal Gas Law
- 2.6: The Gaussian Distribution of One Component of the Molecular Velocity
- 2.7: The Maxwell-Boltzmann Distribution of Molecular Speeds in 3 Dimensions
- 2.8: Intermolecular Interactions Correction to the Translational Partition Function
- 2.9: Ortho and Para Hydrogen
- 2.10: The Equipartition Principle
- 2.11: Molar Heat Capacities

3: Quantum Mechanics

- 3.1: Quantum Operators Represent Classical Variables
- 3.2: Eigenfunctions of Operators are Orthogonal
- 3.3: Commuting Operators Allow Infinite Precision
- 3.4: The Quantum Mechanical Free Particle
- 3.5: The Energy Levels of a Rigid Rotor
- 3.6: The Variational Method
- 3.7: Linear Variational Method and the Secular Determinant
- 3.8: Perturbation Theory Expresses the Solutions in Terms of Solved Problems
- 3.9: Electron Spin, Indistinguishability and Slater Determinants
- 3.10: Band Structure

4: Spectroscopy

- 4.1: Spectroscopic Selection Rules
- 4.2: Rotational Spectroscopy of Diatomic Molecules
- 4.3: Rotational Spectra of Polyatomic Molecules
- 4.4: Harmonic Oscillator
- 4.5: Hermite Polynomials are either Even or Odd Functions
- 4.6: The Harmonic Oscillator and Infrared Spectra
- 4.7: Vibrational Overtones
- 4.8: Rotations Accompany Vibrational Transitions

- 4.9: Unequal Spacings in Vibration-Rotation Spectra
- 4.10: Electronic Spectra Contain Electronic, Vibrational, and Rotational Information
- 4.11: The Franck-Condon Principle
- 4.12: Electronically Excited Molecules can Relax by a Number of Processes
- 4.13: Raman Spectroscopy
- 4.14: The Dynamics of Transitions can be Modeled by Rate Equations
- 4.15: Beer's Law
- 4.16: A Two-Level System Cannot Achieve a Population Inversion
- 4.17: Population Inversion can be Achieved in a Three-Level System
- 4.18: What is Inside a Laser?
- 4.19: The Helium-Neon Laser
- 4.20: Modern Applications of Laser Spectroscopy
- 4.21: Broadening Mechanisms

5: Moving Molecules and Chemical Kinetics

- 5.1: Classical Model of Ideal Gas Pressure
- 5.2: Collisions
- 5.3: The Frequency of Collisions with a Wall
- 5.4: Transport of Matter and Energy in Perfect Gases
- 5.5: Stokes-Einstein-Sutherland Equation
- 5.6: The Rate of Bimolecular Gas-Phase Reaction Can Be Estimated Using Hard-Sphere Collision Theory and an Energy-Dependent Reaction Cross Section
- 5.7: A Reaction Cross Section Depends Upon the Impact Parameter
- 5.8: The Rate Constant for a Gas-Phase Chemical Reaction May Depend on the Orientations of the Colliding Molecules
- 5.9: The Internal Energy of the Reactants Can Affect the Cross Section of a Reaction
- 5.10: A Reactive Collision Can Be Described in a Center-of-Mass Coordinate System
- 5.11: Reactions Can Produce Vibrationally Excited Molecules
- 5.12: Reactive Collisions Can be Studied Using Crossed Molecular Beam Machines
- 5.13: The Velocity and Angular Distribution of the Products of a Reactive Collision
- 5.14: Not All Gas-Phase Chemical Reactions are Rebound Reactions
- 5.15: The Potential-Energy Surface Can Be Calculated Using Quantum Mechanics
- 5.16: Equilibrium Constants in Terms of Partition Functions
- 5.17: Statistical Mechnanical Transition State Theory
- 5.18: Chain Reactions
- 5.19: Chain Branching Explosions
- 5.20: Kinetics of Chain Polymerization
- 5.21: Kinetics of Step-Growth Polymerization
- 5.22: Atoms and Molecules can Physisorb or Chemisorb to a Surface
- 5.23: Isotherms are Plots of Surface Coverage as a Function of Gas Pressure at Constant Temperature
- 5.24: Using Langmuir Isotherms to Derive Rate Laws for Surface-Catalyzed Gas-Phase Reactions
- 5.25: The Structure of a Surface is Different from that of a Bulk Solid
- 5.26: The Haber-Bosch Reaction Can Be Surface Catalyzed
- 5.27: Photochemical Kinetics

Index

Glossary

Detailed Licensing

Licensing

1: Your page has been created!

Remove this content and add your own.

- Edit page

  Click the Edit page button in your user bar. You will see a suggested structure for your content. Add your content and hit Save.

1.0.1: Tips:

- Drag and drop

  Drag one or more image files from your computer and drop them onto your browser window to add them to your page.

- Classifications

  Tags are used to link pages to one another along common themes. Tags are also used as markers for the dynamic organization of content in the CXone Expert framework.

- Working with templates

  CXone Expert templates help guide and organize your documentation, making it flow easier and more uniformly. Edit existing templates or create your own.

- Visit for all help topics.

CHAPTER OVERVIEW

1: Thermodynamics

1.1: Review and Setting the Stage
1.2: Additional Measurable Quantities
1.3: Understanding Real Gases Using Measurable Quantities
1.4: Joule-Thompson Coefficient
1.5: Heat Engines
1.6: Multicomponent Phase Diagrams

This page titled 1: Thermodynamics is shared under a CC BY-NC-SA 4.0 license and was authored, remixed, and/or curated by Jonathan Gutow.

1.1: Review and Setting the Stage

1.1.1: Introduction

Using the mathematical properties of state functions we can extend our ability to use thermodynamics combined with physical measurements to make quantitative predictions about the behavior of real systems. This section reviews and defines the mathematics of total differentials and what it means for a total differential to be exact. Then we review the fundamental differentials of thermodynamics. These can be combined with their mathematical properties to generate important partial derivatives that provide rigorous thermodynamic definitions of many useful physical quantities and useful relations between more easily measured and hard to measure thermodynamic quantities.

1.1.2: Total derivatives

A partial derivative of a function F(x_1, x_2 ...), often written as $(\partial F/\partial x_i)_{x_{k_1},x_{k_2}...k_j\neq i}$, can be thought of as the rate of change of F along the direction x_i with all the other coordinates held constant. Geometrically this can be thought of as the tangent to the surface defined by F along the coordinate direction x_i. The *total derivative* (sometimes referred to as the *total differential*) is defined as the sum of all the partial derivatives each multiplied by an infinitesimal change along the coordinate the partial is taken along. This sum is then the infinitesimal change in F for infinitesimal changes along all the coordinates. Assuming F is a function of x_1, x_2 and x_3 yields a total derivative:

$$dF = \left(\frac{\partial F}{\partial x_1}\right)_{x_2,x_3} dx_1 + \left(\frac{\partial F}{\partial x_2}\right)_{x_1,x_3} dx_2 + \left(\frac{\partial F}{\partial x_3}\right)_{x_1,x_2} dx_3 \tag{1.1.1}$$

For a single component closed thermodynamic system (fixed number of moles, n), state functions are always determined when two state variables are defined. In the case of internal energy, we might write $U = f(V,T)$ or $U(V,T)$. If there is a mathematical function that relates the internal energy to these two variables, it is easy to see how U changes when either (or both!) are changed. This can be written as a total differential:

$$dU = \left(\frac{\partial U}{\partial V}\right)_T dV + \left(\frac{\partial U}{\partial T}\right)_V dT \tag{1.1.2}$$

Even without knowing the actually mathematical function relating the variables to the property, we can imagine how to calculate changes in the property from this expression.

$$\Delta U = \int_{V_1}^{V_2} \left(\frac{\partial U}{\partial V}\right)_T dV + \int_{T_1}^{T_2} \left(\frac{\partial U}{\partial T}\right)_V dT$$

In words, this implies that we can think of a change in U occurring due to an *isothermal change* followed by an *isochoric change*. And all we need to know is the slope of the surface in each pathway direction. Clearly, finding ways to measure these derivatives (slopes) is key to being able to calculate thermodynamic changes.

1.1.3: Exact Differentials

Previously we have used the fact that changes in thermodynamic state functions are path independent and noted this is the result of them being exact differentials. Here we define carefully what is required for a differential to be exact.

In general, if a differential can be expressed as

$$df(x,y) = X(x,y)dx + Y(x,y)dy$$

the differential will be an **exact differential** if it follows the **Euler relation**

$$\left(\frac{\partial X}{\partial y}\right)_x = \left(\frac{\partial Y}{\partial x}\right)_y \tag{1.1.3}$$

In order to illustrate this concept, consider $P(V,T)$ using the ideal gas law for a fixed n.

$$P = \frac{nRT}{V}$$

The total differential of P can be written

$$dP = \left(-\frac{nRT}{V^2}\right) dV + \left(\frac{nR}{V}\right) dT \tag{1.1.4}$$

Example 1.1.1: Euler Relation

Does Equation 1.1.4 follow the Euler relation (Equation 1.1.3)?

Solution

Let's confirm!

$$\left[\frac{\partial}{\partial T}\left(-\frac{nRT}{V^2}\right)\right]_V \stackrel{?}{=} \left[\frac{\partial}{\partial V}\left(\frac{nR}{V}\right)\right]_T$$
$$\left(-\frac{nR}{V^2}\right) \stackrel{\checkmark}{=} \left(-\frac{nR}{V^2}\right)$$

dP is, in fact, an exact differential.

The differentials of all of the **thermodynamic functions** that are **state functions** will be exact. Heat and work are not exact differential and dw and dq are called *inexact differentials* instead.

1.1.4: Four fundamental differentials of thermodynamics

The first law of thermodynamics in differential form is:

$$dU = \delta q + \delta w \tag{1.1.5}$$

For a reversible process we have defined the entropy as $dS = \delta q_{rev}/T$ and the reversible work as $\delta w = -P \cdot dV$. Substituting these identities into equation 1.1.5 gives the following differential form of the first law:

$$dU = TdS - PdV \tag{1.1.6}$$

Note that Equation 1.1.6 is valid for a reversible process in which the only work is due to compression/expansion.

The enthalpy is defined as:

$$H = U + PV \tag{1.1.7}$$

From Equation 1.1.7 we can write a differential form of the enthalpy as:

$$dH = dU + PdV + VdP \tag{1.1.8}$$

where we have again used the product rule from calculus on the PV term. Substituting equation 1.1.6 into equation 1.1.8 for the dU term gives another differential relation for dH:

$$dH = TdS - \cancel{PdV} + \cancel{PdV} + VdP = TdS + VdP \tag{1.1.9}$$

Similar arguments, which you should be able to produce, can be made for the state functions G and A. This leads to the four total differentials in table 1.1.1.

Table 1.1.1: the four fundamental differential relations for dU, dH, dG, and dA.

Differential Relation	Equation
dU=TdS−PdV	1.1.6
dH = TdS + VdP	1.1.9
dA=−PdV−SdT	
dG=VdP−SdT	

1.1.5: Some important partial derivatives

From the properties of total and exact differentials plus these fundamental equations we can develop thermodynamically rigorous definitions of thermodynamic quantities in terms of derivatives. Because derivatives reflect rates of change this gives us a handle on measuring these quantities as changes are often measurable even when absolute values of quantities are not.

1.1.5.1: T, V, P and S

Consider equation 1.1.6 from above:

$$dU = TdS - PdV$$

The natural variables of internal energy are thus S and V. So the total differential (dU) in equation 1.1.6 can also be expressed as:

$$dU = \left(\frac{\partial U}{\partial S}\right)_V dS + \left(\frac{\partial U}{\partial V}\right)_S dV \tag{1.1.10}$$

Comparing the two expressions for dU it is apparent that:

$$\left(\frac{\partial U}{\partial S}\right)_V = T \tag{1.1.11}$$

and

$$\left(\frac{\partial U}{\partial V}\right)_S = -P \tag{1.1.12}$$

The relations in equations 1.1.11 and 1.1.12 can be understood as ways to measure the partial derivatives, since T and P are values we can measure. Alternatively, they can be thought of as thermodynamic definitions of T under constant volume conditions and P under constant entropy conditions. For example we can rewrite equation 1.1.11 as:

$$T = \left(\frac{\partial U}{\partial S}\right)_V$$

Likewise the other fundamental differentials of thermodynamics lead to the additional relations between thermodynamic quantities and partial derivatives listed in table 1.1.2. You should be able to recreate the above logic for the other cases.

Table 1.1.2: All the differential relations that can be found by comparing the total differential of U, H, G and A with the four fundamental differentials of thermodynamics.

from dU = TdS - PdV	from dH = TdS + VdP	from dA = -PdV - SdT	from dG = VdP - SdT
$\left(\frac{\partial U}{\partial S}\right)_V = T$	$\left(\frac{\partial H}{\partial S}\right)_P = T$	$\left(\frac{\partial A}{\partial V}\right)_T = -P$	$\left(\frac{\partial G}{\partial P}\right)_T = V$
$\left(\frac{\partial U}{\partial V}\right)_S = -P$	$\left(\frac{\partial H}{\partial P}\right)_S = -V$	$\left(\frac{\partial A}{\partial T}\right)_V = -S$	$\left(\frac{\partial G}{\partial T}\right)_P = -S$

Notice that this means there are multiple thermodynamic definitions of T, P, V and S depending on what is being held constant.

1.1.5.2: Heat Capacities

Two other useful thermochemical quantities we have encountered that can be expressed in terms of partial derivatives are the heat capacities C_P and C_V which can be expressed as

$$C_P = \left(\frac{\partial H}{\partial T}\right)_P$$

and

$$C_V = \left(\frac{\partial U}{\partial T}\right)_V$$

These are properties that can be measured experimentally and tabulated for many substances. These quantities can be used to calculate changes in quantities since they represent the slope of a surface (H or U) in the direction of the specified path (constant P or V). This allows us to use the following kinds of relationships:

$$dH = \left(\frac{\partial H}{\partial T}\right)_p dT$$

and

$$\Delta H = \int \left(\frac{\partial H}{\partial T}\right)_P dT$$

Likewise ΔU can be calculated under constant volume conditions using C_V.

1.1.6: Maxwell Relations

The fact that total differentials of state functions are exact allows us to make some unexpected connections between partial derivatives, which are useful when determining what measurements can be used to determine a particular derivative.

As an example consider dU as written out in equation 1.1.10:

$$dU = \left(\frac{\partial U}{\partial S}\right)_V dS + \left(\frac{\partial U}{\partial V}\right)_S dV$$

Being an exact differential, the Euler relation must hold. Thus:

$$\left[\frac{\partial}{\partial V}\left(\frac{\partial U}{\partial S}\right)_V\right]_S = \left[\frac{\partial}{\partial S}\left(\frac{\partial U}{\partial V}\right)_S\right]_V$$

By substituting using equations 1.1.11 and 1.1.12 (or from table **1.1.2**, we see that

$$\left[\frac{\partial}{\partial V}(T)_V\right]_S = \left[\frac{\partial}{\partial S}(-P)_S\right]_V$$

or

$$\left(\frac{\partial T}{\partial V}\right)_S = -\left(\frac{\partial P}{\partial S}\right)_V$$

This is an example of a **Maxwell Relation**. These are very powerful relationships that allows one to a substitute partial derivatives with a more convenient one.

Similar results can be derived based on the definitions of H, G and A. The results are summarized in table **1.1.3**.

Table **1.1.3**: Maxwell Relations

Function	Differential	Natural Variables	Maxwell Relation
U	$dU = TdS - PdV$	S, V	$\left(\frac{\partial T}{\partial V}\right)_S = -\left(\frac{\partial P}{\partial S}\right)_V$
H	$dH = TdS + VdP$	S, P	$\left(\frac{\partial T}{\partial P}\right)_S = \left(\frac{\partial V}{\partial S}\right)_P$
A	$dA = -PdV - SdT$	V, T	$\left(\frac{\partial P}{\partial T}\right)_V = \left(\frac{\partial S}{\partial V}\right)_T$
G	$dG = VdP - SdT$	P, T	$\left(\frac{\partial V}{\partial T}\right)_P = -\left(\frac{\partial S}{\partial P}\right)_T$

The Maxwell relations are extraordinarily useful in deriving the dependence of thermodynamic values on the state variables of P, T, and V.

1.1.7: Partial derivative reciprocal and cyclic relations

Two more mathematical manipulations involving partial derivatives are also very useful when working with thermodynamics. These relations are valid as long as each variable in the total derivative are differentiable functions of the other variables (for more discussion of this see "Partial differential relations" on Wikipedia.org and the links and references included there). This is

essentially the requirement for being able to write a total differential, thus the relations described below are valid for relationships based on the fundamental differentials of thermodynamics.

The **reciprocal relation** is

$$1 = \left(\frac{\partial z}{\partial y}\right)_x \left(\frac{\partial y}{\partial z}\right)_x \quad \text{or} \quad \left(\frac{\partial z}{\partial y}\right)_x = \frac{1}{\left(\frac{\partial y}{\partial z}\right)_x} \tag{1.1.13}$$

As the choice of label for each variable is arbitrary this could equally well be stated as:

$$\left(\frac{\partial x}{\partial y}\right)_z = \frac{1}{\left(\frac{\partial y}{\partial x}\right)_z}$$

Derivation of the reciprocal rule

Consider a system that is described by three variables, and for which one can write a mathematical constraint on the variables

$$F(x, y, z) = 0$$

Under these circumstances, one can specify the state of the system varying only two parameters independently because the third parameter will have a fixed value. As such one could define two functions: $z(x, y)$ and $y(x, z)$.

This allows one to write the total differentials for dz and dy as follows

$$dz = \left(\frac{\partial z}{\partial x}\right)_y dx + \left(\frac{\partial z}{\partial y}\right)_x dy \tag{1.1.14}$$

and

$$dy = \left(\frac{\partial y}{\partial x}\right)_z dx + \left(\frac{\partial y}{\partial z}\right)_x dz \tag{1.1.15}$$

Substituting the Equation 1.1.15 expression into Equation 1.1.14:

$$dz = \left(\frac{\partial z}{\partial x}\right)_y dx + \left(\frac{\partial z}{\partial y}\right)_x \left[\left(\frac{\partial y}{\partial x}\right)_z dx + \left(\frac{\partial y}{\partial z}\right)_x dz\right] \tag{1.1.16}$$

$$= \left(\frac{\partial z}{\partial x}\right)_y dx + \left(\frac{\partial z}{\partial y}\right)_x \left(\frac{\partial y}{\partial x}\right)_z dx + \left(\frac{\partial z}{\partial y}\right)_x \left(\frac{\partial y}{\partial z}\right)_x dz \tag{1.1.17}$$

Collecting dz terms on one side and dy terms on the other yields:

$$\left[1 - \left(\frac{\partial z}{\partial y}\right)_x \left(\frac{\partial y}{\partial z}\right)_x\right] dz = \left[\left(\frac{\partial z}{\partial x}\right)_y + \left(\frac{\partial z}{\partial y}\right)_x \left(\frac{\partial y}{\partial x}\right)_z\right] dx \tag{1.1.18}$$

Because dz and dx can vary independently the the quantities in square brackets must equal zero. The reciprocal relation is derived from the left-hand-side:

$$1 - \left(\frac{\partial z}{\partial y}\right)_x \left(\frac{\partial y}{\partial z}\right)_x = 0 \implies \left(\frac{\partial z}{\partial y}\right)_x \left(\frac{\partial y}{\partial z}\right)_x = 1$$

The **cyclic relation** (sometimes called the *triple product rule*) is:

$$\left(\frac{\partial x}{\partial y}\right)_z \left(\frac{\partial y}{\partial z}\right)_x \left(\frac{\partial z}{\partial x}\right)_y = -1 \tag{1.1.19}$$

This is useful because it allows any one of the three partial derivatives to be expressed as a fraction involving the other two partial derivatives especially when combined with the reciprocal rule this can be very useful.

Example 1.1.1

Imagine you are working with a real gas and have equipment to measure T and P and V and the ability to control T and V, but no way to maintain the sample at a constant pressure as T and V vary. What two measurements can be combined to yield $\left(\frac{\partial V}{\partial T}\right)_P$?

Solution

From the cyclic relation we can write:

$$\left(\frac{\partial V}{\partial T}\right)_P \left(\frac{\partial T}{\partial P}\right)_V \left(\frac{\partial P}{\partial V}\right)_T = -1$$

Isolating the partial derivative of interest on the left-hand-side and using the reciprocal relation to invert the constant V derivative yields:

$$\left(\frac{\partial V}{\partial T}\right)_P = -\frac{\left(\frac{\partial P}{\partial T}\right)_V}{\left(\frac{\partial P}{\partial V}\right)_T}$$

Notice that the two derivatives on the right-hand-side require measuring pressure while varying T (and holding V constant) or varying V (and holding T constant). These are conditions that can be met with the equipment at hand. We have made no assumptions about whether the gas is ideal or not.

Derivation of the cyclic relation

This right-hand-side of equation 1.1.18 implies:

$$\left(\frac{\partial z}{\partial x}\right)_y + \left(\frac{\partial z}{\partial y}\right)_x \left(\frac{\partial y}{\partial x}\right)_z = 0$$

This rearranges to:

$$\left(\frac{\partial z}{\partial x}\right)_y = -\left(\frac{\partial z}{\partial y}\right)_x \left(\frac{\partial y}{\partial x}\right)_z$$

Using the reciprocal rule to rewrite the right-hand-side yields:

$$\left(\frac{\partial z}{\partial x}\right)_y = -\frac{1}{\left(\frac{\partial y}{\partial z}\right)_x \left(\frac{\partial x}{\partial y}\right)_z}$$

Multiplying through by the the denominator on the right-hand-side results in the cyclic relation:

$$\left(\frac{\partial x}{\partial y}\right)_z \left(\frac{\partial y}{\partial z}\right)_x \left(\frac{\partial z}{\partial x}\right)_y = -1$$

1.1.8: Exercises

1. Write out the derivation of all the relations in table **1.1.1**.
2. Write out the logic to develop the relations in table **1.1.2**.
3. Write out the derivation of all the Maxwell relations in table **1.1.3**.
4. Starting with the fundamental differential expression for dU divide through by dV to get an expression for $\left(\frac{\partial U}{\partial V}\right)_T$. Then use a Maxwell relation to show that you can rewrite it to $\left(\frac{\partial U}{\partial V}\right)_T = T\left(\frac{\partial P}{\partial T}\right)_V - P$, which contains easily measurable quantities.

This page titled 1.1: Review and Setting the Stage is shared under a CC BY-NC-SA 4.0 license and was authored, remixed, and/or curated by Jonathan Gutow.

- **4.2: Total and Exact Differentials** by Patrick Fleming is licensed CC BY-NC-SA 4.0.
- **1.6: The Gibbs and Helmholtz Energy** by Serge L. Smirnov and James McCarty is licensed CC BY-NC-SA 4.0.
- **6.2: Combining the First and Second Laws - Maxwell's Relations** by Patrick Fleming is licensed CC BY-NC-SA 4.0.

- **4.1: Prelude to Putting the First Law to Work** by Patrick Fleming is licensed CC BY-NC-SA 4.0.
- **4.3: Compressibility and Expansivity** by Patrick Fleming is licensed CC BY-NC-SA 4.0.

1.2: Additional Measurable Quantities

1.2.1: Introduction

In addition to the measurable sample specific quantities C_v and C_P there are a few other useful sample specific thermodynamic quantities that can be measured, tabulated and fit to functional forms for calculating properties of real samples. These are discussed below. What your should notice is that just like the heat capacities these are intensive properties and defined in terms of a derivative (change).

1.2.2: Isothermal Compressibility (κ_T)

A very important property of a substance is how compressible it is. Gases are very compressible, so when subjected to high pressures, their volumes decrease significantly. Solids and liquids however are not as compressible. However, they are not entirely incompressible. High pressure will lead to a decrease in volume, even if it is only slight. Compressibility varies significantly from among substances even in the liquid and solid phases.

To quantify just how compressible substances are, it is necessary to define the property. The **isothermal compressibility** is defined by the fractional differential change in volume due to a change in pressure.

$$\kappa_T \equiv -\frac{1}{V}\left(\frac{\partial V}{\partial P}\right)_T \tag{1.2.1}$$

The negative sign is important in order to keep the value of κ_T positive, since an increase in pressure will lead to a decrease in volume. The $1/V$ term is needed to make the property intensive so that it can be tabulated in a useful manner.

Gases at high enough temperatures and low enough pressures (near ambient conditions for the gases you are familiar with) behave close to ideally. We can calculate κ_T for and idea gas by directly taking the derivative:

$$V = \frac{nRT}{P}$$

So remembering that for an ideal gas $\frac{nRT}{PV} = 1$:

$$\kappa_T = -\frac{1}{V}\left(\frac{\partial V}{\partial P}\right)_T = -\frac{1}{V}\left(\frac{\partial}{\partial P}\right)_T \frac{nRT}{P} = \frac{nRT}{P^2V} = P^{-1}$$

So near ambient conditions κ_T for gases is $(10^5\ \text{Pa})^{-1} = 10^{-5}\ \text{Pa}^{-1} \approx 1\ \text{atm}^{-1} \approx 1\ \text{bar}^{-1}$. The isothermal compressibility for liquids and solids are much smaller being in the range of $10^{-5}\ \text{atm}^{-1}$ for liquids and $10^{-7}\ \text{atm}^{-1}$ for solids.

1.2.3: Thermal expansion coefficient (α)

Another very important property of a substance is how its volume will respond to changes in temperature. Again, gases respond profoundly to changes in temperature (think Charles' Law!) whereas solids and liquid will have more modest (but not negligible) responses to changes in temperature. (For example, If mercury or alcohol didn't expand with increasing temperature, we wouldn't be able to use those substances in thermometers.)

The definition of the **thermal expansion coefficient** (more accurately the *isobaric thermal expansion coefficient*) is

$$\alpha \equiv \frac{1}{V}\left(\frac{\partial V}{\partial T}\right)_P \tag{1.2.2}$$

As was the case with the compressibility factor, the $1/V$ term is needed to make the property intensive, and thus able to be tabulated in a useful fashion. In the case of expansion, volume tends to increase with increasing temperature, so the partial derivative is positive.

Gases at high enough temperatures and low enough pressures (near ambient conditions for the gases you are familiar with) behave close to ideally. We can calculate α for and idea gas by directly taking the derivative:

$$V = \frac{nRT}{P}$$

So:

$$\alpha = \frac{1}{V}\left(\frac{\partial V}{\partial T}\right)_P = \frac{1}{V}\left(\frac{\partial}{\partial T}\right)_P \frac{nRT}{P} = \frac{nR}{PV} = T^{-1}$$

Near room temperature this yields a value of $(298\ K)^{-1}$ = 0.00336 K^{-1}. This apparently small number is actually large. For comparison with some solids and liquids see table **1.2.1**.

Table **1.2.1**: A sampling of thermal expansion coefficients at 20 ˚C (from Wikipedia.org, https://en.wikipedia.org/wiki/Therma...ious_materials)

Solids (K^{-1})		Liquids (K^{-1})	
Al	69 x 10^{-6}	ethanol	0.000750
C (diamond)	3 x 10^{-6}	water	0.000207
Si	9 x 10^{-6}		

Example 1.2.1: Using the reciprocal and cyclic partial derivative relations to find useful relationships among thermodynamic quantities

Derive an expression for

$$\frac{\alpha}{\kappa_T}. \tag{1.2.3}$$

in terms of derivatives of thermodynamic functions using the definitions in Equations 1.2.1 and 1.2.2.

Solution

Substituting Equations 1.2.1 and 1.2.2 into the Equation 1.2.3

$$\frac{\alpha}{\kappa_T} = \frac{\frac{1}{V}\left(\frac{\partial V}{\partial T}\right)_P}{-\frac{1}{V}\left(\frac{\partial V}{\partial P}\right)_T}$$

Simplifying (canceling the $1/V$ terms and using the recipricol relation to invert the partial derivative in the denominator) yields

$$\frac{\alpha}{\kappa_T} = -\left(\frac{\partial V}{\partial T}\right)_P \left(\frac{\partial P}{\partial V}\right)_T$$

Applying the cyclic relation to the product on the right allows it to be expressed as a single (and also measurable derivative):

$$\frac{\alpha}{\kappa_T} = \left(\frac{\partial P}{\partial T}\right)_V$$

1.2.4: Adiabatic compressibility (κ_S)

In his seminal work, *Philosophiae Naturalis Principia Mathematica* (Newton, 1723), Isaac Newton (1643 - 1727)[1] calculated the speed of sound through air, assuming that sound was carried by isothermal compression waves. His calculated value of 949 m/s was about 15% smaller than experimental determinations. He accounted for the difference by pointing to “non-ideal effects”. But it turns out that his error, albeit an understandable one (since sound waves do not appear to change bulk air temperatures) was that the compression waves are adiabatic, rather than isothermal. As such, there are small temperature oscillations that occur due to the adiabatic compression followed by expansion of the gas carrying the sound waves. The oversight was correct by Pierre-Simon Laplace (1749 – 1827).[2]

LaPlace modeled the compression waves using the **adiabatic compressibility**, κ_S defined by

$$\kappa_S = -\frac{1}{V}\left(\frac{\partial V}{\partial P}\right)_S$$

Since the entropy is defined by

$$dS = \frac{dq_{rev}}{T}$$

it follows that any adiabatic pathway ($dq = 0$) is also **isentropic** ($dS = 0$), or proceeds at constant entropy.

> *Adiabatic pathways are also isentropic.*

Using what we know about thermodynamics and the behaviors of partial derivatives we can quantitatively describe why realizing the compression is adiabatic increases the value calculated for the speed of sound. We will start with the formula for the speed of sound in a gas (see for example https://en.wikipedia.org/wiki/Speed_...ound#Equations for explanation of form):

$$v_{sound} = \sqrt{\frac{1}{\rho\kappa}}$$

where κ is the compressibility. As noted above using the adiabatic compressibility yields a higher speed of sound. Thus $\kappa_S < \kappa_T$, which we can show.

Example 1.2.2: Showing that $\kappa_S < \kappa_T$

Show that $\kappa_S < \kappa_T$ using known thermodynamic properties and derivative relations.

Solution

We begin by expanding the description of κ_S by using the cyclic partial derivative relation. Applying this, the adiabatic compressibility can be expressed

$$\kappa_S = \frac{1}{V}\left(\frac{\partial V}{\partial S}\right)_P\left(\frac{\partial S}{\partial P}\right)_V$$

followed by using the reciprocal relation:

$$\kappa_S = \frac{1}{V}\frac{\left(\frac{\partial S}{\partial P}\right)_V}{\left(\frac{\partial S}{\partial V}\right)_P}$$

Using a simple chain rule, the partial derivatives can be expanded to get something a little easier to evaluate:

$$\kappa_S = \frac{1}{V}\frac{\left(\frac{\partial S}{\partial T}\right)_V\left(\frac{\partial T}{\partial P}\right)_V}{\left(\frac{\partial S}{\partial T}\right)_P\left(\frac{\partial T}{\partial V}\right)_P} \tag{1.2.4}$$

The utility here is that

$$\left(\frac{\partial S}{\partial T}\right)_V = \frac{C_V}{T} \tag{1.2.5}$$

$$\left(\frac{\partial S}{\partial T}\right)_P = \frac{C_P}{T} \tag{1.2.6}$$

This means that Equation 1.2.4 simplifies to

$$\kappa_S = \frac{C_V}{C_P}\left(\frac{1}{V}\frac{\left(\frac{\partial T}{\partial P}\right)_V}{\left(\frac{\partial T}{\partial V}\right)_P}\right)$$

Simplifying what is in the parenthesis yields

$$\kappa_S = \frac{C_V}{C_P}\left(\frac{1}{V}\left(\frac{\partial T}{\partial P}\right)_V\left(\frac{\partial V}{\partial T}\right)_P\right)$$

$$\kappa_S = \frac{C_V}{C_P}\left(-\frac{1}{V}\left(\frac{\partial V}{\partial P}\right)_T\right)$$

$$\kappa_S = \frac{C_V}{C_P}\kappa_T$$

Because it includes PV work, C_P is always bigger than C_V, so $\frac{C_V}{C_P} < 1$ making κ_S smaller than κ_T.

Note

The above derivation also allows calculation of κ_S from readily measured quantities.

1.2.4.1: References

1. Isaac Newton, Wikipedia.org, https://en.wikipedia.org/wiki/Isaac_Newton.

2. O'Connor and Robertson, "Pierre-Simon Laplace", https://mathshistory.st-andrews.ac.u...phies/Laplace/.

1.2.5: Internal pressure (π_T)

Another useful derivative quantity is the **internal pressure**. Going back to the expression for changes in internal energy that stems from assuming that U is a function of V and T (or $U(V,T)$ for short)

$$dU = \left(\frac{\partial U}{\partial V}\right)_T dV + \left(\frac{\partial U}{\partial T}\right)_V dT$$

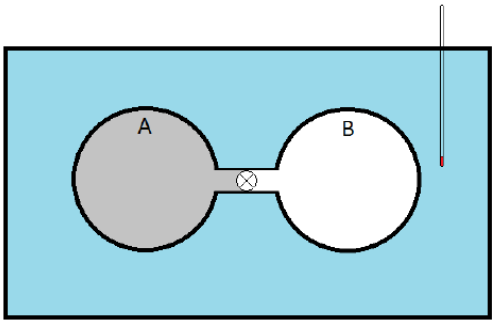
one quickly recognizes one of the terms as the constant volume heat capacity, C_V. And so the expression can be re-written

$$dU = \left(\frac{\partial U}{\partial V}\right)_T dV + C_V dT$$

But what about the first term? The partial derivative is a coefficient called the “internal pressure”, and given the symbol π_T.

$$\pi_T = \left(\frac{\partial U}{\partial V}\right)_T$$

James Prescott Joule (1818-1889) recognized that π_T should have units of pressure (Energy/volume = pressure) and designed an experiment to measure it.



He immersed two copper spheres, A and B, connected by a stopcock. Sphere A is filled with a sample of gas while sphere B was evacuated. The idea was that when the stopcock was opened, the gas in sphere A would expand ($\Delta V > 0$) against the vacuum in sphere B (doing no work since $P_{ext} = 0$. The change in the internal energy could be expressed

$$dU = \pi_T dV + C_V dT$$

But also, from the first law of thermodynamics

$$dU = dq + dw$$

Equating the two

$$\pi_T dV + C_V dT = dq + dw$$

and since $dw = 0$

$$\pi_T dV + C_V dT = dq$$

Joule concluded that $dq = 0$ (and $dT = 0$ as well) since he did not observe a temperature change in the water bath which could only have been caused by the metal spheres either absorbing or emitting heat. And because $dV > 0$ for the gas that underwent the expansion into an open space, π_T must also be zero! In truth, the gas did undergo a temperature change, but it was too small to be detected within his experimental precision. An additional problem with this experiment is that unless the second container is of infinite volume the pressure the gas is expanding against steadily increases as gas moves to container B.

π_T is generally not zero and can be calculated from easily measurable quantities. This is shown below making use of what we know about differentials and Maxwell's relations.

The fundamental differential for U is:

$$dU = TdS - PdV \tag{1.2.7}$$

We are looking for

$$\pi_T = \left(\frac{\partial U}{\partial V}\right)_T$$

Dividing equation 1.2.7 by dV and holding T constant yields:

$$\left(\frac{\partial U}{\partial V}\right)_T = T\left(\frac{\partial S}{\partial V}\right)_T - P\left(\frac{\partial V}{\partial V}\right)_T$$

The last derivative is 1, so this simplifies to:

$$\left(\frac{\partial U}{\partial V}\right)_T = T\left(\frac{\partial S}{\partial V}\right)_T - P$$

The derivative $\left(\frac{\partial S}{\partial V}\right)_T$ is not easy to measure, so we want to express it in terms of more easily measurable quantities. Looking at the Maxwell relations, you will find the one from the dA fundamental equation $\left(\frac{\partial P}{\partial T}\right)_V = \left(\frac{\partial S}{\partial V}\right)_T$ suits our purpose. Making the substitution yields.

$$\left(\frac{\partial U}{\partial V}\right)_T = T\left(\frac{\partial P}{\partial T}\right)_V - P \tag{1.2.8}$$

Using what we showed in example 1.2.1, $\left(\frac{\partial P}{\partial T}\right)_V = \frac{\alpha}{\kappa_T}$, we can substitute into equation 1.2.8 to get a general expression in terms of easily measured quantities for the internal pressure of any substance (solid, liquid or gas):

$$\pi_T = \left(\frac{\partial U}{\partial V}\right)_T = T\frac{\alpha}{\kappa_T} - P$$

Note that since α and κ_T are defined to be positive this implies that π_T is positive for "low" (near ambient for atmospheric gases) and negative at "high" pressure.

Example 1.2.3: Showing that $\pi_T = 0$ for an ideal gas

Show that for an ideal gas $\pi_T = \left(\frac{\partial U}{\partial V}\right)_T = 0$.

Solution

For an ideal gas $P = nRT/V$, so it is easy to show that

$$\left(\frac{\partial P}{\partial T}\right)_V = \frac{nR}{V} \tag{1.2.9}$$

so combining Equations 1.2.8 and 1.2.9 together to get

$$\left(\frac{\partial U}{\partial V}\right)_T = \frac{nRT}{V} - P \tag{1.2.10}$$

And since also because $P = nRT/V$, then Equation 1.2.10 simplifies to

$$\left(\frac{\partial U}{\partial V}\right)_T = P - P = 0$$

So while Joule's observation was consistent with limiting ideal behavior, his result was really an artifact of his experimental uncertainty masking what actually happened.

Example 1.2.4: Deriving π_T for a van der Waals gas

What is the internal pressure of a van der Waals gas?

Solution

For a van der Waals gas,

$$P = \frac{nRT}{V - nb} - \frac{an^2}{V^2} \tag{1.2.11}$$

so

$$\left(\frac{\partial P}{\partial T}\right)_V = \frac{nR}{V - nb} \tag{1.2.12}$$

and

$$\left(\frac{\partial U}{\partial V}\right)_T = T\frac{nR}{V - nb} - P \tag{1.2.13}$$

Substitution of the expression for P (Equation 1.2.11) into this Equation 1.2.13

$$\left(\frac{\partial U}{\partial V}\right)_T = \frac{an^2}{V^2}$$

1.2.6: Summary of useful measurable derivatives

Table **1.2.2**: The useful measurable derivatives.

Definitions	Alternative Expressions
$\kappa_T = -\frac{1}{V}\left(\frac{\partial V}{\partial P}\right)_T$	
$\alpha = \frac{1}{V}\left(\frac{\partial V}{\partial T}\right)_P$	
$\kappa_S = -\frac{1}{V}\left(\frac{\partial V}{\partial P}\right)_S$	
$\pi_T = \left(\frac{\partial U}{\partial V}\right)_T$	$\pi_T = \left(\frac{\partial U}{\partial V}\right)_T = T\frac{\alpha}{\kappa_T} - P$
$C_P = \left(\frac{\partial H}{\partial T}\right)_P$	$C_P = T\left(\frac{\partial S}{\partial T}\right)_P$
$C_V = \left(\frac{\partial U}{\partial T}\right)_V$	$C_V = T\left(\frac{\partial S}{\partial T}\right)_V$

1.2.7: Exercises

1. Starting with the fundamental differential expression for dH divide through by dT and hold P constant to get an expression for $\left(\frac{\partial H}{\partial T}\right)_P$. Use this to show that both expressions for C_p in table **1.2.2** are valid.
2.

1.2.8: Contributors

- Jonathan Gutow, UW Oshkosh
- Patrick Fleming, Cal State Eastbay

This page titled 1.2: Additional Measurable Quantities is shared under a CC BY-NC-SA 4.0 license and was authored, remixed, and/or curated by Jonathan Gutow.

- **4.3: Compressibility and Expansivity** by Patrick Fleming is licensed CC BY-NC-SA 4.0.
- **5.8: Adiabatic Compressibility** by Patrick Fleming is licensed CC BY-NC-SA 4.0.
- **4.4: The Joule Experiment** by Patrick Fleming is licensed CC BY-NC-SA 4.0.
- **4.1: Prelude to Putting the First Law to Work** by Patrick Fleming is licensed CC BY-NC-SA 4.0.

1.3: Understanding Real Gases Using Measurable Quantities

1.3.1: Introduction

Combining thermodynamics with measurable quantities allows us to predict the the thermodynamic behavior of real substances not just ideal ones. This significantly extends the usefulness of thermodynamics. In this section we will consider some examples of how real gases behave differently than ideal gases.

1.3.2: Adiabatic volume changes

For an ideal gas we have shown that $\pi_T = 0$. This allows us to state that $dU = \pi_T dV + C_V dT = C_V dT$. dU is also $dU = dq + dw$, but dq = 0 under adiabatic conditions so combining these we have rigorously shown that for an ideal gas:

$$C_V dT = dw. \tag{1.3.1}$$

whereas for a real gas where $\pi_T \neq 0$ the relationship is:

$$\pi_T dV + C_V dT = dw. \tag{1.3.2}$$

1.3.2.1: Case 1: Against zero pressure (irreversible)

If the gas expands against zero pressure it does no work and dw = 0.

Ideal gas case

Equation 1.3.1 becomes:

$$C_V dT = 0.$$

As $C_V > 0$ this implies that dT = 0, so the gas does not change temperature.

Real gas case

Equation Equation 1.3.2 becomes:

$$\pi_T dV + C_V dT = 0.$$

This rearranges to:

$$\pi_T dV = -C_V dT.$$

Collecting the measured quantities on one side and the differentials on the other yields:

$$\left(\frac{dT}{dV}\right)_S = -\frac{\pi_T}{C_V}.$$

In this case the subscript S is used to indicate adiabatic (isentropic) conditions. $C_V > 0$ and in the density range where attractions dominate $\pi_T > 0$. Thus the temperature will drop when a real gas expands against a vacuum. If $\pi_T < 0$, the situation at very high densities where repulsions dominate, the temperature could increase upon expansion.

This result can also be written in terms of the easily measurable α and κ_T using our previous result, $\pi_T = T\frac{\alpha}{\kappa_T} - P$, resulting in:

For a real gas expanding against a vacuum:

$$\left(\frac{dT}{dV}\right)_S = -\frac{1}{C_V}\left(T\frac{\alpha}{\kappa_T} - P\right).$$

1.3.2.2: Case 2: Against a non-zero pressure (irreversible)

In this case $dw = -P_{ext} dV$, where P_{ext} is a constant external pressure that either allows expansion or causes compression.

Ideal gas case

Equation 1.3.1 becomes:

$$C_V dT = -P_{ext} dV$$

which rearranges to:

$$\left(\frac{dT}{dV}\right)_S = -\frac{P_{ext}}{C_V}. \tag{1.3.3}$$

So an expansion of an ideal gas against a constant pressure will result in a temperature drop. The rate of drop is determined by the ratio of the external pressure and the constant volume heat capacity of the gas.

Real gas case

Equation 1.3.2 becomes:

$$\pi_T dV + C_V dT = -P_{ext} dV.$$

Collecting like differentials on the same sides produces:

$$(\pi_T + P_{ext}) dV = -C_V dT.$$

Collecting the differentials on the left and other factors on the right under adiabatic conditions:

$$\left(\frac{\partial T}{\partial V}\right)_S = -\frac{\pi_T + P_{ext}}{C_V}. \tag{1.3.4}$$

In the regime where $\pi_T > 0$ the numerator in equation 1.3.4 is more positive than in equation 1.3.3 by π_T. Thus, a real gas would be expected to cool more on expanding against a constant pressure than an ideal gas. If $\pi_T < 0$ then the real gas would cool less than an ideal gas. As in the previous instance we can substitute in for π_T in terms of α and κ_T.

For a real gas expanding adiabatically against a constant pressure:

$$\left(\frac{\partial T}{\partial V}\right)_S = -\frac{\left(T\frac{\alpha}{\kappa_T} - P\right) + P_{ext}}{C_V}.$$

1.3.2.3: Case 3: Reversible volume change

In the previous two examples we considered how temperature changed during an irreversible change in volume. During a reversible adiabatic change the pressure and volume must change in sync. A good way to understand this is to evaluate the partial derivative

$$\left(\frac{\partial V}{\partial P}\right)_S$$

This can be expanded by using the cyclic relation followed by an application of the reciprocal relation:

$$\left(\frac{\partial V}{\partial P}\right)_S = -\frac{\left(\frac{\partial V}{\partial S}\right)_P}{\left(\frac{\partial P}{\partial S}\right)_V}.$$

Expanding the two derivatives on the right-hand-side makes the equation easier to interpret:

$$\left(\frac{\partial V}{\partial P}\right)_S = -\frac{\left(\frac{\partial V}{\partial T}\right)_P \left(\frac{\partial T}{\partial S}\right)_P}{\left(\frac{\partial P}{\partial T}\right)_V \left(\frac{\partial T}{\partial S}\right)_V}. \tag{1.3.5}$$

Remembering that $dS = \frac{dq_{rev}}{T}$, which means at constant P $dS = \frac{C_P dT}{T} \implies \left(\frac{\partial S}{\partial T}\right)_P = \frac{C_P}{T}$ and likewise at constant V $\left(\frac{\partial S}{\partial T}\right)_V = \frac{C_V}{T}$, equation 1.3.5 can be simplified to:

$$\left(\frac{\partial V}{\partial P}\right)_S = -\frac{C_V}{C_P}\left(\frac{\partial V}{\partial T}\right)_P \left(\frac{\partial T}{\partial P}\right)_V.$$

$$= \frac{C_V}{C_p}\left(\frac{\partial V}{\partial P}\right)_T \tag{1.3.6}$$

Or defining $\gamma = C_p/C_V$, Equation 1.3.6 can be easily rearranged to

$$\gamma\left(\frac{\partial V}{\partial P}\right)_S = \left(\frac{\partial V}{\partial P}\right)_T = -V\kappa_T \tag{1.3.7}$$

Ideal gas case

For an ideal gas $\kappa_T = P^{-1}$ (at ambient conditions $\kappa_T \approx 10^{-5} Pa^{-1}$). So, substituting into equation 1.3.7 gives us:

$$\gamma\left(\frac{\partial V}{\partial P}\right)_S = -\frac{V}{P}$$

which is in a form we can rearrange to integrate. Separation of variables yields:

$$\gamma\frac{dV}{V} = -\frac{dP}{P}.$$

Integration (assuming that γ is independent of volume) yields

$$\gamma\int_{V_1}^{V_2}\frac{dV}{V} = -\int_{P_1}^{P_2}\frac{dP}{P}.$$

Integrating both sides yields

$$\gamma\ln\left(\frac{V_2}{V_1}\right) = -\ln\left(\frac{P_2}{P_1}\right) \quad \text{or} \quad \gamma\ln\left(\frac{V_2}{V_1}\right) = \ln\left(\frac{P_1}{P_2}\right),$$

which is easily manipulated to show that

$$P_1V_1^\gamma = P_2V_2^\gamma$$

or

$$PV^\gamma = \text{constant}$$

the behavior of an ideal gas along an adiabat.

Real gas case

In this case we do not have a closed form expression for κ_T, although we could use an empirical gas equation such as the virial expansion, van der Waals or others.

Consider again equation 1.3.7 but rearranged to put all the constants on one side:

$$\left(\frac{\partial V}{\partial P}\right)_S = -\frac{V\kappa_T}{\gamma}$$

In the case of real gases intermolecular attractions dominate except at high density (low T and/or high P). Imagine increasing the pressure of a "low" density real gas. Increasing the pressure increases the density, which lowers the average potential energy (closer together, so more attraction). In an adiabatic system the total energy (potential + kinetic) must remain fixed. If the potential energy is reduced then the kinetic energy must increase, which increases the pressure. Thus, a given change in pressure requires less of a change in volume. The conclusion is that $\kappa_T(real) < \kappa_T(ideal)$ and that we see a smaller volume change for a given pressure change with real gases.

Closed form expressions for how P and V vary for significant changes in real gases are difficult to come up with because of the temperature dependence of κ_T, which is often only available with good accuracy via direct measurements. For example consider the van der Waals empirical real gas equation:

$$\left(P + \frac{a}{\bar{V}^2}\right)\left(\bar{V} - b\right) = RT, \tag{1.3.8}$$

where a and b are the van der Waals coefficients dependent on the identity of the gas and $\bar{V}$ is the molar volume of the gas at the particular P and T combination. This is a cubic equation in $\bar{V}$ so it is difficult to solve for $\bar{V}$ and then take the derivative with respect to P to find κ_T. However, we can use the reciprocal properties of derivatives to avoid having to do as much work, yet get a functional form of $\kappa_T = \frac{-1}{V}\left(\frac{\partial V}{\partial P}\right)_T$. The trick is to realize we can solve easily for P and then just invert the derivative $\left(\frac{\partial P}{\partial V}\right)_T$ to get a valid expression for what we want as illustrated below.

$$P = \frac{RT}{\bar{V} - b} - \frac{a}{\bar{V}^2}$$

Taking the derivative yields:

$$\left(\frac{\partial P}{\partial \bar{V}}\right)_T = -\frac{RT}{\left(\bar{V} - b\right)^2} + \frac{2a}{\bar{V}^3}.$$

Inverting yields:

$$\left(\frac{\partial \bar{V}}{\partial P}\right)_T = \frac{\bar{V}^3\left(\bar{V} - b\right)^2}{-RT\bar{V}^3 + 2a\left(\bar{V} - b\right)^2}.$$

Notice the temperature dependence. In an adiabatic process the temperature also changes with the volume, so a functional form of T(P, V) must be found in order to integrate over a significant volume change for a real gas.

1.3.3: Isothermal changes

Isothermal changes are what $\kappa_T = -\frac{1}{V}\left(\frac{\partial V}{\partial P}\right)_T$ and $\pi_T = \left(\frac{\partial U}{\partial V}\right)_T$ quantify. As shown previously from the general result

$$\pi_T = \left(\frac{\partial U}{\partial V}\right)_T = T\frac{\alpha}{\kappa_T} - P,$$

we know that for an ideal gas $\pi_T = 0$, and, since α and κ_T are defined to be positive, that $\pi_T > 0$ for real gases unless the pressure is very high.

This gives us a handle on how U changes under isothermal (dT = 0) conditions:

$$dU = dq + dw = \pi_T dV + C_V dT = \pi_T dV.$$

Ideal gas case ($\pi_T = 0$): dU = 0, which implies ΔU = 0 for all isothermal changes of an ideal gas.

Real gas case: $dU \propto dV$. Thus, in the "low" pressure regime where $\pi_T > 0$, U increases with increasing volume and decreases with decreasing volume. In the "high" pressure regime where $\pi_T < 0$, the opposite is true.

This page titled 1.3: Understanding Real Gases Using Measurable Quantities is shared under a CC BY-NC-SA 4.0 license and was authored, remixed, and/or curated by Jonathan Gutow.

- **5.8: Adiabatic Compressibility** by Patrick Fleming is licensed CC BY-NC-SA 4.0.

1.4: Joule-Thompson Coefficient

1.4.1: Introduction

A useful derivative for understanding cooling or heating of gases when they expand is the Joule-Thomson coefficient (μ_{JT}). In 1852, working with William Thomson (who would later become Lord Kelvin), Joule conducted an experiment in which they pumped gas at a steady rate through a lead pipe that was cinched to create a constriction. On the upstream side of the constriction, the gas was at a higher pressure than on the downstream side of the constriction. Also, the temperature of the gas was carefully monitored on either side of the constriction. The cooling that they observed as the gas expanded from a high pressure region to a lower pressure region was extremely important and lead to a common design of modern refrigerators.

1.4.2: Definition

Not all gases undergo a cooling effect upon expansion. It depends on the the pressure, temperature and the identity of the gas. Some gases, such as hydrogen and helium, will experience a warming effect upon expansion under conditions near room temperature and pressure. The direction of temperature change can be determined by measuring the Joule-Thomson coefficient, μ_{JT}. This coefficient has the definition

$$\mu_{JT} \equiv \left(\frac{\partial T}{\partial P}\right)_H$$

This is a useful derivative because it appears in the expression for the infinitesimal change of H with respect to pressure and temperature:

$$dH = \left(\frac{\partial H}{\partial P}\right)_T dP + \left(\frac{\partial H}{\partial T}\right)_P dT \tag{1.4.1}$$

You should recognize the second derivative as C_P. Using the cyclic derivative relationship the first derivative can be rewritten to depend on C_P and μ_{JT}.

$$\left(\frac{\partial H}{\partial P}\right)_T = -\frac{1}{\left(\frac{\partial P}{\partial T}\right)_H \left(\frac{\partial T}{\partial H}\right)_P}$$

Recognizing that the differentials on the bottom are the inverse of C_P and μ_{JT} leads to:

$$\left(\frac{\partial H}{\partial P}\right)_T = -\mu_{JT} C_P. \tag{1.4.2}$$

This allows dH to be written in terms of measurable quantities:

$$dH = -\mu_{JT} C_P dP + C_P dT \tag{1.4.3}$$

1.4.3: Measurement of μ_{JT}

The Joule-Thomson coefficient can be measured by recording the adiabatic temperature drop or increase a gas undergoes for a given pressure drop. This can be visualized as two pistons moving as in figure **1.4.1**) to maintain the pressures on either side as constants. The apparatus is insulated to make it adiabatic. This is clearly an adiabatic process, but is isenthalpic, as indicated in the definition?

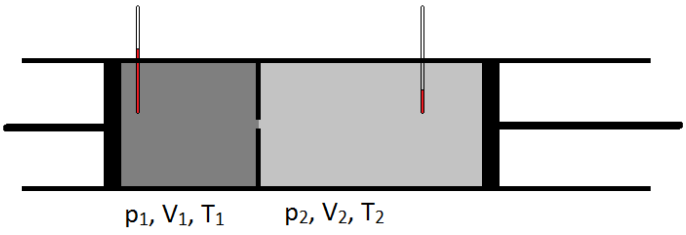


Figure **1.4.1**:

This process is isenthalpic as shown below.[1]

Since the gas expands adiabatically, q = 0. Thus, $\Delta U = w$. Imagine starting with all the gas on the high pressure (up stream) side. The initial conditions are P_1, V_1 and T_1. After all the gas has passed through it will be at P_2, V_2 and T_2. The work on the upstream side was:

$$w_1 = -P_1 \Delta V_1 = -P_1(V_{1f} - V_{1i}) = -P_1(0 - V_1) = P_1 V_1$$

On the downstream side the work is:

$$w_2 = -P_2 \Delta V_2 = -P_2(V_{2f} - V_{2i}) = -P_2(V_2 - 0) = -P_2 V_2.$$

Summing these together gives us the total work and ΔU:

$$\Delta U = U_2 - U_1 = w_1 + w_2 = P_1 V_1 - P_2 V_2.$$

Collecting all the upstream quantities on one side and the downstream on the other yields:

$$U_2 + P_2 V_2 = U_1 + P_1 V_1. \tag{1.4.4}$$

Since H = U + PV equation 1.4.4 means that the enthalpy on the two sides is the same, making the process isenthalpic.

In an actual laboratory setting constant flow of gas at a fixed pressure and temperature into the high pressure side and removal of gas from the low pressure side is used. An alternative to measuring the temperature change is to measure the isothermal Joule_Thomson coefficient $\left(\frac{\partial H}{\partial P}\right)_T$ (equation 1.4.2) directly by determining how much heat is needed to keep the temperatures on the two sides equal. Equation 1.4.2 can then be used to calculate μ_{JT}.

1.4.3.1: References

1. P. Atkins and J. De Paula, *Physical Chemistry*, 9th Ed. (W.H. Freeman and Co., New York, 2010), Pp. 79 - 83.

1.4.4: Real gas behavior

The typical behavior of the Joule-Thomson coefficient can be summarized in Figure 1.4.2. At the combinations of T and P for which $\mu_{JT} > 0$ (inside the shaded region), the sample will cool upon expansion. At those P and T conditions outside of the shaded region, where $\mu_{JT} < 0$, the gas will undergo a temperature increase upon expansion. And along the boundary, a gas will undergo neither a temperature increase not decrease upon expansion. For a given pressure, there are typically two temperatures at which μ_{JT} changes sign. These are the upper and lower inversion temperatures.

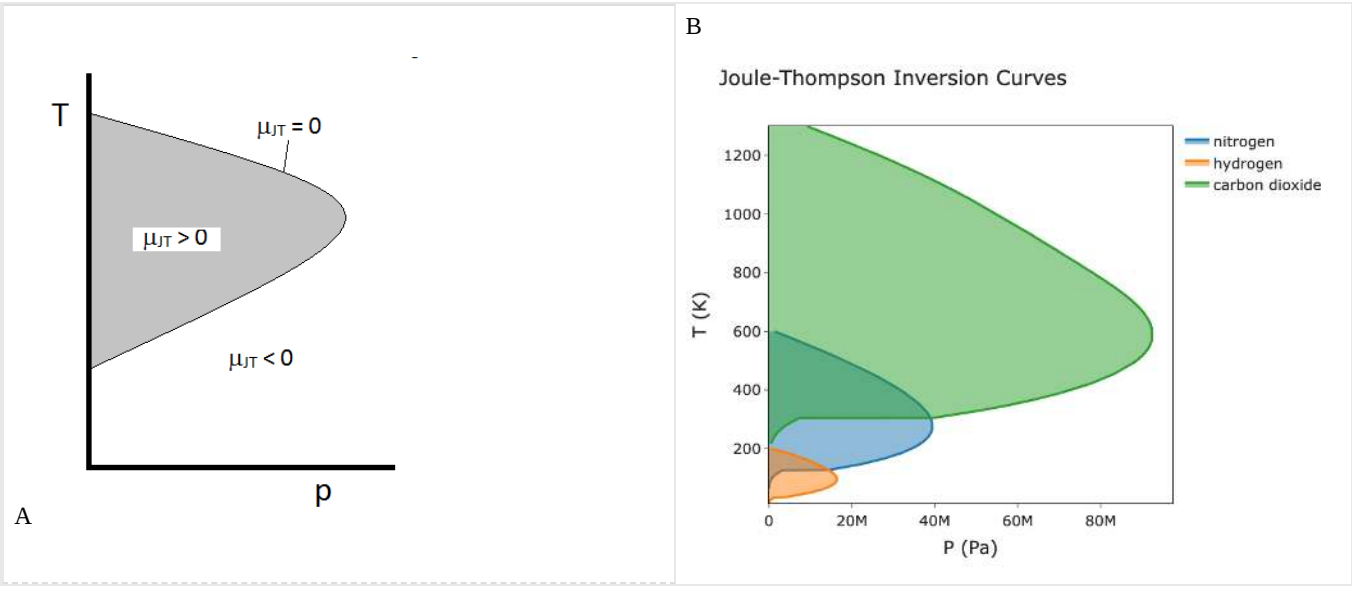


Figure 1.4.2: A) The typical behavior of the Joule-Thomson coefficient at different temperatures and pressures. B) Inversions curves for nitrogen, hydrogen and carbon dioxide. Based on values calculated using the CoolProp code, which uses Helmholtz-energy-explicit equations of state.

Joule-Thompson cooling is used in the Linde (you may have heard of a company by that name) refrigeration technique to liquefy atmospheric gases. The gas to be cooled is pumped through a cooling coil inside an insulated container. The end of the coil is open to the box. The gas that expands through a throttle out of the end of the coil cools as long as the temperature and pressure are within the cooling region ($\mu_{JT} > 0$). This cooler gas cools the gas within the coil and is then pumped out of the insulated container. The gas pumped out of the container is compressed to raise its temperature above ambient and run through a heat exchanger to cool it back down to close to ambient. This is then run through the coil inside again. Eventually, the gas coming out the throttle is so cool that it condenses and drips to the bottom of the insulated container, where it can be collected.

1.4.5: Relation of μ_{JT} to other measurable quantities

Recall that equation 1.4.2 gives us a relation between μ_{JT} and a derivative of the enthalpy:

$$\left(\frac{\partial H}{\partial P}\right)_T = -\mu_{JT} C_P.$$

From the fundamental differential dH = TdS + VdP we can divide by dP while holding T constant to get:

$$\left(\frac{\partial H}{\partial P}\right)_T = T\left(\frac{\partial S}{\partial P}\right)_T + V,$$

where we have used the general result that du/du = 1. Looking at the Maxwell relations you will recognize that $\left(\frac{\partial S}{\partial P}\right)_T = -\left(\frac{\partial V}{\partial T}\right)_P$. So:

$$\left(\frac{\partial H}{\partial P}\right)_T = -T\left(\frac{\partial V}{\partial T}\right)_P + V = -TV\alpha + V = V(1 - T\alpha).$$

Setting this equal to $-\mu_{JT} C_P$:

$$V(1 - T\alpha) = -\mu_{JT} C_P \implies \mu_{JT} = \frac{V}{C_P}(T\alpha - 1)$$

For an ideal gas, $\alpha = 1/T$, so $\mu_{JT} = 0$. Thus, gases will only show non-zero values for μ_{JT} when they deviate from ideal behavior.

1.4.6: Contributors

- Jonathan Gutow, UW Oshkosh
- Patrick Fleming, Cal State Eastbay

This page titled 1.4: Joule-Thompson Coefficient is shared under a CC BY-NC-SA 4.0 license and was authored, remixed, and/or curated by Jonathan Gutow.

- **4.5: The Joule-Thomson Effect** by Patrick Fleming is licensed CC BY-NC-SA 4.0.

1.5: Heat Engines

1.5.1: Introduction

Heat and work are both forms of transferring energy, and under the right circumstance, one form may be transformed into the other. However, the second law of thermodynamics puts a limitation on this. To go from work to heat is called dissipation and there is no limitation on this at all. In fact it was through dissipation (by friction) that we discovered that heat and work were both forms of energy. There is, however, a limitation on converting heat to work. In this section we will begin by considering the theoretical Carnot cycle which uses only reversible processes. From past analyses we know that reversible processes yield the maximum work possible from a gas expansion. Thus, the efficiency of the Carnot cycle is the upper limit to the efficiency of conversion of heat into work.

1.5.2: The Carnot cycle

The idealized Carnot cycle involves four steps as illustrated in figure 1.5.1.

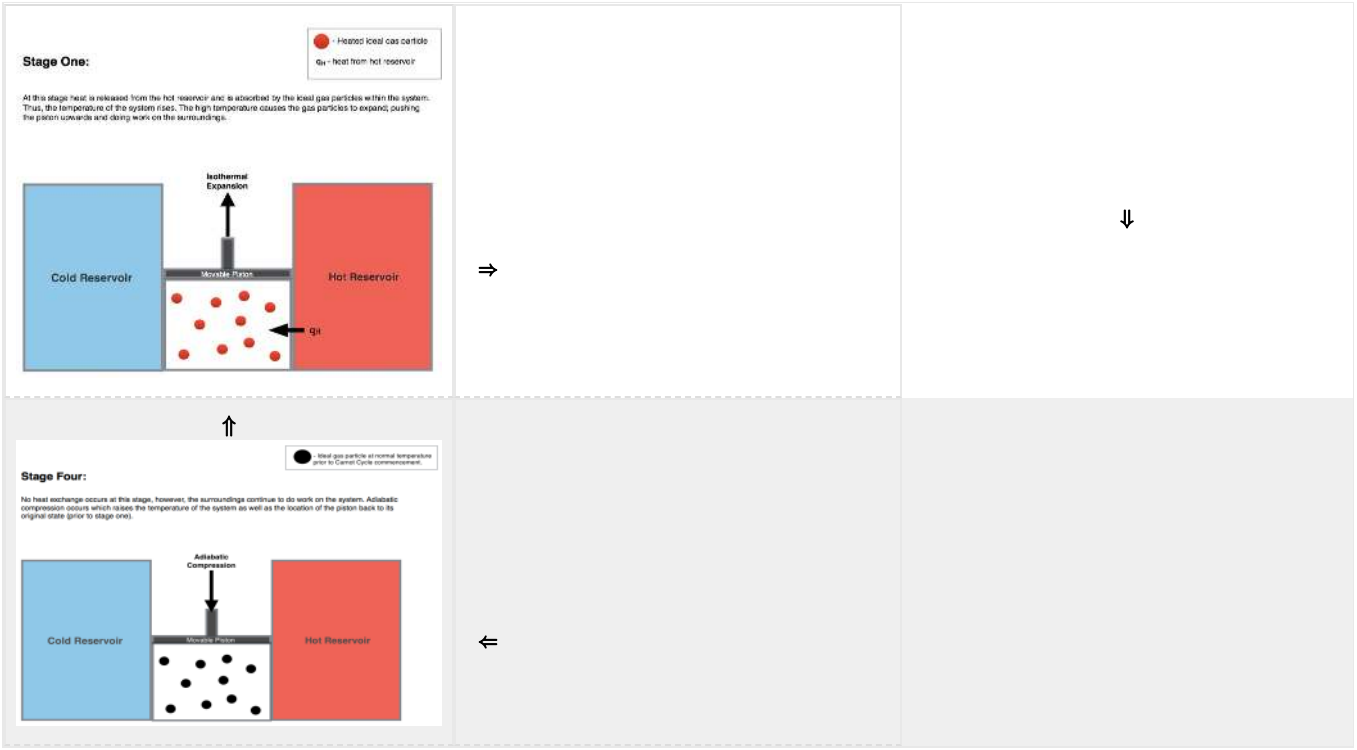


Figure 1.5.1: The four reversible steps in the Carnot cycle. **Step 1** starting at high pressure and low volume (A) and expanding isothermally (heat in from the hot reservoir) to a lower pressure and larger volume (B). **Step 2** starting at (B) and expanding adiabatically (no thermal contact with either reservoir) to an even lower pressure and larger volume (C). **Step 3** starting at (C) and being compressed isothermally (heat out to the cold reservoir) to a higher pressure and lower volume (D). **Step 4** starting at (D) being compressed back to the initial pressure and volume (A) adiabatically (no thermal contact with reservoirs). Figures courtesy of BlyumJ, CC BY-SA 4.0 , via Wikimedia Commons.

One way to imagine the heat exchange happening in the process is to imagine that the piston containing the working gas is separated from the cold and hot reservoirs by barriers that can shift from insulating to heat conducting frictionlessly. A realistic physical approximation to this would be movable barriers where one part is insulating foam and another a heat conductor such as copper metal.

This idealized cycle is shown on a PV diagram in figure 1.5.2.

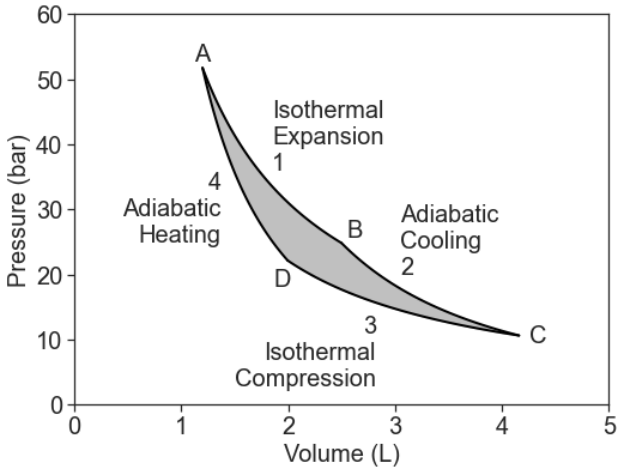


Figure 1.5.2: PV diagram for the Carnot cycle.

We can analyze the heat total heat and work of this cycle assuming an ideal gas.This cycle forms the 4-stage Carnot cycle heat engine. The cycle consists of:

1. Isothermal expansion at the hot temperature, T_h. As we have shown for an ideal gas an isothermal change leads to zero change in internal energy. Thus:

$$\Delta U_1 = w_1 + q_h = 0.$$

2. During adiabatic cooling from T_h to T_c no heat is exchanged. Thus:

$$\Delta U_2 = w_2.$$

3. Isothermal compression at the cold temperature, T_c:

$$\Delta U_3 = w_3 + q_c = 0$$

4. Adiabatic heating from T_c to T_h:

$$\Delta U_4 = w_4$$

The total four-step process produces work because $w_{hot} > w_{cold}$, where $w_{hot} = w_1 + w_2$ and $w_{cold} = w_3 + w_4$. The work is the integral under the upper curves minus the lower curves, i.e.the surface *area in between*.

Sadi Carnot

Sadi Carnot was a French engineer at the beginning of the 19th century. He considered a cyclic process involving a cylinder filled with gas. This cycle the Carnot cycle contributed greatly to the development of thermodynamics and the improvement of the steam engine. Carnot demonstrated that the cold temperature on the right is as important as the heat source on the left in defining the possible efficiency of a heat engine

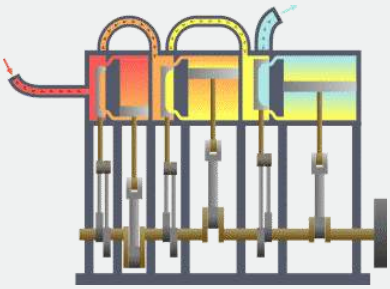


Figure 20.7.2 : Animation of a typical vertical triple-expansion engine. (CC SA-BY 2.5; Emoscopes).

1.5.3: Efficiency

Of course we spend good money on the fuel to start the cycle by heating things up. So how much work do we get for the heat we put in? In other words, we want to know how efficient our heat engine is. The efficiency, η of a heat engine is:

$$\eta = \frac{|w_{\text{cycle}}|}{q_h} = \frac{q_h + q_c}{q_h} = 1 + \frac{q_c}{q_h}$$

To get the work of the cycle, we can make use of internal energy as a state function. As the path is circular the circular integrals for U is zero:

$$\begin{aligned} \oint dU &= \Delta U_{\text{cycle}} \\ &= \sum \Delta U_i \\ &= w_1 + q_h + w_2 + w_3 + q_c + w_4 \\ &= 0 \end{aligned}$$

Rearranging:

$$\begin{aligned} q_h + q_c &= -w_1 - w_2 - w_3 - w_4 \\ &= -w_{\text{cycle}} \end{aligned}$$

An ideal engine would take $q_h \rightarrow q_c$ with 100% efficiency. The work of the cycle will be equivalent to the heat transfer. For ideal gases:

1. $w_1 = -RT_h \ln\left(\frac{V_B}{V_A}\right) = -q_h$
2. $dU = \delta w = C_V dT \rightarrow w_2 = C_V (T_c - T_h)$
3. $w_3 = -RT_c \ln\left(\frac{V_D}{V_C}\right) = -q_c$
4. $w_4 = C_V (T_h - T_c)$

Finding an expression for w_{cycle}:

$$\begin{aligned} w_{\text{cycle}} &= -RT_h \ln\left(\frac{V_B}{V_A}\right) + C_V (T_c - T_h) - RT_c \ln\left(\frac{V_D}{V_C}\right) + C_V (T_h - T_c) \\ &= -RT_h \ln\left(\frac{V_B}{V_A}\right) - RT_c \ln\left(\frac{V_D}{V_C}\right) = -R(T_h - T_c) \ln\left(\frac{V_B}{V_A}\right) \end{aligned}$$

The last simplification step used the fact that $(V_B/V_A) = (V_C/V_D) = (V_D/V_C)^{-1}$ because the two adiabats involve changes between the same high and low temperatures plus our gas is ideal making $P_c V_c^{\gamma} = P_h V_h^{\gamma}$.

We have an expression for work, so we can evaluate the efficiency, η. The efficiency of the Carnot engine is:

$$\eta = \frac{|w_{\text{cycle}}|}{q_h} = \frac{R(T_h - T_c) \ln\left(\frac{V_B}{V_A}\right)}{RT_h \ln\left(\frac{V_B}{V_A}\right)} = \frac{T_h - T_c}{T_h} = 1 - \frac{T_c}{T_h}$$

Paths (2) and (4) are adiabats, so we can also use entropy, S, to get the same solution:

$$\oint dS = \frac{q_h}{T_h} + \frac{q_c}{T_c} = 0$$

Therefore:

$$\frac{q_c}{q_h} = -\frac{T_c}{T_h}$$

And we get that:

$$\eta = 1 + \frac{q_c}{q_h} = 1 - \frac{T_c}{T_h} \tag{1.5.1}$$

As you see we can only get full efficiency if T_{cold} is 0 K, which is never (i.e., we always waste energy). Another implication is that if $T_c = T_h$ then **no work** can be obtained, no matter how much energy is available in the from of heat. Or in other words, if one

dissipates work into heat isothermally, *none* of it can be retrieved. Equation 1.5.1 is not very forgiving at all. Imagine that you have a heat source of 400 K (a superheated pool of water, e.g. a geyser) and you are dumping the waste heat into a river near room temperature at 300 K. The best efficiency you'll ever get is:

$$\eta = 1 - \frac{300}{400} = 25\%$$

Sadly, you'd be dumping three quarters of your energy as heat in the river (and that is best case scenario as there are always more losses, e.g. due to friction).

> This is another illustration of the second law of thermodynamics. For a process to move forward entropy must be created in the Universe. In the case of heat engines this means that some of the heat must end up as waste heat in the Universe. Thus heat cannot be converted to work with 100% efficiency.

1.5.4: Heat pumps

So getting our work from heat is hard and always less than 100% successful. The other way around should be easy. After all, we can dissipate work into heat freely even under isothermal conditions!

What happens if we let the heat engine run backwards? Consider reversing all the flows in the above diagram. Obviously we must *put in work* to make the cycle run in reverse. The heat will now flow from cold to hot, say from your cold garden into your nice and warm apartment. The amount of heat you get in your humble abode will be the sum of all the work (say 100 Joules) you dissipate *plus* the heat you pumped out of the garden (say 300 Joules). Thus if you are willing to pay for the energy you dissipate (100 Joules), you may well end up with a total of 400 Joules of heat in your apartment! Obviously if it is heat you are after, this is a better deal than just dissipating the work in your apartment (by burning some oil). Then you'd only get 100 J for your precious buck.

Dissipating it as electrical heating is even worse because you would:

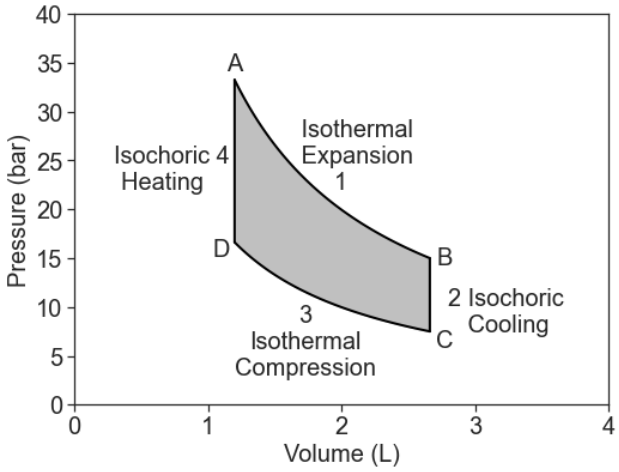
1. first burn (a lot more!) oil to generate heat;
2. use this heat to produce electrical work at great expense because a lot of the heats gets dumped at the low temperature side;
3. dissipate the work again in your apartment (without using it to pump any heat out of the garden).

Refrigerators are also heat pumps. They heat the kitchen by pumping heat from its innards to the kitchen. If I keep the door open, however, all it does is dissipate precious electrical work, because the pumped heat will flow back into its innards and spoil the milk.

1.5.5: More realistic cycles

1.5.5.1: Stirling

Let's consider another type of heat engine, the Stirling engine. The Stirling engine uses a circular reversible path in an ideal PV diagram:



The path consists of four steps:

1. *Isothermal* expansion at the hot temperature T_h:

$$q_1 = q_h = -w$$

and we get work **out** (i.e., negative work):

$$w_h = -RT_h \ln\left(\frac{V_B}{V_A}\right)$$

2. *Isochoric cooling* from T_h to T_c (with constant C_V):

$$q_2 = \frac{C_V}{\Delta T} \tag{1.5.2}$$

3. *Isothermal* compression at the cold temperature T_c:

$$q_3 = q_c = -w$$

and we must put work **in** (i.e., positive work):

$$w_c = -RT_c \ln\left(\frac{V_D}{V_C}\right) = RT_c \ln\left(\frac{V_B}{V_A}\right)$$

4. *Isochoric heating* from T_c to T_h (with constant C_V):

$$q_4 = -\frac{C_V}{\Delta T} \tag{1.5.3}$$

Notice that this gray area *vanishes* if $T_h = T_c$. Obviously how cold the cold side is of great importance! The amount of work is also equal to the difference in the heat picked up at high temperature q_h and dumped at low temperature q_c. The isochoric heats cancel. The problem is that q_c is only zero if the cold temperature is 0 K. That means that we can never get all the heat we pick up at high temperatures to come out as work.

1.5.5.2: Otto

This cycle is quite close to what occurs in an internal combustion automobile engine. The cycle starts with the compressed fuel-air mixture at P_A, V_A and T_A.

1. The fuel is then ignited and assumed to heat at constant volume to T_h.
2. The heated gas then expands adiabatically (isentropicly) to V_B, P_B and T_B.
3. The gas then cools to T_C while V_B is maintained. This last step is a simplification of exhausting of the spent combustion products and replacement by a new fuel-air mixture, which usually requires an additional piston cycle to force out the exhaust and suck in the fresh fuel-air mixture.
4. The fuel-air mixture is adiabatically compressed to the initial P_A, V_A and T_A.

Analysis of the cycle shows that the efficiency is equal to:

$$\eta = 1 - \left(\frac{V_A}{V_B}\right)^{(C_P - C_V) \div C_V} = 1 - \left(\frac{V_A}{V_B}\right)^{\gamma - 1}. \tag{1.5.4}$$

This is why high compression ratio engines are desirable. The higher the compression ratio the higher T_h and thus the higher the efficiency. The ratio is limited by the available materials for constructing the engine and the properties of the fuel used. Typical modern high compression engines operate with compression ratios 12:1 (V_B:V_A) or slightly greater.[1] This limits their thermodynamic maximum efficiency. Assume the best case scenario where the working gas is an ideal monatomic gas (no internal degrees of freedom to absorb the energy, so it all ends up a kinetic energy generating pressure). For ideal gases, $C_P = (C_V + nR)$. For a monatomic ideal gas $C_V = \frac{3}{2}nR$, so :

$$\eta = 1 - \left(\frac{1}{12}\right)^{\frac{2}{3}} = 0.81.$$

This looks pretty good. But there are two problems: 1) most of the gases are at least diatomics with ideal values of $C_V = \frac{5}{2}nR$ or nonlinear polyatomics with values of $C_V = 3nR$; 2) there are additional frictional and mechanical losses. Assuming ideal polyatomic molecules we would expect a maximum efficiency of:

$$\eta = 1 - \left(\frac{1}{12}\right)^{\frac{1}{3}} = 0.56.$$

Actual automobiles achieve in the 20 - 30% range of conversion of thermal energy to vehicle motion. This compares very poorly with the round trip efficiency of 80+% when storing solar energy in batteries and then using it to drive electric motors in an EV. This is why even using electricity generated by burning fossil fuels in modern electric generation facilities, which can get thermal efficiencies close to 60%,[2] EV's are more energy efficient than ICE automobiles.

Under *ideal operating conditions* where the adiabatic expansion in step 2 cools the gases to T_C, so no additional heat is wasted in cooling the gases to T_C in step 3 (a "warmed up" engine should be close), you can that the efficiency depends only on the minimum T_C exhaust gas temperature and the maximum T_h of the gases, just as for the Carnot cycle:

$$\eta(\text{otto ideal}) = 1 - \frac{T_c}{T_h}. \tag{1.5.5}$$

1.5.6: References

1. "Compression ratio", Wikipedia.org. https://en.wikipedia.org/wiki/Compression_ratio. Accessed Aug. 31, 2025.

2. "Combined cycle power plant", Wikipedia.org. https://en.wikipedia.org/wiki/Combin...le_power_plant. Accessed Aug. 31, 2025.

1.5.7: Contributors

- Jerry LaRue
- Jonathan Gutow, UW Oshkosh

This page titled 1.5: Heat Engines is shared under a CC BY-NC-SA 4.0 license and was authored, remixed, and/or curated by Jonathan Gutow.

- **20.7: Thermodynamics Provides Insight into the Conversion of Heat into Work** by Jerry LaRue is licensed CC BY-NC-SA 4.0.

1.6: Multicomponent Phase Diagrams

1.6.1: Introduction

As might be expected multicomponent phase diagrams are more complex than phase diagrams for pure substances. These multicomponent phase diagrams are useful for understanding how distillation works and the behavior of mixtures. We will start with quantifying the number of possible phases that can coexist under particular constraints in a system and then discuss phase separation and distillation.

1.6.2: Gibbs Phase Rule

The **Gibbs phase rule** describes the number of compositional and phase variables that can be varied freely for a system at equilibrium. We will call these the degrees of freedom (F). Given a system of C components that can form P different phases and two state variables to vary (pressure and temperature), if there were no constraints we would have F = CP + 2 degrees of freedom.

The first constraint is that for each phase present in a system, the mole fraction of all but one component can be varied independently. This is because, the relationship

$$\sum_i \chi_i = 1$$

places a constraint on the last mole fraction. Thus, we lose one degree of freedom for each phase that is present. This leads to: F = 2 + CP - P.

The second constraint comes from the fact that the chemical potential of all the phases in equilibrium must be the same. There are P-1 equations of the form $\mu_A = \mu_B$, where A and B represent different phases, specifying this constraint. Thus for each component we lose another P-1 degrees of freedom. This leads to: F = 2 + CP - P -C(P-1).

Simplification leads to the common form of the Gibbs phase rule.

$$\begin{aligned} F &= 2 + PC - P - C(P-1) \\ &= 2 + PC - P - PC + C \\ &= 2 + C - P \end{aligned} \tag{1.6.1}$$

Equation 1.6.1 is the Gibbs phase rule.

Example 1.6.1:

Show that the maximum number of phases that can co-exist at equilibrium for a single component system is $P = 3$.

Solution

The maximum number of components will occur when the number of degrees of freedom is zero.

$$\begin{aligned} 0 &= 2 + 1 - P \\ P &= 3 \end{aligned}$$

Note: This shows that there can never be a “quadruple point” for a single component system!

Because a single component system at its triple point has no degrees of freedom, the triple point makes a very convenient physical condition at which to define a temperature. For example, the International Practical Temperature Scale of 1990 (IPT-90) uses the triple points of hydrogen, neon, oxygen, argon, mercury, and water to define several low temperatures. (The calibration of a platinum resistance thermometer at the triple point of argon, for example, is described by Strouse (Strouse, 2008)). The advantage to using a triple point is that the compound sets both the temperature and pressure, rather than forcing the researcher to set a pressure and *then* measure the temperature of a phase change, introducing an extra parameter than can introduce uncertainty into the measurement.

As suggested by the Gibbs Phase Rule, the most important variables describing a mixture are pressure, temperature and composition. In the case of single component systems, composition is not important so only pressure and temperature are typically

depicted on a phase diagram. However, for mixtures with two components, the composition is of vital import, so there is generally a choice that must be made as to whether the other variable to be depicted is temperature or pressure.

Temperature-composition diagrams are very useful in the description of binary systems, many of which will form two-phase compositions at a variety of temperatures and compositions.

1.6.3: Partially Miscible Liquids

A pair of liquids is considered partially miscible if there is a set of compositions over which the liquids will form a two-phase liquid system. This is a common situation and is the general case for a pair of liquids where one is polar and the other non-polar (such as water and vegetable oil.) Another case that is commonly used in the organic chemistry laboratory is the combination of diethyl ether and water. In this case, the differential solubility in the immiscible solvents allows the two-phase liquid system to be used to separate solutes using a separatory funnel method.

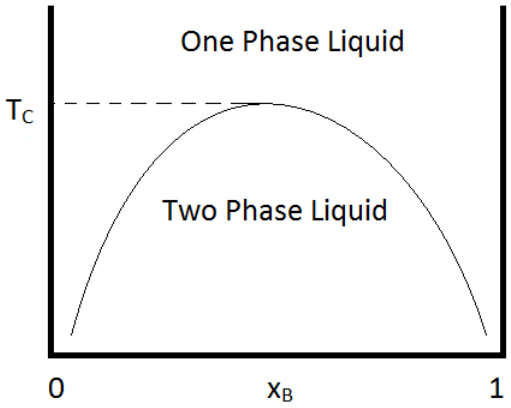


Figure **1.6.1** :

As is the case for most solutes, their solubility is dependent on temperature. For many binary mixtures of immiscible liquids, miscibility increases with increasing temperature. And then at some temperature (known as the upper critical temperature), the liquids become miscible in all compositions. An example of a phase diagram that demonstrates this behavior is shown in Figure **1.6.1**. An example of a binary combination that shows this kind of behavior is that of methyl acetate and carbon disufide, for which the critical temperature is approximately 230 K at one atmosphere (Ferloni & Spinolo, 1974). Similar behavior is seen for hexane/nitrobenzene mixtures, for which the critical temperature is 293 K.

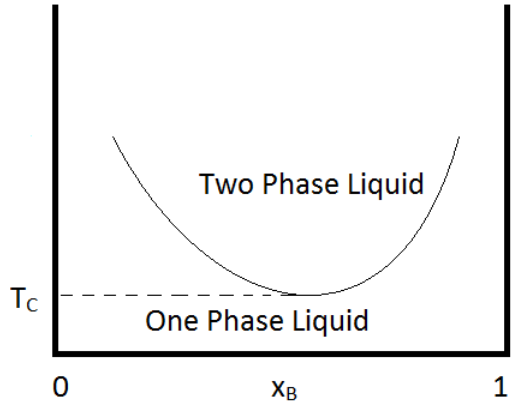


Figure **1.6.2** :

Another condition that can occur is for the two immiscible liquids to become completely miscible below a certain temperature, or to have a lower critical temperature. An example of a pair of compounds that show this behavior is water and trimethylamine. A typical phase diagram for such a mixture is shown in Figure **1.6.2**. Some combinations of substances show both an upper and lower critical temperature, forming two-phase liquid systems at temperatures between these two temperatures. An example of a combination of substances that demonstrate the behavior is nicotine and water.

1.6.4: The Lever Rule

The composition and amount of material in each phase of a two phase liquid can be determined using the **lever rule**. This rule can be explained using the following diagram.

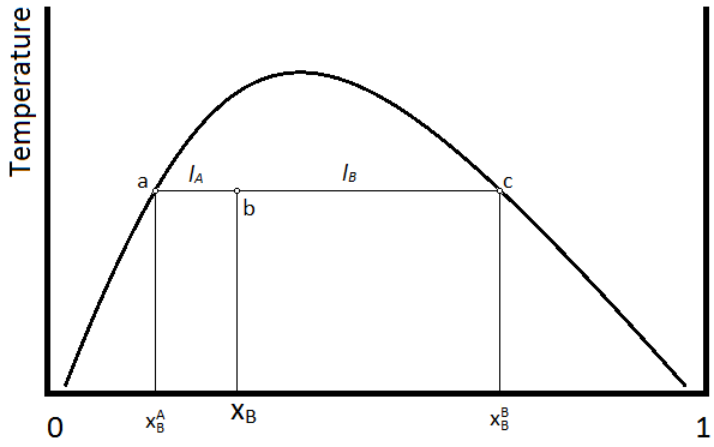


Figure **1.6.3** :

Suppose that the temperature and composition of the mixture is given by point b in the above diagram. The horizontal line segment that passes through point b, is terminated at points a and c, which indicate the compositions of the two liquid phases. Point a indicates the mole faction of compound B (χ_B^A) in the layer that is predominantly A, whereas the point c indicates the composition (χ_B^B)of the layer that is predominantly compound B. The relative amounts of material in the two layers is then inversely proportional to the length of the tie-lines a-b and b-c, which are given by l_A and l_B respectively. In terms of mole fractions,

$$l_A = \chi_B - \chi_B^A$$

and

$$l_B = \chi_B^B - \chi_B$$

The number of moles of material in the A layer (n_A) and the number of moles in the B layer (n_B) are inversely proportional to the lengths of the two lines l_A and l_B.

$$n_A l_A = n_B l_B$$

Or, substituting the above definitions of the lengths l_A and l_B, the ratio of these two lengths gives the ratio of moles in the two phases.

$$\frac{n_A}{n_B} = \frac{l_B}{l_A} = \frac{\chi_B^B - \chi_B}{\chi_B - \chi_B^A}$$

1.6.5: Distillation

Distillation can be understood in terms of the *lever rule*, which provides a simple way of determining the relative *quantities* (not just the compositions) of two phases in equilibrium. The plot below shows the boiling point diagram of a simple binary mixture of composition ①. At the temperature corresponding to the tie line, the composition of the liquid corresponds to ② (more A than B) and that of the vapor to ③ (more B than A or "enriched" in B).

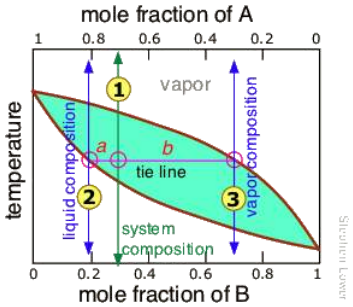


Figure **1.6.4**:

The relative quantities of the liquid and the vapor we identified above are given by the lengths of the tie-line segments labeled *a* and *b*. Thus in this particular example, in which *b* is about four times longer than *a*, we can say that the mole ratio of vapor (of composition 3) to liquid (composition 2) is 4.

1.6.5.1: Fractional Distillation

Now if we collect and condense the vapor, we will have a new liquid with composition enriched in B. If we re-vaporize it at the lower boiling temperature of this new liquid we create a new vapor that is even more enriched in B. Repeating this process is called fractional distillation. To make this more concrete, suppose you want to separate a liquid mixture composed of 20 mole-% B and 80 mole-% A, with A being the more volatile.

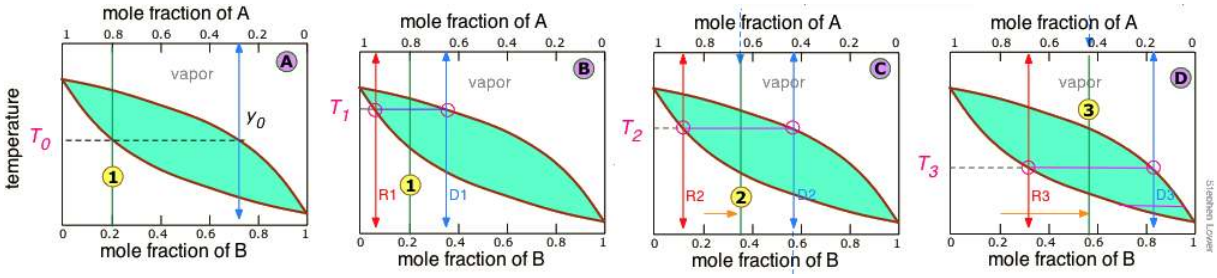


Figure **1.6.5**: Steps in Fractional Distillation

A As we heat the mixture whose overall composition is indicated by 1, the first vapor is formed at T_0 and has the composition y_0, found by extending the horizontal dashed line until it meets the vapor curve. This vapor is clearly enriched in B; if it is condensed, the resulting liquid will have a mole fraction $x_B > 0.7$.

B As the liquid continues to boil, the boiling temperature rises. When it reaches T_1, we will have boiled away half of the liquid. At this point, the "system" composition (liquid plus vapor) is still the same (1), but is now equally divided between the liquid, which we call "residue" R_1, and the condensed vapor, the *distillate* D_1.

> *How do we know it is equally divided? We have picked T_1 so that the tie line is centered on the system concentration, so by the lever rule, R_1 and D_1 contain equal numbers of moles.*

C We now take the condensed liquid D_1 having the composition 2, and distill half of it, obtaining distillate of composition D_2.

D .. and then carry out yet another distillation, this time using D_3 as our feedstock.

E Our four-stage fractionation has enriched the more volatile solute from 20 to slightly over 80 mole-percent in D_4. The less volatile component A is most concentrated in R_1. R_2 through R_4 are thrown away (but not down the sink, please!)

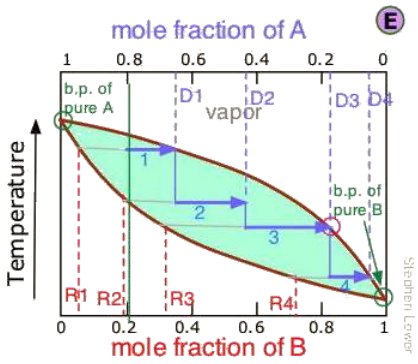


Figure **1.6.6**: Boiling point diagrams illustrating fractional distillation"

This may be sufficient for some purposes, but we might wish to do much better, using perhaps 1000 stages instead of just 4. What could be more tedious?

1.6.5.2: Fractionation with reflux

Not to worry! The multiple successive distillations can be carried out "virtually" by inserting a *fractionating column* between the boiling flask and the condenser. The key is that the boiling point of each fraction enriched in the more volatile component is lower than the previous fraction. So as we go up the column to lower temperatures the condensation - vaporization cycle repeats.

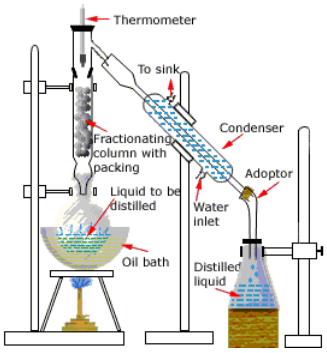


Figure **1.6.7**:

These columns are made with indentations or are filled with materials that provide a large surface area extending through the vertical temperature gradient (higher temperature near the bottom, lower temperature at the top.) The idea is that hot vapors condense at various levels in the column and the resulting liquid drips down (*refluxes*) to a lower level where it is vaporized, which corresponds roughly to a re-distillation. *Vigreux columns* having multiple indentations are widely used. Simple columns can be made by filling a glass tube with beads, short glass tubes, or even stainless steel kitchen-type scouring pads. More elaborate ones have spinning steel ribbons.

1.6.5.3: Separation efficiency: theoretical plates

The operation of fractionating columns can best be understood by reference to a bubble-cap column. The one shown here consists of four sections, or "plates" through which hot vapors rise and bubble up through pools of condensate that collect on each plate. The intimate contact between vapor and liquid promotes equilibration and re-distillation at successively higher temperatures at each higher plate in the column. Unlike the case of the step-wise fractional distillation we discussed above, none of the intermediate residues is thrown away; they simply drip down back into the pot where their fractionation journey begins again, always leading to a further concentration of the less-volatile component in the remaining liquid. At the same time, the vapor emerging from the top plate (5) provides a continuing flow of volatile-enriched condensate, although in diminishing quantities as it is depleted in the boiling pot.

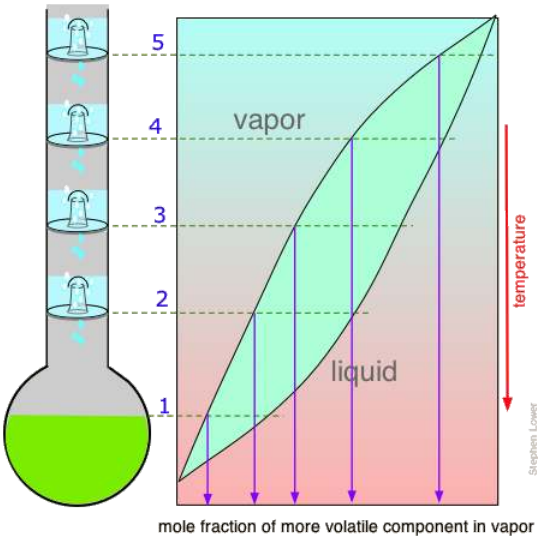


Figure **1.6.8**:

If complete equilibrium is attained between the liquid and vapor at each stage, then we can describe the system illustrated above as providing "five theoretical plates" of separation (remember that the pot represents the first theoretical plate.) Equilibrium at each stage requires a steady-state condition in which the quantity of vapor moving upward at each stage is equal to the quantity of liquid draining downward — in other words, the column should be operating in total reflux, with no net removal of distillate. So any real distillation process will be operated at a reflux ratio that provides optimum separation in a reasonable period of time.

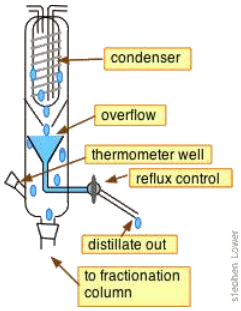


Figure **1.6.9**: Reflux ratio can be adjusted by placing a special control head on top of the fractionation column. The laboratory-type device shown here illustrates the general concept. Reflux control is mainly of importance in large-scale industrial operations.

Some of the more advanced laboratory-type devices (such as some spinning-steel band columns) are said to offer up to around 200 theoretical plates of separating power.

1.6.6: Azeotropes: the Limits of Distillation

The boiling point diagrams presented in the foregoing section apply to solutions that behave in a reasonably ideal manner — that is, to solutions that do not deviate too far from Raoult's law. As we explained above, mixtures of liquids whose intermolecular interactions are widely different do not behave ideally, and may be impossible to separate by ordinary distillation. The reason for this is that under certain conditions, the compositions of the liquid and of the vapor in equilibrium with it become identical, precluding any further separation. These cross-over points appear as "kinks" in the boiling point diagrams.

1.6.6.1: High- and low-boiling azeotropes

Thus in this boiling point diagram for a mixture exhibiting a positive deviation from Raoult's law, successive fractionations of mixtures correspond to either ① or ② bring the distillation closer to the azeotropic composition indicated by the dashed vertical line. Once this point is reached, further distillation simply yields more of the same "high-boiling" azeotrope.

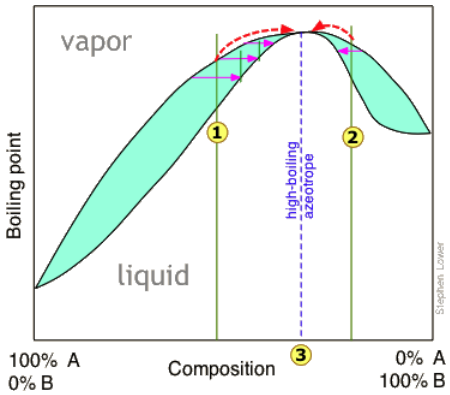


Figure **1.6.10**: High Boiling Azeotrope

Distillation of a mixture having a negative deviation from Raoult's law leads to a similar stalemate, in this case yielding a "low-boiling" azeotrope. High- and low-boiling azeotropes are commonly referred to as *constant-boiling mixtures*, and they are more common than most people think.

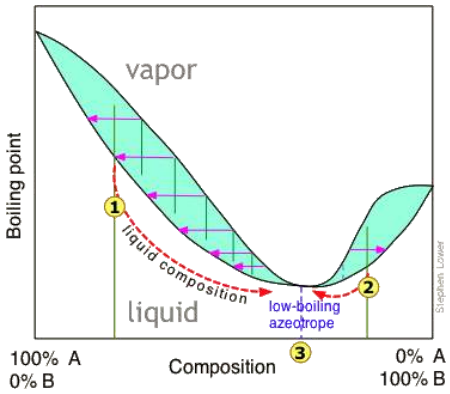


Figure **1.6.11**: Low Boiling Azeotrope

An example of a common low boiling azeotrope is water + ethanol, which yields ~96% by weight ethanol as the limit of purification by simple fractional distillation.

1.6.7: Phase diagrams including multiphase liquids and solids

It is possible that when the temperature is lowered enough below the boiling points of the solutions the liquid could undergo phase separation as in figures **1.6.1** and **1.6.3**. Thus you could have a more complex diagram that looks something like the figure below. Exactly how the various boundaries relate depends on the particular system. For example the two phase liquid region boundary could touch the two phase vapor boundaries at the low-boiling azeotrope point in the figure.

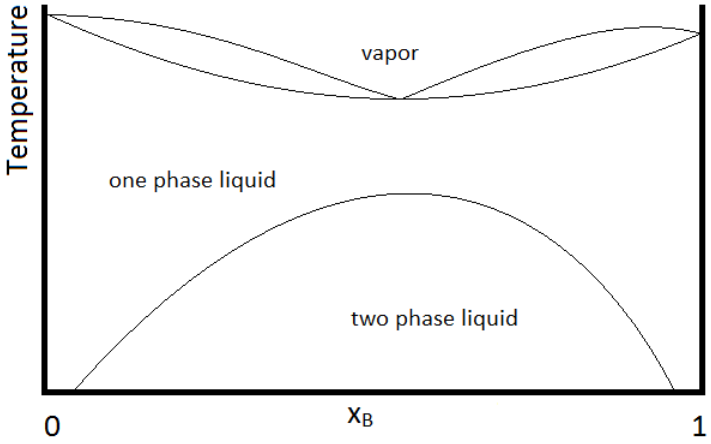


Figure **1.6.12**: Phase diagram for a binary solution with the boiling point of a low boiling azeotrope that is higher then when components are miscible (single phase).

Solids mixtures can also exhibit different phase compositions. A phase diagram for two immiscible solids and the liquid phase (which is miscible in all proportions) is shown in the figure below. The point labeled "e_2" is the **eutectic point**, meaning the composition for which the mixture of the two solids has the lowest melting point. The four main regions can be described as below:

- Two-phase solid
- (Region I) Solid (mostly A) and liquid (A and B)
- (Region II) Solid (mostly B) and liquid (A and B)
- Single phase liquid (A and B)

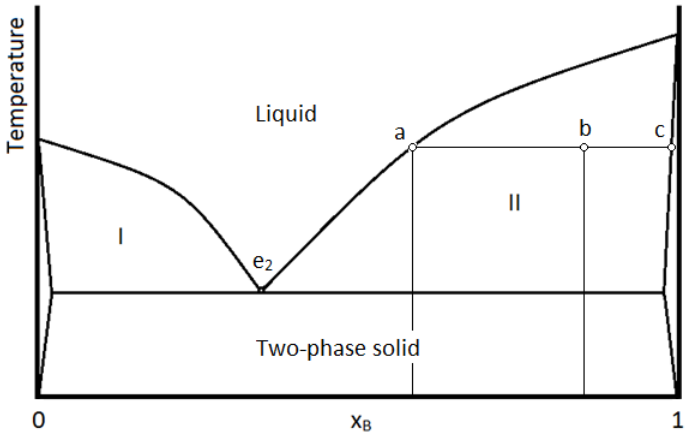


Figure **1.6.13**: Phase diagram of a two-component system that exhibits an eutectic point.

The unlabeled regions on the sides of the diagram indicate regions where one solid is so miscible in the other, that only a single phase solid forms. This is different than the "two-phase solid" region where there are two distinct phases, meaning there are regions (crystals perhaps) that are distinctly mostly A or B, even though they are intermixed within on another. Region I contains two phases: a solid phase that is mostly compound A, and a liquid phase which contains both A and B. A sample in region II (such as the temperature/composition combination depicted by point b) will consist of two phases: 1 is a liquid mixture of A and B with a composition given by that at point a, and the other is a single phase solid that is mostly pure compound B, but with traces of A entrained within it. As always, the lever rule applies in determining the relative amounts of material in the two phases.

Many other additional complexities exist in the phase diagrams for binary mixtures of solids, liquids or gases. Even more complexity is found as expected from the Gibb's phase rule in diagrams of ternary and higher mixtures.

Keep in mind that the diagrams we have been looking at are slices of multi-dimensional spaces where surfaces (1 dimension less than the number of degrees of freedom) separate the different phase regions.

This page titled 1.6: Multicomponent Phase Diagrams is shared under a CC BY-NC-SA 4.0 license and was authored, remixed, and/or curated by Jonathan Gutow.

- **8.3: Criterion for Phase Equilibrium** by Patrick Fleming is licensed CC BY-NC-SA 4.0.
- **8.6: Phase Diagrams for Binary Mixtures** by Patrick Fleming is licensed CC BY-NC-SA 4.0.
- **8.9: Distillation** by Stephen Lower is licensed CC BY 3.0. Original source: http://www.chem1.com/acad/webtext/virtualtextbook.html.
- **8.9: Solid-Liquid Systems - Eutectic Points** by Patrick Fleming is licensed CC BY-NC-SA 4.0.

CHAPTER OVERVIEW

2: Statistical Mechanics

2.1: Microcanonical and Canonical Ensembles
2.2: Statistical Thermodynamic Functions
2.3: Microconanonical (q molecular) Versus Canonical (Q) Partition Functions
2.4: From Quantum States to Partition Functions
2.5: Derivation of Ideal Gas Law
2.6: The Gaussian Distribution of One Component of the Molecular Velocity
2.7: The Maxwell-Boltzmann Distribution of Molecular Speeds in 3 Dimensions
2.8: Intermolecular Interactions Correction to the Translational Partition Function
2.9: Ortho and Para Hydrogen
2.10: The Equipartition Principle
2.11: Molar Heat Capacities

This page titled 2: Statistical Mechanics is shared under a CC BY-NC-SA 4.0 license and was authored, remixed, and/or curated by Jonathan Gutow.

2.1: Microcanonical and Canonical Ensembles

2.1.1: Introduction

Statistical thermodynamics (statistical mechanics) is our connection between the microscopic behavior and properties of matter and macroscopic thermodynamic behavior. Statistical thermodynamics involves calculating weighted averages of the microscopic behavior of the constituents of the system of interest to arrive at the macroscopic properties of the system. To do these calculations we must decide which parameters we will allow to vary and which will be held constant. We will use statistical concepts to average over the quantities that can vary. In the language of statistical mechanics this means choosing which ensemble to work with. There are many, but we will consider only two.

2.1.2: Definition of an ensemble

An ensemble is an *imaginary* replication of the system of interest so that every possible arrangement of the quantities that can vary exist in one of the replications. As an example consider a system consisting of three quantum mechanical particles (A, B and C) each with a ground state and two equally spaced excited state in an isolated system (fixed volume and insulated from the surroundings). If the system contains enough energy for three quanta of excitation we can identify all the different arrangements of energy that use all of it. They are shown below using * to indicate a quantum of excitation:

A* B* C*	A** B C*	A** B* C
	A B** C*	A* B** C
	A B* C**	A* B C**

There is only one real system, which would be found in one of these seven arrangements, but each one of the possible arrangements is part of the *imaginary* ensemble representing the system. Another name for an arrangement is a microstate.

When building an ensemble, we will make the *a priori* (before hand) assumption that any microstate that satisfies our constraints is equally likely. This means that if we take many measurements of the distribution of the quanta we will get each of the microstates 1/7 of the time.

2.1.3: Microcanonical ensemble and a statistical definition of entropy

The example ensemble above is a very small **microcanonical ensemble**, which are isolated systems with the total energy of the system (E), volume (V) and number of particles (N) held constant. In the above example we said nothing about the volume, but because the particles are isolated from the rest of the universe they must be contained is some isolated volume.

Notice that six of the arrangements have one doubly excited molecule, one singly excited molecule and one unexcited (ground state) molecule. If the molecules are indistinguishable any one of these microstates is equivalent (the same configuration or macrostate). This means one doubly excited, one singly excited and one unexcited molecule is the most likely configuration for us to measure (6/7 of the time). Enumeration is the hard way to find the most likely distribution. This is equivalent to the statistical problem of distributing objects among bins, which has a well known solution. From statistics if n_i objects are in bin i and there are N total objects and k bins (meaning i = 0, 1, 2, ... k-1) the weight (W) is the number of ways of distributing those particles in groups of n_i into the k bins:

$$W = \frac{N!}{n_1! n_2!, \ldots}. \tag{2.1.1}$$

Think of the energy levels (0, 1 or 2 quanta) as the bins. In the first case all the particles are in the 1 quanta of excitation bin: $n_1 = 3$ and $n_0 = n_2 = 0$. This yields:

$$W_1 = \frac{3!}{3!0!0!} = \frac{3 \cdot 2 \cdot 1}{3 \cdot 2 \cdot 1 \cdot 1 \cdot 1} = 1.$$

In the second case 1 particle is in the 0 state, one in the 1 state and one in the 2 state:

$$W_2 = \frac{3!}{1!1!1!} = \frac{3 \cdot 2 \cdot 1}{1 \cdot 1 \cdot 1} = 6.$$

Because we have only two excited states there are no more bins and thus no other configurations. The total number of microstates is just the sums of all the weights ($W_1 + W_2 = 7$).

Entropy is a measure of disorder. A higher weighting for a configuration corresponds to more ways of getting the configuration and therefore more disorder. Thus, we would expect a larger W to indicate higher entropy. The other property that entropy must have is that it is additive. If we have two systems with entropies S_A and S_B the total entropy $S_{tot} = S_A + S_B$. But the total number of configurations we can make with two systems with W_A and W_B is $W_{tot} = W_A W_B$. Thus we need a definition in terms of weights that is additive, but also consistent with the fact that the weight of a combined system should be the product of the weights of the individual systems.

Example 2.1.1: Number of microstates of a larger system made of two isolated systems

Show that the number of microstates available goes as the product of the number of microstates when a new system is constructed of two isolated systems each in a configuration with W = 2.

Solution

Call the microstates in system 1 A and B and in system 2 C and D. The combinations we can make are: AC, AD, BC and BD for a total of 4 distinct microstates = 2x2 = W_1W_2.

The solution is to utilize the properties of logs. In particular ln(ab) = ln(a) + ln(b). We will define the statistical entropy of a particular configuration as $S_i = k_B \ln W_i$, where k_B = Boltzmann constant. This means that $S_A + S_B = k_B \ln(W_A) + k_B \ln(W_B) = k_B \ln(W_A W_B)$, satisfying both the statistical and thermodynamic requirements for an entropy.

Thus for a microcanonical ensemble the entropy is:

$$S = k_B ln W = k_B ln \left(\frac{N!}{\prod_i n_i!} \right) = k_B \left(ln N! - \sum_i ln(n_i!) \right). \tag{2.1.2}$$

Real systems have huge numbers of particles making the factorials impractical. Luckily, there is a very good approximation $\ln x! \approx x \ln x - x$ called Stirling's approximation, which has very small fractional errors for large x. Applying this we can rewrite equation 2.1.2 as:

$$S = k_B \left(N ln N - N - \sum_i (n_i ln(n_i) - n_i) \right). \tag{2.1.3}$$

Since $\sum_i n_i = N$ this simplifies further to:

$$\begin{aligned} S = k_B \left(N ln N - \sum_i n_i ln(n_i) \right) &= k_B \left(\sum_i n_i ln N - \sum_i n_i ln(n_i) \right) \\ &= k_B \left(\sum_i n_i ln N - n_i ln(n_i) \right) \\ = k_B \left(\sum_i n_i ln \left(\frac{N}{n_i} \right) \right) = -k_B \left(\sum_i n_i ln \left(\frac{n_i}{N} \right) \right) &= -N k_B \left(\sum_i \frac{n_i}{N} ln \left(\frac{n_i}{N} \right) \right). \end{aligned} \tag{2.1.4}$$

Notice that the fractions $\frac{n_i}{N}$ is the fraction of the total molecules that will be found in the energy level i. Although nice and compact this is still not a very practical way of calculating the entropy if N and thus i are large. The traditional approach is to apply the method of Lagrange multipliers to constrain the energy to our fixed value and maximize the number of microstates. Instead we will develop more generally useful expressions by working with the canonical ensemble.

2.1.4: Canonical ensemble[1]

This ensemble is used for constant temperature systems. The volume (V), number particles (N) and temperature (T) of the system are constant. This is a chemically useful way to describe a system. In most cases chemical systems consist of a container in

equilibrium with the surroundings, which have a particular temperature. At any given time the system can exchange energy with the surroundings as long as the temperature of the system remains in equilibrium with the surroundings. This is less constrained than the microcanonical ensemble where the system has a fixed total energy. By using the canonical ensemble we will be able to use the thermodynamic definition of temperature to get a very general expression for the entropy of the system. From there we will be able to go on to derive general statistical expressions for other thermodynamic quantities.

Our discussion begins by applying the idea of the weight of our configurations in a more general way. The trick is to express this weight in terms of the surroundings, which are so much larger than the system that we can use an approximate Taylor series expansion to express the entropy without significant error.

For this system in contact with the surroundings, which is part of the Universe, the total energy is fixed at $E_T = E_{sur} + E_{sys}$. We will refer to a particular energy configuration of the system as E_i. Thus for a particular E_i $E_{sur} = E_T - E_i$.

Start by considering the canonical equivalent of the microcanonical ratio $\frac{n_i}{N}$, which we will call $P(i)$:

$$P(i) = \frac{\text{number of ways of getting the system with energy } E_i}{\text{all ways of arranging} E_T} = \frac{W_{sur}(E_{sur})}{W_T(E_T)} \tag{2.1.5}$$

To convert this to a more useful general expression we need to express the entropy of the surroundings in terms of the total energy, E_T, and the energy of the system, E_i. Then we will use that to express P(i) in terms of E_i.

2.1.4.1: The entropy of the surroundings

From the Boltzmann definition of entropy we have:

$$S_{sur} = k_B ln W_{sur}(E_{sur}).$$

Now consider expanding S_{sur} in a Taylor series about E_T.

$$S_{sur}(E_{sur}) \approx S_{sur}(E_T) + \left(\frac{\partial S_{sur}}{\partial E_{sur}}\right)_{V,N} |_{E_T}(E_T - E_{sur}) \tag{2.1.6}$$

This is approximate because we have only kept the first term of the Taylor series. However, $E_{sur} = E_T - E_i$ and $E_i << E_T$ so the error from dropping higher order terms will be negligible.

We can re-express the derivative in terms of the system energy, E_i, using the fact that E_T is a constant and $E_{sur} = E_T - E_i$. This implies the differential

$dE_{sur} = d(E_T - dE_i) = 0 - dE_i$.

We also need to convert dS_{sur} to a differential in terms of the system. First write it as the differential of the Boltzmann entropy:

$$dS_{sur} = d(k_B ln W_{sur}(E_{sur}))$$

The W_{sur} can be replaced by using the fact that weights multiply. Thus $W_T(E_T) = W_{sur}(E_{sur})W_i(E_i) \Rightarrow W_{sur}(E_{sur}) = W_T(E_T)/W_i(E_i)$. Substituting this in:

$$dS_{sur} = d\left(k_B ln\left(\frac{W_T(E_T)}{W_i(E_i)}\right)\right) = d\left(k_B ln W_T(E_T) - k_B ln W_i(E_i)\right) = 0 - d(k_B ln W_i(E_i)) = -dS_i.$$

Substituting the differentials and $E_{sur} = E_T - E_i$ into equation 2.1.6:

$$S_{sur}(E_T - E_i) \approx S_{sur}(E_T) + \left(\frac{\partial S_i}{\partial E_i}\right)_{V,N} |_{E_T}(E_T - (E_T - E_i))$$

From thermodynamics we know that $\left(\frac{\partial U}{\partial S}\right)_{V,N} = T$. The energy $E_i = U_i - U_i(0)$, where $U_i(0)$ is the constant internal energy of the system that it has at absolute 0. Thus $\left(\frac{\partial E_i}{\partial S_i}\right)_{V,N} = \left(\frac{\partial U}{\partial S}\right)_{V,N} = T$. Replacing the derivative with 1/T our expression for $S_{sur}(E_T - E_i)$ can be further simplified to:

$$S_{sur}(E_T - E_i) \approx S_{sur}(E_T) - \frac{E_i}{T} \tag{2.1.7}$$

2.1.4.2: P(i) in a generally useful form

Our goal is to find a general form of P(i) (equation 2.1.5) that we can use to calculate system thermodynamic quantities. We start by assuming that our approximation in calculating $S_{sur}(E_T - E_i)$ is accurate so we have:

$$S_{sur}(E_T - E_i) = S_{sur}(E_T) - \frac{E_i}{T} \implies k_B ln W_{sur}(E_{sur}) = k_B ln W_{sur}(E_T) - \frac{E_i}{T}$$
$$\implies k_B ln\left(\frac{W_{sur}(E_{sur})}{W_{sur}(E_T)}\right) = -\frac{E_i}{T} \implies \frac{W_{sur}(E_{sur})}{W_{sur}(E_T)} = exp\left(-\frac{E_i}{k_B T}\right)$$
$$\implies W_{sur}(E_{sur}) = W_{sur}(E_T) exp\left(-\frac{E_i}{k_B T}\right).$$

We can substitute this into our original expression for P(i) (equation 2.1.5) to get:

$$P(i) = \frac{W_{sur}(E_{sur})}{W_T(E_T)} = \frac{W_{sur}(E_T)}{W_T(E_T)} exp\left(-\frac{E_i}{k_B T}\right) \tag{2.1.8}$$

As P(i) is a probability it must be normalized. So,

$$\sum_{i=1}^{\infty} P(i) = \sum_{i=1}^{\infty} \frac{W_{sur}(E_T)}{W_T(E_T)} exp\left(-\frac{E_i}{k_B T}\right) = 1. \tag{2.1.9}$$

Because E_T is a constant the fraction of weights on the right hand side can be removed from the sum:

$$\frac{W_{sur}(E_T)}{W_T(E_T)} \sum_{i=1}^{\infty} exp\left(-\frac{E_i}{k_B T}\right) = 1 \implies \frac{W_{sur}(E_T)}{W_T(E_T)} = \frac{1}{\sum_{i=1}^{\infty} exp\left(-\frac{E_i}{k_B T}\right)}. \tag{2.1.10}$$

Substituting this final result into P(i) yields:

$$P(i) = \frac{W_{sur}(E_T)}{W_T(E_T)} exp\left(-\frac{E_i}{k_B T}\right) = \frac{exp\left(-\frac{E_i}{k_B T}\right)}{\sum_{i=1}^{\infty} exp\left(-\frac{E_i}{k_B T}\right)} \tag{2.1.11}$$

This is entirely in terms of the energy of the configuration i. The sum on the bottom is referred to as Q(T), the canonical partition function. It is the normalization constant. The larger Q(T) the more energy states are accessible. Q(T) is the key parameter necessary to calculate thermodynamic quantities. You may also notice that P(i) looks like the Boltzmann energy distribution. This is the more general canonical probability distribution.

2.1.4.3: References

1. This discussion is based on Section 2.4 of A. Cooksy *Physical Chemistry: Thermodynamics* (Pearson Education, Inc. Columbus, OH, 2014).

This page titled 2.1: Microcanonical and Canonical Ensembles is shared under a CC BY-NC-SA 4.0 license and was authored, remixed, and/or curated by Jonathan Gutow.

2.2: Statistical Thermodynamic Functions

2.2.1: Introduction

With an expression for the canonical distribution we can derive statistical expressions for thermodynamic functions and variables. In this section we derive expressions for many of them. For reference our canonical expressions are:

$$Q(T) = \sum_{i=1}^{\infty} exp\left(-\frac{E_i}{k_B T}\right) \tag{2.2.1}$$

and

$$P(i) = \frac{exp\left(-\frac{E_i}{k_B T}\right)}{Q(T)} \tag{2.2.2}$$

2.2.2: U

The thermodynamic internal energy U will be the sum of the zeropoint energy, U_o, and the thermal energy accounted for by statistical thermodynamics. The thermal energy is the mean energy of the system. This can be expressed as the sum of all the possible energy configurations each multiplied by their individual probability. Thus,

$$U - U_o = \langle E \rangle = \sum_{i=0}^{\infty} E_i P(i) = \frac{1}{Q} \sum_{i=0}^{\infty} E_i exp\left(\frac{-E_i}{k_B T}\right) \tag{2.2.3}$$

We can re-express this in terms of only Q and constants by recognizing how the derivative of Q with respect to T at constant volume is related to <E>.

$$\left(\frac{\partial Q}{\partial T}\right)_V = \left(\frac{\partial}{\partial T}\right)_V \left(\sum_{i=1}^{\infty} exp\left(-\frac{E_i}{k_B T}\right)\right) = \frac{1}{k_B T^2} \left(\sum_{i=1}^{\infty} E_i exp\left(-\frac{E_i}{k_B T}\right)\right) \tag{2.2.4}$$

Notice that the sum in the equation is the same as in the sum for U-U_o. If we divide by Q and multiply by $k_B T^2$ we convert this equation to:

$$\frac{k_B T^2}{Q}\left(\frac{\partial Q}{\partial T}\right)_V = \frac{1}{Q} \sum_{i=1}^{\infty} E_i exp\left(-\frac{E_i}{k_B T}\right).$$

The right-hand-side of the above equation is the same at equation 2.2.3. We can combine this with (dln(u)/dx) = 1/u(du/dx) to get two equivalent expressions for the internal energy:

$$U - U_o = \frac{k_B T^2}{Q}\left(\frac{\partial Q}{\partial T}\right)_V = k_B T^2 \left(\frac{\partial ln Q}{\partial T}\right)_V \tag{2.2.5}$$

2.2.3: S

Recall that $dq_{rev} = C_V dT$ and $dS = \frac{dq_{rev}}{T}$. So we can get the S - S_o as the integral from T = 0 to T' of dS, where T' is the temperature of interest:

$$S - S_o = \int_0^{T'} \frac{C_V}{T} dT. \tag{2.2.6}$$

From classical thermodynamics $\left(\frac{\partial U}{\partial T}\right)_V = C_V$. Combined with equation 2.2.5 and noting that dU_o= 0 the integral becomes:

$$S - S_o = \int_0^{T'} \frac{1}{T} \frac{\partial}{\partial T} \left(k_B T^2 \frac{\partial ln Q}{\partial T} \right)_V dT \tag{2.2.7}$$
$$= \int_0^{T'} \frac{1}{T} \left[k_B T^2 \left(\frac{\partial^2 \ln Q}{\partial T^2} \right)_V + 2 k_B T \left(\frac{\partial \ln Q}{\partial T} \right)_V \right] dT$$
$$= k_B \int_0^{T'} T \left(\frac{\partial^2 \ln Q}{\partial T^2} \right)_V dT + 2 k_B \int_0^{T'} \left(\frac{\partial \ln Q}{\partial T} \right)_V dT$$
$$= k_B \int_0^{T'} T \left(\frac{\partial^2 \ln Q}{\partial T^2} \right)_V dT + 2 k_B ln Q(T') - 2 k_B ln Q(0)$$

The remaining integral can be done using integration by parts ($\int u dv = uv - \int v du$) with u = T and $dv = \left(\frac{\partial^2 \ln Q}{\partial T^2} \right)_V dT$.

$$S - S_o = k_B T' \left(\frac{\partial \ln Q}{\partial T} \right)_V - k_B \int_0^{T'} \left(\frac{\partial \ln Q}{\partial T} \right)_V dT + 2 k_B ln Q(T') - 2 k_B ln Q(0) \tag{2.2.8}$$
$$= k_B T' \left(\frac{\partial \ln Q}{\partial T} \right)_V - k_B ln Q(T') + k_B ln Q(0) + 2 k_B ln Q(T') - 2 k_B ln Q(0)$$
$$= k_B T' \left(\frac{\partial \ln Q}{\partial T} \right)_V + k_B ln Q(T') - k_B ln Q(0)$$

The last term accounts for the residual entropy at T = 0 K, so is S_o, which cancels out on both sides. Dropping the T' now that the integration is complete we have:

$$S = k_B T \left(\frac{\partial \ln Q}{\partial T} \right)_V + k_B ln Q(T). \tag{2.2.9}$$

The first term is $(U-U_o)/T$ (see equation 2.2.5). Thus, we can also write this as:

$$S = \frac{U - U_o}{T} + k_B ln Q(T). \tag{2.2.10}$$

2.2.4: A

Helmholtz free energy A is defined as

$$A = U - TS\ . \tag{2.2.11}$$

Using our equations for U - U_o (2.2.5)and S (2.2.10) we can get a statistical expression for A - A_o.

$$A - A_o = U - U_o - T \left[\frac{U - U_o}{T} + k_B ln Q \right] = -k_B T ln Q \tag{2.2.12}$$

2.2.5: Pressure

The simplest route to P is to note that $P = -\left(\frac{\partial A}{\partial V}\right)_T$. From equation 2.2.12 it then follows that

$$P = k_B T \left(\frac{\partial \ln Q}{\partial V} \right)_T . \tag{2.2.13}$$

2.2.6: H

H = U + PV. From equation 2.2.13:

$$PV = V k_B T \left(\frac{\partial \ln Q}{\partial V} \right)_T = k_B T \left(\frac{\partial \ln Q}{\partial \ln V} \right)_T . \tag{2.2.14}$$

Substituting into the equation for H for U (equation 2.2.5)and PV we get:

$$H - H_o = U - U_o + PV = k_B T \left[\left(\frac{\partial \ln Q}{\partial \ln T} \right)_V + \left(\frac{\partial \ln Q}{\partial \ln V} \right)_T \right]. \tag{2.2.15}$$

Connoisseurs will notice the beautiful symmetry of this equation.

2.2.7: G

From the definitions of H (2.2.15) we can also compute G,

$$G - G_o = H - H_o - TS = -k_B T \left[lnQ - \left(\frac{\partial lnQ}{\partial \ln V} \right)_T \right]. \tag{2.2.16}$$

This page titled 2.2: Statistical Thermodynamic Functions is shared under a CC BY-NC-SA 4.0 license and was authored, remixed, and/or curated by Jonathan Gutow.

- **4.2: The Relation of State Functions to the Partition Function** by Gunnar Jeschke is licensed CC BY-NC 3.0. Original source: https://ethz.ch/content/dam/ethz/special-interest/chab/physical-chemistry/epr-dam/documents/education/statistical-thermodynamics/stat_TD.pdf.

2.3: Microconanonical (q molecular) Versus Canonical (Q) Partition Functions

2.3.1: Introduction

The canonical expressions for thermodynamic quantities require calculating Q. We want to be able to use what we know about the microscopic (quantum) behavior of molecules to do this. Thus, we need to connect Q to the microscopic (quantum) energy levels. The microcanonical q is defined it in terms of the energy levels of the molecules in the system. So, our goal is to determine the connection between the two partition functions.

2.3.2: Total energy of a system

> To make our notation more compact we will use the common formalism of using the substitution $\beta = \frac{1}{k_B T}$.

A system, such as a container of gas, can consist of a large number of particles. Their energies are additive so in a sytem with total energy E_i:

$$E_i = \epsilon_i(1) + \epsilon_i(2) + \epsilon_i(3) + \cdots$$

Each of the molecules can have their energy distributed over their respective internal energy states (e.g., vibrations, rotations, etc.). This means that each $\epsilon_i(k)$ is already a summation over the states of the molecule. Thus,

$$E_i = \sum_{i,k,j} \epsilon_{i,k,j},$$

where i is the canonical energy index, k indicates the particle and j the energy state of the particle.

2.3.3: Q versus q

When calculating Q it should not matter which order we sum over the possible energy combinations of quantum levels, just that we include them all. Thus, assuming all the molecules are **distinguishable** (e.g. in a crystal they could be identified by position), we can get the canonical partition function as:

$$Q(N,V,\beta) = \sum_i e^{-\beta E_i} = \sum_i exp\left(-\beta \sum_{j,k} \epsilon_{i,j,k}\right).$$

Because it does not matter whether we sum over the states of the system or all the individual states of the molecules we can instead write this as the product of the sums for each of the molecules:

$$Q(N,V,\beta) = \left(\sum_j e^{\beta\epsilon_j}\right)\left(\sum_j e^{\beta\epsilon_j}\right)\left(\sum_j e^{\beta\epsilon_j}\right)\ldots$$

Where each factor is for a different molecule (different k). Each of the sums is a microcanonical q, where the summation is over molecular energy states rather than system energies of a canonical ensemble. So, compactly we have:

$$Q(N,V,\beta) = \prod_k q_k$$

If the energy states of all the particles are the same, then the equation simplifies to:

$$Q(N,V,\beta) = [q(V,\beta)]^N \tag{2.3.1}$$

We can do this if, for example, the particles are embedded in a crystal where we can distinguish them by their location.

However, under most conditions, full knowledge of each member of an ensemble is missing and hence we have to operate with a more reduced knowledge. This is demonstrated via a simple model of two particles in a two-energy level system in Figure **2.3.1**. Each particle (red or blue) can occupy either the $E_1 = 0$ energy level or the $E_2 = \epsilon$ energy level resulting in four possible states that describe the system. The corresponding partition function for this system is then:

$$Q_{\text{distinguishable}} = e^0 + e^{-\beta\epsilon} + e^{-\beta\epsilon} + e^{-2\beta\epsilon} = q^2 \tag{2.3.2}$$

and is just the molecular partition function (q) squared.

$$q^2 = q_{blue}q_{red} = (e^0 + e^{-\beta\epsilon})(e^0 + e^{-\beta\epsilon})$$

because each particle can occupy either the 0 or ϵ state.

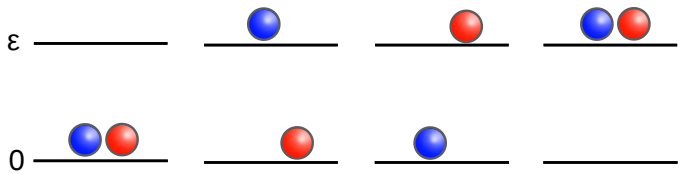


Figure 2.3.1: Four different states can exist for a two-level system with two distinguishable particles (red and blue balls). (CC BY 4.0; Delmar Larsen via LibreTexts)

However, if the two particles are indistinguishable (e.g., both the same color as in Figure 2.3.2) then while four different combinations can be generated like in Figure 2.3.1, there is no discernible way to separate the two middle states. Hence, there are effectively only three states observable for this system.

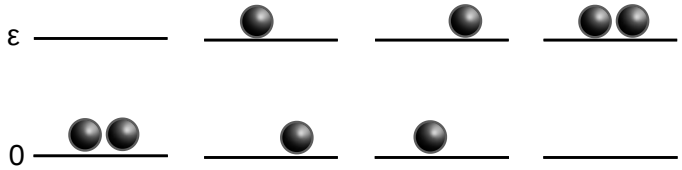


Figure 2.3.2: Three different states can exist for a two-level system with two indistinguishable particles (black balls). The two middle states are indescernable and represent a single state with one particle exited and the other in the ground state. (CC BY 4.0; Delmar Larsen via LibreTexts)

The corresponding partition function for this system can be constructed:

$$Q(N,V,\beta) = e^0 + e^{-\beta\epsilon} + e^{-2\beta\epsilon} \neq q^2 \tag{2.3.3}$$

and this is not equal to the square of the molecular partition function. If Equation 2.3.1 were used to describe the indistinguishable particle case, then it would overestimate the number of observable states. From combinatorics, using q^N for a large N-particle system of indistinguishable particles will overestimate the number of states by a factor of $N!$. Therefore Equation 2.3.2 requires a slight modification to account for this over counting.

$$Q(N,V,\beta) = \frac{\sum_i e^{-\beta E_i}}{N!} \tag{2.3.4}$$

If we have N molecules, we can perform $N!$ permutations that should not affect the outcome. To avoid over counting (making sure we do not count each state more than once), the partition function becomes:

$$Q(N,V,\beta) = \frac{q(V,\beta)^N}{N!} \tag{2.3.5}$$

Note

As you may have noticed, using Equation 2.3.4 to estimate of Q for the two-indistinguishable particle discussed case above with $N = 2$ is incorrect (i.e., Equation 2.3.4 is not equal to Equation 2.3.3). That is because the $N!$ factor is only applicable for large N.

This page titled 2.3: Microconanonical (q molecular) Versus Canonical (Q) Partition Functions is shared under a CC BY-NC-SA 4.0 license and was authored, remixed, and/or curated by Jonathan Gutow.

- 17.6: The Partition Function of Distinguishable, Independent Molecules is the Product of the Molecular Partition Functions by Jerry LaRue is licensed CC BY 4.0.

- **17.7: Partition Functions of Indistinguishable Molecules Must Avoid Over Counting States** by Delmar Larsen, Jerry LaRue is licensed CC BY 4.0.

2.4: From Quantum States to Partition Functions

2.4.1: Introduction

From quantum mechanics we know that to a first approximation the total energy of the molecule can be separated into four independent contributions (translation, vibration, rotation and electronic).

$$\epsilon = \epsilon_{trans} + \epsilon_{vib} + \epsilon_{rot} + \epsilon_{elec}.$$

So summing over all the possible energy microstates of the molecule and shortening the subscripts to the first letter we have:

$$q = \sum_{t,v,r,e} e^{-\beta(\epsilon_t+\epsilon_v+\epsilon_r+\epsilon_e)} = \sum_{t,v,r,e} e^{-\beta\epsilon_t}e^{-\beta\epsilon_v}e^{-\beta\epsilon_r}e^{-\beta\epsilon_e} \tag{2.4.1}$$
$$= \sum_t e^{-\beta\epsilon_t}\sum_v e^{-\beta\epsilon_v}\sum_r e^{-\beta\epsilon_r}\sum_e e^{-\beta\epsilon_e} = q_{trans}q_{vib}q_{rot}q_{elec}$$

Where we have used that $e^{a+b} = e^a e^b$.

Thus, we need to develop expressions for the partition functions of the individual molecular degrees of freedom. Then they can be combined to calculate a molecular q, which can be used to calculate the canonical Q. The forms of Q are included below as a reminder.

indistinguishable particles	**distinguishable particles**
$Q(N,V,\beta) = \frac{q(V,\beta)^N}{N!}.$ (2.4.2)	$Q(N,V,\beta) = [q(V,\beta)]^N.$ (2.4.3)

2.4.2: Translational partition function

Let us consider the translational partition function of a monatomic gas particle confined to a cubic box of length L. The particle inside the box has translational energy levels given by:

$$E_{\text{trans}} = \frac{h^2\left(n_x^2+n_y^2+n_z^2\right)}{8mL^2}$$

where n_x, n_y and n_z are the quantum numbers in the three directions. The translational partition function is given by:

$$q_{\text{trans}} = \sum_i e^{-\epsilon_i/kT}$$

which is the product of translational partition functions in the three dimensions. We can write the translation partition function as the product of the translation partition function for each direction:

$$q_{\text{trans}} = q_x q_y q_z \tag{2.4.4}$$
$$= \sum_{n_x=1}^{\infty} e^{-\epsilon_x/kT}\sum_{n_y=1}^{\infty} e^{-\epsilon_y/kT}\sum_{n_z=1}^{\infty} e^{-\epsilon_z/kT} \tag{2.4.5}$$

Since the levels are very closely spaced (continuous), we can replace each sum in Equation 2.4.5 with an integral. For example:

$$q_x = \sum_{n_x=1}^{\infty} e^{-\epsilon_x/kT} \tag{2.4.6}$$
$$\approx \int_{n_x=1}^{\infty} e^{-\epsilon_x/kT}dn_x \tag{2.4.7}$$

and after substituting the energy for the relevant dimension:

$$\epsilon_x = \frac{h^2n_x^2}{8mL^2}$$

we can extend the lower limit of integration in the approximation of Equation 2.4.7:

$$q_x = \int_1^{\infty} e^{-\frac{h^2 n_x^2}{8mL^2kT}} dn_x \approx \int_0^{\infty} e^{-\frac{h^2 n_x^2}{8mL^2kT}} dn_x$$

We then use the following solved Gaussian integral:

$$\int_o^{\infty} e^{-an^2} dn = \sqrt{\frac{\pi}{4a}}$$

with the following substitution:

$$a = \frac{h^2}{8mL^2kT}$$

we get:

$$q_x = \sqrt{\frac{\pi}{4a}} = \sqrt{\frac{2\pi mkT}{h^2}} L$$

or more commonly presented as:

$$q_x = \frac{L}{\Lambda}$$

where Λ is the **de Broglie wavelength** and is given by

$$\Lambda = \frac{h}{\sqrt{2\pi mkT}}$$

Multiplying the expressions for q_x, q_y and q_z (Equation 2.4.4) and using V as the volume of the box L^3, we arrive at:

$$q_{\text{trans}} = \left(\frac{2\pi mkT}{h^2}\right)^{3/2} V = \frac{V}{\Lambda^3} \tag{2.4.8}$$

This is usually a very large number (10^{20}) for volumes of 1 cm^3 for small molecular masses. This means that such a large number of translational states are accessible and available for occupation by the molecules of a gas.

Example

Calculate the translational partition function of an I_2 molecule at 300K. Assume V to be 1 liter.

Solution

Mass of I_2 is $2 \times 127 \times 1.6606 \times 10^{-27} kg$

$$\begin{aligned} 2\pi mkT &= 2 \times 3.1415 \times (2 \times 127 \times 1.6606 \times 10^{-27}\, kg) \times 1.3807 \times 10^{-23}\, J/K \times 300K \\ &= 1.0969 \times 10^{-44}\, J\, kg \end{aligned}$$

$$\begin{aligned} \Lambda &= \frac{h}{\sqrt{2\pi mkT}} \\ &= \frac{6.6262 \times 10^{-34}\, J\, s}{\sqrt{1.0969 \times 10^{-44}\, J\, kg}} = 6.326 \times 10^{-12}\, m \end{aligned}$$

The via Equation 2.4.8

$$q_{\text{trans}} = \frac{V}{\Lambda^3} = \frac{1000 \times 10^{-6} m^3}{(6.326 \times 10^{-12}\, m)^3} = 3.95 \times 10^{30}$$

This means that 3.95×10^{30} quantum states are thermally accessible to the molecular system

Contributors and Attributions

- www.chem.iitb.ac.in/~bltembe/pdfs/ch_3.pdf

2.4.3: Rotational partition function

The rotational energy levels of a **diatomic molecule** modeled as a rigid body (no vibrations) rotating in three dimensions are the solutions to the quantum mechanical particle on a sphere. This is essentially the same problem as finding the angular components of an electron in a one electron atom and results in solutions that are the spherical harmonics specified by two quantum numbers. When talking about a rotating body the quantum numbers are called J = 0, 1, 2... (instead of ℓ as in the case of electronic states) and $-J \leq m_J \leq J$ (instead of m_ℓ). Just as for the electron the energies only depend on J and are given in wavenumbers (cm^{-1}) as:

$$E_{rot}(J) = \tilde{B}J(J+1) \tag{2.4.9}$$

where:

$$\tilde{B} = \frac{h}{8\pi^2 Ic}$$

Here, $\tilde{B}$ is the rotational constant expressed in cm^{-1}, c = speed of light in cm/s, and I is the moment of inertia of the molecule given by μR^2 for a diatomic, and μ is the reduced mass, and R the bond length (assuming rigid rotor approximation). The rotational energy levels in Joules are given by:

$$E_j = \frac{J(J+1)h^2}{8\pi^2 I}$$

The energies can be also expressed in terms of the rotational temperature, Θ_{rot}, defined as:

$$\Theta_{rot} = \frac{h^2}{8\pi^2 I k_B} \tag{2.4.10}$$

The interpretation of θ_{rot} is as an estimate of the temperature at which thermal energy ($\approx k_B T$) is comparable to the spacing between rotational energy levels. At about this temperature the population of excited rotational levels becomes important. See Table 1.

Table **2.4.1**: Select Rotational Temperatures. In each case the value refers to the most common isotopic species.

Molecule	H_2	N_2	O_2	F_2	HF	HCl	CO_2	HBr	CO
Θ_{rot}	87.6	2.88	2.08	1.27	30.2	15.2	0.561	12.2	2.78

In the summation for the expression for rotational partition function (q_{rot}) we can do an explicit summation:

$$q_{rot} = \sum_{j=0} (2J+1)e^{-E_J/k_B T} \tag{2.4.11}$$

if only a finite number of terms contribute. The factor $(2J+1)$ for each term in the expansion accounts for the degeneracy of a rotational state J due to m_J. For each allowed energy E_J from Equation 2.4.9 there are $(2J+1)$ eigenstates. The Boltzmann factor must be multiplied by $(2J+1)$ to properly account for the degeneracy these states:

$$(2J+1)e^{-E_J/k_B T}$$

If the rotational energy levels are very close to one another, we can integrate similar to what we did for q_{trans} previously to get:

$$q_{rot} = \int_0^\infty (2J+1)e^{-\tilde{B}J(J+1)/k_B T} dJ$$

This integration can easily be done by substituting $x = J(J+1)$ and $dx = (2J+1)dJ$:

$$q_{rot} = \frac{k_B T}{\tilde{B}} \tag{2.4.12}$$

For a homonuclear diatomic molecule, rotating the molecule by 180° brings the molecule into a configuration which is *indistinguishable* from the original configuration. This leads to an over counting of the accessible states. To correct for this, we

divide the partition function by σ, which is called the **symmetry number** and is equal to the distinct number of ways by which a molecule can be brought into identical configurations by rotations. The rotational partition function becomes:

$$q_{\text{rot}} = \frac{k_B T}{\tilde{B}\sigma} \tag{2.4.13}$$

or commonly expressed in terms of Θ_{rot}:

$$q_{\text{rot}} = \frac{T}{\Theta_{\text{rot}}\sigma} \tag{2.4.14}$$

Example 2.4.1

What is the rotational partition function of H_2 at 300 K?

Solution

For simplicty, we are ignoring the fact that there are actually two forms of H_2 (ortho and para) that depend on whether the nuclear spins are parallel or anti-parallel.

1. Using the integral approximation:

The value of $\tilde{B}$ for H_2 is 60.864 cm^{-1}. The value of $k_B T$ in cm^{-1} can be obtained by dividing it by hc, i.e., which is $k_B T/hc = 209.7\ cm^{-1}$ at 300 K. $\sigma = 2$ for a homonuclear molecule. Therefore from Equation 2.4.13,

$$\begin{aligned} q_{\text{rot}} &= \frac{k_B T}{\tilde{B}\sigma} \\ &= \frac{209.7\ cm^{-1}}{(2)(60.864\ cm^{-1})} \\ &= 1.723 \end{aligned}$$

Since the rotational frequency of H_2 is quite large, only the first few rotational states are accessible at 300 K.

2. Using explicit summation up to 10 terms:

The full expression without numbers substituted in is:

$$\begin{aligned} q_{rot} = \frac{1}{\sigma} \\ \left[1 + 3e^{-\frac{2B}{Tk_B}} + 5e^{-\frac{6B}{Tk_B}} + 7e^{-\frac{12B}{Tk_B}} + 9e^{-\frac{20B}{Tk_B}} + 11e^{-\frac{30B}{Tk_B}} + 13e^{-\frac{42B}{Tk_B}} + 15e^{-\frac{56B}{Tk_B}}\right. \\ \left. + 17e^{-\frac{72B}{Tk_B}} + 19e^{-\frac{90B}{Tk_B}} + 21e^{-\frac{110B}{Tk_B}}\right] = 1.8996. \end{aligned} \tag{2.4.15}$$

The sum was done using a symbolic algebra system to generate the expression and then substitute in for B and $k_B T$ to get a number. To check that 10 terms is enough, we can calculate just the last term to see its size:

$$\frac{21}{\sigma} exp\left(-\frac{110B}{Tk_B}\right) = \frac{21}{2} exp\left(-\frac{110(60.864 cm^{-1})}{209.7 cm^{-1}}\right) = 1.5 \times 10^{-12}. \tag{2.4.16}$$

Thus, 10 terms was plenty to get to negligible contributions. Notice that the explicit sum yields a value that is a little higher (~10%) than the integral approximation. The integral approximation will show better agreement to the actual value calculated by explicit summation the smaller the ratio Θ_{rot}/T becomes.

For molecules with smaller rotational constants significant population is found in rotational states above 1. The figure below shows the population distribution at room temperature for HCl $\tilde{B} \approx 10 cm^{-1}$.

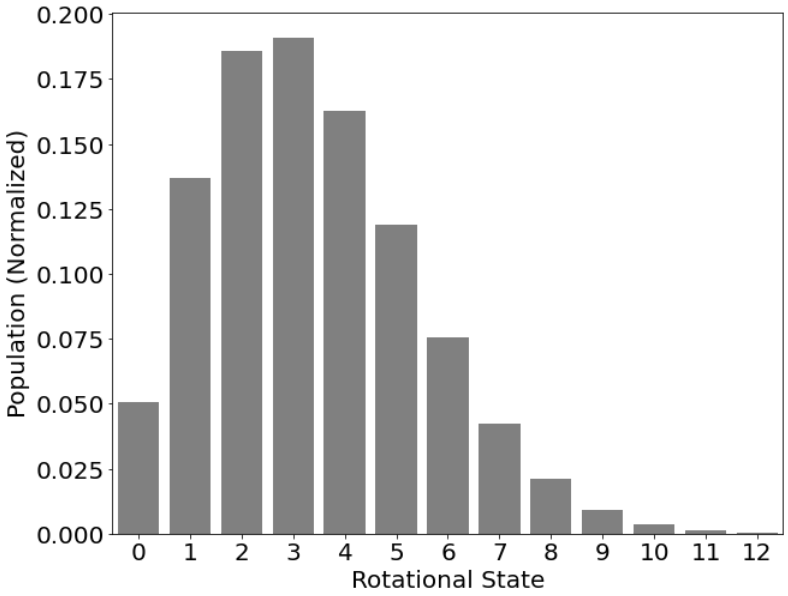


Figure 2.4.1: The normalized rotational population of HCl at room temperature.

Contributors and Attributions

- www.chem.iitb.ac.in/~bltembe/pdfs/ch_3.pdf

2.4.3.1: Rotational partition function of nonlinear polyatomics

Nonlinear molecules have an additional two moments of inertia and thus a more complicated arrangements of rotational quantum states. A similar analysis to the diatomic yields an approximate expression that depends on all three of the rotational constants (A, B and C):

$$q_{rot} \approx \frac{1}{\sigma}\left(\frac{\pi k_B^3 T^3}{ABC}\right)^{1/2} \tag{2.4.17}$$

The proper symmetry number can be arrived at from the symmetry classification of the molecule, but is simply a count of the number of ways of rotating the molecule onto itself. If you are familiar with symmetry classifications this information is summarized in the table below:

Table 2.4.2: Symmetry numbers σ corresponding to symmetry point groups. Table from Jeshke 6.4.

Group	σ	Group	σ	Group	σ	Group	σ
C_1, C_i, C_s, $C_{\infty v}$	1	$D_{\infty h}$	2	T, T_d	12	O_h	24
C_n, C_{nv}, C_{nh}	n	D_n, D_{nh}, D_{nd}	$2n$	S_n	$n/2$	I_h	60

2.4.4: Vibrational partition function

The vibrational energy levels of a diatomic approximated as a quantum harmonic oscillator are given by:

$$E_v = (\mathrm{v} + 1/2)h\nu$$

where is ν the vibrational frequency and v is the vibrational quantum number. In this case, it is easy to sum the geometric series shown below:

$$\begin{aligned} q_{\text{vib}} &= \sum_{\mathrm{v}=0}^{\infty} exp\left(\frac{-(\mathrm{v}+1/2)h\nu}{k_B T}\right) \\ &= e^{-h\nu/(2k_B T)}\left(1 + e^{-h\nu/(k_B T)} + e^{-2h\nu/(k_B T)} + \ldots\right) \end{aligned}$$

or rewritten as:

$$q_{\text{vib}} = e^{-h\nu/(2k_BT)}\left(1 + x + x^2 + x^3 + ...\right) \tag{2.4.18}$$

where $x = e^{-h\nu/(2k_BT)}$. Given the following power series expansion:

$$\frac{1}{1-x} = 1 + x + x^2 + x^3 + x^4 + ...$$

Equation 2.4.18 can be rewritten as:

$$q_{\text{vib}} = e^{-h\nu/(2k_BT)}\left(\frac{1}{1-x}\right)$$

or:

$$q_{\text{vib}} = \frac{e^{-h\nu/(2k_BT)}}{1 - e^{-h\nu/(k_BT)}} \tag{2.4.19}$$

If the zero of energy scale is at $h\nu/(2k_BT)$, then Equation 2.4.19 can be rewritten as:

$$q_{\text{vib}} = \frac{1}{1 - e^{-h\nu/(k_BT)}} \tag{2.4.20}$$

A vibrational temperature Θ_{vib} may be defined as:

$$\Theta_{\text{vib}} = \frac{h\nu}{k_B}$$

where ν is the vibrational frequency. Θ_{vib} is a good way to express the *stiffness* of the vibrating bond in units of the Boltzmann constant.

Table **2.4.3** : Representative molecular data for a few diatomics

Molecule	g	Bond Length (pm)	ω (cm^{-1})	Θ_{vib} (K)	$\tilde{B}$ (cm^{-1})	Θ_{rot} (K)	Force constant k (dynes/cm)	D_0 (kcal/mol)
H_2	1	0.7474	4400	6332	60.9	87.6	5.749	103.2
D_2	1	0.7415	3118	4487	30.45	43.8	5.77	104.6
N_2	1	1.097	2358	3393	2.001	2.99	22.94	225.1
O_2	3	1.207	1580	2274	1.446	2.08	11.76	118.0
Cl_2	1	1.987	560	805	0.244	0.351	3.2	57.0
CO	1	1.128	2170	3122	1.931	2.78	19.03	255.8
NO	2	1.15	190	2719	1.695	2.45	15.7	150.0
HCl	1	1.275	2938	4227	10.44	15.02	4.9	102.2
HI	1	1.609	2270	3266	6.46	9.06	3.0	70.5
Na_2	1	3.096	159	229	0.154	0.221	0.17	17.3
K_2	1	3.979	92.3	133	0.0561	0.081	0.10	11.8

Example 18.4.1

The vibrational frequency of of I_2 is $214.57\ cm^{-1}$. Calculate the vibrational partition function of I_2 at 300 K.

Solution:

$$\frac{h\nu}{k_BT} = \frac{214.57}{209.7} = 1.0232$$

so

$$e^{-h\nu/k_BT} = 0.3595$$

and

$$q_{\text{vib}} = \frac{1}{1-0.3595} = 1.561$$

This implies, as before, that very few vibrational states are accessible and much less than rotation states and many orders less than translation states.

2.4.4.1: Vibrational Populations

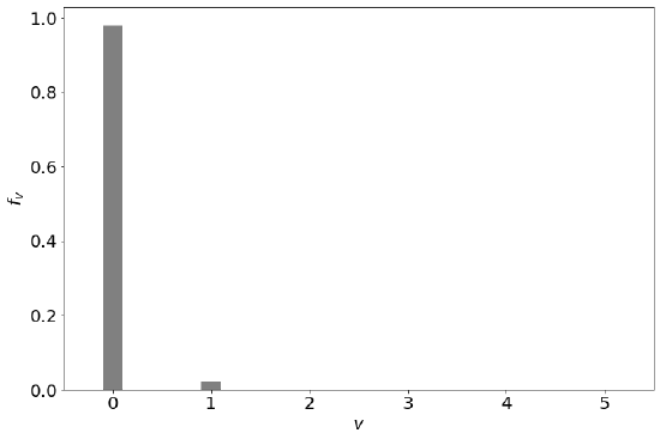
We can calculate the fraction of molecules in each vibrational state. The fraction of molecules in the vth vibrational state is given by:

$$f_v = \frac{e^{-h\nu(v+\frac{1}{2})/k_BT}}{q_{\text{vib}}}$$

Substituting in Equation 2.4.19, we get:

$$\begin{aligned} f_v &= \left(1-e^{-h\nu/k_BT}\right)e^{-h\nu v/k_BT} \\ &= \left(1-e^{-\Theta_{\text{vib}}/T}\right)e^{-\Theta_{\text{vib}}v/T} \end{aligned} \tag{2.4.21}$$

We can plot the fraction molecules in each vibrational state.



The vibrational population of Cl_2 at 300 K. Most of the molecules are in the ground vibrational state, $v = 0$.

From the figure, we can see that most of the Cl_2 molecules are in the ground vibrational state at room temperature (300 K). This is true for most molecules. Only molecules with very weak bonds and low vibrational temperatures will populate a significant fraction of molecules in excited vibrational states.

Contributors and Attributions

- www.chem.iitb.ac.in/~bltembe/pdfs/ch_3.pdf

2.4.4.2: Vibrational partition functions of polyatomic molecules

For polyatomic molecules, the independent vibrational motions are referred to as normal modes of vibration. The vibrational energy is then the sum of the energies for each normal mode:

$$E_{vib} = \sum_i^{\alpha} \left(v_i + \frac{1}{2} \right) h\nu$$

where ν_i is the vibrational frequency for the ith normal mode and α is the number of vibration degrees of freedom. A linear molecule has $3n - 5$ vibrational degrees of freedom and a nonlinear molecule has $3n - 6$ vibrational degrees of freedom. Because the normal modes are independent of each other, we can take our results from previous sections:

$$q_{vib} = \prod_i^{\alpha} q_i = \prod_i^{\alpha} \frac{1}{1 - e^{-h\nu_i/kT}}. \tag{2.4.22}$$

2.4.5: Electronic partition function

Writing the electronic energies as $E_1, E_2, E_3, ...$ with corresponding degeneracies $g_1, g_2, g_3, ...$ The electronic partition function is then given by the following summation:

$$q_{el}(T) = g_1 e^{-E_1/kT} + g_2 e^{-E_2/kT} + g_3 e^{-E_3/kT} + ... \tag{2.4.23}$$

Usually, the differences in electronic energies are significantly greater than thermal energy kT:

$$kT \ll E_1 < E_2 < E_3$$

If we treat the lowest energy electronic state E_1 as the reference value of zero of energy, the electronic partition function (Equation 2.4.23) can be approximated as:

$$q_{elec}(T) = g_1 + g_2 e^{-E_2/kT} + g_3 e^{-E_3/kT} + ... \tag{2.4.24}$$

Typically electronic states are tens of thousands of wave numbers above the ground state. For example, the first excited electronic state of nitric oxide (NO) is ~40,000 cm^{-1}. Using this value:

$$\frac{E_2}{kT} = \frac{40000 \text{ cm}^{-1}}{kT} = \frac{10^4 \text{ K}}{T}$$

That means, that even at 1,000 K, the value of the second term in 2.4.24 is:

$$g_2 e^{-10} = g_2 4.5 \times 10^{-5}$$

The result is that the higher electronic states are not accessible under ordinary temperatures. There are some cases, however, where the first excited state lies much closer to the ground state, but these are the exception rather than the rule.

Example 2.4.1

Find the electronic partition of H_2 at 300 K.

Solution

The lowest electronic energy level of H_2 is near $-32\ eV$ and the next level is about $5\ eV$ higher. Taking -32 eV as the zero (or reference value of energy), then

$$q_{el} = e_0 + e^{-5eV/kT} + ...$$

At 300 K, T = 0.02\; eV and

$$q_{el} = 1 + e^{-200} + ...$$
$$\approx 1.0$$

Where all terms other than the first are essentially 0. This implies that $q_{el} = 1$.

The physical meaning of the result from Example 2.4.1 is that only the ground electronic state is generally thermally accessible at room temperature.

Contributors and Attributions

- www.chem.iitb.ac.in/~bltembe/pdfs/ch_3.pdf

This page titled 2.4: From Quantum States to Partition Functions is shared under a CC BY-NC-SA 4.0 license and was authored, remixed, and/or curated by Jonathan Gutow.

- **18.1: Translational Partition Functions of Monotonic Gases** is licensed CC BY-NC-SA 4.0.
- **18.5: Most Molecules are Rotationally Excited at Ordinary Temperatures** is licensed CC BY-NC-SA 4.0.
- **18.6: Rotational Partition Functions of Diatomic Gases Contain a Symmetry Number** is licensed CC BY-NC-SA 4.0.
- **18.4: Most Molecules are in the Ground Vibrational State** is licensed CC BY-NC-SA 4.0.
- **6.4: Rotational Partition Function** by Gunnar Jeschke is licensed CC BY-NC 3.0. Original source: https://ethz.ch/content/dam/ethz/special-interest/chab/physical-chemistry/epr-dam/documents/education/statistical-thermodynamics/stat_TD.pdf.
- **18.7: Vibrational Partition Functions of Polyatomic Molecules Include the Partition Function for Each Normal Coordinate** is licensed CC BY-NC-SA 4.0.
- **18.2: Most Atoms are in the Ground Electronic State** is licensed CC BY-NC-SA 4.0.

2.5: Derivation of Ideal Gas Law

Introduction

Statistical mechanics allows us to prove that the ideal gas law is valid for structureless non-interacting particles (no intermolecular forces, rotations or vibrations), in other words ideal monatomic gases. To do this we combine the statistical thermodynamics definition of P:

$$P = k_B T \left(\frac{\partial \ln Q}{\partial V} \right)_T . \tag{2.5.1}$$

with the calculation of the partition function for an ideal monatomic gas.

Q of ideal monatomic gas

The only contributions to the energy of an ideal monatomic gas are the translational degree(s) of freedom as they contain no vibrating bonds and no shape to rotate. Real monatomic gases behave close to ideally because their attractions are weak and near room temperature only their electronic ground states are populated. Thus, the only q contributing to Q is q_{trans}. As all the molecules are identical we have:

$$Q_{ideal} = \frac{q_{trans}^N}{N!}. \tag{2.5.2}$$

From before:

$$q_{trans} = \left(\frac{2\pi m k_B T}{h^2} \right)^{3/2} V = \frac{V}{\Lambda^3}. \tag{2.5.3}$$

Substituting in we get:

$$Q_{ideal} = \frac{V^N}{\Lambda^{3N} N!}. \tag{2.5.4}$$

Calculating P (ideal gas)

Thus,

$$lnQ = NlnV - 3Nln\Lambda - lnN! \implies \left(\frac{\partial lnQ}{\partial V} \right)_T = \frac{N}{V}, \tag{2.5.5}$$

because the last two terms in lnQ are independent of volume.

Substituting into equation 2.5.1 yields:

$$P = \frac{N k_B T}{V} = \frac{nRT}{V}. \tag{2.5.6}$$

Showing that ideal gas law behavior is what is expected for non-interacting particles.

2.5: Derivation of Ideal Gas Law is shared under a not declared license and was authored, remixed, and/or curated by LibreTexts.

2.6: The Gaussian Distribution of One Component of the Molecular Velocity

2.6.1: Introduction

For translation in one dimension (e.g. the x dimension) the probability distribution of energies is:

$$P(\epsilon_x) = \frac{exp\left(\frac{-\epsilon_x}{k_BT}\right)}{q_x}, \tag{2.6.1}$$

where

$$q_x = \sqrt{\frac{2\pi mkT}{h^2}}L.$$

As kinetic energy = (1/2)mv^2 we can write the probability of energy (2.6.1) in terms of the x-component of the velocity (v_x) as:

$$P(\epsilon_x) = \frac{exp\left(\frac{-mv_x^2}{2k_BT}\right)}{q_x}.$$

To do calculations on velocity it is necessary to get $P(v_x)$ not $P(\epsilon_x)$. Luckily the only part of the expression above for $P(\epsilon_x)$ that depends on ϵ_x is q_x, the partition function, which is just the normalization constant for the distribution. Thus we can start our analysis of the velocity distribution by calculating a new normalization constant when integrating over all the possible velocities, $-\infty < v_x < \infty$. The distribution we must normalize is then:

$$P(v_x) = Nexp\left(\frac{-mv_x^2}{2k_BT}\right), \tag{2.6.2}$$

where N is our unknown normalization constant.

2.6.2: Normalized velocity distribution (Maxwell-Boltzmann distribution)

Normalization requires that:

$$1 = \int_{-\infty}^{\infty} P(v_x)dv_x = N\int_{-\infty}^{\infty} \exp\left(\frac{-mv_x^2}{2k_BT}\right)dv_x \implies N = \frac{1}{\int_{-\infty}^{\infty}\exp\left(\frac{-mv_x^2}{2k_BT}\right)dv_x} \tag{2.6.3}$$

The expression can be simplified by letting $\alpha = \frac{m}{2k_BT}$:

$$N\int_{-\infty}^{\infty}\exp\left(-\alpha v_x^2\right)dv_x = 1$$

A table of definite integrals says that

$$\int_{-\infty}^{\infty} e^{-ax^2}dx = \sqrt{\frac{\pi}{a}}$$

So

$$N\sqrt{\frac{\pi}{\alpha}} = 1$$

Thus,

$$N = \sqrt{\frac{\alpha}{\pi}} = \left(\frac{m}{2\pi k_BT}\right)^{1/2}$$

And thus the normalized distribution function is given by

$$P(v_x) = \left(\frac{m}{2\pi k_BT}\right)^{1/2}\exp\left(-\frac{mv_x^2}{2k_BT}\right) \tag{2.6.4}$$

Many texts use $f(v_x)$ instead of $P(v_x)$. We have used $P(v_x)$ for consistency with our usage of P(x) for probabililty of x in statistical mechanics.

2.6.3: Average velocity versus average speed

Calculating the average velocity in the x direction

A value that is useful is the average velocity in the x direction. Using the probability distribution, the average value of v_x is given by

$$\langle v_x \rangle = \int_{-\infty}^{\infty} v_x P(v_x) dv_x$$

This integral will, by necessity, be zero. This must be the case as the distribution is symmetric, so that half of the molecules are traveling in the +x direction, and half in the –x direction. These motions will have to cancel. So, a more satisfying result will be given by considering the magnitude of v_x, which gives the speed in the x direction. Since this cannot be negative, and given the symmetry of the distribution, the problem becomes

$$\langle |v_x| \rangle = 2 \int_{0}^{\infty} v_x P(v_x) dv_x$$

In other words, we will consider only half of the distribution, and then double the result to account for the half we ignored.

For simplicity, we will write the distribution function as

$$P(v_x) = N \exp(-\alpha v_x^2)$$

where

$$N = \left(\frac{m}{2\pi k_B T} \right)^{1/2}$$

and

$$\alpha = \frac{m}{2k_B T}.$$

A table of definite integrals shows

$$\int_{0}^{\infty} x e^{-ax^2} dx = \frac{1}{2a}$$

so

$$\langle |v_x| \rangle = 2N \left(\frac{1}{2\alpha} \right) = \frac{N}{\alpha}$$

Substituting our definitions for N and α produces

$$\langle |v_x| \rangle = \left(\frac{m}{2\pi k_B T} \right)^{1/2} \left(\frac{2k_B T}{m} \right) = \left(\frac{2k_B T}{\pi m} \right)^{1/2}$$

This expression indicates the average speed for motion in one direction.

It is important to note that equation 2.6.4 describes the distribution function for one component of the molecular ***velocity***. Because a molecule is able to move in a positive or a negative direction, the range of one component of the molecular velocity (v_x in this case) is $-\infty$ to ∞. This distribution of velocities is a Gaussian distribution of velocities, as shown in Figure **2.6.1** .

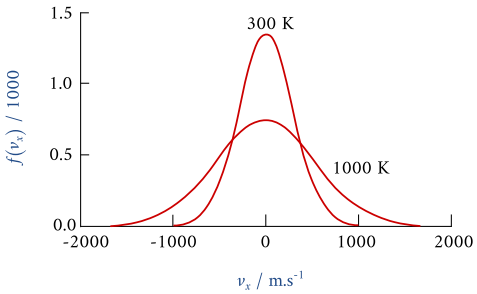


Figure 2.6.1 : Distribution of the x component of the velocity of a nitrogen molecule at 300 K and 1000 K. (CC BY-NC; Ümit Kaya via LibreTexts)

As we will see the distribution of molecular ***speeds*** accounting for motion in three dimensions is not a Gaussian distribution.

Contributors and Attributions

- Patrick E. Fleming (Department of Chemistry and Biochemistry; California State University, East Bay)
- Tom Neils (Grand Rapids Community College, editing)
- J. Gutow (UW-Oshkosh)

This page titled 2.6: The Gaussian Distribution of One Component of the Molecular Velocity is shared under a CC BY-NC-SA 4.0 license and was authored, remixed, and/or curated by Jonathan Gutow.

- **27.2: The Gaussian Distribution of One Component of the Molecular Velocity** is licensed CC BY-NC-SA 4.0.

2.7: The Maxwell-Boltzmann Distribution of Molecular Speeds in 3 Dimensions

2.7.1: Introduction

If we were to plot the number of molecules whose velocities fall within a series of narrow ranges, we would obtain a slightly asymmetric curve known as a *velocity distribution*. The peak of this curve would correspond to the *most probable* velocity. This velocity distribution curve is known as the *Maxwell-Boltzmann distribution*, but is frequently referred to only by Boltzmann's name. The **Maxwell-Boltzmann distribution law** was first worked out around 1860 by the great Scottish physicist, **James Clerk Maxwell** (1831-1879), who is better known for discovering the laws of electromagnetic radiation. Later, the Austrian physicist **Ludwig Boltzmann** (1844-1906) put the relation on a sounder theoretical basis and simplified the mathematics somewhat. Boltzmann pioneered the application of statistics to the physics and thermodynamics of matter and was an ardent supporter of the atomic theory of matter at a time when it was still not accepted by many of his contemporaries.

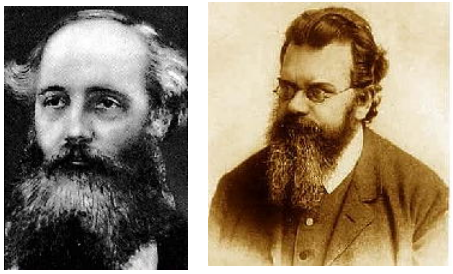


Figure **2.7.1** : Maxwell (left) and Boltzmann (right) are responsible for describing the velocity distribution of gas molecules

2.7.2: Maxwell-Boltzmann velocity distribution in 3-D

Previously, we saw that the distribution function for molecular speeds in the x direction is given by:

$$P(v_x) = \underbrace{\sqrt{\frac{m}{2\pi k_B T}}}_{\text{normalization term}} \underbrace{\exp\left(\frac{-mv_x^2}{2k_B T}\right)}_{\text{exponential term}} \tag{2.7.1}$$

The distribution along the y and z coordinates is the same. As probabilities multiply, we expect the distribution in 3-D to be the product:

$$\begin{aligned} P(v_x, v_y, v_z) &= P(v_x)P(v_y)P(v_z) \\ &= \sqrt{\frac{m}{2\pi k_B T}} \exp\left(\frac{-mv_x^2}{2k_B T}\right) \sqrt{\frac{m}{2\pi k_B T}} \exp\left(\frac{-mv_y^2}{2k_B T}\right) \sqrt{\frac{m}{2\pi k_B T}} \exp\left(\frac{-mv_z^2}{2k_B T}\right) \\ &= \left(\frac{m}{2\pi k_B T}\right)^{\frac{3}{2}} \exp\left(\frac{-mv_x^2}{2k_B T}\right) \exp\left(\frac{-mv_y^2}{2k_B T}\right) \exp\left(\frac{-mv_z^2}{2k_B T}\right) \\ &= \left(\frac{m}{2\pi k_B T}\right)^{\frac{3}{2}} \exp\left(\frac{-m(v_x^2 + v_y^2 + v_z^2)}{2k_B T}\right). \end{aligned} \tag{2.7.2}$$

Using normal vector magnitude properties (or simply using the Pythagorean Theorem), we know that

$$v^2 = v_x^2 + v_y^2 + v_z^2,$$

where v is the length of the velocity vector (the particle speed ignoring the direction of travel). So, equation 2.7.2 can be rewritten in terms of the particle speed as:

$$P(v_x, v_y, v_z) = \left(\frac{m}{2\pi k_B T}\right)^{\frac{3}{2}} \exp\left(\frac{-mv^2}{2k_B T}\right). \tag{2.7.3}$$

This expression provides the probability of a particular molecular velocity with the components (v_x, v_y and v_z), but we are looking for the probability of a speed with magnitude $v = \sqrt{v_x^2 + v_y^2 + v_z^2}$. In his 1860 paper ("Illustrations of the dynamical theory of gases. Part 1. On the motions and collisions of perfectly elastic spheres", 1860), Maxwell applied a transformation of coordinate system

from Cartesian coordinates (x, y, z) to spherical polar coordinates (v, θ, ϕ) to integrate over all the velocities with the same magnitude v. In this new coordinate system, v represents the magnitude of the velocity (or the speed) and all of the directional data is carried in the angles θ and ϕ. The infinitesimal volume unit becomes

$$dx\,dy\,dz = v^2 \sin(\theta)\,dv\,d\theta\,d\phi$$

Applying this transformation of coordinates and integrating over the angles **Maxwell's distribution** took the following form

$$P(v) = 4\pi v^2 \left(\frac{m}{2\pi k_B T}\right)^{3/2} \exp\left(\frac{-mv^2}{2k_B T}\right) \tag{2.7.4}$$

Integration over all directions to obtain the distribution

$$P(v) = \int_0^{\pi}\int_0^{2\pi} \left(\frac{m}{2\pi k_B T}\right)^{3/2} \exp\left(\frac{-mv^2}{2k_B T}\right) v^2 \sin\theta d\phi d\theta$$
$$= \left(\frac{m}{2\pi k_B T}\right)^{3/2} \exp\left(\frac{-mv^2}{2k_B T}\right) \underbrace{\int_0^{\pi}\int_0^{2\pi} v^2 \sin\theta d\phi d\theta}_{=4\pi v^2}$$

This equation is rearranged to give

$$P(v) = 4\pi v^2 \left(\frac{m}{2\pi k_B T}\right)^{3/2} \exp\left(\frac{-mv^2}{2k_B T}\right)$$

This function can be thought of as having three basic parts to it: **a normalization constant** (N), a velocity dependence (v^2), and an exponential term that contains the kinetic energy ($\frac{1}{2}mv^2$).

2.7.3: Velocity distributions depend on temperature and mass

Higher temperatures allow a larger fraction of molecules to acquire greater amounts of kinetic energy, causing the Boltzmann plots to spread out. Figure **2.7.2** shows how the Maxwell-Boltzmann distribution is affected by temperature. At lower temperatures, the molecules have less energy. Therefore, the speeds of the molecules are lower and the distribution has a smaller range. As the temperature of the molecules increases, the distribution flattens out. Because the molecules have greater energy at higher temperature, the molecules are moving faster.

Notice how the left ends of the plots are anchored at zero velocity (there will always be a few molecules that happen to be at rest.) As a consequence, the curves flatten out as the higher temperatures make additional higher-velocity states of motion more accessible. The area under each plot is the same for a constant number of molecules.

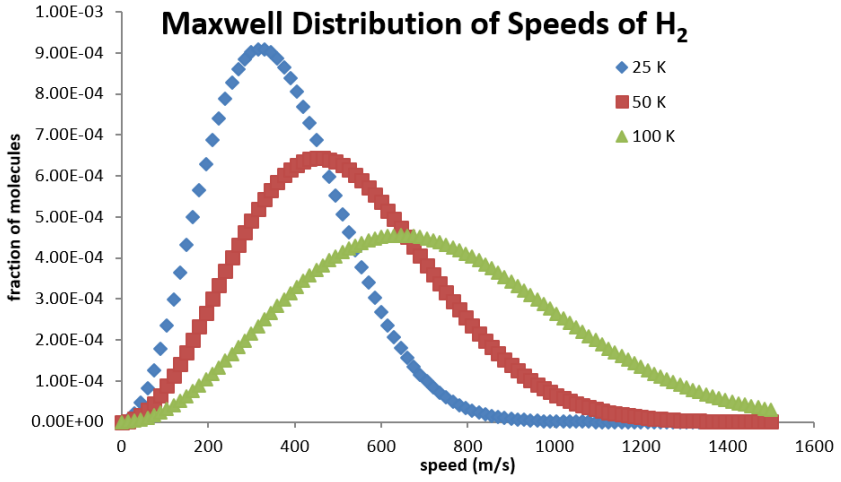


Figure **2.7.2**: Maxwell Distribution of speeds for hydrogen molecules at differing temperatures.

Calculating the Average Speed

Using the Maxwell distribution as a distribution of probabilities, the average molecular speed in a sample of gas molecules can be determined.

$$\begin{aligned}\langle v\rangle &= \int_{-\infty}^{\infty} v\,P(v)dv \\ &= \int_{-\infty}^{\infty} v\,4\pi\sqrt{\left(\frac{m}{2\pi k_BT}\right)^3}v^2\exp\left(\frac{-mv^2}{2k_BT}\right)\,dv \\ &= 4\pi\sqrt{\left(\frac{m}{2\pi k_BT}\right)^3}\int_{-\infty}^{\infty} v^3\exp\left(\frac{-mv^2}{2k_BT}\right)\,dv\end{aligned}$$

The following can be found in a table of integrals:

$$\int_0^{\infty} x^{2n+1}e^{-ax^2}dx = \frac{n!}{2a^{n+1}}$$

So

$$\langle v\rangle = 4\pi\sqrt{\left(\frac{m}{2\pi k_BT}\right)^3}\left[\frac{1}{2\left(\frac{m}{2k_BT}\right)^2}\right]$$

Which simplifies to

$$\langle v\rangle = \left(\frac{8k_BT}{\pi m}\right)^{1/2}$$

Note: the value of $\langle v\rangle$ is twice that of $\langle v_x\rangle$ which was derived in an earlier example!

$$\langle v\rangle = 2\langle v_x\rangle$$

Example 27.3.1 :

What is the average value of the squared speed according to the Maxwell distribution law?

Solution:

$$\begin{aligned}\langle v^2\rangle &= \int_{-\infty}^{\infty} v^2\,P(v)dv \\ &= \int_{-\infty}^{\infty} v^2\,4\pi\sqrt{\left(\frac{m}{2\pi k_BT}\right)^3}v^2\exp\left(\frac{-mv^2}{2k_BT}\right)\,dv \\ &= 4\pi\sqrt{\left(\frac{m}{2\pi k_BT}\right)^3}\int_{-\infty}^{\infty} v^4\exp\left(\frac{-mv^2}{2k_BT}\right)\,dv\end{aligned}$$

A table of integrals indicates that

$$\int_0^{\infty} x^{2n}e^{-ax^2}dx = \frac{1\cdot 3\cdot 5\ldots(2n-1)}{2^{n+1}a^n}\sqrt{\frac{\pi}{a}}$$

Substitution (noting that $n = 2$) yields

$$\langle v^2\rangle = 4\pi\sqrt{\left(\frac{m}{2\pi k_BT}\right)^3}\left[\frac{1\cdot 3}{2^3\left(\frac{m}{2k_BT}\right)^2}\sqrt{\frac{\pi}{\left(\frac{m}{2k_BT}\right)}}\right]$$

which simplifies to

$$\langle v^2\rangle = \frac{3k_BT}{m}$$

Note: The square root of this average squared speed is called the **root mean square** (RMS) speed, and has the value

$$v_{rms} = \sqrt{\langle v^2 \rangle} = \left(\frac{3k_BT}{m}\right)^{1/2}$$

All molecules have the same kinetic energy ($\frac{1}{2}mv^2$) at the same temperature, so the fraction of molecules with higher velocities will increase as m, the molecular weight, decreases. Figure **2.7.3** shows the dependence of the Maxwell-Boltzmann distribution on molecule mass. On average, heavier molecules move more slowly than lighter molecules. Therefore, heavier molecules will have a smaller speed distribution, while lighter molecules will have a speed distribution that is more spread out.

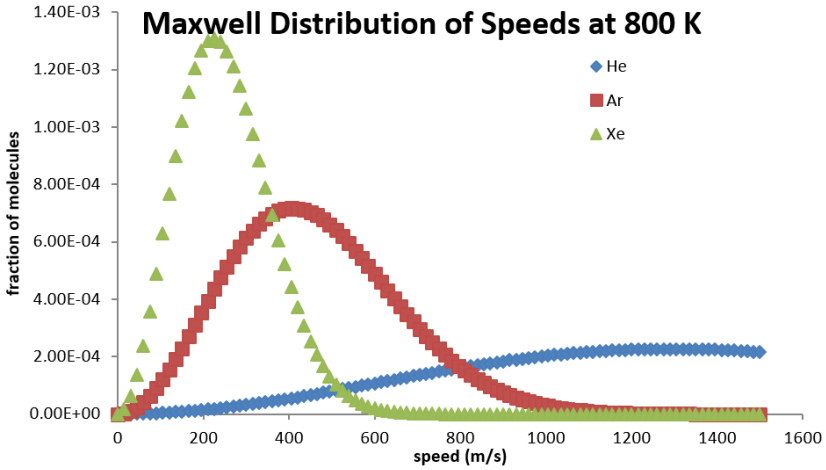


Figure **2.7.3**: Maxwell Distribution of speeds at 800 K for different gasses of differing molecular masses.

2.7.4: Summary of important speed expressions

Three speed expressions are commonly derived from the Maxwell-Boltzmann distribution:

- the average speed (calculated above)
- the root-mean-square speed (calculated above), and
- the most probable speed.

The **most probable speed** is the maximum value on the distribution plot. This is established by finding the velocity when the derivative of Equation **2.7.4** is zero

$$\frac{dP(v)}{dv} = 0$$

which using molar mass instead of molecular mass is:

$$v_{mp} = \sqrt{\frac{2RT}{M}} \tag{2.7.5}$$

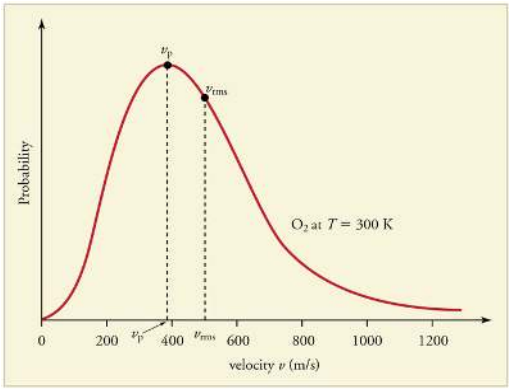


Figure 2.7.(4) : The Maxwell-Boltzmann distribution is shifted to higher speeds and is broadened at higher temperatures. from OpenStax. The speed at the top of the curve is called the most probable speed because the largest number of molecules have that

speed.

The **average speed** is the sum of the speeds of all the molecules divided by the number of molecules. In terms of the molar mass rather than molecular mass this is expressed as:

$$v_{avg} = \bar{v} = \int_0^\infty vP(v)dv = \sqrt{\frac{8RT}{\pi M}}.$$

The **root-mean-square speed** is square root of the average speed-squared. In terms of the molar mass rather than molecular mass this is expressed as:

$$v_{rms} = \bar{v^2} = \sqrt{\frac{3RT}{M}}$$

where R is the gas constant, T is the absolute temperature and M is the molar mass of the gas.

It *always* follows that for gases that follow the Maxwell-Boltzmann distribution:

$$v_{mp} < v_{avg} < v_{rms}$$

2.7.5: Problems

1. Using the Maxwell-Boltzman function, calculate the fraction of argon gas molecules with a speed of 305 m/s at 500 K.
2. If the system in problem 1 has 0.46 moles of argon gas, how many molecules have the speed of 305 m/s?
3. Calculate the values of C_{mp}, C_{avg}, and C_{rms} for xenon gas at 298 K.
4. From the values calculated above, label the Boltzmann distribution plot with the approximate locations of (C_{mp}\), C_{avg}, and C_{rms}.
5. What will have a larger speed distribution, helium at 500 K or argon at 300 K? Helium at 300 K or argon at 500 K? Argon at 400 K or argon at 1000 K?

2.7.5.1: Answers

1. 0.00141
2. 3.92×10^{20} argon molecules
3. c_{mp} = 194.27 m/s, c_{avg} = 219.21 m/s, c_{rms} = 237.93 m/s
4. As stated above, C_{mp} is the most probable speed, thus it will be at the top of the distribution curve. To the right of the most probable speed will be the average speed, followed by the root-mean-square speed.
5. Hint: Use the related speed expressions to determine the distribution of the gas molecules: helium at 500 K. helium at at 300 K. argon at 1000 K.

2.7.6: Sources

1. Dunbar, R.C. Deriving the Maxwell Distribution *J. Chem. Ed.* **1982**, *59*, 22-23.
2. Peckham, G.D.; McNaught, I.J.; Applications of the Maxwell-Boltzmann Distribution *J. Chem. Ed*. **1992**, *69*, 554-558.
3. Chang, R. *Physical Chemistry for the Biosciences*, 25-27.
4. HyperPhysics: http://hyperphysics.phy-astr.gsu.edu...maxspe.html#c3

Contributors and Attributions

- Prof. David Blauch (Davidson College)
- Stephen Lower, Professor Emeritus (Simon Fraser U.) Chem1 Virtual Textbook
- Adam Maley (Hope College)
- Patrick E. Fleming (Department of Chemistry and Biochemistry; California State University, East Bay)
- Stephanie Schaertel (Grand Valley State University)
- Tom Neils (Grand Rapids Community College, editing)
- J. Gutow (UW-Oshkosh)

This page titled 2.7: The Maxwell-Boltzmann Distribution of Molecular Speeds in 3 Dimensions is shared under a CC BY-NC-SA 4.0 license and was authored, remixed, and/or curated by Jonathan Gutow.

- **27.3: The Distribution of Molecular Speeds is Given by the Maxwell-Boltzmann Distribution** is licensed CC BY-NC-SA 4.0.

2.8: Intermolecular Interactions Correction to the Translational Partition Function

2.8.1: Introduction

In ideal gases the only contribution to the energy of the molecules is the kinetic energy of the molecules. But in gases where the molecules interact (attract or repel each other), the energy also depends on the relative position of the molecules. The discussion that follows shows how this can be incorporated into the translational partition function. This discussion largely follows that found in Cooksy's *Physical Chemistry: Thermodynamics, Statistical Mechanics, & Kinetics* section 3.4.[1]

2.8.2: The time behavior missing from the quantum description of q

In deriving q_{trans} from the quantum energy levels we used the time independent quantum solutions for a particle trapped in a three dimensional box:

$$E_{\text{trans}} = \frac{h^2\left(n_x^2+n_y^2+n_z^2\right)}{8mL^2}.$$

In this formulation the energy of a particle only depends on the quantum state it is in.These quantum states do not have any time dependence. Using the assumption that the states are close together we converted the summation over the quantum states to integration over the quantum numbers, yielding the following equation for q_{trans}:

$$q_{trans} = \int_0^\infty exp\left(-\frac{h^2n_x^2}{8mL^2k_BT}\right)dn_x \int_0^\infty exp\left(-\frac{h^2n_y^2}{8mL^2k_BT}\right)dn_y \int_0^\infty exp\left(-\frac{h^2n_z^2}{8mL^2k_BT}\right)dn_z.$$

This only requires integration in a three dimensional space defined by the axes of the three quantum numbers (n_x, n_y, n_z), because the energy of the particles is time-independent.

We, however, want to capture the averaging over the time-dependent motion of the molecules, because this determines how far apart they are on average and thus the strength of the intermolecular interactions. In this case we have six coordinates we will need to integrate over to capture the energetics of the system: the velocities (v_x, v_y, v_z) and positions (X, Y, Z). The difficult way to do this would be to resort to the time-dependent quantum mechanics of the system to capture the relative positions and velocities in the time-dependent wavefunctions of the particles. We will follow a somewhat easier classical route that depends on the classical velocities and positions.

2.8.3: Switching from our quantum number coordinates to v_x, v_y, v_z, X, Y and Z

Since the coordinates are orthogonal we will do the transformation along one coordinate and take the product of three coordinates as we did when deriving the quantum expression.

From quantum mechanics:

$$\epsilon_x = \frac{h^2n_x^2}{8mL^2} \tag{2.8.1}$$

Classically:

$$\epsilon_x = \frac{1}{2}mv_x^2 \tag{2.8.2}$$

Combining these yields:

$$\epsilon_x = \frac{h^2n_x^2}{8mL^2} = \frac{1}{2}mv_x^2.$$

To convert between the n_x and v_x coordinates solve for one and take the derivative with respect to the other to find how their infinitessimal volume elements are related:

$$\frac{h^2n_x^2}{8mL^2} = \frac{1}{2}mv_x^2 \implies n_x^2 = \frac{4m^2L^2}{h^2}v_x^2 \implies n_x = \pm\frac{2mL}{h}v_x$$
$$\implies \frac{dn_x}{dv_x} = \pm\frac{2mL}{h} \implies dn_x = \pm\frac{2mL}{h}dv_x.$$

Substituting the classical energy (equation 2.8.2) for the quantum energy in the integral for q_x and replacing dn_x by the scaled volume element in v_x space we get:

$$q_x = \int_0^\infty exp\left(-\frac{h^2 n_x^2}{8mL^2 k_B T}\right) dn_x = \frac{1}{2}\int_{-\infty}^{\infty} exp\left(-\frac{mv_x^2}{2k_B T}\right)\frac{2mL}{h} dv_x \\ = \frac{mL}{h}\int_{-\infty}^{\infty} exp\left(-\frac{mv_x^2}{2k_B T}\right) dv_x, \tag{2.8.3}$$

where the factor of (1/2) accounts for extending the integral to $-\infty$ to capture the fact that $-\infty < v_x < \infty$.

Multiplying three of these together to get three dimensions gives us:

$$q_{trans} = q_x q_y q_z = \left(\frac{m}{h}\right)^3 L^3 \int_{-\infty}^{\infty}\int_{-\infty}^{\infty}\int_{-\infty}^{\infty} exp\left(-\frac{m(v_x^2+v_y^2+v_z^2)}{2k_B T}\right) dv_x dv_y dv_z, \tag{2.8.4}$$

This captures the kinetic energy, but we also want to account for the energy depending on the separation. Thus, we need to expand our integration coordinates to depend on position as well as velocity. For compactness we will rewrite the energy simply as ϵ and note that since the triple integral

$$\frac{1}{V}\int_o^L\int_o^L\int_o^L dXdYdZ = 1,$$

we can multiply by that without changing the value of our integral. Thus we now have:

$$q_{trans} = \left(\frac{m}{h}\right)^3 L^3 \frac{1}{V}\int_o^L\int_o^L\int_o^L\int_{-\infty}^{\infty}\int_{-\infty}^{\infty}\int_{-\infty}^{\infty} exp\left(-\frac{\epsilon}{k_B T}\right) dv_x dv_y dv_z dXdYdZ, \tag{2.8.5}$$

2.8.4: Separating the translational kinetic energy from the distance dependent potential of interaction

The expression for q_{trans} in equation 2.8.5 can be rewritten to separate the kinetic energy part (K) and the interaction potential (I) by setting $\epsilon = K + I$ and noting that $L^3 = V$:

$$q_{trans} = \left(\frac{m}{h}\right)^3 \int_o^L\int_o^L\int_o^L\int_{-\infty}^{\infty}\int_{-\infty}^{\infty}\int_{-\infty}^{\infty} exp\left(-\frac{K+I}{k_B T}\right) dv_x dv_y dv_z dXdYdZ \\ = \int_o^L\int_o^L\int_o^L exp\left(-\frac{I}{k_B T}\right) dXdYd \\ Z\left[\left(\frac{m}{h}\right)^3 \int_{-\infty}^{\infty}\int_{-\infty}^{\infty}\int_{-\infty}^{\infty} exp\left(-\frac{K}{k_B T}\right) dv_x dv_y dv_z\right] = q_I' q_K'. \tag{2.8.6}$$

The first triple integral contains all the distance dependent interaction potential energy and the second triple integral is a volume independent kinetic energy contribution to the partition function. The kinetic energy triple integral evaluates to:

$$q_K' = \left(\frac{2\pi mkT}{h^2}\right)^{3/2}, \tag{2.8.7}$$

which, as expected from the way we divided up the integrations, is the quantum q_{trans}/V. Thus q'_K has units of 1/volume. The interaction triple integral can be difficult to evaluate analytically and depends on the potential of interaction. But there are a few things to note:

- When there is no interaction, making I = 0, the interaction potential integral reduces to:

$$q_I' = \int_o^L\int_o^L\int_o^L exp\left(-\frac{0}{k_B T}\right) dXdYdZ = \int_o^L\int_o^L\int_o^L dXdYdZ = V,$$

recovering the time-independent quantum result of:

$$q_{trans} = \left(\frac{2\pi mkT}{h^2}\right)^{3/2} V.$$

- If the interaction is attractive I < 0 and the triple integrals will yield a multiplier on the partition function that is greater than the volume. So, q_{trans} when attractions dominate will be larger than for the ideal case.

- If the interaction is repulsive I > 0 and the triple integrals will yield a multiplier on the partition function that is less than the volume. In this case q_{trans} will be less than for the ideal case.

2.8.5: References

1. A. Cooksy *Physical Chemistry: Thermodynamics, Statistical Mechanics, & Kinetics* (Pearson Education, Inc. Columbus, OH, 2014).

2.8.6: Contributors

- J. Gutow (UW-Oshkosh)

This page titled 2.8: Intermolecular Interactions Correction to the Translational Partition Function is shared under a CC BY-NC-SA 4.0 license and was authored, remixed, and/or curated by Jonathan Gutow.

2.9: Ortho and Para Hydrogen

The molecules of hydrogen can exist in two forms depending on the spins on the two hydrogen nuclei. If both the nuclear spins are parallel, the molecule is called ortho and if the spins are antiparallel, it is referred to as para (in disubstituted benzene, **para** refers to the two groups at two opposite ends, while in **ortho**, they are adjacent or "parallel" to each other). The spin on the hydrogen nucleus has a magnitude of $\frac{1}{2}\hbar$. The presence of nuclear spins leads to very interesting consequences for the populations of the rotational states and on a macroscopic scale, has consequences on measured entropies and heat capacities as well. The total partition function of $\mathbf{H_2}$ can be written as:

$$q_{\text{tot}} = q_{\text{elec}} q_{\text{vib}} q_{\text{rot}} q_{\text{trans}} q_{\text{nuc}}$$

where, the subscripts refer to the respective motions. After "half" a rotation, the nuclei are superimposed on each other. Since a proton is a spin half nucleus, the total wave function must be antisymmetic with respect to the exchange of the particles. i.e.:

$$\psi(1,2) = -\psi(2,1)$$

The translational motion refers to the motion of the molecular center of mass and has no influence on the symmetry of the nuclear wave function. Vibrational motion depends on the magnitude of the internuclear distance and has no effect on the particle exchange. The electronic motion also has no effect on the symmetry properties of the nuclear wave function. Therefore, the product of the nuclear spin and rotational wave functions must be antisymmetric with respect to the particle exchange. For the nuclear spin functions, there are four combinations. One combination is a singlet:

$$|\psi_{\nu,s}\rangle = \alpha(1)\beta(2) - \alpha(2)\beta(1)$$

And the other three combinations are the three states of a triplet:

$$|\psi_{\nu,s}\rangle = \alpha(1)\alpha(2)$$
$$|\psi_{\nu,s}\rangle = \alpha(1)\beta(2) + \alpha(2)\beta(1)$$
$$|\psi_{\nu,s}\rangle = \beta(1)\beta(2)$$

The rotational wavefunctions (ψ_r) are given in terms of the associated Legendre polynomials $P_l^{|m|}(x)$ where $x = \cos\theta$:

$$|\psi_r\rangle = e^{im\phi} P_l^{|m|}(\cos\theta) \tag{2.9.1}$$

with:

$$P_l^{(m)}(x) = \left(1 - x^2\right)^{|m/2} \frac{d^{|m|} P_l(x)}{dx^{m|}} \tag{2.9.2}$$

$$P_l(x) = \frac{1}{2^l l!} \frac{d^l \left(x^2 - 1\right)^l}{dx^l} \tag{2.9.3}$$

When the nuclei are interchanged, θ becomes $\pi - \theta$ and φ is changed to $\varphi + \pi$. The polynomials change as:

$$P_l(-x) = (-1)' P_l(x); \quad P_l^{|m|}(-x) = (-1)^{l-|m|||} P_l^{|m|}(x) \tag{2.9.4}$$

The exponential function changes as:

$$e^{im(\phi+\pi)} = e^{im\pi} e^{im\varphi} = (-1)^{|m|} e^{im\varphi} \tag{2.9.5}$$

Therefore, the rotational wave function changes as:

$$P_l(-x) = (-1)^l P_l(x) \tag{2.9.6}$$

$$P_l^{|m|}(-x) = (-1)^{l-|m|} P_l^{|m|}(x) \tag{2.9.7}$$

- $|\psi_r\rangle$ is symmetrical for even J, and
- $|\psi_r\rangle$ is antisymmetrical for odd J

Combining the nuclear spin and the rotational parts, we see that, the product ψ_r, ψ_m must be antisymmetrical (with respect to the exchange of nuclei) for half integral nuclear spins and symmetrical for integral spins. To accomplish this, the singlet nuclear states

(para) must be combined with the even rotational functions and the triplet nuclear states must be combined with the odd rotational states. The rotational partition functions for ortho and para hydrogens are, thus:

$$q_{\text{ortho}} = q_{\nu,t} q_{r,\text{odd}} = 3 \sum_{J=1,3,5,\ldots} (2J+1) e^{-J(J+1)\Theta_R/T} \tag{2.9.8}$$

and:

$$q_{\text{para}} = q_{\nu,\,s}\, q_{r,\text{even}} = 1 \sum_{J=0,2,4,\ldots} (2J+1) e^{-J(J+1)\Theta_R/T} \tag{2.9.9}$$

where Θ_R is the rotational temperature defined previously. The total partition function consisting both ortho and para hydrogens is given by:

$$q_{\text{rot},nu} = 1 \sum_{j=0.2.4} (2J+1) e^{-J(J+1)\Theta_k/T} + 3 \sum_{j=1,3,5,n} (2J+1) e^{-J(J+1)\Theta_R/T} \tag{2.9.10}$$

The ratio of ortho to para hydrogens at thermal equilibrium is given by:

$$\frac{N_o}{N_p} = \frac{3 \sum_{j=1,2,3\ldots} (2J+1) e^{-J(J+1)\Theta_R/T}}{\sum_{j=0} 2(2J+1) e^{-J(J+1)\Theta_R/T}} \tag{2.9.11}$$

At high temperature, the two summations become equal and therefore, the high temperature limit of N_o/N_p is 3. At low temperature, the ratio becomes:

$$\frac{N_o}{N_p} = \frac{3\left(3e^{-2\Theta_k/T} + \ldots\ldots\right)}{1\left(1 + 5e^{-5\Theta_n/T} + \ldots\right)} \rightarrow 0, \text{ as } T \rightarrow 0 \tag{2.9.12}$$

A good experimental verification of the above analysis is a comparison between the calculated rotational heat capacities at constant volume (C_V) rot, nu (calculated from:

$$C_V = \frac{\partial \langle E \rangle}{\partial T}$$

where:

$$\langle E \rangle = \frac{\partial \ln q_{\text{rot},\nu}}{\partial \beta}$$

The heat capacities are shown as a function of temperature in Figure 18.10.1 .

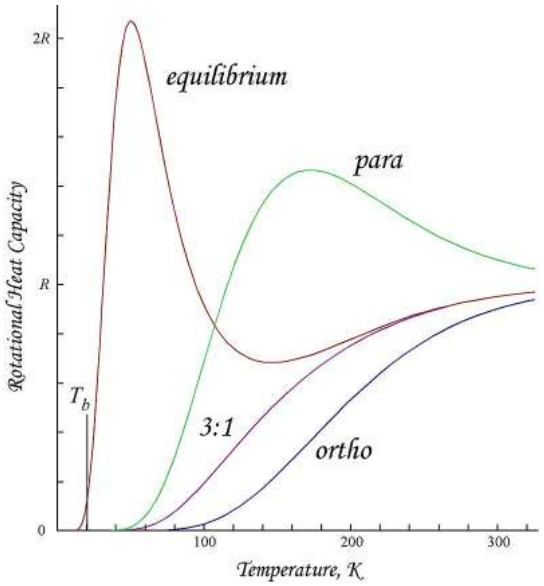


Figure 18.10.1 : The heat capacities of o- and p- hydrogens as a function of temperature. The curve marked Exp depicts the experimental data, the curve eq represents the data for an equilibrated mixture of o- and p- at a given temperature and the curves o- and p-represent the heat capacities of pure o- and pure p- hydrogens. (CC-SA-BY 3.0; Gadolinist).

The purple curve marked 3:1 gives the experimental data, the curve eq represents the data for an equilibrated mixture of o- and p- at a given temperature. The curves o- and p- represent the heat capacities of pure o- and pure p- hydrogens calculated from the o- and p- partition functions given by Equations 2.9.8 and 2.9.9 respectively. Initially it was a puzzle as to why the experimental data differs from the calculated values. In fact, the experimental data seemed to agree very well with the following equation:

$$(C_V)_{\text{rot},\nu} = \frac{3}{4}(C_V)_{\text{rot},\nu}(\text{ortho}) + \frac{1}{4}(C_V)_{\text{rot},\nu}(\text{para}) \tag{2.9.13}$$

The reason for this is that, when $\mathbf{H_2}$ is cooled down from a higher temperature, the ortho:para ratio continues to remain 0.75 / 0.25 (the high temperature value) because the $\textbf{ortho} \rightarrow \textbf{para}$ interconversion rate is very very small and we do not reach the equilibrium composition unless a catalyst such as activated charcoal is added to the gas mixture. Equation 2.9.13 corresponds to a “frozen high temperature mixture” of ortho:para hydrogens. In the presence of the catalyst, the experiments also give the curve labeled as eq in the graph. This in indeed a very nice case where the experiments support not only the methods of statistical thermodynamics but also of the antisymmetry principle for bosons and fermions. If we consider the case of $^{16}\mathbf{O_2}$, where the nuclear spins are zero, the rotational wave function has to be symmetric as only symmetric wave functions are permitted for bosons. Thus, only even rotational states contribute to the partition function:

$$q_{\text{rot},V}(^{16}\mathbf{O_2}) = \sum_{J=0,2,4,\ldots} (2J+1)e^{-J(J+1)\theta_R/T}$$

Contributors and Attributions

- www.chem.iitb.ac.in/~bltembe/pdfs/ch_3.pdf

2.9: Ortho and Para Hydrogen is shared under a CC BY-NC-SA 4.0 license and was authored, remixed, and/or curated by LibreTexts.

- **18.10: Ortho and Para Hydrogen** is licensed CC BY-NC-SA 4.0.

2.10: The Equipartition Principle

2.10.1: Introduction

The law of equipartition of energy states that each quadratic term in the classical expression for the energy contributes $\frac{1}{2}k_BT$ to the average thermal energy per molecule. Here, k_B is the Boltzmann constant, and T is the temperature in Kelvin. For instance, the motion of an atom has three degrees of freedom (number of ways of absorbing energy), corresponding to the x, y and z components of its velocity. Since these velocities appear quadratically in the kinetic energy ($KE = \frac{1}{2}mv^2$), every atom has an average kinetic energy of $\frac{3}{2}k_BT$ in thermal equilibrium.

The number of degrees of freedom (DOF) of a polyatomic gas molecule is $3N$ where N is the number of atoms in the molecule. This is equal to number of coordinates for the system (e.g. for N = two atoms you would have x, y, z for each atom yielding 3(2) = 6 DOF). For molecules we usually do not consider the x, y and z velocity of each atom. Instead we divide the molecular motion into 3 translational DOF corresponding to the x, y and z velocity of the molecular center-of-mass, rotational DOF, and vibrational DOF (also referred to as vibrational modes). There are two distinct cases for how the degrees of freedom are divided among rotation and vibration:

- **Linear molecules** have 3 translational DOF and 2 rotational DOF, corresponding to rotation about the two axes perpendicular to the molecular axis (the bond in a simple diatomic). This means the remaining 3N - 5 DOF are vibrations (e.g. in a diatomic this gives us 3(2) - 5 = 1 vibrational DOF, the bond stretch).
- **Nonlinear molecules** have have 3 translational DOF and 3 rotational DOF, corresponding to rotation about three orthogonal internal axes. This means the remaining 3N - 6 DOF are vibrations (e.g. in a pentatomic molecule such as methane this gives us 3(5) - 6 = 9 vibrational DOF).

2.10.2: Translations

The translational DOF have a classical energy of

$$\epsilon_{trans} = \frac{1}{2}m\left(v_x^2 + v_y^2 + v_z^2\right). \tag{2.10.1}$$

Based on the classical energy the equipartion principle gives us an average molecular contribution to the thermal energy of $3\left(\frac{1}{2}k_BT\right)$, because there are 3 quadratic terms.

Let us compare that to the translational contribution to the average energy based on statistical mechanics. From statistical mechanics the average energy in a DOF is:

$$\langle E_{DOF}\rangle = k_BT^2\left(\frac{\partial ln q_{DOF}}{\partial T}\right)_V \tag{2.10.2}$$

Introducing the translational partition function derived earlier, Equation 2.10.2 becomes

$$\langle E_{trans}\rangle = k_BT^2\left(\frac{\partial}{\partial T}\right)_V ln\left(\frac{2\pi mk_BT}{h^2}\right)^{3/2}V = \frac{3}{2}k_BT$$

Thus, the translational degrees of freedom in three dimensions satisfy the equipartition theorem with each translational degree providing $\frac{1}{2}k_BT$ of energy.

2.10.3: Rotations

The classical expression for the rotational energy of a diatomic or linear molecule, using I as the moment of inertia and ω_i as the angular velocity around axis i, is

$$E_{rot} = \frac{1}{2}I(\omega_x^2 + \omega_y^2). \tag{2.10.3}$$

For a nonlinear molecule the classical rotational energy is

$$E_{rot} = \frac{1}{2}(I_x\omega_x^2 + I_y\omega_y^2 + I_z\omega_z^2). \tag{2.10.4}$$

Thus based on equipartion and the number of quadratic terms, we would expect <E_{rot}>(linear) = k_BT and <E_{rot}>(nonlinear) = $\frac{3}{2}k_BT$.

Again using equation 2.10.2 we can do the calculation of the average rotational energy based on statistical mechanics. Except for very small molecules or low temperatures we can use the "high" temperature limiting integrated value for the rotational partition function. For the linear case we have:

$$q_{rot}(\text{linear}) = \frac{k_BT}{\sigma B}. \tag{2.10.5}$$

Substituting in to 2.10.2 yields:

$$\langle E_{rot}(\text{linear})\rangle = k_BT^2\left(\frac{\partial}{\partial T}\right)_V ln\left(\frac{k_BT}{\sigma B}\right) = k_BT. \tag{2.10.6}$$

For the nonlinear case:

$$q_{rot}(\text{nonlinear}) = \frac{1}{\sigma}\left(\frac{\pi k_B^3T^3}{ABC}\right)^{1/2}. \tag{2.10.7}$$

Substituting in to 2.10.2 yields:

$$\langle E_{rot}(\text{nonlinear})\rangle = k_BT^2\left(\frac{\partial}{\partial T}\right)_V ln\left(\frac{1}{\sigma}\left(\frac{\pi k_B^3T^3}{ABC}\right)^{1/2}\right) = \frac{3}{2}k_BT. \tag{2.10.8}$$

As long as the temperature is reasonably high and the molecules are not H_2, rotational degrees of freedom give a value of $\frac{1}{2}k_BT$ for each rotational DOF in accordance with the equipartition principle. When this is true (almost always) the rotational DOF are said to be "active". In cases where the modes are not "active" direct summation of the partition function is necessary to calculate the actual average thermal energy per molecule.

2.10.4: Vibrations

The classical expression for the one dimensional vibrational energy is

$$E_{vib} = ½kx^2 + ½\mu v_x^2, \tag{2.10.9}$$

where k is the vibrational spring constant (not k_B), μ is the reduced mass of the vibrating mass and v_x is the velocity of the vibrating mass. the two quadratic terms suggest we expect to get $\langle E_{vib}\rangle = k_BT$ for each vibrational degree of freedom.

Again using equation 2.10.2 we can do the calculation of the average vibrational energy based on statistical mechanics. The vibrational partition function for a single mode is:

$$q_{\text{vib}} = \frac{1}{1-e^{-h\nu/(k_BT)}} \tag{2.10.10}$$

Substituting in to 2.10.2 yields:

$$\langle E_{vib}\rangle = k_BT^2\left(\frac{\partial}{\partial T}\right)_V ln\left(\frac{1}{1-e^{-h\nu/(k_BT)}}\right) = \frac{k_BT^2}{k_BT^2}h\nu\frac{e^{-h\nu/(k_BT)}}{1-e^{-h\nu/(k_BT)}}. \tag{2.10.11}$$

This can be simplified by dividing both numerator and denominator of by $e^{-h\nu/k_BT}$

$$\langle E_{vib}\rangle = h\nu\left(\frac{1}{e^{h\nu/k_BT}-1}\right) \tag{2.10.12}$$

Equation 2.10.12 is applicable at all temperatures, but if $h\nu/k_BT \ll 1$ (i.e., the high temperature limit), then the exponential in the denominator can be expanded

$$e^{h\nu/k_BT} - 1 \approx 1 + h\nu/k_BT - 1 = h\nu/k_BT \tag{2.10.13}$$

and Equation 2.10.12 becomes

$$\langle E_{vib} \rangle \approx \cancel{h\nu} \left(\frac{1}{\cancel{h\nu}/k_B T} \right)$$

$$\langle E_{vib} \rangle \approx k_B T \tag{2.10.14}$$

with each vibrational degree providing $k_B T$ of energy (since there are two quadratic terms in energy of a harmonic oscillator, kinetic energy and potential energy).

At high temperature the equipartition theorem is valid (the vibrational mode is "active"), but at low temperature, the expansion in Equation 2.10.13 fails (or more terms are required). In this case, only a few vibrational states are occupied making the mode "inactive" and the equipartition principle is not applicable to the vibrational contribution to the thermal energy.

2.10.5: Overall thermal energy

Accounting for the fact that vibrational degrees of freedom are often not active we can create a more realistic equation for the total thermal energy than just assuming $k_B T$ from each vibrational mode, $\frac{3}{2} k_B T$ from translation and $k_B T$ from rotation in the linear case or $\frac{3}{2} k_B T$ for the nonlinear case.

$$E^*_{eqpart} = \frac{3}{2} k_B T + \frac{D_{rot}}{2} k_B T + D^*_{vib} k_B T, \tag{2.10.15}$$

where D_{rot} is the number of rotational degrees of freedom (2 for linear, 3 for nonlinear) and D^*_{vib} is the number of active vibrational degrees of freedom. Only very low frequency vibrational modes below 200 cm^{-1} are active near room temperature.

2.10.6: References

1. Thermodynamics and Statistical Mechanics, Greiner W., Neise, Stocker, Springer, 2001
2. Physical Chemistry, 5th ed., Atkins P., W. H. Freeman and Company, 1994.

Contributors and Attributions

- Zane Sterkewolf (UC Davis)
- www.chem.iitb.ac.in/~bltembe/pdfs/ch_3.pdf
- Sudarson S Sinha (Tel Aviv University)
- J. Gutow (UW-Oshkosh)

This page titled 2.10: The Equipartition Principle is shared under a CC BY-NC-SA 4.0 license and was authored, remixed, and/or curated by Jonathan Gutow.

- **18.11: The Equipartition Principle** is licensed CC BY-NC-SA 4.0.

2.11: Molar Heat Capacities

2.11.1: Introduction

Heat capacity at constant volume C_V, is defined as

$$C_V = \left(\frac{\partial U}{\partial T}\right)_V, \tag{2.11.1}$$

and heat capacity at constant pressure C_P, is defined as

$$C_P = \left(\frac{\partial H}{\partial T}\right)_P. \tag{2.11.2}$$

The statistical definitions of U and H in terms of the canonical partition function Q are:

$$U = k_B T^2 \left(\frac{\partial lnQ}{\partial T}\right)_V + U_o \tag{2.11.3}$$

and

$$H = k_B T^2 \left(\frac{\partial \ln Q}{\partial T}\right)_V + V k_B T \left(\frac{\partial \ln Q}{\partial V}\right)_T + H_o. \tag{2.11.4}$$

Substituting into equations 2.11.1 and 2.11.2 we get statistical expressions for for the heat capacities:

$$C_V = \left(\frac{\partial}{\partial T}\right)_V \left(k_B T^2 \left(\frac{\partial lnQ}{\partial T}\right)_V + U_o\right) = \left(\frac{\partial}{\partial T}\right)_V \left(k_B T^2 \left(\frac{\partial lnQ}{\partial T}\right)_V\right), \tag{2.11.5}$$

and

$$\begin{aligned} C_P &= \left(\frac{\partial}{\partial T}\right)_P \left(k_B T^2 \left(\frac{\partial \ln Q}{\partial T}\right)_V + V k_B T \left(\frac{\partial \ln Q}{\partial V}\right)_T + H_o\right) \\ &= \left(\frac{\partial}{\partial T}\right)_P \left(k_B T^2 \left(\frac{\partial \ln Q}{\partial T}\right)_V + V k_B T \left(\frac{\partial \ln Q}{\partial V}\right)_T\right). \end{aligned} \tag{2.11.6}$$

These expressions are general and apply to molecules that have no intermolecular interactions as well as those that are strongly interacting. Calculating Q for interacting particles is challenging (see for example the discussion on the impact of interactions on just the translational contribution to the partition function), so we will limit ourselves to some specific cases where the interactions are unimportant or easier to predict.

We will consider pure samples, so all the particles are identical. If the sample is gas phase this means that:

$$Q(gas) = \frac{q_{trans}^N q_{rot}^N q_{vib}^N q_{elec}^N}{N!}, \tag{2.11.7}$$

where N = the number of molecules in the sample, q_{trans} is the microcanonical translational partition function, q_{rot} is the microcanonical rotational partition function, q_{vib} is the microcanonical vibrational partition function and q_{elec} is the microcanonical electronic partition function. In the solid phase where the molecules are distinguishable by their location the 1/N! is dropped and translation and rotation are not possible:

$$Q(solid) = q_{vib}^N q_{elec}^N. \tag{2.11.8}$$

2.11.2: Heat capacity of gases

Equations 2.11.5 and 2.11.6 depend on the lnQ. So taking the ln of equation 2.11.7 we get:

$$lnQ(gas) = N ln q_{trans} + N ln q_{rot} + N ln q_{vib} + N ln q_{elec} - ln N!. \tag{2.11.9}$$

So,

$$C_V = \left(\frac{\partial}{\partial T}\right)_V \left(k_B T^2 \left(\frac{\partial lnQ}{\partial T}\right)_V\right) \tag{2.11.10}$$
$$= \left(\frac{\partial}{\partial T}\right)_V \left(k_B T^2 \left(\frac{\partial}{\partial T}\right)_V (Nlnq_{trans} + Nlnq_{rot} + Nlnq_{vib} + Nlnq_{elec} - lnN!)\right)$$
$$= \left(\frac{\partial}{\partial T}\right)_V \left(k_B T^2 \left(N\left(\frac{\partial lnq_{trans}}{\partial T}\right)_V + N\left(\frac{\partial lnq_{rot}}{\partial T}\right)_V + N\left(\frac{\partial lnq_{vib}}{\partial T}\right)_V + N\left(\frac{\partial lnq_{elec}}{\partial T}\right)_V - 0\right)\right)$$
$$= \left(\frac{\partial}{\partial T}\right)_V N\left[k_B T^2 \left(\frac{\partial lnq_{trans}}{\partial T}\right)_V + k_B T^2 \left(\frac{\partial lnq_{rot}}{\partial T}\right)_V + k_B T^2 \left(\frac{\partial lnq_{vib}}{\partial T}\right)_V + k_B T^2 \left(\frac{\partial lnq_{elec}}{\partial T}\right)_V\right].$$

Each term in the square brackets is just the average energy of each particular type of molecular motion ($\langle E_k \rangle$, where k = trans, rot, vib or elec). In our discussion of equipartition of energy among the different types of molecular motion we developed expressions for these if the molecules do not interact strongly. Inserting the expressions from that discussion converts equation 2.11.10 to:

$$C_V = \left(\frac{\partial}{\partial T}\right)_V N\left[\frac{3}{2}k_B T + \frac{D_{rot}}{2}k_B T + D^*_{vib}k_B T\right], \tag{2.11.11}$$

where D_{rot} is the number of rotational degrees of freedom (2 for linear and 3 for nonlinear molecules) and D^*_{vib} is the number of active (low frequency) vibrational degrees of freedom. We have also assumed that the electronic states are far enough apart that lnq_{elec} is a constant, giving a derivative of zero. Setting N = N_A (Avogadro's number) and taking the remaining derivative with respect to T gives us an equipartition expression for the molar constant volume heat capacity of a gas:

$$C_{Vm} = \frac{3}{2}R + \frac{D_{rot}}{2}R + D^*_{vib}R = \left(\frac{3}{2} + \frac{D_{rot}}{2} + D^*_{vib}\right)R, \tag{2.11.12}$$

where we have used $N_A k_B = R$, the gas constant. Additionally, we know that for an ideal gas that $C_{Pm} = C_{Vm} + R$ giving us an equivalent equipartition expression for the molar constant pressure heat capacity of a gas:

$$C_{Pm} = \left(\frac{5}{2} + \frac{D_{rot}}{2} + D^*_{vib}\right)R, \tag{2.11.13}$$

Thus we predict that:

- A monatomic gas (no rotations and no vibrations) will have a $C_{Vm} = (3/2)R = 12.47$ J mol^{-1} K^{-1} and $C_{Pm} = (5/2)R = 20.79$ J mol^{-1} K^{-1}.
- A linear molecule with no low frequency vibrations will have a $C_{Vm} = (5/2)R = 20.79$ J mol^{-1} K^{-1} and $C_{Pm} = (7/2)R = 29.10$ J mol^{-1} K^{-1}.
- A nonlinear molecule with no low frequency vibrations will have a $C_{Vm} = 3R = 24.94$ J mol^{-1} K^{-1} and $C_{Pm} = 4R = 33.26$ J mol^{-1} K^{-1}.
- If some vibrations are active C_{Vm} will be increased by $D^*_{vib}R$.

The table below collects some heat capacities for a selection of gases under standard conditions (298 K). You will notice that these simple predictions are very good in many cases

Table 2.11.1: Heat capacities for a selection of gases under standard conditions (298 K). Monatomic gases are in blue, linear molecules in red and nonlinear molecules in purple. Values from the resource table Extended Thermodynamic Properties and the CoolProp software package.

Gas	C_{Vm} (J mol^{-1} K^{-1})	C_{Pm} (J mol^{-1} K^{-1})
Monatomic Gases		
He	12.47	20.79
Ar	12.47	20.79
Xe	12.53	21.02
Linear Molecules (including diatomics)		
H_2	20.52	28.84
HCl	20.98	29.51
O_2	21.07	29.43
N_2	20.82	29.17
CO	20.83	29.19
CO_2	28.93	37.44
Nonlinear Molecules		
H_2O (g)	25.33	33.67
NH_3	27.97	36.82
CH_4	27.40	35.80
SF_6	88.72	97.03

The experimental values are generally higher than the estimates, except for the case of H_2, which has such a large rotational constant that at room temperature only some of the lowest excited rotational states are accessible. This leads to even the rotational degrees of freedom of H_2 to being less then completely "active". Making a good estimate for H_2 requires using the full summation for q_{rot}.

Some other discrepancies to notice:

- Xe which has significant dispersion attractions has a higher heat capacity then predicted for a monatomic gas.
- Other than H_2 linear molecules have heat capacities above the prediction. The heavier the atoms in the molecule, the lower the vibrational frequencies and the more vibrations contribute to the heat capacity.
- For nonlinear molecules, again, the heavier the atoms in the molecule, the lower the vibrational frequencies and the more vibrations contribute to the heat capacity.

Despite these discrepancies, the agreement is very good for such a simple model. Switching to explicit summation to calculate the partitions functions would make the predictions for molecules without significant attractions (non-polar molecules with relatively weak dispersion interactions) quite close.

Example 2.11.1: CO_2 vs. NO_2

The predicted molar constant volume heat capacity for the linear CO_2 (with three translational and two rotational degrees of freedom) is $5/2R$ ($20.79\ JK^{-1}mol^{-1}$).

The experimental value is 28.93 J K^{-1}mol^{-1}.

The estimated molar constant volume heat capacity for NO_2 (a bent molecule, with three translational and three rotational degrees of freedom) is $3R$ ($24.94\ JK^{-1}mol^{-1}$).

The experimental value is 29.5 J K^{-1}mol^{-1}.

Both the experimental values are higher than estimated, suggesting that vibrations do contribute to some extent. Especially for CO_2, the deviation is significant. This suggests that the bigger deviation in the prediction of molar heat capacities is probably due to the existence of the lower frequency-bending vibration in carbon dioxide.

2.11.2.1: Temperature dependence of gas phase heat capacities

Our simple model (equation 2.11.13) assumes the rotational degrees of freedom contribute to the heat capacity. However, k_BT has to be much greater than the spacing between the quantum energy levels for this to be true. If this is not satisfied, the heat capacity will be reduced. If the gaseous state could be maintained down to near absolute zero even the translational degrees of freedom would not contribute and the heat capacity would drop to zero. Any degree of freedom with energy spacings greater than k_BT are considered to be **inactive** or **frozen out**; this is the situation for the vibrational degrees of freedom at room temperature and that is why the usual assumption is that they will not contribute. As we lower the temperature rotations will cease to contribute as well. The figure below presents an idealized plot of the heat capacity of a gas versus temperature.

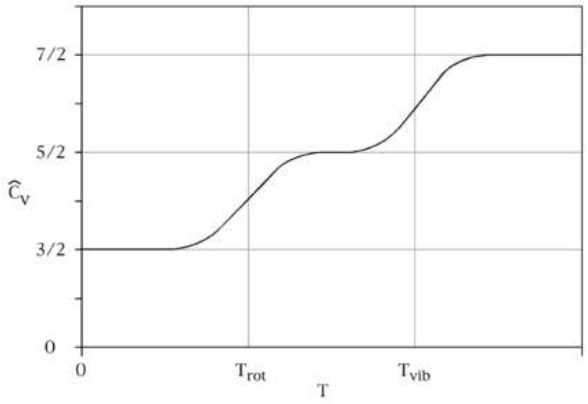


Figure **2.11.1** : Idealized plot of the molar specific heat of a diatomic gas against temperature, with C_{Vm} ($\hat{C}_V$) in units of R. It agrees with the value (7/2)R predicted by equipartition at high temperatures (where R is the gas constant), but decreases to (5/2)R and then (3/2)R at lower temperatures, as the vibrational and rotational modes of motion are "frozen out". (Public domain; PD-Self)

2.11.3: Heat capacity of solids

We will consider Einsteins model for monatomic solids. Einstein proposed a simple model for such substances whereby the atoms only have vibrational energy (each atom can vibrate in three perpendicular directions around its lattice position). Specifically, the 'Einstein Solid Model' assumes that the atoms act like three-dimensional harmonic oscillators (with the vibrational motion of each atom in each perpendicular dimension entirely independent). This is equivalent to assuming that electronic states do not contribute so equation 2.11.8 becomes:

$$Q(solid) = q_{vib}^N. \tag{2.11.14}$$

Near room temperature and for heavy atoms, such as most metals, the vibrations will be low frequency and thus "active". Following the same argument made for gases, this leads to just the last term in equation 2.11.11 and 2.11.12. As we are assuming three active vibrational degrees of freedom, we expect the molar heat capacity for solid pure elements near room temperature to be:

$$C_{Vm} \approx 3R = 24.94 Jmol^{-1}K^{-1}.$$

In the early 1800s, two French scientists by the names of Pierre Louis Dulong and Alexis Therese Petit empirically discovered the same remarkable result. The Dulong-Petit Law is normally expressed in terms of the specific heat capacity (C_s) and the molar mass (M) of the metal

$$C_sM = C_{Vm} \approx 25(JK^{-1}mol^{-1}) \tag{2.11.15}$$

where C_s represents how much heat is required to raise the temperature of 'one gram' of that substance by one degree Kelvin. Dulong and Petit, as well as other scientists of their time, used this famous relationship as a means of establishing more accurate values for the atomic weight of metallic elements (by instead measuring the specific heat capacity of the element and using the Dulong-Petit relationship, which is a relatively simple method of establishing weights in comparison to the more disputable gravimetric methods that were being used at the time to establish the equivalent weights of elements).

Because only vibrations are involved it is relatively straightforward to derive the full temperature dependent expression for the heat capacity of the 'Einstein Solid Model' through statistical mechanics. The average vibrational energy of a 1-D harmonic oscillator is:

$$\langle E_{vib} \rangle = \frac{h\nu}{e^{h\nu/k_BT} - 1} = \frac{k_B\Theta_{vib}}{e^{\Theta_v/T} - 1}. \tag{2.11.16}$$

Taking the derivative with respect to temperature to get C_{Vm} and converting from per molecule to per mole we get:

$$C_{V,m}^{1-D} = R\left(\frac{\Theta_v}{T}\right)^2 \left(\frac{e^{-\Theta_v/2T}}{1 - e^{-\Theta_v/T}}\right)^2 \tag{2.11.17}$$

where R is the universal gas constant, T is absolute temperature, and Θ_v is called the 'characteristic vibrational temperature' of the oscillator, h represents Plank's constant and k_B is Boltzmann's constant.

Since the vibrations in each dimension are assumed to be independent, the expression for the constant volume molar heat capacity of a 'three-dimensional' Einstein Solid is obtained by simply multiplying Equation 2.11.17 by three;

$$C_{V,m}^{3-D} = 3R\left(\frac{\Theta_v}{T}\right)^2 \left(\frac{e^{-\Theta_v/2T}}{1 - e^{-\Theta_v/T}}\right)^2 \tag{2.11.18}$$

The temperature variation of the heat capacity of most metallic solids is well described by equation 2.11.18. Furthermore, plots of equation 2.11.18 as a function of temperature for metals with widely varying vibrational frequencies reveal that the heat capacity always approaches the same asymptotic limit of $3R$ at high temperatures. Stated another way, at high temperatures

$$\lim_{T\to\infty}\left[\left(\frac{\Theta_v}{T}\right)^2 \left(\frac{e^{-\Theta_v/2T}}{1 - e^{-\Theta_v/T}}\right)^2\right] = 1 \tag{2.11.19}$$

and Equation 2.11.18 reduces to the value we got previously:

$$\lim_{T\to\infty}\left[C_{V,m}^{3D}\right] = 3R \tag{2.11.20}$$

In addition to predicting the high temperature limit correctly the model also predicts correctly that the heat capacity will approach zero as $T \to 0K$. The denominator in equation 2.11.18 approaches zero more slowly than the numerator.

2.11.4: Exercises

Consult the CRC Handbook of Chemistry and Physics (CRC Press: Boca Raton, FL) or other reliable source of data and compile a table of specific heat capacities for a large number of elements that are known to exist as monoatomic solids at room temperature. Also look up and record the molar mass of these elements. The elements that you consider should be restricted to those appearing in groups 1-14 of the periodic table. Make sure you generate a fairly large list which includes a number of elements that are normally considered as metallic in character (such as copper, iron, sodium, lithium, gold, platinum, barium, and aluminum), but also some non-metallic elements that are nonetheless monoatomic isotropic solids (such as carbon-diamond, beryllium, boron, and silicon). Heat capacities that are usually reported in the literature are not actual constant volume heat capacities (C_v), but are instead constant pressure heat capacities (C_p). Fortunately, C_p and C_v are essentially equal for simple solids (within the level of precision that we consider in this exercise), and you can assume that the values from the CRC Handbook represent C_s.

1. Enter the element name, the specific heat capacity, and the molar mass of each element in a your favorite data analysis tool. Calculate the product of specific heat and molar mass for each element and calculate how much this product differs from the Dulong-Petit prediction (express your result as a percent difference relative to $3R$).
2. Assess the generality of the Dulong-Petit law in an alternate way by generating a plot of specific heat as a function of reciprocal Molar Mass (C_s versus $1/M$), which should be linear with a slope equal to 3R if the data behave according to Equation 2.11.15.

3. Inspect your results from 1 and 2 above and identify any elements that significantly deviate from the Dulong-Petit law. When they occur, do deviations tend to be smaller or larger than 3R? Does the degree of deviation from the Dulong-Petit law seem to correlate with periodic trends in metallic (or covalent) bonding for these elements? Do deviations tend to occur more readily for elements of smaller or higher atomic weight? Explain how the type of bonding and the magnitude of the atomic weight can lead to deviations from the arguments made in Equations 2.11.15-2.11.20 above.
4. Use the plotting method that you employed in step 2 above as a means of determining a value for the universal gas constant (R) - but make sure you throw-out any specific heat data for elements that you suspect do not fall within the limit $\Theta_v \ll 298\,K$. Calculate the percent error in the value of R that you determine.
5. Verify that the limit expressed in Equation 2.11.19 above is true (HINT: expand each of the exponential terms in a power series and note that higher-order terms are negligible in the limit $T \gg \Theta_v$).

This page titled 2.11: Molar Heat Capacities is shared under a CC BY-NC-SA 4.0 license and was authored, remixed, and/or curated by Jonathan Gutow.

- **18.11: The Equipartition Principle** is licensed CC BY-NC-SA 4.0.
- **Specific Heat Capacities and the Dulong-Petit Law** by Tandy Grubbs is licensed CC BY-NC-SA 4.0.

CHAPTER OVERVIEW

3: Quantum Mechanics

3.1: Quantum Operators Represent Classical Variables
3.2: Eigenfunctions of Operators are Orthogonal
3.3: Commuting Operators Allow Infinite Precision
3.4: The Quantum Mechanical Free Particle
3.5: The Energy Levels of a Rigid Rotor
3.6: The Variational Method
3.7: Linear Variational Method and the Secular Determinant
3.8: Perturbation Theory Expresses the Solutions in Terms of Solved Problems
3.9: Electron Spin, Indistinguishability and Slater Determinants
3.10: Band Structure

This page titled 3: Quantum Mechanics is shared under a not declared license and was authored, remixed, and/or curated by Jonathan Gutow.

3.1: Quantum Operators Represent Classical Variables

Learning Objectives

- Understand how the correspondence principle argues that a unique quantum operator exist for every classical observable.
- Recognize several of the commonly used quantum operators

Introduction

Quantum mechanics can be formulated as a mathematical model based on a series of postulates. The first being that the wavefunction completely specifies the state and thus properties of the system.

Postulate I: Information content of the Wavefunction

The state of a system is completely specified by ψ, the wavefunction for the system that satisfies the quantum wave equation for the system (for example the time independent Schrödinger equation $\hat{H}\psi = E\psi$). Thus, everything that can be known about the system can be extracted (calculated) from ψ.

Operators for observables

The second postulate specifies how observable information can be calculated from ψ. An observable is a dynamic variable of a system that can be experimentally measured (e.g., position, momentum and kinetic energy). In systems governed by classical mechanics, it is a real-valued function (never complex), however, in quantum physics, every observable in quantum mechanics is represented by an independent operator that is used to obtain physical information about the observable from the wavefunction. It is a general principle of quantum mechanics that there is an operator for every physical observable. For an observable that is represented in classical physics by a function $Q(x, p)$, the corresponding operator is $Q(\hat{x}, \hat{p})$.

Postulate II: The Correspondence Principle

For every observable property of a system there is a corresponding quantum mechanical operator. This is often referred to as the **Correspondence Principle**.

Classical dynamical variables, such as x (position) and p (momentum), are represented in quantum mechanics by *linear operators* which act on the wavefunction. Starting with the quantum operators for position and momentum we can construct others such as kinetic energy (T) by analogy with the classical physical relations. The quantum operator for position in one dimension is $\hat{x}$ which represents multiplication by position x. So:

$$\hat{x}\psi = x\psi.$$

The classical operator for position of a particle in three dimensions is just the set of coordinates x, y, and z, which is written as a vector, r:

$$\vec{r} = (x, y, z) = x\vec{i} + y\vec{j} + z\vec{k} \tag{3.1.1}$$

Thus, we write the quantum operator as:

$$\hat{\vec{r}} = (\hat{x}, \hat{y}, \hat{z}) = \hat{x}\vec{i} + \hat{y}\vec{j} + \hat{z}\vec{k} = x\vec{i} + y\vec{j} + z\vec{k} \tag{3.1.2}$$

Notice that because the operator for a position is just multiplication by position the classical and quantum operator are effectively the same.

The operator for a component of linear momentum is

$$\hat{p}_x = -i\hbar\frac{\partial}{\partial x}. \tag{3.1.3}$$

In three dimensions

$$\hat{p} = -i\hbar\left(\frac{\partial}{\partial x}, \frac{\partial}{\partial y}, \frac{\partial}{\partial z}\right) = -i\hbar\nabla \tag{3.1.4}$$

Classically the momentum is $p_x = mv_x$, m = mass and v_x = velocity. The classical kinetic energy in one dimension is $T_x = (1/2)mv_x^2$ or substituting in momentum, $p_x = mv_x$

$$T_x = \frac{p_x^2}{2m}. \tag{3.1.5}$$

Substituting in the quantum momentum operator $\hat{p}_x$ for p_x in equation 3.1.5 yields the quantum operator for the kinetic energy observable in one dimension:

$$\hat{T}_x = \frac{1}{2m}\hat{p}_x^2 = -\frac{\hbar^2}{2m}\frac{\partial^2}{\partial x^2}. \tag{3.1.6}$$

In three dimensions

$$\hat{T} = \frac{1}{2m}\hat{p}^2 = \frac{-\hbar^2}{2m}\nabla\cdot\nabla = \frac{-\hbar^2}{2m}\nabla^2 = \frac{-\hbar^2}{2m}\left(\frac{\partial^2}{\partial x^2} + \frac{\partial^2}{\partial y^2} + \frac{\partial^2}{\partial z^2}\right). \tag{3.1.7}$$

The total energy operator is called the Hamiltonian operator, $\hat{H}$ and consists of the kinetic energy operator plus the potential energy operator $\hat{V}$, which is just multiplication by the potential energy function.

$$\hat{H} = \hat{T} + \hat{V} = -\frac{\hbar^2}{2m}\nabla^2 + \hat{V}(x, y, z) \tag{3.1.8}$$

The Hamiltonian Operator

The Hamiltonian operator is named after the Irish mathematician William Hamilton and comes from the his formulation of Classical Mechanics that is based on the total energy:

$$\hat{H} = \hat{T} + \hat{V}$$

rather than Newton's second law,

$$\vec{F} = m\vec{a}$$

In many cases only the kinetic energy of the particles and the electrostatic or Coulomb potential energy due to their charges are considered, but in general all terms that contribute to the energy appear in the Hamiltonian. These additional terms account for such things as external electric and magnetic fields and magnetic interactions due to magnetic moments of the particles and their motion.

Table 3.1.1 : Some common Operators in Quantum Mechanics

Name	Observable Symbol	Operator Symbol	Operation
Position (in 1D)	x	$\hat{x}$	Multiply by x
Position (in 3D)	$\vec{r}$	$\hat{r}$	Multiply by $\vec{r}$
Momentum (in 1D)	p_x	$\hat{p}_x$	$-i\hbar\frac{d}{dx}$
Momentum (in 3D)	$\vec{p}$	$\hat{p}$	$-i\hbar\left[\hat{i}\ \frac{d}{dx}+\hat{j}\frac{d}{dy}+\hat{k}\frac{d}{dz}\right]$
Kinetic Energy (in 1D)	T_x	$\hat{T}_x$	$\frac{-\hbar^2}{2m}\frac{d^2}{dx^2}$
Kinetic Energy (in 3D)	T	$\hat{T}$	$\frac{-\hbar^2}{2m}\left[\frac{d^2}{dx^2}+\frac{d^2}{dy^2}+\frac{d^2}{dz^2}\right]$ Which can be simplified to $\frac{-\hbar^2}{2m}\nabla^2$
Potential Energy (in 1D)	$V(x)$	$\hat{V}(x)$	Multiply by $V(x)$
Potential Energy (in 3D)	$V(x,y,z)$	$\hat{V}(x,y,z)$	Multiply by $V(x,y,z)$
Total Energy	H	$\hat{H}$	$\frac{-\hbar^2}{2m}\nabla^2+V(x,y,z)$
Angular Momentum (x axis component)	L_x	$\hat{L}_x$	$-i\hbar\left[y\frac{d}{dz}-z\frac{d}{dy}\right]$
Angular Momentum (y axis component)	L_y	$\hat{L}_y$	$-i\hbar\left[z\frac{d}{dx}-x\frac{d}{dz}\right]$
Angular Momentum (z axis component)	L_z	$\hat{L}_z$	$-i\hbar\left[x\frac{d}{dy}-y\frac{d}{dx}\right]$

3.1: Quantum Operators Represent Classical Variables is shared under a CC BY-NC-SA 4.0 license and was authored, remixed, and/or curated by LibreTexts.

- **4.2: Quantum Operators Represent Classical Variables** is licensed CC BY-NC-SA 4.0.

3.2: Eigenfunctions of Operators are Orthogonal

Learning Objectives

- Understand the properties of a Hermitian operator and their associated eigenstates
- Recognize that all experimental obervables are obtained by Hermitian operators

Consideration of the quantum mechanical description of the particle-in-a-box exposed two important properties of quantum mechanical systems. We saw that the eigenfunctions of the Hamiltonian operator are orthogonal, and we also saw that the position and momentum of the particle could not be determined exactly. We now examine the generality of these insights by stating and proving some fundamental theorems. These theorems use the Hermitian property of quantum mechanical operators that correspond to observables, which is discuss first.

3.2.1: Hermitian Operators

Since the eigenvalues of a quantum mechanical operator correspond to measurable quantities, the eigenvalues must be real, and consequently a quantum mechanical operator must be Hermitian. To prove this, we start with the premises that ψ and ϕ are functions, $\int d\tau$ represents integration over all coordinates, and the operator $\hat{A}$ is **Hermitian** by definition if

$$\int \psi^* \hat{A} \phi \, d\tau = \int (\hat{A}^* \psi^*) \phi \, d\tau \tag{3.2.1}$$

This equation means that the complex conjugate of $\hat{A}$ can operate on ψ^* to produce the same result after integration as $\hat{A}$ operating on ϕ, followed by integration. To prove that a quantum mechanical operator $\hat{A}$ is Hermitian, consider the eigenvalue equation and its complex conjugate.

$$\hat{A}\psi = a\psi \tag{3.2.2}$$

$$\hat{A}^* \psi^* = a^* \psi^* = a\psi^* \tag{3.2.3}$$

Note that $a^* = a$ because the eigenvalue is real. Multiply Equation 3.2.2 and 3.2.3 from the left by ψ^* and ψ, respectively, and integrate over the full range of all the coordinates. Note that ψ is normalized. The results are

$$\int \psi^* \hat{A} \psi \, d\tau = a \int \psi^* \psi \, d\tau = a \tag{3.2.4}$$

$$\int \psi \hat{A}^* \psi^* \, d\tau = a \int \psi \psi^* \, d\tau = a \tag{3.2.5}$$

Since both integrals equal a, they must be equivalent.

$$\int \psi^* \hat{A} \psi \, d\tau = \int \psi \hat{A}^* \psi^* \, d\tau \tag{3.2.6}$$

The operator acting on the function,

$$\hat{A}^* \psi^* = \phi$$

produces a new function. Since functions commute, the right hand side of equation 3.2.6 can be rewritten as

$$\int \psi \hat{A}^* \psi^* \, d\tau = \int \psi \phi \, d\tau = \int \phi \psi \, d\tau = \int (\hat{A}^* \psi^*) \psi d\tau.$$

Thus equation 3.2.6 can be rewritten as

$$\int \psi^* \hat{A} \psi \, d\tau = \int \left(\hat{A}^* \psi^* \right) \psi \, d\tau \tag{3.2.7}$$

Thus, $\hat{A}$ satisfies the criterion for being Hermitian in equation 3.2.1.

This shows that **operators that produce eigenvalues that are real numbers are Hermitian.**

3.2.2: Orthogonality

Two wavefunctions, $\psi_1(x)$ and $\psi_2(x)$, are said to be *orthogonal* if

$$\int_{-\infty}^{\infty} \psi_1^* \psi_2 \, dx = 0. \tag{3.2.8}$$

Orthogonality Theorem

Eigenfunctions of a Hermitian operator are orthogonal if they have different eigenvalues.

Because of this theorem, we can identify orthogonal functions easily without having to integrate or conduct an analysis based on symmetry or other considerations.

Proof

ψ and φ are two eigenfunctions of the operator Â with real eigenvalues a_1 and a_2, respectively. Since the eigenvalues are real, $a_1^* = a_1$ and $a_2^* = a_2$.

$$\hat{A}\psi = a_1\psi$$

$$\hat{A}^*\phi^* = a_2\phi^*$$

Multiply the first equation by ϕ^* and the second by ψ and integrate.

$$\int \phi^* \hat{A}\psi \, d\tau = a_1 \int \phi^* \psi \, d\tau$$

$$\int \psi \hat{A}^* \phi^* \, d\tau = a_2 \int \psi \phi^* \, d\tau \tag{3.2.9}$$

Subtract the two equations above to obtain

$$\int \phi^* \hat{A}\psi \, d\tau - \int \psi \hat{A}^* \phi^* \, d\tau = (a_1 - a_2) \int \phi^* \psi \, d\tau \tag{3.2.10}$$

The left-hand side of Equation 3.2.10 is zero because $\hat{A}$ is Hermitian yielding

$$0 = (a_1 - a_2) \int \phi^* \psi \, d\tau \tag{3.2.11}$$

If a_1 and a_2 in Equation 3.2.11 are not equal, then the integral **must** be zero. This result proves that **nondegenerate eigenfunctions** of the same operator are orthogonal.

□

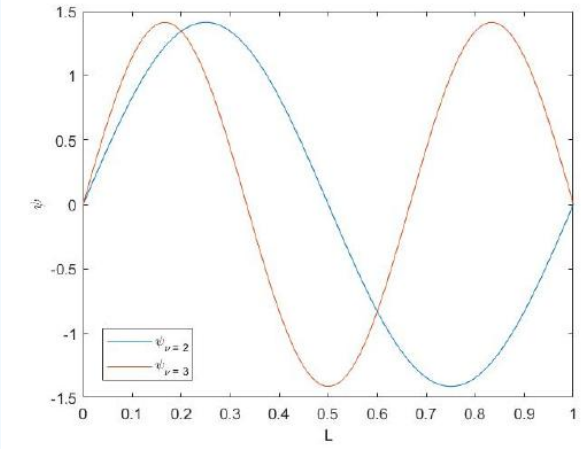
In other words, eigenstates of an Hermitian operator corresponding to *different* eigenvalues are automatically *orthogonal*.

Example4.5.1

Draw graphs and use them to show that the particle-in-a-box wavefunctions for $\psi(n = 2)$ and $\psi(n = 3)$ are orthogonal to each other.

Solution

The two PIB wavefunctions are qualitatively similar when plotted



These wavefunctions are orthogonal when

$$\int_{-\infty}^{\infty} \psi(n=2)\psi(n=3)dx = 0$$

and when the PIB wavefunctions are substituted this integral becomes

$$\int_0^L \sqrt{\frac{2}{L}} \sin\left(\frac{2n}{L}x\right) \sqrt{\frac{2}{L}} \sin\left(\frac{2n}{L}x\right) dx = ?$$

$$\frac{2}{L}\int_0^L \sin\left(\frac{2}{L}x\right) \sin\left(\frac{3}{L}x\right) = ?$$

We can expand the integrand using trigonometric identities to help solve the integral, but it is easier to take advantage of the symmetry of the integrand, specifically, the $\psi(n=2)$ wavefunction is even (blue curves in above figure) and the $\psi(n=3)$ is odd (purple curve). Their product (even times odd) is an odd function and the integral over an odd function is zero. Therefore $\psi(n=2)$ and $\psi(n=3)$ wavefunctions are orthogonal.

This can be repeated an infinite number of times to confirm the entire set of PIB wavefunctions are mutually orthogonal as the Orthogonality Theorem guarantees.

3.2.3: Orthogonality of Degenerate Eigenstates

Consider two eigenstates of $\hat{A}$, ψ_a and ψ'_a, which correspond to the *same* eigenvalue, a. Such eigenstates are termed **degenerate**. The above proof of the orthogonality of different eigenstates fails for degenerate eigenstates. Note, however, that *any* linear combination of ψ_a and ψ'_a is also an eigenstate of $\hat{A}$ corresponding to the eigenvalue a. Thus, even if ψ_a and ψ'_a are not orthogonal, we can always choose two linear combinations of these eigenstates which are orthogonal. For instance, if ψ_a and ψ'_a are properly normalized, we can define the **overlap integral**

$$S = \int_{-\infty}^{\infty} \psi_a^* \psi'_a dx, \tag{3.2.12}$$

It is easily demonstrated (see below) that

$$\psi''_a = \frac{|S|}{\sqrt{1-|S|^2}} \left(\psi_a - S^{-1}\psi'_a\right) \tag{3.2.13}$$

is a properly normalized eigenstate of $\hat{A}$, corresponding to the eigenvalue a, which is orthogonal to ψ_a. It is straightforward to generalize the above argument to three or more degenerate eigenstates. Hence, we conclude that the eigenstates of a Hermitian operator are, or can be chosen to be, **mutually orthogonal.**

Theorem: Gram-Schmidt Orthogonalization

Degenerate eigenfunctions are **not** automatically orthogonal, but can be made so mathematically via the Gram-Schmidt Orthogonalization.

The above theorem argues that if the eigenvalues of two eigenfunctions are the same then the functions are said to be degenerate and linear combinations of the degenerate functions can be formed that will be orthogonal to each other. Since the two eigenfunctions have the same eigenvalues, the linear combination also will be an eigenfunction with the same eigenvalue. The proof of this theorem shows us one way to produce orthogonal degenerate functions.

Proof that orthogonal wavefunctions can be constructed from non-orthogonal degenerate wavefunctions

Both the bra-ket $\langle|\rangle$ notation and normal integral notation are shown.

If ψ_a and ψ_a' are degenerate, but not orthogonal, we can define a new composite wavefunction $\Phi = \psi_a' - S\psi_a$ where S is the overlap integral:

$$S = \langle \psi_a | \psi_a' \rangle = \int_{-\infty}^{\infty} \psi_a^* \psi_a' dx$$

then ψ_a and Φ will be orthogonal.

$$\langle \psi_a | \Phi \rangle = \langle \psi_a | \psi_a' - S\psi_a \rangle = \int \psi_a^* (\psi_a' - S\psi_a) d\tau \tag{3.2.14}$$

$$= \cancel{\langle \psi_a | \psi_a' \rangle}^{S} - S \cancel{\langle \psi_a | \psi_a \rangle}^{1} = \cancel{\int \psi_a^* \psi_a' d\tau}^{S} - S \cancel{\int \psi_a^* \psi_a d\tau}^{1}$$

$$= S - S = 0$$

Thus, ψ_a and Φ will be orthogonal.

□

Exercise 4.5.2

Find N that normalizes ψ if $\psi = N(\varphi_1 - S\varphi_2)$ where φ_1 and φ_2 are normalized wavefunctions and S is their overlap integral.

$$S = \langle \varphi_1 | \varphi_2 \rangle$$

Answer

Remember that to normalize an arbitrary wavefunction, we find a constant N such that $\langle \psi | \psi \rangle = 1$. This equates to the following procedure:

$$\langle \psi | \psi \rangle = \langle N(\varphi_1 - S\varphi_2) | N(\varphi_1 - S\varphi_2) \rangle = 1$$

$$N^2 \langle (\varphi_1 - S\varphi_2) | (\varphi_1 - S\varphi_2) \rangle = 1$$

$$N^2 \left[\cancel{\langle \varphi_1 | \varphi_1 \rangle}^{1} - S \cancel{\langle \varphi_2 | \varphi_1 \rangle}^{S} - S \cancel{\langle \varphi_1 | \varphi_2 \rangle}^{S} + S^2 \cancel{\langle \varphi_2 | \varphi_2 \rangle}^{1} \right] = 1$$

$$N^2 (1 - S^2 \cancel{- S^2 + S^2}) = 1$$

$$N^2 (1 - S^2) = 1$$

therefore

$$N = \frac{1}{\sqrt{1 - S^2}}$$

We conclude that the eigenstates of operators are, or can be chosen to be, **mutually orthogonal**.

Contributors and Attributions

- Richard Fitzpatrick (Professor of Physics, The University of Texas at Austin)

3.2: Eigenfunctions of Operators are Orthogonal is shared under a CC BY-NC-SA 4.0 license and was authored, remixed, and/or curated by LibreTexts.

- **4.5: Eigenfunctions of Operators are Orthogonal** is licensed CC BY-NC-SA 4.0.

3.3: Commuting Operators Allow Infinite Precision

Learning Objectives

- To connect the Heisenberg Uncertainty principle to the commutation relations.
- Develop proficiency in calculating the commutator of two operators.

If two operators commute then both quantities can be measured at the same time with infinite precision, if not then there is a tradeoff in the accuracy in the measurement for one quantity vs. the other. This is the mathematical representation of the Heisenberg Uncertainty principle.

3.3.1: Commuting Operators

One important property of operators is that the order of operation matters. Thus in general

$$\hat{A}\hat{E}f(x) \neq \hat{E}\hat{A}f(x)$$

unless the two operators **commute**. Two operators commute if the following equation is true:

$$\left[\hat{A},\hat{E}\right] = \hat{A}\hat{E} - \hat{E}\hat{A} = 0$$

To determine whether two operators commute first operate $\hat{A}\hat{E}$ on a function $f(x)$. Then operate $\hat{E}\hat{A}$ the same function $f(x)$. If the same answer is obtained subtracting the two functions will equal zero and the two operators will commute.on

If two operators commute, then they can have the same set of eigenfunctions. By definition, two operators $\hat{A}$ and $\hat{B}$ commute if the effect of applying $\hat{A}$ then $\hat{B}$ is the same as applying $\hat{B}$ then $\hat{A}$, i.e.

$$\hat{A}\hat{B} = \hat{B}\hat{A}.$$

For example, the operations brushing-your-teeth and combing-your-hair commute, while the operations getting-dressed and taking-a-shower do not. This theorem is very important. If two operators commute and consequently have the same set of eigenfunctions, then the corresponding physical quantities can be evaluated or measured exactly simultaneously with no limit on the uncertainty. As mentioned previously, the eigenvalues of the operators correspond to the measured values.

If $\hat{A}$ and $\hat{B}$ commute and ψ is an eigenfunction of $\hat{A}$ with eigenvalue b, then

$$\hat{B}\hat{A}\psi = \hat{A}\hat{B}\psi = \hat{A}b\psi = b\hat{A}\psi \tag{3.3.1}$$

Equation 3.3.1 says that $\hat{A}\psi$ is an eigenfunction of $\hat{B}$ with eigenvalue b, which means that when $\hat{A}$ operates on ψ, it cannot change ψ. At most, $\hat{A}$ operating on ψ can produce a constant times ψ.

$$\hat{A}\psi = a\psi \tag{3.3.2}$$

$$\hat{B}(\hat{A}\psi) = \hat{B}(a\psi) = a\hat{B}\psi = ab\psi = b(a\psi) \tag{3.3.3}$$

Equation 3.3.3 shows that Equation 3.3.2 is consistent with Equation 3.3.1. Consequently ψ also is an eigenfunction of $\hat{A}$ with eigenvalue a.

Example 3.3.1

Do the following pairs of operators commute?

a. $\hat{A} = \dfrac{d}{dx}$ and $\hat{E} = x^2$
b. $\hat{B} = \dfrac{h}{x}$ and $\hat{C}\{f(x)\} = f(x) + 3$
c. $\hat{J} = 3x$ and $\hat{O} = x^{-1}$

Solution a

This requires evaluating $\left[\hat{A},\hat{E}\right]$, which requires solving for $\hat{A}\{\hat{E}f(x)\}$ and $\hat{E}\{\hat{A}f(x)\}$ for arbitrary wavefunction $f(x)$ and asking if they are equal.

$$\hat{A}\{\hat{E}f(x)\} = \hat{A}\{x^2 f(x)\} = \frac{d}{dx}\{x^2 f(x)\} = 2xf(x) + x^2 f'(x)$$

From the product rule of differentiation.

$$\hat{E}\{\hat{A}f(x)\} = \hat{E}\{f'(x)\} = x^2 f'(x)$$

Now ask if they are equal

$$\left[\hat{A},\hat{E}\right] = 2xf(x) + x^2 f'(x) - x^2 f'(x) = 2xf(x) \neq 0$$

Therefore the two operators do not commute.

Solution b

This requires evaluating $\left[\hat{B},\hat{C}\right]$ like in Example 3.3.1 .

$$\hat{B}\{\hat{C}f(x)\} = \hat{B}\{f(x)+3\} = \frac{h}{x}(f(x)+3) = \frac{hf(x)}{x} + \frac{3h}{x}$$

$$\hat{C}\{\hat{B}f(x)\} = \hat{C}\{\frac{h}{x}f(x)\} = \frac{hf(x)}{x} + 3$$

Now ask if they are equal

$$\left[\hat{B},\hat{C}\right] = \frac{hf(x)}{x} + \frac{3h}{x} - \frac{hf(x)}{x} - 3 \neq 0$$

The two operators do **not** commute.

Solution c

This requires evaluating $\left[\hat{J},\hat{O}\right]$

$$\hat{J}\{\hat{O}f(x)\} = \hat{J}\{f(x)3x\} = f(x)3x/x = 3f(x)$$

$$\hat{O}\{\hat{J}f(x)\} = \hat{O}\{\frac{f(x)}{x}\} = \frac{f(x)3x}{x} = 3f(x)$$

$$\left[\hat{J},\hat{O}\right] = 3f(x) - 3f(x) = 0$$

Because the difference is zero, the two operators commute.

3.3.2: General Heisenberg Uncertainty Principle

Although it will not be proven here, there is a general statement of the uncertainty principle in terms of the commutation property of operators. If two operators $\hat{A}$ and $\hat{B}$ do not commute, then the uncertainties (standard deviations σ) in the physical quantities associated with these operators must satisfy

$$\sigma_A \sigma_B \geq \frac{1}{2}\left|\int \psi^*[\hat{A}\hat{B} - \hat{B}\hat{A}]\psi\, d\tau\right| \text{ or } \frac{1}{2}\left|\langle\psi^*|[\hat{A}\hat{B} - \hat{B}\hat{A}]|\psi\rangle\right| \tag{3.3.4}$$

where the the square brackets inside the integral is called the **commutator**, and $\left|\ \right|$ signifies the modulus or absolute value. If $\hat{A}$ and $\hat{B}$ commute, then the right-hand-side of Equation 3.3.4 is zero, so either or both σ_A and σ_B could be zero, and there is no restriction on the uncertainties in the measurements of the eigenvalues a and b. If $\hat{A}$ and $\hat{B}$ do not commute, then the right-hand-side of Equation 3.3.4 will not be zero, and neither σ_A nor σ_B can be zero unless the other is infinite. Consequently, both a and b cannot be eigenvalues of the same wavefunctions and cannot be measured simultaneously to arbitrary precision.

? Exercise3.3.1

Show that the commutator for position and momentum in one dimension equals $-i\hbar$ and that the right-hand-side of Equation 3.3.4 therefore equals $\hbar/2$ giving $\sigma_x\sigma_{px} \geq \frac{\hbar}{2}$.

3.3.3: Applications

Operators are very common with a variety of purposes. They are used to figure out the energy of a wavefunction using the Schrödinger Equation.

$$\hat{H}\psi = E\psi$$

They also help to explain observations made in the experimentally. An example of this is the relationship between the magnitude of the angular momentum and the components.

$$\left[\hat{L}^2, \hat{L}_x^2\right] = \left[\hat{L}^2, \hat{L}_y^2\right] = \left[\hat{L}^2, \hat{L}_z^2\right] = 0$$

However the components do not commute themselves. An additional property of commuters that commute is that both quantities can be measured simultaneously. Thus, the magnitude of the angular momentum and ONE of the components (usually z) can be known at the same time however, NOTHING is known about the other components.

> *The physical quantities corresponding to operators that commute can be measured simultaneously to any precision.*

3.3.2A Example

Determine whether the following two operators commute:

$$\hat{K} = \alpha \int [1]^{[\infty]} d[x]$$

and

$$\hat{H} = d/dx$$

Solution

Evaluate

$$\left[\hat{K}, \hat{H}\right]$$

3.3.2B Example

Determine whether the following two operators commute:

$$\hat{I} = 5$$

and

$$\hat{L} = \int_{[1]}^{[\infty]} d[x]$$

Solution

The identity operator, $\hat{I}$ is a real number and commutes with everything. Thus, these two operators commute. We can also directly evaluate the commutator:

$$\left[\hat{I}, \hat{L}\right]$$

$$\left[\hat{I}, \hat{L}\right] f(x) = 5\int_1^\infty f(x)d(x) - \int_1^\infty 5f(x)d(x) = 0$$

3.3.2C? Exercise

Show that the components of the angular momentum do not commute.

$$\hat{L}_x = -i\hbar\left[-\sin\left(\phi\frac{\delta}{\delta\theta}\right) - \cot(\Theta)\cos\left(\phi\frac{\delta}{\delta\phi}\right)\right]$$

$$\hat{L}_y = -i\hbar\left[\cos\left(\phi\frac{\delta}{\delta\theta}\right) - \cot(\Theta)\cos\left(\phi\frac{\delta}{\delta\phi}\right)\right]$$

$$\hat{L}_z = -i\hbar\frac{\delta}{\delta\theta}$$

Solution

This requires evaluating the following commucators:

$$\left[\hat{L}_z, \hat{L}_x\right] = i\hbar\hat{L}_y$$

$$\left[\hat{L}_x, \hat{L}_y\right] = i\hbar\hat{L}_z$$

$$\left[\hat{L}_y, \hat{L}_z\right] = i\hbar\hat{L}_x$$

3.3.4: Contributors

- David M. Hanson, Erica Harvey, Robert Sweeney, Theresa Julia Zielinski
- J. Gutow (UW-Oshkosh)

3.3.5: References

1. Gohberg, I. Basic Operator Theory; Birkhäuser: Boston, 2001
2. McQuarrie, D.A. Quantum Chemistry, 2nd Edition; University Science Books:Sausalito, 2008
3. Schechter, M. Operator Methods in Quantum Mechanics; Dover Publications, 2003

This page titled 3.3: Commuting Operators Allow Infinite Precision is shared under a CC BY-NC-SA 4.0 license and was authored, remixed, and/or curated by David M. Hanson, Erica Harvey, Robert Sweeney, Theresa Julia Zielinski via source content that was edited to the style and standards of the LibreTexts platform.

- **4.6: Commuting Operators Allow Infinite Precision** by David M. Hanson, Erica Harvey, Robert Sweeney, Theresa Julia Zielinski is licensed CC BY-NC-SA 4.0. Original source: https://web.archive.org/web/20200619182410/http://www.chemeddl.org.

3.4: The Quantum Mechanical Free Particle

Learning Objectives

- To desribe the quantum mechanical free particle
- To recognize the application of the heisenburg uncertainty principle applied to the free particle
- To identify the lack of quantization of the free particle and understand why.

The simplest system in quantum mechanics has the potential energy $V = 0$ everywhere. This is called a **free particle** since it has no forces acting on it. We consider the one-dimensional case, with motion only in the x-direction, giving the time-independent Schrödinger equation

$$-\frac{\hbar^2}{2m}\frac{d^2\psi(x)}{dx^2} = E\psi(x) \tag{3.4.1}$$

or more simply

$$\hat{H}\psi(x) = E\psi(x) \tag{3.4.2}$$

with

$$\hat{H} = -\frac{\hbar^2}{2m}\frac{d^2}{dx^2} \tag{3.4.3}$$

Total derivatives can be used since there is one independent variable. The equation simplifies to

$$\psi''(x) + k^2\psi(x) = 0 \tag{3.4.4}$$

with the definition

$$k^2 \equiv \frac{2mE}{\hbar^2} \tag{3.4.5}$$

Possible solutions of Equation 3.4.4 are

$$\psi(x) = const\begin{Bmatrix}\sin(kx)\\ \cos(kx)\\ e^{\pm ikx}\end{Bmatrix} \tag{3.4.6}$$

There is no restriction on the value of k. Thus a free particle, even in quantum mechanics, can have any non-negative value of the energy

$$E = \frac{\hbar^2k^2}{2m} \geq 0 \tag{3.4.7}$$

The energy levels in this case are *not* quantized and correspond to the same continuum of kinetic energy shown by a classical particle.

Example 3.4.1: Eigenstates of the Hamiltonian of a free particle

Consider for a free particle (i.e., $V(x) = 0$) moving in one dimension.

a. Demonstrate that $\sin(kx)$, $\cos(kx)$, and $e^{\pm ikx}$ are indeed eigenfunctions of $\hat{H}$.
b. What are their corresponding eigenstates?
c. What are the energies not quantized?

? Exercise 3.4.1

Consider for a free particle (i.e., $V(x) = 0$) moving in one dimension.

a. Demonstrate that $\cos(kx)$ and $e^{\pm ikx}$ are eigenfunctions of $\hat{H}$.
b. What are their corresponding eigenstates?
c. Is momentum quantized for a free particle?

It is of interest also to consider the x-component of linear momentum for the free-particle solutions (Equation 3.4.6). The eigenvalue equation for momentum is

$$\hat{p}_x\psi(x) = -i\hbar\frac{d\psi(x)}{dx} = p\psi(x) \tag{3.4.14}$$

where we have denoted the momentum eigenvalue as p.

It is easily shown that neither of the functions $\sin kx$ or $\cos kx$ from Equation 3.4.6 is an eigenfunction of $\hat{p}_x$. However, $e^{\pm ikx}$ are both eigenfunctions with eigenvalues $p = \pm\hbar k$, respectively. Evidently the momentum p can take on any real value between -∞ and +∞. The kinetic energy, equal to $E = p^2/2m$, can correspondingly have any value between 0 and +∞.

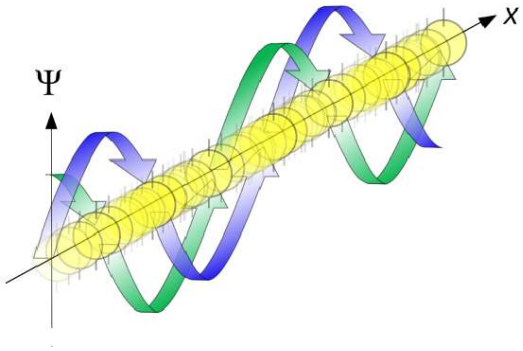


Figure 3.4.1: Propagation of quantum free particle (i.e. de Broglie waves) in 1D space. The real part of the complex amplitude is blue and imaginary part is green. The probability (shown as the yellow opacity) of finding the particle at a given point x is spread out evenly over space, there is no definite position of the particle. (Public Domain; Maschen).

> *A free particle, even in quantum mechanics, can have any non-negative value of the energy*

✓ Example 3.4.2: Eigenstates of Momentum of a Free Particle

Consider for a free particle (i.e., $V(x) = 0$) moving in one dimension.

a. Demonstrate that $e^{\pm ikx}$ are eigenfunctions of $\hat{p}_x$.
b. What are their corresponding eigenstates?

? Exercise 3.4.2

Show that neither $\sin kx$ nor $\cos kx$ are eigenstates of $\hat{p}_x$ for a free particle (i.e., $V(x) = 0$) moving in one dimension.

3.4.1: Superpositions

The functions $\sin kx$ and $\cos kx$, while not eigenfunctions of $\hat{p}_x$, are each *superpositions* of the two eigenfunctions $e^{\pm ikx}$, by virtue of the trigonometric identities

$$\cos(kx) = \frac{1}{2}(e^{ikx} + e^{-ikx}) \tag{3.4.15}$$

and

$$\sin(kx) = \frac{1}{2i}(e^{ikx} - e^{-ikx}) \tag{3.4.16}$$

The eigenfunction e^{ikx} for $k > 0$ represents the particle moving from left to right on the *x-axis* (blue curve in Figure **3.4.2**) with momentum $p > 0$. Correspondingly, e^{-ikx} represents motion from right to left with $p < 0$ (red curve in Figure **3.4.2**).

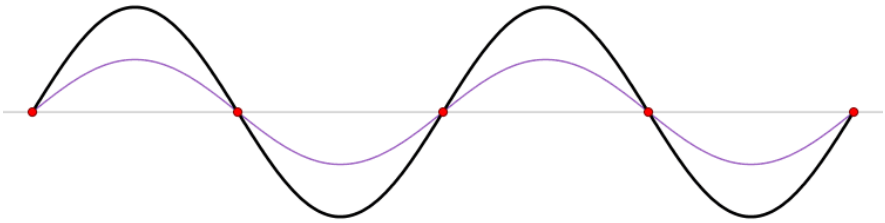


Figure **3.4.2**: Two waves traveling in opposite directions across the same medium combine linearly. In this animation, both waves have the same wavelength and the sum of amplitudes results in a standing wave. (Public Domain; LucasVB)

The functions $\sin(kx)$ and $\cos(kx)$ represent *standing waves*, obtained by superposition of opposing complex waves. Although these two trigonometry functions are not eigenfunctions of $\hat{p}_x$, they *are* eigenfunctions of $\hat{p}_x^2$ and hence they are eigenfunctions of the Hamiltonian operator $\hat{H}$.

Not every wavefunction is an eigenstate

It is important to note that while $\sin kx$ nor $\cos kx$ are **not** eigenstates of momentum, these functions can be decomposed into a combination of functions that are eigenstates (Equation **3.4.14** and **3.4.16**). The ability to decompose wavefunctions into (linear) combinations of eigenstates is used throughout quantum mechanics and will be discussed in more detail in further Sections.

3.4.2: Wavepackets - The Superposition Principle in Action

Consider the wavefunction corresponding to a free electron traveling through a cathode ray tube. The electron leaves the cathode, shoots through the vacuum, and impinges on the screen. At an intermediate point in this process, it is moving through the vacuum and the wavefunction must be nonzero over some volume, but zero in the places the electron has not possibly reached yet, and zero in the places it has definitely left.

However, if the electron has a precise energy (which is all kinetic energy), it also has a precise *momentum*. De Broglie argued that this necessarily implies that the electron wave has a precise *wavelength*. However, since it is a free particle ($V = 0$, the only wave with a *precise* wavelength λ has the form

$$\psi(x,t) = Ae^{i(kx-\omega t)} \tag{3.4.17}$$

where $k = \frac{2\pi}{\lambda}$ and $\omega = 2\pi\nu$. The wavefunctions of Equation **3.4.17** are the solutions to the full time-dependent Schrödinger equation (not just the spatial component discussed above).

The problem with using the wavefunctions of Equation **3.4.17** to represent free particles is that plane sine waves extend to infinity in both spatial directions, so cannot represent a particle whose wavefunction is nonzero in a limited region of space. Physically, that it must have a wavefunction that goes to zero far away in either direction. A localized wavefunction of this type is called a "**wavepacket**". We shall discover that a wavepacket can be constructed by adding plane waves together. To represent a localized particle, we must superpose waves having different wavelengths. Now, the plane waves we add together will individually be solutions of the Schrödinger equation.

The Schrödinger Equation is a Linear Differential Equation

As discussed in previously for a classical wave equation, it quantum equivalent, i.e., Schrödinger equation (both time dependent and independent), are *linear* equations. That is, if $\psi_1(x,y,z,t), \psi_2(x,y,z,t)$ are both solutions of the equation, then so is

$$\psi(x,y,z,t) = c_1\psi_1(x,y,z,t) + c_2\psi_2(x,y,z,t) \tag{3.4.18}$$

where c_1 and c_2 are arbitrary constants, as is easy to check. We previously called this property the **Principle of Superposition**.

The essential point is that in Schrödinger's equation every term contains a factor ψ, but no term contains a factor ψ^2 (or a higher power). That is what is meant by a "linear" equation. If the equation *did* contain a constant term, or a term including ψ^2, superposition wouldn't work—the sum of two solutions to the equation would not itself be a solution to the equation.

In fact, we have been assuming this linearity all along: when we analyze interference and diffraction of waves, we just add the two wave amplitudes at each spot. For the double slit, we take it that if the wave radiating from one slit satisfies the wave equation, then adding the two waves together will give a new wave which also satisfies the equation.

3.4.3: Building Wavepackets

If we add together two sine waves with frequencies close together, we get "beats." This pattern can be viewed as a string of wavepackets. For example considering adding to sine waves together with spatial and temporal frequencies of $(k \pm \Delta k)$ and $(\omega \pm \Delta\omega)$, respectively.

$$\sin\left[(k-\Delta k)x-(\omega-\Delta\omega)t\right]+\sin\left[(k+\Delta k)x-(\omega+\Delta\omega)t\right]) \tag{3.4.19}$$

If we use the trigonometric addition formula, the sum in Equation 3.4.19 can be simplified to

$$2\sin(kx-\omega t)\cos\left[(\Delta k)x-(\Delta\omega)t\right] \tag{3.4.20}$$

Equation 3.4.20 exhibits the phenomenon of beats between waves close in frequency. The first term, $\sin(kx-\omega t)$, oscillates at the average of the two frequencies. It is modulated by the slowly varying second term, often called the "**envelope function**", which oscillates once over a spatial extent of order $\pi/\Delta k$. This is the distance over which waves initially in phase at the origin become completely out of phase. Of course, going a further distance of order $\pi/\Delta k$, the waves will become synchronized again.

That is, beating two close frequencies together breaks up the continuous wave into a series of packets, the beats. To describe a single electron moving through space, we need a single packet. This can be achieved by superposing waves having a continuous distribution of wavelengths, or wave numbers within of order Δk, say, of k. In this case, the waves will be out of phase after a distance of order $\pi/\Delta k$, but since they have many different wavelengths, they will never get back in phase again.

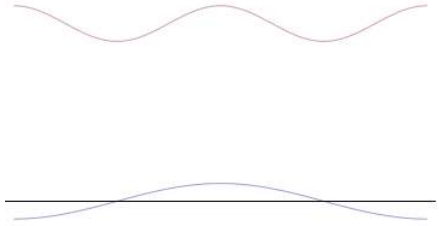


Figure **3.4.3**: The superposition of several plane waves to form a wave packet. This wave packet becomes increasingly localized with the addition of many waves. The Fourier transform is a mathematical operation that separates a wave packet into its individual plane waves. Note that the waves shown here are real for illustrative purposes only, whereas in quantum mechanics the wavefunction is generally complex. (Public Domain; Teply).

We have seen how two sine waves of equal amplitude close together in frequency produce beats: if the waves are in phase at the origin, as we go along the *x*-axis they gradually fall out of phase, and cancel each other at a distance $x = \frac{\pi}{2\Delta}$, where 2Δ is the difference in k of the two $\sin kx$ waves (Figure **3.4.3**). (For the moment, we are ignoring the time development of these waves: we're just looking at t = 0.). If we continue along the *x*-axis to $\frac{\pi}{\Delta}$, the two waves will be back in phase again, this is the next beat. Now, if instead of adding *two* waves, we add *many* waves, all of different k, but with the k's taken from some small interval of size of order Δk, and all these waves are in phase at the origin, then, again, they will all stay more or less in phase for a distance of order $x = \frac{\pi}{2\Delta}$.

However, as we proceed past that point, the chances of them all getting back in phase again get rapidly smaller as we increase the number of different waves. This wavepacket perspective of a free particle is shown in Figure **3.4.4**, where the wavefunction amplitude (both real and imaginary) is localized and tapers off on either side (contrast this image with Figure **3.4.1** that exhibits uniform amplitude over all space since it is an oscillatory eigenfunction.

Gaussian Wavepackets

Fortunately, there is a simple explicit mathematical realization of the addition of plane waves to form a localized function: the *Gaussian wavepacket:*

$$\psi(x, t=0) = A \underbrace{e^{ik_0 x}}_{\text{oscillating term}} \overbrace{e^{-x^2/2\Delta^2}}^{\text{Gaussian envelope}} \tag{3.4.21}$$

where k_0 is an average wavenumber. Topically, the equation for Gaussian wavepackets has an oscillating term with a Gaussian envelope function. This wavepacket wavefunction may be used to represent a localized electron with a negligible probability of finding the electron outside in a small section of length dx at x(Figure **3.4.3**).

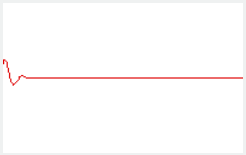


Figure **3.4.4**: A time-dependent (moving) gaussian wavepacket (real or imaginary part). (Public Domain; Wikipedia)

3.4: The Quantum Mechanical Free Particle is shared under a CC BY-NC-SA 4.0 license and was authored, remixed, and/or curated by Michael Fowler & Seymour Blinder.

- **3.4: The Quantum Mechanical Free Particle** by Michael Fowler, Seymour Blinder is licensed CC BY-NC-SA 4.0.

3.5: The Energy Levels of a Rigid Rotor

Learning Objectives

- Compare the classical and quantum rigid rotor in three dimensions
- Demonstrate how to use the Separation of Variable technique to solve the 3D rigid rotor Schrödinger Equation
- Identify and interpret the two quantum numbers for a 3D quantum rigid rotor including the range of allowed values
- Describe the wavefunctions of the 3D quantum rigid rotor in terms of nodes, average displacements and most probable displacements
- Describe the energies of the 3D quantum rigid rotor in terms of values and degeneracies

Rigid rotor means when the distance between particles do not change as they rotate. A rigid rotor only approximates a rotating diatomic molecular if vibration is ignored.

3.5.1: The Classical Rigid Rotor in 3D

The **rigid rotor** is a mechanical model that is used to explain rotating systems. The linear rigid rotor model consists of two point masses located at fixed distances from their center of mass. The fixed distance between the two masses and the values of the masses are the only characteristics of the rigid model. However, for many actual diatomics this model is too restrictive since distances are usually not completely fixed and corrections on the rigid model can be made to compensate for small variations in the distance. Even in such a case the rigid rotor model is a useful model system to master.

For a rigid rotor, the total energy is the sum of kinetic (T) and potential (V) energies

$$E_{tot} = T + V \tag{3.5.1}$$

The potential energy, V, is set to 0 because the distance between particles does not change within the rigid rotor approximation. However, In reality, $V \neq 0$ because even though the average distance between particles does not change, the particles still vibrate. The rigid rotor approximation greatly simplifys our discussion.

Since $V = 0$ then $E_{tot} = T$ and we can also say that:

$$T = \frac{1}{2}\sum m_i v_i^2 \tag{3.5.2}$$

However, we have to determine v_i in terms of rotation since we are dealing with rotation motion. Since,

$$\omega = \frac{v}{r} \tag{3.5.3}$$

where ω is the **angular velocity**, we can say that:

$$v_i = \omega X r_i \tag{3.5.4}$$

Thus we can rewrite Equation 3.5.2 as:

$$T = \frac{1}{2}\sum m_i v_i \left(\omega X r_i\right) \tag{3.5.5}$$

Since ω is a scalar constant, we can rewrite Equation 3.5.5 as:

$$T = \frac{\omega}{2}\sum m_i \left(v_i X r_i\right) = \frac{\omega}{2}\sum l_i = \omega\frac{L}{2} \tag{3.5.6}$$

where l_i is the **angular momentum** of the ith particle, and L is the angular momentum of the *entire system*. Also, we know from physics that,

$$L = I\omega \tag{3.5.7}$$

where I is the moment of inertia of the rigid body relative to the axis of rotation. We can rewrite Equation 3.5.2 as

$$T = \omega \frac{I\omega}{2} = \frac{1}{2} I\omega^2 \tag{3.5.8}$$

Equation 3.5.8 shows that the energy of the rigid rotor scales with increasing angular frequency (i.e., the faster is rotates) and with increasing moment of inertia (i.e, the inertial resistance to rotation). Also, as expected, the classical rotational energy is not quantized (i.e., all possible rotational frequencies are possible).

We can also express the rotational energy in terms of L (equation 3.5.7). Just as with linear momentum if we square it and divide by 2I, we get T:

$$\frac{L^2}{2I} = \frac{I^2\omega^2}{2I} = \frac{I\omega^2}{2} = T. \tag{3.5.9}$$

3.5.2: The Quantum Rigid Rotor in 3D

It is convenient to discuss rotation with in the spherical coordinate system rather than the Cartesian system (Figure 5.8.1).

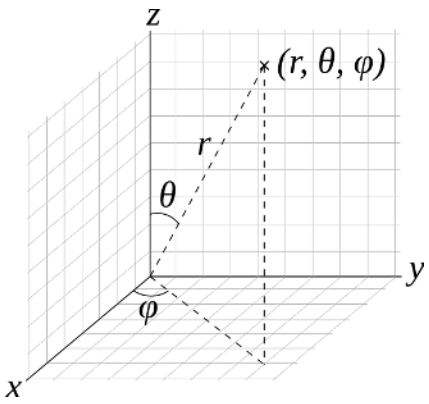


Figure 5.8.1 : The spherical coordinate system in terms of the Cartesian system. (Public Domain; Andeggs via Wikipedia).

To solve the Schrödinger equation for the rigid rotor, we will separate the variables and form single-variable equations that can be solved independently. Only two variables θ and φ are required in the rigid rotor model because the bond length, r, is taken to be the constant r_0. We first write the rigid rotor wavefunctions as the product of a theta-function depending only on θ and a phi-function depending only on φ

$$|\psi(\theta,\varphi)\rangle = |\Theta(\theta)\Phi(\varphi)\rangle \tag{3.5.10}$$

We then substitute the product wavefunction and the Hamiltonian written in spherical coordinates into the Schrödinger Equation 3.5.11

$$\hat{H}|\Theta(\theta)\Phi(\varphi)\rangle = E|\Theta(\theta)\Phi(\varphi)\rangle \tag{3.5.11}$$

to obtain

$$-\frac{\hbar^2}{2\mu r_0^2}\left[\frac{\partial}{\partial r_0} r_0^2 \frac{\partial}{\partial r_0} + \frac{1}{\sin\theta}\frac{\partial}{\partial\theta}\sin\theta\frac{\partial}{\partial\theta} + \frac{1}{\sin^2\theta}\frac{\partial^2}{\partial\varphi^2}\right]|\Theta(\theta)\Phi(\varphi)\rangle = E|\Theta(\theta)\Phi(\varphi)\rangle \tag{3.5.12}$$

Since $r = r_0$ is constant for the **rigid rotor** and does not appear as a variable in the functions, the partial derivatives with respect to r are zero; i.e. the functions do not change with respect to r. We also can substitute the symbol I for the moment of inertia, μr_0^2 in the denominator of the left hand side of Equation 3.5.12, to give

$$-\frac{\hbar^2}{2I}\left[\frac{1}{\sin\theta}\frac{\partial}{\partial\theta}\sin\theta\frac{\partial}{\partial\theta} + \frac{1}{\sin^2\theta}\frac{\partial^2}{\partial\varphi^2}\right]|\Theta(\theta)\Phi(\varphi)\rangle = E|\Theta(\theta)\Phi(\varphi)\rangle \tag{3.5.13}$$

Equation 3.5.9 tells us that the energy of a rotating body is $L^2/(2I)$. Thus we can identify the $-\hbar^2$ multiplied by the expression in square brackets as $\hat{L}^2$, the square of the total angular momentum operator:

$$\hat{L}^2 = -\hbar^2\left[\frac{1}{\sin\theta}\frac{\partial}{\partial\theta}\sin\theta\frac{\partial}{\partial\theta} + \frac{1}{\sin^2\theta}\frac{\partial^2}{\partial\varphi^2}\right]. \tag{3.5.14}$$

To begin the process of the Separating of Variables technique, multiply each side of Equation 3.5.13 by $\frac{2I}{\hbar^2}$ and $\frac{-\sin^2\theta}{\Theta(\theta)\Phi(\varphi)}$ to give

$$\frac{1}{\Theta(\theta)\Phi(\varphi)}\left[\sin\theta\frac{\partial}{\partial\theta}\sin\theta\frac{\partial}{\partial\theta}+\frac{\partial^2}{\partial\varphi^2}\right]\Theta(\theta)\Phi(\varphi)=\frac{-2IE\sin^2\theta}{\hbar^2} \tag{3.5.15}$$

Simplify the appearance of the right-hand side of Equation 3.5.15 by defining a parameter λ:

$$\lambda=\frac{2IE}{\hbar^2}. \tag{3.5.16}$$

Note that this λ has no connection to a wavelength; it is merely being used as an algebraic symbol for the combination of constants shown in Equation 3.5.16.

Inserting λ, evaluating partial derivatives, and rearranging Equation 3.5.15 produces

$$\frac{1}{\Theta(\theta)}\left[\sin\theta\frac{\partial}{\partial\theta}\left(\sin\theta\frac{\partial}{\partial\theta}\right)\Theta(\theta)+\left(\lambda\sin^2\theta\right)\Theta(\theta)\right]=-\frac{1}{\Phi(\varphi)}\frac{\partial^2}{\partial\varphi^2}\Phi(\varphi) \tag{3.5.17}$$

? Exercise 5.8.1

Carry out the steps leading from Equation 3.5.15 to Equation 3.5.17. Keep in mind that, if y is not a function of x,

$$\frac{dy}{dx}=y\frac{d}{dx}$$

Equation 3.5.17 says that the function on the left, depending only on the variable θ, always equals the function on the right, depending only on the variable φ, for all values of θ and φ. The only way two different functions of independent variables can be equal for all values of the variables is if both functions are equal to a constant (review separation of variables). We call this constant m_J^2 because soon we will need the square root of it. The two differential equations to solve are the θ-equation

$$\sin\theta\frac{d}{d\theta}\left(\sin\theta\frac{d}{d\theta}\right)\Theta(\theta)+\left(\lambda\sin^2\theta-m_J^2\right)\Theta(\theta)=0 \tag{3.5.18}$$

and the φ-equation

$$\frac{d^2}{d\varphi^2}\Phi(\varphi)+m_J^2\Phi(\varphi)=0 \tag{3.5.19}$$

The partial derivatives have been replaced by total derivatives because only a single variable is involved in each equation.

> *Often m_J is referred to as just m for convenience.*

? Exercise 5.8.2

Show how Equations 3.5.18 and 3.5.19 are obtained from Equation 3.5.17.

3.5.2.1: Solving the φ Equation

The φ-equation is similar to the Schrödinger Equation for the free particle. Since we already solved this previously, we immediately write the solutions:

$$\Phi_m(\varphi)=Ne^{\pm im_J\varphi} \tag{3.5.20}$$

where we introduce the number m to track how many wavelengths of the wavefunction occur around one rotation (similar to the wavelength description of the Bohr atom).

? Exercise 5.8.3

Substitute Equation 3.5.20 into Equation 3.5.19 to show that it is a solution to that differential equation.

Answer

Substitute

$$\Phi_m(\varphi) = \mathrm{N}e^{\pm im_J\varphi}$$

into

$$\frac{d^2}{d\varphi^2}\Phi(\varphi) + m_J^2\Phi(\varphi) = 0$$

$$\begin{aligned}\frac{d^2}{d\varphi^2}\Phi_\mathrm{m}(\varphi) + m_J^2\Phi_\mathrm{m}(\varphi) =& \frac{d}{d\varphi}\left(\mathrm{N}\left(\pm im_J\right)e^{\pm im_J\varphi}\right) + m_J^2\Phi_\mathrm{m}(\varphi)\\ =& \mathrm{N}\left(\pm im_J\right)^2 e^{\pm im_J\varphi}\Big) + m_J^2\left(\mathrm{N}e^{\pm im_J\varphi}\right)\\ =& -\mathrm{N}m_J^2 e^{\pm im_J\varphi} + \mathrm{N}m_J^2 e^{\pm im_J\varphi} = 0\end{aligned}$$

Thus

$$\Phi_m(\varphi) = Ne^{\pm im_J\varphi}$$

is a solution to the differential equations.

The normalization condition, Equation 3.5.21 is used to find a value for N that satisfies Equation 3.5.20.

$$\int_0^{2\pi} \Phi^*(\varphi)\Phi(\varphi)d\varphi = 1 \tag{3.5.21}$$

The range of the integral is only from 0 to 2π because the angle φ specifies the position of the internuclear axis relative to the x-axis of the coordinate system and angles greater than 2π do not specify additional new positions.

? Exercise 5.8.4

Use the normalization condition in Equation 3.5.21 to demonstrate that $N = 1/\sqrt{2\pi}$.

Answer

We need to evaluate Equation 3.5.21 with $\psi(\varphi) = Ne^{\pm imJ\varphi}$

$$\begin{aligned}\psi^*(\varphi)\psi(\varphi) &= Ne^{+imJ\varphi}Ne^{-imJ\varphi}\\ &= N^2\end{aligned}$$

$$1 = \int_0^{2\pi} N^*Nd\varphi = 1$$

$$N^2(2\pi) = 1$$

$$N = \sqrt{1/2\pi}$$

Values for m are found by using a **cyclic boundary condition**. The cyclic boundary condition means that since φ and $\varphi + 2\varphi$ refer to the same point in three-dimensional space, $\Phi(\varphi)$ must equal $\Phi(\varphi + 2\pi)$, i.e.

$$e^{im_J\varphi} = e^{im_J(\varphi+2\pi)} \tag{3.5.22}$$

$$= e^{im_J\varphi}e^{im_J2\pi} \tag{3.5.23}$$

For the equality in Equation 3.5.23 to hold, $e^{im_J2\pi}$ must equal 1, which is true only when

$$m_J = \cdots, -3, -2, -1, 0, 1, 2, 3, \cdots \tag{3.5.24}$$

In other words m_J can equal **any positive or negative integer or zero.**

? Exercise 5.8.5 : Cyclic Boundary Conditions

Use Euler's Formula to show that $e^{im_J 2\pi}$ equals 1 for m_J equal to zero or any positive or negative integer.

Thus, the Φ function is

$$\Phi_{m_J}(\varphi) = \sqrt{\frac{1}{2\pi}} e^{\pm i m_J \varphi}$$

with

$$m_J = 0, \pm 1, \pm 2, \cdots$$

3.5.2.2: Solving the $\Theta(\theta)$ Equation

Finding the $\Theta(\theta)$ functions that are solutions to the θ-equation (Equation 3.5.18) is a more complicated process. Solutions are found to be a set of power series called *Associated Legendre Functions* (Table M2), which are power series of trigonometric functions, i.e., products and powers of sine and cosine functions. The $\Theta(\theta)$ functions, along with their normalization constants, are shown in the third column of Table **3.5.1** .

Table **3.5.1** : Spherical Harmonic Wavefunctions

m_J	J	$\Theta_J^{m_J}(\theta)$	$\Phi(\varphi)$	$Y_J^{m_J}(\theta,\varphi)$
0	0	$\frac{1}{\sqrt{2}}$	$\frac{1}{\sqrt{2\pi}}$	$\frac{1}{\sqrt{4\pi}}$
0	1	$\sqrt{\frac{3}{2}}\cos\theta$	$\frac{1}{\sqrt{2\pi}}$	$\sqrt{\frac{3}{4\pi}}\cos\theta$
1	1	$\sqrt{\frac{3}{4}}\sin\theta$	$\frac{1}{\sqrt{2\pi}}e^{i\varphi}$	$\sqrt{\frac{3}{8\pi}}\sin\theta e^{i\varphi}$
-1	1	$\sqrt{\frac{3}{4}}\sin\theta$	$\frac{1}{\sqrt{2\pi}}e^{-i\varphi}$	$\sqrt{\frac{3}{8\pi}}\sin\theta e^{-i\varphi}$
0	2	$\sqrt{\frac{5}{8}}(3\cos^2\theta-1)$	$\frac{1}{\sqrt{2\pi}}$	$\sqrt{\frac{5}{16\pi}}(3\cos^2\theta-1)$
1	2	$\sqrt{\frac{15}{4}}\sin\theta\cos\theta$	$\frac{1}{\sqrt{2\pi}}e^{i\varphi}$	$\sqrt{\frac{15}{8\pi}}\sin\theta\cos\theta e^{i\varphi}$
-1	2	$\sqrt{\frac{15}{4}}\sin\theta\cos\theta$	$\frac{1}{\sqrt{2\pi}}e^{-i\varphi}$	$\sqrt{\frac{15}{8\pi}}\sin\theta\cos\theta e^{-i\varphi}$
2	2	$\sqrt{\frac{15}{16}}\sin^2\theta$	$\frac{1}{\sqrt{2\pi}}e^{2i\varphi}$	$\sqrt{\frac{15}{32\pi}}\sin^2\theta e^{2i\varphi}$
-2	2	$\sqrt{\frac{15}{16}}\sin^2\theta$	$\frac{1}{\sqrt{2\pi}}e^{2i\varphi}$	$\sqrt{\frac{15}{32\pi}}\sin^2\theta e^{-2i\varphi}$

The solution to the θ-equation requires that λ in Equation 3.5.17 be given by

$$\lambda = J(J+1) \tag{3.5.25}$$

where

$$J \geq |m_J| \tag{3.5.26}$$

J can be 0 or any positive integer greater than or equal to m_J. Each pair of values for the quantum numbers, J and m_J, identifies a rotational state with a wavefunction (Equation 3.5.10) and energy (below). Equation 3.5.26 means that J controls the allowed values of m_J.

> *Each pair of values for the quantum numbers, J and m_J, identifies a rotational state and hence a specific wavefunction with associated energy.*

The combination of Equations 3.5.16 and 3.5.25 reveals that the energy of this system is quantized.

$$E = \frac{\hbar^2 \lambda}{2I} = J(J+1)\frac{\hbar^2}{2I} \tag{3.5.27}$$

From the fact that $E = L^2/(2I)$ this also implies that we know the quantum angular momentum:

$$L^2 = \hbar^2 J(J+1) \text{ or } L = \hbar\sqrt{J(J+1)}. \tag{3.5.28}$$

Using Equation 3.5.27, you can construct a rotational energy level diagram (Figure 5.8.2). For simplicity, use energy units of $\frac{\hbar^2}{2I}$.

- $J = 0$: The lowest energy state has $J = 0$ and $m_J = 0$. This state has an energy $E_0 = 0$. There is only **one state** with this energy, i.e. one set of quantum numbers, one wavefunction, and one set of properties for the molecule.
- $J = 1$: The next energy level is $J = 1$ with energy $\frac{2\hbar^2}{2I}$. There are **three states** with this energy because m_J can equal +1, 0, or -1. These different states correspond to different orientations of the rotating molecule in space. States with the same energy are said to be degenerate. The degeneracy of an energy level is the number of states with that energy. The degeneracy of the $J = 1$ energy level is 3 because there are three states with the energy $\frac{2\hbar^2}{2I}$.
- $J = 2$: The next energy level is for $J = 2$. The energy is $\frac{6\hbar^2}{2I}$, and there are **five states** with this energy corresponding to $m_J = +2, +1, 0, -1, -2$. The energy level degeneracy is five. Note that the spacing between energy levels increases as J increases. Also note that the degeneracy increases. The degeneracy is always $2J + 1$ because m_J ranges from $+J$ to $-J$ in integer steps, including 0.

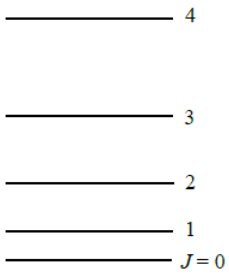


Figure 5.8.2 : Energy spacing for a rigid rotor (in 3D). Notice the energy depends only on J and not depend on m_J. That is, the energy of the rotor is not affected by its orientation.

> *Each allowed energy of rigid rotor is $(2J + 1)$-fold degenerate. Hence, there exist $(2J + 1)$ different wavefunctions with that energy.*

? Exercise 5.8.6

Compute the energy levels for a rotating molecule for $J = 0$ to $J = 5$ using units of $\frac{\hbar^2}{2I}$.

Answer

This rotating molecule can be assumed to be a rigid rotor molecule. From solving the Schrödinger equation for a rigid rotor we have the relationship for energies of each rotational eigenstate (Equation 3.5.27):

$$E = J(J+1)(\hbar^2/2I)$$

Using this equation, we can plug in the different values of the J quantum number so that

- For J=0, $E = (0)(1)(\hbar^2/2I) = 0$
- For J=1, $E = (1)(2)(\hbar^2/2I) = 2(\hbar^2/2I)$
- For J=2, $E = (2)(3)(\hbar^2/2I) = 6(\hbar^2/2I)$
- For J=3, $E = (3)(4)(\hbar^2/2I) = 12(\hbar^2/2I)$
- For J=4, $E = (4)(5)(\hbar^2/2I) = 20(\hbar^2/2I)$
- For J=5, $E = (5)(6)(\hbar^2/2I) = 30(\hbar^2/2I)$

This shows that as J increases, the energy levels get farther apart (Figure 5.8.2).

Exercise 5.8.7

For $J = 0$ to $J = 5$, identify the degeneracy of each energy level and the values of the m_J quantum number that go with each value of the J quantum number. Construct a rotational energy level diagram including $J = 0$ through $J = 5$. Label each level with the appropriate values for the quantum numbers J and m_J.

Answer

The diagram below is not to scale. J = 0 is the lowest energy and J = 5 is the highest energy. The spacing gets larger as J increases.

m_J is an integer in the range $-J \leq m_J \leq J$, thus for any J there are 2J +1 possible m_J.

J = 5 m_J =-5 m_J =-4 m_J =-3 m_J =-2 m_J =-1 m_J = 0 m_J = 1 m_J = 2 m_J =3 m_J =4 m_J =5

J = 4 m_J =-4 m_J =-3 m_J =-2 m_J =-1 m_J = 0 m_J = 1 m_J = 2 m_J =3 m_J =4

J = 3 m_J =-3 m_J =-2 m_J =-1 m_J = 0 m_J = 1 m_J = 2 m_J =3

J = 2 m_J =-2 m_J =-1 m_J = 0 m_J = 1 m_J = 2

J = 1 m_J =-1 m_J = 0 m_J = 1

J = 0 m_J = 0

Interpretation of Quantum Numbers for a Rigid Rotor

The m_J quantum number reflects the component of the angular momentum along the z direction (and hence is sometimes called the azimuthal quantum number). For a fixed value of J, the different values of m_J reflect the different **directions** the angular momentum vector could be pointing – for large, positive m_J the angular momentum is mostly along +z; if m_J is zero the angular momentum is orthogonal to z. Physically, the energy of the rotation does not depend on the direction, which is reflected in the fact that the energy depends only on J (Equation 3.5.27), which measures the length of the vector, not its direction given by m_J.

Example 5.8.7 : Molecular Oxygen

Calculate $J = 0$ to $J = 1$ rotational transition of the O_2 molecule with a bond length of 121 pm.

Solution

$$E = \frac{\hbar^2}{I} = \frac{\hbar^2}{\mu r^2}$$

$$\mu_{O2} = \frac{m_O m_O}{m_O + m_O} = \frac{(15.9994)(15.9994)}{15.9994 + 15.9994} = 7.9997$$

convert from atomic units to kilogram using the conversion: 1 au = 1.66 x 10^{-27} kg. Plug and chug.

$$E = 5.71 \times 10^{-27}\ Joules$$

3.5.3: Spherical Harmonics

A wavefunction that is a solution to the rigid rotor Schrödinger Equation (Equation 3.5.10) can be written as a single function $Y(\theta, \varphi)$, which is called a spherical harmonic function.

$$Y_J^{m_J}(\theta, \varphi) = \Theta_J^{|m_J|}(\theta)\Phi_{m_J}(\varphi) \tag{3.5.29}$$

The spherical harmonic wavefunction is labeled with m_J and J because its functional form depends on both of these quantum numbers. These functions are tabulated above for $J = 0$ through $J = 2$ and for $J = 3$ in the Spherical Harmonics Table (M4) Polar

plots of some of the θ-functions are shown in Figure 5.8.3 .

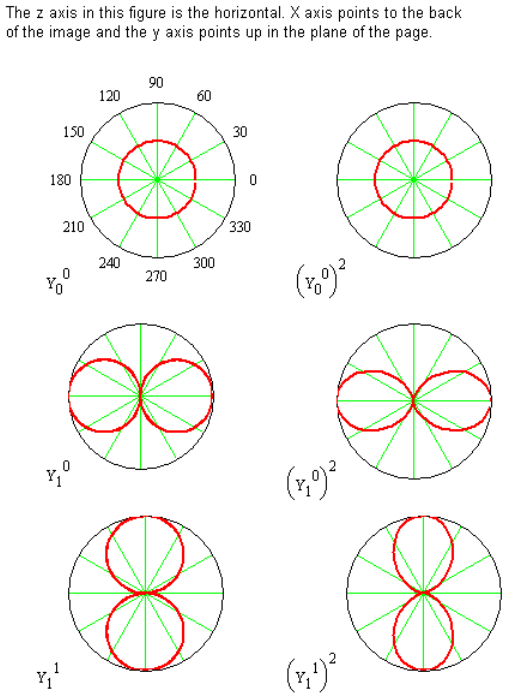


Figure 5.8.3 : Polar plots in which the distance from the center gives the value of the function Y for the indicated angle θ.

The two-dimensional space for a rigid rotor is defined as the surface of a sphere of radius r_0, as shown in Figure 5.8.2 .

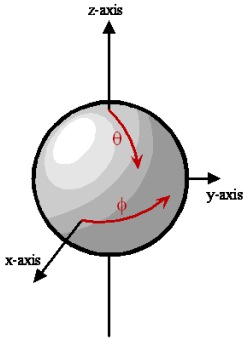


Figure 5.8.4 : Space for a rigid rotor is restricted to the surface of a sphere of radius r_0. The only degrees of freedom are motions along θ or φ on the surface of the sphere.

The probability of finding the internuclear axis at specific coordinates θ_0 and φ_0 within an infinitesimal area ds on this curved surface is given by

$$Pr\left[\theta_0, \varphi_0\right] = Y_J^{m_J*}(\theta_0, \varphi_0) Y_J^{m_J}(\theta_0, \varphi_0) ds \tag{3.5.30}$$

where the area element ds is centered at θ_0 and φ_0.

Within the Copenhagen interpretation of wavefunctions, the absolute square (or modulus squared) of the rigid rotor wavefunction $Y_J^{m_J*}(\theta, \varphi) Y_J^{m_J}(\theta, \varphi)$ gives the probability density for finding the internuclear axis oriented at θ to the z-axis and φ to the x-axis. In spherical coordinates the area element used for integrating θ and φ is

$$ds = \sin\theta \, d\theta \, d\varphi \tag{3.5.31}$$

? Exercise 5.8.8

Use calculus to evaluate the probability of finding the internuclear axis of a molecule described by the $J = 1$, $m_J = 0$ wavefunction somewhere in the region defined by a range in θ of 0° to 45°, and a range in of 0° to 90°. Note that a double integral will be needed. Sketch this region as a shaded area on Figure 5.8.3 .

Consider the significance of the probability density function by examining the $J = 1$, $m_J = 0$ wavefunction. The Spherical Harmonic for this case is

$$Y_1^0 = \sqrt{\frac{3}{4\pi}} \cos\theta \tag{3.5.32}$$

The polar plot of $(Y_1^0)^2$ is shown in Figure 5.8.3 . For $J = 1$ and $m_J = 0$, the probability of finding the internuclear axis is independent of the angle φ from the x-axis, and greatest for finding the internuclear axis along the z-axis, but there also is a probability for finding it at other values of θ as well. So, although the internuclear axis is not always aligned with the z-axis, the probability is highest for this alignment. Also, since the probability is independent of the angle φ, the internuclear axis can be found in any plane containing the z-axis with equal probability.

The $J = 1$, $m_J = 0$ function is 0 when θ = 90°. Therefore, the entire xy-plane is a **node**. This fact means the probability of finding the internuclear axis in this particular horizontal plane is 0 in contradiction to our classical picture of a rotating molecule. In the classical picture, a molecule rotating in a plane perpendicular to the xy-plane must have the internuclear axis lie in the xy-plane twice every revolution, but the quantum mechanical description says that the probability of being in the xy-plane is zero. This conclusion means that molecules are not rotating in the classical sense, but they still have some, but not all, of the properties associated with classical rotation. The properties they retain are associated with angular momentum.

? Exercise 5.8.9

For each state with $J = 0$ and $J = 1$, use the function form of the Y spherical harmonics and Figure 5.8.1 to determine the most probable orientation of the internuclear axis in a diatomic molecule, i.e., the most probable values for θ and θ.

? Exercise 5.8.10

Write a paragraph describing the information about a rotating molecule that is provided in the polar plot of $Pr[\theta, \theta]$ for the $J = 1$, $m_J = \pm 1$ state in Figure 5.8.1 . Compare this information to the classical picture of a rotating object.

3.5.4: Summary

There are two quantum numbers that describe the quantum behavior of a rigid rotor in three-deminesions: J is the total angular momentum quantum number and m_J is the z-component of the angular momentum. The spherical harmonics called $Y_J^{m_J}$ are functions whose probability $|Y_J^{m_J}|^2$ has the well known shapes of the s, p and d orbitals etc learned in general chemistry.

3.5.5: References

1. Anderson, J.M. Introduction to Quantum Chemistry, 1969, W.A. Benjamin, Inc, pg.91-100.
2. Atkins, Peter and de Paula, Julio. Physical Chemistry for the Life Sciences. New York: W.H. Freeman and Company. p. 515.

Contributors and Attributions

- Ian Huh
- David M. Hanson, Erica Harvey, Robert Sweeney, Theresa Julia Zielinski ("Quantum States of Atoms and Molecules")
- Mark Tuckerman (New York University)
- MIT OpenCourseWare (Robert Guy Griffin and Troy Van Voorhis)

3.5: The Energy Levels of a Rigid Rotor is shared under a CC BY-NC-SA 4.0 license and was authored, remixed, and/or curated by LibreTexts.

- **5.8: The Energy Levels of a Rigid Rotor** is licensed CC BY-NC-SA 4.0.

3.6: The Variational Method

Learning Objectives

- Appreciate the complexity of solving muliti-electron atoms
- Characterize multi-electron interactions within shielding and penetration concepts
- Use the variational method as an approximation to study insolvable problems
- User variational method to evaluate the effective nuclear charge for a specific atom

In this section we introduce the powerful and versatile variational method and use it to improve the approximate solutions we found for the helium atom using the independent electron approximation.

3.6.1: The True (Experimentally Determined) Energy of the Helium Atom

The helium atom has two electrons bound to a nucleus with charge $Z = 2$. The *successive* removal of the two electrons can be considered stepwise:

$$\mathrm{He} \xrightarrow{I_1} \mathrm{He}^+ + e^- \xrightarrow{I_2} \mathrm{He}^{++} + 2e^- \tag{3.6.1}$$

The *first ionization energy* I_1 is the minimum energy required to remove the first electron from helium gas and is experimentally determined:

$$I_1 = -E_{1s}(\mathrm{He}) = 24.59\ eV$$

While the second ionization energy, I_2 can be experimentally determined, it can also be calculated exactly from the hydrogen atom solutions since He^+ is a hydrogen-like ion with $Z = 2$. Hence, we have

$$\begin{aligned} I_2 &= -E_{1s}(\mathrm{He}^+) \\ &= \frac{Z^2}{2n^2} \\ &= 54.42\ \mathrm{eV} \end{aligned}$$

The energy of the three separated particles on the right side of Equation 3.6.1 is zero (by definition). Therefore the ground-state energy of helium atom is given by

$$\begin{aligned} E_{true} &= -(I_1 + I_2) \\ &= -79.02\ \mathrm{eV}. \end{aligned}$$

which can be expressed in terms of the ***Rydberg*** constant ($R_H = 13.6\ eV$) that also describes the lowest energy of the hydrogen atom

$$E_{true} = -5.8066\, R_H$$

We will attempt to reproduce this **true value**, as close as possible, by different theoretical approaches (all approximations).

3.6.2: The "Ignorance is Bliss" Approximation

The Hamiltonian for the Helium atom is:

$$\hat{H} = -\frac{\hbar^2}{2m_e}\nabla^2_{el_1} - \frac{\hbar^2}{2m_e}\nabla^2_{el_2} - \frac{Ze^2}{4\pi\epsilon_0 r_1} - \frac{Ze^2}{4\pi\epsilon_0 r_2} + \cancel{\frac{e^2}{4\pi\epsilon_0 r_{12}}} \tag{3.6.2}$$

If we simply *ignore* the electron-electron repulsion term, then Equation 3.6.2 can be simplified to

$$\hat{H} \approx -\frac{\hbar^2}{2m_e}\nabla^2_{el_1} - \frac{Ze^2}{4\pi\epsilon_0 r_1} - \frac{\hbar^2}{2m_e}\nabla^2_{el_2} - \frac{Ze^2}{4\pi\epsilon_0 r_2} \tag{3.6.3}$$

$$\approx h_1(r_1) + h_2(r_2) \tag{3.6.4}$$

where h_1 and h_2 are one electron Hamiltonians for electron 1 and 2, respectively, and are just the hydrogen-like Hamiltonians. The approximation in Equation 3.6.4 is convenient since electron 1 is *separable* from electron 2, so that the two-electron wavefunction is approximated as a product to two one-electron wavefunctions:

$$\Psi_{total} = \psi_{el_1}\psi_{el_2} \tag{3.6.5}$$

or in braket notation

$$|\Psi_{total}\rangle = \hat{H}|\psi_{el_1}\psi_{el_2}\rangle \tag{3.6.6}$$

With some operator algebra, something important arises - the one electron energies are **additive**:

$$\hat{H}\Psi_{total} = (\hat{H}_{el_1} + \hat{H}_{el_2})\psi_{n\ el_1}\psi_{n\ el_2} = (E_{n_1} + E_{n_2})\psi_{n\ el_1}\psi_{n\ el_2}$$

or in bra-ket notation

$$\begin{aligned}\hat{H}|\Psi_{total}\rangle &= \hat{H}|\psi_{el_1}\psi_{el_2}\rangle \\ &= (E_{n_1} + E_{n_2})|\psi_1\psi_2\rangle\end{aligned}$$

The energy for a ground state Helium atom (both electrons in lowest state) is then

$$\begin{aligned}E_{He_{1s}} &= \underbrace{E_{n_1}}_{\text{energy of single electron in helium}} + \underbrace{E_{n_2}}_{\text{energy of single electron in helium}} \\ &= -R_H\left(\frac{Z^2}{1}\right) - R_H\left(\frac{Z^2}{1}\right) \\ &= -8R_H\end{aligned}$$

This approximation significantly overestimates the true energy of the helium atom $E_{He_{1s}} = -5.8066\ R$. This is a poor approximation and we need to address electron-electron repulsion properly (or better at least).

3.6.3: Shielding and Penetration

One way to take electron-electron repulsion into account is to modify the form of the wavefunction. A logical modification is to change the nuclear charge, Z, in the wavefunctions to an effective nuclear charge (Z_{eff}), from +2 to a smaller value. The rationale for making this modification is that one electron partially shields the nuclear charge from the other electron, as shown in Figure 3.6.1 .

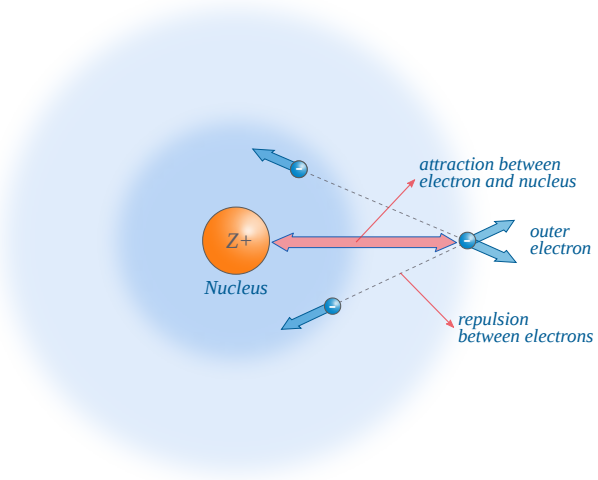


Figure 3.6.1 : Electron-electron shielding leading to a reduced effective nuclear charge. The attractive force of the nucleus on the outer electron is partially countered by the repulsive force between inner electrons and the outer electron. (CC BY-SA; Ümit Kaya via LibreTexts)

A region of negative charge density between one of the electrons and the +2 nucleus makes the potential energy between them more positive (decreases the attraction between them). We can effect this change mathematically by using $\zeta < 2$ in the wavefunction expression. If the shielding were complete, then Z_{eff} would equal 1. If there is no shielding, then $Z_{eff} = 2$. So a way to take into account the electron-electron interaction is by saying it produces a shielding effect. The shielding is not zero, and it is not complete, so the effective nuclear charge varies between one and two.

In general, a theory should be able to make predictions in advance of knowledge of the experimental result. Consequently, a principle and method for choosing the best value for Z_{eff} or any other adjustable parameter that is to be optimized in a calculation is needed. The Variational Principle provides the required criterion and method and says that the best value for any variable parameter in an approximate wavefunction is the value that gives the **lowest energy for the ground state**; i.e., the value that minimizes the energy. The variational method is the procedure that is used to find the lowest energy and the best values for the variable parameters.

3.6.4: A Better Approximation: The Variational Method

The variational method is one way of finding approximations to the lowest energy eigenstate or ground state, and some excited states. This allows calculating approximate wavefunctions and is the variational principle. The method consists in choosing a "trial wavefunction" depending on one or more parameters, and finding the values of these parameters for which the expectation value of the energy is the lowest possible. The wavefunction obtained by fixing the parameters to such values is then an approximation to the ground state wavefunction, and the expectation value of the energy in that state is an **upper bound** to the ground state energy.

The variational principle means that the expectation value for the binding energy obtained using an approximate wavefunction and the exact Hamiltonian operator will be higher than or equal to the true energy for the system. This idea is really powerful. When implemented, it permits us to find the best approximate wavefunction from a given wavefunction that contains one or more adjustable parameters, called a **trial wavefunction**. A mathematical statement of the variational principle is

$$E_{trial} \geq E_{true} \tag{3.6.7}$$

where

$$E_{trial} = \frac{\langle \psi_{trial} | \hat{H} | \psi_{trial} \rangle}{\langle \psi_{trial} | \psi_{trial} \rangle} \tag{3.6.8}$$

$$= \frac{\int \psi^*_{trial} \hat{H} \psi_{trial} d\tau}{\int \psi^*_{trial} \psi_{trial} d\tau} \tag{3.6.9}$$

Equation 3.6.7 is called the variational theorem and states that for a time-independent Hamiltonian operator, any trial wavefunction will have an variational energy (i.e., expectation value) that is **greater than or equal** to the true ground state wavefunction corresponding to the given Hamiltonian (Equation 3.6.7). Because of this, the variational energy is an upper bound to the true ground state energy of a given molecule. The general approach of this method consists in choosing a "trial wavefunction" depending on one or more parameters, and finding the values of these parameters for which the expectation value of the energy is the lowest possible (Figure 3.6.2).

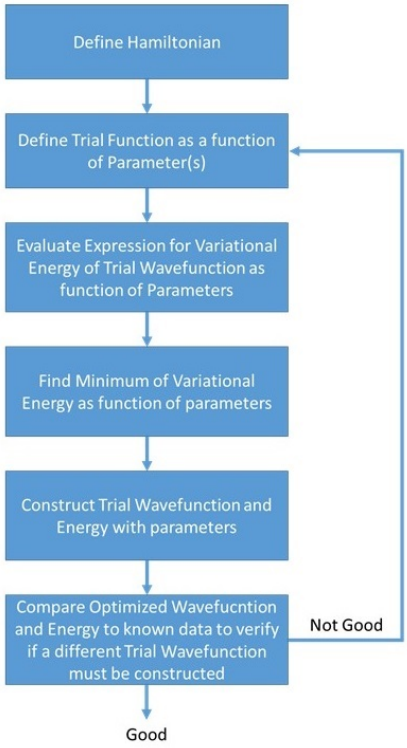


Figure **3.6.2** : Simplified algorithmic flowchart of the Variational Method approximation

> *The variational energy E_{trial} is only equal to the true energy E_{true} when the the corresponding trial wavefunction ψ_{trial} is equal to the true wavefunction ψ_{true}.*

3.6.5: Application to the Helium atom Ground State

Often the expectation values (numerator) and normalization integrals (denominator) in Equation 3.6.9 can be evaluated analytically. For the case of the He atom, let's consider the trial wavefunction as the product wavefunction given by Equation 3.6.10 (this is called the **orbital approximation**),

$$\psi(r_1, r_2) \approx \varphi(r_1)\varphi(r_2) \tag{3.6.10}$$

The adjustable or variable parameter in the trial wavefunction is the effective nuclear charge ζ, and the Hamiltonian is the complete form given below (Note: quantum calculations typically refer to effective nuclear charge as ζ rather than Z_{eff} as we used previously).

$$\hat{H} = -\frac{\hbar^2}{2m}\nabla_1^2 - \frac{\zeta e^2}{4\pi\epsilon_0 r_1} - \frac{\hbar^2}{2m}\nabla_2^2 - \frac{\zeta e^2}{4\pi\epsilon_0 r_2} + \frac{e^2}{4\pi\epsilon_0 r_{12}} \tag{3.6.11}$$

the adjustable or variable parameter in the trial wavefunction is the effective nuclear charge ζ (would be equal to $\zeta = 2$ if fully unshielded), and the Hamiltonian is the complete form. When the expectation value for the trial energy (Equation 3.6.9) is evaluated for helium, the result is a variational energy that depends on the adjustable parameter, ζ.

$$E_{trial}(\zeta) = \frac{\mu e^4}{4\epsilon_0^2 h}\left(\zeta^2 - \frac{27}{8}\zeta\right) \tag{3.6.12}$$

This function is plotted in Figure **3.6.3** as a function of ζ. According to the variational principle (Equation 3.6.7), the minimum value of the energy on this graph is the best approximation of the true energy of the system, and the associated value of ζ is the best value for the adjustable parameter.

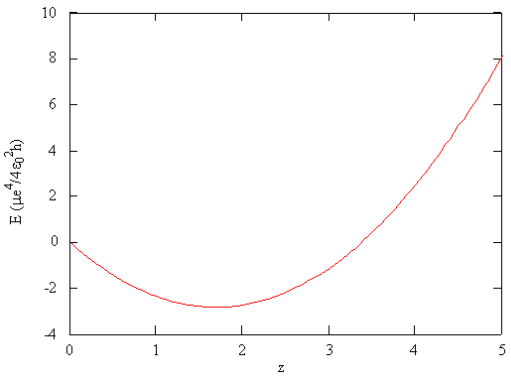


Figure **3.6.3** : Graph of trial energies for helium atom as a function of the adjustable parameter ζ in Equation **3.6.12** that represents the effective nuclear charge felt by the electrons.

Using the mathematical function for the energy of a system, the minimum energy with respect to the adjustable parameter can be found by taking the derivative of the energy with respect to that parameter, setting the resulting expression equal to zero, and solving for the parameter, in this case ζ. This is a standard method in calculus for finding maxima and minima.

? Exercise 3.6.1

Find the value for ζ that minimizes the helium binding energy for the product trial wavefunction in Equation **3.6.10** with the Hamiltonian in Equation **3.6.11**. and compare the binding energy to the experimental value. What is the percent error in the calculated value?

Solution

The variational method requires following the workflow in Figure **3.6.2** .

- Step 1: Define the Hamiltonian - This is given by Equation **3.6.11**.
- Step 2: Define the trial wavefunction as a function of at least one parameter - This is given by Equation **3.6.10**.
- Step 3: Evaluate variational energy (E_{trial} integral (Equation **3.6.9**) - This procedure was already above in Equation **3.6.12**.
- Step 4: Minimize the variational energy as a function of the parameter(s) - Following the standard approach to find extrema in calculus, evaluate the derivative of E_{trial} with respect to ζ and set to zero:

$$\frac{dE_{trial}}{d\zeta} = \frac{\mu e^4}{4\epsilon_0^2 h}\left(2\zeta - \frac{27}{8}\right) = 0$$

then solve for the roots of this polynomial

$$2\zeta - \frac{27}{8} = 0$$

or

$$\zeta = \frac{27}{16} \approx 1.6875$$

- Step 5-6: The question does not ask for the optimized wavefunction (Step 5) or to compare the result with the true value to evaluate the quality of the approximation (Step 6). We can skip these steps.

From Exercise **3.6.1** , the $\zeta = 1.6875$ and the approximate energy we calculate using this approximation method, E_{approx} = -77.483 eV. Table **3.6.1** shows that a substantial improvement in the accuracy of the computed binding energy is obtained by using shielding to account for the electron-electron interaction. Including the effect of electron shielding in the wavefunction reduces the error in the binding energy to about 2%. This idea is very simple, elegant, and significant.

Table **3.6.1** : Comparison of the results of three approximation methods to experiment.

Method	He binding energy (eV)
"Ignorance is Bliss" Approximation (neglect repulsion between electrons)	-108.8
Variational method with variable effective charge	-77.483
Experimental	-79.0

The improvement we have seen in the total energy calculations using a variable parameter ζ indicates that an important contribution of electron-electron interaction or repulsion to the total binding energy arises from the fact that each electron shields the nuclear charge from the other electron. It is reasonable to assume the electrons are independent; i.e., that they move independently, but the shielding must be taken into account in order to fine-tune the wavefunctions. The inclusion of optimizable parameters in the wavefunction allows us to develop a clear physical image of the consequences of our variation calculation. Calculating energies correctly is important, and it is also important to be able to visualize electron densities for multi-electron systems. In the next two sections, we take a temporary break from our consideration of approximation methods in order to examine multi-electron wavefunctions more closely.

3.6: The Variational Method is shared under a CC BY-NC-SA 4.0 license and was authored, remixed, and/or curated by LibreTexts.

- **7.1: The Variational Method Approximation** by David M. Hanson, Erica Harvey, Robert Sweeney, Theresa Julia Zielinski is licensed CC BY-NC-SA 4.0. Original source: https://web.archive.org/web/20200619182410/http://www.chemeddl.org.

3.7: Linear Variational Method and the Secular Determinant

Learning Objectives

- Understand how the variational method can be expanded to include trial wavefunctions that are a linear combination of functions with coefficients that are the parameters to be varied.
- To be able to construct secular equations to solve the minimization procedure intrinsic to the variational method approach.
- To map the secular equations into the secular determinant
- To understand how the Linear Combination of Atomic Orbital (LCAO) approximation is a specific application of the linear variational method.

A special type of variation widely used in the study of molecules is the so-called **linear variation function**, where the trial wavefunction is a linear combination of N linearly independent functions (often atomic orbitals) that not the eigenvalues of the Hamiltonian (since they are not known). For example

$$|\psi_{trial}\rangle = \sum_{j=1}^{N} a_j |\phi_j\rangle \tag{3.7.1}$$

and

$$\langle\psi_{trial}| = \sum_{j=1}^{N} a_j^* \langle\phi_j| \tag{3.7.2}$$

In these cases, one says that a 'linear variational' calculation is being performed.

Linear Variational Basis Functions

The set of functions $\{\phi_j\}$ are called the 'linear variational' basis functions and are nothing more than members of a set of functions that are convenient to deal with. However, they are typically not arbitrary and are usually selected to address specific properties of the system:

- to obey all of the boundary conditions that the exact state $|\psi_{trial}\rangle$ obeys,
- to be functions of the the same coordinates as $|\psi_{trial}\rangle$,
- to be of the same symmetry as $|\psi_{trial}\rangle$, and
- to be convenient to evaluate Hamiltonian terms elements $\langle\phi_i|H|\phi_j\rangle$.

Beyond these conditions, nothing other than effort can limit the selection and number of such basis functions in the expansions in Equations 3.7.1 and 3.7.2.

As discussed in Section 7.1, the variational energy for a generalized trial wavefunction is

$$E_{trial} = \frac{\langle\psi_{trial}|\hat{H}|\psi_{trial}\rangle}{\langle\psi_{trial}|\psi_{trial}\rangle} \tag{3.7.3}$$

Substituting Equations 3.7.1 and 3.7.2 into Equation 3.7.3 involves addressing the numerator and denominator individually. For the numerator, the integral can be expanded thusly:

$$\langle\psi_{trial}|H|\psi_{trial}\rangle = \sum_{i}^{N}\sum_{j}^{N} a_i^* a_j \langle\phi_i|H|\phi_j\rangle. \tag{3.7.4}$$

$$= \sum_{i,j}^{N,N} a_i^* a_j \langle\phi_i|H|\phi_j\rangle. \tag{3.7.5}$$

We can rewrite the following integral in Equation 3.7.5 as a function of the basis elements (not the trial wavefunction) as

$$H_{ij} = \langle\phi_i|H|\phi_j\rangle$$

So the numerator of the right side of Equation 3.7.3 becomes

$$\langle \psi_{trial}|H|\psi_{trial}\rangle = \sum_{i,j}^{N,N} a_i^* a_j H_{ij} \tag{3.7.6}$$

Similarly, the denominator of the right side of Equation 3.7.3 can be expanded

$$\langle \psi_{trial}|\psi_{trial}\rangle = \sum_{i,j}^{N,N} a_i^* a_j \langle \phi_i|\phi_j\rangle \tag{3.7.7}$$

We often simplify the integrals on the right side of Equation 3.7.7 as

$$S_{ij} = \langle \phi_i|\phi_j\rangle$$

where S_{ij} are **overlap integrals** between the different $\{\phi_j\}$ basis functions. Equation 3.7.7 is thus expressed as

$$\langle \psi_{trial}|\psi_{trial}\rangle = \sum_{i,j}^{N,N} a_i^* a_j S_{ij} \tag{3.7.8}$$

Orthonormality of Basis Functions

There is no explicit rule that the $\{\phi_j\}$ functions have to be **orthogonal** or **normalized** functions, although they often are selected that way for convenience. Therefore, *a priori*, S_{ij} does not have to be δ_{ij}.

Substituting Equations 3.7.6 and 3.7.8 into the variational energy formula (Equation 3.7.3) results in

$$E_{trial} = \frac{\sum_{i,j}^{N,N} a_i^* a_j H_{ij}}{\sum_{i,j}^{N,N} a_i^* a_j S_{ij}} \tag{3.7.9}$$

For such a trial wavefunction as Equation 3.7.1, the variational energy depends quadratically on the 'linear variational' a_j coefficients. These coefficients can be varied to find the optimized trial wavefunction ($|\psi_{trial}\rangle$) that approximates the true wavefunction ($|\psi\rangle$) that we cannot analytically solve for.

3.7.1: Minimizing the Variational Energy

The expression for variational energy (Equation 3.7.9) can be rearranged

$$E_{trial} \sum_{i,j}^{N,N} a_i^* a_j S_{ij} = \sum_{i,j}^{N,N} a_i^* a_j H_{ij} \tag{3.7.10}$$

The optimum coefficients are found by searching for minima in the variational energy landscape spanned by varying the $\{a_i\}$ coefficients (Figure **3.7.1**).

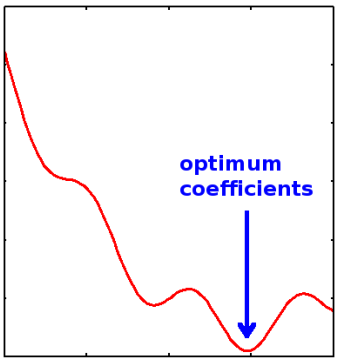


Figure 3.7.1 : Linear Variational Principle in action. Two (or more) wavefunctions are mixed by linear combination. The coefficients a_1, a_2 determine the weight each of them is given. The optimum coefficients are found by searching for minima in the potential landscape spanned by a_1 and a_2. (CC BY-SA-NC; Rudolf Winter; Aberystwyth University).

We want to minimize the energy with respect to the linear coefficients $\{a_i\}$, which requires that

$$\frac{\partial E_{trial}}{\partial a_i} = 0$$

for all i.

Differentiating both sides of Equation 3.7.10 for the kth coefficient gives,

$$\frac{\partial E_{trial}}{\partial a_k} \sum_{i,j}^{N,N} a_i^* a_j S_{ij} + E_{trial} \sum_i \sum_j \left[\frac{\partial a_i^*}{\partial a_k} a_j + \frac{\partial a_j}{\partial a_k} a_i^* \right] S_{ij} \tag{3.7.11}$$
$$= \sum_{i,j}^{N,N} \left[\frac{\partial a_i^*}{\partial a_k} a_j + \frac{\partial a_j}{\partial a_k} a_i^* \right] H_{ij}$$

Since the coefficients are independent

$$\frac{\partial a_i^*}{\partial a_k} = \delta_{ik}$$

and

$$S_{ij} = S_{ji}$$

and also since the Hamiltonian is a Hermitian Operator (see below)

$$H_{ij} = H_{ji}$$

then Equation 3.7.11 simplifies to

$$\frac{\partial E_{trial}}{\partial a_k} \sum_i \sum_j a_i^* a_j S_{ij} + 2E_{trial} \sum_i a_i S_{ik} = 2 \sum_i a_i H_{ik} \tag{3.7.12}$$

At the minimum variational energy, when

$$\frac{\partial E_{trial}}{\partial a_k} = 0$$

then Equation 3.7.12 gives

$$\sum_i^N a_i (H_{ik} - E_{trial} S_{ik}) = 0 \tag{3.7.13}$$

for all k. The equations in 3.7.13 are called the **Secular Equations**.

Hermitian Operators

Hermitian operators are operators that satisfy the general formula

$$\langle \phi_i | \hat{A} | \phi_j \rangle = \langle \phi_j | \hat{A} | \phi_i \rangle \tag{3.7.14}$$

If that condition is met, then $\hat{A}$ is a Hermitian operator. For any operator that generates a real eigenvalue (e.g., observables), then that operator is Hermitian. The Hamiltonian $\hat{H}$ meets the condition of a Hermitian operator. Equation 3.7.14 can be rewriten as

$$A_{ij} = A_{ji}^*$$

where

$$A_{ij} = \langle \phi_i | \hat{A} | \phi_j \rangle$$

and

$$A_{ji} = \langle \phi_j | \hat{A} | \phi_i \rangle$$

Therefore, when applied to the Hamiltonian operator

$$H_{ij}^* = H_{ji}.$$

If the functions $\{|\phi_j\rangle\}$ are orthonormal, then the overlap matrix S reduces to the unit matrix (one on the diagonal and zero every where else) and the Secular Equations in Equation 3.7.13 reduces to the more familiar Eigenvalue form:

$$\sum_i^N H_{ij} a_j = E_{trial} a_i. \tag{3.7.15}$$

Hence, the secular equation, in either form, have as many eigenvalues E_i and eigenvectors $\{C_{ij}\}$ as the dimension of the H_{ij} matrix as the functions in $|\psi_{trail}\rangle$ (Example 3.7.1). It can also be shown that between successive pairs of the eigenvalues obtained by solving the secular problem at least one exact eigenvalue must occur (i.e.,$E_{i+1} > E_{exact} > E_i$, for all i). This observation is referred to as '*the bracketing theorem*'.

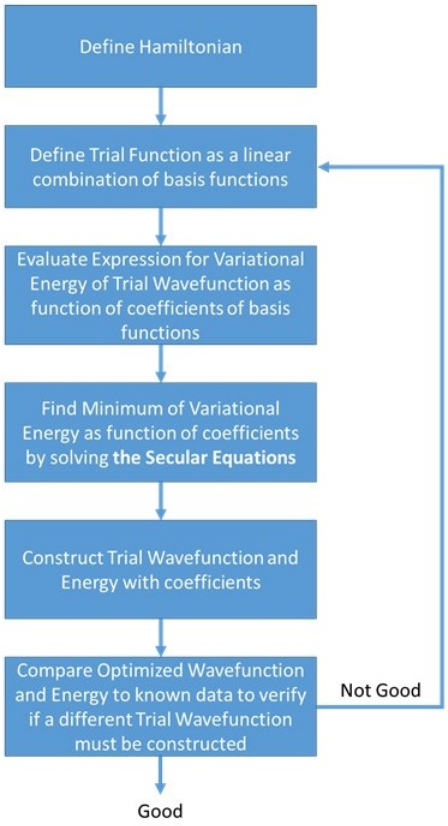


Figure 7.2.2 : Simplified algorithmic flowchart of the linear Variational Method approximation. Compared to the similar algorithmic flowchart for the "normal" Variational Method approximation.

Variational methods, in particular the linear variational method, are the most widely used approximation techniques in quantum chemistry. To implement such a method one needs to know the Hamiltonian H whose energy levels are sought and one needs to construct a trial wavefunction in which some 'flexibility' exists (e.g., as in the linear variational method where the a_j coefficients can be varied). This tool will be used to develop several of the most commonly used and powerful molecular orbital methods in chemistry.

3.7.2: The Secular Determinant

From the secular equations with an orthonormal functions (Equation 3.7.15), we have k simultaneous secular equations in k unknowns. These equations can also be written in matrix notation, and for a non-trivial solution (i.e. $c_i \neq 0$ for all i), the determinant of the secular matrix must be equal to zero.

$$|H_{ik}-ES_{ik}| = 0 \tag{3.7.16}$$

Properties of Determinants

- The determinant is a **real** number, it is **not** a matrix.
- The determinant can be a negative number.
- It is **not** associated with absolute value at all except that they both use vertical lines.
- The determinant **only** exists for square matrices (2×2, 3×3, ..., $n \times n$). The determinant of a 1×1 matrix is that single value in the determinant.
- The inverse of a matrix will exist only if the determinant is not zero.

Expanding Determinants

The determinant can be evaluated using an expansion method involving minors and cofactors. Before we can use them, we need to define them. It is the product of the elements on the main diagonal minus the product of the elements off the main diagonal. In the case of a 2×2 matrix, the specific formula for the determinant is

$$|A| = \begin{vmatrix} a & b \\ c & d \end{vmatrix} = ad - bc.$$

Similarly, suppose we have a 3×3 matrix A, and we want the specific formula for its determinant $|A|$:

$$\begin{aligned} |A| = \begin{vmatrix} a & b & c \\ d & e & f \\ g & h & i \end{vmatrix} &= a \begin{vmatrix} e & f \\ h & i \end{vmatrix} - b \begin{vmatrix} d & f \\ g & i \end{vmatrix} + c \begin{vmatrix} d & e \\ g & h \end{vmatrix} \\ &= aei + bfg + cdh - ceg - bdi - afh. \end{aligned}$$

To solve Equation 3.7.16, the determinate should be expanded and then set to zero. That generates a polynomial (called a **characteristic equation**) that can be directly solved with linear algebra methods or numerically.

3.7.1 Example : A Simple Two Component Basis Set

If $|\psi_{trial}\rangle$ is a linear combination of two functions. In math terms,

$$|\psi_{trial}\rangle = \sum_{n=1}^{N=2} a_n |f_n\rangle = a_1|\phi_1\rangle + a_2|\phi_2\rangle$$

then the secular determinant (Equation 3.7.16), in matrix formulation would look like this

$$\begin{vmatrix} H_{11} - E_{trial}S_{11} & H_{12} - E_{trial}S_{12} \\ H_{12} - E_{trial}S_{12} & H_{22} - E_{trial}S_{22} \end{vmatrix} = 0$$

Solution

First the approximate energies are found by finding the roots of the characteristic polynomial from the secular determinant (equation 3.7.16). These E_{trial} can then be inserted into the secular equations 3.7.13 to solve for the coefficients in the linear combination of functions.

$$a_1^2 H_{11} + 2a_1 a_2 H_{12} + a_2^2 H_{22} = 0$$

and

$$a_1(H_{12} - E_{trial}S_{12}) + a_2(H_{22} - E_{trial}S_{22}) = 0$$

Equation 3.7.16 can be solved to obtain the energies E. When arranged in order of increasing energy, these provide approximations to the energies of the first k states (each having an energy higher than the true energy of the state by virtue of the variation theorem). To find the energies of a larger number of states we simply use a **greater number** of basis functions $\{\phi_i\}$ in the trial wavefunction (Example 3.7.1). To obtain the approximate wavefunction for a particular state, we substitute the appropriate energy into the secular equations and solve for the coefficients a_i.

Using this method it is possible to find all the coefficients $a_1 \ldots a_k$ in terms of one coefficient; normalizing the wavefunction provides the absolute values for the coefficients.

3.7.2 Example : Linear Combination of Atomic Orbitals (LCAO) Approximation

Trial wavefunctions that consist of linear combinations of simple functions

$$|\psi(r)\rangle = \sum_i a_i |\phi_i(r)\rangle$$

form the basis of the Linear Combination of Atomic Orbitals (LCAO) method introduced by Lennard and Jones and others to compute the energies and wavefunctions of atoms and molecules. The functions $\{|\phi_i\rangle\}$ are selected so that matrix elements can be evaluated analytically. Two basis sets of atomic orbitals functions can be used: Slater type and Gaussian type:

Slater orbitals using Hydrogen-like wavefunctions

$$|\phi_i\rangle = Y_l^m(\theta,\phi)e^{-\alpha r}$$

and Gaussian orbitals of the form

$$|\phi_i\rangle = Y_l^m(\theta,\phi)e^{-\alpha r^2}$$

are the most widely used forms, where $Y_l^m(\theta,\phi)$ are the spherical harmonics that represent the angular part of the atomic orbitals. Gaussian orbitals form the basis of many quantum chemistry computer codes.

This page titled 3.7: Linear Variational Method and the Secular Determinant is shared under a CC BY-NC-SA 4.0 license and was authored, remixed, and/or curated by Claire Vallance via source content that was edited to the style and standards of the LibreTexts platform.

- **7.2: Linear Variational Method and the Secular Determinant** by Claire Vallance is licensed CC BY-NC-SA 4.0. Original source: http://vallance.chem.ox.ac.uk/pdfs/SymmetryLectureNotes.pdf.

3.8: Perturbation Theory Expresses the Solutions in Terms of Solved Problems

Learning Objectives

- Use perturbation theory to approximate the energies of systems as a series of perturbation of a solved system.
- Use perturbation theory to approximate the wavefunctions of systems as a series of perturbation of a solved system.

It is easier to compute the changes in the energy levels and wavefunctions with a scheme of successive corrections to the zero-field values. This method, termed **perturbation theory**, is the single most important method of solving problems in quantum mechanics and is widely used in atomic physics, condensed matter and particle physics. Perturbation theory is another approach to finding approximate solutions to a problem, by starting from the exact solution of a related, simpler problem. A critical feature of the technique is a middle step that breaks the problem into "solvable" and "perturbation" parts. Perturbation theory is applicable if the problem at hand cannot be solved exactly, but can be formulated by adding a "small" term to the mathematical description of the exactly solvable problem.

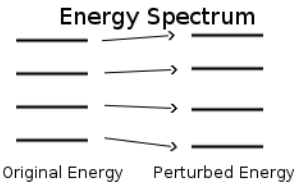


Figure 7.4.1 : Perturbed Energy Spectrum. (CC BY-SA 2.0, Frontier via Wikipedia)

We begin with a Hamiltonian $\hat{H}^0$ having known eigenstates and eigenenergies:

$$\hat{H}^o|n^o\rangle = E_n^o|n^o\rangle \tag{3.8.1}$$

The task is to find how these eigenstates and eigenenergies change if a small term H^1 (an external field, for example) is added to the Hamiltonian, so:

$$(\hat{H}^0 + \hat{H}^1)|n\rangle = E_n|n\rangle \tag{3.8.2}$$

That is to say, on switching on $\hat{H}^1$ changes the wavefunctions:

$$\underbrace{|n^o\rangle}_{\text{unperturbed}} \Rightarrow \underbrace{|n\rangle}_{\text{Perturbed}} \tag{3.8.3}$$

and energies (Figure 7.4.1):

$$\underbrace{E_n^o}_{\text{unperturbed}} \Rightarrow \underbrace{E_n}_{\text{Perturbed}} \tag{3.8.4}$$

> *The basic assumption in perturbation theory is that H^1 is sufficiently small that the leading corrections are the same order of magnitude as H^1 itself, and the true energies can be better and better approximated by a successive series of corrections, each of order H^1/H^o compared with the previous one.*

The strategy is to **expand** the true wavefunction and corresponding eigenenergy as series in $\hat{H}^1/\hat{H}^o$. These series are then fed into Equation 3.8.2, and terms of the same order of magnitude in $\hat{H}^1/\hat{H}^o$ on the two sides are set equal. The equations thus generated are solved one by one to give progressively more accurate results.

To make it easier to identify terms of the same order in $\hat{H}^1/\hat{H}^o$ on the two sides of the equation, it is convenient to introduce a dimensionless parameter λ which always goes with $\hat{H}^1$, and then expand both eigenstates and eigenenergies as power series in λ,

$$|n\rangle = \sum_i^m \lambda^i |n^i\rangle \tag{3.8.5}$$

$$E_n = \sum_{i=0}^m \lambda^i E_n^i \tag{3.8.6}$$

where m is how many terms in the expansion we are considering. The ket $|n^i\rangle$ is multiplied by λ^i and is therefore of order $(H^1/H^o)^i$.

> *λ is purely a bookkeeping device: we will set it equal to 1 when we are through! It's just there to keep track of the orders of magnitudes of the various terms.*

For example, in first order perturbation theory, Equations 3.8.5 are truncated at $m = 1$ (and setting $\lambda = 1$):

$$|n\rangle \approx |n^o\rangle + |n^1\rangle \tag{3.8.7}$$

$$E_n \approx E_n^o + E_n^1 \tag{3.8.8}$$

However, let's consider the general case for now. Adding the full expansions for the eigenstate (Equation 3.8.5) and energies (Equation 3.8.6) into the Schrödinger equation for the perturbation Equation 3.8.2 in

$$(\hat{H}^o + \lambda \hat{H}^1)|n\rangle = E_n|n\rangle \tag{3.8.9}$$

we have

$$(\hat{H}^o + \lambda \hat{H}^1)\left(\sum_{i=0}^m \lambda^i |n^i\rangle\right) = \left(\sum_{i=0}^m \lambda^i E_n^i\right)\left(\sum_{i=0}^m \lambda^i |n^i\rangle\right) \tag{3.8.10}$$

We're now ready to match the two sides term by term in powers of λ. Note that the zeroth-order term, of course, just gives back the unperturbed Schrödinger Equation (Equation 3.8.1).

Let's look at Equation 3.8.10 with the first few terms of the expansion:

$$(\hat{H}^o + \lambda \hat{H}^1)\left(|n^o\rangle + \lambda|n^1\rangle\right) = \left(E_n^0 + \lambda E_n^1\right)\left(|n^o\rangle + \lambda|n^1\rangle\right) \tag{3.8.11}$$

$$\begin{aligned} \hat{H}^o|n^o\rangle + \lambda\hat{H}^1|n^o\rangle + \lambda H^o|n^1\rangle + \lambda^2\hat{H}^1|n^1\rangle = {} & E_n^0|n^o\rangle + \lambda E_n^1|n^o\rangle \\ & + \lambda E_n^0|n^1\rangle + \lambda^2 E_n^1|n^1\rangle \end{aligned} \tag{3.8.12}$$

Collecting terms in order of λ and coloring to indicate different orders

$$\begin{aligned} & \underset{\text{zero order}}{\hat{H}^o|n^o\rangle} \\ & + \underset{\text{1st order}}{\lambda(\hat{H}^1|n^o\rangle + \hat{H}^o|n^1\rangle)} + \underset{\text{2nd order}}{\lambda^2\hat{H}^1|n^1\rangle} = \underset{\text{zero order}}{E_n^0|n^o\rangle} + \underset{\text{1st order}}{\lambda(E_n^1|n^o\rangle + E_n^0|n^1\rangle)} + \underset{\text{2nd order}}{\lambda^2 E_n^1|n^1\rangle} \end{aligned} \tag{3.8.13}$$

If we expanded Equation 3.8.10 further we could express the energies and wavefunctions in higher order components.

3.8.1: Zero-Order Terms ($\lambda = 0$)

Collecting the zero order terms in the expansion (black terms in Equation 3.8.13) results in just the Schrödinger Equation for the unperturbed system

$$\hat{H}^o|n^o\rangle = E_n^o|n^o\rangle \tag{3.8.14}$$

3.8.2: First-Order Expression of Energy ($\lambda = 1$)

The summations in Equations 3.8.5, 3.8.6, and 3.8.10 can be truncated at any order of λ. For example, the first order perturbation theory has the truncation at $\lambda = 1$. Matching the terms that linear in λ (red terms in Equation 3.8.13) and setting $\lambda = 1$ on both sides of Equation 3.8.13:

$$\hat{H}^o|n^1\rangle + \hat{H}^1|n^o\rangle = E_n^o|n^1\rangle + E_n^1|n^o\rangle \tag{3.8.15}$$

Equation 3.8.15 is the key to finding the first-order change in energy E_n^1. Taking the **inner product** of both sides with $\langle n^o|$:

$$\langle n^o|\hat{H}^o|n^1\rangle + \langle n^o|\hat{H}^1|n^o\rangle = \langle n^o|E_n^o|n^1\rangle + \langle n^o|E_n^1|n^o\rangle \tag{3.8.16}$$

since operating the zero-order Hamiltonian on the bra wavefunction (this is just the Schrödinger equation; Equation 3.8.14) is

$$\langle n^o|\hat{H}^o = \langle n^o|E_n^o \tag{3.8.17}$$

and via the orthonormality of the unperturbed $|n^o\rangle$ wavefunctions both

$$\langle n^o|n^o\rangle = 1 \tag{3.8.18}$$

and Equation 3.8.8 can be simplified

$$\cancel{E_n^o\langle n^o|n^1\rangle} + \langle n^o|H^1|n^o\rangle = \cancel{E_n^o\langle n^o|n^1\rangle} + E_n^1\cancel{\langle n^o|n^o\rangle^1} \tag{3.8.19}$$

since the unperturbed set of eigenstates are orthogonal (Equation 3.8.18) and we can cancel the other term on each side of the equation, we find that

$$E_n^1 = \langle n^o|\hat{H}^1|n^o\rangle \tag{3.8.20}$$

> *The first-order change in the energy of a state resulting from adding a perturbing term $\hat{H}^1$ to the Hamiltonian is just the **expectation value** of $\hat{H}^1$ in the **unperturbed** wavefunctions.*

That is, the first order energies (Equation 3.8.15) are given by

$$E_n \approx E_n^o + E_n^1 \tag{3.8.21}$$

$$\approx \underbrace{E_n^o + \langle n^o|H^1|n^o\rangle}_{\text{First Order Perturbation}} \tag{3.8.22}$$

3.8.1A ✔ Example : A Perturbed Particle in a Box

Estimate the energy of the ground-state and first excited-state wavefunction within first-order perturbation theory of a system with the following potential energy

$$V(x) = \begin{cases} V_o & 0 \le x \le L \\ \infty & x < 0 \text{ and } x > L \end{cases}$$

Solution

The first step in any perturbation problem is to write the Hamiltonian in terms of a unperturbed component that the solutions (both eigenstates and energy) are known and a perturbation component (Equation 3.8.2). For this system, the unperturbed Hamilonian and solutions is the particle in an infiinitely high box and the perturbation is a shift of the potential within the box by V_o.

$$\hat{H}^1 = V_o$$

Using Equation 3.8.20 for the first-order term in the energy of the ground-state

$$E_n^1 = \langle n^o|H^1|n^o\rangle$$

with the wavefunctions known from the particle in the box problem

$$|n^o\rangle = \sqrt{\frac{2}{L}}\sin\left(\frac{n\pi}{L}x\right)$$

At this stage we can do two problems independently (i.e., the ground-state with $|1\rangle$ and the first excited-state $|2\rangle$). However, in this case, the first-order perturbation to any particle-in-the-box state can be easily derived.

$$E_n^1 = \int_0^L \sqrt{\frac{2}{L}}\sin\left(\frac{n\pi}{L}x\right) V_o \sqrt{\frac{2}{L}}\sin\left(\frac{n\pi}{L}x\right) dx$$

or better yet, instead of evaluating this integrals we can simplify the expression

$$E_n^1 = \langle n^o|H^1|n^o\rangle = \langle n^o|V_o|n^o\rangle = V_o\langle n^o|n^o\rangle = V_o$$

so via Equation 3.8.22, the energy of each perturbed eigenstate is

$$\begin{aligned} E_n &\approx E_n^o + E_n^1 \\ &\approx \frac{h^2}{8mL^2}n^2 + V_o \end{aligned}$$

While this is the first order perturbation to the energy, it is also the exact value.

3.8.1B ✔ Example : An Even More Perturbed Particle in a Box

Estimate the energy of the ground-state wavefunction within first-order perturbation theory of a system with the following potential energy

$$V(x) = \begin{cases} V_o & 0 \le x \le L/2 \\ \infty & x < 0 \; and \; x > L \end{cases}$$

Solution

As with Example 7.4.1 , we recognize that unperturbed component of the problem (Equation 3.8.2) is the particle in an infinitely high well. For this system, the unperturbed Hamiltonian and solution is the particle in an infinitely high box and the perturbation is a shift of the potential within half a box by V_o. This is essentially a step function.

Using Equation 3.8.20 for the first-order term in the energy of the any state

$$\begin{aligned} E_n^1 &= \langle n^o|H^1|n^o\rangle \\ &= \int_0^{L/2}\sqrt{\frac{2}{L}}\sin\left(\frac{n\pi}{L}x\right)V_o\sqrt{\frac{2}{L}}\sin\left(\frac{n\pi}{L}x\right)dx + \int_{L/2}^{L}\sqrt{\frac{2}{L}}\sin\left(\frac{n\pi}{L}x\right)0\sqrt{\frac{2}{L}}\sin\left(\frac{n\pi}{L}x\right)dx \end{aligned}$$

The second integral is zero and the first integral is simplified to

$$E_n^1 = \frac{2}{L}\int_0^{L/2} V_o \sin^2\left(\frac{n\pi}{L}x\right)dx$$

this is evaluated to

$$\begin{aligned} E_n^1 &= \frac{2V_o}{L}\left[\frac{-1}{2\frac{\pi n}{a}}\cos\left(\frac{n\pi}{L}x\right)\sin\left(\frac{n\pi}{L}x\right) + \frac{x}{2}\right]_0^{L/2} \\ &= \frac{2V_o}{\cancel{L}}\frac{\cancel{L}}{4} = \frac{V_o}{2} \end{aligned}$$

The energy of each perturbed eigenstate, via Equation 3.8.22, is

$$\begin{aligned} E_n &\approx E_n^o + \frac{V_o}{2} \\ &\approx \frac{h^2}{8mL^2}n^2 + \frac{V_o}{2} \end{aligned}$$

3.8.3: First-Order Expression of Wavefunction ($\lambda = 1$)

The general expression for the first-order change in the *wavefunction* is found by taking the inner product of the first-order expansion (Equation 3.8.15) with the bra $\langle m^o|$ with $m \neq n$,

$$\langle m^o|H^o|n^1\rangle + \langle m^o|H^1|n^o\rangle = \langle m^o|E_n^o|n^1\rangle + \langle m^o|E_n^1|n^o\rangle \tag{3.8.23}$$

Last term on right side of Equation 3.8.23

The last integral on the right hand side of Equation 3.8.23 is zero, since $m \neq n$ so

$$\langle m^o|E_n^1|n^o\rangle = E_n^1\langle m^o|n^o\rangle \tag{3.8.24}$$

and

$$\langle m^o|n^0\rangle = 0 \tag{3.8.25}$$

First term on right side of Equation 3.8.23

The first integral is more complicated and can be expanded back into the H^o

$$E_m^o\langle m^o|n^1\rangle = \langle m^o|E_m^o|n^1\rangle = \langle m^o|H^o|n^1\rangle \tag{3.8.26}$$

since

$$\langle m^o|H^o = \langle m^o|E_m^o \tag{3.8.27}$$

so

$$\langle m^o|n^1\rangle = \frac{\langle m^o|H^1|n^o\rangle}{E_n^o - E_m^o} \tag{3.8.28}$$

and therefore the wavefunction corrected to first order is:

$$|n\rangle \approx |n^o\rangle + |n^1\rangle \tag{3.8.29}$$

$$\approx |n^o\rangle + \underbrace{\sum_{m\neq n} \frac{|m^o\rangle\langle m^o|H^1|n^o\rangle}{E_n^o - E_m^o}}_{\text{First Order Perturbation Theory}} \tag{3.8.30}$$

Equation 3.8.30 is essentially is an expansion of the unknown wavefunction correction as a **linear combination** of known unperturbed wavefunctions 3.8.32:

$$|n\rangle \approx |n^o\rangle + |n^1\rangle \tag{3.8.31}$$

$$\approx |n^o\rangle + \sum_{m\neq n} c_{m,n}|m^o\rangle \tag{3.8.32}$$

with the expansion coefficients determined by

$$c_{m,n} = \frac{\langle m^o|H^1|n^o\rangle}{E_n^o - E_m^o} \tag{3.8.33}$$

This is justified since the set of original zero-order wavefunctions forms a **complete basis set** that can describe any function.

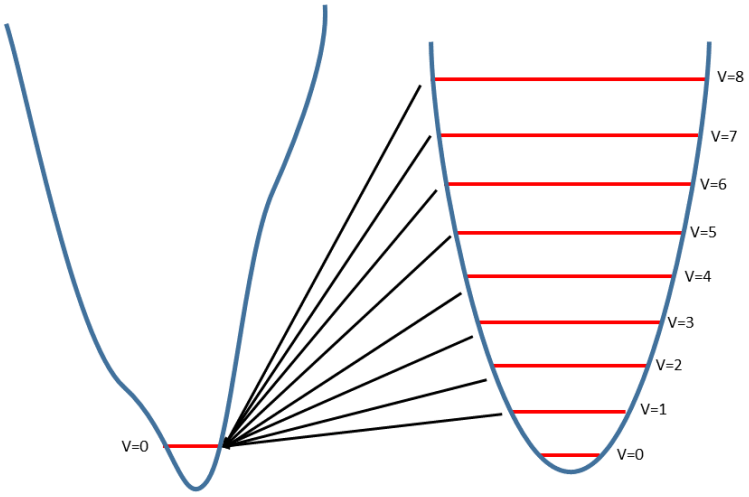


Figure 7.4.2 : The first order perturbation of the ground-state wavefunction for a perturbed (left potential) can be expressed as a linear combination of all excited-state wavefunctions of the unperturbed potential (Equation 3.8.32), shown as a harmonic oscillator in this example (right potential). Note that the ground-state harmonic oscillator wavefunction is not part of this expression and all wavefunctions need to be included in the expression, not just the first eight wavefunctions shown here. (CC BY 4.0; Delmar Larsen)

Calculating the first order perturbation to the wavefunctions is in general an infinite sum of off diagonal matrix elements of $\boldsymbol{H^1}$ (Figure 7.4.2).

- However, the denominator argues that terms in this sum will be weighted by states that are of **comparable energy**. That means in principle, these sum can be truncated easily based off of some criterion.
- Another point to consider is that many of these matrix elements will equal zero depending on the symmetry of the $\{|n^o\rangle\}$ basis and $\boldsymbol{H^1}$ (e.g., some $\langle m^o|H^1|n^o\rangle$ integrals in Equation 3.8.30 could be zero due to the integrand having an odd symmetry; see Example 7.4.3).

> *The denominators in Equation 3.8.30 argues that terms in this sum will be preferentially dictated by states that are of **comparable energy**. That is, eigenstates that have energies significantly greater or lower than the unperturbed eigenstate will weakly contribute to the perturbed wavefunction.*

Example 7.4.2 : A Harmonic Oscillator with a Cubic Perturbation

Estimate the energy of the ground-state wavefunction associated with the Hamiltonian using perturbation theory

$$\hat{H} = \frac{-\hbar}{2m}\frac{d^2}{dx^2} + \frac{1}{2}kx^2 + \epsilon x^3$$

Solution

The first step in a perturbation theory problem is to identify the reference system with the known eigenstates and energies. For this example, this is clearly the harmonic oscillator model.

Energy

The first steps in flowchart for applying perturbation theory (Figure 7.4.1) is to separate the Hamiltonian of the difficult (or unsolvable) problem into a solvable one with a perturbation. For this case, we can rewrite the Hamiltonian as

$$\hat{H}^o + \hat{H}^1$$

where

- $\hat{H}^o$ is the Hamitonian for the standard Harmonic Oscillator with **known** eigenstates and eigenenergies

$$\hat{H}^{(0)} = \frac{-\hbar}{2m}\frac{d^2}{dx^2} + \frac{1}{2}kx^2$$

- $\hat{H}^1$ is the pertubtiation

$$\hat{H}^1 = \epsilon x^3$$

The first order perturbation is given by Equation 3.8.20, which for this problem is

$$E_n^1 = \langle n^o | \epsilon x^3 | n^o \rangle$$

Notice that the integrand has an odd symmetry (i.e., $f(x) = -f(-x)$) with the perturbation Hamiltonian being odd and the ground state harmonic oscillator wavefunctions being even. So

$$E_n^1 = 0$$

This means to first order pertubation theory, this cubic terms does not alter the ground state energy (via Equation 3.8.22). However, this is not the case if second-order perturbation theory were used, which is more accurate (not shown).

Wavefunction

Calculating the first order perturbation to the wavefunctions (Equation 3.8.30) is more difficult than energy since multiple integrals must be evaluated (an infinite number if symmetry arguments are not applicable). The harmonic oscillator wavefunctions are often written in terms of Q, the unscaled displacement coordinate:

$$|\Psi_v(x)\rangle = N_v'' H_v(\sqrt{\alpha}Q) e^{-\alpha Q^2/2}$$

with α

$$\alpha = 1/\sqrt{\beta} = \sqrt{\frac{k\mu}{\hbar^2}}$$

and

$$N_v'' = \sqrt{\frac{1}{2^v v!}} \left(\frac{\alpha}{\pi}\right)^{1/4}$$

Let's consider only the first six wavefunctions that use these Hermite polynomials $H_v(x)$:

- $H_0 = 1$
- $H_1 = 2x$
- $H_2 = -2 + 4x^2$
- $H_3 = -12x + 8x^3$
- $H_4 = 12 - 48x^2 + 16x^4$
- $H_5 = 120x - 160x^3 + 32x^5$

The first order perturbation to the ground-state wavefunction (Equation 3.8.30)

$$|0^1\rangle = \sum_{m \neq 0}^{5} \frac{|m^o\rangle\langle m^o|H^1|0^o\rangle}{E_0^o - E_m^o} \tag{3.8.34}$$

given these truncated wavefunctions (we should technically use the infinite sum) and that we are considering only the ground state with $n = 0$:

$$|0^1\rangle = \frac{\langle 1^o|H^1|0^o\rangle}{E_0^o - E_1^o}|1^o\rangle + \frac{\langle 2^o|H^1|0^o\rangle}{E_0^o - E_2^o}|2^o\rangle + \frac{\langle 3^o|H^1|0^o\rangle}{E_0^o - E_3^o}|3^o\rangle + \frac{\langle 4^o|H^1|0^o\rangle}{E_0^o - E_4^o}|4^o\rangle + \frac{\langle 5^o|H^1|0^o\rangle}{E_0^o - E_5^o}|5^o\rangle$$

We can use symmetry of the perturbation and unperturbed wavefunctions to solve the integrals above. We know that the unperturbed harmonic oscillator wavefunctions $\{|n^0\}\rangle$ alternate between even (when v is even) and odd (when v is odd) as shown previously. Since the perturbation is an odd function, only when $m = 2k + 1$ with $k = 1, 2, 3$ would these integrals be non-zero (i.e., for $m = 1, 3, 5, ...$).

So of the original five unperturbed wavefunctions, only $|m=1\rangle$, $|m=3\rangle$, and $|m=5\rangle$ mix to make the first-order perturbed ground-state wavefunction so

$$|0^1\rangle = \frac{\langle 1^o|H^1|0^o\rangle}{E_0^o - E_1^o}|1^o\rangle + \frac{\langle 3^o|H^1|0^o\rangle}{E_0^o - E_3^o}|3^o\rangle + \frac{\langle 5^o|H^1|0^o\rangle}{E_0^o - E_5^o}|5^o\rangle$$

At this stage, the integrals have to be manually calculated using the defined wavefuctions above, which is left as an exercise. Notice that each unperturbed wavefunction that can "mix" to generate the perturbed wavefunction will have a reciprocally decreasing contribution (w.r.t. energy) due to the growing denominator in Equation 3.8.34.

? Exercise 7.4.3 : Harmonic Oscillator with a Quartic Perturbation

Use perturbation theory to estimate the energy of the ground-state wavefunction associated with this Hamiltonian

$$\hat{H} = \frac{-\hbar}{2m}\frac{d^2}{dx^2} + \frac{1}{2}kx^2 + \gamma x^4.$$

3.8.4: Second-Order Terms ($\lambda = 2$)

There are higher energy terms in the expansion of Equation 3.8.5 (e.g., the blue terms in Equation 3.8.13), but are not discussed further here other than noting the whole perturbation process is an infinite series of corrections that ideally converge to the correct answer. It is truncating this series as a finite number of steps that is the approximation. The general approach to perturbation theory applications is giving in the flowchart in Figure 7.4.1 .

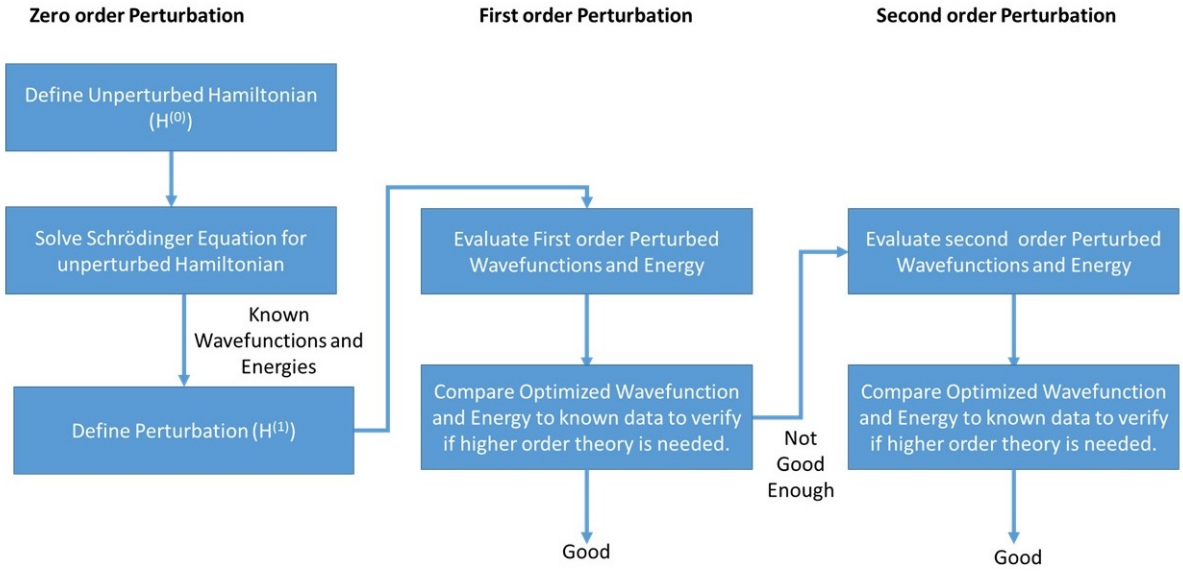


Figure 7.4.1 : Simplified algorithmic flowchart of the Perturbation Theory approximation showing the first two perturbation orders. The process can be continued to third and higher orders. (CC BY 4.0; Delmar Larsen)

Perturbation Theory Does not always Work

It should be noted that there *are* problems that cannot be solved using perturbation theory, even when the perturbation is very weak, although such problems are the exception rather than the rule. One such case is the one-dimensional problem of free particles perturbed by a localized potential of strength λ. Switching on an arbitrarily weak attractive potential causes the $k = 0$ free particle wavefunction to drop below the continuum of plane wave energies and become a localized bound state with binding energy of order λ^2. However, changing the sign of λ to give a repulsive potential there is no bound state, the lowest energy plane wave state stays at energy zero. Therefore the energy shift on switching on the perturbation **cannot** be represented as a power series in λ, the strength of the perturbation.

3.8: Perturbation Theory Expresses the Solutions in Terms of Solved Problems is shared under a CC BY-NC-SA 4.0 license and was authored, remixed, and/or curated by LibreTexts.

- **7.4: Perturbation Theory Expresses the Solutions in Terms of Solved Problems** by Delmar Larsen is licensed CC BY-NC-SA 4.0.

3.9: Electron Spin, Indistinguishability and Slater Determinants

3.9.1: Introduction

Because electrons in an atom or molecule are indistinguishable from each other quantum properties cannot depend on which electron is in which of the occupied quantum states. This has consequences for what functional forms are valid for the wavefunction of an orbital that includes the spacial and spin components. These consequences underlie the concepts of multiplet configurations (singlets, doublets, triplets, etc...).

3.9.2: Now Back to Electrons (The Orbital Approximation again)

The generic multi-electron atom including terms for the additional electrons with a general charge Z; e.g.

$$V(r_1) = -\frac{Ze^2}{4\pi\epsilon_0 r_1} \tag{3.9.1}$$

So the electronic Hamiltonian for the multi-electron system becomes

$$\hat{H} = -\frac{\hbar^2}{2m_e}\sum_i^N \nabla_i^2 + \sum_i^N V(r_i) + \sum_{i>j}^N V(r_{ij}) \tag{3.9.2}$$

We predict that exact solutions to the multi-electron Schrödinger equation would consist of a family of multi-electron wavefunctions, each with an associated energy eigenvalue, i.e.,

$$|\psi_a(r_1, r_2, \cdots r_N)\rangle \tag{3.9.3}$$

with energy E_a and

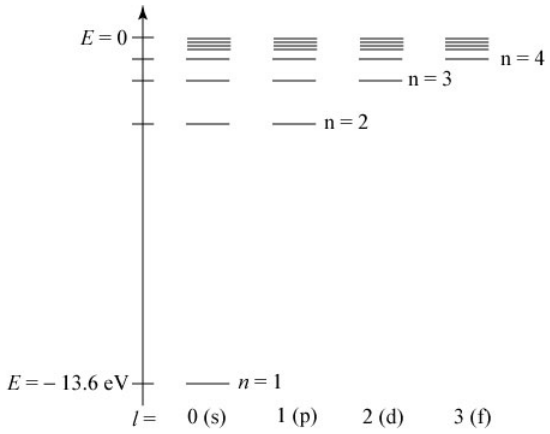
$$|\psi_b(r_1, r_2, \cdots r_N)\rangle \tag{3.9.4}$$

with energy E_b and

$$|\psi_c(r_1, r_2, \cdots r_N)\rangle \tag{3.9.5}$$

with energy E_c etc.

The fact that electrons interact through their Coulomb repulsion means that an exact wavefunction for a multi-electron system would be a single function that depends **simultaneously** upon the coordinates of all the electrons; i.e., a multi-electron wavefunction. These wavefunctions and energies would describe the ground and excited states of the multi-electron atom, just as the hydrogen wavefunctions and their associated energies describe the ground and excited states of the hydrogen atom. We would predict quantum numbers to be involved, as well.



For hydrogen, the wavefunctions are just the orbitals. For multi-electrons, the corresponding wavefunctions are combinations of orbitals that look and feel like hydrogenic wavefunctions, but are not.

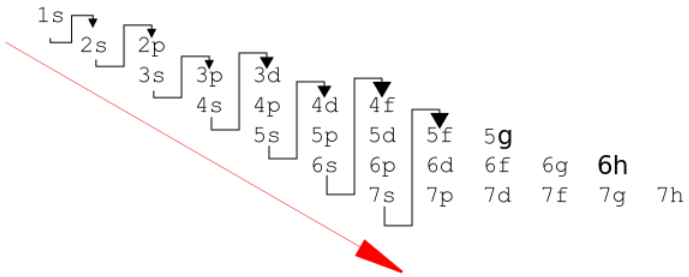
Unfortunately, the Coulomb repulsion terms make it impossible to find an exact solution to the Schrödinger equation for many-electron atoms.

> *The most basic approximations to the exact solutions involve writing a multi-electron wavefunction as a simple product of single-electron orbitals, and obtaining the energy of the atom in the state described by that wavefunction as the sum of the energies of the one-electron components.*

By writing the multi-electron wavefunction as a product of single-electron functions, we conceptually transform a multi-electron atom into a collection of individual electrons located in individual functions whose spatial characteristics and energies can be separately identified. For atoms, these single-electron functions are called **atomic orbitals**.

$$|\psi(r_1, r_2, \cdots, r_i)\rangle \approx |\phi_1(r_1)\phi_2(r_2)\cdots\phi_i(r_i)\rangle \tag{3.9.6}$$

Knowing the orbitals of a particular species provides information about the sizes, shapes, directions, symmetries, and energies of those regions of space that are **available** to the electrons (i.e., the complete set of orbitals that are available). This knowledge does **not** determine into which orbitals the electrons are placed. It is by describing the electronic configurations (i.e., orbital occupancies such as $1s^2 2s^2 2p^2$ or $1s^2 2s^2 2p^1 3s^1$) appropriate to the energy range under study that one focuses on how the electrons **occupy the orbitals** (scaled by the effective nuclear charge).



The approximate order of filling of atomic orbitals, following the arrows from 1s to 7p. (After 7p the order includes orbitals outside the range of the diagram, starting with 8s.) (CC BY-SA; Sharayanan)

Using the information from the figure above it is possible to arrange the orbitals in an order that **approximately** reflects increasing energy which is useful to figure out the orbital occupancies using a few simple rules.

The Aufbau Principle is not Entirely Correct - It is only a guideline!

So unfortunately, it seems that even though most of the effects which combine to result in the observed electronic configurations are known, there is no qualitative way to predict where the configurations are going to mismatch with the aufbau principle or the energy levels of the orbitals. The aufbau principle is most decidedly wrong for practically every atom with respect to the placement of the orbital energy levels, but incredibly it happens to predict the configuration of the valence shell for most atoms.

3.9.3: Electronic Configurations

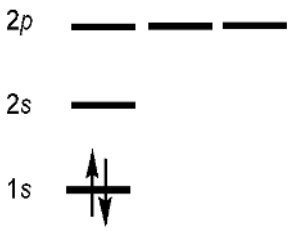
Specification of a particular occupancy of the set of orbitals available to the system gives an **electronic configuration**.

3.9.3.1: Helium Atom

The helium atom has the $1s^2$ electronic configuration (and the Li^+ ions). This configuration can describe a single **spinorbital**:

$$|1s(1)\uparrow 1s(2)\downarrow\rangle \quad \text{or} \quad |1s(1)\alpha 1s(2)\beta\rangle$$

Within the orbital approximation (Equation 3.9.6) each electron resides is in a spinorbital with an spatial orbital part (involving n, l and m_l) quantum numbers and a spin part (involving the m_s quantum number). We know there are two different values of m_s from general chemistry.



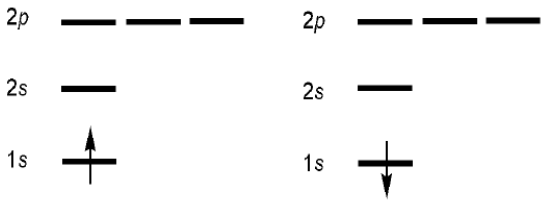
3.9.3.2: Hydrogen Atom

The hydrogen atom has the $1s^1$ electronic configuration for the hydrogen atom (and the He^{+1} and the Li^{+2} ions). This configuration can describe two possible **spinorbital** combinations:

$$|1s(1)\uparrow\rangle \quad \text{or} \quad |1s(1)\alpha\rangle$$

or

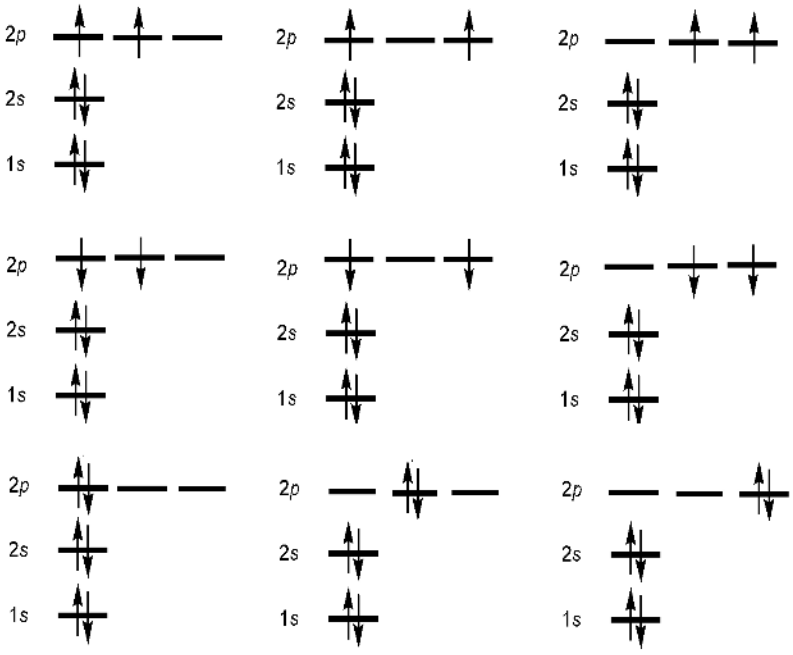
$$|1s(1)\downarrow\rangle \quad \text{or} \quad |1s(1)\beta\rangle$$



3.9.3.3: Carbon Atom

- $1s^2 2s^2 2p^2$ is an electronic configuration for the carbon atom (and the N^{+1} and the O^{+2} ions)

This configuration represents situations in which the electrons occupy low-energy orbitals of the system and, as such, are likely to contribute strongly to the true ground and low-lying excited states and to the low-energy states of molecules formed from these atoms or ions.



Specification of an electronic configuration does not, however, specify a particular electronic state of the system (i.e., which orbital is occupied). For the electronic configuration of carbon with $1s^2 2s^2 2p^2$, there are many ways in which the 2p orbitals can be occupied by the two electrons. As a result, there are a total of multiple "microstates" which cluster into energetically distinct **levels**, lying within this single configuration.

> *To address these levels, we need to discuss electron spin and the fourth Quantum Number!*

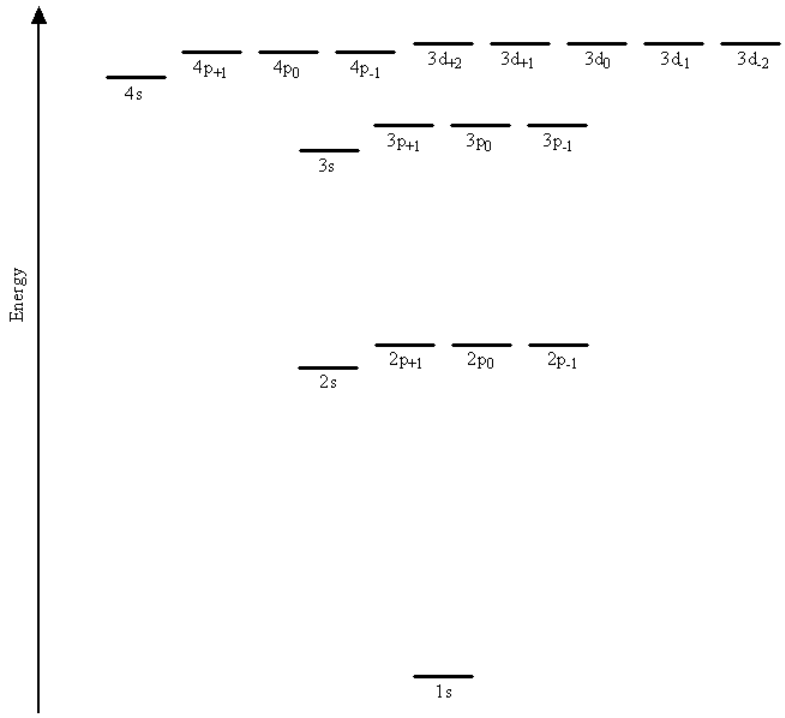
3.9.4: Complete the Quantum Number Tetrad: spin-orbitals

Hydrogenic spin-orbitals used as components of multi-electron systems are identified in the same way as they are for the hydrogen atom. Each spin-orbital consists of a spatial wavefunction, specified by the the quantum numbers (n, ℓ, and m_ℓ) and denoted 1s, 2s, 2p, 3s, 3p, 3d, etc, multiplied by a spin function, specified by the quantum number ms and denoted α or β.

The subscript on the argument of the spatial function reveals which electron is being described (r_1 is a vector that refers to the coordinates of electron 1, for example.) No argument is given for the spin function. An example of a spin-orbital for electron 2 in a $3p_z$ orbital:

$$|\phi_{3p_z}\alpha(r_2)\rangle = \phi_{3,1,0}(r_2)\alpha \tag{3.9.7}$$

The basic mathematical functions and thus the general shapes and angular momenta for hydrogenic orbitals are the same as those for hydrogen orbitals.



Ordering of energy levels for **Ar**. Energy level differences are not to scale.

The energy of each electron now depends not only on its principle quantum number, n, but also on its angular momentum quantum number, ℓ.

3.9.5: Pauli Exclusion Principle

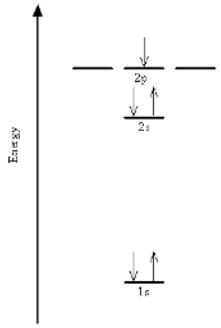
Three rules apply for predicting the *ground state* configuration of an atom:

1. **The Pauli Exclusion Principle:** There is one more quantum number called the *spin quantum number* m_s that can take values +½ or -½ (for electrons). *No two electrons can have the same four quantum numbers* so an orbital can "hold" only two electrons. (i.e., only two electrons can be described by the same spacial wave function). This rule cannot be broken.
2. **The Aufbau principle:** Electron configurations are built up by filling the lowest energy orbitals first (provided the energy differences are significant). Remember this rule applies to the ground state; *excited* configurations that do not violate the Pauli

principle are possible.

3. **Hund's (first) rule:** Where orbitals have the same energy (are degenerate) or nearly so, they will be filled one electron in each, with parallel spins, before pairing begins. Other configurations are *excited* states, i.e., not forbidden.

The mathematical analog of these steps is the construction of the approximate multi-electron wavefunction as a **product** of the single-electron "atomic" spin-orbitals. For example, the configuration of the boron atom, shown schematically in the energy level diagram, is written in shorthand form as $\mathbf{1s^2 2s^2 2p^1}$. The degeneracy of the 2s and 2p orbitals is **broken by the electron-electron interactions** in multi-electron systems.



Orbital energy level diagram that represents the electron configuration of the boron atom. Orbital energy differences are approximately scaled.

Rather than showing the individual spin-orbitals in the diagram or in the shorthand notation, we commonly say that up to two electrons can be described by each spatial orbital, one with spin function α (electron denoted by an arrow pointing up) and the other with spin function β (arrow pointing down). This restriction is a manifestation of the Pauli Exclusion Principle mentioned above.

3.9.6: Indistinguishability

We will use the following statement as a guide to keep our explorations focused on the development of a clear picture of the multi-electron atom: “When a multi-electron wavefunction is built as a product of single-electron wavefunctions, the corresponding concept is that exactly one electron’s worth of charge density is described by each atomic spin-orbital.”

A subtle, but important part of the conceptual picture is that the electrons in a multi-electron system are not distinguishable from one another by any experimental means. Since the electrons are indistinguishable, the probability density we calculate by squaring the modulus of our multi-electron wavefunction also cannot change when the electrons are interchanged (permuted) between different orbitals. In general, if we interchange two identical particles, the world does not change. As we will see below, this requirement leads to the idea that the world can be divided into two types of particles based on their behavior with respect to permutation or interchange.

We could symbolically write an approximate two-particle wavefunction as $|\psi(r_1, r_2)\rangle$. This could be, for example, a two-electron wavefunction for helium. To exchange the two particles, we simply substitute the coordinates of particle 1 (r_1) for the coordinates of particle 2 (r_2) and vice versa, to get the new wavefunction $|\psi(r_1, r_2)\rangle$. This new wavefunction **must** have the property that

$$\begin{aligned} |\psi(r_1, r_2)|^2 &= \psi(r_2, r_1)^* \psi(r_2, r_1) \\ &= \psi(r_1, r_2)^* \psi(r_1, r_2) \end{aligned}$$

This will be true only if the wavefunctions before and after permutation are related by a factor of $e^{i\phi}$,

$$\psi(r_1, r_2) = e^{i\phi} \psi(r_2, r_1) \tag{3.9.8}$$

so that when squared

$$\left(e^{-i\phi} \psi(r_1, r_2)^*\right) \left(e^{i\phi} \psi(r_1, r_2)^*\right) = \psi(r_1, r_2)^* \psi(r_1, r_2) \tag{3.9.9}$$

If we exchange or permute two identical particles twice, we are (by definition) back to the original situation. If each permutation changes the wavefunction by $e^{i\phi}$, the double permutation must change the wavefunction by $e^{i\phi} e^{i\phi}$. Since we then are back to the original state, the effect of the double permutation must equal 1; i.e.,

$$e^{i\phi} e^{i\phi} = e^{i2\phi} = 1 \tag{3.9.10}$$

which is true only if $\phi = 0$ or an integer multiple of π. The requirement that a double permutation reproduce the original situation limits the acceptable values for $e^{i\phi}$ to either +1 (when $\phi = 0$) or -1 (when $\phi = \pi$). Both possibilities are found in nature.

3.9.6.1: Bosons (symmetric)

The behavior of some particles requires that the wavefunction be symmetric with respect to permutation ($e^{i\phi} = +1$). A wavefunction that is symmetric with respect to electron interchange is one whose output does NOT change sign when the electron coordinates are interchanged, as shown below.

$$\psi(r_2, r_1) = e^{i\phi}\psi(r_1, r_2) = +\psi(r_1, r_2) \tag{3.9.11}$$

These particles are called bosons and have integer spin such as deuterium nuclei, photons, and gluons.

3.9.6.2: Fermions (antisymmetric)

The behavior of other particles requires that the wavefunction be antisymmetric with respect to permutation ($e^{i\phi} = -1$). A wavefunction that is antisymmetric with respect to electron interchange is one whose output changes sign when the electron coordinates are interchanged, as shown below.

$$\psi(r_2, r_1) = e^{i\phi}\psi(r_1, r_2) = -\psi(r_1, r_2) \tag{3.9.12}$$

These particles, called fermions, have half-integer spin and include **electrons**, protons, and neutrinos.

Example 3.9.1: A "Bad" Wavefunction for Helium Atom

Blindly following the first statement of the Pauli Exclusion Principle, that each electron in a multi-electron atom **must** be described by a different spin-orbital, we try constructing a simple product wavefunction for helium using two different spin-orbitals. Both have the 1s spatial component, but one has spin function α and the other has spin function β so the product wavefunction matches the form of the ground state electron configuration for He, $1s^2$.

$$|\psi(\mathbf{r}_1, \mathbf{r}_2)\rangle = |\phi_{1s\alpha}(\mathbf{r}_1)\phi_{1s\beta}(\mathbf{r}_2)\rangle \tag{3.9.13}$$

After permutation of the electrons, this becomes

$$|\psi(\mathbf{r}_2, \mathbf{r}_1)\rangle = |\phi_{1s\alpha}(\mathbf{r}_2)\phi_{1s\beta}(\mathbf{r}_1)\rangle \tag{3.9.14}$$

which is different from the starting function since $\phi_{1s\alpha}$ and $\phi_{1s\beta}$ are different spin-orbital functions. However, an antisymmetric function must produce the same function multiplied by (–1) after permutation, and that is not the case here.

Mathematically, when we switch the two we want we want (since they are fermions)

$$|\psi(\mathbf{r}_2, \mathbf{r}_1)\rangle = -|\psi(\mathbf{r}_1, \mathbf{r}_2)\rangle \tag{3.9.15}$$

and when writing out the wavefunctions:

$$|\phi_{1s\alpha}(\mathbf{r}_2)\phi_{1s\beta}(\mathbf{r}_1)\rangle \neq -|\phi_{1s\alpha}(\mathbf{r}_1)\phi_{1s\beta}(\mathbf{r}_2)\rangle \tag{3.9.16}$$

Therefore the wavefunction in Equation 3.9.13 is not a good wavefunction. We must try something else.

To avoid getting a totally different function when we permute the electrons, we can make **a linear combination of functions**. A very simple way of taking a linear combination involves making a new function by simply adding or subtracting functions. The function that is created by subtracting the right-hand side of Equation 3.9.14 from the right-hand side of Equation 3.9.13 has the desired antisymmetric behavior. The $2^{-1/2}$ constant on the left-hand side accounts for the fact that the total wavefunction must be normalized.

$$|\psi(\mathbf{r}_1, \mathbf{r}_2)\rangle = \frac{1}{\sqrt{2}}[\phi_{1s\alpha}(\mathbf{r}_1)\phi_{1s\beta}(\mathbf{r}_2) - \phi_{1s\alpha}(\mathbf{r}_2)\phi_{1s\beta}(\mathbf{r}_1)] \tag{3.9.17}$$

Does this satisfy the antisymmetric requirement for electron exchange:

$$|\psi(\mathbf{r}_1,\mathbf{r}_2)\rangle \stackrel{?}{=} -|\psi(\mathbf{r}_2,\mathbf{r}_1)\rangle \tag{3.9.18}$$

$$\begin{aligned} &\frac{1}{\sqrt{2}}[\phi_{1s\alpha}(\mathbf{r}_1)\phi_{1s\beta}(\mathbf{r}_2)-\phi_{1s\alpha}(\mathbf{r}_2)\phi_{1s\beta}(\mathbf{r}_1)] \\ \stackrel{?}{=}&-\frac{1}{\sqrt{2}}[\phi_{1s\alpha}(\mathbf{r}_2)\phi_{1s\beta}(\mathbf{r}_1)-\phi_{1s\alpha}(\mathbf{r}_1)\phi_{1s\beta}(\mathbf{r}_2)] \end{aligned} \tag{3.9.19}$$

simplify

$$\begin{aligned} &\frac{1}{\sqrt{2}}[\phi_{1s\alpha}(\mathbf{r}_1)\phi_{1s\beta}(\mathbf{r}_2)-\phi_{1s\alpha}(\mathbf{r}_2)\phi_{1s\beta}(\mathbf{r}_1)] \\ \stackrel{\checkmark}{=}&+\frac{1}{\sqrt{2}}[\phi_{1s\alpha}(\mathbf{r}_1)\phi_{1s\beta}(\mathbf{r}_2)-\phi_{1s\alpha}(\mathbf{r}_2)\phi_{1s\beta}(\mathbf{r}_1)] \end{aligned} \tag{3.9.20}$$

So we have a proper anti-symmetric wavefunction where the wavefunctions are do not depend on the label we assign to each electron. If we had chosen the linear combination to be

$$|\psi(\mathbf{r}_1,\mathbf{r}_2)\rangle = \frac{1}{\sqrt{2}}[\phi_{1s\alpha}(\mathbf{r}_1)\phi_{1s\beta}(\mathbf{r}_2)+\phi_{1s\alpha}(\mathbf{r}_2)\phi_{1s\beta}(\mathbf{r}_1)] \tag{3.9.21}$$

we would have found that it does not work because it is symmetric with respect to exchange of electrons

$$|\psi(\mathbf{r}_2,\mathbf{r}_1)\rangle = \frac{1}{\sqrt{2}}[\phi_{1s\alpha}(\mathbf{r}_2)\phi_{1s\beta}(\mathbf{r}_1)+\phi_{1s\alpha}(\mathbf{r}_1)\phi_{1s\beta}(\mathbf{r}_2)] = |\psi(\mathbf{r}_1,\mathbf{r}_2)\rangle. \tag{3.9.22}$$

So just like the possibilities with the spins parallel ($\alpha\alpha$ or $\beta\beta$) this is not a good spin-spatial wavefunction for the electrons both in the 1s orbital. We have thus shown that for a full orbital (2 electrons) they must be paired. This is not true if the electrons are in different orbitals (degenerate or of different energies).

As an example we will consider the first excited state of He. The electronic configuration of the first excited state of He is $1s^1 2s^1 2p^0$ and we can envision four microstates for this configuration. As expected, the wavefunctions associated for of these microstate must satisfy indistinguishability requirement just like the ground state.

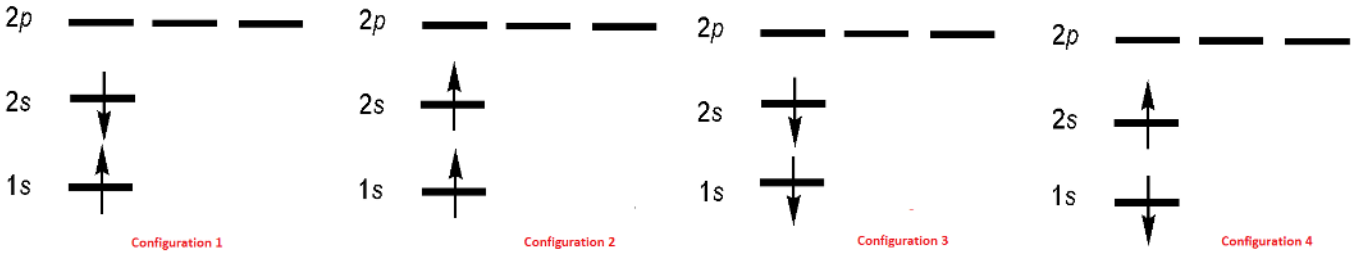


Figure : Electron configurations for first-excited state of the helium atom.

These electron configurations are used to construct four possible excited-state two-electron wavefunctions, where we will write them as a product of spatial and spin parts to make it clear which part is antisymmetric (factor with the "-" sign):

$$|\psi_1(\mathbf{r}_1,\mathbf{r}_2)\rangle = \frac{1}{2}\underbrace{[\varphi_{1s}(1)\varphi_{2s}(2)+\varphi_{1s}(2)\varphi_{2s}(1)]}_{\text{spatial component}}\underbrace{[\alpha(1)\beta(2)-\alpha(2)\beta(1)]}_{\text{spin component}} \tag{3.9.23}$$

$$|\psi_2(\mathbf{r}_1,\mathbf{r}_2)\rangle = \frac{1}{\sqrt{2}}\underbrace{[\varphi_{1s}(1)\varphi_{2s}(2)-\varphi_{1s}(2)\varphi_{2s}(1)]}_{\text{spatial component}}\underbrace{[\alpha(1)\alpha(2)]}_{\text{spin component}} \tag{3.9.24}$$

$$|\psi_3(\mathbf{r}_1,\mathbf{r}_2)\rangle = \frac{1}{\sqrt{2}}\underbrace{[\varphi_{1s}(1)\varphi_{2s}(2)-\varphi_{1s}(2)\varphi_{2s}(1)]}_{\text{spatial component}}\underbrace{[\alpha(1)\beta(2)+\alpha(2)\beta(1)]}_{\text{spin component}} \tag{3.9.25}$$

$$|\psi_4(\mathbf{r}_1,\mathbf{r}_2)\rangle = \frac{1}{2}\underbrace{[\varphi_{1s}(1)\varphi_{2s}(2)-\varphi_{1s}(2)\varphi_{2s}(1)]}_{\text{spatial component}}\underbrace{[\beta(1)\beta(2)]}_{\text{spin component}} \tag{3.9.26}$$

All four wavefunctions are antisymmetric as required for fermionic wavefunctions (which is left to an exercise). Wavefunctions $|\psi_2\rangle$ and $|\psi_4\rangle$ correspond to the two electrons both having spin up or both having spin down (Configurations 2 and 3 in Figure , respectively). Wavefunctions $|\psi_1\rangle$ and $|\psi_3\rangle$ are combinations: antisymmetric (Configuration 1 - Configuration 4) and symmetric (Configuration 1 + 4). That is, a single electron configuration does not describe the wavefunction.

Notice that the first combination has a symmetric spatial wavefunction while the other three use the antisymmetric spacial wavefunction. The multiplicity is the number of different spin functions that can be combined with a spatial wavefunction to produce a valid wavefunction. Thus the $|\psi_1\rangle$ represents a **singlet** and the $|\psi_2\rangle$, $|\psi_3\rangle$ and $|\psi_4\rangle$, which all have the same anti-symmetric spacial part, represent a **triplet**.

For many electrons, this ad hoc construction procedure would obviously become unwieldy. However, there is an elegant way to construct an antisymmetric wavefunction for a system of N identical particles.

3.9.7: Slater Determinants as a way to "Hardwire" Indistinguishability into the Wavefunction

A linear combination that describes an appropriately antisymmetrized multi-electron wavefunction for any desired orbital configuration is easy to construct for a two-electron system. However, interesting chemical systems usually contain more than two electrons. For these multi-electron systems, a relatively simple scheme for constructing an antisymmetric wavefunction from a product of one-electron functions is to write the wavefunction in the form of a determinant. John Slater introduced this idea so the determinant is called a **Slater determinant**.

The Slater determinant for the two-electron wavefunction of helium is

$$|\psi(\mathbf{r}_1,\mathbf{r}_2)\rangle = \frac{1}{\sqrt{2}}\begin{vmatrix}\phi_{1s}(1)\alpha(1) & \phi_{1s}(1)\beta(1)\\ \phi_{1s}(2)\alpha(2) & \phi_{1s}(2)\beta(2)\end{vmatrix} \tag{3.9.27}$$

We can introduce a shorthand notation for the arbitrary **spin-orbital**

$$\phi_{i\alpha}(\mathbf{r}) = \phi_i\alpha \tag{3.9.28}$$

or

$$\phi_{i\beta}(\mathbf{r}) = \phi_i\beta \tag{3.9.29}$$

as determined by the m_s quantum number. A shorthand notation for the determinant in Equation 3.9.27 is then

$$|\psi(\mathbf{r}_1,\mathbf{r}_2)\rangle = 2^{-\frac{1}{2}}Det|\phi_{1s\alpha}(\mathbf{r}_1)\phi_{1s\beta}(\mathbf{r}_2)| \tag{3.9.30}$$

The determinant is written so the electron coordinate changes in going from one row to the next, and the spin orbital changes in going from one column to the next. The advantage of having this recipe is clear if you try to construct an antisymmetric wavefunction that describes the orbital configuration for uranium! Note that the normalization constant is $(N!)^{-\frac{1}{2}}$ for N electrons.

The generalized Slater determinant for a multi-electron atom with N electrons is then

$$|\psi(\mathbf{r}_1,\mathbf{r}_2,\dots,\mathbf{r}_N)\rangle = \frac{1}{\sqrt{N!}}\begin{vmatrix}\phi_1(\mathbf{r}_1) & \phi_2(\mathbf{r}_1) & \cdots & \phi_N(\mathbf{r}_1)\\ \phi_1(\mathbf{r}_2) & \phi_2(\mathbf{r}_2) & \cdots & \phi_N(\mathbf{r}_2)\\ \vdots & \vdots & \ddots & \vdots\\ \phi_1(\mathbf{r}_N) & \phi_2(\mathbf{r}_N) & \cdots & \phi_N(\mathbf{r}_N)\end{vmatrix} \tag{3.9.31}$$

3.9.8: Contributors

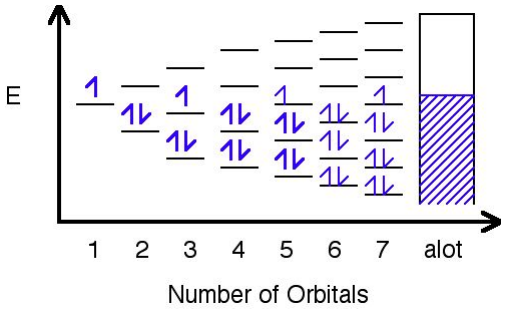
- David M. Hanson
- Erica Harvey
- Robert Sweeney
- Theresa Julia Zielinski
- Delmar Larson
- Jonathan Gutow

This page titled 3.9: Electron Spin, Indistinguishability and Slater Determinants is shared under a CC BY-NC-SA 4.0 license and was authored, remixed, and/or curated by Jonathan Gutow.

- **8.6: Antisymmetric Wavefunctions can be Represented by Slater Determinants** by David M. Hanson, Erica Harvey, Robert Sweeney, Theresa Julia Zielinski is licensed CC BY-NC-SA 4.0.

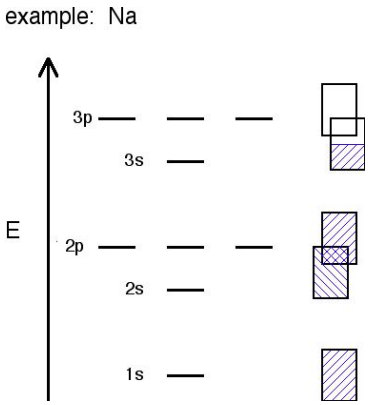
3.10: Band Structure

Band Theory was developed with some help from the knowledge gained during the quantum revolution in science. In 1928, Felix Bloch had the idea to take the quantum theory and apply it to solids. In 1927, Walter Heitler and Fritz London discovered bands- very closely spaced orbitals with not much difference in energy.



In this image, orbitals are represented by the black horizontal lines, and they are being filled with an increasing number of electrons as their amount increases. Eventually, as more orbitals are added, the space in between them decreases to hardly anything, and as a result, a band is formed where the orbitals have been filled.

Different metals will produce different combinations of filled and half filled bands.



Sodium's bands are shown with the rectangles. Filled bands are colored in blue. As you can see, bands may overlap each other (the bands are shown askew to be able to tell the difference between different bands). The lowest unoccupied band is called the conduction band, and the highest occupied band is called the valence band.

Bands will follow a trend as you go across a period:

- In Na, the 3s band is 1/2 full.
- In Mg, the 3s band is full.
- In Al, the 3s band is full and the 3p ban is 1/2 full... and so on.

The probability of finding an electron in the conduction band is shown by the equation:

$$P = \frac{1}{e^{\Delta E/RT} + 1} \tag{3.10.1}$$

The ΔE in the equation stands for the change in energy or energy gap. T stands for the temperature, and R is a bonding constant. That equation and this table below show how the bigger the difference in energy is, or gap, between the valence band and the conduction band, the less likely electrons are to be found in the conduction band. This is because they cannot be excited enough to make the jump up to the conduction band.

ELEMENT	ΔE(kJ/mol) of energy gap	# of electrons/cm^3 in conduction band	insulator, or conductor?
C (diamond)	524 (big band gap)	10^{-27}	insulator
Si	117 (smaller band gap, but not a full conductor)	10^{9}	semiconductor
Ge	66 (smaller band gap, but still not a full conductor)	10^{13}	semiconductor

Conductors, Insulators and Semiconductors

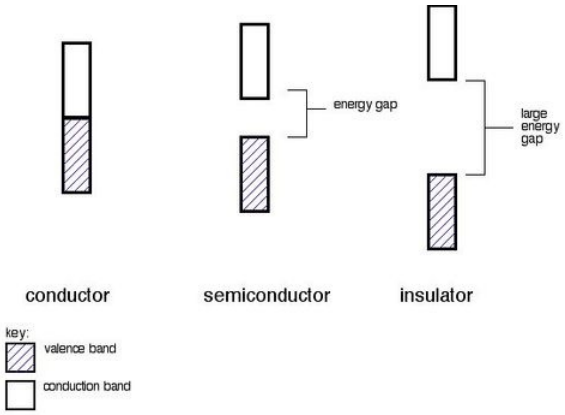


Diagram comparing conductor, semiconductor, and insulator energy bands. Conductor has overlapping bands; semiconductor has small gap; insulator has large gap. Key: valence and conduction bands.

A. Conductors

Metals are conductors. There is no band gap between their valence and conduction bands, since they overlap. There is a continuous availability of electrons in these closely spaced orbitals.

B. Insulators

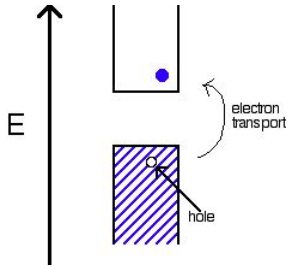
In insulators, the band gap between the valence band the the conduction band is so large that electrons cannot make the energy jump from the valence band to the conduction band.

C. Semiconductors

Semiconductors have a small energy gap between the valence band and the conduction band. Electrons can make the jump up to the conduction band, but not with the same ease as they do in conductors. There are two different kinds of semiconductors: **intrinsic** and **extrinsic**.

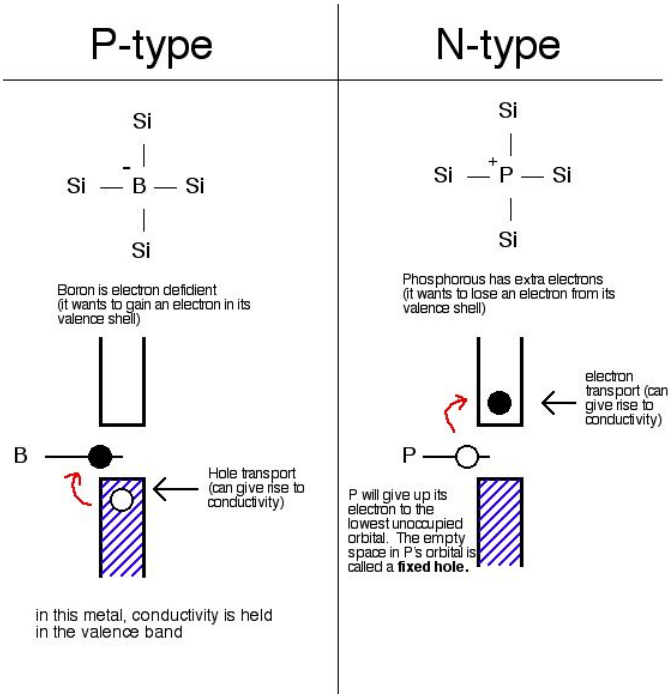
i. Intrinsic Semiconductors

An intrinsic semiconductor is a semiconductor in its pure state. For every electron that jumps into the conduction band, the missing electron will generate a hole that can move freely in the valence band. The number of holes will equal the number of electrons that have jumped.



ii. Extrinsic Semiconductors

In extrinsic semiconductors, the band gap is controlled by purposefully adding small impurities to the material. This process is called **doping**. Doping, or adding impurities to the lattice can change the electrical conductivity of the lattice and therefore vary the efficiency of the semiconductor. In extrinsic semiconductors, the number of holes will not equal the number of electrons jumped. There are two different kinds of extrinsic semiconductors, p-type (positive charge doped) and n-type (negative charge doped).



? Exercise 3.10.1

How do you distinguish between a valence band and a conduction band?

Answer

The valence band is the highest band with electrons in it, and the conduction band is the highest band with no electrons in it.

? Exercise 3.10.2

Is the energy gap between an insulator smaller or larger than the energy gap between a semiconductor?

Answer

Larger

Exercise 3.10.3

What two methods bring conductivity to semiconductors?

Answer

Electron transport and hole transport

Exercise 3.10.4

You are more likely to find electrons in a conduction band if the energy gap is smaller/larger?

Answer

Smaller

References

1. Petrucci, Harwood, Herring, Madura. GENERAL CHEMISTRY Principles and Modern Applications 9th Edition. Macmillan Publishing Co: New Jersey. 1989.
2. Moore, John T. Chemistry Made Simple. Random House Inc: New York. 2004.

3.10: Band Structure is shared under a CC BY-NC 4.0 license and was authored, remixed, and/or curated by Jim Clark & Sierra Blair.

- **Band Structure** by Jim Clark, Sierra Blair is licensed CC BY-NC 4.0.

CHAPTER OVERVIEW

4: Spectroscopy

4.1: Spectroscopic Selection Rules
4.2: Rotational Spectroscopy of Diatomic Molecules
4.3: Rotational Spectra of Polyatomic Molecules
4.4: Harmonic Oscillator
4.5: Hermite Polynomials are either Even or Odd Functions
4.6: The Harmonic Oscillator and Infrared Spectra
4.7: Vibrational Overtones
4.8: Rotations Accompany Vibrational Transitions
4.9: Unequal Spacings in Vibration-Rotation Spectra
4.10: Electronic Spectra Contain Electronic, Vibrational, and Rotational Information
4.11: The Franck-Condon Principle
4.12: Electronically Excited Molecules can Relax by a Number of Processes
4.13: Raman Spectroscopy
4.14: The Dynamics of Transitions can be Modeled by Rate Equations
4.15: Beer's Law
4.16: A Two-Level System Cannot Achieve a Population Inversion
4.17: Population Inversion can be Achieved in a Three-Level System
4.18: What is Inside a Laser?
4.19: The Helium-Neon Laser
4.20: Modern Applications of Laser Spectroscopy
4.21: Broadening Mechanisms

This page titled 4: Spectroscopy is shared under a not declared license and was authored, remixed, and/or curated by Jonathan Gutow.

4.1: Spectroscopic Selection Rules

4.1.1: Introduction

Once we know what energy a given transition would have, we can ask, “Which transitions between energy levels or states are possible?”

4.1.2: Calculating the transition probability

Clearly the transitions cannot violate the Pauli Exclusion Principle; that is, they cannot produce an electron configuration with three electrons in the same orbital. Besides the Pauli Exclusion Principle, there are additional restrictions that result from the nature of the interaction between electromagnetic radiation and matter. These restrictions are summarized by spectroscopic selection rules. These rules tell whether or not a transition from one state to another state is possible.

To obtain these selection rules, we consider light as consisting of perpendicular oscillating electric and magnetic fields. The magnetic field interacts with magnetic moments and causes transitions seen in electron spin resonance and nuclear magnetic resonance spectroscopies. The oscillating electric field interacts with electrical charges, i.e. the positive nuclei and negative electrons that comprise an atom or molecule, and cause the transitions seen in UV-Visible, atomic absorption, infrared and fluorescence spectroscopies.

The energy of interaction, E, between a system of charged particles and an electric field ϵ is given by the scalar product of the electric field and the dipole moment, μ, for the system. Both of these quantities are vectors.

$$E = -\mu \cdot \epsilon \tag{4.1.1}$$

The dipole moment is defined as the summation of the product of the charge q_j times the position vector r_j for all charged particles j.

$$\mu = \sum_j q_j r_j \tag{4.1.2}$$

Example 4.1.1

Calculate the dipole moment of HCl from the following information. The position vectors below use Cartesian coordinates (x, y, z), and the units are pm. What fraction of an electronic charge has been transferred from the chlorine atom to the hydrogen atom in this molecule? $r_H = (124.0, 0, 0)$, $r_{Cl} = (-3.5, 0, 0)$, $q_H = 2.70x10^{-20}C, q_{Cl} = -2.70x10^{-20}C$.

Example 4.1.2

Sketch a diagram for Exercise 4.1.1 showing the coordinate system, the HCl molecule and the dipole moment.

To calculate an expectation value for this interaction energy, we need to evaluate the expectation value integral.

$$\langle E \rangle = \int \psi_n^* (-\hat{\mu} \cdot \hat{\epsilon}) \psi_n d\tau \tag{4.1.3}$$

The $\int d\tau$ symbol simply means integrate over all coordinates. The operators $\hat{\mu}$ and $\hat{\epsilon}$ are vectors and are the same as the classical quantities, μ and ϵ.

Usually the wavelength of light used in electronic spectroscopy is very long compared to the length of a molecule. For example, the wavelength of green light is 550 nm, which is much larger than molecules, which are closer to 1 nm in size. The magnitude of electric field then is essentially constant over the length of the molecule, and ϵ can be removed from the integration since it is constant wherever ψ is not zero. In other words, ψ is finite only over the volume of the molecule, and the electric field is constant over the volume of the molecule. What remains for the integral is the expectation value for the permanent dipole moment of the molecule in state n, namely,

$$\langle \mu \rangle = \int \psi_n^* \hat{\mu} \psi_n d\tau \tag{4.1.4}$$

so

$$E = -\langle \mu \rangle \cdot \epsilon \tag{4.1.5}$$

Example 4.1.3

Verify that the vectors in the scalar product in Equation 4.1.5 commute by expanding $\mu \cdot \epsilon$ and $\epsilon \cdot \mu$. Use particle-in-a-box wave functions with HCl charges and coordinates.

Equation 4.1.5 shows that the strength or energy of the interaction between a charge distribution and an electric field depends on the dipole moment of the charge distribution.

To obtain the strength of the interaction that causes transitions between states, the transition dipole moment is used rather than the dipole moment. The transition dipole moment integral is very similar to the dipole moment integral in Equation 4.1.4 except the two wavefunctions are different, one for each of the states involved in the transition. Two different states are involved in the integral because the transition dipole moment integral has to do with the magnitude of the interaction with the electric field that causes a transition between the two states. For a transition where the state changes from ψ_i to ψ_f, the transition dipole moment integral is

$$\langle \mu \rangle_T = \int \psi_f^* \hat{\mu} \psi_i d\tau = \mu_T \tag{4.1.6}$$

Just like the probability density is given by the absolute square of the wavefunction, the probability for a transition as measured by the absorption coefficient is proportional to the absolute square $\mu_T^* \mu_T$ of the transition dipole moment, which is calculated using Equation 4.1.6. Since taking the absolute square always produces a positive quantity, it does not matter whether the transition moment itself is positive, negative, or imaginary. The transition dipole moment integral and its relationship to the absorption coefficient and transition probability can be derived from the time-dependent Schrödinger equation. Here we only want to introduce the concept of the transition dipole moment and use it to obtain selection rules and relative transition probabilities for the particle-in-a-box. Later it will be applied to other systems that we will be considering.

If $\mu_T = 0$ then the interaction energy is zero and no transition occurs or is possible between states characterized by ψ_i and ψ_f. Such a transition is said to be forbidden, or more precisely, electric-dipole forbidden. In fact, the electric-dipole electric-field interaction is only the leading term in a multipole expansion of the interaction energy, but the higher order terms in this expansion usually are not significant. It becomes important to consider the higher order terms if the light intensity is very high, as can happen with focused high power laser light. If μ_T is large, then the probability for a transition and the absorption coefficient are large.

It is very useful to be able to tell whether a transition is possible, $\mu_T \neq 0$, or not possible, $\mu_T = 0$, without having to evaluate integrals. Properties of the wavefunctions such as symmetry or angular momentum can be used to determine the conditions that must exist for the transition dipole moment to be finite, i.e. not zero. Statements called spectroscopic selection rules summarize these conditions. Selection rules do not tell us how probable or intense a transition is. They only tell us whether a transition is possible or not possible.

For the particle-in-a-box model, we need to consider the transition moment integral for one electron. According to Equation 4.1.2, the dipole moment operator for an electron in one dimension is –ex since the charge is –e and the electron is located at x.

$$\mu_T = -e \int_0^L \psi_f^*(x) x \psi_i(x) dx \tag{4.1.7}$$

This is the integral that must be evaluated for various particle-in-a-box wavefunctions to see which transitions are allowed (i.e. $\mu_T \neq 0$) and forbidden ($\mu_T = 0$) and to determine the relative strengths of the allowed transitions.

4.1.3: Using symmetry to analyze selection rules

It generally requires much work and time to evaluate integrals analytically or even numerically on a computer. Our time, computer time, and work can be saved if we can identify by inspection when integrals are zero. The determination of when integrals are zero leads to spectroscopic selection rules and provides a better understanding of them. Here we use graphs to examine properties of the wavefunctions for a particle-in-a-box to determine when the transition dipole moment integral is zero and thereby obtain the

spectroscopic selection rules for this system. These considerations are completely general and can be applied to any integrals. We essentially determine whether integrals are zero or not by drawing pictures and thinking. What could be easier?

Consider the case for a transition from orbital $n = 1$ to orbital $n = 2$ of a molecule described by the particle-in-a-box model. These two wavefunctions are shown in Figure **4.1.1** as $f1$ and $f2$, respectively. For the curves shown on the left in the figure, we defined the box to have unit length, L = 1, and infinite potential barriers at $x = 0$ and $x = L$ as we did previously, so the particle is trapped between 0 and L. For the curves shown on the right, $g1$ and $g2$, we put the origin of the coordinate system halfway between the potential barriers, i.e. at the center of the box. The barriers have not moved and the particle has not changed, but our description of the position of the barriers and the particle has changed. We now say the barriers are located at $x = -L/2$ and $x = +L/2$, and the particle is trapped between $-L/2$ and $+L/2$.

Clearly the wavefunctions in Figure **4.1.1** look the same for these two choices of coordinate systems. The appearance of the wavefunctions doesn't depend on the coordinate system we have chosen or on our labels since the wavefunctions tell us about the probability of finding the particle. This probability does not change when we change the coordinate system or relabel the axis. The names of these functions do change, however. In Figure **4.1.1***a*, they both are sine functions. In Figure **4.1.1***b*, one is a cosine function and the other is a sine function multiplied by -1.

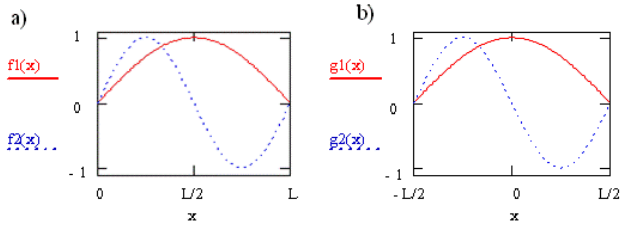


Figure **4.1.1**: Wavefunctions for quantum state n=1 and quantum state n=2 in the two different coordinate systems.

Exercise 4.1.1

Sketch $(f_1(x))^2$ and $(g_1(x))^2$. What do you observe? Sketch $(f_2(x))^2$ and $(g_2(x))^2$. What do you observe? What is the significance with respect to the probability given by both f(x) and g(x)?

We moved the origin of the coordinate system to the center of the box to take advantage of the symmetry properties of these functions. By symmetry, we mean the correspondence in form on either side of a dividing point, line, or plane. As we shall see, the analysis of the symmetry is straightforward if the origin of the coordinate systems coincides with the dividing point, line, or plane. Since the right and left halves of the box or molecule represented by the box are the same, the square of the wavefunction for x > 0 must be the same as the square of the wavefunction for x < 0. Since the box is symmetrical, the probability density, ψ^2, for the particle distribution also must be symmetrical because there is no reason for the particle to be located preferentially on one side or the other.

The transition moment integral for the particle-in-a-box involves three functions (ψ_f, ψ_i, and x) that are multiplied together at each point x to form the integrand. These three functions for i = 1 and f = 2 are plotted on the left in Figure **4.1.2**. The integrand is the product of these three functions and is shown on the right in the figure. The integral is the area between the integrand and the zero on the y-axis. Clearly this area and thus also the value of the integral is not zero. The integral is negative because ψ_2 is negative for x > 0 and x is negative for x < 0. Since $\mu_T \neq 0$, the transition from ψ_1 to ψ_2 is allowed. As we previously mentioned in this chapter, and will see again later, the absorption coefficient is proportional to the absolute square of μ_T so it is acceptable for the transition moment integral to be negative. It even could involve $\sqrt{-1}$. Taking the absolute square makes both negative and imaginary quantities positive.

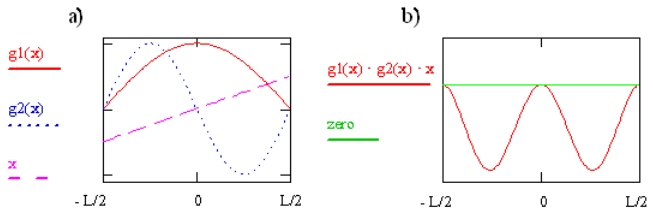


Figure **4.1.2**: Functions (a) and integrand (b) of the transition moment integral for the transition from quantum state n = 1 to quantum state n = 2.

Exercise 4.1.2

Write the expression or function for the integrand that is plotted on the right side of Figure **4.1.7** in terms of x, sine, and cosine functions. Use your function to explain why the integrand is 0 at x = 0 and has minima at x = + 0.25L and - 0.25L. Sketch the corresponding probability function.Where are the peaks in the probability function?

Now consider the transition moment integral for quantum state n = 1 to quantum state n = 3. In Figure **4.1.3**, the wavefunctions and the x operator are shown on the left side, and the integrand is shown on the right side. For this case we see that the integrand for x < 0 is the negative of the integrand for x > 0. This difference in sign means the net positive area for x > 0 is canceled by the net negative area for x < 0, so the total area and the transition moment integral are zero. We therefore conclude that the transition from n = 1 to n = 3 is forbidden.

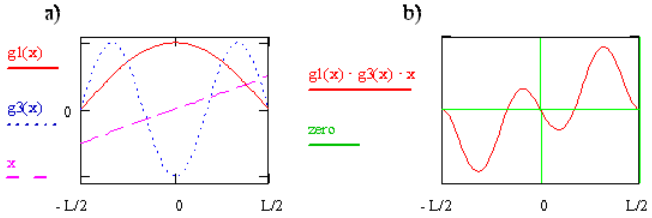


Figure **4.1.3**: Functions (a) and integrand (b) of the transition moment integral for the transition from quantum state n = 1 to quantum state n = 3.

Exercise 4.1.3

Write the expression or function for the integrand that is plotted on the right side of Figure **4.1.8** in terms of x and cosine functions. Use your function to explain why the integrand is zero at x = 0, why is it negative just above x = 0, and why as x goes from 0 to –0.5, the integrand first is positive and then negative.

In spectroscopy some special terms are used to describe the symmetry properties of wavefunctions. The terms symmetric, **gerade**, and even describe functions like $f(x) = x^2$ and $\psi_1(x)$ for the particle-in-a-box that have the property $f(x) = f(-x)$, i.e. the function has the same values for x > 0 and for x < 0. The terms antisymmetric, **ungerade**, and odd describe functions like $f(x) = x$ and $\psi_2(x)$ for the particle-in-a-box that have the property $f(x) = -f(-x)$, i.e. the function for $x > 0$ is has values that are opposite in sign compared to the function for x < 0. Gerade and ungerade are German words meaning even and odd and are abbreviated as g and u. Note that antisymmetric does not mean non-symmetric.

If an integrand is u, then the integral is zero! It is zero because the contribution from $x > 0$ is cancelled by the contribution from $x < 0$, as shown by the example in Figure **4.1.8**. An integrand will be u if the product of the functions comprising it is u. The following rules make it possible to quickly identify whether a product of two functions is u.

$$g \cdot g = g, u \cdot u = g, g \cdot u = u \tag{4.1.8}$$

These rules are the same as those for multiplying +1 for g and -1 for u. The validity of these rules can be seen by examining Figures **4.1.1** and **4.1.1**. If an integrand consists of more than two functions, the rules are applied to pairs of functions to obtain the

symmetry of their product, and then applied to pairs of the product functions, and so forth, until one obtains the symmetry of the integrand.

Exercise 4.1.4

Use Mathcad or some other software to draw graphs of $x^2, -x^2, x^3, and -x^3$ as a function of x. Which of these functions are g and which are u? Is the product function $x^2 \cdot x^3 g$ or u? How about $x^2 \cdot -x^2 \cdot x^3 and x^2 \cdot x^3 \cdot -x^3$?

Exercise 4.1.5

Label each function in Figures Figure 4.1.2 and Figure 4.1.3 as g or u. Also label the integrands.

Exercise 4.1.6

Use symmetry arguments to determine which of the following transitions between quantum states are allowed for the particle-in-a-box:

a. $n = 2$ to $n = 3$
b. $n = 2$ to $n = 4$.

Symmetry properties of functions allow us to identify when the transition moment integral and other integrals are zero. This symmetry-based approach to integration can be generalized and becomes even more powerful when concepts taken from mathematical Group Theory are used. With the tools of Group Theory, one can examine symmetry properties in three-dimensional space for complicated molecular structures. A group-theoretical analysis helps understand features in molecular spectra, predict products of chemical reactions, and simplify theoretical calculations of molecular structures and properties.

4.1.4: Atomic selection rules

The selection rules for promoting a single electron moving from one atomic orbital to another via the absorption or emission of light are

$$\Delta l = \pm 1 \text{ and } \Delta m_l = 0, \pm 1 \tag{4.1.9}$$

These selection rules arise from the conservation fo angular momentum during a spectroscopic transition and the fact that a photon has a spin 1.

These basic selection rules are complicated by the fact that the orbital angular momentum l and the spin angular momentum are actually coupled. Although that coupling is important for understanding the details of atomic spectroscopy we will ignore this coupling. This coupling gets very complicated as atoms get heavier because the many electron interactions make our orbital approximation worse and thus the quantum number l, based on the hydrogen atom model, is no longer a good quantum number. Up to the point where the validity of the l quantum number breaks down the states are historically labeled by what are called **term symbols** such as $^2P_{1/2}$, where the left superscript describes the multiplicity of the state (2S + 1) , 'P' the total angular momentum (L = 1, like a p orbital. If L = 0 we would use 'S') and the subscript indicates the particular vector sum of L and S.

Sodium D Line

One notable atomic spectral line of sodium vapor is the so-called D-line, which may be observed directly as the sodium flame-test line and also the major light output of low -pressure sodium lamps (these produce pressure sodium lamps (these produce an unnatural yellow). The D-line is one of the classified Fraunhofer lines in Sodium vapor in the upper layers of lines. Sodium vapor in the upper layers of the sun creates a dark line in the emitted spectrum of electromagnetic radiation by absorbing visible light in a band of wavelengths around 589.5 nm. This wavelength corresponds to transitions in atomic sodium in which the valence-electron transitions from a 3s to 3p electronic state. This is allowed because $\Delta l = +1 = \ell_p - \ell_s = 1 - 0$.

Closer examination of the visible spectrum of atomic sodium reveals that the D-line actually consists of two lines called the D_1 and D_2 lines at 589 6 nm and 589.0 nm, respectively. The splitting between these lines arises because of spin-orbit coupling. Na has one unpaired electron ($S = ½$), with possible spin angular momentums of +1/2 and - 1/2. If we consider the $S \rightarrow P$

transition, then for the excited state, P, we have $L = 1$. Thus, there are two possibilities for the total L + S, often called J $J = 3/2$ or $J = 1/2$.

Applying the simple selection rules (equation 4.1.9), we can specify which transitions can occur. For example consider an electron in the 3s orbital transitioning to the 3d orbital. This would require l = 0 going to l = 2, this yields $\Delta l = 2$ so is not allowed, because the absorption of a photon only provides 1 unit of angular momentum not 2. On the other had it would be possible to go from a 3p (l = 1) to the 3d (l = 2). However, it is not possible to go from any p-orbital to any d-orbital. Consider starting in the p-orbital specified by $m_l = -1$. The selection rules require that $\Delta m_l = 0, \pm 1$. Thus the final m_l values that are possible are: $m_l = -2, -1 and 0$. Thus the d-orbitals with (m_l = 1 and 2\) are not accessible via a single photon absorption from the p, $m_l = -1$ state. The restrictions based on m_l are illustrated in the figure below.

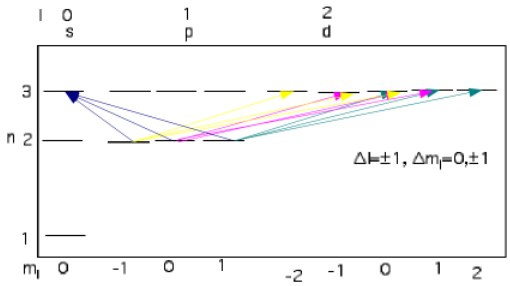


Figure 4.1.4: A diagram (Grotrain diagram) indicating the allowed single photon excitations (absorptions) from the 2p orbitals going to orbitals in the n = 3 shell. Notice that because of the $\Delta l = \pm 1$ constraint the final states must be s or d orbitals. They cannot be p orbitals. The $\Delta m_l = 0, \pm 1$ constraint means that any of the p's can end up in the s orbital, but each p can only go to 3 of the 5 d's.

This page titled 4.1: Spectroscopic Selection Rules is shared under a CC BY-NC-SA 4.0 license and was authored, remixed, and/or curated by Jonathan Gutow.

- **4.5: The Transition Dipole Moment and Spectroscopic Selection Rules** by David M. Hanson, Erica Harvey, Robert Sweeney, Theresa Julia Zielinski is licensed CC BY-NC-SA 4.0. Original source: https://web.archive.org/web/20200619182410/http://www.chemeddl.org.
- **4.7: Using Symmetry to Identify Integrals that are Zero** by David M. Hanson, Erica Harvey, Robert Sweeney, Theresa Julia Zielinski is licensed CC BY-NC-SA 4.0. Original source: https://web.archive.org/web/20200619182410/http://www.chemeddl.org.
- **8.11: Using Atomic Term Symbols to Interpret Atomic Spectra** by David M. Hanson, Erica Harvey, Robert Sweeney, Theresa Julia Zielinski is licensed CC BY-NC-SA 4.0.

4.2: Rotational Spectroscopy of Diatomic Molecules

The permanent electric dipole moments of polar molecules can couple to the electric field of electromagnetic radiation. This coupling induces transitions between the rotational states of the molecules. The energies that are associated with these transitions are detected in the far infrared and microwave regions of the spectrum. For example, the microwave spectrum for carbon monoxide shown below in figure **4.2.1** spans a frequency range of 100 to 1200 GHz, which corresponds to 3 - 40 cm^{-1}.

The selection rules for the rotational transitions are derived from the transition moment integral by using the spherical harmonic functions and the appropriate dipole moment operator, $\hat{\mu}$.

$$\mu_T = \int Y_{J_f}^{m_f *} \hat{\mu} Y_{J_i}^{m_i} \sin\theta \, d\theta \, d\varphi \tag{4.2.1}$$

Evaluating the transition moment integral involves a bit of mathematical effort. This evaluation reveals that the transition moment depends on the square of the dipole moment of the molecule, μ^2 and the rotational quantum number, J, of the initial state in the transition,

$$\mu_T = \mu^2 \frac{J+1}{2J+1} \tag{4.2.2}$$

and that the selection rules for rotational transitions are

$$\Delta J = \pm 1 \tag{4.2.3}$$

$$\Delta m_J = 0, \pm 1 \tag{4.2.4}$$

For $\Delta J = +1$, a photon is absorbed; for $\Delta J = -1$ a photon is emitted.

Exercise 4.2.1

Explain why your microwave oven heats water but not air. Hint: draw and compare Lewis structures for components of air and for water.

The energies of the rotational levels are given by Equation 4.2.5,

$$E = J(J+1)\frac{\hbar^2}{2I} \tag{4.2.5}$$

and each energy level has a degeneracy of $2J+1$ due to the different m_J values.

Exercise 4.2.2

Use the rotational energy level diagram for $J = 0$, $J = 1$, and $J = 2$ that you produced in Exercise **4.2.9**, and add arrows to show all the allowed transitions between states that cause electromagnetic radiation to be absorbed or emitted.

4.2.1: Transition Energies

The transition energies for absorption of radiation are given by

$$E_{photon} = \Delta E_{states} \tag{4.2.6}$$

$$= E_f - E_i \tag{4.2.7}$$

$$= h\nu \tag{4.2.8}$$

$$= hc\bar{\nu} \tag{4.2.9}$$

Substituted Equation 4.2.5 into Equation 4.2.9

$$h\nu = hc\bar{\nu} \tag{4.2.10}$$

$$= J_f(J_f+1)\frac{\hbar^2}{2I} - J_i(J_i+1)\frac{\hbar^2}{2I} \tag{4.2.11}$$

Since microwave spectroscopists use frequency, and infrared spectroscopists use wavenumber units when describing rotational spectra and energy levels, both ν and $\bar{\nu}$ are included in Equation 4.2.11, and J_i and J_f are the rotational quantum numbers of the initial (lower) and final (upper) levels involved in the absorption transition. When we add in the constraints imposed by the selection rules, J_f is replaced by $J_i + 1$, because the selection rule requires $J_f - J_i = 1$ for absorption. The equation for absorption transitions then can be written in terms of the quantum number J_i of the initial level alone.

$$h\nu = hc\bar{\nu} = 2(J_i + 1)\frac{\hbar^2}{2I} \tag{4.2.12}$$

Divide Equation 4.2.12 by h to obtain the frequency of the allowed transitions,

$$\nu = 2B(J_i + 1) \tag{4.2.13}$$

where B, the rotational constant for the molecule, is defined as

$$B = \frac{\hbar^2}{2hI} \tag{4.2.14}$$

Exercise 4.2.3

Complete the steps going from Equation 4.2.11 to Equation 4.2.14 and identify the units of B at the end.

Exercise 4.2.4

Infrared spectroscopists use units of wave numbers. Rewrite the steps going from Equation 4.2.11 to Equation 4.2.14 to obtain expressions for $\hbar\nu$ and B in units of wave numbers. Note that to convert B in Hz to B in cm^{-1}, you simply divide the former by c.

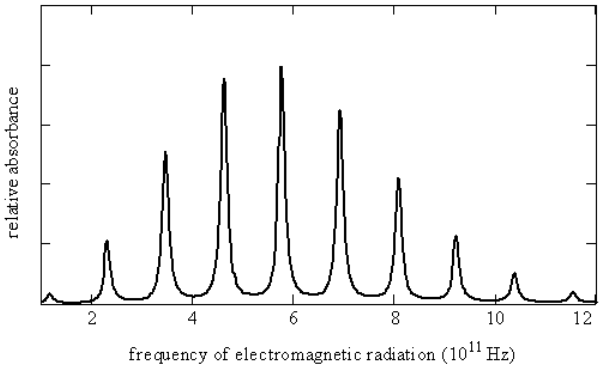


Figure 4.2.1 shows the rotational spectrum of $^{12}{}^{16}CO$ as a series of nearly equally spaced lines. The line positions ν_J, line spacings, and the maximum absorption coefficients (γ_{max}), the absorption coefficients associated with the specified line position) for each line in this spectrum are given here in Table 4.2.1.

Table 4.2.1: Rotational Transitions in $^{12}{}^{16}CO$ at 40 K

J	ν_J(MHz)	Spacing from previous line(MHz)	γ_{max}
0	115,271.21	0	0.0082
1	230,538.01	115,266.80	0.0533
2	345,795.99	115,257.99	0.1278
3	461,040.76	115,244.77	0.1878
4	576,267.91	115,227.15	0.1983
5	691,473.03	115,205.12	0.1618
6	806,651.78	115,178.68	0.1064
7	921,799.55	115,147.84	0.0576
8	1,036,912.14	115,112.59	0.0262
9	1,151,985.08	115,072.94	0.0103

Let's try to reproduce Figure **4.2.1** from the data in Table **4.2.1** by using the quantum theory that we have developed so far. Equation **4.2.13** predicts a pattern of exactly equally spaced lines. The lowest energy transition is between $J_i = 0$ and $J_f = 1$ so the first line in the spectrum appears at a frequency of $2B$. The next transition is from $J_i = 1$ to $J_f = 2$ so the second line appears at $4B$. The spacing of these two lines is 2B. In fact the spacing of all the lines is $2B$ according to this equation, which is consistent with the data in Table **4.2.1** showing that the lines are very nearly equally spaced. The difference between the first spacing and the last spacing is less than 0.2%.

Exercise 4.2.5

Use Equation **4.2.13** to prove that the spacing of any two lines in a rotational spectrum is $2B$. That is, derive $\nu_{J_i+1} - \nu_{J_i} = 2B$.

4.2.2: Non-Rigid Rotor Effects

Centrifugal stretching of the bond as J increases causes the decrease in the spacing between the lines in an observed spectrum. This decrease shows that the molecule is not really a rigid rotor. As the rotational angular momentum increases with increasing J, the bond stretches. This stretching increases the moment of inertia and decreases the rotational constant. Centrifugal stretching is exactly what you see if you swing a ball on a rubber band in a circle (Figure **4.2.1**).



Figure **4.2.1**: In the absence of the spring, the particles would fly apart. However, the force exerted by the extended spring pulls the particles onto a periodic, oscillatory path. (CC BY-SA 3.0; Cleonis).

The effect of centrifugal stretching is smallest at low J values, so a good estimate for B can be obtained from the $J = 0$ to $J = 1$ transition. From B, a value for the bond length of the molecule can be obtained since the moment of inertia that appears in the definition of B, Equation **4.2.14**, is the reduced mass times the bond length squared.

Exercise 4.2.6

Use the frequency of the $J = 0$ to $J = 1$ transition observed for carbon monoxide to determine a bond length for carbon monoxide.

When the centrifugal stretching is taken into account quantitatively, the development of which is beyond the scope of the discussion here, a very accurate and precise value for B can be obtained from the observed transition frequencies because of their high precision. Rotational transition frequencies are routinely reported to 8 and 9 significant figures.

As we have just seen, quantum theory successfully predicts the line spacing in a rotational spectrum. An additional feature of the spectrum is the line intensities. The lines in a rotational spectrum do not all have the same intensity, as can be seen in Figure 4.2.1.1 and Table 4.2.1. The maximum absorption coefficient for each line, γ_{max}, is proportional to the magnitude of the transition moment, μ_T which is given by Equation 4.2.2, and to the population difference between the initial and final states, Δn. Since Δn is the difference in the number of molecules present in the two states per unit volume, it is actually a difference in number density.

$$\gamma_{max} = C_{\mu T} \cdot \Delta n \tag{4.2.15}$$

where $C_{\mu T}$ includes constants obtained from a more complete derivation of the interaction of radiation with matter.

The dependence on the number of molecules in the initial state is easy to understand. For example, if no molecules were in the $J = 7$, $m_J = 0$ state, no radiation could be absorbed to produce a $J = 7$, $m_J = 0$ to $J = 8$, $m_J = 0$ transition. The dependence of the line intensity on the population of the final state is explained in the following paragraphs.

When molecules interact with an electromagnetic field (i.e., a photon), they can be driven from one state to another with the absorption or emission of energy. Usually there are more molecules in the lower energy state and the absorption of radiation is observed as molecules go from the lower state to the upper state. This situation is the one we have encountered up to now. In some situations, there are more molecules in the upper state and the emission of radiation is observed as molecules are driven from the upper state to the lower state by the electromagnetic field. This situation is called population inversion, and the process is called stimulated emission. Stimulated emission is the reason lasers are possible. Laser is an acronym for light amplification by stimulated emission of radiation. Even in the absence of an electromagnetic field, atoms and molecules can lose energy spontaneously and decay from an upper state to a lower energy state by emitting a photon. This process is called spontaneous emission. Stimulated emission therefore can be thought of as the inverse of absorption because both processes are driven by electromagnetic radiation, i.e. the presence of photons.

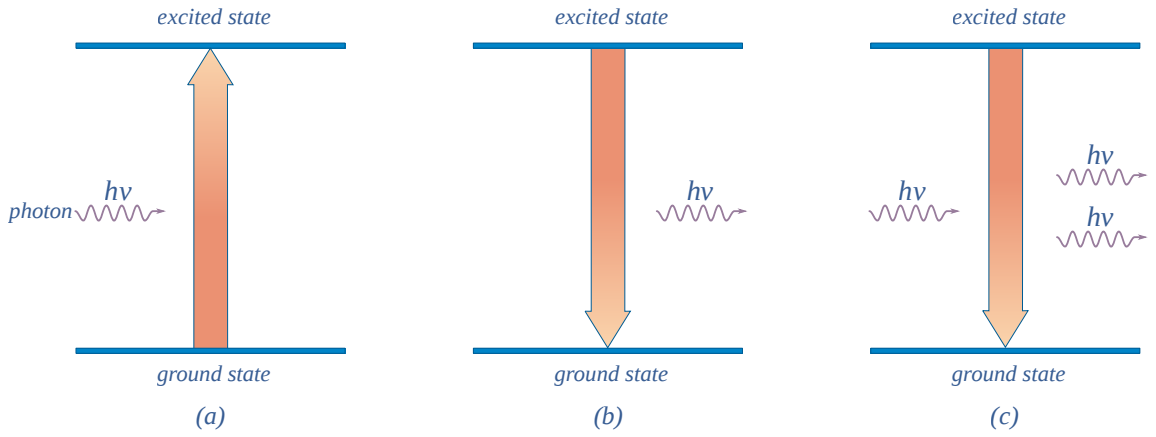


Figure 4.2.2: a) In absorption, an incident photon $h\nu$ is absorbed by the system and drives the system from the ground state to an excited state. b) In spontaneous emission, a photon is produced when the system goes from an excited state to the ground state. c) In stimulated emission, an incident photon is not absorbed, but drives the system from an excited state to the ground state, accompanied by release of a second photon.

Whether absorption or stimulated emission is observed when electromagnetic radiation interacts with a sample depends upon the population difference, Δn, of the two states involved in the transition. For a rotational transition,

$$\Delta n = n_J - n_{J+1} \tag{4.2.16}$$

where n_J represents the number of molecules in the lower state and n_{J+1} represents the number in the upper state per unit volume. If this difference is 0, there will be no net absorption or stimulated emission because they exactly balance. If this difference is positive, absorption will be observed; if it is negative, stimulated emission will be observed.

We can develop an expression for Δn that uses only the population of the initial state, n_J, and the Boltzmann factor. The Boltzmann factor allows us to calculate the population of a higher state given the population of a lower state, the energy gap between the states and the temperature. Multiply the right-hand side of Equation 4.2.16 by n_J/n_J to obtain

$$\Delta n = \left(1 - \frac{n_{J+1}}{n_J}\right) n_J \tag{4.2.17}$$

Next recognize that the ratio of populations of the states is given by the Boltzmann factor which when substituted into yields

$$\Delta n = \left(1 - e^{\frac{-h\nu_J}{kT}}\right) n_J \tag{4.2.18}$$

where $h\nu_J$ is the energy difference between the two states. For the rigid rotor model

$$\nu_J = 2B(J+1) \tag{4.2.19}$$

so Equation 4.2.18 can be rewritten as

$$\Delta n = \left(1e^{\frac{-2hB(J+1)}{kT}}\right) n_J \tag{4.2.20}$$

Equation expresses the population difference between the two states involved in a rotational transition in terms of the population of the initial state, the rotational constant for the molecule, B, the temperature of the sample, and the quantum number of the initial state.

To get the number density of molecules present in the initial state involved in the transition, n_J, we multiply the fraction of molecules in the initial state, F_J, by the total number density of molecules in the sample, n_{total}.

$$n_J = F_J \cdot n_{total} \tag{4.2.21}$$

The fraction F_J is obtained from the rotational partition function.

$$F_J = (2J+1)\left(\frac{hB}{kT}\right)\left(e^{\frac{-2hB(J+1)}{kT}}\right) \tag{4.2.22}$$

The exponential is the Boltzmann factor that accounts for the thermal population of the energy states. The factor $2J+1$ in this equation results from the degeneracy of the energy level. The more states there are at a particular energy, the more molecules will be found with that energy. The (hB/kT) factor results from normalization to make the sum of F_J over all values of J equal to 1. At room temperature and below only the ground vibrational state is occupied; so all the molecules (n_{total}) are in the ground vibrational state. Thus the fraction of molecules in each rotational state in the ground vibrational state must add up to 1.

Exercise 4.2.7

Show that the numerator, $J(J+1)hB$ in the exponential of Equation 4.2.22 is the energy of level J.

Exercise 4.2.8: Hydrogen Chloride

Calculate the relative populations of the lowest ($J = 0$) and second ($J = 1$) rotational energy level in the HCl molecule at room temperature. Do the same for the lowest and second vibrational levels of HCl. Compare the results of these calculations. Are Boltzmann populations important to vibrational spectroscopy? Are Boltzmann populations important for rotational spectroscopy?

Now we put all these pieces together and develop a master equation for the maximum absorption coefficient for each line in the rotational spectrum, which is identified by the quantum number, J, of the initial state. Start with Equation 4.2.15 and replace μ_T using Equation 4.2.2.

$$\gamma_{max} = C\left(\mu^2 \frac{J+1}{2J+1}\right) \cdot \Delta n \tag{4.2.23}$$

Then replace Δn using Equation 4.2.20.

$$\gamma_{max} = C\left(\mu^2 \frac{J+1}{2J+1}\right)\left(e^{\frac{-2hB(J+1)}{kT}}\right) n_J \tag{4.2.24}$$

Finally replace nJ using Equations 4.2.21 and 4.2.22 to produce

$$= C\left[\mu^2 \frac{J+1}{2J+1}\right]\left[e^{\frac{-2hB(J+1)}{kT}}\right]\left[(2J+1)\left(\frac{hB}{kT}\right)\left(e^{\frac{-2hB(J+1)}{kT}}\right)\right]^{\gamma_{max}} n_{total} \tag{4.2.25}$$

Equation 4.2.25 enables us to calculate the relative maximum intensities of the peaks in the rotational spectrum shown in Figure 4.2.2, assuming all molecules are in the lowest energy vibrational state, and predict how this spectrum would change with temperature. The constant C includes the fundamental constants ϵ_o, c and h, that follow from a more complete derivation of the interaction of radiation with matter. The complete theory also can account for the line shape and width and includes an additional radiation frequency factor.

$$C = \frac{2\pi}{3\epsilon_0 ch} \tag{4.2.26}$$

In the spectrum shown in Figure 4.2.1.1, the absorption coefficients for each peak first increase with increasing J because the difference in the populations of the states increases and the factor $(J+1)$ increases. Notice that the denominator in the factor resulting from the transition moment cancels the degeneracy factor $2J+1$. After the maximum the second Boltzmann factor, which is a decreasing exponential as J increases, dominates, and the intensity of the peaks drops to zero. Exploration of how well Equation 4.2.25 corresponds to the data in Table 4.2.1 and discovering how a rotational spectrum changes with temperature are left to an end-of-the-chapter activity.

Exercise 4.2.9

Why does not the first Boltzmann factor in Equation 4.2.25 cause the intensity to drop to zero as J increases.

This page titled 4.2: Rotational Spectroscopy of Diatomic Molecules is shared under a CC BY-NC-SA 4.0 license and was authored, remixed, and/or curated by David M. Hanson, Erica Harvey, Robert Sweeney, Theresa Julia Zielinski via source content that was edited to the style and standards of the LibreTexts platform.

- **7.6: Rotational Spectroscopy of Diatomic Molecules** by David M. Hanson, Erica Harvey, Robert Sweeney, Theresa Julia Zielinski is licensed CC BY-NC-SA 4.0. Original source: https://web.archive.org/web/20200619182410/http://www.chemeddl.org.

4.3: Rotational Spectra of Polyatomic Molecules

Quick Review of Diatomic Rotation

As discussed previously, the Schrödinger equation for the angular motion of a rigid (i.e., having fixed bond length R) diatomic molecule is

$$\frac{\hbar^2}{2\mu}\left[\frac{1}{R^2\sin\theta}\frac{\partial}{\partial\theta}\left(\sin\theta\frac{\partial}{\partial\theta}\right)+\frac{1}{R^2\sin^2\theta}\frac{\partial^2}{\partial\varphi^2}\right]|\psi\rangle = E|\psi\rangle$$

or

$$\frac{L^2}{2\mu R^2}|\psi\rangle = E|\psi\rangle$$

The Hamiltonian in this problem contains only the kinetic energy of rotation; no potential energy is present because the molecule is undergoing unhindered "free rotation". The angles θ and φ describe the orientation of the diatomic molecule's axis relative to a laboratory-fixed coordinate system, and μ is the reduced mass of the diatomic molecule

$$\mu = \frac{m_1 m_2}{m_1 + m_2}$$

The eigenvalues corresponding to each eigenfunction are straightforward to find because H_{rot} is proportional to the L^2 operator whose eigenvalues have already been determined. The resultant rotational energies are given as:

$$E_J = \frac{\hbar^2 J(J+1)}{2\mu R^2} = BJ(J+1) \tag{4.3.1}$$

and are independent of M. B is the rotational constant. Thus each energy level is labeled by J and is $2J+1$-fold degenerate (because M ranges from $-J$ to J). The rotational energy in Equation 4.3.1 can be expressed in terms of the moment of inertia I

$$I = \sum_i m_i R_i^2 \tag{4.3.2}$$

where m_i is the mass of the ith atom and R is its distance from the center of mass of the molecule. This moment of inertia replaces μR^2 in the denominator of Equation 4.3.1:

$$E_J = \frac{\hbar^2 J(J+1)}{2I} = BJ(J+1) \tag{4.3.3}$$

4.3.1: Rotation of Polyatomic Molecules

In contrast to diatomic molecules (Equation 4.3.2), the rotational motions of polyatomic molecules in three dimensions are characterized by multiple moments of inertia. typically reflected in an 3×3 inertia tensor. It is common in rigid body mechanics to express in these moments of inertia in *lab-based Cartesian coordinates* via a notation that explicitly identifies the x, y, and z axes such as I_{xx} and I_{xy}, for the components of the inertia tensor.

$$I = \begin{bmatrix} I_{xx} & I_{xy} & I_{xz} \\ I_{yx} & I_{yy} & I_{yz} \\ I_{xx} & I_{xy} & I_{zz} \end{bmatrix} \tag{4.3.4}$$

The components of this tensor can be assembled into a matrix given by

$$I_{xx} = \sum_{k=1}^{N} m_k(y_k^2 + z_k^2)$$

$$I_{yy} = \sum_{k=1}^{N} m_k(x_k^2 + z_k^2)$$

$$I_{zz} = \sum_{k=1}^{N} m_k (x_k^2 + y_k^2)$$

$$I_{yx} = I_{xy} = -\sum_{k=1}^{N} m_k x_k y_k$$

$$I_{zx} = I_{xz} = -\sum_{k=1}^{N} m_k x_k z_k$$

$$I_{zy} = I_{yz} = -\sum_{k=1}^{N} m_k y_k z_k.$$

The rotational motions of polyatomic molecules are characterized by moments of inertia that are defined in a *molecule based coordinates* with axes that are labeled a, b, and c. Measured in the body frame the inertia matrix (Equation 4.3.4) is a constant real symmetric matrix, which can be decomposed into a diagonal matrix, given by

$$I = \begin{pmatrix} I_a & 0 & 0 \\ 0 & I_b & 0 \\ 0 & 0 & I_c \end{pmatrix}$$

These labels are assigned so that I_c is the **largest** principal moment of inertia with an order of the three moments set as

$$I_a < I_b < I_c$$

The rotational kinetic energy operator for a rigid non-linear polyatomic molecule is then expressed as

$$H_{rot} = \frac{J_a^2}{2I_a} + \frac{J_b^2}{2I_b} + \frac{J_c^2}{2I_c} \tag{4.3.5}$$

The components of the quantum mechanical angular momentum operators along the three principal axes are:

$$J_a = -i\hbar \cos\chi \left[\cot\theta \frac{\partial}{\partial\chi} - (\sin\theta)^{-1} \frac{\partial}{\partial\varphi} \right] - -i\hbar \sin\chi \frac{\partial}{\partial\theta} \tag{4.3.6}$$

$$J_b = i\hbar \sin\chi \left[\cot\theta \frac{\partial}{\partial\chi} - (\sin\theta)^{-1} \frac{\partial}{\partial\varphi} \right] - -i\hbar \cos\chi \frac{\partial}{\partial\theta} \tag{4.3.7}$$

$$J_c = -\frac{ih\partial}{\partial\chi} \tag{4.3.8}$$

The angles θ, φ, and χ are the **Euler angles** needed to specify the orientation of the rigid molecule relative to a laboratory-fixed coordinate system. The corresponding square of the total angular momentum operator J^2 can be obtained as

$$J^2 = J_a^2 + J_b^2 + J_c^2 \tag{4.3.9}$$

$$= -\frac{\partial^2}{\partial\theta^2} - \cot\theta \frac{\partial}{\partial\theta} - \left(\frac{1}{\sin\theta} \right) \left(\frac{\partial^2}{\partial\varphi^2} + \frac{\partial^2}{\partial\chi^2} - 2\cos\theta \frac{\partial^2}{\partial\varphi\partial\chi} \right) \tag{4.3.10}$$

and the component along the lab-fixed Z axis is

$$J_Z = -ih \frac{\partial}{\partial\varphi}.$$

4.3.2: Spherical Tops

When the three principal moment of inertia values are identical, the molecule is termed a spherical top. In this case, the total rotational energy Equation 4.3.5 can be expressed in terms of the total angular momentum operator J^2

$$H_{rot} = \frac{J^2}{2I}$$

As a result, the eigenfunctions of H_{rot} are those of J^2 (and J_a as well as J_Z both of which commute with J_2 and with one another; J_Z is the component of J along the lab-fixed Z-axis and commutes with J_a because

$$J_Z = -ih\frac{\partial}{\partial\varphi}$$

and

$$J_a = -ih\frac{\partial}{\partial\chi}$$

act on different angles. The energies associated with such eigenfunctions are

$$E(J,K,M) = \frac{\hbar^2 J(J+1)}{2I^2}$$

for all K (i.e., J a quantum numbers) ranging from -J to J in unit steps and for all M (i.e., J Z quantum numbers) ranging from -J to J. Each energy level is therefore $(2J+1)^2$ degenarate because there are $2J+1$ possible K values and $2J+1$ possible M values for each J. The eigenfunctions of J^2, J_Z and J_a, $|J,M,K>$ are given in terms of the set of rotation matrices $D_{J,M,K}$:

$$|J,M,K\rangle = \sqrt{\frac{2J+1}{8\pi^2}} D^*_{J,M,K}(\theta,\varphi,\chi)$$

which obey

$$J^2|J,M,K\rangle = \hbar^2 J(J+1)|J,M,K\rangle$$

$$J_a|J,M,K\rangle = \hbar K|J,M,K\rangle$$

$$J_Z|J,M,K\rangle = \hbar M|J,M,K\rangle$$

4.3.3: Symmetric Tops

Symmetrical tops are molecules with two rotational axes that have the same inertia and one unique rotational axis with a different inertia. Symmetrical tops can be divided into two categories based on the relationship between the inertia of the unique axis and the inertia of the two axes with equivalent inertia. If the unique rotational axis has a greater inertia than the degenerate axes the molecule is called an **oblate symmetrical top** (Figure 13.8.1). If the unique rotational axis has a lower inertia than the degenerate axes the molecule is called a **prolate symmetrical top**. For simplification think of these two categories as either frisbees for oblate tops or footballs for prolate tops.

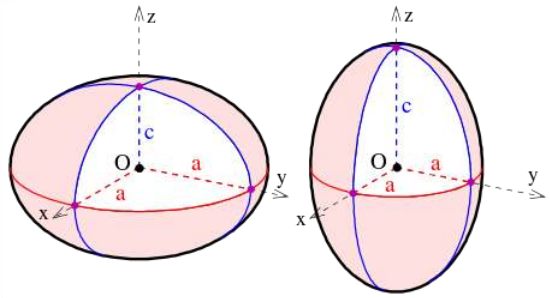


Figure 13.8.1 : The assignment of semi-axes on a spheroid. It is oblate if $c < a$ (left) and prolate if $c > a$ (right). (CC BY-SA 4.0; Ag2gaeh)

Again, the rotational kinetic energy, which is the full rotational Hamiltonian, can be written in terms of the total rotational angular momentum operator J^2 and the component of angular momentum along the axis with the unique principal moment of inertia.

For prolate tops, Equation 4.3.5 becomes

$$H_{rot} = \frac{J^2}{2I} + J_a^2\left(\frac{1}{2I_a} - \frac{1}{2I}\right)$$

For oblate tops, Equation 4.3.5 becomes

$$H_{rot} = \frac{J^2}{2I} + J_c^2\left(\frac{1}{2I_c} - \frac{1}{2I}\right)$$

As a result, the eigenfunctions of H_{rot} are those of J^2 and J_a or J_c (and of J_Z), and the corresponding energy levels.

The energies for prolate tops are

$$E(J,K,M) = \frac{h^2 J(J+1)}{2I^2} + h^2 K^2 \left(\frac{1}{2I_a} - \frac{1}{2I}\right)$$

and the energies for oblate tops are

$$E(J,K,M) = \frac{h^2 J(J+1)}{2I2} + h^2 K^2 \left(\frac{1}{2I_c} - \frac{1}{2I}\right)$$

again for K and M (i.e., J_a or J_c and J_Z quantum numbers, respectively) ranging from $-J$ to J in unit steps. Since the energy now depends on K, these levels are only $2J+1$ degenerate due to the $2J+1$ different M values that arise for each J value. The eigenfunctions $|J,M,K>$ are the same rotation matrix functions as arise for the spherical-top case.

4.3.4: Asymmetric Tops

The rotational eigenfunctions and energy levels of a molecule for which all three principal moments of inertia are distinct (a **asymmetric top**) can not easily be expressed in terms of the angular momentum eigenstates and the J, M, and K quantum numbers. However, given the three principal moments of inertia I_a, I_b, and I_c, a matrix representation of each of the three contributions to the general rotational Hamiltonian in Equation 4.3.5 can be formed within a basis set of the $\{|J,M,K\rangle\}$ rotation matrix functions. This matrix will **not** be diagonal because the $|J,M,K\rangle$ functions are not eigenfunctions of the asymmetric top H_{rot}. However, the matrix can be formed in this basis and subsequently brought to diagonal form by finding its eigenvectors {C n, J,M,K } and its eigenvalues $\{E_n\}$. The vector coefficients express the asymmetric top eigenstates as

$$\psi_n(\theta,\varphi,\chi) = \sum_{J,M,K} C_{n,J,M,K} |J,M,K\rangle$$

Because the total angular momentum J^2 still commutes with H_{rot}, each such eigenstate will contain only one J-value, and hence Ψ_n can also be labeled by a J quantum number:

$$\psi_{n,J}(\theta,\varphi,\chi) = \sum_{M,K} C_{n,J,M,K} |J,M,K\rangle$$

To form the only non-zero matrix elements of H_{rot} within the $|J,M,K\rangle$ basis, one can use the following properties of the rotation-matrix functions:

$$\langle j,\rangle = \langle j,\rangle = 1/2 < j,\rangle = h2[J(J+1) - K2],$$

$$\langle j,\rangle = h^2 K^2$$

$$\langle j\rangle = -\langle j\rangle = h^2[J(J+1) - K(K\pm1)]1/2[J(J+1) - (K\pm1)(K\pm2)]1/2\langle j\rangle = 0$$

Each of the elements of J_c^2, J_a^2, and J_b^2 must, of course, be multiplied, respectively, by $1/2I_c$, $1/2I_a$, and $1/2I_b$ and summed together to form the matrix representation of H_{rot}. The diagonalization of this matrix then provides the asymmetric top energies and wavefunctions.

This page titled 4.3: Rotational Spectra of Polyatomic Molecules is shared under a CC BY-NC-SA 4.0 license and was authored, remixed, and/or curated by Jack Simons.

- **13.8: Rotational Spectra of Polyatomic Molecules** by Jack Simons is licensed CC BY-NC-SA 4.0.

4.4: Harmonic Oscillator

4.4.1: Introduction

The harmonic oscillator is a model which has several important applications in both classical and quantum mechanics. It serves as a prototype in the mathematical treatment of such diverse phenomena as elasticity, acoustics, AC circuits, molecular and crystal vibrations, electromagnetic fields and optical properties of matter.

4.4.2: Classical Oscillator

A simple realization of the harmonic oscillator in classical mechanics is a particle which is acted upon by a restoring force proportional to its displacement from its equilibrium position. Considering motion in one dimension, this means

$$F = -kx \tag{4.4.1}$$

Such a force might originate from a spring which obeys Hooke's law, as shown in Figure **4.4.1**. According to Hooke's law, which applies to real springs for sufficiently small displacements, the restoring force is proportional to the displacement—either stretching or compression—from the equilibrium position.

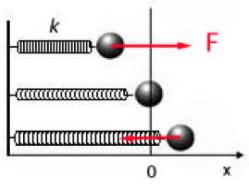


Figure **4.4.1**: Spring obeying Hooke's law.

The *force constant* k is a measure of the stiffness of the spring. The variable x is chosen equal to zero at the equilibrium position, positive for stretching, negative for compression. The negative sign in Equation 4.4.1 reflects the fact that F is a *restoring* force, always in the opposite sense to the displacement x.

Applying Newton's second law to the force from Equation 4.4.1, we find x

$$F = m\frac{d^2x}{dx^2} = -kx \tag{4.4.2}$$

where m is the mass of the body attached to the spring, which is itself assumed massless. This leads to a differential equation of familiar form, although with different variables:

$$\ddot{x}(t) + \omega^2 x(t) = 0 \tag{4.4.3}$$

with

$$\omega^2 \equiv \frac{k}{m} \tag{4.4.4}$$

The dot notation (introduced by Newton himself) is used in place of primes when the independent variable is time. The general solution to Equation 4.4.3 is

$$x(t) = A\sin\omega t + B\cos\omega t \tag{4.4.5}$$

which represents periodic motion with a sinusoidal time dependence. This is known as *simple harmonic motion* and the corresponding system is known as a *harmonic oscillator*. The oscillation occurs with a constant angular frequency

$$\omega = \sqrt{\frac{k}{m}} \text{ radians per second} \tag{4.4.6}$$

This is called the *natural frequency* of the oscillator. The corresponding *circular (or angular) frequency* in Hertz (cycles per second) is

$$\nu = \frac{\omega}{2\pi} = \frac{1}{2\pi}\sqrt{\frac{k}{m}} \text{ Hz} \tag{4.4.7}$$

The general relation between force and potential energy in a conservative system in one dimension is

$$F = \frac{-dV}{dx} \tag{4.4.8}$$

Thus the potential energy of a harmonic oscillator is given by

$$V(x) = \frac{1}{2}kx^2 \tag{4.4.9}$$

which has the shape of a parabola, as drawn in Figure **4.4.2**. A simple computation shows that the oscillator moves between positive and negative turning points $\pm x_{max}$ where the total energy E equals the potential energy $\frac{1}{2}kx_{max}^2$ while the kinetic energy is momentarily zero. In contrast, when the oscillator moves past $x = 0$, the kinetic energy reaches its maximum value while the potential energy equals zero.

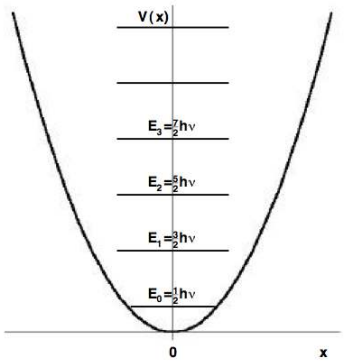


Figure **4.4.2**: Potential energy function and first few energy levels for harmonic oscillator.

4.4.3: Harmonic Oscillator in Quantum Mechanics

Given the potential energy in Equation 4.4.9, we can write down the Schrödinger equation for the one-dimensional harmonic oscillator:

$$-\frac{\hbar^2}{2m}\frac{d^2\psi(x)}{dx^2} + \frac{1}{2}kx^2\psi(x) = E\psi(x) \tag{4.4.10}$$

This equation is challenging to solve for ψ because the potential varies with position and is less than infinity in all of space. This means the particle can be found at any x between $\pm\infty$. Solutions for it have been found by others by what are essentially sophisticated guess and check methods. The results are:

$$\psi_n(x) = \left(\frac{\sqrt{\alpha}}{2^n n!\sqrt{\pi}}\right)^{1/2} H_n(\sqrt{\alpha}x)e^{-\alpha x^2/2} \tag{4.4.11}$$

where

$$\alpha = \sqrt{\frac{mk}{\hbar^2}} \tag{4.4.12}$$

and $H_n(\xi)$, with $\xi = \sqrt{\alpha}x$ represents the Hermite polynomial of degree n. The first few Hermite polynomials are

$$H_0(\xi) = 1 \tag{4.4.13}$$

$$H_1(\xi) = 2\xi \tag{4.4.14}$$

$$H_2(\xi) = 4\xi^2 - 2 \tag{4.4.15}$$

$$H_3(\xi) = 8\xi^3 - 12\xi \tag{4.4.16}$$

The four lowest harmonic-oscillator eigenfunctions are plotted in Figure **4.4.3**. Note the topological resemblance to the corresponding particle-in-a-box eigenfunctions.

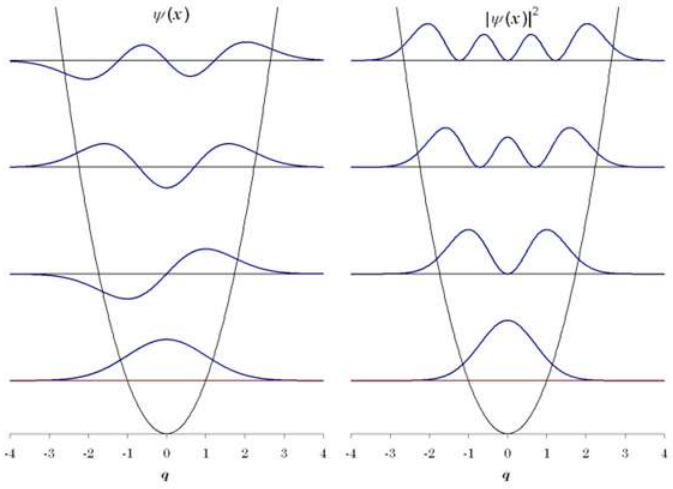


Figure 4.4.3: Harmonic oscillator eigenfunctions for n=0, 1, 2, 3 and probability densities. **Two things to note**: these wavefunctions do not reach zero until x = ±∞; a particle represented by any of these wavefunctions have a probability of being in the classically forbidden regions where the energy is less than the potential energy (the particle exhibits tunneling).

The eigenvalues are given by the simple formula

$$E_n = \left(n + \frac{1}{2}\right)\hbar\omega \tag{4.4.17}$$

where ω is as defined in equation 4.4.6. These energy levels are drawn in Figure 4.4.2, on the same scale as the potential energy. The ground-state energy $E_0 = \frac{1}{2}\hbar\omega$ is greater than the classical value of zero, again a consequence of the uncertainty principle. This means that the oscillator is always oscillating.

Note that the difference between successive energy eigenvalues has a constant value

$$\Delta E = E_{n+1} - E_n = \hbar\omega = h\nu \tag{4.4.18}$$

This is reminiscent of Planck's formula for the energy of a photon. It comes as no surprise then that the quantum theory of radiation has the structure of an assembly of oscillators, with each oscillator representing a mode of electromagnetic waves of a specified frequency.

4.4.4: Contributors and Attributions

- Seymour Blinder (Professor Emeritus of Chemistry and Physics at the University of Michigan, Ann Arbor)
- Jonathan Gutow (UW Oshkosh).

This page titled 4.4: Harmonic Oscillator is shared under a CC BY-NC-SA 4.0 license and was authored, remixed, and/or curated by Jonathan Gutow.

- **Harmonic Oscillator** is licensed CC BY-NC-SA 4.0.

4.5: Hermite Polynomials are either Even or Odd Functions

Learning Objectives

- Understand key properties of the Hermite polynomials including orthogonality and symmetry.
- Be proficient at using symmetries of integrands to quickly solve integrals.

Hermite polynomials were defined by Laplace (1810) though in scarcely recognizable form, and studied in detail by Chebyshev (1859). Chebyshev's work was overlooked and they were named later after Charles Hermite who wrote on the polynomials in 1864 describing them as new. They were consequently not new although in later 1865 papers Hermite was the first to define the multidimensional polynomials. The first six Hermite polynomial are plotted in Figure 5.7.1 .

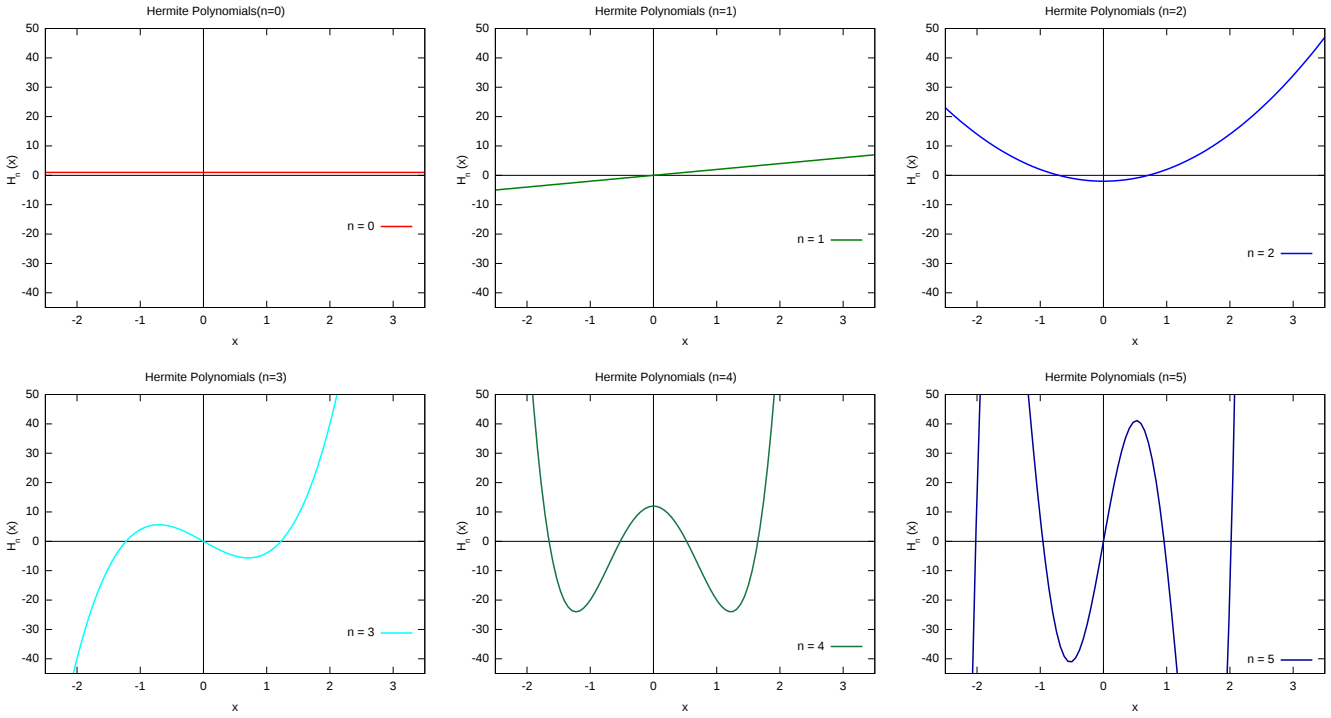


Figure 5.7.1 : The first six Hermite polynomials $H_n(x)$. (CC BY-SA 3.0 Unported; Alessio Damato, Vulpecula and others via Wikipedia)

Generating Formula

Any Hermite polynomial $H_n(x)$ can be generated from a previous one $H_{n-1}(x)$ via the following using the recurrence relation

$$H_{n+1}(x) = 2xH_n(x) - 2nH_{n-1}(x). \tag{4.5.1}$$

4.5.1: Hermite Polynomials are Symmetric

Let $f(x)$ be a real-valued function of a real variable.

- Then f is **even** if the following equation holds for all x and -x in the domain of f

$$f(x) = f(-x)$$

- Then f is **odd** if the following equation holds for all x and -x in the domain of f

$$-f(x) = f(-x)$$

Even and odd are terms used to describe particularly well-behaved functions. An *even* function is symmetric about the y-axis (Figure 5.7.2 ; left). That is, if we reflect the graph of the function in the y-axis, then it does not change. Formally, we say that f is

even if, for all x and $-x$ in the domain of f, we have

$$f(-x) = f(x)$$

Two examples of even functions are $f(x) = x^2$ and $f(x) = \cos x$.

An *odd* function has rotational symmetry of order two about the origin (Figure 5.7.2 ; middle). That is, if we rotate the graph of the function 180° about the origin, then it does not change. Formally, we say that ff is odd if, for all x and $-x$ in the domain of f, we have

$$f(-x) = -f(x)$$

Examples of odd functions are $f(x) = x^3$ and $f(x) = \sin x$.

Naturally, not all functions can be classified as even or odd. For example $f = x^3 + 1$ shown in the right side of Figure 5.7.2 , is neither.

> You can also think of these properties as symmetry conditions at the origin. More symmetries in 3D space are discussed in Group Theory.

Without proof, we can identify several key features involving multiplication properties of even and odd functions:

- The product of two **even** functions is an **even** function.
- The product of two **odd** functions is an **even** function.
- The product of an **even** function and an **odd** function is an odd function.

This can be shown graphically as a product table like that in Table 5.7.1 .

Table 5.7.1 : Product table of 1D Functions

Product table	Odd Function (anti-symmetric)	Even Function (symmetric)	No symmetry (neither)
Odd Function (anti-symmetric)	Even Function (symmetric)	Odd Function (anti-symmetric)	who knows
Even Function (symmetric)	Odd Function (anti-symmetric)	Even Function (symmetric)	who knows
No symmetry (neither)	who knows	who knows	who knows

Notice that the Hermite polynomials in Figure 5.7.1 oscillate from even to odd. We can take advantage of that aspect in our calculation of Harmonic Oscillator wavefunctions. Hermite Polynomial is an even or odd function depends on its degree n. Based on

$$H_n(-x) = (-1)^n H_n(x) \tag{4.5.2}$$

- $H_n(x)$ is an even function, when n is even.
- $H_n(x)$ is an odd function, when n is odd.

4.5.2: Integration over Symmetric Functions

You often consider integrals of the form

$$I = \int_{-a}^{a} f(x)\,\mathrm{d}x$$

If f is odd or even, then sometimes you can make solving this integral easier. For example, we can rewrite that integral in the following way:

$$I = \int_{-a}^{a} f(x)\,\mathrm{d}x = \int_{-a}^{0} f(x)\,\mathrm{d}x + \int_{0}^{a} f(x)\,\mathrm{d}x \tag{4.5.3}$$

$$= \int_{0}^{a} f(-x)\,\mathrm{d}x + \int_{0}^{a} f(x)\,\mathrm{d}x \tag{4.5.4}$$

For an even function, we have $f(-x) = f(x)$ and Equation 4.5.4 can be simplified

$$I = \int_0^a f(-x)\,dx + \int_0^a f(x)\,dx$$
$$= 2\int_0^a f(x)\,dx$$

For an odd function, we have $f(-x) = -f(x)$ and Equation 4.5.4 can be simplified

$$I = -\int_0^a f(x)\,dx + \int_0^a f(x)\,dx$$
$$= 0$$

That's what it means to simplify the integration: the integral of an odd or even function over the interval $[-L, L]$ can be put into a nicer form (and sometimes we can see that it vanishes without ever computing an integral).

Example 5.7.1

Technically, evaluating the orthogonality of Hermite polynomials requires integrating over the $\exp(-x^2)$ weight function (Equations 4.5.5 and 4.5.6).

Solution

For the Hermite polynomials $H_n(x)$, the relevant inner product (using Dirac Notation)

$$\langle f, g\rangle = \int_{-\infty}^{\infty} f(x)g(x)\exp(-x^2)\,dx$$

While the $H_2(x)H_3(x)$ product is indeed an odd function (Table 5.7.1), while $exp(-x^2)$ is even. Their product is odd, and thus $\langle f, g\rangle$ certainly ought to be zero.

Symmetry is an important aspect of quantum mechanics and mathematics, especially in calculating integrals. Using this symmetry, integrals can be identified to be equal to zero without explicitly solving them. For example, the integral of an odd integrand over all possible values will **always** be zero irrespective of the exact nature of the function:

$$\int_{-\infty}^{\infty} f(x)\,dx = 0$$

This simplifies calculations greatly as demonstrated in the following chapters.

4.5.3: Hermite Polynomials are Orthogonal

Hermite polynomials $H_n(x)$ are *n*th-degree polynomials for *n* = 0, 1, 2, 3 and form an orthogonal set of functions for the weight function $e^{-x^2/2}$. The exact relation is:

$$\int_{-\infty}^{\infty} H_m(x)H_n(x)e^{-x^2/2}dx = 0 \tag{4.5.5}$$

if $m \neq n$ and

$$\int_{-\infty}^{\infty} H_m(x)H_n(x)e^{-x^2/2}dx = 2^n n!\sqrt{\pi} \tag{4.5.6}$$

if $m = n$.

This will not be proved, but can the demonstrated using any of the Hermite polynomials listed in the previous section. The orthogonality property becomes important when solving the Harmonic oscillator problems. Note that the integral of Equation 4.5.6 is important for normalizing the quantum harmonic oscillator wavefunctions discussed in last Section.

Example 5.7.2 : Hermite Polynomials are Orthogonal

Demonstrate that $H_2(x)$ and $H_3(x)$ are orthogonal.

Solution

We need to confirm

$$\int_{-\infty}^{\infty} H_2(x)H_3(x)dx = 0$$

or when substituted

$$\int_{-\infty}^{\infty} (4x^2-2)(8x^3-12x)dx = 0$$

because it says I need to show it's orthogonal on $[-\infty,\infty]$ or we can just evaluate it on a finite interval $[-L,L]$, where L is a constant.

$$\begin{aligned}\int_{-L}^{L}(4x^2-2)(8x^3-12x)dx &= 8\left(\frac{2x^6}{3}-2x^4+\frac{3x^2}{2}\right)\Bigg|_{-L}^{L}\\ &= 8\left(\frac{2L^6}{3}-2L^4+\frac{3L^2}{2}\right)-8\left(\frac{2(-L)^6}{3}-2(-L)^4+\frac{3(-L)^2}{2}\right)\\ &= 0.\end{aligned}$$

4.5.4: Concluding

Hermite polynomials are a component in the harmonic oscillator wavefunction that dictates the symmetry of the wavefunctions. If your integration interval is symmetric around 0, then the integral over *any* integrable odd function is zero, no exception. Therefore as soon as you've found that your integrand is odd and your integration interval is symmetric, you're done. Also, for general functions, if you can easily split them into even and odd parts, you only have to consider the integral over the even part for symmetric integration intervals.

Another important property is that the product of two even or of two odd functions is even, and the product of an even and an odd function is odd. For example, if ff is even, $x \mapsto f(x)\sin(x)$ is odd, and therefore the integral over it is zero (provided it is well defined).

This page titled 4.5: Hermite Polynomials are either Even or Odd Functions is shared under a CC BY-SA license and was authored, remixed, and/or curated by Delmar Larsen.

- **5.7: Hermite Polynomials are either Even or Odd Functions** by Delmar Larsen is licensed CC BY-SA 4.0.

4.6: The Harmonic Oscillator and Infrared Spectra

Learning Objectives

- Understand how the quantum harmonic oscillator model can be used to interpret the infrared spectra of diatomic molecules
- Understand the origin of the transition moment integral and selection rules and how they are related

Infrared (IR) spectroscopy is one of the most common and widely used spectroscopic techniques employed mainly by inorganic and organic chemists due to its usefulness in determining structures of compounds and identifying them. Chemical compounds have different chemical properties due to the presence of different functional groups. IR spectroscopy is one of the most common and widely used spectroscopic techniques. Absorbing groups in the infrared region absorb within a certain wavelength region. The absorption peaks within this region are usually sharper when compared with absorption peaks from the ultraviolet and visible regions. In this way, IR spectroscopy can be very sensitive to determination of functional groups within a sample since different functional group absorbs different particular frequency of IR radiation. Also, each molecule has a characteristic spectrum often referred to as the fingerprint. A molecule can be identified by comparing its absorption peak to a data bank of spectra. IR spectroscopy is very useful in the identification and structure analysis of a variety of substances, including both organic and inorganic compounds. It can also be used for both qualitative and quantitative analysis of complex mixtures of similar compounds.

4.6.1: IR Spectroscopy

Transitions between vibrational energy levels can be induced about by absorption or emission of radiation. To understand this, knowledge of both the initial and final eigenstates is needed. The energy of the vth eigenstate of a harmonic oscillator can be written as

$$E_v = \left(v + \frac{1}{2}\right) \frac{h}{2\pi}\sqrt{\frac{k}{\mu}} \tag{4.6.1}$$

where h is Planck's constant and v is the vibrational quantum number and ranges from 0, 1, 2, 3,..., ∞. Equation 4.6.1 is often rewritten as

$$E_v = \left(v + \frac{1}{2}\right) h\nu_m \tag{4.6.2}$$

where ν_m is the vibrational frequency of the vibration. Equation 4.6.2 is often written as

$$E_v = \left(v + \frac{1}{2}\right) \hbar\omega$$

where ω is the angular frequency (i.e., $2\pi\nu$).

Transitions in vibrational energy levels can be brought about by absorption of radiation, provided the energy of the radiation ($h\nu_{photon}$) **exactly** matches the difference in energy ($\Delta E_{vv'}$) between the vibrational quantum state v to quantum state v'. This can be expressed as

$$\begin{aligned} h\nu_{photon} &= \Delta E_{vv'} \\ &= E_{v'} - E_v \\ &= \left(v' + \frac{1}{2}\right) h\nu_m - \left(v + \frac{1}{2}\right) h\nu_m \\ &= (v' - v)\, h\nu_m \end{aligned} \tag{4.6.3}$$

Let's consider only transitions between adjacent eigenstates (discussed in more details below) so

$$v' - v = \pm 1$$

which is positive if an IR photon is absorbed and negative if it is emitted. For the absorption of a IR photon, Equation 4.6.3 simplifies to

$$h\nu_{photon} = h\nu_m$$
$$= \frac{h}{2\pi}\sqrt{\frac{k}{\mu}} \tag{4.6.4}$$

The frequency of radiation ν_{photon} that will bring about this change is **identical** to the classical vibrational frequency of the bond ν.

The Wavenumber as a Unit of Energy

The cm^{-1} is the wavenumber scale and it can also be defined as 1/wavelength in cm. A wavenumber is often used due to its direct relationship with both frequency and energy. The frequency of the absorbed radiation causes the molecular vibrational frequency for the absorption process:

$$\bar{\nu}(cm^{-1}) = \frac{1}{\lambda(\mu m)} \times 10^4 \left(\frac{\mu m}{cm}\right) \tag{4.6.5}$$
$$= \frac{\nu\,(Hz)}{c\,(cm/s)} \tag{4.6.6}$$

Equation 4.6.3 can be modified so that the radiation can be expressed in wavenumbers

$$\tilde{\nu}_m = \frac{1}{2\pi c}\sqrt{\frac{k}{\mu}} \tag{4.6.7}$$

where c is the velocity of light (cm/s) and $\tilde{\nu}$ is the wavenumber of an absorption maximum (cm^{-1}).

Example 5.5.1: Hydrogen Halides

The force constants for typical diatomic molecules are in the range between 400 to 2000 $N \cdot m^{-1}$.

Molecule	HF	HCl	HBr	HI	CO	NO
Force constant, k ($N.m^{-1}$)	970	480	410	320	1860	1530

For the diatomic molecules listed above, calculate the following:

a. angular frequency ($rad \cdot s^{-1}$)
b. natural frequency (Hz)
c. period (s)
d. separation between energy levels
e. wavelength λ of the electromagnetic radiation absorbed in the transition $v = 0 \rightarrow v = 1$.

Solution

For **HCl**:

a. angular frequency

$$\omega = 5.45 \times 10^{14} rad \cdot s^{-1}$$

b. natural frequency:

$$\nu = \frac{\omega}{2\pi} = 8.68 \times 10^{13}$$

c. period (s):

$$T = \frac{1}{\nu} = 1.15 \times 10^{-14}$$

d. separation between energy levels:

$$\Delta E = E_{v=1} - E_{v=0} = \hbar\omega = 5.75 \times 10^{-20}\ J$$

e. wavelength λ of the electromagnetic radiation absorbed in the transition $v = 0 \rightarrow v = 1$:

$$3.46 \times 10^{-6}\, m$$

The electromagnetic radiation released (and absorbed) for vibrations is primarily in the infrared (IR) part of the spectrum. Calculating the above properties for the other molecules remains as an exercise.

Note: We did not designate the specific isotopes in the hydrogen halides above because that information was not required to solve these questions.

IR deals with the interaction between a molecule and radiation from the electromagnetic region ranging (4000- 40 cm^{-1}). The IR region of the electromagnetic spectrum ranges in wavelength from 2 -15 μm. Conventionally the IR region is subdivided into three regions (Table 5.5.1): near IR, mid IR and far IR. Most of the IR used originates from the mid IR region.

Table 5.5.1: Regions of the IR Spectrum

Region	Wavelength	Wavenumbers ($\tilde{\nu}$), cm^{-1}	Frequencies (v), HZ
Near	0.78 -2.5	12800 - 4000	3.8 x 10^{14} - 1.2 x 10^{14}
Middle	2.5 - 50	4000 - 200	3.8 x 10^{14} - 1.2 x 10^{14}
Far	50 -100	200 -10	3.8 x 10^{14} - 1.2 x 10^{14}
Most Used	2.5 -15	4000 -670	3.8 x 10^{14} - 1.2 x 10^{14}

? Example 5.5.2: Hydrogen Chloride

The $H^{35}Cl$ equilibrium bond length is 0.127 nm and the $v = 0$ to $v = 1$ transition is observed in the infrared at 2,886 cm^{-1}. Compute the vibrational energy of $H^{35}Cl$ in its lowest state.

a. Compute the classical limit for the stretching of the HCl bond from its equilibrium length in this state.
b. What percent of the equilibrium bond length is this extension?

Solution

The H–Cl bond length is $0.127\,nm = 1.27 \times 10^{-10} m$ and the IR transition is observed at $2886\,cm^{-1}$. We first convert this to Hertz

$$2886\,cm^{-1}(3 \times 10^{10} cm/s) = 8.646 \times 10^{13} s^{-1} = 8.646 \times 10^{13}\,Hz$$

The equations for the energy of the vth eigenstate of a harmonic oscillator is

$$E_v = (v + 1/2)\hbar\omega$$

So the ground state ($v = 0$) energy is

$$E_0 = \frac{1}{2}\hbar\omega$$

with

$$\begin{aligned}\omega &= 2\pi\nu \\ &= 5.54 \times 10^{14}\, rad/s\end{aligned}$$

We can then extra the ground state vibrational energy (aka zero-point energy) from

$$\begin{aligned}E_o &= \frac{1}{2}\hbar\omega \\ &= \frac{1}{2}\hbar(5.54 \times 10^{14} rad/s) \\ &= 2.916 \times 10^{-20}\ J\end{aligned}$$

The classical limit of the stretch is denoted as Q_0, this can be equated as potential energy in relation to the total E_0 found above as, at E_0, all of the energy would be potential energy in the form of the stretch. In comparison to the classic spring potential

$$V = \frac{1}{2}kQ_0^2$$

As described above, we can relate the two as

$$\frac{1}{2}\hbar\omega = \frac{1}{2}kQ_0^2$$

or,

$$2.916 \times 10^{-20} J = \frac{1}{2}481Q_0^2$$

where $Q_0 = 1.10 \times 10^{-11} m = 0.0110\, nm$.

Lastly, this classical limit to length can be compared to the equilibrium bond length by a simple relation of

$$\begin{aligned} \textbf{Percent bond length} &= \frac{Q_0}{x_{eq}} \times 100\% \\ &= \frac{0.0110\, nm}{0.127\, nm} \times 100\% \\ &= 8.66\% \end{aligned}$$

4.6.2: Selection Rules for IR Transitions

Photons can be absorbed or emitted, and the harmonic oscillator can transition from one vibrational energy state to another. Which transitions between vibrational states are allowed? When discussing the Bohr hydrogen atom in Chapter 1, we identified multiple transitions between different states as being responsible for the line spectra emission of the hydrogen atom. No limitations were identified so that any transition between any starting state and ending state was possible and this resulted in a complex pattern in the spectra. As we will identify later on, when considering mulit-electron atoms, there are **selection rules** that limits which transitions will be observed (i.e., are allowed).

A similar situation exist for the harmonic oscillator and IR transitions and a set of selection rules must be satisfied to ensure a particular transition is allowed. Selection rules result from evaluating a **transition moment integral** that expresses the probability of a transition from the v to the v' eigenstates:

$$\mu_T = \langle \psi_{v'} | \hat{\mu}(x) | \psi_v \rangle \tag{4.6.8}$$

$$= \int_{-\infty}^{\infty} \psi_{v'}^*(x) \hat{\mu}(x) \psi_v(x) dx \tag{4.6.9}$$

When the transition moment integral is zero for two specific eigenstates (i.e., $\psi_v(x)$ and $\psi_v'(x)$), then the probability of observing that transition is zero. In this case, this transition is called a **forbidden transition** (i.e., it will not be obversed). Transitions with low probabilities are call "weakly allowed transitions" since they will have small amplitudes in spectra and transitions with high probabilities are "strongly allowed transitions" and will exhibit high amplitudes in spectra.

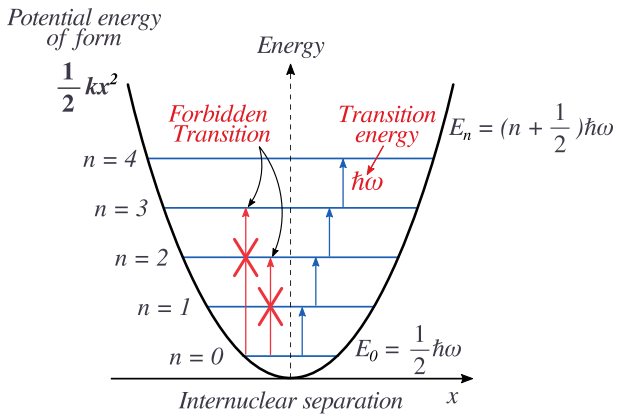


Figure 5.5.1: Possible transitions for a harmonic oscillator. Allowed transitions are labeled with blue arrows and forbidden transitions are labeled with red arrows. (CC BY-NC; Ümit Kaya via LibreTexts)

To evaluate Equation 4.6.9, we need to express the dipole moment operator, $\hat{\mu}$, in terms of the magnitude of the vibration x. The dipole moment operator is defined as

$$\hat{\mu} = \sum_{electrons} e\vec{r} + \sum_{nuclei} q\vec{R} \tag{4.6.10}$$

where the two sums are over all the electrons and nuclei and involve the particle charge ($-e$ or q) multiplying the position vector ($\vec{r}$ or $\vec{R}$, respectively). We can obtain this dipole moment operator in terms of the magnitude of the displacement coordinate, x, in a simple way by using a **Taylor series expansion** for the dipole moment around the equlibrium position ($x = 0$).

$$\hat{\mu}(x) = \mu_{x=0} + \left.\frac{d\mu(x)}{dx}\right|_{x=0} x + \left.\frac{d^2\mu(x)}{dx^2}\right|_{x=0} x^2 + \cdots \tag{4.6.11}$$

Retaining only the first two terms and substituting into Equation 4.6.9 produces

$$\mu_T = \mu_{x=0} \int_{-\infty}^{\infty} \psi_{v'}(x)\psi_v(x)dx + \left.\frac{d\mu(x)}{dx}\right|_{x=0} \int_{-\infty}^{\infty} x\psi^*_{v'}(x)\psi_v(x)dx \tag{4.6.12}$$

where $\mu_{x=0}$ is the **dipole moment** of the molecule when the nuclei are at their equilibrium positions, and

$$\left.\frac{d\mu(x)}{dx}\right|_{x=0}$$

is the *linear* change in the dipole moment due to the displacement of the nuclei in the normal mode. The derivative is the linear change because it multiplies x and not a higher power of x in Equation 4.6.11. Both μ and

$$\left.\frac{d\mu(x)}{dx}\right|_{x=0}$$

are moved outside of the integral because they are constants that no longer depend on x because they are evaluated at $x = 0$.

The integral in the first term in Equation 4.6.12 is 0 because any two harmonic oscillator wavefunctions are *orthogonal*. The integral in the second term of Equation 4.6.12 is zero except when $v' = v \pm 1$ as demonstrated in Exercise 5.5.1 . Also note that the second term is zero if

$$\left.\frac{d\mu(x)}{dx}\right|_{x=0} = 0 \tag{4.6.13}$$

Hence we can identify two "rules" that need to be satisfied for an IR photon to be absorb (or emitted) by a vibrating molecule.

Rules for IR Absorption

For IR absorption to occur two conditions must be met:

1. There must be a **change** in the dipole moment of the molecule as a result of a molecular vibration (or rotation). The change (or oscillation) in the dipole moment allows interaction with the alternating electrical component of the IR radiation. Symmetric molecules (or bonds) do not absorb IR radiation since there is no dipole moment.
2. If the frequency of the radiation ν_{photon} matches the natural frequency of the vibration (ν_m), the IR photon can be absorbed and the amplitude of the vibration increases.

? Exercise 5.5.1

Use one of the Hermite polynomial recursion relations to verify that the second integral in Equation 4.6.12 is 0 unless $v' = v \pm 1$.

If we are to observe absorption of infrared radiation due to a vibrational transition in a molecule, the transition moment cannot be zero. This condition requires that the dipole moment derivative Equation 4.6.13 **cannot** be zero and that the vibrational quantum number change by one unit. The normal coordinate motion must cause the dipole moment of the molecule to change in order for a molecule to absorb infrared radiation. If the normal coordinate oscillation does not cause the dipole moment to change then $\mu_T = 0$ and no infrared absorption is observed. So we can

$$\underbrace{\Delta v = \pm 1}_{\text{For allowed transitions}} \tag{4.6.14}$$

Consider oxygen and nitrogen molecules. Because they are symmetrical, their dipole moments are zero, $\mu = 0$. Since the vibrational motion (only bond stretching for a diatomic molecule) preserves this symmetry, the change in the dipole moment due to the vibrational motion also is zero, $\frac{d\mu(x)}{dx} = 0$. Consequently, oxygen and nitrogen do not absorb infrared radiation as a result of vibrational motion.

? Exercise 5.5.2

Explain why the molar absorptivity or molar extinction coefficients (ϵ) in Beer's Law for the IR absorption of some vibrations are greater than others.

Answer

Qualitatively, if the probability of transition is large, then the molar absorptivity is large. And similar if the transition were not allowed, then there will be no intensity and no observed peak in the spectrum. Transitions can be "partially allowed" as well, and these bands appear with a lower intensity than the full allowed transitions.

When looking at the Beer's Law

$$A = \epsilon\, c\, l$$

where A is absorbance. ϵ is the molar absorptivity, c is the molar concentration and l is the optical path length

We are only looking at the change in the molar absorptivity as the IR absorptions of vibrations vary. To do this we have to look at the transition moment integral

$$\mu_T = \langle \psi_{v'} | \hat{\mu}(x) | \psi_v \rangle$$

When the transition moment integral is zero, there is no transition as it is not allowed under the selection rules. This means that the IR is not absorbing any vibrations and therefore the molar absorptivity is zero, which means that absorbance according to Beer's Law is zero. As the transition moment integral increases, the molar absorptivity also increases and the overall absorbance increases.

The case $v' = v + 1$ corresponds to going from one vibrational state to a higher energy one by absorbing a photon with energy $h\nu$. The case $v' = v - 1$ corresponds to a transition that emits a photon with energy $h\nu$. In the harmonic oscillator model infrared spectra are very simple; only the fundamental transitions, $\Delta = \pm 1$, are allowed. The associated transition energy is $\hbar\omega$, according to

Equation 4.6.4. The transition energy is the change in energy of the oscillator as it moves from one vibrational state to another, and it equals the photon energy.

$$\begin{aligned}\Delta E &= E_{final} - E_{initial} \\ &= h\nu_{photon} \\ &= \hbar\omega_{oscillator}\end{aligned}$$

For perfect harmonic oscillators, the only possible allowed transitions are $\Delta = \pm 1$ with all other transitions forbidden (Figure 5.5.1). This conclusion predicts that the vibrational absorption spectrum of a diatomic molecule consists of a single line since the energy levels are equally spaced in the harmonic oscillator model (Figure 5.5.1). If the vibration were anharmonic, then the levels would not be equally spaced and then transitions from $v = 0$ to $v = 1$ and from $v = 1$ to $v = 2$, etc. would occur at different frequencies.

> *Only the fundamental transitions, $\Delta = \pm 1$, are observed in infrared spectra within harmonic oscillator model.*

The actual IR spectrum is more complex, especially at high resolution. There is a fine structure due to the rotational states of the molecule. These states will be discussed in the next chapter. The spectrum is enriched further by the appearance of lines due to transitions corresponding to $\Delta = \pm n$ where $n > 1$. These transitions are called **overtone** transitions and their appearance in spectra despite being forbidden in the harmonic oscillator model is due to the anharmonicity of molecular vibrations. Anharmonicity means the potential energy function is not strictly the harmonic potential. The first overtone, $\Delta v = 2$, generally appears at a frequency slightly less than twice that of the fundamental, i.e. the frequency due to the $\Delta v = 1$ transition.

? Exercise 5.5.3: Hydrogen Chloride

Compute the approximate transition frequencies in wavenumber units for the first and second overtone transitions in HCl given that the fundamental is at 2,886 cm^{-1}.

This page titled 4.6: The Harmonic Oscillator and Infrared Spectra is shared under a CC BY-NC-SA 4.0 license and was authored, remixed, and/or curated by David M. Hanson, Erica Harvey, Robert Sweeney, Theresa Julia Zielinski.

- **5.5: The Harmonic Oscillator and Infrared Spectra** by David M. Hanson, Erica Harvey, Robert Sweeney, Theresa Julia Zielinski is licensed CC BY-NC-SA 4.0.

4.7: Vibrational Overtones

Although the harmonic oscillator proves useful for modeling lower energy levels, like $v = 0, 1$, it fails at higher numbers of v. It not only fails to properly model atomic bonds and dissociations, but also is unable to match spectra showing additional lines that are not accounted for in the harmonic oscillator model.

4.7.1: Anharmonicity

Until this point, we have been using the harmonic oscillator to describe the internuclear potential energy of the vibrational motion. Fundamental vibrational frequencies of a molecule corresponds to a transition of $\Delta v = \pm 1$. While this is a decent approximation, bonds do not behave like they do in the Harmonic Oscillator approximation (Figure **4.7.1**). For example, the parabolic potential of the Harmonic Oscillator approximation means that the vibrations can hold any amount of energy and bonds can stretch to any length, while in real molecules if the atoms are too far apart the bond will dissociate.

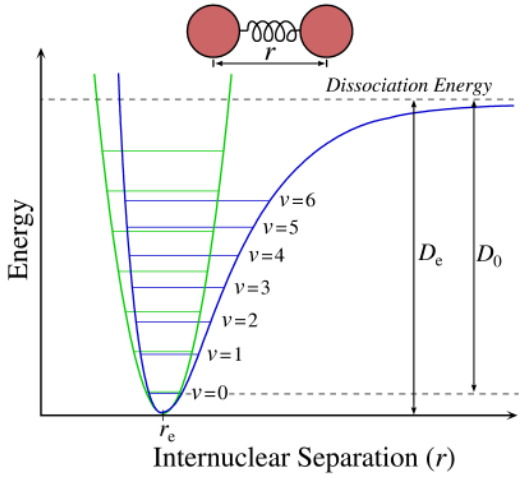


Figure **4.7.1** : Pictured above is the Harmonic Oscillator approximation (green parabola) superimposed on the anharmonic oscillator (blue curve) on a potential energy diagram. V(R) is the potential energy of a diatomic molecule and R is the radius between the centers of the two atoms. Towards the left is compression of the bond, towards the right is extension. (CC BY-SA 3.0; Created by Mark Somoza March 26 2006).

As you can see in Figure **4.7.1** , the harmonic oscillator potential well (in green) only roughly fits over the more accurate anharmonic oscillator well (in blue). The blue curve accounts for dissociation at large R values, which the green curve does not even remotely cover. However, this is just one important difference between the harmonic and anharmonic (real) oscillators.

The real potential energy can be expanded in the Taylor series.

$$V(R) = V(R_e) + \frac{1}{2!}\left(\frac{d^2V}{dR^2}\right)_{R=R_e}(R-R_e)^2 + \frac{1}{3!}\left(\frac{d^3V}{dR^3}\right)_{R=R_e}(R-R_e)^3 + \frac{1}{4!}\left(\frac{d^4V}{dR^4}\right)_{R=R_e}(R-R_e)^4 + \ldots \tag{4.7.1}$$

This expansion was discussed in detail previously. The first term in the expansion is ignored since the derivative of the potential at R_e is zero (i.e., at the bottom of the well). The Harmonic Oscillator approximation only uses the next term, the quadratic term, in the series

$$V_{HO}(R) \approx V(R_e) + \frac{1}{2!}\left(\frac{d^2V}{dR^2}\right)_{R=R_e}(R-R_e)^2$$

or in terms of a spring constant, ignoring the absolute energy term($V(R_e)$) and defining r to equal the displacement from equilibrium ($r = R - R_e$), then we get the "standard" harmonic oscillator potential:

$$V_{HO}(R) = \frac{1}{2}kr^2$$

Alternatively, the expansion in Equation 4.7.1 can be shortened to the cubic term

$$V(x) = \frac{1}{2}kr^2 + \frac{1}{6}\gamma r^3 \tag{4.7.2}$$

where

- $V(x_0) = 0$, and $r = R - R_0$.
- k is the harmonic force constant, and
- γ is the first (i.e., cubic) *anharmonic* term

It is important to note that this approximation is only good for R near R_0.

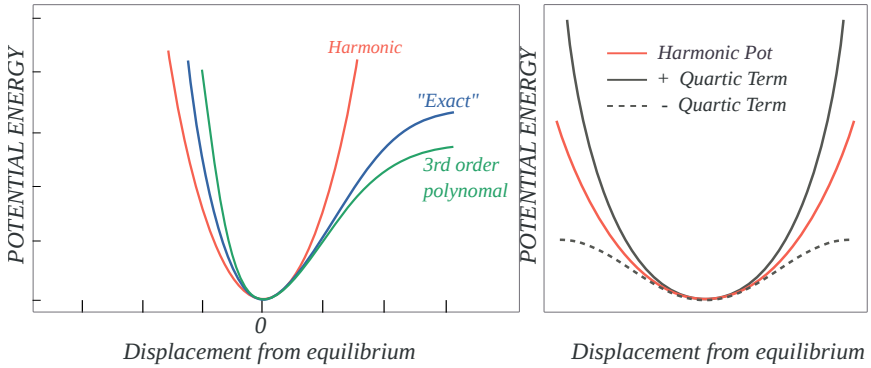


Figure 4.7.2 : (left) Deviation from simple harmonic potential approximation (red curve) of true/exact potential (blue curve) with cubic term (green). (right) Expansion with positive or negative quartic terms. (CC BY-NC; Ümit Kaya via LibreTexts)

The harmonic oscillator approximation gives by the following energies:

$$E_v = \tilde{\nu}\left(v + \frac{1}{2}\right)$$

When the cubic term in the expansion (Equation 4.7.2) is included, and the Schrödinger equation is solved using perturbation theory this gives:

$$E_v = \tilde{\nu}\left(v + \frac{1}{2}\right) - \tilde{\chi_e}\tilde{\nu}\left(v + \frac{1}{2}\right)^2$$

where $\tilde{\chi_e}$ is the **anharmonicity constant**. It is much smaller than 1, which makes sense because the terms in the Taylor series approach zero. This is why, although E_v technically includes all of the Taylor series, we only concern ourselves with the first and second terms. The rest are so small and barely add to the total and thus can be ignored. To get a more accurate approximation, more terms can be included, but otherwise, can be ignored. Almost all diatomics have experimentally determined $\frac{d^2V}{dx^2}$ for their lowest energy states. H_2, Li_2, O_2, N_2, and F_2 have had terms up to $n < 10$ determined of Equation 4.7.1.

4.7.2: Overtones

The Harmonic Oscillator approximation predicts that there will be only one line in the spectrum of a diatomic molecule, while experimental data shows there is in fact one dominant line--**the fundamental**--and other weaker lines. How can we account for these extra lines?

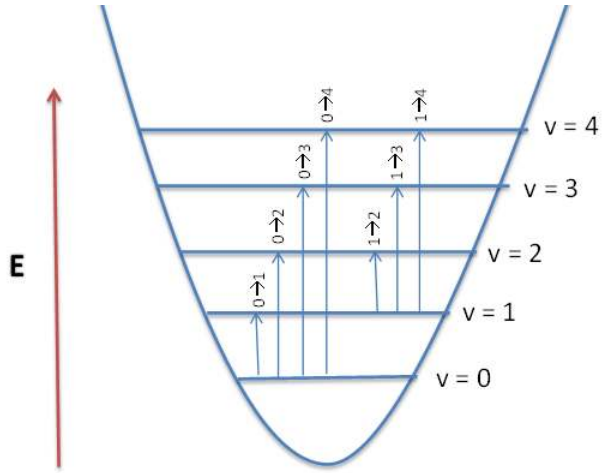


Figure **4.7.3** : A diagram for a vibrating diatomic molecule. The levels denoted by vibrational quantum numbers v represent the potential energy for the harmonic (quadratic) oscillator. The transition $0 \rightarrow 1$ is the fundamental, transitions $0 \rightarrow n$ (n>1) are called overtones, and transitions $1 \rightarrow n$ (n > 1) are called hot transitions (hot bands).

Any resonant frequency above the fundamental frequency is referred to as an *overtone*. In the IR spectrum, overtone bands are multiples of the fundamental absorption frequency. As you can recall, the energy levels in the Harmonic Oscillator approximation are evenly spaced apart. Energy is proportional to the frequency absorbed, which in turn is proportional to the wavenumber, the first overtone that appears in the spectrum will be twice the wavenumber of the fundamental. That is, first overtone $v = 0 \rightarrow 2$ is (approximately) twice the energy of the fundamental, $v = 0 \rightarrow 1$.

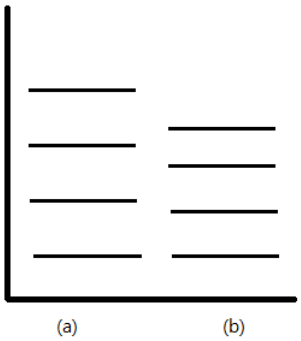


Figure **4.7.4** : An exaggerated view of the energy levels. (a) would be the harmonic oscillator, with the evenly spaced out energy levels. (b) would be the anharmonic, with the energy levels compressing until they converge.

The levels are not equally spaced, like in the harmonic oscillator, but decrease as v increases, until it ultimately converges, as implied by Figure **4.7.4**. Also as a result of anharmonicity, the $\Delta v = \pm 1$ selection rule is no longer valid and v can be any number. This leads to the observation of higher order transitions, or **overtones**, which result from the transition of the ground state to higher energy levels.

Anharmonic Oscillator Selection Rules

For the anharmonic oscillator, the selection rule is $\Delta V = \textbf{any number}$. That is, there are no selection rules (for state to state transitions)

Overtones occur when a vibrational mode is excited from $v = 0$ to $v = 2$ (the first overtone) or $v = 0$ to $v = 3$ (the second overtone). The fundamental transitions, $v = \pm 1$, are the most commonly occurring, and the probability of overtones rapidly decreases as $\Delta v > \pm 1$ gets bigger. Based on the harmonic oscillator approximation, the energy of the overtone transition will be approximately v times the fundamental associated with that particular transition. The anharmonic oscillator calculations show that the overtones are usually less than a multiple of the fundamental frequency. Overtones are generally not detected in larger molecules.

This is demonstrated with the vibrations of the diatomic **HCl** in the gas phase:

Table **4.7.1** : HCl vibrational spectrum.

Transition	$\tilde{\nu}_{obs}$ [cm^{-1}]	$\tilde{\nu}_{obs}$ Harmonic [cm^{-1}]	$\tilde{\nu}_{obs}$ Anharmonic [cm^{-1}]
$0 \rightarrow 1$ (fundamental)	2885.9	2885.9	2,885.3
$0 \rightarrow 2$ (first overtone)	5668.0	5771.8	5,665.0
$0 \rightarrow 3$ (second overtone)	8347.0	8657.7	8,339.0
$0 \rightarrow 4$ (third overtone)	10 923.1	11 543.6	10,907.4
$0 \rightarrow 5$ (fourth overtone)	13 396.5	14 429.5	13,370

We can see from Table **4.7.1** that the anharmonic frequencies correspond much better with the observed frequencies, especially as the vibrational levels increase. Because the energy levels and overtones are closer together in the anharmonic model, they are also more easily reached. This means that there is a higher chance of that level possibly being occupied, meaning it can show up as additional, albeit weaker intensity lines (the weaker intensity indicates a smaller probability of the transition occuring).

? Exercise 13.5.1

HCl has a fundamental band at 2885.9 cm^{-1} and an overtone at 5668.1 cm^{-1} Calculate $\tilde{\nu}$ and $\tilde{\chi_e}$.

? Exercise 13.5.2

Write out the Taylor series, and comment on the trend in the increasing terms. Using a test number x, please add terms 3, 4, and 5, then compare this to term 2. How do they compare? We have seen that the anharmonic terms increase the accuracy of our oscillator approximation. Why don't we care so much about terms past the second?

4.7.3: References

1. Infrared and Raman Spectra of Inorganic and Coordination Compounds. Part A: Theory and Applications in Inorganic Chemistry; Part B: Application in Coordination, Organometallic, and Bioinorganic Chemistry, 5th Edition (Nakamoto, Kazuo)
2. Lyle McAfee Journal of Chemical Education 2000 77 (9), 1122
3. Stuart, Barbara. *Infrared Spectroscopy: Fundamentals and Applications.* Wiley, 2004. Print.

This page titled 4.7: Vibrational Overtones is shared under a CC BY 4.0 license and was authored, remixed, and/or curated by Alexandra Holmes & Hannah Toru Shay.

- **13.5: Vibrational Overtones** by Alexandra Holmes, Hannah Toru Shay is licensed CC BY 4.0.

4.8: Rotations Accompany Vibrational Transitions

4.8.1: Introduction

The vibrational spectra of a diatomic molecules in the gas phase also contains closely-spaced (1-10 cm^{-1} difference) transitions attributable to rotational transitions that accompany the vibrational transitions. This is because a molecule can undergo simultaneous vibrational and rotational transitions upon absorption or emission of a single photon. Since vibrational energy states are separated by more than 1 - 10 cm^{-1}, the rotational energy states can be superimposed upon the vibrational energy states.

We treat the molecule's **vibrations** as those of a harmonic oscillator (ignoring anharmonicity). Thus we will assume the energy of a vibration is quantized in discrete levels and given by

$$E_v = h\nu\left(v + \frac{1}{2}\right)$$

Where v is the vibrational quantum number and can have integer values 0, 1, 2..., and ν is the frequency of the vibration given by:

$$\nu = \frac{1}{2\pi}\left(\frac{k}{\mu}\right)^{\frac{1}{2}}$$

where k is the force constant and μ is the reduced mass of a diatomic molecule with atom masses m_1 and m_2, given by

$$\mu = \frac{m_1 m_2}{m_1 + m_2} \tag{4.8.1}$$

We treat the molecule's **rotations** as those of a rigid rotor (ignoring centrifugal distortion). The energy of a rotation is also quantized in discrete levels given by

$$E_r = \frac{h^2}{8\pi^2 I}J(J+1)$$

In which I is the moment of inertia, given by

$$I = \mu r^2$$

where μ is the reduced mass (Equation 4.8.1) and r is the equilibrium bond length.

Experimentally, frequencies or wavenumbers are measured rather than energies, and dividing by h or hc gives more commonly seen transition energies in these units, $F(J)$ using the rotational quantum number J and the rotational constant B in either frequency

$$F(J) = \frac{E_r}{h} = \frac{h}{8\pi^2 I}J(J+1) = BJ(J+1)$$

or wavenumbers

$$\tilde{F}(J) = \frac{E_r}{hc} = \frac{h}{8\pi^2 cI}J(J+1) = \tilde{B}J(J+1)$$

> It is important to note in which units one is working since the rotational constant is always represented as B, whether in frequency or wavenumbers.

The total energy of the combined rotation-vibration state, $S(v, J)$, can be written as the sum of the vibrational energy and the rotational energy

$$S(v, J) = G(v) + F(J)$$

where $G(v)$ represents the energy of the harmonic oscillator, ignoring anharmonic components and $S(J)$ represents the energy of a rigid rotor, ignoring centrifugal distortion.

From this, we can derive

$$S(v, J) = \nu_0 \left(v + \frac{1}{2}\right) + BJ(J+1)$$

4.8.2: Selection Rules

Rotational and vibrational transitions of molecules can be used to determine useful information such as the bond length. In order do this the quantum states involved in each transition must be identified. This requires analyzing the **rovibrational spectra**.

- **Vibrational Transition Selection Rules**: At room temperature, typically only the lowest energy vibrational state v= 0 is populated, so typically v_0 = 0 and Δv = +1. The full selection rule is technically that Δv = ±1, however here we assume energy can only go upwards because of the lack of population in the upper vibrational states. Keep in mind that since this selection rule requires the dipole moment of the molecule to change during the transition homonuclear diatomics do not exhibit IR active vibrational transitions.
- **Rotational Transition Selection Rules**: At room temperature (thermal energies of about ~ 208 cm^{-1}), states with J≠0 can be populated since they have small energy differences between neighboring states compared to the thermal energy. This contrasts with vibrational levels, where the energy spacing is large compared to the available thermal energy. Since a photon contains one quantum **of angular momentum** and we abide by the principle of **conservation of angular momentum,** the selection rule is ΔJ = ±1, just as it is for pure rotational transitions.

Because $\Delta J \neq 0$ we will not see the rovibrational transition v = 0, J = 0 to v=1, J =0, unless there is some other way of using the one unit of angular momentum from the absorbed photon. Thus, this pure vibrational transition is not observed for closed shell heteronuclear diatomics. The pure vibrational transition $\Delta J = 0$, called the Q-branch, can be observed for open shell species where the angular momentum can be used to flip the unpaired electron spin. The $\Delta J = \pm 1$ selection rule gives rise to an R-branch (when $\Delta J = +1$) and a P-branch ($\Delta J = -1$). Each line of the branch is labeled R(J) or P(J), where J represents the value of the lower state rotational quantum number (see figure 4.8.1).

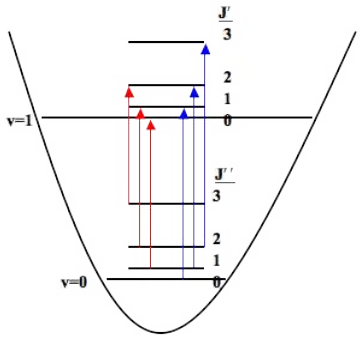


Figure 4.8.1 : Rotation-Vibration Transitions. Rotational transitions are on the order of 1-10 cm^{-1}, while vibrational transitions are on the order of 1000 cm^{-1}. The difference of magnitude between the energy transitions allow rotational levels to be superimposed within vibrational levels.

4.8.2.1: R-branch

The R branch is when ΔJ = +1 (i.e. the rotational quantum number in the ground state is one less than the rotational quantum number in the excited state). Assuming the rotational constant does not change between the ground and excited vibrational states, we can calculate the observed transition energies as follows:

$$\Delta E(R(J)) = \Delta E_{vib} + \Delta E_{rot} = h\nu_0 + hB\left[J'(J'+1) - J''(J''+1)\right] \quad (4.8.2)$$

$$= h\nu_0 + hB\left[(J+1)(J+2) - J(J+1)\right] \quad (4.8.3)$$

$$= h\nu_0 + 2hB(J+1), \quad (4.8.4)$$

where $h\nu_0$ is the vibrational transition energy, B is the rotational constant, and J is the initial rotational quantum number (J" in figure 4.8.1).

4.8.2.2: P-branch

The P branch is when ΔJ = -1 (i.e. the rotational quantum number in the ground state is one more than the rotational quantum number in the excited state). Assuming the rotational constant does not change between the ground and excited vibrational states,

we can calculate the observed transition energies as follows:

$$\Delta E(P(J)) = \Delta E_{vib} + \Delta E_{rot} = h\nu_0 + hB[J'(J'+1) - J''(J''+1)] \quad (4.8.5)$$

$$= h\nu_0 + hB[(J-1)J - J(J+1)] \quad (4.8.6)$$

$$= h\nu_0 - 2hBJ \quad (4.8.7)$$

4.8.2.3: Q-branch

The Q branch is when ΔJ = 0 (i.e. the rotational quantum number in the ground state is the same as the rotational quantum number in the excited state). Assuming the rotational constant does not change between the ground and excited vibrational states the rotational energy will not change so:

$$\Delta E(Q(J)) = \Delta E_{vib} + \Delta E_{rot} = h\nu_0 + 0 \quad (4.8.8)$$

$$= h\nu_0 \quad (4.8.9)$$

The Q-branch can be observed in polyatomic molecules and diatomic molecules with electronic angular momentum in the ground electronic state, e.g. nitric oxide, NO. Most diatomics are closed shell and do not exhibit a Q branch. If a Q branch exists it will consist of lots of closely spaced lines rather than a single line because the rotational constant in the excited state will not be exactly the same as in the ground vibrational state due to the slight elongation of the bond as the vibrational excitation increases.

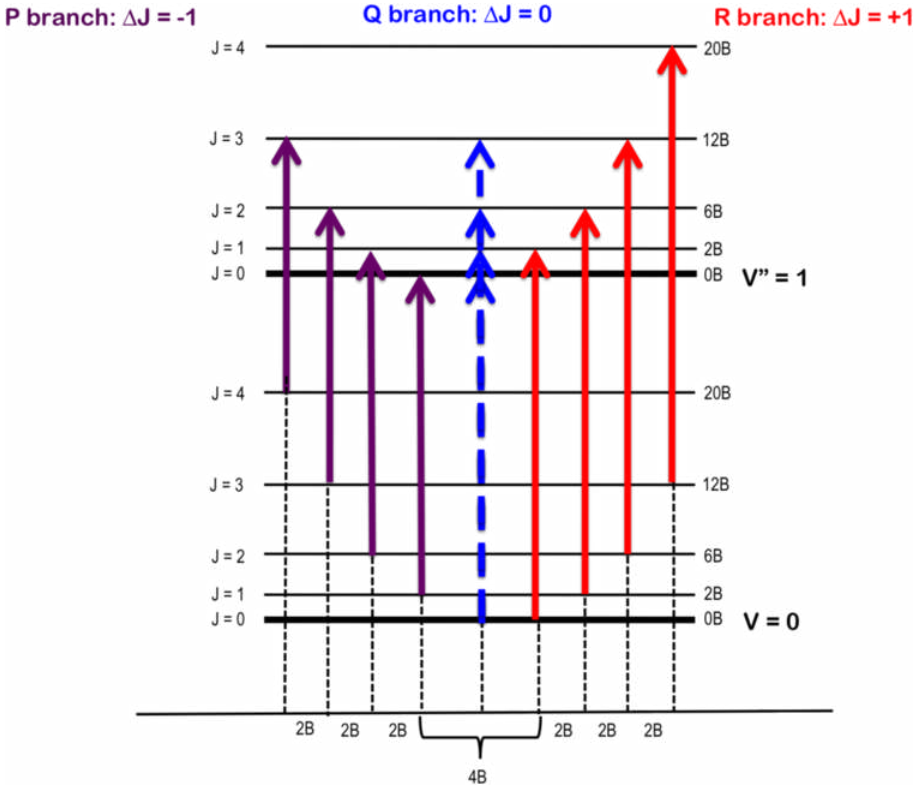


Figure **4.8.2** : Cartoon depiction of rotational energy levels, J, imposed on vibrational energy levels, v. The transitions between levels that would result in the P- and R-branches are depicted in purple and red, respectively, in addition to the theoretical Q-branch line in blue.

As seen in Figure **4.8.2** , the lines of the P-branch (represented by purple arrows) and R-branch (represented by red arrows) are separated by specific multiples of B (i.e, $2B$), thus the bond length can be deduced without the need for pure rotational spectroscopy.

4.8.3: The predicted spectrum

The spectrum we expect, based on the conditions described above, consists of lines equidistant in energy from one another, separated by a value of $2B$. The *relative* intensity of the lines is a function of the rotational populations of the ground states (i.e. the

intensity is proportional to the number of molecules available to make the transition). The *overall* intensity of the lines also depends on the vibrational transition dipole moment.

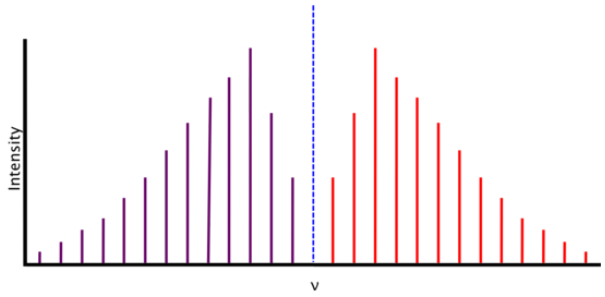


Figure **4.8.3** : A cartoon depiction of an ideal rovibrational spectrum.

In Figure **4.8.3** , between $P(1)$ and $R(0)$ lies the zero gap, where the the first lines of both the P- and R-branch are separated by $4B$, assuming that the rotational constant B is equal for both energy levels. The zero gap is also where we would expect the Q-branch, depicted as the dotted line, if it is allowed.

From statistical mechanics the fraction of the population in each J state will be:

$$f(J) = \frac{(2J+1)exp\left(\frac{-E_J}{k_BT}\right)}{\sum_{J=0}^{\infty} exp\left(\frac{-E_J}{k_BT}\right)} = \frac{(2J+1)exp\left(\frac{-B(J(J+1)}{k_BT}\right)}{\sum_{J=0}^{\infty} exp\left(\frac{-B(J(J+1)}{k_BT}\right)}, \tag{4.8.10}$$

where the 2J + 1 factor comes from the degeneracy of the rotational state. This is just the Boltzmann distribution of populations. The sum on the bottom of equation 4.8.10 is the partition function which is approximately $q_{rot} = \frac{k_BT}{B}$ (see the rotational partition function). By substituting in for the sum with q_{rot} and taking the derivative with respect to J, one finds that there is a value for J where the population reaches a maximum as seen in the cartoon illustration.

This page titled 4.8: Rotations Accompany Vibrational Transitions is shared under a CC BY 4.0 license and was authored, remixed, and/or curated by Joya Cooley & Jonathan Gutow@University of Wisconsin - Oshkosh.

- **13.2: Rotations Accompany Vibrational Transitions** by Joya Cooley is licensed CC BY 4.0.

4.9: Unequal Spacings in Vibration-Rotation Spectra

We find that real rovibrational spectra do not exhibit the equal spacing expectations from the treatment in the previous section and look more like the idealized spectrum in Figure 4.9.1 . As energy increases, the R-branch lines become increasingly similar in energy (i.e., the lines move closer together) and as energy decreases, the P-branch lines become increasingly dissimilar in energy (i.e. the lines move farther apart). This is attributable to two phenomena: *rotational-vibrational coupling* and *centrifugal distortion*.

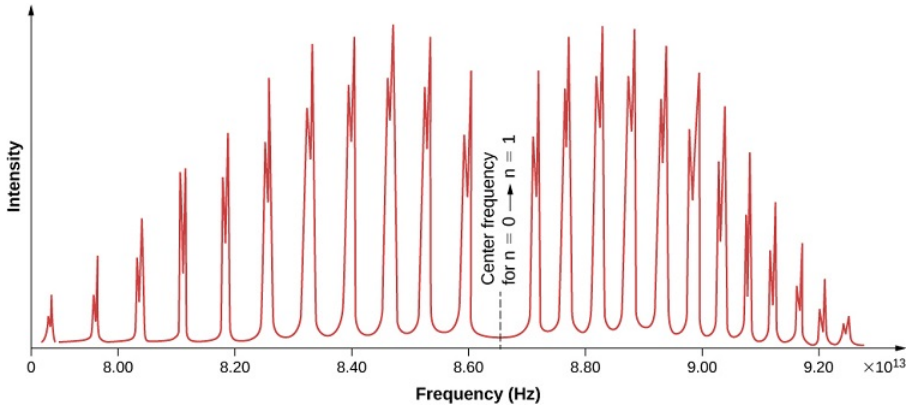


Figure 4.9.1 : Absorption spectrum of hydrogen chloride (**HCl**) from the $n = 0$ to $n = 1$ vibrational levels. The discrete peaks indicate a quantization of the angular momentum of the molecule. The bands to the left indicate a decrease in angular momentum, whereas those to the right indicate an increase in angular momentum. (CC-SA; OpenStax).

Experimental data shows that the P branch has closer spaces between the lines as the frequencies decrease while R branch has further spaces between the lines as the frequencies increase. On the spectrum, R region is on the left and P region is on the right separated by a large gap in between. There are other graphs show differently, but the regions can be labeled using their spacing characteristic discussed below.

Vibration-Rotation Interaction

Consider the rotational constant for a rigid rotator $\tilde{B} = h/8\pi^2 c\mu R_e^2$ where $\tilde{B}$ is the rotational constant, and R_e^2 is the bond length. It is clear from the equation that $\tilde{B}$ depends on R_e^2 in a inverse manner, so $\tilde{B}$ will decrease as R_e^2 increase, and vice versa.

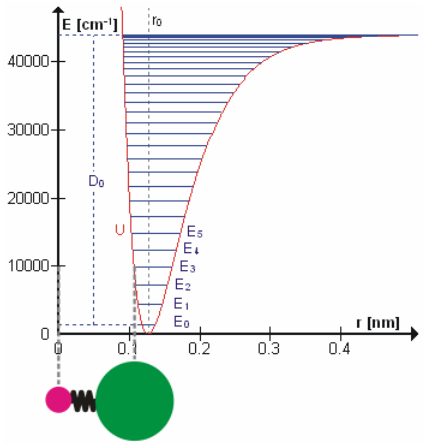


Figure 4.9.2 : Anharmonic Oscillator and Bond Length. Figure used with permission from Wikipedia.

Vibrational state and the bond length also possess a relationship, and that is bond length, R_e^2, will increase as the vibrational state, v increases. High vibrational states have large vibrational amplitudes (the amplitude can be visualized as the distance from one side to the other on the harmonic-oscillator parabola, and higher states has greater distance). On a potential graph, imagine a diatomic molecule with one of the atom fixed at the origin, the bond is along the x-axis, and the molecule vibrate toward and away from the origin along x-axis. The range at how much the bond can stretch or squeeze depend on the vibrational amplitude. So, at high vibrational state (thus high amplitude), the bond can squeeze in and stretch out more (just a little more) on the regular harmonic-

oscillator potential, but it can stretch out greatly on an anharmonic oscillator. That's why bond length increase with vibrational state.

> **Note**
>
> The two relationship established above
>
> - $\tilde{B} \propto R_e^2$ (inversely proportional)
>
> and
>
> - $R_e^2 \propto v$ (directly proportional)
>
> Therefore,
>
> - $\tilde{B} \propto v$ (inversely proportional)
>
> The rotational constant dependent on the vibrational state is denoted as $\tilde{B}_v$, and the dependence of $\tilde{B}$ on v is the vibrational-rotational interaction.

Let's calculate the frequencies of R and P Branches with vibrational dependent rotational constants. The energies of the rigid rotator-harmonic oscillator is

$$\tilde{E}_{v,J} = G(v) + F(J) = \tilde{\nu}(v + \frac{1}{2}) + \tilde{B}J(J+1)$$

or in term of $\tilde{B}_v$

$$\tilde{E}_{v,J} = \tilde{\nu}\left(v + \frac{1}{2}\right) + \tilde{B}_v J(J+1)$$

According to the vibration-rotation interaction, $\tilde{B}_1 < \tilde{B}_0$ because $R_e^2(v=1) > R_e^2(v=0)$. Hence, the frequencies of rovibrational transitions from $v = 0 \rightarrow 1$ can be calculated as the following:

For R branch, allowed $J = 0, 1, 2, ...$

$$\tilde{\nu}_R(\Delta J = +1) = \tilde{E}_{1,J+1} - \tilde{E}_{0,J}$$

$$= \frac{3}{2}\tilde{\nu} + \tilde{B}_1(J+1)(J+2) - \frac{1}{2}\tilde{\nu} - \tilde{B}_0 J(J+1)$$

$$= \tilde{\nu} + 2\tilde{B}_1 + (3\tilde{B}_1 - \tilde{B}_0)J + (\tilde{B}_1 - \tilde{B}_0)J^2$$

For P branch, allowed $J = 1, 2, 3, ...$

$$\tilde{\nu}_P(\Delta J = -1) = \tilde{E}_{1,J-1} - \tilde{E}_{0,J}$$

$$= \tilde{\nu} - (\tilde{B}_1 + \tilde{B}_0)J + (\tilde{B}_1 - \tilde{B}_0)J^2$$

Decrease in Spacing of Lines in the R Branch with Increasing J

A closer look at

$$\tilde{\nu}_R = \tilde{\nu} + 2\tilde{B}_1 + (3\tilde{B}_1 - \tilde{B}_0)J + (\tilde{B}_1 - \tilde{B}_0)J^2$$

shows that the last term in the parentheses $(\tilde{B}_1 - \tilde{B}_0)$ will be always negative because $\tilde{B}_1 < \tilde{B}_0$, and it also multiplies with J^2, so the square term $(\tilde{B}_1 - \tilde{B}_0)J^2$ will give a larger negative value for increasing J. As a result, $\tilde{\nu}_R = \tilde{\nu}+$(smaller and smaller value) as J increase. Because the rotational frequencies keep getting smaller, the spacing between lines in R branch decreases as J increases.

Increasing in Spacing of Lines in the P Branch with Decreasing J

Using the same analysis as above,

$$\tilde{\nu}_P = \tilde{\nu} - (\tilde{B}_1 + \tilde{B}_0)J + (\tilde{B}_1 - \tilde{B}_0)J^2$$

shows that the last term in the parentheses $(\tilde{B}_1 - \tilde{B}_0)$ will be always negative because $\tilde{B}_1 < \tilde{B}_0$, and it also multiplies with J^2, so the square term $(\tilde{B}_1 - \tilde{B}_0)J^2$ will give a larger negative value even for decreasing J. As a result, $\tilde{\nu}_R = \tilde{\nu}$–(smaller and smaller value) as J decreases. Because the rotational frequencies keep getting larger, the spacing between lines in P branch increase as J decreases.

References

1. McQuarrie, Donald A. Quantum Chemistry. New York: University Science Books, 2007.
2. Hollas, M. J. *Modern spectroscopy*. (3rd ed.). Chichester: John Wiley & Sons, 1996.
3. Hollas, M. J. *Basic atomic and molecular spectroscopy*. Cambridge: The Royal Society of Chemistry, 2002.
4. Herzberg, G. *Molecular spectra and molecular structure*. (2nd ed.). New York: Prentice-Hall, 1950.
5. Fetterolf, Monty L. Enhanced Intensity Distribution Analysis of the Rotational–Vibrational Spectrum of HCl. J. Chem. Ed. **2007**, *84*, 1064. DOI: 10.1021/ed084p1062

4.9: Unequal Spacings in Vibration-Rotation Spectra is shared under a CC BY-NC-SA 4.0 license and was authored, remixed, and/or curated by Joya Cooley & Dayton Dang.

- **13.3: Unequal Spacings in Vibration-Rotation Spectra** by Dayton Dang, Joya Cooley is licensed CC BY-NC-SA 4.0.

4.10: Electronic Spectra Contain Electronic, Vibrational, and Rotational Information

4.10.1: Introduction

If the photon energies are high enough (generally visible or shorter wavelength) absorption or emission of the light by a molecule can lead to electronic transitions. Just as rotational transitions can combine with the more closely spaced rotational transitions to create rovibrational spectra, electronic spectra can exhibit simultaneous changes in electronic, vibrational and rotational states of the molecule.

4.10.2: Electron Transitions are not Purely Electronic

We have thus far studied *rovibrational transitions*--that is, transitions involving both the vibrational and rotational states. Similarly, electronic transitions tend to accompany both rotational and vibrational transitions. These are often portrayed as an electronic potential energy cure with the vibrational level drawn on each curve. *Additionally, each vibrational level has a set of rotational levels associated with it.*

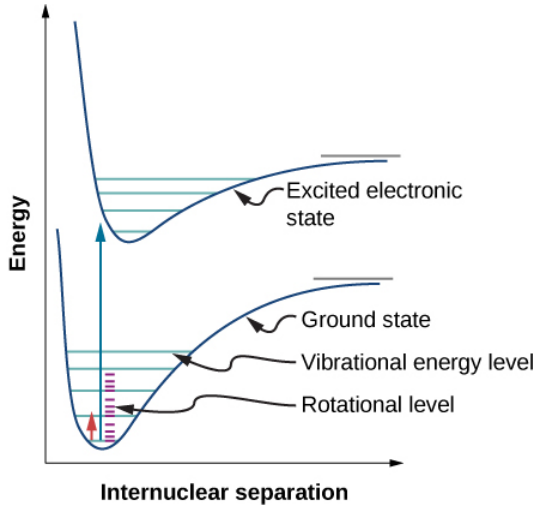


Figure **4.10.1** : Three types of energy levels in a diatomic molecule: electronic, vibrational, and rotational. If the vibrational quantum number (v) changes by one unit, then the rotational quantum number (J) changes by one unit. (CC BY 3.0; OpenStax).

Recall that in the Born-Oppenheimer approximation, nuclear kinetic energies can be ignored (e.g., fixed) to solve for electronic wavefunctions and energies, which are much faster than rotation or vibration. As such, it is important to note that unlike rovibrational transitions, electronic transitions aren't dependent on rotational or vibrational transitions and are assumed to be separate. Therefore, when using an anharmonic oscillator-nonrigid rotator approximation (and excluding translational energy), the total energy of a diatomic is:

$$\tilde{E}_{total} = \tilde{\nu}_{el} + G(v) + F(J) \tag{4.10.1}$$

where $\tilde{\nu}_{el}$ is the electronic transition energy change in wavenumbers, $G(v)$ is the vibrational energy with energy level v (assuming anharmonic oscillator), and $F(J)$ is the rotational energy, assuming a nonrigid rotor. Equation 4.10.1 can be expanded accordingly:

$$\tilde{E}_{total} = \underbrace{\tilde{\nu}_{el}}_{\text{electronic}} + \underbrace{\tilde{\nu}_e\left(v+\frac{1}{2}\right) - \tilde{\chi}_e\tilde{\nu}_e\left(v+\frac{1}{2}\right)^2}_{\text{vibrational}} + \underbrace{\tilde{B}J(J+1) - \tilde{D}J^2(J+1)^2}_{\text{rotational}} \tag{4.10.2}$$

Notice that both the vibration constant ($\tilde{\nu}_e$) and anharmonic constant ($\tilde{\chi}_e$) are electronic state dependent (and hence the rotational constants would be too, but are ignored here). Since rotational energies tend to be so small compared to electronic, their effects are minimal and are typically ignored when we do calculations and are referred to as *vibronic* transitions.

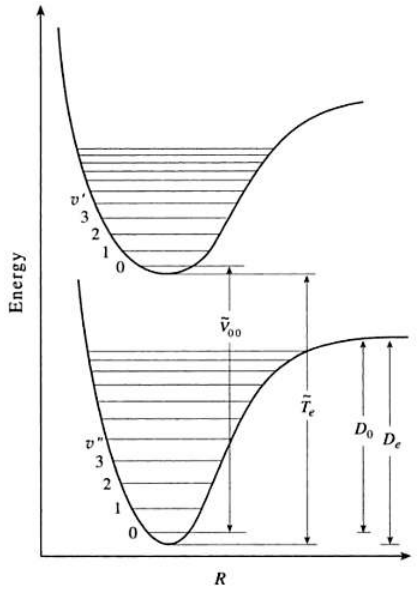


Figure **4.10.2** : As you can see, electronic transitions involve two energy potential wells! The vibrational levels are included, but rotational levels are excluded.

The eigenstate-to-eigenstate transitions (e.g., $\mathbf{1 \rightarrow 2}$) possible are numerous and have absorption lines at

$$\tilde{\nu}_{obs} = \tilde{E}_2 - \tilde{E}_1 \tag{4.10.3}$$

and for simplification, we refer to constants associated with these states as $|'\rangle$ and $|''\rangle$, respectively. So Equation 4.10.3 is

$$\tilde{\nu}_{obs} = E''\tilde{(v'')} - E'\tilde{(v')}$$

Also important to note that typically vibronic transitions are usually the result of the vibrational $v' = 0$ vibratonal state. Within this assumption and excluding the rotational contributions (due to their low energies), Equation 4.10.2 can be used with Equation 4.10.3 to get

$$\tilde{\nu}_{obs} = \tilde{T}_{el} + \left(\frac{1}{2}\tilde{\nu}'_e - \frac{1}{4}\tilde{\chi}'_e\tilde{\nu}'_e\right) - \left(\frac{1}{2}\tilde{\nu}''_e - \frac{1}{4}\tilde{\chi}''_e\tilde{\nu}''_e\right) + \tilde{\nu}'_e v'' - \tilde{\chi}'_e\tilde{\nu}'_e v''(v''+1) \tag{4.10.4}$$

A common transition of importance is the $\tilde{\nu}_{00}$, which is the $\mathbf{0 \rightarrow 0}$ transition and include no vibrational change. For this case, equation 4.10.4 is then

$$\tilde{\nu}_{00} = \tilde{T}_{el} + \left(\frac{1}{2}\tilde{\nu}'_e - \frac{1}{4}\tilde{\chi}'_e\tilde{\nu}'_e\right) - \left(\frac{1}{2}\tilde{\nu}''_e - \frac{1}{4}\tilde{\chi}''_e\tilde{\nu}''_e\right)$$

This is the lowest energy possible to observe in an electronic transition although it may be of low intensity as discussed in the following section.

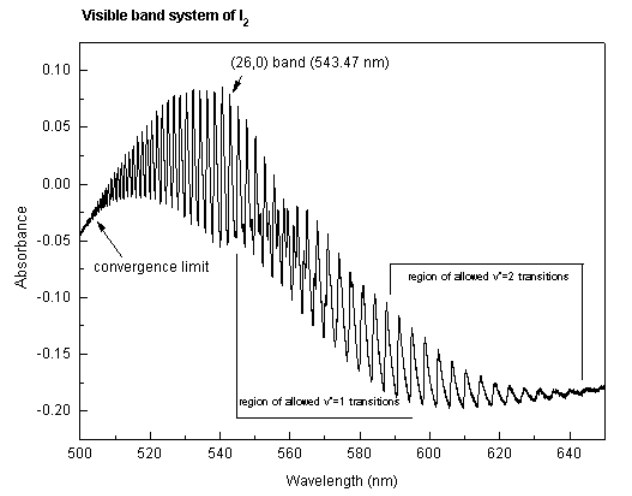
Iodine

The absorption spectrum of iodine yields information about the excited state well rather than the ground state well (notice that equation 4.10.4 depends primarily on excited state parameters).

Recall that as v' increases, the vibrational energy spacing decreases. At the upper edge of the well, the vibrational energy spacing decreases to 0, which means that the energies form a continuum rather than being quantized. It is at this limit that **bond dissociation occurs**. The energy required to dissociate the bond is actually D'_o rather than D'_e because the molecule cannot have less than **the zero point energy**.

The vibrational-electronic spectrum of I_2 in the region from 500-650 nm displays a large number of well-defined bands which, for the most part, correspond to v'<-- 0 transitions connecting the v" = 0 vibrational level of the ground electronic state (denoted as $X^1\Sigma^+$) to many different vibrational levels v' of the excited $B^3\Pi$ electronic state. Under the conditions of this experiment (i.e., low resolution), the rotational lines within each band are not resolved. However, the peaks may be identified

as R-branch band heads (1). For a molecule as heavy as I_2, the position of each band head is within a few tenths of one cm^{-1} of the band origin (2), and for the purposes of this discussion, the distinction between the two may be ignored. The general features of the absorption spectrum are shown below:



Each small bump, or peak, such as the (26,0) band labelled on the spectrum, corresponds to a transition between two vibrational levels and is called a *band*. Each band is comprised of several hundred *lines*, each of which involves different upper and lower rotational quantum numbers; as mentioned, these lines are not resolved in the spectrum. The region of maximum absorption in each band is caused by many of these lines falling together; it is called the *band head*. The set of all of these bands is referred to as the *visible band system* of I_2.

If the sample is hot, then excited vibrational levels of the ground state may be populated, and these also will absorb light. The *hot bands* arising from absorption from v''=1 and v''=2 are shown very approximately on the absorption spectrum above.

This page titled 4.10: Electronic Spectra Contain Electronic, Vibrational, and Rotational Information is shared under a CC BY-SA 4.0 license and was authored, remixed, and/or curated by Jonathan Gutow.

- **13.6: Electronic Spectra Contain Electronic, Vibrational, and Rotational Information** is licensed CC BY-SA 4.0.

4.11: The Franck-Condon Principle

Learning Objectives

- To explain the vibrational fine structure in electronic spectroscopy for bound excited states in terms of the Franck-Condon approximation
- To calculate the vibrational progressions (Franck-Condon factors) in a single displaced harmonic oscillator vibronic system.

4.11.1: Introduction

The **Franck-Condon Principle** describes the intensities of vibronic transitions, or the absorption or emission of a photon. It states that when a molecule is undergoing an electronic transition, such as ionization, the nuclear configuration of the molecule experiences no significant change. This is due in fact that nuclei are much more massive than electrons and the electronic transition takes place faster than the nuclei can respond. When the nucleus realigns itself with the new electronic configuration, the theory states that it must undergo a vibration.

If we picture the vertical transition from ground to excited electronic state as occurring from a vibrational wavefunction that gives a probability distribution of finding the nuclei in a give region of space we can determine the probability of a given vibrational level from the overlap integral $S_{v',v}$ which gives the overlap of the vibrational wavefunction in the ground and excited state. The v' quantum numbers refer to the ground state and the v quantum numbers refer to the excited state. The transition probability can be separated into electronic and nuclear parts using the Condon approximation.

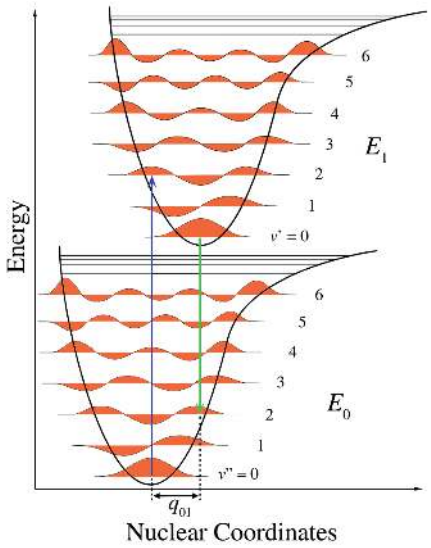


Figure **4.11.1** : Franck–Condon principle energy diagram. Since electronic transitions are very fast compared with nuclear motions, vibrational levels are favored when they correspond to a minimal change in the nuclear coordinates. The potential wells are shown favoring transitions between $v = 0$ and $v' = 2$. (CC-SA-BY-3.0; Samoza).

In Figure **4.11.1** , the nuclear axis shows a consequence of the internuclear separation and the vibronic transition is indicated by the blue and green vertical arrows. This figure demonstrates three things:

1. An absorption leads to a higher energy state,
2. fluorescence leads to a lower energy state, and
3. the shift in nuclear coordinates between the ground and excited state is indicative of a new equilibrium position for the nuclear interaction potential. The fact that the fluorescence arrow is shorter than the absorption indicates that it has less energy, or that its wavelength is longer.

The Classical Condon approximation

Condon approximation is the assumption that the electronic transition occurs on a time scale short compared to nuclear motion so that the transition probability can be calculated at a fixed nuclear position.

The **rapid electronic excitation** results in the change of electronic state without a change in molecular geometry. This is called a **vertical transition**. Notice that when the transition is from, for example, the v = 0 equilibrium geometry in the ground state the molecular geometry will not be the equilibrium geometry in the excited state. Classically this would mean that after the transition the molecule would be vibrationally excited. Because real molecules are quantum systems it really means that a vibrationally excited state is more likely.

The Franck-Condon Principle explains the relative intensities of vibronic transitions by relating the probability of a vibrational transition to the overlap of the vibrational wavefunctions. The probability of a vibrational transition occurring is the square of the transition dipole expectation value:

$$\begin{aligned} P_{i\rightarrow f} &= |\langle \psi^*_{final}|\mu|\psi_{initial}\rangle|^2 \\ &= \left|\int \psi^*_{final}\mu\psi_{initial}d\tau\right|^2 \end{aligned}$$

Within the Franck-Condon approximation, the nuclei are considered "fixed" during electronic transitions. Thus, electronic transitions can be considered vertical transitions on electronic potential energy curves (vertical transitions in Figure **4.11.1**).

The Quantum Franck-Condon Principle

The Franck-Condon Principle has both a Classical and Quantum application. Classically, the Franck–Condon principle is the approximation that an electronic transition is most likely to occur without changes in the positions of the nuclei in the molecular entity and its environment. The resulting state is called a Franck–Condon state, and the transition involved, a vertical transition. The quantum mechanical formulation of this principle is that the intensity of a vibronic transition is proportional to the square of the overlap integral between the vibrational wavefunctions of the two states that are involved in the transition.

The Franck-Condon principle is based on the Born-Oppenheimer approximation, which allows separation of the electronic q and nuclear Q wavefunctions given the total wavefunction.

$$|\psi_{total}(Q,q) = |\psi_{nuc}(Q)\rangle\psi_{el}(Q;q)\rangle$$

Since the transition operator, $\hat{\mu}(q)$, is dependent only on the electronic component, the nuclear components can be separated from the transition moment integral that dictates the probability of the transition occurring:

$$\langle\psi^*_{total,f}|\hat{\mu}|\psi_{total,i}\rangle = \langle\psi^*_{nuc,f}|\langle\psi^*_{el,f}|\mu|\psi_{el,i}\rangle|\psi_{nuc,i}\rangle \tag{4.11.1}$$

$$= \underbrace{\langle\psi^*_{nuc,f}|\psi_{nuc,i}\rangle}_{\text{nuclear overlap}}\langle\psi^*_{el,f}|\mu|\psi_{el,i}\rangle \tag{4.11.2}$$

If the nuclear overlap integral is zero for this transition, then the transition will not be observed, irrespective of the magnitude of the electronic factor.

4.11.2: S_{00} Transition Evaluated within Harmonic Oscillator Model

The nuclear overlap for the zero-zero transition S_{00} can be calculated quite simply using the definition of the Gaussian form of the harmonic oscillator wavefunctions.

The zero-point wavefunction in the ground electronic state is

$$|\psi(R)\rangle = |\left(\frac{\alpha}{\pi}\right)^{1/4} e^{-\alpha(R-R_e)^2/2}\rangle$$

The zero-point wavefunction in the excited electronic state is

$$|\psi(R)\rangle = |\left(\frac{\alpha}{\pi}\right)^{1/4} e^{-\alpha(R-Q_e)^2/2}\rangle$$

where

- $\alpha = \frac{\sqrt{mk}}{\hbar}$

- R_e is the equilibrium bond length in the ground electronic state
- Q_e is the equilibrium bond length in the excited electronic state

The nuclear overlap integral is

$$S_{00} = \langle \psi^*_{nuc,f} | \psi_{nuc,i} \rangle = \sqrt{\frac{\alpha}{\pi}} \int_{\infty}^{\infty} e^{-\alpha(R-R_e)^2/2} e^{-\alpha(R-Q_e)^2/2} dR \tag{4.11.3}$$

The exponent in Equation 4.11.3 can be expanded as

$$S_{00} = \sqrt{\frac{\alpha}{\pi}} \int_{\infty}^{\infty} e^{-\alpha(2R^2 - RR_e - 2RQ_e + R_e^2 + Q_e^2)/2} dR \tag{4.11.4}$$

and we use

$$(R_e + Q_e)^2 = R_e^2 + Q_e^2 + 2R_eQ_e$$

and

$$(R_e - Q_e)^2 = R_e^2 + Q_e^2 - 2R_eQ_e$$

to substitute and complete the square inside the integral. We can express

$$R_e^2 + Q_e^2 = \frac{1}{2}[(R_e + Q_e)^2 + (R_e - Q_e)^2].$$

Thus, the integral in Equation 4.11.4 is

$$S_{00} = \sqrt{\frac{\alpha}{\pi}} e^{-\alpha(R_e - Q_e)^2/4} \int_{-\infty}^{\infty} e^{-\alpha\{R - 1/2(R_e + Q_e)\}^2} dR$$

The integral is a **Gaussian integral**. You can show that if we let $z = \sqrt{\alpha}\{R - 1/2(R_e + Q_e)\}$ then $dz = \sqrt{\alpha} dR$ and the integral becomes

$$S_{00} = \sqrt{\frac{\alpha}{\pi}} e^{-\alpha(R_e - Q_e)^2/4} \frac{1}{\sqrt{\alpha}} \int_{-\infty}^{\infty} e^{z^2} dz \tag{4.11.5}$$

this integral has been solved already, from a table of integrals, Equation 4.11.5 becomes

$$S_{00} = e^{-\alpha(R_e - Q_e)^2/4} \tag{4.11.6}$$

We would follow the same procedure to calculate that overlap of the zeroth level vibration in the ground to the first excited vibrational level of the excited state: S_{01}.

4.11.3: S_{01} Transition Evaluated within Harmonic Oscillator Model

To calculate the overlap of zeroth ground state level ($v = 0$) with the first excited state level ($v' = 1$) we use the Hermite polynomial $H_1(x) = 2x$ for describing the excited state wavefunction (see here for a review on harmonic oscillator wavefunctions). Here $x = \sqrt{\alpha}(R - Q_e)$.

$$S_{01} = \langle \psi^*_{nuc,f} | \psi_{nuc,i} \rangle \tag{4.11.7}$$

with the zero-point wavefunction in the ground electronic state is

$$|\psi(R)\rangle = \left| \left(\frac{\alpha}{\pi}\right)^{1/4} e^{-\alpha(R-R_e)^2/2} \right\rangle$$

The first excited-state wavefunction in the excited electronic state is

$$|\psi(R)\rangle = \left| \left(\frac{\alpha}{\pi}\right)^{1/4} \sqrt{\alpha} 2(R - Q_e) e^{-\alpha(R-Q_e)^2/2} \right\rangle$$

The overlap of zeroth ground state level with the first excited state level (Equation 4.11.7) is then

$$S_{01} = \frac{1}{\sqrt{2}}\sqrt{\frac{\alpha}{\pi}}\int_{-\infty}^{\infty} e^{-\alpha(R-R_e)^2/2}\sqrt{\alpha}2(R-Q_e)e^{-\alpha(R-Q_e)^2/2}$$

and

$$S_{01} = \sqrt{\frac{2\alpha^2}{\pi}}e^{-\alpha(R_e-Q_e)^2/4}\int_{-\infty}^{\infty}(R-Q_e)e^{-\alpha\{R-1/2(R_e+Q_e)^2\}}$$

The same substitutions can be made as above so that the integral can be written as (not shown and to be demonstrated in a homework exercises) and the final result is

$$S_{01} = \sqrt{\frac{\alpha^2}{2}}(R_e-Q_e)e^{-\alpha(R_e-Q_e)^2/4} \tag{4.11.8}$$

We could continue and calculate that overlap of the zeroth level in the ground state with all the higher light vibrational levels: S_{02}, S_{03}, etc. Each term corresponds to a transition with a different energy since the vibrational levels have different energies. The absorption band then has the appearance of a progression (a Franck-Condon progression) of transitions between different levels each with its own probability.

4.11.4: Franck-Condon Progressions

To understand the significance of the above formula for the FC factor, let us examine a ground and excited state potential energy surface at $T = 0$ Kelvin. Shown below are two states separated by 8,000 cm^{-1} in energy. This is energy separation between the bottoms of their potential wells, but also between the respective zero-point energy levels. Let us assume that the wavenumber of the vibrational mode is 1,000 cm^{-1} and that the bond length is increased due to the fact that an electron is removed from a bonding orbital and placed in an anti-bonding orbital upon electronic excitation.

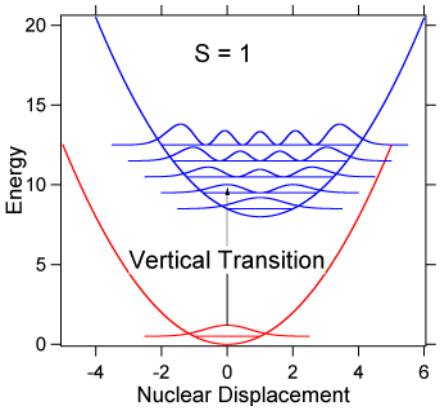


Figure **4.11.2** : Wavefunctions transitions for a harmonic oscillator model system with moderate separation (S=1).

According to the above model for the Franck-Condon factor we would generate a "stick" spectrum (Figure **4.11.3**) where each vibrational transition is infinitely narrow and transition can only occur when $E = h\nu$ exactly. For example, the potential energy surfaces were given for S = 1 and the transition probability at each level is given by the sticks (black) in the figure below.

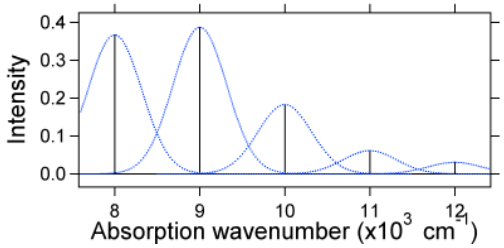


Figure **4.11.3** : Stick spectrum, dressed with Gaussians, for the moderate separation (S=1) harmonic oscillator system from Figure **4.11.2**. The lowest energy transition v = 0 to v = 0 transtion.

The dotted Gaussians that surround each stick give a more realistic picture of what the absorption spectrum should look like. In this first place each energy level (stick) will be given some width by the fact that the state has a finite lifetime. Such broadening is

called homogeneous broadening since it affects all of the molecules in the ensemble in a similar fashion. There is also broadening due to small differences in the environment of each molecule. This type of broadening is called inhomogeneous broadening. Regardless of origin the model above was created using a Gaussian broadening

The nuclear displacement between the ground and excited state determines the shape of the absorption spectrum. Let us examine both a smaller and a larger excited state displacement. If $S = ½$ and the potential energy surfaces in this case are:

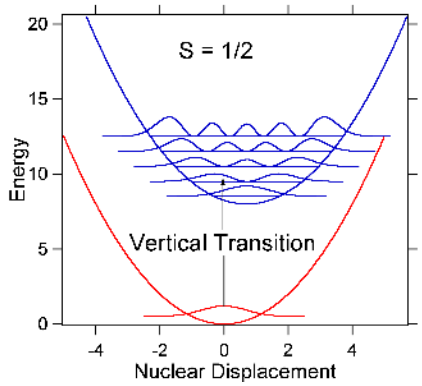


Figure **4.11.4** : Wavefunctions transitions for a harmonic oscillator model system with small displacement (S=1/2).

For this case the "stick" spectrum has the appearance in Figure **4.11.5**

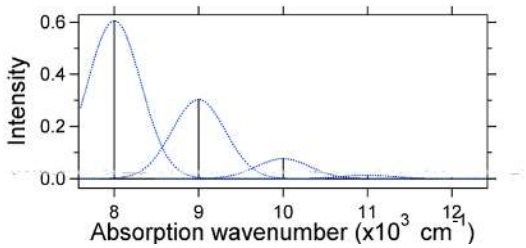


Figure **4.11.5** : Stick spectrum, dressed with Gaussians, for the small displacement (S=1/2) harmonic oscillator system from Figure **4.11.4**.

Note that the zero-zero or $S_{0,0}$ vibrational transition is much large in the case where the displacement is small.

> As a general rule of thumb the S constant gives the ratio of the intensity of the $v = 2$ transition to the $v = 1$ transition. In this case since $S = 0.5$, the $v = 2$ transition is 0.5 the intensity of $v = 1$ transition.

As an example of a larger displacement the disposition of the potential energy surfaces for S = 2 is shown below.

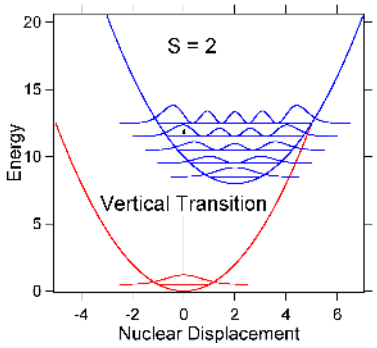


Figure **4.11.6** : Wavefunctions transitions for a harmonic oscillator model system with strong displacement (S=2).

The larger displacement results in decreased overlap of the ground state level with the v = 0 level of the excited state. The maximum intensity will be achieved in higher vibrational levels as shown in the stick spectrum.

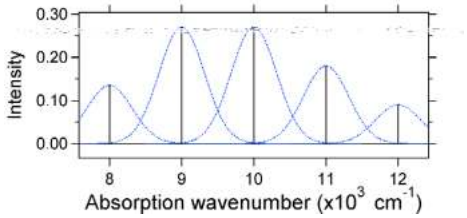


Figure **4.11.7** : Stick spectrum, dressed with Gaussians, for the large displacement (S=2) harmonic oscillator system from Figure **4.11.6**.

The absorption spectra plotted below all have the same integrated intensity, however their shapes are altered because of the differing extent of displacement of the excited state potential energy surface.

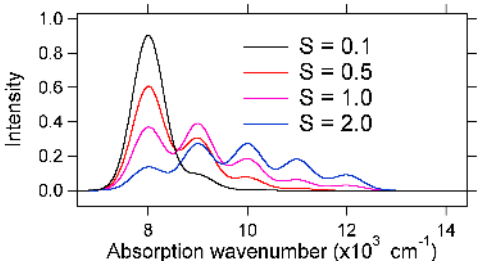


Figure **4.11.8** : Stick spectra, dressed with Gaussians, for the small to large displacements in harmonic oscillator system described above.

So the nature of the relative vibronic band intensities can tell us whether there is a displacement of the equilibrium nuclear coordinate that accompanied a transition. When will there be an increase in bond length (i.e., $Q_e > R_e$)? This occurs when an electron is promoted from a bonding molecular orbital to a non-bonding or anti-bonding molecular orbitals (i.e., when the bond order is less in the excited state than the ground state).

4.11.5: References

1. J.M. Luis, D.M. Bishop, B. Kirtman. *A different approach for calculating Franck–Condon factors including anharmonicity.* J. Chem. Phys., 120 (2004), pp. 813–822.
2. Atkins, Peter and Julio de Paula. Physical Chemistry for the Life Sciences. 2006. New York, NY: W.H. Freeman and Company. p. 563-564
3. Franck-Condon Principle. 1996, 68, 2243. IUPAC Compendium of Chemical Terminology 2nd Edition (1997). www.iupac.org/goldbook/F02510.pdf
4. E.Rabinowitch and Govindjee. Light Absorption and Fate of Excitation of Energy. 1969. Franck-Condon Principle. http://www.life.uiuc.edu/govindjee/b...em494/Abs.html

---

This page titled 4.11: The Franck-Condon Principle is shared under a CC BY-NC-SA 4.0 license and was authored, remixed, and/or curated by Stefan Franzen & Matthew Ziering.

- **13.7: The Franck-Condon Principle** by Matthew Ziering, Stefan Franzen is licensed CC BY-NC-SA 4.0.

4.12: Electronically Excited Molecules can Relax by a Number of Processes

4.12.1: Introduction

To understand fluorescence, phosphorescence and how lasers work we must first describe how a molecule in an excited state can relax back to the ground state because the light emitted is influenced by these relaxation processes. The two radiative decay pathways for an excited molecule are fluorescence and phosphorescence. Fluorescence differs from phosphorescence in that the energy transition that is responsible for fluorescence does not involve a change in electron spin multiplicity. Thus fluorescence lifetimes are short (10^{-9} - 10^{-6} s). In phosphorescence, there is a change in electron spin multiplicity, resulting in a longer lifetime of the excited state (second to minutes). A description of electron spin and the differences between singlet and triplet states will clarify the difference between fluorescence and phosphorescence.

4.12.2: Spin Multiplicity - Singlet and Triplet Excited States

The Pauli Exclusion principle states that two electrons in an atom cannot have the same four quantum numbers (n, l, m_l, m_s). Therefore, because two electrons can occupy each orbital, these two electrons must have opposite spin states. These opposite spin states are called spin pairing. Because of this spin pairing, most molecules are diamagnetic, and are not attracted or repelled by an external magnetic or electric field. Molecules that contain unpaired electrons (free radicals) do have magnetic moments that are attracted to an external magnetic or electric field.

A molecule is said to be in a singlet state when all the electron spins are paired in the molecular electronic state, and the electronic energy levels do not split when the molecule is exposed to a magnetic field. A doublet state occurs when there is an unpaired electron that gives two possible orientations when exposed to a magnetic field and imparts different energies to the system. A singlet or a triplet state can form when one electron is excited to a higher energy level. In an excited singlet state, the promoted electron retains the spin orientation it had in the ground state (i.e., paired). In a triplet excited state, the promoted electron undergoes a change in spin, and so has the same spin orientation (parallel) to the unpaired electron that remains in the ground state orbital. The difference between the spins of ground singlet, excited singlet, and excited triplet is shown in Figure **4.12.1**. The terms singlet, doublet and triplet are derived using the equation for multiplicity, 2S+1, where S is the total spin angular momentum (sum of all the electron spins). Individual spins are denoted as spin up (s = +1/2) or spin down (s = -1/2). If we were to calculate the multiplicity for the singlet ground state or the singlet excited state, the equation would be

$$2(+1/2 + -1/2) + 1 = 2(0) + 1 = 1$$

In a similar fashion, the spin multiplicity for the triplet excited state can be calculated as

$$2(+1/2 + +1/2) + 1 = 2(1) + 1 = 3$$

which gives a triplet state as expected.

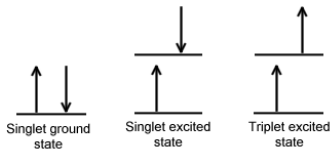


Figure **4.12.1**: Spin in the ground and excited states (Tyler Matthews - Paint Shop Pro, Public Domain, https://commons.wikimedia.org/w/inde...curid=64926546)

The difference between a molecule in the ground and the triplet excited state is that the molecule is diamagnetic in the ground state and paramagnetic in the triplet excited state. This difference in spin state makes the transition from singlet to triplet (or triplet to singlet) less likely than the singlet-to-singlet transitions. For this reason, the lifetime of the triplet state is longer than the lifetime of the singlet state by a factor of roughly 10^4 seconds. The transition from ground to excited triplet state has a low probability of occurring, thus these absorption bands are less intense than singlet-singlet state absorption bands. However, an excited triplet state can be populated from an excited singlet state of certain molecules. Jablonski diagrams can be used to explain transitions such as this that occur in photoluminescence molecules.

4.12.3: Jablonski Diagrams

Aleksander Jablonski was a Polish academic who devoted his life to the study of molecular absorbance and emission of light. He developed a graphic representation that shows the possible consequences of applying photons from the visible spectrum of light to a particular molecule. These schematics are referred to as Jablonski diagrams.

A Jablonski diagram is an energy diagram, arranged with energy on a vertical axis. The energy levels can be quantitatively denoted, but most of these diagrams use energy levels schematically. The rest of the diagram is arranged into columns. Every column usually represents a specific spin multiplicity for a particular species. However, some diagrams divide energy levels within the same spin multiplicity into different columns. Within each column, horizontal lines represent eigenstates for that particular molecule. Bold horizontal lines are representations of the limits of electronic energy states. Within each electronic energy state are multiple vibrational energy states that may be coupled with the electronic state. Usually only a portion of these vibrational eigenstates are represented due to the massive number of possible vibrations in a molecule. Each of these vibrational energy states can be subdivided even further into rotational energy levels; however, typical Jablonski diagrams omit such intense levels of detail.

Through the use of straight and wavy lines, these figures show transitions between eigenstates that occur from the exposure of a molecule to a particular wavelength of light. Straight lines show the conversion between a photon of light and the energy of an electron. Wavy lines show nonradiative transitions of electrons. Within a Jablonski diagram several different pathways show how an electron may accept and then dissipate the energy from a photon. Thus, most diagrams start with arrows originating from the ground electronic state and finish with arrows returning to the ground electronic state.

The Jablonski diagram drawn below is a partial energy diagram that represents the energy of a photoluminescent molecule in its different energy states. The lowest and darkest horizontal line represents the ground-state electronic energy of the molecule which is the singlet state labeled as S_o. At room temperature, a majority of the molecules are in this state. The thicker lines on the left labeled S_1, S_2 , and S_3 represent the excited electronic states for the molecule in the singlet state. The thicker lines on the right labeled T_1, T_2, and T_3 represent excited triplet states.

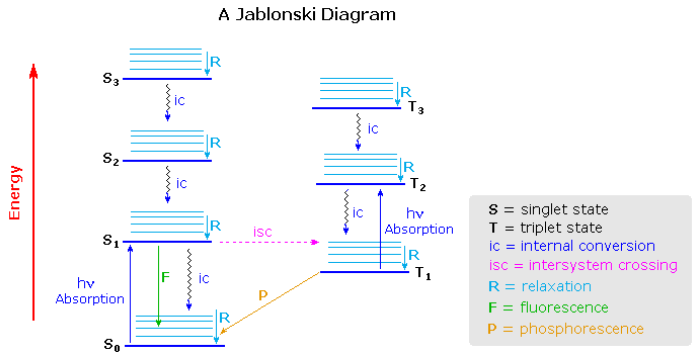


Figure **4.12.2**: Partial Jablonski Diagram for Absorption, Fluorescence, and Phosphorescence. (Bill Reusch, Michigan State University).

4.12.4: Deactivation Processes

A molecule that is excited can return to the ground state by several combinations of mechanical steps that will be described below and shown in Figure **4.12.2**.The deactivation process of fluorescence and phosphorescence involve an emission of a photon radiation as shown by the straight arrow in Figure **4.12.2**. The wiggly arrows in Figure **4.12.2** are deactivation processes without the use of radiation. The favored deactivation process is the route that is most rapid and spends the least time in the excited state. If the rate constant for relaxation is more favorable in the radiationless path, the fluorescence will be less intense or absent.

4.12.4.1: Relaxation and Fluorescence

Often, when an excited state species relaxes, giving off a photon, the wavelength of the photon is different from the one that initially led to excitation. When this happens, the photon is invariably red-shifted; its wavelength is longer than the initial one. This situation is called "fluorescence" (Figure **4.12.3**).

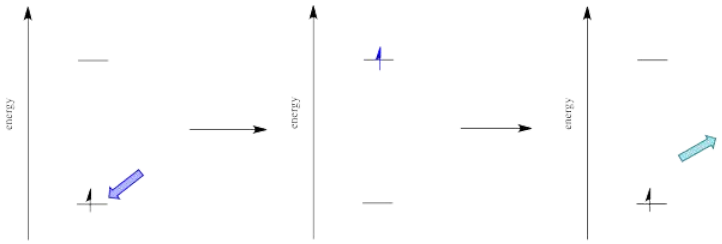


Figure 4.12.3: The absorption of purple light by a ground state particle, leading to the creation of an excited state particle. This excited state particle then emits blue light as it returns to the ground state.

How can that be? Isn't energy quantized? How is the molecule suddenly losing some of the energy that the original photon brought with it? This energy discrepancy is related to the Franck-Condon principle from the previous page. When an electron is promoted to an electronic excited state, it often ends up in an excited vibrational state as well (Figure 4.12.4). Vibrational energy, however, is not exchanged exclusively by means of photons. It can be gained or lost through molecular collisions and heat transfer.

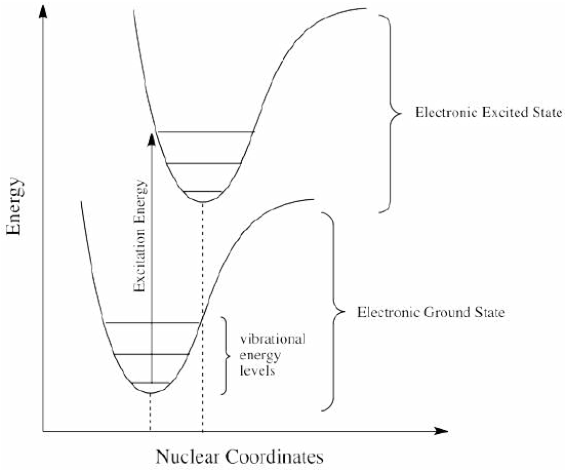


Figure 4.12.4: Transition from the ground state to an excited vibrational state within the excited electronic state.

Thus, an excited state molecule with an electron in a high-energy vibrational level within an excited electronic state might simply re-emit a photon of exactly the same wavelength as the one that was absorbed. But the excited electron is much more likely to relax into the lowest vibrational state within the excited electronic state, losing some of that initial excitation energy as heat. When the electron relaxes to this lower vibrational state, the energy gap between this excited state and the ground state is a little smaller. The photon that is emitted upon fluorescence will have lower energy and longer wavelength than a photon emitted from the original, higher vibrational level, excited state. See Figure 4.12.5.

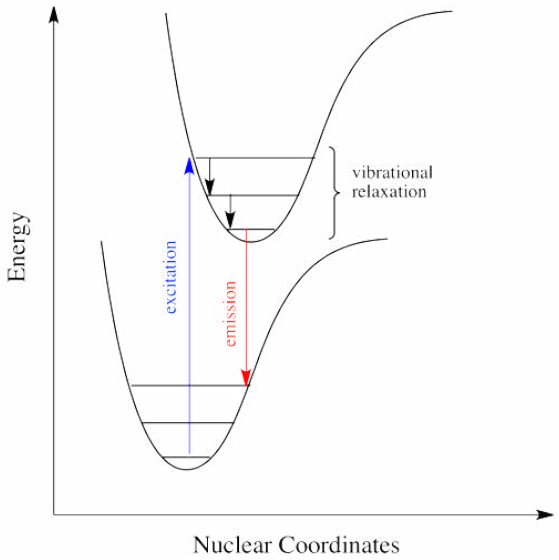


Figure 4.12.5: Excitation, followed by vibrational relaxation, and then emission.

Figure 4.12.6 shows the fluorescence transitions of a hypothetical diatomic molecule in which the equilibrium bond length of the ground state and the first singlet excited state are identical. In this molecule all absorptions involve transitions from the lowest vibrational level of the electronic ground state ($v'' = 0$) to various vibrational levels in the excited electronic state. Because vibrational relaxation occurs more rapidly than fluorescence, the fluorescence spectrum is composed of lines showing transitions from the lowest vibrational level of the excited state ($v' = 0$) to various vibrational levels in the electronic ground state.

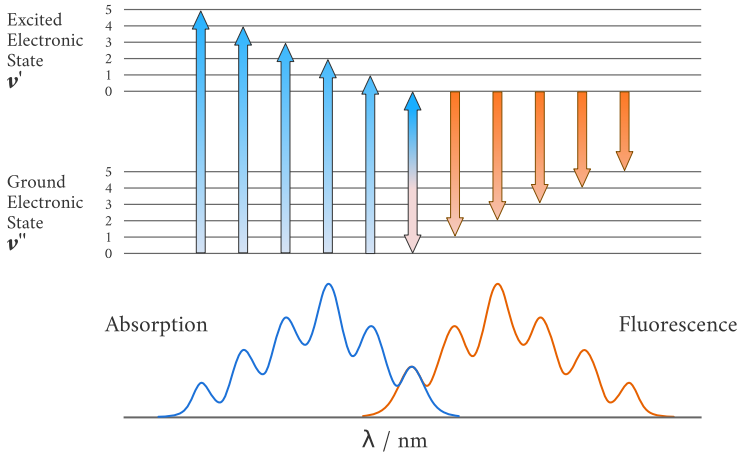


Figure 4.12.6: Absorption and fluorescence transitions in a hypothetical diatomic molecule in which the equilibrium bond length of the ground state is equal to the equilibrium bond length of the excited state. (CC BY-NC; Ümit Kaya, via LibreTexts)

Just how does a molecule undergo vibrational relaxation? Vibrational energy is the energy used to lengthen or shorten bonds, or to widen or squeeze bond angles. Given a big enough molecule, some of this vibrational energy could be transferred into bond lengths and angles further away from the electronic transition. Otherwise, if the molecule is small, it may transfer some of its energy in collisions with other molecules. In molecules, as one molecule drops to a lower vibrational state, the other will hop up to a higher vibrational state with the energy it gains. In Figure 4.12.7 below, the red molecule is in an electronic excited and vibrational state. In a collision, it transfers some of its vibrational energy to the blue molecule.

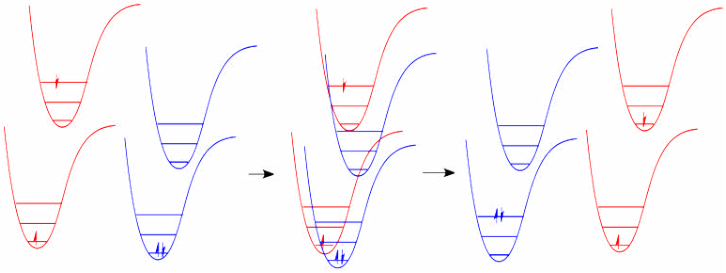


Figure **4.12.7**: The transfer of vibrational energy (heat) through a collision.

Note

There are many examples of energy being transferred this way in everyday life. In a game of pool, one billiard ball can transfer its energy to another, sending it toward the pocket. Barry Bonds can transfer a considerable amount of energy through his bat into a baseball, sending it out of the park, just as Serena Williams can send a whole lot of energy whizzing back at her sister.

Exercise 4.12.1

How does the energy of an electronic absorption compare to other processes? To find out, you might consider the excitation of an entire mole of molecules, rather than a single molecule absorbing a single photon. Calculate the energy in kJ/mol for the following transitions.

a. absorbance at 180 nm (ultraviolet)
b. absorbance at 476 nm (blue)
c. absorbance at 645 nm (red)

Answer

One method to carry out this calculation: $\frac{1}{x\text{nm}} \times \frac{1\,\text{nm}}{1x10^{-9}\,\text{m}} \times 6.626x10^{-34}\text{Js} \times \frac{3.000x10^{8}\text{m}}{\text{s}} \times \frac{6.022x10^{23}\text{photons}}{1.000\text{mole}} \times \frac{1\text{kJ}}{1000\text{J}}$

a. 665.0 kJ/mol
b. 251.5 kJ/mol
c. 185.6 kJ/mol

Exercise 4.12.2

How does the energy of an excitation between vibrational states compare to that of an electronic excitation? Typically, infrared absorptions are reported in cm^{-1}, which is simply what it looks like: the reciprocal of the wavelength in cm. Because wavelength and frequency are inversely related, wavenumbers are considered a frequency unit. Calculate the energy in kJ/mol for the following transitions.

a. absorbance at 3105 cm^{-1}
b. absorbance at 1695 cm^{-1}
c. absorbance at 963 cm^{-1}

Answer

One method to carry out this calculation: $x\text{cm}^{-1} \times \frac{100\,\text{cm}}{1\,\text{m}} \times 6.626x10^{-34}\text{Js} \times \frac{3.000x10^{8}\text{m}}{\text{s}} \times \frac{6.022x10^{23}\text{photons}}{1.000\text{mole}} \times \frac{1\text{kJ}}{1000\text{J}}$

a. 37.14 kJ/mol
b. 20.27 kJ/mol
c. 11.52 kJ/mol

By comparing these answers with those from Exercise **4.12.1**, we can see that the energy difference between vibrational states is an order of magnitude less than the energy difference between electronic states.

4.12.4.2: Internal Conversion

If electrons can get to a lower energy state, and give off a little energy at a time, relaxing to lower and lower vibrational levels, do they need to give off a photon at all? Maybe they can relax all the way down to the ground state via vibrational relaxation. That is certainly the case. Given many vibrational energy levels, and an excited state that is low enough in energy so that some of its lower vibrational levels overlap with some of the higher vibrational levels of the ground state, an electron can relax from an excited electronic state back to the ground state without releasing a photon (Figure \(\PageIndex{8}).

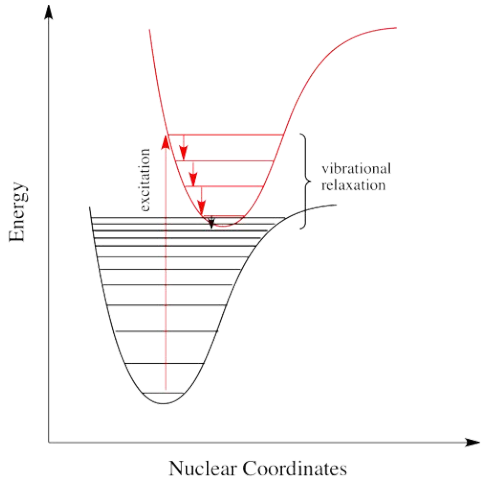


Figure **4.12.8**: Relaxation of an excited state particle to the ground state through the nonradiative process of internal conversion.

This event is called a "radiationless transition", because it occurs without release of a photon. The electron simply slides over from a low vibrational state of the excited electronic state to a high vibrational state of the electronic ground state. If the electron simply keeps dropping a vibrational level at a time back to the ground state, the process is called **"internal conversion"**.

Internal conversion has an important consequence. Because the absorption of UV and visible light can result in energy transfer into vibrational states, much of the energy that is absorbed from these sources is converted into heat. That can be a good thing if you happen to be a marine iguana trying to warm up in the sun after a plunge in the icy Pacific. It can also be a tricky thing if you are a process chemist trying to scale up a photochemical reaction for commercial production of a pharmaceutical, because you have to make sure the system has adequate cooling available.

4.12.4.3: Intersystem Crossing

Intersystem crossing is a process that leads to the electron getting caught between the excited state and the ground state. Just as, little by little, vibrational relaxation can lead the electron back onto the ground state energy surface, it can also lead the electron into states that are intermediate in energy in which the spin multiplicity has changed.

For example, suppose an organic molecule undergoes electronic excitation. Generally, organic molecules have no unpaired electrons. Their ground states are singlet states. According to one of the selection rules for electronic excitation, the excited state must also have no unpaired electrons. In other words, the spin on the electron that gets excited is the same after excitation as it was before excitation.

However, that's not the lowest possible energy state for that electron. When we think about atomic orbital filling, there is a rule that governs the spin on the electrons in degenerate orbitals: in the lowest energy state, **spin is maximized** (Hund's rule). In other words, when we draw a picture of the valence electron configuration of nitrogen, we show nitrogen's three p electrons each in its own orbital, with their spins parallel.



Figure **4.12.9**: The diagram on the left shows the energetically stable quartet spin state. The diagram on the right shows the less stable doublet spin state.

In Figure **4.12.9**, the diagram on the left, with three unpaired electrons, all with parallel spins, shows a nitrogen in the quartet spin state. This is the most stable state. Having one of those spins point the other way would result in a different, higher energy spin

state. The diagram on the right shows a different a different spin state, in which one pair of electrons in the p level is spin-paired, one up and one down, even though they are in different p orbitals. That would leave one electron without an opposite partner, so the nitrogen would be in a doublet spin state. The spin state on the left is **lower** in energy than the state on the right. That's just one of the rules of quantum mechanics (**Hund's rule**): maximize spin when degenerate orbitals are singly occupied.

A similar argument can be made for a molecule with the triplet state lower in energy than the singlet state, as shown in Figure 4.12.10. Why didn't the electron get excited to the triplet state in the first place? That is a forbidden (unlikely) electronic transition. But sliding down vibrationally onto the triplet state from the singlet excited state is not, because it doesn't involve absorption or emission of a photon.

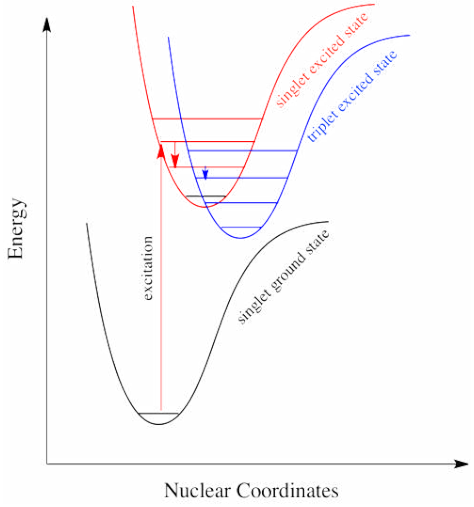


Figure 4.12.10: Intersystem crossing from a singlet excited state to a triplet excited state.

Intersystem crossing can have important consequences in reaction chemistry because it allows access to triplet states that are not normally available in many molecules. Because triplet states feature unpaired electrons, their reactivity is often typified by radical processes. That means an added suite of reactions can be accessed via this process.

4.12.4.4: Phosphorescence: A Radiationless Transition Followed by Emission

Intersystem crossing is one way a system can end up in a triplet excited state. Even though this state is lower in energy than a singlet excited state, it cannot be accessed directly via electronic excitation because that would violate the spin selection rule $\Delta S = 0$. Once intersystem crossing has occurred, the process of reattaining the ground state slows down dramatically. The quick way back to ground state is to emit a photon. But because that would involve a change in spin state, it is not allowed. Realistically speaking, that means it takes a long time. By "a long time", we might mean a few seconds, several minutes, or possibly even hours. Eventually, the electron can drop back down, accompanied by the emission of a photon. This situation is called "phosphorescence" (Figure \(\PageIndex{11}).

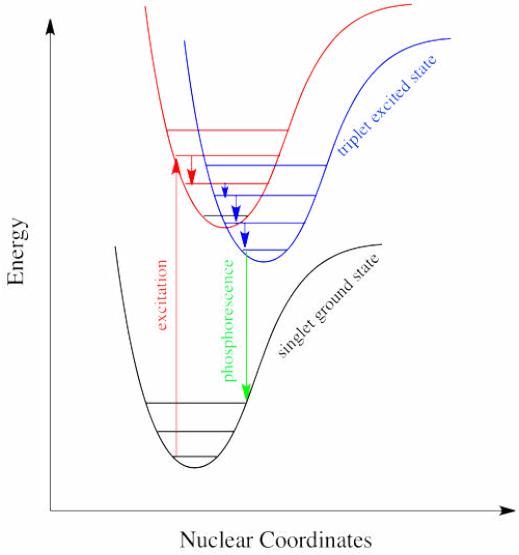


Figure 4.12.11: The process of phosphorescence - excitation, followed by vibrational relaxation, intersystem crossing, and phosphorescence.

Many plants and animals use phosphorescence as a means of signaling. Molecules that display phosphorescence are also often incorporated into toys and shirts so that they will glow in the dark.

4.12.4.5: External Conversion

Deactivation of the excited electronic state may also involve the interaction and energy transfer between the excited state and the solvent or solute in a process called **external conversion.** Low temperature and high viscosity lead to enhanced fluorescence because they reduce the number of collision between molecules, thus slowing down this type of deactivation process.

4.12.5: Absorption and Emission Rates

The table below compares the absorption and emission rates of fluorescence and phosphorescence. The rate of photon absorption is very rapid. Fluorescence emission occurs at a slower rate. Since the triplet to singlet (or reverse) is a forbidden transition, meaning it is less likely to occur than the singlet-to-singlet transition, the rate of triplet to singlet is typically slower. Therefore, phosphorescence emission requires more time than fluorescence.

Table 4.12.1 : Rates of Absorption and Emission comparison.

Process	Radiative Process?	Transition	Timescale (sec)
Light Absorption (Excitation)	yes	$S_0 \rightarrow S_n$	ca. 10^{-15} (instantaneous)
Internal Conversion	no	$S_n \rightarrow S_1$	10^{-14} to 10^{-11}
Vibrational Relaxation	no	$S_n^* \rightarrow S_n$	10^{-12} to 10^{-10}
Intersystem Crossing	no	$S_1 \rightarrow T_1$	10^{-11} to 10^{-6}
Fluorescence	yes	$S_1 \rightarrow S_0$	10^{-9} to 10^{-6}
Phosphorescence	yes	$T_1 \rightarrow S_0$	10^{-3} to 100
Non-Radiative Decay to Ground State (Internal Conversion)	no	$S_1 \rightarrow S_0$ $T_1 \rightarrow S_0$	10^{-7} to 10^{-5} 10^{-3} to 100

4.12.6: References

1. D. A. Skoog, et al. "Principles of Instrumental Analysis" 6th Edition, Thomson Brooks/Cole. 2007

2. D. C. Harris and M.D. Bertolucci "Symmetry and Spectroscopy, An Introduction to Vibrational and Electronic Spectroscopy" Dover Publications, Inc., New York. 1989.

Contributors and Attributions

- Chris P Schaller, Ph.D., (College of Saint Benedict / Saint John's University)
- Diana Wong (UCD)
- Tom Neils (Grand Rapids Community College)

4.12: Electronically Excited Molecules can Relax by a Number of Processes is shared under a CC BY-NC-SA 4.0 license and was authored, remixed, and/or curated by LibreTexts.

- **15.1: Electronically Excited Molecules can Relax by a Number of Processes** is licensed CC BY-NC-SA 4.0.

4.13: Raman Spectroscopy

4.13.1: What is Raman Spectroscopy

Raman spectroscopy is a powerful tool for determining chemical species. As with other spectroscopic techniques, Raman spectroscopy detects certain interactions of light with matter. In particular, this technique exploits the existence of Stokes and Anti-Stokes scattering to examine molecular structure. When radiation in the near infrared (NIR) or visible range interacts with a molecule, several types of scattering can occur. Three of these can be seen in the energy diagram in Figure **4.13.1**.

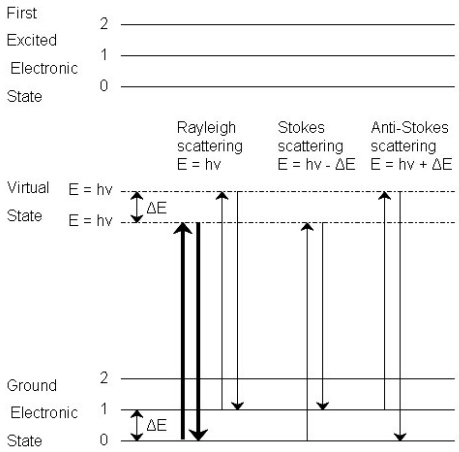


Figure **4.13.1**: Three types of scattering by a molecule excited by a photon with energy E = hν. The most common transition is marked with bold arrows.

In all three types of scattering, an incident photon of energy hν raises the molecule from a vibrational state to one of the infinite number of virtual states located between the ground and first electronic states. The type of scattering observed is dependent on how the molecule relaxes after excitation.

4.13.1.1: **Rayleigh Scattering**

1. The molecule is excited to any virtual state.
2. The molecule relaxes back to its original state.
3. The photon is scattered elastically, leaving with its original energy.

4.13.1.2: **Stokes Scattering**

1. The molecule is excited to any virtual state.
2. The molecule relaxes back to a higher vibrational state than it had originally.
3. The photon leaves with energy hν-ΔE and has been scattered inelastically.

4.13.1.3: **Anti-Stokes Scattering**

1. The molecule begins in a vibrationally excited state.
2. The molecule is excited to any virtual state.
3. The molecule relaxes back to a lower vibrational state than it had originally.
4. The photon leaves with energy hν+ΔE, and has been scattered superelastically.

Rayleigh scattering is by far the most common transition, due to the fact that no change has to occur in the vibrational state of the molecule. The anti-Stokes transition is the least common, as it requires the molecule to be in a vibrationally excited state before the photon is incident upon it. Due to the lack of intensity of the anti-Stokes signal and filtering requirements that eliminate photons with incident energy and higher, generally only Stokes scattering is used in Raman measurements. The relative intensities of Rayleigh, Stokes and anti-Stokes scattering can be seen in Figure **4.13.2**.

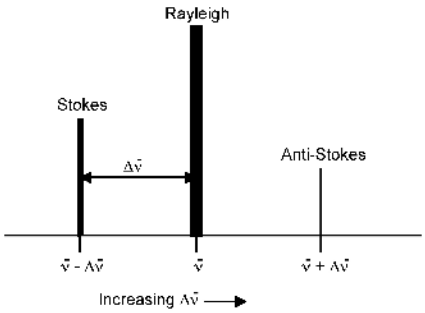


Figure **4.13.2** Location and relative intensity (indicated by peak height and width) of the Stokes and anti-Stokes scattering relative to Rayleigh scattering.

Raman spectroscopy observes the change in energy between the incident and scattered photons associated with the Stokes and anti-Stokes transitions. This is typically measured as the change in the wavenumber (cm-1), from the incident light source. Because Raman measures the change in wavenumber, measurements can be taken using a source at any wavelength; however, near infrared and visible radiation are commonly used. Photons with ultraviolet wavelengths could work as well, but tend to cause photodecomposition of the sample.

4.13.2: Comparison between Raman and Infrared Spectroscopy

Raman spectroscopy sounds very much like infrared (IR) spectroscopy; however, IR examines the wavenumber at which a functional group has a vibrational mode, while Raman observes the shift in vibration from an incident source. The Raman frequency shift is identical to the IR peak frequency for a given molecule or functional group. As mentioned above, this shift is independent of the excitation wavelength, giving versatility to the design and applicability of Raman instruments.

The cause of the vibration is also mechanistically different between IR and Raman. This is because the two operate on different sets of selection rules. IR absorption requires a dipole moment or change in charge distribution to be associated with the vibrational mode. Only then can photons of the same energy as the vibrational state of molecule interact. A schematic of this can be seen in Figure **4.13.3**.



Figure **4.13.3** A change in dipole moment is required for a vibrational mode to be IR active.

Raman signals, on the other hand, due to scattering, occur because of a molecule's polarizability, illustrated in Figure **4.13.4**. Many molecules that are inactive or weak in the IR will have intense Raman signals. This results in often complementary techniques.

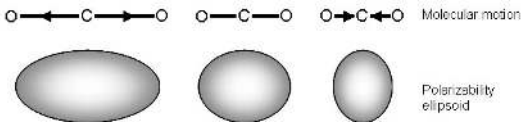


Figure **4.13.4** A change in the polarizability of a bond is required for a vibrational mode to be Raman active.

4.13.3: What does Raman Spectroscopy Measure?

Raman activity depends on the polarizability of a bond. This is a measure of the deformability of a bond in an electric field. This factor essentially depends on how easy it is for the electrons in the bond to be displaced, inducing a temporary dipole. When there is a large concentration of loosely held electrons in a bond, the polarizability is also large, and the group or molecule will have an intense Raman signal. Because of this, Raman is typically more sensitive to the molecular framework of a molecule rather than a specific functional group as in IR. This should not be confused with the polarity of a molecule, which is a measure of the separation of electric charge within a molecule. Polar molecules often have very weak Raman signals due to the fact that electronegative atoms hold electrons so closely.

Raman spectroscopy can provide information about both inorganic and organic chemical species. Many electron atoms, such as metals in coordination compounds, tend to have many loosely bound electrons, and therefore tend to be Raman active. Raman can provide information on the metal ligand bond, leading to knowledge of the composition, structure, and stability of these complexes.

This can be particularly useful in metal compounds that have low vibrational absorption frequencies in the IR. Raman is also very useful for determining functional groups and fingerprints of organic molecules. Often, Raman vibrations are highly characteristic to a specific molecule, due to vibrations of a molecule as a whole, not in localized groups. The groups that do appear in Raman spectra have vibrations that are largely localized within the group, and often have multiple bonds involved.

4.13.4: What is Surface-Enhanced Raman Spectroscopy

Raman measurements provide useful characterization of many materials. However, the Raman signal is inherently weak (less than 0.001% of the source intensity), restricting the usefulness of this analytical tool. Placing the molecule of interest near a metal surface can dramatically increase the Raman signal. This is the basis of surface-enhanced Raman spectroscopy (SERS). There are several factors leading to the increase in Raman signal intensity near a metal surface

1. The distance to the metal surface.
    - Signal enhancement drops off with distance from the surface.
    - The molecule of interest must be close to the surface for signal enhancement to occur.
2. Details about the metal surface: morphology and roughness.
    - This determines how close and how many molecules can be near a particular surface area.
3. The properties of the metal.
    - Greatest enhancement occurs when the excitation wavelength is near the plasma frequency of the metal.
4. The relative orientation of the molecule to the normal of the surface.
    - The polarizability of the bonds within the molecule can be affected by the electrons in the surface of the metal.

4.13.4.1: Surface-Enhanced Raman Spectroscopy for the Study of Surface Chemistry

The ever-rising interest in nanotechnology involves the synthesis and application of materials with a very high surface area to volume ratio. This places increasing importance on understanding the chemistry occurring at a surface, particularly the surface of a nanoparticle. Slight modifications of the nanoparticle or its surrounding environment can greatly affect many properties including the solubility, biological toxicity, and reactivity of the nanomaterial. Noble metal nanomaterials are of particular interest due to their unique optical properties and biological inertness.

One tool employed to understand the surface chemistry of noble metal nanomaterial, particularly those composed of gold or silver is *surface-enhanced Raman spectroscopy* (SERS). Replacing a metal surface with a metal nanoparticle increases the available surface area for the adsorption of molecules. Compared to a flat metal surface, a similar sample size using nanoparticles will have a dramatically stronger signal, since signal intensity is directly related to the concentration of the molecule of interest. Due to the shape and size of the structure, the electrons in the nanoparticle oscillate collectively when exposed to incident electromagnetic radiation. This is called the *localized surface plasmon resonance* (LSPR) of the nanoparticle. The LSPR of the nanoparticles boosts the Raman signal intensity dramatically for molecules of interest near the surface of the nanoparticle. In order to maximize this effect, a nanoparticle should be selected with its resonant wavelength falling in the middle of the incident and scattered wavelengths.

The overall intensity enhancement of SERS can be as large as a factor of 10^6, with the surface plasmon resonance responsible for roughly four orders of magnitude of this signal increase. The other two orders of magnitude have been attributed to chemical enhancement mechanisms arising charge interactions between the metal particle and the adsorbate or from resonances in the adsorbate alone, as discussed above.

4.13.4.1.1: Why is SERS Useful for Studying Surface Chemistry?

Traditionally, SERS uses nanoparticles made of conductive materials, such as gold, to learn more about a particular molecule. However, of interest in many growing fields that incorporate nanotechnology is the structure and functionalization of a nanoparticle stabilized by some surfactant or capping agent. In this case, SERS can provide valuable information regarding the stability and surface structure of the nanoparticle. Another use of nanoparticles in SERS is to provide information about a ligand's structure and the nature of ligand binding. In many applications it is important to know whether a molecule is bound to the surface of the nanoparticle or simply electrostatically interacting with it.

4.13.5: Sample Preparation and Instrumental Details

The standard Raman instrument is composed of three major components. First, the instrument must have an illumination system. This is usually composed of one or more lasers. The major restriction for the illumination system is that the incident frequency of light must not be absorbed by the sample or solvent. The next major component is the sample illumination system. This can vary widely based on the specifics of the instrument, including whether the system is a standard macro-Raman or has micro-Raman capabilities. The sample illumination system will determine the phase of material under investigation. The final necessary piece of a Raman system is the spectrometer. This is usually placed 90° away from the incident illumination and may include a series of filters or a monochromator. An example of a macro-Raman and micro-Raman setup can be Figure **4.13.5** and Figure **4.13.6**. A macro-Raman spectrometer has a spatial resolution anywhere from 100 μm to one millimeter while a micro-Raman spectrometer uses a microscope to magnify its spatial resolution.

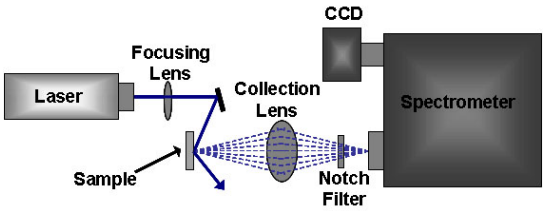


Figure **4.13.5** Schematic of a macro-Raman spectrometer.

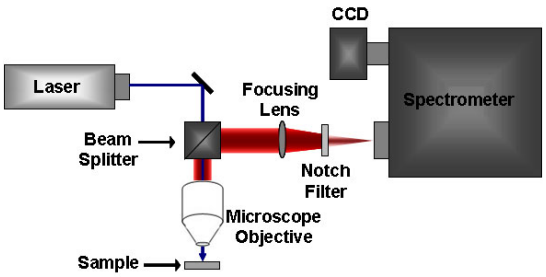


Figure **4.13.6** Schematic of a micro-Raman spectrometer where illumination and collection are performed through microscope objective.

This page titled 4.13: Raman Spectroscopy is shared under a CC BY 4.0 license and was authored, remixed, and/or curated by Pavan M. V. Raja & Andrew R. Barron (OpenStax CNX) via source content that was edited to the style and standards of the LibreTexts platform.

- **4.3: Raman Spectroscopy** by Pavan M. V. Raja & Andrew R. Barron is licensed CC BY 4.0. Original source: http://cnx.org/contents/ba27839d-5042-4a40-afcf-c0e6e39fb45425.2.

4.14: The Dynamics of Transitions can be Modeled by Rate Equations

4.14.1: The Interaction of Light with Atoms

In 1916, Albert Einstein proposed that there are three processes occurring in the formation of an atomic spectral line. The three processes are referred to as spontaneous emission, stimulated emission, and absorption (figure **4.14.1**).

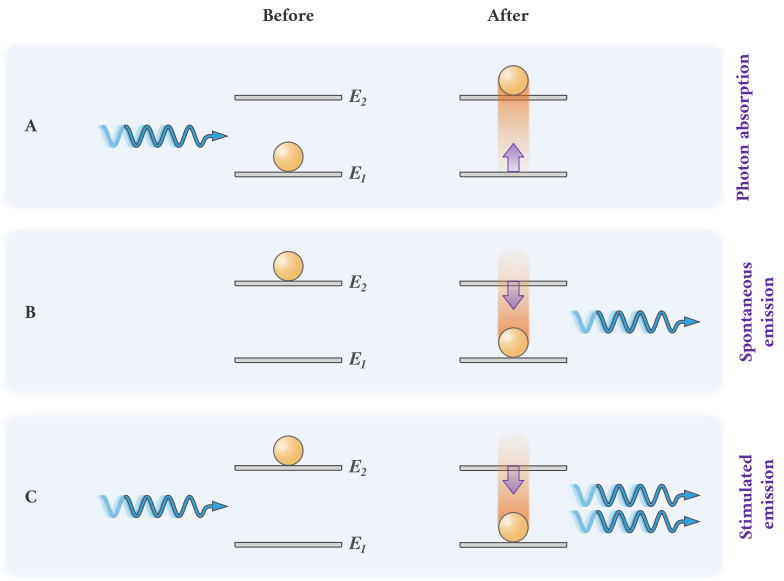


Figure **4.14.1**: The three processes that can occur during the formation of a spectral line. A) Absorption of a photon, leading to the promotion of an electron to a higher electronic energy level. B) The spontaneous emission of a photon created by the relaxation of an electron back to the ground state. C) The stimulated emission of a photon created by the influence of a passing photon, accompanied by the relaxation of an electron back to the ground state. (CC BY-NC 4.0; Ümit Kaya via LibreTexts)

For now, let's make our discussion as simple as possible, by assuming we are talking about the interaction of light with an atom that has only two energy levels. There is a collection of these atoms present, and they are in an assortment of states, some in the ground state, and some in "the" excited state. Our discussion of photon emission to this point has generally centered around *spontaneous emission*, the triggering of which we attributed to a perturbation in the hamiltonian that comes from (if nothing else) vacuum fluctuations.

Suppose some of these atoms spontaneously emit photons, and now the collection of atoms is not sitting in a total vacuum, but is in the presence of many photons as well. We now consider what effects these present photons can have on the atoms. The answer depends upon which state the atom is in when it encounters the photon. If the atom is in the ground state, then it can absorb the photon and go to the excited state. If the atom is in its excited state, it can't absorb the photon, but the time-varying EM fields of the photon present a nice perturbation to the electron's hamiltonian (at just the right frequency!) to induce the emission of a photon. This is called *stimulated emission*. The photon that induces the emission is unaffected by the interaction, and continues on its merry way. The emitted photon naturally has the same frequency as the passing photon (the energy gap assured this), but it also emerges moving in the same direction as, *and in phase with* the stimulating photon.

It turns out that if a photon happens by two of these atoms, the first in the ground state and the second in the excited state, the probability that it will be absorbed by the first is equal to the probability that it will stimulate emission in the other – neither of these results is preferred over the other. Now consider a collection of these atoms in a state of some fixed total energy. This total energy comes from the number of atoms in the ground state multiplied by the energy of that state, plus the number of atoms in the excited state multiplied by the number of atoms in that state. The populations of these two states subject to the constraint of the total energy can be shown to be a function that depends upon the energy difference of the two states and the temperature of the

collection of atoms. Specifically, if N_1 is the number of atoms in the ground state, N_2 is the number of atoms in the excited state, and the energy difference is ΔE, then the following relation holds:

$$N_1 = N_2 e^{\frac{\Delta E}{k_B T}},$$

where T is the temperature and k_B is Boltzmann's constant. Clearly N_1 is greater than N_2, but how much greater? We can do a very quick calculation of this using an approximation that at room temperature, the constant $k_B T$ is about 140 eV. Let's assume that the energy difference between two energy states of an atom is on the order of 1eV. Then the number of ground state atoms would exceed the number of excited state atoms by a factor of $e^{40} = 2.4\times10^{17}$!

Thus, a photon passing through this collection has an equal probability of being absorbed or stimulating emission if it happens by an atom prepared for one of those actions. But there are so many more atoms available to absorb the photon, that this has a much greater chance of happening. While waiting for a photon to stimulate emission, an atom in an excited state will impatiently emit a photon spontaneously, which will then be much more likely to be absorbed than stimulate emission, and things continue like this, with some atoms spontaneously sending out photons while others absorb them.

4.14.2: Einstein Coefficients

Einstein proposed a separate rate equation for each of the three processes described above. The rate of each process is proportional to the number of particles in either the ground state (absorption) or the excited state (emission). Each rate is also proportional to the spectral radiant energy density, ρ_ν, which is a measure of the radiant energy density (ρ) per unit frequency of the light associated with the transition. Thus, $\rho_\nu = \frac{d\rho}{d\nu}$, and has units of $\frac{J \cdot s}{m^3}$. With each process there is also an associated Einstein coefficient, which is a proportionality constant.

4.14.2.1: Photon absorption

Absorption is the process by which a photon is absorbed by the atom, causing an electron to jump from a lower energy level to a higher one (figure **4.14.1***a*). The process is described by the Einstein coefficient $B_{12}\left(\frac{m^3}{J \cdot s^2}\right)$, which gives the probability per unit time per unit spectral radiance of the radiation field that an electron in state 1 with energy E_1 will absorb a photon with an energy $E_2 - E_1 = h\nu_{12}$ and jump to state 2 with energy E_2. If $N_1(t)$ is the number density of atoms in state 1, then the change in the number density of atoms in state 1 per unit time due to absorption will be

$$-\frac{dN_1(t)}{dt} = B_{12}\rho_\nu(\nu_{12})N_1(t)$$

If only absorption occurred, the increase of the excited state population as a function of time is equal to the decrease of the ground state population as a function of time.

4.14.2.2: Spontaneous emission

Spontaneous emission is the process by which an electron "spontaneously" (i.e. without any outside influence) decays from a higher energy level to a lower one (figure **4.14.1***b*). The process is described by the Einstein coefficient $A_{21}(s^{-1})$, which gives the probability per unit time that an electron in state 2 with energy E_2 will decay spontaneously to state 1 with energy E_1, emitting a photon with an energy $E_2 - E_1 = h\nu_{21}$. Due to the energy-time uncertainty principle, the transition actually produces photons within a narrow range of frequencies called the spectral linewidth. If $N_2(t)$ is the number density of atoms in state 2, then the change in the number density of atoms in state 2 per unit time due to spontaneous emission will be

$$-\frac{dN_2(t)}{dt} = A_{21}N_2(t)$$

The same process results in increasing of the population of the state 1:

$$\frac{dN_1(t)}{dt} = A_{21}N_2(t)$$

4.14.2.3: Stimulated emission

Stimulated emission (also known as induced emission) is the process by which an electron is induced to jump from a higher energy level to a lower one by the presence of electromagnetic radiation at (or near) the frequency of the transition (figure **4.14.1***c*). From

the thermodynamic viewpoint, this process must be regarded as negative absorption. The process is described by the Einstein coefficient $B_{21}\left(\frac{m^3}{J \cdot s^2}\right)$, which gives the probability per unit time per unit spectral radiance of the radiation field that an electron in state 2 with energy E_2will decay to state 1 with energy E_1, emitting a photon with an energy $E_2 - E_1 = h\nu_{21}$. The change in the number density of atoms in state 1 per unit time due to induced emission will be

$$\frac{dN_1(t)}{dt} = B_{21}\rho_\nu(\nu_{21})N_2(t)$$

4.14.3: The Relationship between A_{21}, B_{12}, and B_{21}

In 1900, Max Planck derived a formula for the energy density per unit bandwidth of a blackbody radiator by making the assumption that only discrete energies are allowed. His work agreed with known experimental data, and it is one of the fundamental ideas of quantum mechanics. More specifically, the spectral energy density per unit bandwidth, $\rho_\nu(\nu_{12})$ in units $\frac{J \cdot s}{m^3}$, is given by

$$\rho_\nu(\nu_{12}) = \frac{8\pi h}{c^3}\frac{\nu_{12}^3}{e^{(h\nu_{12})/(k_BT)} - 1} \tag{4.14.1}$$

In a given sample of atoms exposed to radiation of the correct frequency all three processes will be occurring simultaneously. Thus the rate of change of the populations of the two states will be

$$-\frac{dN_1(t)}{dt} = \frac{dN_2(t)}{dt} = B_{12}\rho_\nu(\nu_{12})N_1(t) - A_{21}N_2(t) - B_{21}\rho_\nu(\nu_{21})N_2(t) \tag{4.14.2}$$

If we assume that the two energy states are in thermal equilibrium, then N_1 and N_2 are constant, and thus

$$-\frac{dN_1(t)}{dt} = \frac{dN_2(t)}{dt} = B_{12}\rho_\nu(\nu_{12})N_1(t) - A_{21}N_2(t) - B_{21}\rho_\nu(\nu_{21})N_2(t) = 0 \tag{4.14.3}$$

Upon solving for $\rho_\nu(\nu_{12})$, we get

$$\rho_\nu(\nu_{12}) = \frac{A_{21}}{(N_1(t)/N_2(t))B_{12} - B_{21}} \tag{4.14.4}$$

Recall that in this equation N_1/N_2 represents the electron density in the lower energy state divided by the electron density in the upper state at equilibrium. This quantity is a function of temperature. Assuming many allowed energy states, the number of occupied states decreases exponentially with temperature, as per Boltzmann statistics.

$$N_2/N_1 = \frac{g_2}{g_1}e^{(-h\nu_{12})/(k_BT)} \tag{4.14.5}$$

The quantity $\frac{g_2}{g_1}$ represents the degeneracy level, which is the number of allowed electrons in the upper state over the number of allowed electrons in the lower state. In this expression, g_1 and $g2$ are unitless measures of the number of ways electrons can occupy an energy states. Upon rearrangement, equation 4.14.5 becomes

$$N_1/N_2 = \frac{g_1}{g_2}e^{(h\nu_{12})/(k_BT)} \tag{4.14.6}$$

Equations 4.14.6 and 4.14.4 can be combined to get

$$\rho_\nu(\nu_{12}) = \frac{A_{21}}{\left(\frac{g_1}{g_2}e^{(h\nu_{12})/(k_BT)}\right)B_{12} - B_{21}} \tag{4.14.7}$$

which can be rearranged to

$$\rho_\nu(\nu_{12}) = \frac{\frac{A_{21}}{B_{21}}}{\left(\frac{g_1B_{12}}{g_2B_{21}}e^{(h\nu_{12})/(k_BT)}\right) - 1} \tag{4.14.8}$$

One expression for the energy density per unit bandwidth of this system is given by Equation 4.14.1. Equation 4.14.8 gives a second expression for the energy density per unit bandwidth, and it was found by considering the relative rates of absorption, spontaneous emission, and stimulated emission. These equations can be combined to relate the rates of the different processes.

$$\frac{8\pi h}{c^3}\frac{\nu_{12}^3}{e^{(h\nu_{12})/(k_BT)}-1}=\frac{\frac{A_{21}}{B_{21}}}{\left(\frac{g_1B_{12}}{g_2B_{21}}e^{(h\nu_{12})/(k_BT)}\right)-1} \tag{4.14.9}$$

The above equation is true for the conditions

$$\frac{A_{21}}{B_{21}}=\frac{8\pi h\nu_{12}^3}{c^3} \tag{4.14.10}$$

and

$$\frac{g_1B_{12}}{g_2B_{21}}=1 \tag{4.14.11}$$

If we know one of the Einstein coefficients, we can quickly calculate the other two Einstein coefficients using equations 4.14.10 and 4.14.11.

These equations also provide further insight into the operation of lasers and other devices based on stimulated emission. The overall nonequilibrium upper state population rate is given by

$$\frac{dN_2(t)}{dt}=-A_{21}N_2-B_{21}\rho_\nu(\nu_{21})N_2+B_{21}\frac{g_2}{g_1}\rho_\nu(\nu_{12})N_1 \tag{4.14.12}$$

which can be simplified with some algebra.

$$\frac{dN_2(t)}{dt}=-A_{21}N_2-B_{21}\rho_\nu(\nu_{12})\left(N_2-\frac{g_2}{g_1}N_1\right) \tag{4.14.13}$$

The term in parenthesis is the net upper state population. Optical amplification and lasing can only occur when the term in parenthesis is positive. The condition

$$N_2-\frac{g_2}{g_1}N_1>0 \tag{4.14.14}$$

is called a population inversion. It only occurs when enough energy is being supplied to the system, by optical, electrical, or thermal means, so that there are more electrons in the upper energy level than the lower energy level. This situation cannot be achieved for a two-level system, as will be shown in the next section. However, in section 15.4, it will be shown that this situation can be achieved if the system has more than two levels.

4.14.4: Contributors

- Andrea M. Mitofsky (Trine University)
- Tom Weideman (University of California, Davis)
- Wikipedia (https://en.Wikipedia.org/wiki/Einstein_coefficients)
- Tom Neils (Grand Rapids Community College)

4.14: The Dynamics of Transitions can be Modeled by Rate Equations is shared under a CC BY-NC-SA 4.0 license and was authored, remixed, and/or curated by LibreTexts.

- **15.2: The Dynamics of Transitions can be Modeled by Rate Equations** is licensed CC BY-NC-SA 4.0.

4.15: Beer's Law

4.15.1: Absorbance and Concentration

When monochromatic electromagnetic radiation passes through an infinitesimally thin layer of sample of thickness *dx*, it experiences a decrease in its power of *dP* (Figure 4.15.1). From the Einstein rate model for absorption and emission of light, when the light intensity is low enough that saturation is not reached (negligible stimulated emission) and the energy level separation is large enough that essentially all the population is in the ground state the rate of photon absorption is:

$$\frac{dN_g}{dt} = B\rho N_g$$

where N_g is the number of species in the ground state, B is the Einstein B coefficient and ρ is the radiant energy density of the photons at the absorption frequency in (units of Js/m^3). This means that the probability of absorbing a photon is proportional to the number of molecules the light encounters multiplied by the energy density. As the energy density is just proportional to the power of the light beam (P, units of W/m^2), through $\rho = P/c$. We can write the infinitesimal change in the light intensity dP:

$$dP = -\epsilon P N_g,$$

Where ϵ is the proportionality constant. In any given slice of sample of thickness dx the light will encounter N_g = CAdx absorbers (C = concentration, A = cross-sectional area of the light beam). Substituting this into the above equation and absorbing the area of the beam into our constant we get:

$$dP = -\epsilon APCdx = -\alpha PCdx,$$

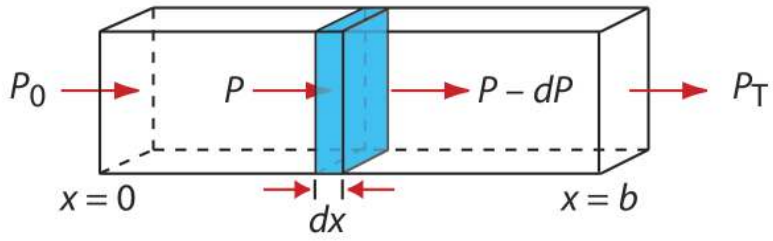


Figure 4.15.1. Factors used to derive the Beer's law.

Dividing through by P shows that the fractional decrease in power is proportional to the sample's thickness and to the analyte's concentration, *C*; thus

$$-\frac{dP}{P} = \alpha C dx \tag{4.15.1}$$

where *P* is the power incident on the thin layer of sample and α is a proportionality constant. Integrating the left side of Equation 4.15.1 over the sample's full thickness

$$-\int_{P=P_0}^{P=P_t} \frac{dP}{P} = \alpha C \int_{x=0}^{x=b} dx$$

$$\ln \frac{P_0}{P_T} = \alpha b C \tag{4.15.2}$$

converting from ln to log, and substituting into the equation relating transmittance to absorbance

$$A = -\log T = -\log \frac{P_T}{P_0}$$

gives

$$A = \alpha b C \tag{4.15.3}$$

where *a* is the analyte's absorptivity with units of cm^{-1} conc^{-1}. If we express the concentration using molarity, then we replace *a* with the molar absorptivity, ε, which has units of cm^{-1} M^{-1}.

$$A = \varepsilon b C \tag{4.15.4}$$

The absorptivity and the molar absorptivity are proportional to the probability that the analyte absorbs a photon of a given energy. As a result, values for both a and ε depend on the wavelength of the absorbed photon.

Example 4.15.1

A 5.00×10^{-4} M solution of analyte is placed in a sample cell that has a pathlength of 1.00 cm. At a wavelength of 490 nm, the solution's absorbance is 0.338. What is the analyte's molar absorptivity at this wavelength?

Solution

Solving Equation 4.15.4 for ϵ and making appropriate substitutions gives

$$\varepsilon = \frac{A}{bC} = \frac{0.338}{(1.00\text{ cm})\left(5.00 \times 10^{-4}\text{ M}\right)} = 676\text{ cm}^{-1}\text{ M}^{-1}$$

Exercise 4.15.1

A solution of the analyte from Example 4.15.1 has an absorbance of 0.228 in a 1.00-cm sample cell. What is the analyte's concentration?

Answer

Making appropriate substitutions into Beer's law

$$A = 0.228 = \varepsilon b C = \left(676\text{ M}^{-1}\text{ cm}^{-1}\right)(1\text{ cm})C$$

and solving for C gives a concentration of 3.37×10^{-4} M.

Equation 4.15.3 and Equation 4.15.4, which establish the linear relationship between absorbance and concentration, are known as Beer's law. Calibration curves based on Beer's law are common in quantitative analyses.

As is often the case, the formulation of a law is more complicated than its name suggests. This is the case, for example, with Beer's law, which also is known as the Beer-Lambert law or the Beer-Lambert-Bouguer law. Pierre Bouguer, in 1729, and Johann Lambert, in 1760, noted that the transmittance of light decreases exponentially with an increase in the sample's thickness.

$$T \propto e^{-b}$$

Later, in 1852, August Beer noted that the transmittance of light decreases exponentially as the concentration of the absorbing species increases.

$$T \propto e^{-C}$$

Together, and when written in terms of absorbance instead of transmittance, these two relationships make up what we know as Beer's law.

4.15.2: Beer's Law and Multicomponent Samples

We can extend Beer's law to a sample that contains several absorbing components. If there are no interactions between the components, then the individual absorbances, A_i, are additive. For a two-component mixture of analyte's X and Y, the total absorbance, A_{tot}, is

$$A_{tot} = A_X + A_Y = \varepsilon_X b C_X + \varepsilon_Y b C_Y$$

Generalizing, the absorbance for a mixture of n components, A_{mix}, is

$$A_{mix} = \sum_{i=1}^{n} A_i = \sum_{i=1}^{n} \varepsilon_i b C_i \tag{4.15.5}$$

4.15.3: Limitations to Beer's Law

Beer's law suggests that a plot of absorbance vs. concentration—we will call this a Beer's law plot—is a straight line with a *y*-intercept of zero and a slope of ab or εb. In some cases a Beer's law plot deviates from this ideal behavior (see Figure 4.15.2).

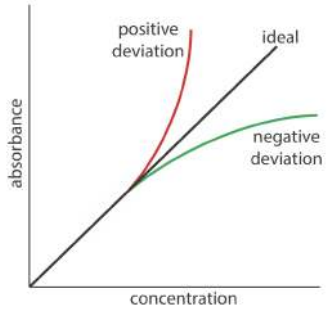


Figure 4.15.2. Plots of absorbance vs. concentration showing positive and negative deviations from the ideal Beer's law relationship, which is a straight line.

4.15.3.1: Fundamental Limitations to Beer's Law

Beer's law is a limiting law that is valid only for low concentrations of analyte. There are two contributions to this fundamental limitation to Beer's law. At higher concentrations the individual particles of analyte no longer are independent of each other. The resulting interaction between particles of analyte may change the analyte's absorptivity. A second contribution is that an analyte's absorptivity depends on the solution's refractive index. Because a solution's refractive index varies with the analyte's concentration, values of a and ε may change. For sufficiently low concentrations of analyte, the refractive index essentially is constant and a Beer's law plot is linear.

The other fundamental limit is that the light intensity must be low enough that stimulated emission (saturation of the transition) can be ignored.

4.15.3.2: Instrumental Limitations to Beer's Law

There are two principal instrumental limitations to Beer's law: stray radiation and non-polychromatic radiation.

Stray radiation is the first contribution to instrumental deviations from Beer's law. Stray radiation arises from imperfections in the wavelength selector that allow light to enter the instrument and to reach the detector without passing through the sample. Stray radiation adds an additional contribution, P_{stray}, to the radiant power that reaches the detector; thus

$$A = -\log \frac{P_T + P_{stray}}{P_0 + P_{stray}}$$

For a small concentration of analyte, P_{stray} is significantly smaller than P_0 and P_T, and the absorbance is unaffected by the stray radiation. For higher concentrations of analyte, less light passes through the sample and P_T and P_{stray} become similar in magnitude. This results is an absorbance that is smaller than expected, and a negative deviation from Beer's law.

The second limitation is that Beer's law assumes that radiation reaching the sample is of a single wavelength—that is, it assumes a purely monochromatic source of radiation. Even the best wavelength selector, however, passes radiation with a small, but finite effective bandwidth. Let's assume we have a line source that emits light at two wavelengths, λ' and λ''. When treated separately, the absorbances at these wavelengths, A' and A'', are

$$A' = -\log \frac{P'_r}{P'_0} = \varepsilon' b C \qquad A'' = -\log \frac{P''_T}{P''_0} = \varepsilon'' b C$$

If both wavelengths are measured simultaneously the absorbance is

$$A = -\log \frac{(P'_T + P''_T)}{(P'_0 + P''_0)}$$

Expanding the logarithmic function of the equation's right side gives

$$A = \log(P_0' + P_0'') - \log(P_T' + P_T'') \tag{4.15.6}$$

Next, we need to find a relationship between P_T and P_0 for any wavelength. To do this, we start with Beer's law

$$A = -\log \frac{P_T}{P_0} = \epsilon b C$$

and then solve for P_T in terms of P_0

$$\log \frac{P_T}{P_0} = -\epsilon b C$$

$$\frac{P_T}{P_0} = 10^{-\epsilon b C}$$

$$P_T = P_0 \times 10^{-\epsilon b C}$$

Substituting this general relationship back into our wavelength-specific equation for absorbance, 4.15.6, we obtain

$$A = \log(P_0' + P_0'') - \log(P_0' \times 10^{-\epsilon b C} + P_0'' \times 10^{-\epsilon b C}) \tag{4.15.7}$$

For monochromatic radiation, we have $\epsilon' = \epsilon'' = \epsilon$ and Equation 4.15.7 simplifies to Beer's law

$$A = -\log(10^{-\epsilon b C}) = \epsilon b C$$

For non-monochromatic radiation, Equation 4.15.7 predicts that the absorbance is smaller than expected if $\epsilon' > \epsilon''$. Polychromatic radiation always gives a deviation from Beer's law, but the effect is smaller if the value of ϵ essentially is constant over the wavelength range passed by the wavelength selector. For this reason, as shown in Figure **4.15.3**, it is better to make absorbance measurements at the top of a broad absorption peak. In addition, the deviation from Beer's law is less serious if the source's effective bandwidth is less than one-tenth of the absorbing species' natural bandwidth [(a) Strong, F. C., III *Anal. Chem.* **1984**, *56*, 16A–34A; Gilbert, D. D. *J. Chem. Educ.* **1991**, *68*, A278–A281]. When measurements must be made on a slope, linearity is improved by using a narrower effective bandwidth.

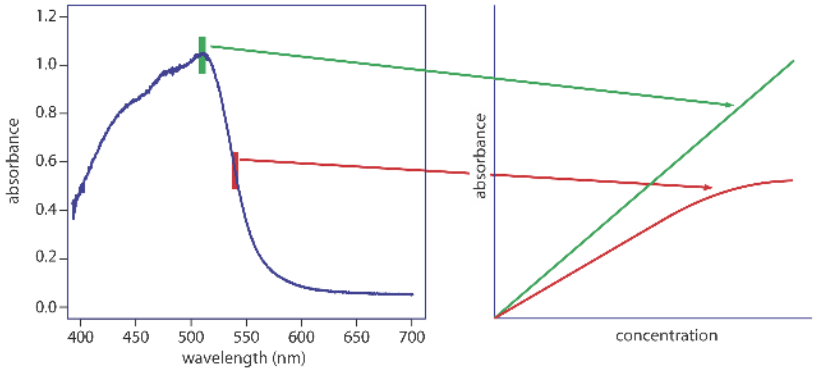


Figure **4.15.3**. Effect of wavelength selection on the linearity of a Beer's law plot. Another reason for measuring absorbance at the top of an absorbance peak is that it provides for a more sensitive analysis. Note that the green Beer's law plot has a steeper slope—and, therefore, a greater sensitivity—than the red Beer's law plot. A Beer's law plot, of course, is equivalent to a calibration curve.

This page titled 4.15: Beer's Law is shared under a CC BY-NC-SA 4.0 license and was authored, remixed, and/or curated by David Harvey.

- **13.2: Beer's Law** by David Harvey is licensed CC BY-NC-SA 4.0.

4.16: A Two-Level System Cannot Achieve a Population Inversion

4.16.1: Introduction

The name laser comes from the acronym for **L**ight **A**mplification by **S**timulated **E**mission of **R**adiation (LASER). As suggested by the name the intensity of incoming light is increased by stimulated emission. As discussed in the dynamic model for absorption and emission of light the population in the excited state of the atom or molecule must exceed that in the lower state for the number of stimulated photons to be larger than the number absorbed. Thus lasing only occurs if there is a population inversion (upper state population larger than the lower state) between the states involved in the transition.

4.16.2: Lasing in Two-Level Systems

Consider a laser medium whose atoms have only two energy states: a ground state and one excited state. In such an idealized atom the only possible transitions are excitation from the ground state to the excited state and de-excitation from the excited state back into ground state. Could such an atom be used to make a laser?

There are several important conditions that our laser must satisfy. First of all, the light that it produces must be coherent. That is to say, it must emit photons that are in-phase with one another. Secondly, it should emit monochromatic light, i.e. photons of the same frequency (or wavelength). Thirdly, it would be desirable if our laser's output were collimated, producing a sharply defined "pencil-like" beam of light (this is not crucial, but clearly a desirable condition). Lastly, it would also be desirable for our laser to be efficient, i.e. the higher the ratio of output energy - to - input energy, the better.

Let us begin by examining the requirements for our first condition for lasing, coherence. This condition is satisfied only when the lasing transition occurs through stimulated emission. As we have already seen, stimulated emission produces identical photons that are of equal energy and phase and travel in the same direction. But for stimulated emission to take place a "passer-by" photon whose energy is just equal to the de-excitation energy must approach the excited atom before it de-excites via spontaneous emission. Typically, a photon emitted by the spontaneous emission serves as the seed to trigger a collection of stimulated emissions. Still, if the lifetime of the excited state is too short, then there will not be enough excited atoms around to undergo stimulated emission. So, the first criteria that we need to satisfy is that the upper lasing state must have a relatively long lifetime, otherwise known as a meta-stable state, with typical lifetimes in the milliseconds range. In addition to the requirement of a long lifetime, we need to ensure that the likelihood of absorption of the "passer-by" photons is minimized. This likelihood is directly related to the ratio of the atoms in their ground state versus those in the excited state. The smaller this ratio, the more likely that the "passer-by" photon will cause a stimulated emission rather than get absorbed. So, to satisfy this requirement, we need to produce a **population inversion**: create more atoms in the excited state than those in the ground state.

Another way of stating the above set of conditions is that the rate of absorption must be less than the rate of stimulated emission

$$\underbrace{B_{21}\rho_\nu(\nu_{21})N_2}_{\text{rate of stimulated emission}} > \underbrace{B_{12}\rho_\nu(\nu_{12})N_1}_{\text{rate of absorption}} \tag{4.16.1}$$

As shown previously, $B_{21} = B_{12}$ and $\rho_\nu(\nu_{12}) = \rho_\nu(\nu_{21})$, thus Equation 4.16.1 becomes

$$N_2 > N_1.$$

Hence, if $N_2 > N_1$ then there is a population inversion.

Achieving population inversion in a two-level system is impossible with photoexcitation because the maximum possible ratio $N_2/N_1 = 1$ within the Einstein model. In that case the stimulated emission and absorption would exactly cancel out and the light beam would pass through without any change in intensity. This is observed with strong laser beams, is called photobleaching and is an example of a situation where Beer's law breaks down. Direct thermal excitation of this system will not work either because the Boltzmann distribution of energy level populations always yields $N_2 < N_1$ for positive temperatures.

$$N_2 = N_1\, e^{\frac{-\Delta E}{k_B T}},$$

Notice that if the temperature were negative (< 0 K) a population inversion could exist. What this implies is that a pair of states involved in lasing can be thought of as being at a negative temperature. This does not mean that the whole system is at a negative

temperature.

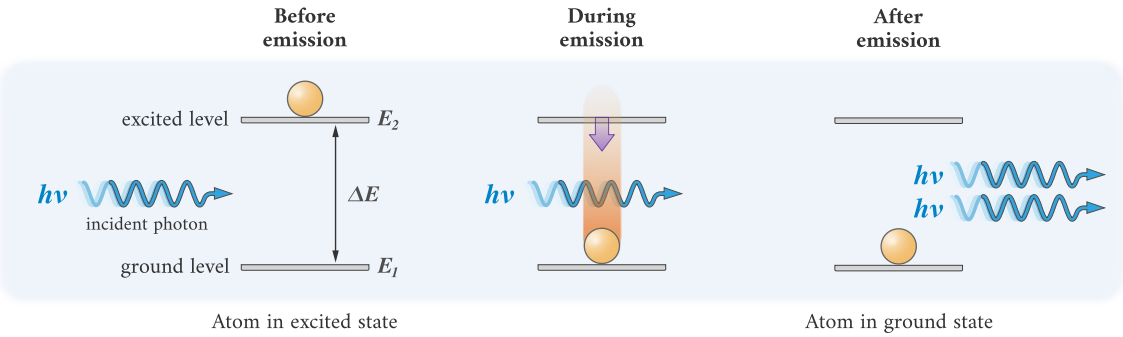


Figure 4.16.1: A purely two-level lasing system cannot lase because there is no way to get more atoms in the excited state than the ground state. In the picture above another photon must already have been absorbed to excite this single atom. Thus, the resulting two photons out are equal to the initial two photons in. (CC BY-NC; Ümit Kaya via LibreTexts)

As we will see more complicated ways of creating the population inversion are necessary.

This page titled 4.16: A Two-Level System Cannot Achieve a Population Inversion is shared under a CC BY-NC-SA 4.0 license and was authored, remixed, and/or curated by Jay Newman, Seyffie Maleki, Tom Neils, Jonathan Gutow@University of Wisconsin - Oshkosh, & Jonathan Gutow@University of Wisconsin - Oshkosh.

- **15.3: A Two-Level System Cannot Achieve a Population Inversion** by Jay Newman, Seyffie Maleki, Tom Neils is licensed CC BY-NC-SA 4.0.

4.17: Population Inversion can be Achieved in a Three-Level System

Optical pumping will at most achieve only an equal population in a two-level system. This is because the probabilities for raising an electron to the upper level and inducing the decay of an electron to the lower level (stimulated emission) are exactly the same! In other words, when both levels are equally populated, the numbers of electrons "going up" and "down" will be the same, so you cannot achieve population inversion which is required for lasers. The solution is to involve a third, metastable level of intermediate energy. The pumping will occur between the two levels with the greatest energy difference, creating a highly populated upper energy level. Two lasing processes are possible once this situation has been obtained. Lasing occurs between the upper level and the intermediate level if the electrons in the upper energy level decay slowly to the intermediate, metastable level, and if the electrons in the intermediate level decay rapidly to the ground state. However, if the electrons in the upper energy level quickly decay into the intermediate level, and the transition from the intermediate level to the ground level is slow, then lasing occurs between the intermediate level and the ground state. In both cases, the lasing frequency has a frequency different than that of the pumping frequency between the ground level and the upper level, so the pumping is off-resonant to the laser transition and will not trigger stimulated emission.

Lasing in Three-Level Systems

The first laser that was demonstrated to operate was a three-level laser, known as **Maiman's ruby laser**.

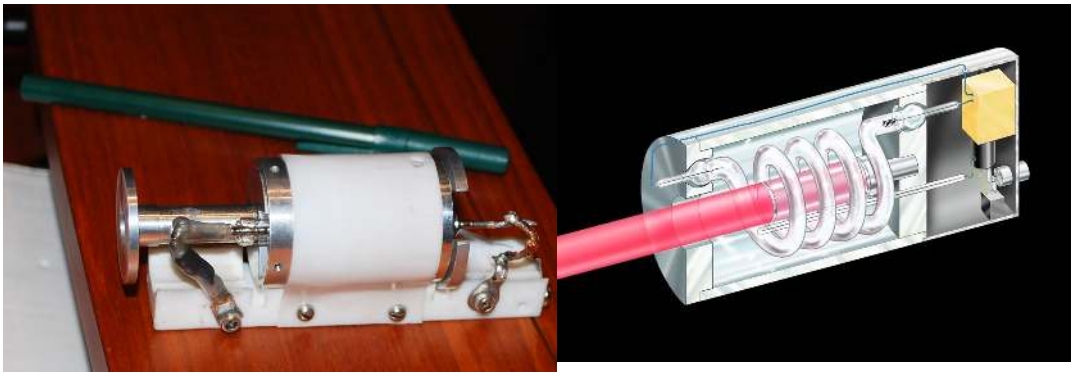


Figure **4.17.1**: (left) A copy of a Maiman laser (CC 0; Guy Immega) (right) Internal view of a Maiman laser (https://commons.wikimedia.org/w/inde...ldid=42317741)

Figure **4.17.1** shows the outside and inside of a three-level laser. A pump causes an excitation from the ground state to the second excited state. This state is a rather short-lived state so that the atom quickly decays into the first excited level. (Atoms in the second excited state may also decay directly back to the ground state, but these atoms can be pumped back to the second excited state again.) The first excited state is a long-lived (i.e. metastable) state which allows the atom to "wait" for the "passer-by" photon while building up a large population of atoms in this state. The lasing transition, in this laser, is due to the decay of the atom from this first excited metastable state to the ground state. If the number of atoms in the ground state exceeds the number of atoms that are pumped into the excited state, then there is a high likelihood that the "lasing photon" will be absorbed and we will not get sustained laser light. The fact that the lower lasing transition is the ground state makes it rather difficult to achieve efficient population inversion. In a ruby laser, this task is accomplished by providing the ruby crystal with a very strong pulsating light source, called a flash lamp. The flash lamp produces a very strong pulse of light that is designed to excite the atoms from their ground state into a short-lived upper level. In this way, the ground state is depopulated and population inversion is achieved until a pulse of laser light is emitted. In the ruby laser, the flash lamp light lasts for about 1/1000 of a second (1 ms) and can be repeated about every second. The duration of the laser pulse is shorter than this, typically 0.1 ms. In some pulsed lasers, the pulse duration can be tailored using special methods to be much shorter than this, down to about 10 fs (where 1 fs = 10^{-15} s or one thousandth of a millionth of a millionth of a second). So, the output of a three-level laser is not continuous but consists of pulses of laser light.

Transition Rates in Three-level Systems

In a three-level system, there are nine (9) events that can occur (Figure **4.17.2**):

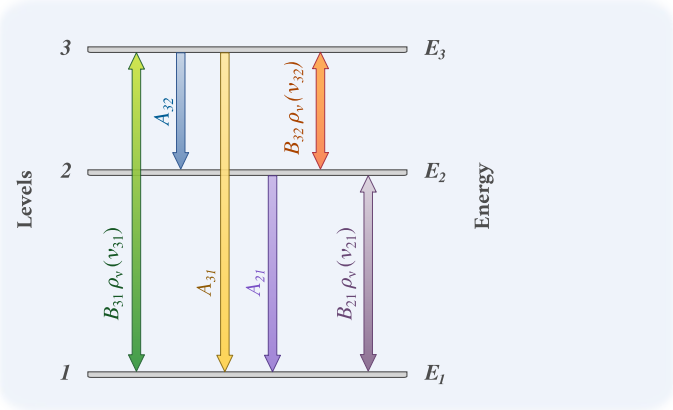


Figure **4.17.2**: The nine possible events in a three-level system. (CC BY-NC; Ümit Kaya via LibreTexts)

a. absorption from level 1 to level 3, as described by $\rho_\nu(\nu_{13})B_{13}N_1$
b. spontaneous emission from level 3 to level 1, as described by $A_{31}N_3$
c. stimulated emission from level 3 to level 1, as described by $\rho_\nu(\nu_{31})B_{31}N_3$
d. spontaneous emission from level 3 to level 2, as described by $A_{32}N_3$
e. stimulated emission from level 3 to level 2 (possible lasing), as described by $\rho_\nu(\nu_{32})B_{32}N_3$
f. absorption from level 2 to level 3, as described by $\rho_\nu(\nu_{23})B_{23}N_2$
g. absorption from level 1 to level 2, as described by $\rho_\nu(\nu_{12})B_{12}N_1$
h. spontaneous emission from level 2 to level 1, as described by $A_{21}N_2$
i. stimulated emission from level 2 to level 1 (possible lasing), as described by $\rho_\nu(\nu_{21})B_{21}N_2$

In most three-level lasers, neither the spontaneous emission from level 3 to level 1, nor the stimulated emission from level 3 to level 1 occur to any significant extent, and so these events are ignored in terms of the kinetics of the lasing process. It is also true that there is no excitation source to cause absorption from level 1 to level 2 other than the possible reabsorption of light emitted from a level 2 to level 1 transition, but this event is unlikely because most atoms in the ground state are pumped up to level 3. Because the pump will be used to drive the absorption from level 1 to level 3, this event is essentially under the control of the experimenter. This leaves a maximum of five events that we need to take into consideration when studying the lasing process.

A Ruby Laser

In a three-level system ruby laser such as that described above, the flash lamp will serve as the pump to repeatedly excite most of the atoms from the ground state to the second excited state. In this laser, lasing occurs due to the stimulated emission from level 2 to level 1 (Figure **4.17.3**.)

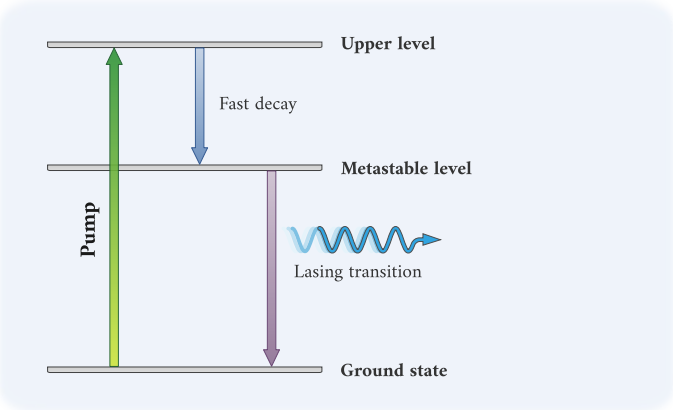


Figure **4.17.3**: Lasing from level 2 to level 1 in a three-level laser. (CC BY-NC; Ümit Kaya via LibreTexts)

Because the lasing will occur from the intermediate, metastable energy level 2, we will focus on the five events that affect its population:

a. absorption from level 2 to level 3, as described by $\rho_\nu(\nu_{32})B_{32}N_2$
b. spontaneous emission from level 3 to level 2, as described by $A_{32}N_3$
c. stimulated emission from level 3 to level 2, as described by $\rho_\nu(\nu_{32})B_{32}N_3$
d. spontaneous emission from level 2 to level 1, as described by $A_{21}N_2$
e. stimulated emission from level 2 to level 1 (lasing), as described by $\rho_\nu(\nu_{21})B_{21}N_2$

In this system, the rate of spontaneous emission from level 3 to level 2 is much more rapid than the rate of absorption from level 2 to level 3, and also much more rapid than the rate of stimulated emission from level 3 to level 2. Thus, any electrons pumped into the upper level are most likely to transition between level 2 and level 3 by spontaneous emission. This means that N_2 is greater than N_1 and thus, population inversion between states 2 and 1 can be achieved. A system of atoms that are able to attain such a population inversion is called a gain medium, and can lase.

A Copper Vapor Laser

In this three-level system, the flash lamp will again, serve as the pump to repeatedly excite most of the atoms from the ground state to the second excited state. However, in this laser, lasing occurs due to the stimulated emission from level 3 to level 2 (Figure 4.17.4).

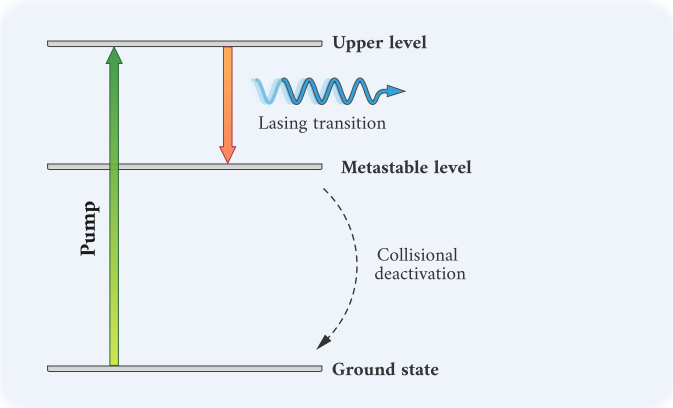


Figure 4.17.4: Lasing from level 3 to level 2 in a three-level laser. (CC BY-NC; Ümit Kaya via LibreTexts)

Because the lasing will occur from the higher energy excited state, we focus on the four events that affect the population ratio between level 3 and level 2:

a. absorption from level 2 to level 3, as described by $\rho_\nu(\nu_{32})B_{32}N_2$
b. spontaneous emission from level 3 to level 2, as described by $A_{32}N_3$
c. stimulated emission from level 3 to level 2 (lasing), as described by $\rho_\nu(\nu_{32})B_{32}N_3$
d. spontaneous emission from level 2 to level 1, as described by $A_{21}N_2$

If we assume that the atoms in the total population will be distributed between the three energy levels, then

$$N_1(t) + N_2(t) + N_3(t) = N_{total}$$

At equilibrium, the population of each level will remain constant, and so

$$0 = \frac{dN_1(t)}{dt} = \frac{dN_2(t)}{dt} = \frac{dN_3(t)}{dt}.$$

Thus,

$$\frac{N_2(t)}{dt} = -\rho_\nu(\nu_{32})B_{32}N_2 + A_{32}N_3 - A_{21}N_2 + \rho_\nu(\nu_{32})B_{32}N_3 = 0 \tag{4.17.1}$$

Rearranging Equation 4.17.1 gives

$$N_2(A_{21} + \rho_\nu(\nu_{32})B_{32}) = N_3(A_{32} + \rho_\nu(\nu_{32})B_{32}) \tag{4.17.2}$$

which rearranges to

$$\frac{N_3}{N_2} = \frac{A_{21} + \rho_\nu(\nu_{32})B_{32}}{A_{32} + \rho_\nu(\nu_{32})B_{32}} \tag{4.17.3}$$

From Equation 4.17.3 we can see that if A_{21} is greater than A_{32}, then N_3 can be greater than N_2. If N_3 is greater than N_2, then population inversion between states 3 and 2 can be achieved. In other words, if atoms in state 2 decay to the ground state more rapidly than atoms in state 3 decay to state 2, there will be a population inversion between states 3 and 2, and the system can lase.

Four-Level Lasers

There are also lasers based on transitions between four energy levels. These lasers can be more efficiently pumped, because the lower level of the lasing transition is not the ground state. Only four-level lasers can provide a continuous lasing output. He-Ne and Nd:YAG lasers are common four-level lasers.

References

D.W. Coutts, in Encyclopedia of Modern Optics, 2005, page 460, https://doi.org/10.1016/B0-12-369395-0/00847-2

4.17: Population Inversion can be Achieved in a Three-Level System is shared under a CC BY-NC-SA 4.0 license and was authored, remixed, and/or curated by Jay Newman, Seyffie Maleki, Tom Neils, & Tom Neils.

- **15.4: Population Inversion can be Achieved in a Three-Level System** by Jay Newman, Seyffie Maleki, Tom Neils is licensed CC BY-NC-SA 4.0.

4.18: What is Inside a Laser?

Most lasers consist of three basic components:

1. the gain medium from which light of a specific frequency is emitted
2. the pump source which provides energy to the gain medium to create the light
3. the laser optical cavity in which the light is amplified by repeatedly passing through the gain medium

4.18.1: The Gain Medium

The gain medium, or active medium, is a collection of atoms or molecules that can undergo stimulated emission. The active medium can be in a gaseous, liquid, or solid form. It can be a pure substance or a solution. Because the emitted light of a laser is created by the transition between two quantized states of the gain medium, laser light is always monochromatic. Laser light is also always coherent, meaning that the light waves emitted by the laser are all in phase.

4.18.1.1: Solids

The first laser, Maiman's ruby laser, described in section 15.4, used a solid rod of synthetic ruby as the gain medium (Figure **4.18.1**).

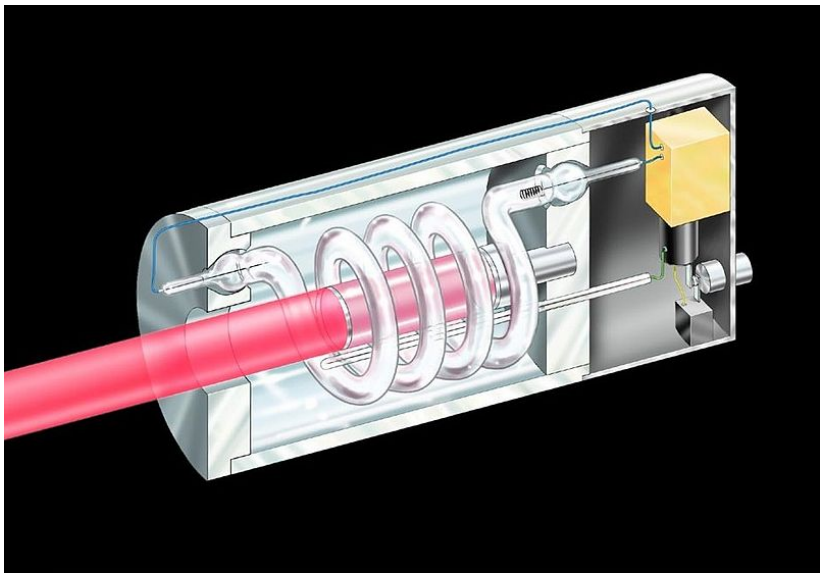


Figure **4.18.1**: Internal view of a Maiman laser (Public Domain; United States Department of Energy via Wikipedia)

Ruby is a gem variety of the mineral corundum, Al_2O_3, in which Cr^{3+} ions replace roughly 0.05% (by mass) of the Al^{3+} ions. The electronic structure of the Cr^{3+} impurities enables to ruby to act as a gain medium. However, synthetic ruby must be used because natural rubies have too many crystal defects. Other solid-state gain media are shown in Table **4.18.1**.

Table **4.18.1**: Solid-phase gain media

Solid-state Host	Active Ion	Wavelength (nm)	Output	Lifetime
Al_2O_3	Ti^{3+}	780	continuous and pulsed	10 fs - 5 ps
Al_2O_3	Cr^{3+}	694.3	pulsed	10 ps
Glass (SiO_2)	Nd^{3+}	1059	pulsed	1 ps
YAG $Y_3Al_5O_{15}$	Nd^{3+}	1064.1	continuous and pulsed	10-150 ps
YLF Y_3LixFy	Nd^{3+}	1054.3	continuous and pulsed	10-100 ps

4.18.1.2: Gases

A basic He-Ne laser is shown in figure **4.18.2**. The gain medium is the gas mixture through which the laser beam passes.

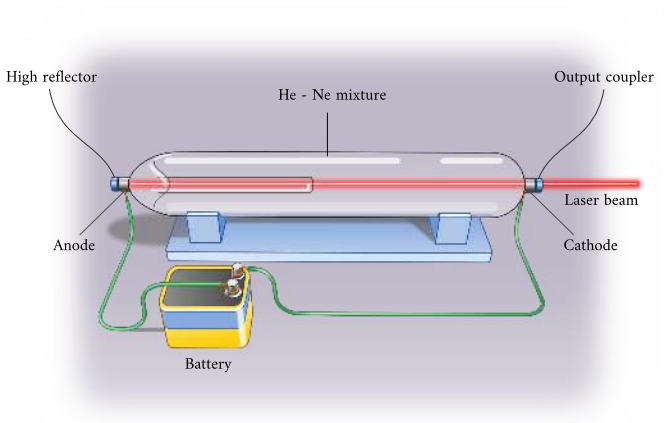


Figure **4.18.2**: Internal view of a He-Ne laser. (CC BY-NC; Ümit Kaya via LibreTexts)

Other common gas-phase media include noble gases and molecules, but also metal cations, and metal atoms as shown in Table **4.18.2.**

Table **4.18.2**: Gas-phase gain media

Gaseous Gain Medium	Wavelength (nm)	Output	Pulse Duration
N_2	337	pulsed	1 ns
Cu	510	pulsed	30 ns
CO_2, He, N_2	tunable near 10,000	pulsed	> 100 ns
He, Ne	3391, 1152, 632, 544	continuous	continuous
He, Cd	441, 325	continuous	continuous
Ar^+	488, 515	continuous	continuous
K^+	647	continuous	continuous.

4.18.1.3: Exciplex Lasers

Exciplex lasers involve the formation of an exciplex, a gaseous species that forms and exists only in an excited state. Because only the upper, excited state can exist, there is no population in the lower, dissociated state, thus a population inversion is obtained. The lasing transition occurs as the excited state exciplex emits its excitation energy and simultaneously falls apart. Two common exciplex lasers are XeCl* (308 nm) and KrF* ((249 nm). These lasers are often referred to as excimer laser, but the term "excimer" refers to an excited dimer, AA*, and so should not be used to describe an exciplex, AB*.

4.18.1.4: Liquid Solutions

Many dye lasers use an organic dye, usually dissolved in a solution, as the gain medium. One advantage of using a dye solution as the gain medium is that it can create a tunable laser, which allows for continuous tuning over a wide range of wavelengths. For example, rhodamine 6G is a dye that can be tuned from 635 nm to 560 nm. The dye solution enters the laser cavity by passing through a cell or by streaming through the air using a dye jet. (Figure **4.18.3**).



Figure **4.18.3**: A dye laser in use. The dye is entering the dye cell through the yellow tube in the left foreground. (CC BY-SA 4.0, By Zaereth - Own work, https://commons.wikimedia.org/w/inde...curid=55762750)

Some common laser dyes other than rhodamine 6G and the rhodamines, include various coumarins, stilbenes, and fluorescein. There are solid state dye lasers (SSDL), in which the dye is dispersed uniformly within a solid polymer matrix.

4.18.2: The Pump Source

For lasing to take place, the gain medium must be pumped into an *excited state* capable of undergoing stimulated emission. The energy required for excitation is often supplied by an electric current or an intense light source, such as a flashlamp or an excitation laser. Diode lasers, excimer lasers, and YAG lasers have all been used as pump sources.

Lasers are categorized as having either a continuous beam or a pulsed beam. In theory, any laser could be run as a pulsed beam laser if the pump source is set to deliver the excitation energy in regularly repeated bursts. Not all lasers can operate as continuous-wave (CW) lasers, though, because there are gain media in which it is not possible to maintain a continuous population inversion. The ruby laser is an example of a laser that cannot produce a continuous wave.

4.18.3: The Laser Optical Cavity

Figure **4.18.4** shows the main components of a generic laser optical (or resonator) cavity. The optical cavity is formed by a pair of mirrors that surround the gain medium and enable feedback of light into the medium. This feedback is critical to the operation of a laser because it is where the amplification of the signal occurs. The gain medium is excited by an external pump source, such as a flash lamp, electric current, or another laser. The output coupler is a partially reflective mirror that allows a portion of the laser radiation to leave the cavity but reflects a majority of the light back through the gain medium. The light trapped between the mirrors forms standing wave structures called modes. Although beyond the scope of this discussion, the reader interested in cavity modes can consult the "Laser Radiation Properties" module.

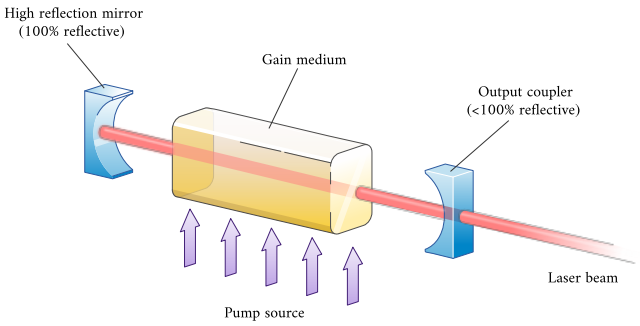


Figure **4.18.4**: A schematic of a generic laser cavity. (CC BY-NC; Ümit Kaya via LibreTexts)

Figure **4.18.5** shows the laser cavity of a tunable dye laser. The laser is tunable because the pump source provides several excitation energies, which result in the creation of several possible energies for the lasing beam. The user chooses the desired lasing energy by means of a tuning element, which is often a movable diffraction grating.

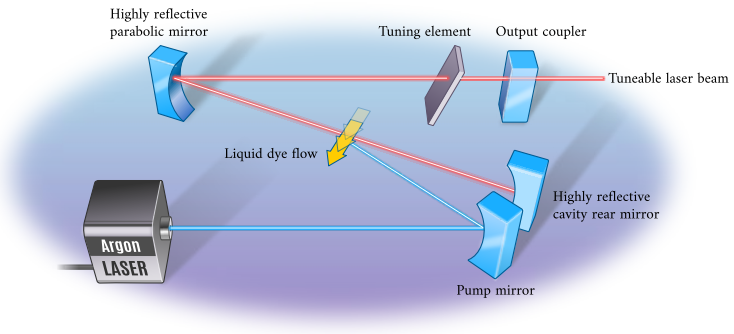


Figure **4.18.5**: A schematic of a dye laser cavity with a dye jet. (CC BY-NC; Ümit Kaya via LibreTexts)

4.18.4: Diode Lasers

Diode lasers do not lase in the same manner as the lasers described above. There is no laser optical cavity, and thus there is no stimulated emission. Diodes made of materials such as GaAs emit light when the recombination of an electron and a hole in a semiconductor releases energy in the form of photons. A population inversion is maintained by rapidly removing the electrons that are falling into the holes of the p-type semiconductor. A pseudo-optical cavity is formed because the semiconductor materials generally have a very high refractive index, causing the photons to be trapped in the crystal of the semiconductor due to the large and abrupt difference in the refractive indices at the surfaces of the crystal. GaAs emits infrared light, but it can be doped to create a material that emits at another wavelength. For example, $GaAs_{0.6}P_{0.4}$ emits red light.

4.18: What is Inside a Laser? is shared under a CC BY-NC-SA 4.0 license and was authored, remixed, and/or curated by LibreTexts.

- **15.5: What is Inside a Laser?** is licensed CC BY-NC-SA 4.0.

4.19: The Helium-Neon Laser

The He-Ne laser was the first continuous-wave (cw) laser invented. A few months after Maiman announced his invention of the pulsed ruby laser, Ali Javan and his associates W. R. Bennet and D. R. Herriott announced their creation of a cw He-Ne laser. This gas laser is a four-level laser that uses helium atoms to excite neon atoms. The atomic transitions in the neon produce the laser light. The most commonly used neon transition in these lasers produces red light at 632.8 nm. These lasers can also produce green and yellow light in the visible region, as well as several UV and IR wavelengths (Javan's first He-Ne operated in the IR at 1152.3 nm). By using highly reflective mirrors designed for one of these many possible lasing transitions, a given He-Ne's output is made to operate at a single wavelength.

He-Ne lasers are not sources of high-power laser light, typically producing a few to tens of mW (milli-Watt, or 10^{-3} W) of power. Probably one of the most important features of these lasers is that they are highly stable, both in terms of their wavelength (mode stability) and intensity of their output light (low jitter in power level). For these reasons, He-Ne lasers are often used to stabilize other lasers. They are also used in applications, such as holography, where mode stability is important. Until the mid-1990's, He-Ne lasers were the dominant type of lasers produced for low-power applications - from range finding to scanning to optical transmission, to laser pointers, etc. Recently, however, other types of lasers, most notably the semiconductor lasers, seem to have won the competition because of reduced costs.

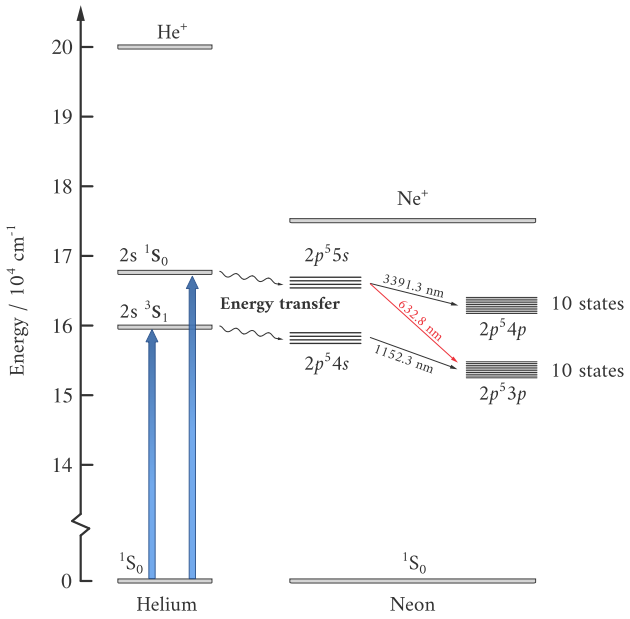


Figure **4.19.1**: An energy level diagram for He and Ne in a He-Ne laser. The pumping creates helium atoms in two excited states. These excited states have energies similar to two sets of four excited states in the Ne atoms. Thus, collisions between the excited He atoms and Ne atoms can lead to nonradiative energy transfer. The excited state Ne atoms have lifetimes that enable a population inversion and lasing. (CC BY-NC; Ümit Kaya via LibreTexts)

The energy level diagram in figure **4.19.1** shows the two excited states of a helium atom, the 2 ^{3}S and 2 ^{1}S, that get populated as a result of electromagnetic pumping. Both of these states are metastable and do not allow de-excitations via radiative transitions. Instead, the helium atoms give off their energy to neon atoms through collisional excitation. In this way, the 4s and 5s levels in neon get populated.

$$He^*(2s^3\,S_1) + Ne(g) \rightarrow He(g) + Ne^*(2p^5 4s)$$

$$He^*(2s^1\,S_0) + Ne(g) \rightarrow He(g) + Ne^*(2p^5 5s)$$

These are the two upper lasing levels, each for a separate set of lasing transitions. Each of these upper lasing levels contains 4 states ($^3P_2$, $^3P_1$, $^3P_0$, $^1P_1$). Radiative decay from the 5s to the 4s levels is forbidden. So, ten states associated with the 4p and 3p levels

serve as the lower lasing levels and rapidly decay into the metastable 3s level. In this way, population inversion is easily achieved in the He-Ne mixture. The 632.8 nm laser transition, for example, involves the 5s and 3p levels, as shown above. Table **4.19.1** lists parameters of several of the Ne transitions.

Table **4.19.1**: Several Lasing Transitions for an Excited State Ne Atom

Transition	λ (nm)	Einstein Coefficient A (s^{-1})	Relative Intensity
$5s^1\ P_1 \rightarrow 3p^3\ P_1$	640.1	0.60×10^6	100
$5s^1\ P_1 \rightarrow 3p^3\ P0$	635.2	0.70×10^6	100
$5s^1\ P_1 \rightarrow 3p^3\ P2$	632.8	6.56×10^6	300
$5s^1\ P_1 \rightarrow 3p^1\ P_1$	629.4	1.35×10^6	100
$5s^1\ P_1 \rightarrow 3p^1\ D_2$	611.8	1.28×10^6	100

In most He-Ne lasers the gas, a mixture of 5 parts helium to 1 part neon, is contained in a sealed glass tube with a narrow (2 to 3 mm diameter) bore as shown above in figure **4.19.2**. Typically the laser's optical cavity mirrors, the high reflector and the output coupler form the two sealing caps for the narrow bore tube. High voltage electrodes create a narrow electric discharge along the length of this tube, which then leads to the narrow beam of laser light.

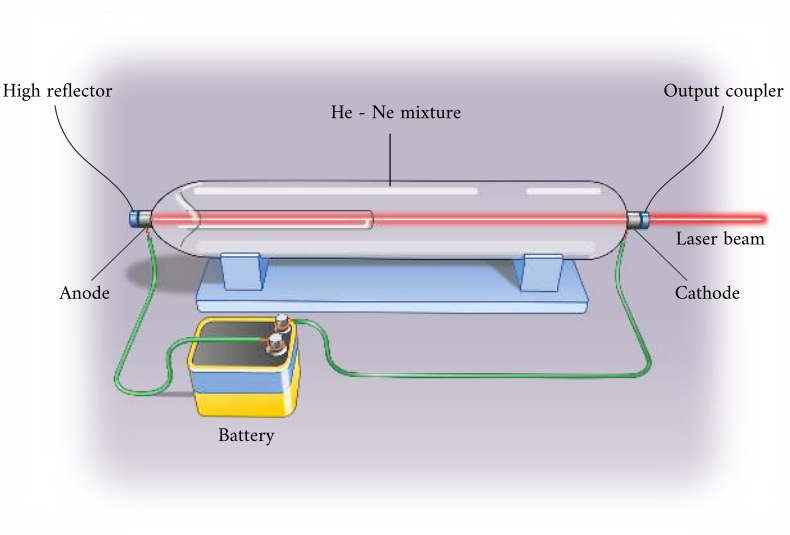


Figure **4.19.2**: A He-Ne laser cavity. (CC BY-NC; Ümit Kaya via LibreTexts)

Many He-Ne lasers also contain a ballast which serves to maintain the desired gas mixture. Since some of the atoms may get embedded in the glass and/or the electrodes as they accelerate within the discharge, in the absence of a ballast the lasing mixture would not last very long. To further prolong the useable life of the laser, some of these lasers also use "getters", often metals such as titanium, that absorb impurities in the gas. Figure **4.19.3** below shows a He-Ne laser with a ballast.

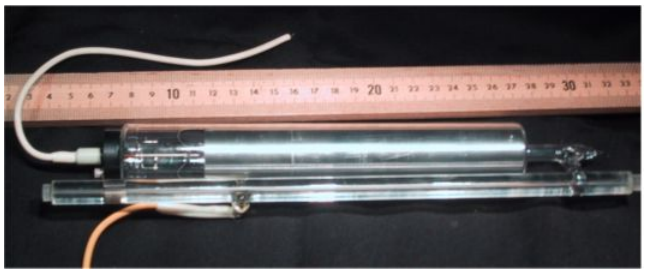


Figure 4.19.3: A commercial He-Ne tube. The thicker cylinder closest to the meter-stick (shown for scale) is the ballast. The thinner tube houses the resonant cavity where the lasing occurs. Notice the two mirrors that seal the two ends of the bore. For mode stability reasons, these mirrors are concave; they serve as the output coupler and the high reflector. (Copyright; author via source)

A typical commercially available He-Ne produces about a few mW of 632.8 nm light with a beam width of a few millimeters at an overall efficiency of near 0.1%. This means that for every 1 Watt of input power from the power supply, 1 mW of laser light is produced. Still, because of their long operating lifetime of 20,000 hours or more and their relatively low manufacturing cost, He-Ne lasers are among the most popular gas lasers.

4.19: The Helium-Neon Laser is shared under a CC BY 4.0 license and was authored, remixed, and/or curated by Jay Newman, Seyffie Maleki, Tom Neils, & Tom Neils.

- **15.6: The Helium-Neon Laser** by Jay Newman, Seyffie Maleki, Tom Neils is licensed CC BY 4.0.

4.20: Modern Applications of Laser Spectroscopy

A Quick Overview

Laser light offers valuable tools to researchers who wish to use the interaction of light with matter to interrogate atomic and molecular systems. Most laser light is characterized by its near monochromaticity (relative to light from other sources), directionality, and coherence [1]. Those characteristics are used in modern laser spectroscopy. The monochromaticity of laser light allows it to be used to probe specific energy changes in atoms and molecules. This ability to select specific wavelengths allows scientists to focus on chosen components in mixtures, including complex reaction mixtures. For example, Park et. al. tracked the dynamics of the reaction of ground state oxygen with ethyl radical by using a 355 nm laser beam to track one of the products of this reaction [2]. Parsons et. al. used near monochromatic laser light sources to achieve state-selective ionization for the study of the products of a photodissociation reaction of atmospheric relevance [3]. Laser monochromaticity can be used to quantify the amount of greenhouse gases in the atmosphere [4]. Even when the samples are not mixtures, monochromaticity allows researchers to gather detailed information about atomic and/or molecular structure. Applications of this type are extremely numerous, including detailed studies of atomic systems [5], semiconductor materials [6], single molecules [7], and biological molecules [8]. Lasers find research applications in art and archeology, where the property of monochromaticity allows specific energies to be probed and laser beam directionality and small spot size curtail destruction of samples [9,10].

Other laser applications focus on the ability of pulsed lasers to provide short pulses. Short-pulsed lasers offer myriad tools for exploring chemical kinetics at a range of timescales, including very short ones. Short-pulse lasers open the opportunity for time-resolved studies of molecular processes such as reaction processes [2,11] and biological processes [12 - 15], and the properties of excited states [16]. Some research applications take advantage of the ability of certain lasers to produce high intensity light. One such application is laser-induced break down spectroscopy (LIBS), in which the high intensity of the laser creates a plasma from solid or liquid samples; that plasma can subsequently be probed [17]. Other techniques that exploit high laser intensities are the nonlinear spectroscopies, where the high intensities of some lasers can produce behaviors in samples that lower-power sources cannot sufficiently stimulate [18,19]. Although most lasers are monochromatic and coherent, some researchers have modified laser light to obtain information from broadband, incoherent laser light [20 – 22], which allows them to probe the response of samples to light that more resembles sunlight (incoherent) than do traditional laser sources [22, 23]. Another possibility is to probe multiple wavelengths with broadband laser sources that are coherent [24].

Conclusion

This brief overview has only skimmed the surface of the vast field of laser spectroscopy. The examples given here are a very small, somewhat arbitrary, and significantly biased subset of the enormous library of published laser-based experiments. References have been chosen to give examples of the topics covered here and have not been extensively reviewed by the author.

Overall, lasers are especially useful as light sources when one or more of the following properties are desired for light in an experiment:

1. A high degree of monochromaticity
2. A well-known central wavelength for a light source
3. A tunable light source
4. Spatial coherence
5. Phase coherence
6. Directionality
7. High intensity
8. Tight focus
9. Short pulses

A particular laser type will not necessarily have all the properties in the list above; however, the menu of available laser types allows a researcher to choose a laser system or systems with the characteristics needed for a particular experiment. New applications of laser spectroscopy and new spectroscopic techniques employing laser light continue to be invented.

References

[1] https://chem.libretexts.org/Bookshelves/Analytical_Chemistry/Supplemental_Modules_(Analytical_Chemistry)/Analytical_Sciences_Digital_Library/JASDL/Courseware/Introduction_to_Lasers/03_Basic_Principles/01_Laser_Radiation_Properties

[2] *J. Phys. Chem. A* 2010, 114, 14, 4891–4895; Publication Date: February 19, 2010; https://doi.org/10.1021/jp910615y

[3] *J. Phys. Chem. A* 2022, 126, 34, 5729–5737; Publication Date: August 22, 2022; https://doi.org/10.1021/acs.jpca.2c04265

[4] https://www.nist.gov/news-events/news/2021/06/nist-laser-comb-systems-now-measure-all-primary-greenhouse-gases-air

[5] R. C. Thompson, 1985 *Rep. Prog. Phys.* **48** 531; https://iopscience.iop.org/article/10.1088/0034-4885/48/4/003

[6] *J. Phys. Chem. A* 2020, 124, 15, 2972–2981; Publication Date: March 23, 2020; https://doi.org/10.1021/acs.jpca.0c00370

[7] *J. Phys. Chem. A* 1997, 101, 45, 8435–8440; Publication Date: November 6, 1997; https://doi.org/10.1021/jp9719063

[8] Jörg Standfuss, Membrane protein dynamics studied by X-ray lasers – or why only time will tell, *Current Opinion in Structural Biology*, Volume 57, 2019, Pages 63-71, ISSN 0959-440X, https://doi.org/10.1016/j.sbi.2019.02.001

[9] https://www.getty.edu/conservation/about/science/laser_mass.html

[10] https://www.laserfocusworld.com/test-measurement/spectroscopy/article/14183101/spectroscopy-uncovers-the-hidden-in-art-and-archaeology

[11] *J. Phys. Chem.* 1996, 100, 31, 12701–12724; Publication Date: August 1, 1996; https://doi.org/10.1021/jp960658s

[12] Hideki Hashimoto, Mitsuru Sugisaki, Masayuki Yoshizawa,

Ultrafast time-resolved vibrational spectroscopies of carotenoids in photosynthesis, *Biochimica et Biophysica Acta - Bioenergetics*, Volume 1847, Issue 1, 2015, Pages 69-78,

ISSN 0005-2728, https://doi.org/10.1016/j.bbabio.2014.09.001.

[13] *J Phys Chem A*. 2003 Oct 9; 107(40): 8208–8214.; Publication Date: June 12, 2003 ; https://doi.org/10.1021/jp030147n

[14] *Biochemistry* 2003, 42, 34, 10054-10059; Publication Date: August 5, 2003; https://doi.org/10.1021/bi034878p

[15] Holzwarth, A. (1989). Applications of ultrafast laser spectroscopy for the study of biological systems. *Quarterly Reviews of Biophysics*, *22*(3), 239-326.

https://doi.org/10.1017/S0033583500002985

[16] *J. Phys. Chem. B* 2015, 119, 29, 9335–9344; Publication Date:November 4, 2014; https://doi.org/10.1021/jp509959n

[17] *Anal. Chem.* 2013, 85, 2, 640–669; Publication Date:November 8, 2012; https://doi.org/10.1021/ac303220r

[18]https://chem.libretexts.org/Bookshelves/Physical_and_Theoretical_Chemistry_Textbook_Maps/Book%3A_Nonlinear_and_Two-Dimensional_Spectroscopy_(Tokmakoff)/00%3A_Front_Matter/05%3A_What_is_Nonlinear_Spectroscopy

[19] Marc Levenson and Satoru Kano, *Introduction to Nonlinear Laser Spectroscopy*, revised edition, 2012, Academic Press, ISBN-13: 978-0124447226, ISBN-10: 0124447228

[20] *J. Phys. Chem. A* 2013, 117, 29, 5926–5954; Publication Date: November 26, 2012; https://doi.org/10.1021/jp310477y

[21] Turner, D., Arpin, P., McClure, S. *et al.* Coherent multidimensional optical spectra measured using incoherent light. *Nat Commun* **4**, 2298 (2013). https://doi.org/10.1038/ncomms3298

[22] *J. Phys. Chem. Lett.* 2012, 3, 21, 3136–3142; Publication Date: October 9, 2012; https://doi.org/10.1021/jz3010317

[23] *J. Phys. Chem. Lett.* 2018, 9, 11, 2946–2955; Publication Date: May 15, 2018; https://doi.org/10.1021/acs.jpclett.8b00874

[24] Muraviev, A.V., Konnov, D. & Vodopyanov, K.L. Broadband high-resolution molecular spectroscopy with interleaved mid-infrared frequency combs. *Sci Rep* **10**, 18700 (2020). https://doi.org/10.1038/s41598-020-75704-3

Contributor

Stephanie Schaertel (Grand Valley State University)

(Thank you to Tom Neils (Grand Rapids Community College) for editing the references)

4.20: Modern Applications of Laser Spectroscopy is shared under a CC BY-NC-SA 4.0 license and was authored, remixed, and/or curated by LibreTexts.

4.21: Broadening Mechanisms

4.21.1: Introduction

Spectral lines are not infinitesimally narrow; they have a finite width. A graph of radiance or intensity per unit wavelength (or frequency) versus wavelength (or frequency) is the *line profile*. There are several causes of line broadening, some internal to the atom or molecule, others external, and each produces its characteristic profile. Some types of profile, for example, have a broad core and small wings; others have a narrow core and extensive, broad wings. Analysis of the exact shape of a line profile may give us information about the physical conditions, such as temperature and pressure, in the system being investigated.

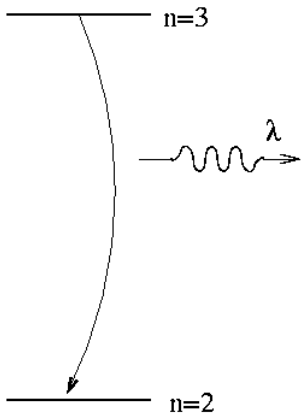
An absorption lineshape can represent the dynamics of the dipole or be broadened by energy relaxation, for instance through coupling to a continuum. However, there are numerous processes that can influence the lineshape. These can be separated by dynamic processes intrinsic to the molecular system, which is termed **homogeneous broadening**, and static effects known as **inhomogeneous broadening**, which can be considered an ensemble averaging effect.

4.21.2: Homogeneous Broadening

Several dynamical mechanisms can potentially contribute to damping and line-broadening. These intrinsically molecular processes, often referred to as homogeneous broadening, are commonly assigned a time scale $T_2 = \gamma^{-1}$.

4.21.2.1: Population Relaxation

Atoms and molecules emit (or absorb) light when their electrons jump from one energy state to another. In the case of the H-alpha line, the transition involves the n=3 and n=2 states of hydrogen.



If we knew the energy difference *exactly*, then we would know the wavelength of the photon *exactly*. However, due to **Heisenberg's Uncertainty Principle,** we do NOT know the energies exactly. One way to look at is that atoms very quickly jump from an excited state to a lower state; that means that you don't have very long to measure the energy in the upper state. The limit on the time available to measure the excited state's energy places a limit on the precision of the energy measurement:

$$\Delta E \Delta t \simeq \hbar$$

The lifetime of hydrogen atoms in their excited states is very short. For example, the lifetime of hydrogen in the $n = 2$ and $n = 3$ states is about 10^{-8} seconds.

Population relaxation refers to decay in the coherence created by the light field as a result of the finite lifetime of the coupled states, and is often assigned a time scale T_1. This can have contributions from radiative decay, such as spontaneous emission, or non-radiative processes such as relaxation as a result of coupling to a continuum.

$$\frac{1}{T_1} = \frac{1}{\tau_{rad}} + \frac{1}{\tau_{NR}} \tag{4.21.1}$$

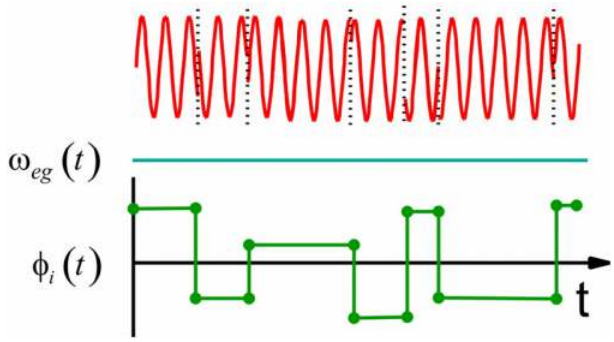
The observed population relaxation time depends on both the relaxation times of the upper and lower states (m and n) being coupled by the field:

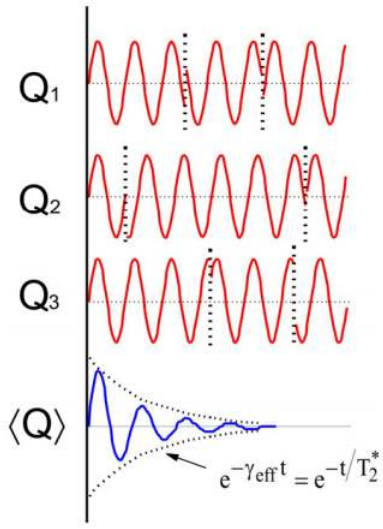
$$1/T_1 = w_{mn} + w_{nm}.$$

When the energy splitting is high compared to k_BT, only the downward rate contributes, which is why the rate is often written $1/2T_1$.

4.21.2.2: Pure Dephasing (Collisional Broadening)

Pure dephasing is characterized by a time constant T_2^* that characterizes the randomization of phase within an ensemble as a result of molecular interactions. This is a dynamic effect in which memory of the phase of oscillation of a molecule is lost as a result of intermolecular interactions that randomize the phase. Examples include collisions in a dense gas, or fluctuations induced by a solvent. This process does not change the population of the states involved.





4.21.2.3: Orientational Relaxation

Orientational relaxation (τ_{or}) also leads to relaxation of the dipole correlation function and to line-broadening. Since the correlation function depends on the projection of the dipole onto a fixed axis in the laboratory frame, randomization of the initial dipole orientations is an ensemble averaged dephasing effect. In solution, this process is commonly treated as an orientational diffusion problem in which τ_{or} is proportional to the diffusion constant.

4.21.2.4: Lineshape of homogeneously broadened transitions

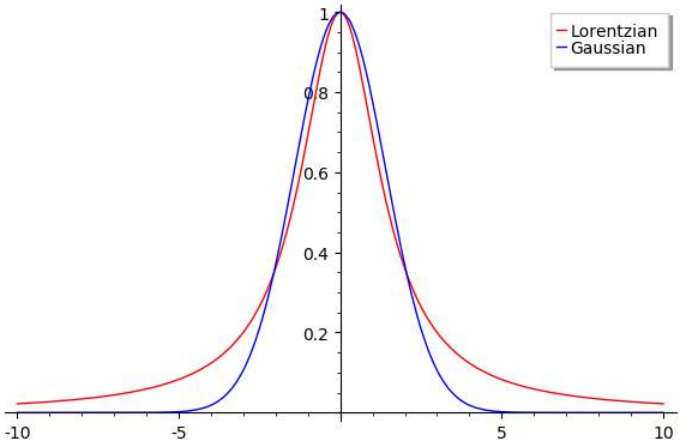
If these homogeneous processes are independent, the rates for different processes contribute additively to the damping and line width:

$$\frac{1}{T_2} = \frac{1}{T_1} + \frac{1}{T_2^*} + \frac{1}{\tau_{or}} = \gamma^{-1} \tag{4.21.2}$$

This type of relaxation results in what is called a Lorentzian line shape:

$$I(\nu) = I_o \frac{\gamma^2}{(\nu - \nu_o)^2 - \gamma^2} \tag{4.21.3}$$

This peak shape has significant intensity far from the peak as shown below in the comparison with a Gaussian shaped peak.



4.21.3: Inhomogeneous Broadening

Absorption lineshapes can also be broadened by a static distribution of frequencies.

4.21.3.1: Doppler broadening

When thermal motion causes a particle to move towards the observer, the emitted radiation will be shifted to a higher frequency. Likewise, when the emitter moves away, the frequency will be lowered. For non-relativistic thermal velocities, the Doppler shift in frequency will be:

$$\nu = \nu_0 \left(1 + \frac{v}{c}\right), \tag{4.21.4}$$

where ν is the observed frequency, ν_0 is the rest frequency, v is the velocity of the emitter towards the observer, and c is the speed of light.

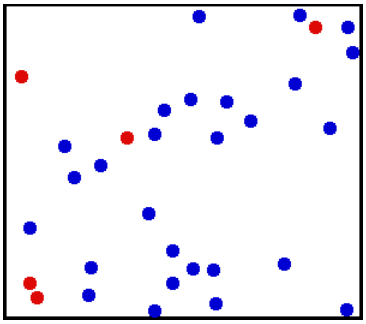


Figure 4.21.1: CMotion of gas molecules. The randomized thermal vibrations of fundamental particles such as atoms and molecules —gives a substance its “kinetic temperature.” . (Public Domain; Greg L via Wikipedia)

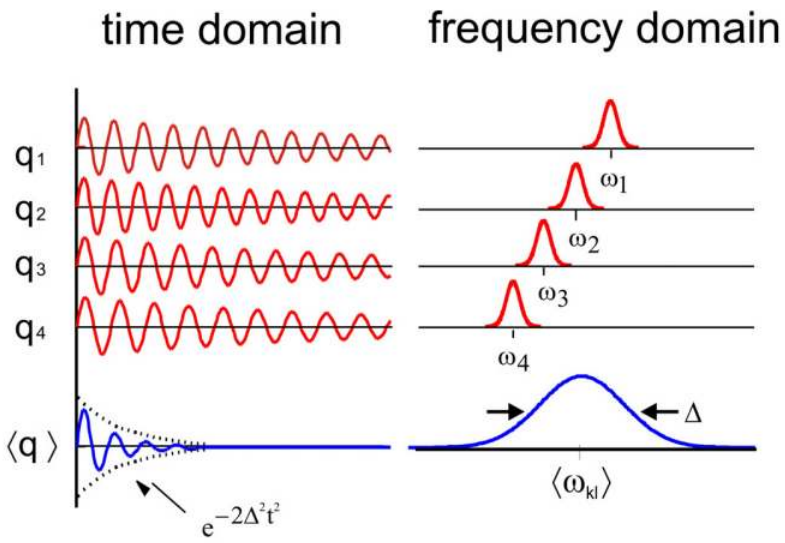
Since there is a distribution of speeds both toward and away from the observer in any volume element of the radiating body, the net effect will be to broaden the observed line. Propagating the Maxwell-Boltzmann Distribution law for velocities of a gas with the Doppler shifting (Equation 4.21.4) results in a line broadening (of a Gaussian distribution).

$$\Delta v_{\text{FWHM}} = \sqrt{\frac{8kT\ln 2}{mc^2}} v_0$$

where FWHM is the full width at half maximum of the line.

4.21.3.2: Static Broadening

If molecules within the ensemble are influenced static environmental variations more than other processes, then the observed lineshape reports on the distribution of environments. This inhomogeneous broadening is a static ensemble averaging effect, which hides the dynamical content in the homogeneous linewidth. The origin of the inhomogeneous broadening can be molecular (for instance a distribution of defects in crystals) or macroscopic (i.e., an inhomogeneous magnetic field in NMR).



The inhomogeneous linewidth is dictated the width of the distribution Δ.

4.21.4: Total Linewidth

The total observed broadening of the absorption lineshape reflects the contribution of all of these effects. All of these effects can be present simultaneously in an absorption spectrum.

4.21: Broadening Mechanisms is shared under a CC BY-NC-SA 4.0 license and was authored, remixed, and/or curated by LibreTexts.

- **2.3: Broadening Mechanisms** is licensed CC BY-NC-SA 4.0.

CHAPTER OVERVIEW

5: Moving Molecules and Chemical Kinetics

5.1: Classical Model of Ideal Gas Pressure
5.2: Collisions
5.3: The Frequency of Collisions with a Wall
5.4: Transport of Matter and Energy in Perfect Gases
5.5: Stokes-Einstein-Sutherland Equation
5.6: The Rate of Bimolecular Gas-Phase Reaction Can Be Estimated Using Hard-Sphere Collision Theory and an Energy-Dependent Reaction Cross Section
5.7: A Reaction Cross Section Depends Upon the Impact Parameter
5.8: The Rate Constant for a Gas-Phase Chemical Reaction May Depend on the Orientations of the Colliding Molecules
5.9: The Internal Energy of the Reactants Can Affect the Cross Section of a Reaction
5.10: A Reactive Collision Can Be Described in a Center-of-Mass Coordinate System
5.11: Reactions Can Produce Vibrationally Excited Molecules
5.12: Reactive Collisions Can be Studied Using Crossed Molecular Beam Machines
5.13: The Velocity and Angular Distribution of the Products of a Reactive Collision
5.14: Not All Gas-Phase Chemical Reactions are Rebound Reactions
5.15: The Potential-Energy Surface Can Be Calculated Using Quantum Mechanics
5.16: Equilibrium Constants in Terms of Partition Functions
5.17: Statistical Mechnanical Transition State Theory
5.18: Chain Reactions
5.19: Chain Branching Explosions
5.20: Kinetics of Chain Polymerization
5.21: Kinetics of Step-Growth Polymerization
5.22: Atoms and Molecules can Physisorb or Chemisorb to a Surface
5.23: Isotherms are Plots of Surface Coverage as a Function of Gas Pressure at Constant Temperature
5.24: Using Langmuir Isotherms to Derive Rate Laws for Surface-Catalyzed Gas-Phase Reactions
5.25: The Structure of a Surface is Different from that of a Bulk Solid
5.26: The Haber-Bosch Reaction Can Be Surface Catalyzed
5.27: Photochemical Kinetics

This page titled 5: Moving Molecules and Chemical Kinetics is shared under a not declared license and was authored, remixed, and/or curated by Jonathan Gutow.

5.1: Classical Model of Ideal Gas Pressure

5.1.1: Introduction

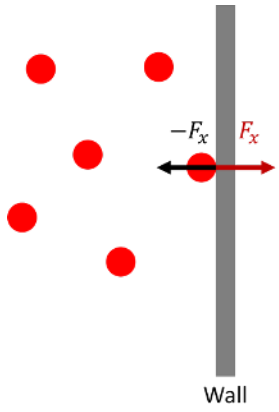
Classical physics can be used to derive the form of the ideal gas law, which can be combined with the root-mean-square average speed from the Maxwell-Boltzmann distribution of speeds (derived classically or via statistical mechanics) to recover the ideal gas law. The discussion of collisions with the walls to produce a pressure provides a place to begin understanding how collisions are involved in the properties of gases.

The assumptions are those of the kinetic molecular theory of gases:

1. Gas particles obey Newton's laws of motion and travel in straight lines unless they collide with other particles or the walls of the container.
2. the particle trajectories and velocities are random.
3. Gas particles are very small compared to the averages of the distances between them.
4. Molecular collisions are perfectly elastic so that kinetic energy is conserved.

5.1.2: Ideal gas law from the kinetic molecular model of gases

Ideal gases have no interactions between the particles, hence, the particles do not exert forces on each other. However, particles do experience a force when they collide with the walls of the container. Let us assume that each collision with a wall is elastic. Let us assume that the gas is in a cubic box of length a and that two of the walls are located at $x = 0$ and at $x = a$. Thus, a particle moving along the x direction will eventually collide with one of these walls and will exert a force on the wall when it strikes it, which we will denote as F_x. Since every action has an equal and opposite reaction, the wall exerts a force $-F_x$ on the particle.



According to Newton's second law, the force $-F_x$ on the particle in this direction gives rise to an acceleration via

$$-F_x = ma_x = m\frac{\Delta v_x}{\Delta t} \tag{5.1.1}$$

Here, t represents the time interval between collisions with the same wall of the box. In an elastic collision, all that happens to the velocity is that it changes sign. Thus, if v_x is the velocity in the x direction before the collision, then $-v_x$ is the velocity after, and $\Delta v_x = -v_x - v_x = -2v_x$, so that

$$-F_x = -2m\frac{v_x}{\Delta t} \tag{5.1.2}$$

Since the particles have no forces acting upon them, except for when they collide iwht the wall container, the particles move at constant speed. Thus, a collision between a particle and, say, the wall at $x = 0$ will not change the particle's speed. Before it strikes this wall again, it will proceed to the wall at $x = a$ first, bounce off that wall, and then return to the wall at $x = 0$. The total distance in the x direction traversed is $2a$, and since the speed in the x direction is always v_x, the interval $\Delta t = \frac{2a}{v_x}$. Consequently, the force is:

$$-F_x = -\frac{mv_x^2}{a} \tag{5.1.3}$$

Thus, the force that the particle exerts on the wall is:

$$F_x = \frac{mv_x^2}{a} \tag{5.1.4}$$

The mechanical definition of pressure is the average force over area:

$$P = \frac{\langle F \rangle}{A} \tag{5.1.5}$$

where $\langle F \rangle$ is the average force exerted by all N particles on a wall of the box of area A. Here $A = a^2$. If we use the wall at $x = 0$ we have been considering, then

$$P = \frac{N\langle F_x \rangle}{a^2} \tag{5.1.6}$$

because we have N particles hitting the wall. Hence:

$$P = \frac{Nm\langle v_x^2 \rangle}{a^3} = \frac{Nm\langle v_x^2 \rangle}{V}, \tag{5.1.7}$$

where we have recognized that $a^3 = V$. Equation 5.1.7 shows that with this simple physical model we predict that the pressure depends on the density of particles (N/V) and the average kinetic energy ($1/2m\langle v_x^2 \rangle$).

To go any further towards the ideal gas law, we need an expression for $\langle v_x^2 \rangle$. From our study of the Maxwell-Boltzmann distribution, we know:

$$\langle v^2 \rangle = \frac{3k_BT}{m}, \tag{5.1.8}$$

where v is the speed in 3 dimensions. From the definition of vector length $v^2 = v_x^2 + v_y^2 + v_z^2 \implies \langle v^2 \rangle = \langle v_x^2 \rangle + \langle v_y^2 \rangle + \langle v_z^2 \rangle$. In addition we know that all three dimensions have the same velocity distribution. Thus, $\langle v^2 \rangle = 3\langle v_x^2 \rangle = 3\langle v_y^2 \rangle = 3\langle v_z^2 \rangle \implies \langle v_x^2 \rangle = \langle v^2 \rangle / 3$. Substituting equation 5.1.8 divided by 3 into equation 5.1.7 for $\langle v_x^2 \rangle$ yields:

$$P = \frac{Nk_BT}{V} = \frac{nRT}{V} \tag{5.1.9}$$

which is the ideal gas law.

Contributors and Attributions

- Mark Tuckerman (New York University)
- Jerry LaRue (Chapman University)
- Jonathan Gutow (UW Oshkosh)

This page titled 5.1: Classical Model of Ideal Gas Pressure is shared under a CC BY-NC-SA 4.0 license and was authored, remixed, and/or curated by Jonathan Gutow.

- **16.1: All Dilute Gases Behave Ideally** is licensed CC BY-NC-SA 4.0.
- **2.3: The Kinetic Molecular Theory of Gases** by Patrick Fleming is licensed CC BY-NC-SA 4.0.

5.2: Collisions

5.2.1: Introduction

Molecular collisions are important in chemical reactions, diffusion and transfer of energy through a sample. Here we consider collisions modeled in a gas of structureless spherical particles to gain a better understanding of some of the implications. We begin by defining the collision cross-section, which provides a quantitative definition of a collision for this simple system. We end by considering how random motion leads to a model for diffusion.

5.2.2: Collision cross-section

Consider two molecules in a system. The probability that they will collide increases with the effective "size" of each particle. However, the size measure that is relevant is the apparent cross-sectional area of encounter where the particles touch. For simplicity, suppose the particles are spherical, which is not a bad approximation for small molecules. The collision cross-section σ_{AB} can be understood as the area of a circle that sweeps out the cylindrical volume within which spherical molecules with a center-to-center distance less than or equal to the sum of their radii collide. Those with centers farther apart do not collide (see figure **5.2.1**). If A and B are hard spheres $\sigma_{AB} = \pi(r_A + r_B)^2$, where 'r' refers to the radius of a sphere.

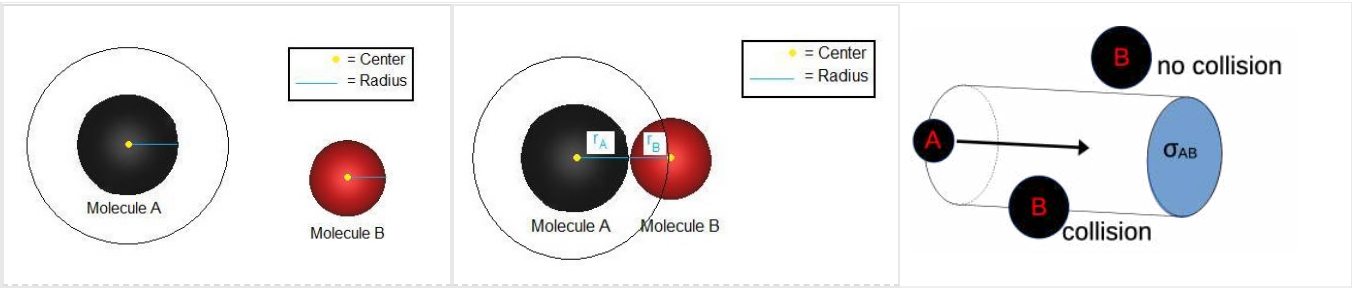


Figure **5.2.1**: (A) no collision; (B) collision; (C) volume swept out by collision cross-section imagining only one particle moving.

This collision cross-section, σ_{AB} is often written in terms of an effective diameter d_{AB} characteristic of both particles. The collision probability increases if both particles have large diameters and decreases if one of them has a smaller diameter than the other. Recognizing the relationship between radius and diameter we can write:

$$d_{AB} = \frac{1}{2}(d_A + d_B) = r_A + r_B$$

and the resulting collision cross section becomes

$$\begin{aligned} \sigma_{AB} &= \pi d_{AB}^2 \\ &= \pi\left(\frac{d_A + d_B}{2}\right)^2 \\ &= \frac{\pi}{4}\left(d_A^2 + 2d_A d_B + d_B^2\right). \end{aligned} \tag{5.2.1}$$

We can rewrite this interms of the cross-sections of each molecule $\sigma = (1/4)\pi d^2$:

$$\begin{aligned} &\frac{1}{4}\left(\sigma_A + 2\sqrt{\sigma_A\sigma_B} + \sigma_B\right) \\ &= \frac{1}{2}\left[\left(\frac{\sigma_A + \sigma_B}{2}\right) + \sqrt{\sigma_A\sigma_B}\right], \end{aligned}$$

which, interestingly, is an average of the two types of averages of the two individual cross sections, the arithmetic and geometric averages!

5.2.3: Average collision Frequency

Consider a system of particles with individual cross sections σ. A particle of cross section σ that moves a distance l in a time Δt will sweep out a cylindrical volume (ignoring the spherical caps) of volume σl (Figure 5.2.2). If the system has a number density ρ, then the number of collisions that will occur is

$$N_{\text{coll}} = \rho \sigma l$$

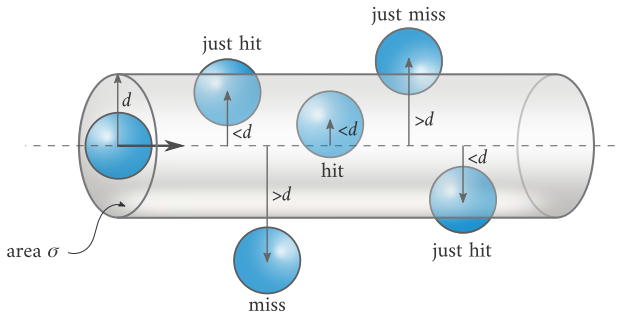


Figure 5.2.2 : Collision cylinder. Any particle that partially overlaps with this volume will experience a collision with a test particle tracing out this volume. (CC BY-NC; Ümit Kaya)

We define the collision frequency for a single molecule, z_A, also known as the average collision rate as $N_{\text{coll}}/\Delta t$, i.e.,

$$z_A = \frac{N_{\text{coll}}}{\Delta t} = \frac{\rho \sigma l}{\Delta t} = \rho \sigma \langle v \rangle \tag{5.2.2}$$

where $\langle v \rangle$ is the average speed of a particle

$$\langle v \rangle = \sqrt{\frac{8 k_B T}{\pi m_A}}$$

Equation 5.2.2 is not quite correct because it is based on the assumption that only the molecule of interest is moving. If we take into account the fact that all of the particles are moving relative to one another, then performing the average over a Maxwell-Boltzmann speed distribution gives

$$\langle v_r \rangle = \langle v_{AB} \rangle = \sqrt{\frac{8 k_B T}{\pi \mu}}.$$

If A and B are the same $\mu = m_A/2$ is the reduced mass. Thus,

$$\langle v_r \rangle = \langle v_{AA} \rangle = \sqrt{2} \langle v \rangle$$

and

$$z_{AA} = \sqrt{2} \rho \sigma \langle v \rangle \ = \rho \sigma \langle v_r \rangle \tag{5.2.3}$$

The reciprocal of z_{AA} is a measure of the average time between collisions for a single molecule.

If the particles are different then:

$$z_{AB} = \rho_{AB} \sigma_{AB} \langle v_r \rangle. \tag{5.2.4}$$

This collision frequency is also sometimes symbolized by γ.

5.2.4: Mean Free Path

The mean free path is the distance a particle will travel, on average, before experiencing a collision event. This is defined as the product of the average speed of a particle and the time between collisions. The former is $\langle v \rangle$, while the latter is $1/z_A$. Hence, we

have

$$\lambda = \frac{\langle v \rangle}{\sqrt{2}\rho\sigma\langle v \rangle} = \frac{1}{\sqrt{2}\rho\sigma}$$

The mean free path can also be described using terms from the ideal gas law, because $\rho = \frac{P \cdot N_A}{R \cdot T}$:

$$\lambda = \frac{R \cdot T}{\sqrt{2} \cdot N_A \cdot \sigma \cdot P}$$

5.2.5: Total collision frequency per unit volume

In equation 5.2.2, z_A represents the collision frequency for one specific molecule in a gas sample. If we wish to calculate the total collision frequency per unit volume, the number density of the molecules, ρ, must be taken into account. The total collision frequency in a sample that contains only A molecules, Z_{AA}, is

$$Z_{AA} = \frac{1}{2}\rho z_A = \frac{1}{2}\sigma\langle v_r \rangle \rho^2 = \frac{\sigma\langle v \rangle \rho^2}{\sqrt{2}}$$

The factor of $\frac{1}{2}$ must be included to avoid double counting collisions between similar molecules. (This is identical reasoning to the fact that there is only one way to roll double 3 with two dice.)

If you have a gas sample that contains A molecules and B molecules, then

$$Z_{AB} = \sigma_{AB}\langle v_r \rangle \rho_A \rho_B \tag{5.2.5}$$

where

$$\sigma_{AB} = \pi\left(\frac{d_A + d_B}{2}\right)^2 \text{ and } \langle v_r \rangle = \sqrt{\frac{8k_BT}{\pi\mu}}$$

Example 5.2.1

Calculate the frequency of hydrogen-hydrogen collisions in a 1.00 cubic centimeter container at 1.00 bar and 298 K.

Solution

The collisional frquency requires knowledge of (1) the number denisty, the average speed (Equation 5.2.5).

The value of σ_{H_2} is 2.30 x 10^{-19} m^2.

The number density:

$$\rho = \left(\frac{N_A P_{H_2}}{RT}\right) = \left(\frac{(6.022x10^{23} mole^{-1})(1.00 \text{ bar})}{(0.08314 L \cdot bar \cdot mol^{-1} \cdot K^{-1})(298 K)}\right)$$
$$= 2.43 \times 10^{22} L^{-1} = 2.43 \times 10^{25} m^{-3}$$

The average speed:

$$\langle \text{v} \rangle = \sqrt{\frac{8\text{R T}}{\pi\text{M}}} = \sqrt{\left(\frac{8(8.314 J \cdot K^{-1})(298 K)}{\pi(0.002016 kg)}\right)} = 1770\frac{m}{s}$$

These are substituted into Equation 5.2.5 to get the collisional frequency

$$Z_{H_2,H_2} = \frac{(2.30x10^{-19} m^2)(1770\frac{m}{s})(2.43x10^{25} m^{-3})^2}{\sqrt{2}}$$
$$= 1.7x10^{35} s^{-1} m^{-3}$$
$$= 1.7 \times 10^{29} s^{-1} cm^{-3}$$

5.2.6: Collision energy

Consider two particles A and B in a system. The kinetic energy of these two particles is

$$K_{AB} = \frac{\mathbf{p}_A^2}{2m_A} + \frac{\mathbf{p}_B^2}{2m_B} \tag{5.2.6}$$

We can describe kinetic energy in terms of center-of-mass ($\mathbf{P}$) and relative momentum ($\mathbf{p}$), which are given by

$$\mathbf{P} = \mathbf{p}_A + \mathbf{p}_B$$

and

$$\begin{aligned} \mathbf{p} &= \text{relative velocity} \times \mu \\ &= (\mathbf{v}_A - \mathbf{v}_B) \times \left(\frac{m_A m_B}{m_A + m_B}\right) \\ &= \frac{m_B \mathbf{p}_A - m_A \mathbf{p}_B}{M} \end{aligned}$$

where

$$M = m_A + m_B$$

is the total mass of the two particles, and

$$\mu = \frac{m_A m_B}{M}$$

is the **reduced mass** of the two particles.

Substituting these terms into equation 5.2.6, we find

$$K_{AB} = \frac{\mathbf{p}_A^2}{2m_A} + \frac{\mathbf{p}_B^2}{2m_B} = \frac{\mathbf{P}^2}{2M} + \frac{\mathbf{p}^2}{2\mu}$$

Note that the kinetic energy separates into a sum of a center-of-mass term and a relative momentum term.

Now the relative position of the two particles is $\mathbf{r} = \mathbf{r}_A - \mathbf{r}_B$ so that the relative velocity is $\dot{\mathbf{r}} = \dot{\mathbf{r}}_A - \dot{\mathbf{r}}_B$ or $\mathbf{v} = \mathbf{v}_A - \mathbf{v}_B$. Thus, if the two particles are approaching each other such that $\mathbf{v}_A = -\mathbf{v}_B$, then $\mathbf{v} = 2\mathbf{v}_A$. However, by equipartitioning the relative kinetic energy, which is mass independent, we get

$$\left\langle \frac{\mathbf{p}^2}{2\mu} \right\rangle = \frac{3}{2} k_B T$$

which is called the *collision energy*

5.2.7: Random Walks

In any system, a particle undergoing frequent collisions will have the direction of its motion changed with each collision and will trace out a path that appears to be random. In fact, if we treat the process as statistical, then, we are, in fact, treating each collision event as a random event, and the particle will change its direction at random times in random ways! Such a path might appear as shown in Figure 5.2.3. Such a path is often referred to as a *random walk path*.

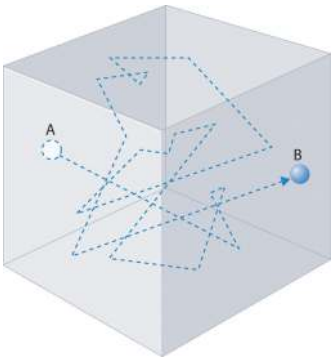


Figure 5.2.3: Random walk path. The Path of a Single Particle in a Gas Sample. The frequent changes in direction are the result of collisions with other gas molecules and with the walls of the container.

In order to analyze such paths, let us consider a random walk in one dimension. We'll assume that the particle move a mean-free path length λ between collisions and that each collision changes the direction of the particles motion, which in one dimension, means that the particle moves either to the right or to the left after each event. This can be mapped onto a metaphoric "coin toss" that can come up heads "H" or tails "T", with "H" causing motion to the right, and "T" causing motion to the left. Let there be N such coin tosses, let i be the number of times "H" comes up and j denote the number of times "T" comes up. Thus, the progress of the particle, which we define as net motion to the right, is given by $(i-j)\lambda$. Letting $k = i-j$, this is just $k\lambda$. Thus, we need to know what the probability is for obtaining a particular value of k in a very large number N of coin tosses. Denote this $P(k)$.

In N coin tosses, the total number of possible sequences of "H" and "T" is 2^N. However, the number of ways we can obtain i heads and j tails, with $i+j=N$ is a binomial coefficient $N!/i!j!$. Now

$$j = N - i = N - (j+k) = N - j - k$$

so that $j = (N-k)/2$. Similarly,

$$i = N - j = N - (i-k) = N - i + k$$

so that $i = (N+k)/2$. Thus, the probability $P(k)$ is

$$P(k) = \frac{N!}{2^N i!j!} = \frac{1}{2^N} \frac{N!}{\left(\frac{N+k}{2}\right)!\left(\frac{N-k}{2}\right)!}$$

We now take the logarithm of both sides:

$$\ln P(k) = \ln N! - \ln 2^N - \ln\left(\frac{N+k}{2}\right)! - \ln\left(\frac{N-k}{2}\right)!$$

and use Stirling's approximation:

$$\ln N! \approx N \ln N - N$$

and write $\ln P(k)$ as

$$\begin{aligned}
\ln P(k) &\approx N\ln N - N - N\ln 2 - \frac{1}{2}(N+k)\ln\frac{1}{2}(N+k) + \frac{1}{2}(N+k) \\
&\quad - \frac{1}{2}(N-k)\ln\frac{1}{2}(N-k) + \frac{1}{2}(N-k) \\
&= N\ln N - N\ln 2 + \frac{1}{2}(N+k)\ln\frac{1}{2} - \frac{1}{2}(N+k)\ln(N+k) \\
&\quad - \frac{1}{2}(N-k)\ln\frac{1}{2} - \frac{1}{2}(N-k)\ln(N-k) \\
&= N\ln N - N\ln 2 + \frac{1}{2}(N+k)\ln 2 - \frac{1}{2}(N+k)\ln(N+k) + \frac{1}{2}(N-k)\ln 2 \\
&\quad - \frac{1}{2}(N-k)\ln(N-k) \\
&= N\ln N - \frac{1}{2}\left[(N+k)\ln(N+k) + (N-k)\ln(N-k)\right]
\end{aligned}$$

Now, write

$$\ln(N+k) = \ln N\left(1+\frac{k}{N}\right) = \ln N + \ln\left(1+\frac{k}{N}\right)$$

and

$$\ln(N-k) = \ln N\left(1-\frac{k}{N}\right) = \ln N + \ln\left(1-\frac{k}{N}\right)$$

We now use the expansions

$$\ln\left(1+\frac{k}{N}\right) = \left(\frac{k}{N}\right) - \frac{1}{2}\left(\frac{k}{N}\right)^2 + \cdots$$
$$\ln\left(1-\frac{k}{N}\right) = -\left(\frac{k}{N}\right) - \frac{1}{2}\left(\frac{k}{N}\right)^2 + \cdots$$

If we stop at the second-order term, then

$$\begin{aligned}\ln P(k) &= N\ln N - \frac{1}{2}(N+k)\left[\ln N + \left(\frac{k}{N}\right) - \frac{1}{2}\left(\frac{k}{N}\right)^2\right] \\ &\quad - \frac{1}{2}(N-k)\left[\ln N - \left(\frac{k}{N}\right) - \frac{1}{2}\left(\frac{k}{N}\right)^2\right] \\ &= -\frac{1}{2}(N+k)\left[\left(\frac{k}{N}\right) - \frac{1}{2}\left(\frac{k}{N}\right)^2\right] + \frac{1}{2}(N-k)\left[\left(\frac{k}{N}\right) + \frac{1}{2}\left(\frac{k}{N}\right)^2\right] \\ &= \frac{1}{2}N\left(\frac{k}{N}\right)^2 - k\left(\frac{k}{N}\right) \\ &= \frac{k^2}{2N} - \frac{k^2}{N} = -\frac{k^2}{2N}\end{aligned}$$

so that

$$P(k) = e^{-k^2/2N}$$

Now, if we let $x = k\lambda$ and $L = \sqrt{N}\lambda$, and if we let x be a continuous random variable, then the corresponding probability distribution $P(x)$ becomes

$$P(x) = \frac{1}{L\sqrt{2\pi}}\, e^{-x^2/2L^2} = \frac{1}{\sqrt{2\pi N\lambda^2}}\, e^{-x^2/2N\lambda^2} \tag{5.2.7}$$

which is a simple Gaussian distribution. Now, N is the number of collisions, which is given by $z_A t$, so we can write the probability distribution for the particle to diffuse a distance x in time t as

$$P(x,t) = \frac{1}{\sqrt{2\pi z_A t\lambda^2}}\, e^{-x^2/2z_A t\lambda^2}$$

Define $D = z_A\lambda^2/2$ as the *diffusion constant*, which has units of (length)^2/time. The distribution then becomes

$$P(x,t) = \frac{1}{\sqrt{4\pi Dt}}\, e^{-x^2/4Dt}$$

Note that this distribution satisfies the following equation:

$$\frac{\partial}{\partial t}P(x,t) = D\frac{\partial^2}{\partial x^2}P(x,t)$$

which is called the diffusion equation. The diffusion equation is, in fact, more general than the Gaussian distribution in Equation 5.2.7. It is capable of predicting the distribution in any one-dimensional geometry subject to any initial distribution $P(x,0)$ and any imposed boundary conditions.

In three dimensions, we consider the three spatial directions to be independent, hence, the probability distribution for a particle to diffuse to a location $\mathbf{r} = (x,y,z)$ is just a product of the three one-dimensional distributions:

$$\mathcal{P}(\mathbf{r}) = P(x)\,P(y)\,P(z) = \frac{1}{(4\pi Dt)^{3/2}}\, e^{-(x^2+y^2+z^2)/4Dt}$$

and if we are only interested in diffusion over a distance r, we can introduce spherical coordinates, integrate over the angles, and we find that

$$P(r,t) = \frac{4\pi}{(4\pi Dt)^{3/2}}\, e^{-r^2/4Dt}$$

This page titled 5.2: Collisions is shared under a CC BY-NC-SA 4.0 license and was authored, remixed, and/or curated by Tom Neils, Mark Tuckerman, Jonathan Gutow, & Jonathan Gutow.

- **27.6: Mean Free Path** by Mark Tuckerman, Tom Neils is licensed CC BY-NC-SA 4.0.

5.3: The Frequency of Collisions with a Wall

5.3.1: Collision frequency per unit area

In the derivation of an expression for the pressure of a gas, it is useful to consider the frequency with which gas molecules collide with the walls of the container. To derive this expression, consider the expression for the "collision volume".

$$V_{col} = v_x \Delta t \ \cdot A$$

in which the product of the velocity v_x and a time interval Δt is multiplied by A, the area of the wall with which the molecules collide.

All of the molecules within this volume, and with a velocity such that the x-component exceeds v_x (and is positive) will collide with the wall. That fraction of molecules is given by

$$N_{col} = \frac{N}{V} \frac{\langle v_x \rangle \Delta t \cdot A}{2},$$

where the factor of (1/2) accounts for the fact that half the molecules are moving away from the wall. Dividing by Δt yields the frequency of collisions with the wall per unit area per unit time:

$$z_w = \frac{N}{V} \frac{\langle v_x \rangle}{2}.$$

This can be rewritten in terms of the average speed in 3 dimensions, $\langle v \rangle$, by making use of results from the Maxwell-Boltzmann speed distributions in one dimension and 3 dimensions. Namely:

$$\langle |v_x| \rangle = \left(\frac{2k_B T}{\pi m} \right)^{1/2} \tag{5.3.1}$$

and

$$\langle v \rangle = \sqrt{\frac{8k_B T}{\pi m}}. \tag{5.3.2}$$

Taking the ratio of these two expression shows that

$$\langle v \rangle = 2 \langle v_x \rangle$$

or

$$\langle v_x \rangle = \frac{1}{2} \langle v \rangle.$$

Thus,

$$z_w = \frac{1}{4} \frac{N}{V} \langle v \rangle = \frac{\langle v \rangle}{4} \rho = \rho \sqrt{\frac{k_B T}{2\pi m}}, \tag{5.3.3}$$

where ρ is the number density (N/V).

5.3.2: Alternative derivation

A different approach to determining z_w is to consider a collision cylinder that will enclose all of the molecules that will strike an area of the wall at an angle θ and with a speed v in the time interval dt. The volume of this collision cylinder is the product of its base area (A) times its vertical height ($v \cos\theta dt$), as shown in figure 5.3.1.

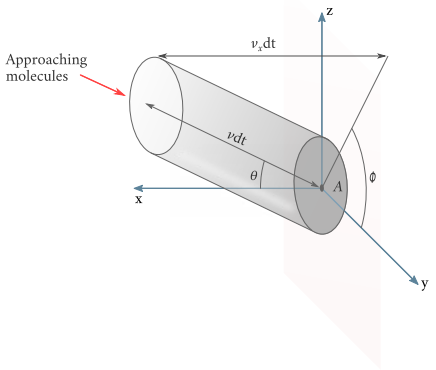


Figure 5.3.1: The collision cylinder for determining the number of collisions of gas molecules with a wall. (CC BY-NC; Ümit Kaya)

The number of molecules in this cylinder is $\rho \cdot A \cdot v \cdot \cos\theta dt$, where ρ is the number density $\frac{N}{V}$. The fraction of molecules that are traveling at a speed between v and $v + dv$ is $F(v)dv$. The fraction of molecules traveling within the solid angle bounded by θ and $\theta + d\theta$ and between ϕ and $\phi + d\phi$ is $\frac{\sin\theta d\theta d\phi}{4\pi}$. Multiplying these three terms together results in the number of molecules colliding with the area A from the specified direction during the time interval dt

$$dN_w = \rho \cdot A \cdot v \cdot \cos\theta\, dt \cdot F(v)dv \cdot \frac{\sin\theta d\theta d\phi}{4\pi}$$

This equation can be rearranged to obtain

$$\frac{1}{A}\frac{dN_w}{dt} = \frac{\rho}{4\pi} vF(v)dv \cdot \cos\theta \sin\theta\, d\theta d\phi = dz_w$$

Integrating this equation over all possible speeds and directions (on the front side of the wall only), we get

$$z_w = \frac{\rho}{4\pi}\int_0^\infty vF(v)dv \cdot \int_0^{\pi/2} \cos\theta \sin\theta\, d\theta \int_0^{2\pi} d\phi$$

The result is that

$$z_w = \frac{1}{A}\frac{dN_w}{dt} = \frac{1}{4}\frac{N}{V}\langle v\rangle = \rho\frac{\langle v\rangle}{4} \tag{5.3.4}$$

Example 27.4.1

Calculate the collision frequency per unit area (Z_w) for oxygen at 25.0°C and 1.00 bar using equation 5.3.4:

$$z_w = \frac{1}{4}\frac{N}{V}\langle v\rangle$$

Solution

N molecules = N_A x n, so that

$$\frac{N}{V} = \frac{(N_A)\cdot n}{V} = \frac{(N_A)\cdot P}{R\cdot T}$$

$$\frac{(6.022x10^{23}\, mole^{-1})(1.00\, bar)}{(0.08319\, L\cdot bar\cdot mole^{-1}\cdot K^{-1})(298\, K)} = 2.43\times 10^{22}\, L^{-1} = 2.43\times 10^{25}\, m^{-3}$$

and

$$\langle v\rangle = \left(\frac{8RT}{\pi M}\right)^{\frac{1}{2}} = \left(\frac{8(8.314 J\cdot K^{-1}\cdot mol^{-1})(298K)}{\pi\cdot(0.031999\, kg)}\right)^{\frac{1}{2}} = 444\, m\cdot s^{-1}$$

Thus

$$z_w = \frac{1}{4}(2.43 \times 10^{25} m^{-3})(444\, m \cdot s^{-1}) \left(\frac{1\, m}{100\, cm}\right)^2 = 2.70 \times 10^{23} s^{-1} \cdot cm^{-2}$$

The factor of N/V is often referred to as the "number density" as it gives the number of molecules per unit volume. At 1 atm pressure and 298 K, the number density for an ideal gas is approximately 2.43 x 10^{19} molecule/cm^3. (This value is easily calculated using the ideal gas law.) By comparison, the average number density for the universe is approximately 1 molecule/cm^3.

Exercise 27.4.1

Calculate the collision frequency per unit area (Z_w) for hydrogen at 25.0°C and 1.00 bar using equation 5.3.4:

$$z_w = \frac{1}{4}\frac{N}{V}\langle v \rangle$$

Answer

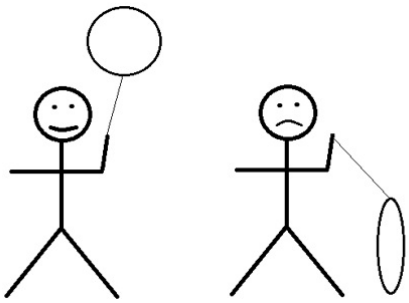
$$\langle v \rangle = 1770\, m \cdot s^{-1}$$

and

$$Z_w = 1.08 \times 10^{24} s^{-1} \cdot cm^{-2}$$

5.3.3: Effusion

Effusion is defined as a loss of material across a boundary. A common example of effusion is the loss of gas inside of a balloon over time.



The rate at which gases will effuse from a balloon is affected by a number of factors. But one of the most important is the frequency with which molecules collide with the interior surface of the balloon. As shown in equation 5.3.3 this is inversely proportional to the mass (m) or molar mass (M) depending on whether you are working on a per-particle or molar basis.

This can be used to compare the relative rates of effusion for gases of different molar masses or measure vapor low vapor pressures.

The Knudsen Cell Experiment

A Knudsen cell is a chamber in which a thermalized sample of gas is kept, but allowed to effuse through a small orifice in the wall. The gas sample can be modeled using the Kinetic Molecular Theory model as a collection of particles traveling throughout the cell, colliding with one another and also with the wall. If a small orifice is present, any molecules that would collide with that portion of the wall will be lost through the orifice.

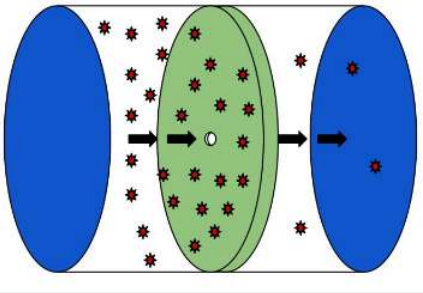
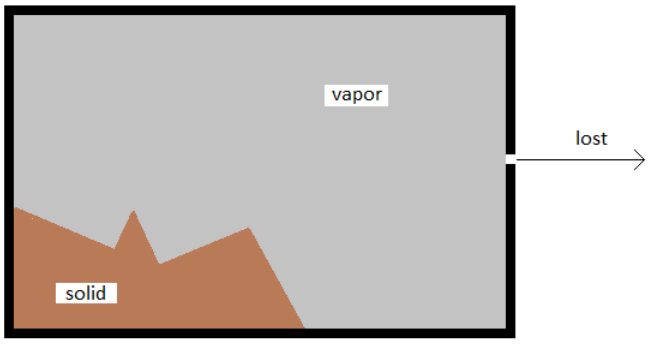


Figure **5.3.2**: Effusion of gas particles through an orifice. (CC BY-SA 3.0; Astrang13).

This makes a convenient arrangement to measure the vapor pressure of the material inside the cell, as the total mass lost by effusion through the orifice will be proportional to the vapor pressure of the substance. The vapor pressure can be related to the mass lost by the expression

$$P = \frac{g}{A\Delta t}\sqrt{\frac{2\pi RT}{M}}$$

where g is the mass lost, A is the area of the orifice, Δt is the time the effusion is allowed to proceed, T is the temperature and M is the molar mass of the compound in the vapor phase. The pressure is then given by P. A schematic of what a Knudsen cell might look like is given below.



5.3.4: Contributors and Attributions

- Patrick E. Fleming (Department of Chemistry and Biochemistry; California State University, East Bay)
- Tom Neils, Grand Rapids Community College
- Jonathan Gutow (UW Oshkosh)

5.3: The Frequency of Collisions with a Wall is shared under a CC BY-NC-SA 4.0 license and was authored, remixed, and/or curated by LibreTexts.

- **27.4: The Frequency of Collisions with a Wall** is licensed CC BY-NC-SA 4.0.
- **2.5: Graham's Law of Effusion** by Patrick Fleming is licensed CC BY-NC-SA 4.0.

5.4: Transport of Matter and Energy in Perfect Gases

5.4.1: Introduction

In this section we will consider the transport of matter and energy in perfect gases to develop a microscopic particulate picture of the processes. Additionally, we will use this model to develop some quantitative predictions on how rates of transport depend on conditions.

By transport we mean the movement of the matter or energy from an initial location in a sample to somewhere else. Two common examples of this are diffusion, where a high concentration of material spreads out until it is evenly distributed, and thermal conduction, where heat energy moves from a hot region to increase the temperature of cooler regions. The rate of this migration through a surface separating one region from the next is quantified by the flux (usually symbolized by $\boldsymbol{J}$). In the simplest form appropriate for transport fluxes, J is a vector perpendicular to the planar surface through which the migration is occurring. The magnitude of the vector is the amount transported per unit time per unit area. In the case of particles using SI units the units would be $s^{-1}m^{-2}$ (particles/s/m^2). See figure **5.4.1**.

5.4.2: Diffusion (matter transport)

Consider the system sketched in figure **5.4.1**. Call the axis perpendicular to the grey plane (parallel to the long sides of the box) z with the positive direction in the direction of the arrow. At any given time particles will be traveling in the direction of the arrow and the opposite direction. In a homogeneous system the number of particles of a given type moving through the plane will be the same each direction. Symbolically this can be represented as a flux in the z direction of:

$$J_z = |J_{+z}| - |J_{-z}| = 0,$$

where the signs on the subscript indicate the direction of the flux. In this formulation we are looking at only at the magnitude in each direction.

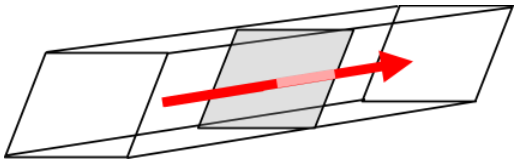


Figure **5.4.1**: Cartoon of flux through a plane surface of area A. The length of the vector represents the magnitude of the flux through the plane per unit time per unit area.

To make the mathematics more straightforward it is best to have a positive flux $\boldsymbol{J_z}$ indicate net flux in the +z direction (direction of arrow).

If the number density (concentration) varies with position (e.g. ρ decreases as we move towards +z) the two fluxes will not balance out. Because the particles are undergoing collisions that might change their trajectory so that even with an initial velocity that would allow them to cross the plane they might not. The maximum average rate they could cross the plane is going to be limited by how many molecules are close enough to the plane that they will not suffer a collision before they cross it. So we need to estimate the number density on each side within one mean free path ($\lambda = (\sqrt{2}\rho\sigma)^{-1}$) of the plane.

First remember that we know how to calculate the rate of collision per unit area with a plane within the kinetic molecular theory. This is just the rate of collision with a wall per unit area:

$$z_w = \frac{1}{4}\frac{N}{V}\langle v\rangle = \frac{\langle v\rangle}{4}\rho = \rho\sqrt{\frac{k_B T}{2\pi m}}, \tag{5.4.1}$$

where <v> is the average velocity, k_B is the Boltzmann constant and m is the particle mass. The upper limit to the flux from one side is z_w, when ρ is the number density at distance λ from the plane.

If the rate of change of the number density (ρ) at the plane is $\frac{d\rho}{dz}|_o$ then the number density at distance λ (one mean free path) to the left of the plane is:

$$\rho_l = \rho_o - \lambda \frac{d\rho}{dz}|_o \tag{5.4.2}$$

and to the right is:

$$\rho_l = \rho_o + \lambda \frac{d\rho}{dz}|_o. \tag{5.4.3}$$

Substituting these number densities into equation 5.4.1 we get the following two expressions:

$$J_{+z} = \frac{\langle v \rangle}{4}\left(\rho_o - \lambda \frac{d\rho}{dz}|_o\right) \tag{5.4.4}$$

and

$$J_{-z} = \frac{\langle v \rangle}{4}\left(\rho_o + \lambda \frac{d\rho}{dz}|_o\right). \tag{5.4.5}$$

As the fluxes are both positive, the total flux is:

$$\begin{aligned} J_z = J_{+z} - J_{-z} = \frac{\langle v \rangle}{4}\left(\rho_o - \lambda \frac{d\rho}{dz}|_o - \rho_o - \lambda \frac{d\rho}{dz}|_o\right) = \frac{\langle v \rangle}{4}\left(-2\lambda \frac{d\rho}{dz}|_o\right) \\ = -\frac{1}{2}\langle v \rangle \lambda \frac{d\rho}{dz}|_o. \end{aligned} \tag{5.4.6}$$

This is an overestimate because some of the particles will have most of their velocity parallel to the plane. This means that some particles will travel so far before crossing the plane that they will undergo a collision that prevents them from crossing the plane. A more careful and much more tedious analysis leads to a factor of 2/3 decrease in the estimate of J_z:

$$J_z = -\frac{1}{3}\langle v \rangle \lambda \frac{d\rho}{dz}|_o. \tag{5.4.7}$$

Fick's law of diffusion states that the observed flux of particles is proportional to the number density gradient and the proportionality constant (the diffusion constant) is symbolized by D:

$$J_z = -D\frac{\partial \rho}{\partial z}. \tag{5.4.8}$$

Thus for our simple gas case:

$$D = \frac{1}{3}\langle v \rangle \lambda = \frac{1}{3}\lambda\sqrt{\frac{8k_BT}{\pi m}} = \frac{1}{3\sqrt{2}\rho\sigma}\sqrt{\frac{8k_BT}{\pi m}}. \tag{5.4.9}$$

So the diffusion constant increases with increased temperature, but decreases as the particles become more massive or the mean free path decreases (higher density or larger particles). In high density systems intermolecular interactions become important and the trends are maintained, but do not exactly follow this simple model.

5.4.3: Thermal conductivity

The coefficient of thermal conductivity κ is the proportionality constant between the temperature gradient and thermal energy flux as defined by the equation:

$$J_z(thermal) = -\kappa \frac{dT}{dz}. \tag{5.4.10}$$

The energy is transported by moving particles, but in this case there is no gradient in the density of particles just the amount of energy the particles have. Thus this time the energy flux $J_z(thermal)$ is:

$$J_z(thermal) = -\frac{1}{3}\langle v \rangle \lambda \rho \frac{d\epsilon}{dz}, \tag{5.4.11}$$

where ϵ is the thermal energy content of a particle and $\rho\epsilon$ is the energy density per unit volume. We can express equation 5.4.11 in terms of $\frac{dT}{dz}$ by using the chain rule:

$$\frac{d\epsilon}{dz} = \frac{d\epsilon}{dT}\frac{dT}{dz}.$$

Substituting this in to equation 5.4.11 yields:

$$J_z(thermal) = -\frac{1}{3}\langle v\rangle \lambda \rho \frac{d\epsilon}{dT}\frac{dT}{dz}. \tag{5.4.12}$$

This can be converted to a more useful form by using the definition of molar heat capacity:

$$C_{V,m} = \left(\frac{dE_m}{dT}\right)_V = N_A\left(\frac{d\epsilon}{dT}\right)_V. \tag{5.4.13}$$

Thus, by substituting $C_{V,m}/N_A$ for $\frac{d\epsilon}{dT}$ in equation 5.4.12 and expanding ρ to (N/V) we get:

$$\begin{aligned} J_z(thermal) &= -\frac{1}{3}\langle v\rangle \lambda \frac{N}{V}\frac{C_{V,m}}{N_A}\frac{dT}{dz} \\ &= -\frac{1}{3}\langle v\rangle \lambda \frac{n}{V}C_{V,m}\frac{dT}{dz} = -\frac{1}{3}\langle v\rangle \lambda [X] C_{V,m}\frac{dT}{dz}, \end{aligned} \tag{5.4.14}$$

where in the last form of the equation [X] is the molar concentration of the gas. Comparing equation 5.4.14 to equation 5.4.10 we see that:

$$\kappa = \frac{1}{3}\langle v\rangle \lambda [X] C_{V,m}. \tag{5.4.15}$$

Expanding this equation out we get:

$$\kappa = \frac{1}{3\sqrt{2}\rho\sigma}\sqrt{\frac{8k_BT}{\pi m}}[X]C_{V,m} = \frac{1}{3\sqrt{2}\sigma}\sqrt{\frac{8k_BT}{\pi m}}\frac{C_{V,m}}{N_A} \tag{5.4.16}$$

using the fact that $\frac{n}{V}C_{V,m} = \rho\frac{C_{V,m}}{N_A}$.

The physical interpretation of equation 5.4.16 is that the thermal conductivity increases with increasing molar heat capacity and temperature, while decreasing as the mass of the particle or their sizes increase. Notice that for a fixed temperature the thermal conductivity does not depend on the gas density (or equivalently pressure in the ideal gas case). Since gases generally have low molar heat capacities they are better insulators than liquids or solids. This is why we make double-paned windows by separating two sheets of glass by dry air or sometimes pure N_2. The lowest heat capacity gases are the noble gases because they are monatomic, meaning they only have kinetic energy contributions to their heat capacity near ambient temperatures. Xe is the best choice for insulation because it is the most massive and the largest diameter of the non-radioactive noble gases. Unfortunately, Xe is relatively rare and thus too expensive to use as the insulating gas in windows and insulators such as expanded foams. Gases only work well as insulators if they are prevented from developing convection currents (wind), so that the energy is only transported diffusively. This is why most gas based insulators (fiberglass, expanded foams, etc) use solids to block convection of the gases.

Equation 5.4.16 shows no pressure dependence for thermal conductivity, yet we know that vacuum jackets (dewar's) are very good insulation. Why? The discrepancy is due to the fact that the preceding analysis ignores the fact that when the pressure is low enough that the mean free path is larger than the gap between the walls, the rate of energy transport becomes proportional to the number of particles available to transport energy across the gap. Thus once the pressure is low enough that the mean free path is greater than the distance between the walls a pressure decrease leads to a decrease in thermal conductivity. An alternative way of thinking about this is that matter is required to transport the thermal energy. When there is no matter no energy can be transported. Dewars work well when gas pressures are < 10^{-9} atm. Dewar performance can be further enhanced by making the interior walls reflective so that less energy is transmitted across the gap by thermal blackbody radiation photons.

5.4.4: Viscosity

Most people are familiar with viscosity from handling liquids of different viscosities. For example, the viscosity of honey is higher than water, meaning the honey resists flowing more than water (colloquially honey is "thicker" than water). Empirically, the relative viscosity of two fluids can be determined by measuring the relative amount of time it takes for the same amount of each fluid to flow non-turbulently through a tube. Viscosity is fundamentally the proportionality constant relating the transfer of momentum perpendicular to the direction of flow. Consider the diagram below of a non-turbulent (Newtonian) flow through a tube

in the x direction. If the bottom of the figure represents a wall of the tube the fluid in immediate contact with the wall is not flowing while each layer as we move towards the center of the tube flows at a faster rate as indicated by the length of the arrows.

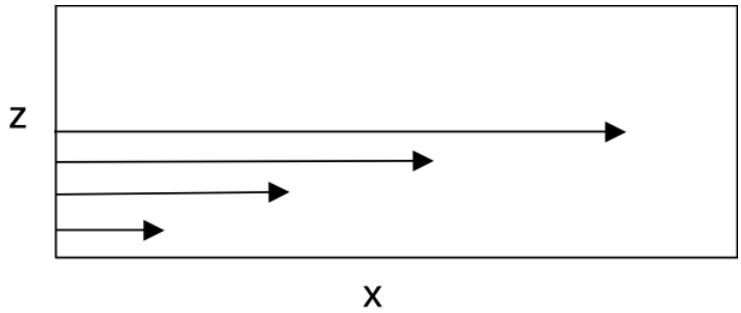


Figure 5.4.2: Cartoon of Newtonian flow of a fluid through a tube in the x direction. The length of the arrows indicate the relative velocities of layers within the tube. At the center of the tube the fluid has the highest velocity.

In each of the layers the particles have different velocities in the x direction ($v_x(z)$). Each $v_x(z)$ has a corresponding x-component of momentum $p_x(z) = mv_x(z)$. Because of thermal motion particles also move randomly in the z direction. Each time a particle moves in the z direction it carries the p_x it had in one layer to a neighboring layer. In this way the x momentum of a layer is reduced by transfer from slower layers and increased by transfer from faster layers. The viscosity η is the proportionality constant between the momentum flux and the change in velocity with z:

$$J_z(x\,momentum) = -\eta\frac{dv_x}{dz}. \tag{5.4.17}$$

As in the case of thermal transfer the momentum is transferred with the matter, but there is no gradient in the amount of matter just the x-component of the momentum (p_x). The amount of matter moving is still the same so:

$$J_z(x\,momentum) = -\frac{1}{3}\langle v\rangle\lambda\rho\frac{dp_x}{dz} = -\frac{1}{3}\langle v\rangle\lambda\rho m\frac{dv_x}{dz}, \tag{5.4.18}$$

where ρp_x is the momentum density per unit volume. Comparing equations 5.4.17 and 5.4.18 we see that:

$$\eta = \frac{1}{3}\langle v\rangle\lambda\rho m = \frac{1}{3}\sqrt{\frac{8k_BT}{\pi m}}\frac{m}{\sqrt{2}\rho\sigma}\rho = \frac{1}{3}\sqrt{\frac{8mk_BT}{\pi}}\frac{1}{\sqrt{2}\sigma}. \tag{5.4.19}$$

This equation implies the viscosity of an idealized gas is independent of the number density, inversely dependent on the size of the particles and proportional to $\sqrt{T}$ or $\sqrt{m}$. Thus, the prediction from this model is that the viscosity of gases increases with temperature! This is observed and is the opposite of what is seen in liquids, where the viscosity decreases with increasing temperature. For gases the viscosity increases with temperature because increasing temperature increases the rate at which particles exchange between layers carrying the momentum of flow between layers, which increases the tendency of the layers to maintain the same velocity. In condensed phases the viscosity is primarily due to intermolecular attractions restricting the flow of particles past each other. Increased temperature disrupts the attractions, thus lowering the viscosity.

5.4.5: References

The contents of this section are based on the following two references:

1. P.W. Atkins, J. de Paula, Physical Chemistry, 7th Ed. (W.H. Freeman and Co. New York, 2002) Pp. 826 - 832.
2. A. Cooksy, Physical Chemistry: Thermodynamics (Pearson Ed. Inc. Columbus, 2014) Pp. 184 - 190.

5.4.6: Contributors

- Jonathan Gutow (UW Oshkosh)

This page titled 5.4: Transport of Matter and Energy in Perfect Gases is shared under a CC BY-NC-SA 4.0 license and was authored, remixed, and/or curated by Jonathan Gutow.

5.5: Stokes-Einstein-Sutherland Equation

5.5.1: Introduction

A useful approximate description of the diffusion constant in a liquid is the Stokes-Einstein-Sutherland equation:

$$D = \frac{k_B T}{6\pi\eta R_{eff}}, \tag{5.5.1}$$

where k_B is the Boltzmann constant, T the temperature in Kelvin, η the viscosity of the solvent and R_{eff} the effective radius of the diffusing particle including any solvent being carried along with the particle. This equation is most often used to estimate D or using measured D and η to calculate R_{eff}. In water this effective radius is often referred to as the hydrodynamic radius.

5.5.2: Derivation

The diffusion constant D is the proportionality constant between the flux (J) and the slope of the concentration (c):

$$J_z = -D\frac{dc}{dz}. \tag{5.5.2}$$

Alternatively, the flux can be thought of as the product of the concentration (c) and a drift speed (s) in the direction of the flux:

$$J_z = sc. \tag{5.5.3}$$

Thus,

$$sc = -D\frac{dc}{dz}. \tag{5.5.4}$$

The drift speed is fixed by the force pushing the particles (the effective potential created by the concentration gradient) and the frictional force resisting movement of the particles through the solvent.

The force created by a potential μ along direction z is:

$$F_{pot} = -\frac{d\mu}{dz}. \tag{5.5.5}$$

In the case of a concentration gradient the appropriate potential is the chemical potential. Assuming an ideal solution the potential is:

$$\mu = \mu_o + RTlnc. \tag{5.5.6}$$

So,

$$F_{pot} = -\frac{d\mu}{dz} = -\frac{d}{dz}\left(\mu_o + RTlnc\right) = \frac{-RT}{c}\frac{dc}{dz}. \tag{5.5.7}$$

This expression is on a per mole basis, but we want to do our calculation on a per particle basis. Dividing the above equation by N_A to acheive this:

$$F_{pot} = \frac{-k_B T}{c}\frac{dc}{dz}. \tag{5.5.8}$$

If we assume sperical particles and that the Stoke's macroscopic rule for the friction experienced by a spherical particle holds for molecule sized particles we have the balancing force as:

$$f = 6\pi\eta R_{eff} s. \tag{5.5.9}$$

Setting the forces in equations 5.5.8 and 5.5.9 equal and solving for $sc = J_z$:

$$\frac{-k_B T}{c}\frac{dc}{dz} = 6\pi\eta R_{eff} s \implies sc = \frac{-k_B T}{6\pi\eta R_{eff}}\frac{dc}{dz}. \tag{5.5.10}$$

Comparing the final expression with equation 5.5.4 we see that:

$$D = \frac{k_B T}{6\pi\eta R_{eff}}. \tag{5.5.11}$$

This page titled 5.5: Stokes-Einstein-Sutherland Equation is shared under a CC BY-NC-SA 4.0 license and was authored, remixed, and/or curated by Jonathan Gutow.

5.6: The Rate of Bimolecular Gas-Phase Reaction Can Be Estimated Using Hard-Sphere Collision Theory and an Energy-Dependent Reaction Cross Section

5.6.1: Collision Frequency using the Hard Sphere Model

For the bimolecular gas-phase reaction

$$\mathrm{Q(g)\ +\ B(g)\ \rightarrow products}$$

the reaction rate is

$$\mathrm{rate} = -\frac{d[Q]}{dt} = k[Q][B]$$

If it is assumed that every collision between Q and B particles results in products, the rate at which molecules collide is equal to the frequency of collisions per unit volume, Z_{QB} (Equation 27.6.4)

$$\mathrm{rate} = Z_{QB} = \sigma_{QB}\langle v_r\rangle \rho_Q \rho_B \tag{5.6.1}$$

Also known as the collision frequency, Z_{QB}, has units of molecules per volume per time, molecules·m^{-3}·s^{-1}. It is possible to obtain a rough estimate of the value of the rate constant, k, from the collision frequency.

Equation 5.6.1 shows the rate on a molecular scale. Generally, Z_{QB} is divided by Avogadro's number, N_0, to obtain the collision frequency on a molar scale

$$\mathrm{rate} = -\frac{d[Q]}{dt} = \frac{Z_{QB}}{N_0} = \frac{\sigma_{QB}\langle v_r\rangle}{N_0}\rho_Q \rho_B$$

To convert the number densities to molar concentrations, we need to realize that

$$\frac{\rho_Q}{N_0} = [Q]$$

then

$$-\frac{d[Q]}{dt} = \frac{Z_{QB}}{N_0} = \frac{\sigma_{QB}\langle v_r\rangle}{N_0}(N_0[Q])(N_0[B])$$

$$-\frac{d[Q]}{dt} = \frac{Z_{QB}}{N_0} = N_0\sigma_{QB}\langle v_r\rangle[Q][B]$$

$$-\frac{d[Q]}{dt} = \frac{Z_{QB}}{N_0} = N_0\sigma_{QB}\sqrt{\frac{8k_BT}{\pi\mu_{QB}}}[Q][B]$$

Thus

$$Z_{QB} = N_0^2\sigma_{QB}\sqrt{\frac{8k_BT}{\pi\mu_{QB}}}[Q][B]$$

and

$$k = N_0\sigma_{QB}\sqrt{\frac{8k_BT}{\pi\mu_{QB}}}$$

where:

- $\langle v_r\rangle$ is the mean relative speed of molecules, which is equal to $\sqrt{\frac{8k_BT}{\pi\mu_{QB}}}$
- ρ_Q and ρ_B are the number densities of Q molecules and B molecules
- N_Q and NB are the numbers of Q molecules and B molecules

- σ_{QB} is the averaged sum of the collision cross sections of molecules Q and B, $\sigma_{QB} = \pi \left(\frac{d_Q + d_B}{2} \right)^2$. The collision cross section represents the collision region presented by one molecule to another. σ_{QB} is often written as πd_{QB}^2.

The units of σ are m^2, the units of N_0 are mole^{-1}, and the units of $\langle v_r \rangle$ are $\frac{m}{s}$. Thus, the units of k are $\frac{m^3}{\text{mole} \cdot s}$

As noted earlier, using this hard-sphere collision theory value for the rate constant is a rough estimate, mainly because the temperature dependence of k is improperly represented in the hard-sphere collision theory prediction. The next sections will describe an initial attempt to correct that error.

5.6.2: Successful Collisions

For a successful collision to occur, the reactant molecules must collide with enough kinetic energy to overcome the repulsions of the electron clouds and to break the existing bonds. To take the energy dependence of a successful collision into account, we will introduce a new reaction cross-section, $\sigma_r(v_r)$, which takes into account the speed of the reactants. Thus

$$k(v_r) = v_r \sigma_r(v_r)$$

The rate constant can be calculated by averaging over a distribution of all speeds, $f(v_r)$

$$k = \int_0^\infty k(v_r) f(v_r) dv_r = \int_0^\infty v_r f(v_r) dv_r \sigma_r(v_r) \tag{5.6.2}$$

$v_r f(v_r) dv_r$ (from the Maxwell-Boltzmann speed distribution) is

$$v_r f(v_r) dv_r = \left(\frac{\mu}{k_B T} \right)^{3/2} \left(\frac{2}{\pi} \right)^{1/2} v_r^3 e^{-\mu v_r^2 / 2 k_B T} dv_r \tag{5.6.3}$$

Equation 5.6.3 presents the rate constant as a function of speed. If we want to compare this version of k with the common, Arrhenius form of k, the dependent variable must be changed from relative speed to relative kinetic energy, E_r. The relationship is

$$E_r = \frac{1}{2} \mu v_r^2 \text{ which rearranges to } v_r = \left(\frac{2E_r}{\mu} \right)^{1/2}$$

Thus,

$$dv_r = \left(\frac{1}{2 \mu E_r} \right)^{1/2} dE_r$$

Substituting v_r and dv_r into equation 5.6.3 gives

$$v_r f(v_r) dv_r = \left(\frac{\mu}{k_B T} \right)^{3/2} \left(\frac{2}{\pi} \right)^{1/2} \left(\frac{2E_r}{\mu} \right)^{3/2} e^{-E_r / k_B T} \left(\frac{1}{2 \mu E_r} \right)^{1/2} dE_r$$

Substituting this equation into equation 5.6.2 and simplifying gives

$$k = \left(\frac{2}{k_B T} \right)^{3/2} \left(\frac{1}{\mu \pi} \right)^{1/2} \int_0^\infty dE_r E_r e^{-E_r / k_B T} \sigma_r(E_r) \tag{5.6.4}$$

We can then assume that the energy dependent reaction cross section $\sigma_r(E_r)$ will include only those molecules which undergo effective collisions with a kinetic energy that is greater than or equal to a minimum sufficient energy, E_0. Thus $\sigma_r(E_r)$ is equal to 0 if $E_r < E_0$ and is equal to σ_{QB} if $E_r \geq E_0$.

Thus we integrate from E_0 to ∞ using the known integral $\int x e^{ax} dx = a^{-2} e^{ax} (ax - 1)$,

$$\begin{aligned} k &= \left(\frac{2}{k_B T} \right)^{3/2} \left(\frac{1}{\mu \pi} \right)^{1/2} \int_{E_0}^\infty dE_r E_r e^{-E_r / k_B T} \sigma_{QB} \\ &= \left(\frac{8 k_B T}{\mu \pi} \right)^{1/2} \sigma_{QB} e^{-E_0 / k_B T} \left(1 + \frac{E_0}{k_B T} \right) \\ &= \langle v_r \rangle \sigma_{QB} \left(1 + \frac{E_0}{k_B T} \right) e^{-E_0 / k_B T}. \end{aligned} \tag{5.6.5}$$

The factors in front of the exponential correspond to the A factor in the Arrhenius equation for the temperature dependence of the rate constant, $k = Aexp\left(\frac{-E_0}{k_BT}\right)$. Notice that this implies that A actually has a temperature dependence with contributions from both the average relative velocities and the relative size of E_0 (E_a) with respect to k_BT. Gas phase kinetics experiments on bimolecular reactions do show variation in the A factor with temperature, although not necessarily the roughly $1/\sqrt{T}$ dependence this simple model implies.

5.6.3: References

Atkins, Peter and Julio de Paula. Physical Chemistry for the Life Sciences. 2006. New York, NY: W.H. Freeman and Company.

5.6.4: Contributor

- Tom Neils, Grand Rapids Community College
- Jonathan Gutow (UW-Oshkosh)

5.6: The Rate of Bimolecular Gas-Phase Reaction Can Be Estimated Using Hard-Sphere Collision Theory and an Energy-Dependent Reaction Cross Section is shared under a CC BY-NC-SA 4.0 license and was authored, remixed, and/or curated by LibreTexts.

- **30.1: The Rate of Bimolecular Gas-Phase Reaction Can Be Estimated Using Hard-Sphere Collision Theory and an Energy-Dependent Reaction Cross Section** is licensed CC BY-NC-SA 4.0.

5.7: A Reaction Cross Section Depends Upon the Impact Parameter

In the previous section, it was assumed that all collisions with sufficient energy would lead to a reaction between the Q and B particles. This is an unrealistic assumption because not all collisions occur with a proper alignment of the particles as shown in Figure **5.7.1**.

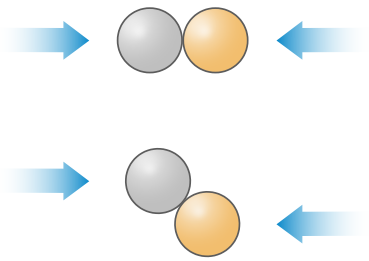


Figure **5.7.1** In the top collision, the particles collide head-on, and thus all of the kinetic energy can be used to overcome electron-electron repulsion and to break bonds. In the bottom collision, the particles collide with a glancing blow so that only part of the kinetic energy is contributed to the reaction process. With collisions involving larger, more complex molecules, there is often a specific molecular orientation required for an effective collision. (CC BY-NC; Ümit Kaya via LibreTexts)

Thus, the energy-dependent reaction cross-section,$\sigma_r(E_r)$, introduced previously is inaccurate and must be modified to take into account the inefficient collisions. One modification is to employ the *line-of-centers* (loc) model for $\sigma_r(E_r)$. This model incorporates the angle of collision relative to the line drawn between the centers of the two colliding particles, as shown in Figure **5.7.2**.

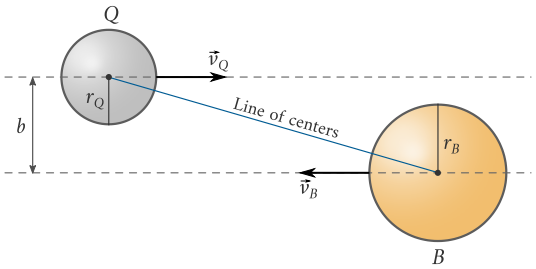


Figure **5.7.2**: This figure shows the geometry of the collision between two particles. The particle velocities are $\vec{v}_Q$ and $\vec{v}_B$. The distance between the paths traveled by the two particle centers is b. (CC BY-NC; Ümit Kaya via LibreTexts)

In this model, and effective collision occurs when $E_{loc} > E_0$ where E_{loc} takes into account the fact that all particle collisions are not head-on collisions. If we define v_r as the relative velocity of approach of particles Q and B, then $v_r = \vec{v}_Q - \vec{v}_B$. The relative kinetic energy, E_r, is then $\frac{1}{2}\mu v_r^2$. From Figure **5.7.2** we can see that the fraction of E_r that can be applied to the collision, (E_{loc}), is dependent upon b, the impact parameter, which is the perpendicular distance between the extrapolated paths traveled by the centers of the particles before the collision occurs. If b is 0, then $E_{loc} = E_r$, but for any other value of b, $E_{loc} < E_r$. If b is greater than the sum of the radii of Q and B, the particles will not collide, and $E_{loc} = 0$. The calculation for determining the exact relationship between the $\sigma_r(E_r)$ and E_r for this line of center model rather complicated, but the result is that $\sigma_r(E_r)$ is equal to 0 if $E_r < E_0$ and is equal to $\sigma_{QB}\left(1 - \frac{E_0}{E_r}\right)$ if $E_r \geq E_0$.

When compared to the simple hard-sphere collision theory, we see that

$$\sigma_r(E_r) = \sigma_{QB} \text{ if } E_r \geq E_0 \text{ (hard-sphere theory)} \tag{5.7.1}$$

$$\sigma_r(E_r) = \sigma_{QB}\left(1 - \frac{E_0}{E_r}\right) \text{ if } E_r \geq E_0 \text{ (line of centers theory)} \tag{5.7.2}$$

If we substitute Equation 5.7.2 into Equation **30.1.4** we get

$$k = \left(\frac{2}{k_B T}\right)^{3/2} \left(\frac{1}{\mu\pi}\right)^{1/2} \int_{E_0}^{\infty} dE_r E_r e^{-E_r/k_B T} \sigma_{QB} \left(1 - \frac{E_0}{E_r}\right)$$
$$= \left(\frac{8k_B T}{\mu\pi}\right)^{1/2} \sigma_{QB} e^{-E_r/k_B T}$$
$$= \langle v_r \rangle \sigma_{QB} e^{-E_r/k_B T}$$

When compared to the simple hard-sphere collision theory, we see that

$$k = \langle v_r \rangle \sigma_{QB} e^{-E_r/k_B T} \left(1 + \frac{E_0}{k_B T}\right) \text{(hard-sphere theory)}$$
$$= \langle v_r \rangle \sigma_{QB} e^{-E_r/k_B T} \text{(line of centers theory)}$$

The line of centers theory expresses k in the same terms as the Arrhenius equation, yet experimental values of k still differ from those predicted by the line of centers model. The errors come about because $\sigma_r(E_r)$ is not accurately described by $\sigma_{QB}\left(1 - \frac{E_0}{E_r}\right)$. More work needs to be done to improve the model for describing A, the Arrhenius factor.

5.7: A Reaction Cross Section Depends Upon the Impact Parameter is shared under a CC BY-NC-SA 4.0 license and was authored, remixed, and/or curated by LibreTexts.

- **30.2: A Reaction Cross Section Depends Upon the Impact Parameter** is licensed CC BY-NC-SA 4.0.

5.8: The Rate Constant for a Gas-Phase Chemical Reaction May Depend on the Orientations of the Colliding Molecules

In the previous section, the simple hard-sphere model for collisions was modified to take into account the fact that not every collision of particles occurred with sufficient energy to result in a reaction. The line of centers model assumed that all colliding particles were spheres, yet we know that this is definitely not the case. Thus, we need to modify the collision model to factor in the orientation of non-spherical particles. Figure 5.8.1 shows an example of properly oriented particles and an example of improperly oriented molecules.

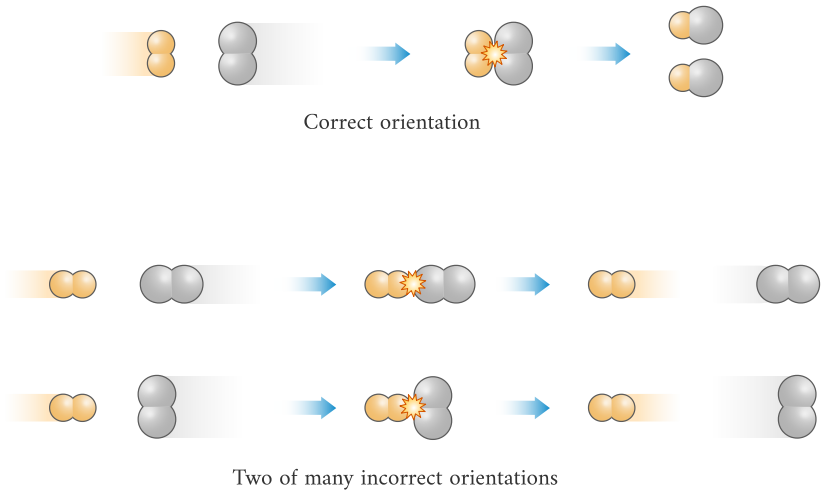


Figure 5.8.1: (top) Molecules colliding with the correct orientation that leads to a successful reaction. (bottom) Molecules colliding in two of the many incorrect orientations that do not lead to a reaction. (CC BY-NC; Ümit Kaya via LibreTexts)

Because proper orientation of colliding molecules is necessary, the hard-sphere collision model overestimates the number of effective collisions. This is one of the factors that leads an incorrect value for A estimated by the hard-sphere collision model.

5.8: The Rate Constant for a Gas-Phase Chemical Reaction May Depend on the Orientations of the Colliding Molecules is shared under a CC BY-NC-SA 4.0 license and was authored, remixed, and/or curated by LibreTexts.

- **30.3: The Rate Constant for a Gas-Phase Chemical Reaction May Depend on the Orientations of the Colliding Molecules** is licensed CC BY-NC-SA 4.0.

5.9: The Internal Energy of the Reactants Can Affect the Cross Section of a Reaction

A further modification of our collision model involves including the internal energy of the colliding gas particles. Recall that the internal energy for a polyatomic gas particle includes electronic, vibrational, and, possibly, rotational energy. It is possible for polyatomic molecules to be in a high enough vibrational state that their vibrational energy alone is greater than E_0. Such molecules would not require any additional translational energy to react. Thus, for a constant total energy, the value of σ_r depends on the vibrational and, to a smaller extent, rotational state of the particle. During a collision between reacting particles, energy can be exchanged between the different degrees of freedom of the particle, so we will need to modify our model to take into account these energy exchanges that occur during a collision. We will see in the next section that using a center-of-mass coordinate system to describe the reaction collision will allow us to incorporate internal energy into our model.

5.9: The Internal Energy of the Reactants Can Affect the Cross Section of a Reaction is shared under a CC BY-NC-SA 4.0 license and was authored, remixed, and/or curated by LibreTexts.

- **30.4: The Internal Energy of the Reactants Can Affect the Cross Section of a Reaction** is licensed CC BY-NC-SA 4.0.

5.10: A Reactive Collision Can Be Described in a Center-of-Mass Coordinate System

We will apply a center-of-mass coordinate system to the bimolecular reaction of ideal gases

$$\mathrm{B(g) + Q(g) \longrightarrow F(g) + G(g)}$$

to develop an improved model for reaction kinetics that produces theoretical values that more closely represent experimental results. In this model, the reactant molecules will travel at velocities $\vec{v}_B$ and $\vec{v}_Q$ before the collision. The product molecules will travel at velocities $\vec{v}_F$ and $\vec{v}_G$ after the collision.

5.10.1: The Velocity and Kinetic Energy of the Center of Mass

The center of mass of two objects must lie along a straight line drawn between the centers of the two objects. Because the two molecules are heading toward each other, the line between them will be changing in size and can be best represented with the vector, $\vec{r}$, where $\vec{r} = \vec{r}_B - \vec{r}_Q$. The pre-reaction center of mass, $\mathbf{R}$ is defined as

$$\mathbf{R} = \frac{m_B \mathbf{r}_B + m_Q \mathbf{r}_Q}{M}$$

where m_B and m_Q are the masses of the individual reactants, and M is the total mass, $m_B + m_Q$.

Velocity is $\frac{d\vec{r}}{dt}$, and so the velocity of the center of mass, $\vec{v}_{cm}$ is

$$\vec{v}_{cm} = \frac{m_B \vec{v}_B + m_Q \vec{v}_Q}{M}$$

The kinetic energy of the reacting system is

$$\mathrm{KE}_{react} = \frac{1}{2} m_B v_B^2 + \frac{1}{2} m_Q v_Q^2$$

This equation can be rewritten as

$$\mathrm{KE}_{react} = \frac{1}{2} M v_{cm}^2 + \frac{1}{2} \mu v_r^2 \tag{5.10.1}$$

Here, μ is the reduced mass and the realtive speed of the colliding particles is $v_r = |\vec{v}_r| = |\vec{v}_B| - |\vec{v}_Q|$. Because we are assuming we have ideal gases, KE_{react} is a constant for the center of mass.

5.10.2: The Reaction

As shown in equation 5.10.1, the kinetic energy of the moving reactants consists of two parts, one due to the relative motion of the two reactant particles, and one due to the motion of the center of mass. The energy due to the motion of the center of mass will not contribute to the reaction, as will soon be shown. Only the energy due to the relative motion of the reacting molecules $\frac{1}{2}\mu v_r^2$ will contribute to overcoming the energy barrier of the energy of the reaction. And only a fraction of that energy will contribute because the molecules are not colliding head-on. Figure 5.10.1 gives a view of the progress of the reaction at several times.

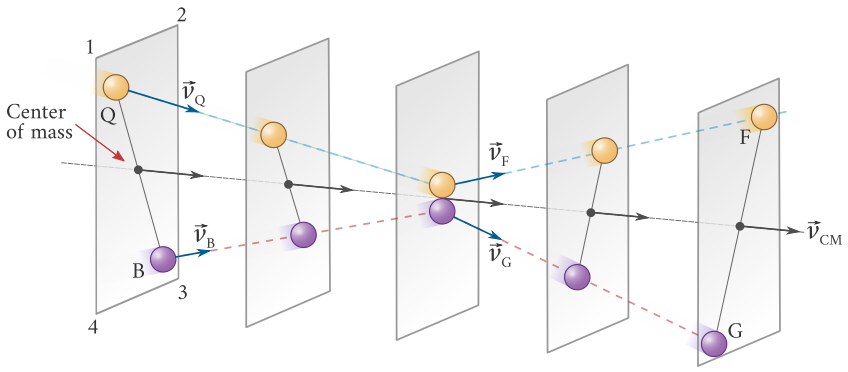


Figure **5.10.1**: A diagram showing the progress of a reaction collision occurring along the path of the center of mass as time passes. The velocity of the center of mass remains constant at all times. The energy that can be contributed towards the reaction by each reactant particles is the component of its own velocity that is co-linear with the collision direction. As shown by Equation **5.10.1**, this energy contribution of the reacting particles is combined in the term $\frac{1}{2}\mu v_r^2$. (CC BY-NC; Ümit Kaya via LibreTexts)

5.10.2.1: Removing the Center of Mass Term

Once **F** and **G** have formed, the post-reaction center of mass, **R** is defined as

$$\mathbf{R} = \frac{m_F\vec{r}_F + m_G\vec{r}_G}{M}$$

where m_F and m_G are the masses of the individual reactants, and M is the total mass, $m_F + m_G$. That means that the velocity of the center of mass, $\vec{v}_{cm}$ is

$$\vec{v}_{cm} = \frac{m_F\vec{v}_F + m_G\vec{v}_G}{M}$$

The kinetic energy of the reacting system is

$$\mathrm{KE}_{react} = \frac{1}{2}m_F v_F^2 + \frac{1}{2}m_G v_G^2$$

This equation can be rewritten as

$$\mathrm{KE}_{react} = \frac{1}{2}M v_{cm}^2 + \frac{1}{2}\mu_P v_{P_r}^2$$

Because the products have different individual masses than the reactants, the reduced mass μ_P and the relative speed v_{P_r} of the products must be denoted as having different values from those of the reactants. The total mass is conserved, however, as is $\vec{v}_{cm}$, the velocity of the center of mass. Because linear momentum must be conserved,

$$m_B\vec{v}_B + m_Q\vec{v}_Q = m_F\vec{v}_F + m_G\vec{v}_G = M\vec{v}_{cm}$$

Because mass is conserved and velocity of the center of mass is constant, the energy contribution of the motion of the center of mass is also constant, and thus does not contribute to the kinetic energy used to attain a successful reaction collision.

5.10.2.2: Estimating the Total Internal Energy

Using the center of mass model for a reaction, we have found the kinetic energy terms for the reactants, $\frac{1}{2}\mu v_r^2$, and products, $\frac{1}{2}\mu_P v_{P_r}^2$. Thus the law of conservation of energy tells us

$$E_{Reactant_{(internal)}} + \frac{1}{2}\mu v_r^2 = E_{Product_{(internal)}} + \frac{1}{2}\mu_P v_{P_r}^2$$

This relationship can be rewritten as

$$E_{Reactant_{(internal)}} + E_{Reactant_{(translational)}} = E_{Product_{(internal)}} + E_{Product_{(translational)}}$$

or

$$E_{R_{(int)}} + E_{R_{(trans)}} = E_{P_{(int)}} + E_{P_{(trans)}}$$

The velocity of the products can be defined based on the laws of conservation of energy and momentum. Unfortunately, the angle between the velocity vector of the reactants $\vec{v}_r$ and the velocity vector of the products $\vec{v}_{P,}$cannot be determined because products molecules can theoretically disperse from the collision in any direction.

5.10: A Reactive Collision Can Be Described in a Center-of-Mass Coordinate System is shared under a CC BY-NC-SA 4.0 license and was authored, remixed, and/or curated by LibreTexts.

- **30.5: A Reactive Collision Can Be Described in a Center-of-Mass Coordinate System** is licensed CC BY-NC-SA 4.0.

5.11: Reactions Can Produce Vibrationally Excited Molecules

As shown at the end of section 30.5, using the center of mass reaction model allows us to state that

$$E_{R_{(int)}} + E_{R_{(trans)}} = E_{P_{(int)}} + E_{P_{(trans)}} \tag{5.11.1}$$

where $E_{R_{(int)}}$ and $E_{P_{(int)}}$ represent the rotational, vibrational, and electronic energies collectively described as the internal energy of the reactants and the products, respectively. If we apply equation 5.11.1 to the well-studied gas-phase reaction

$$\mathbf{F(g) + D_2(g) \longrightarrow DF(g) + D(g)}$$

we can discuss the distribution of a fixed total collision energy between $E_{P_{(int)}}$ and $E_{P_{(trans)}}$. Specifically, if we assume that $\mathbf{F(g)}$ and $\mathbf{D(g)}$ are in their ground electronic states, that $\mathbf{D_2(g)}$ is in its ground rotational, vibrational, and electronic states, and that $\mathbf{DF(g)}$ is in its ground rotational and electronic states, we can focus on the possible vibrational states of the $\mathbf{DF(g)}$ that can be populated. Figure 5.11.1 shows the potential energy curve of the process that is described below.

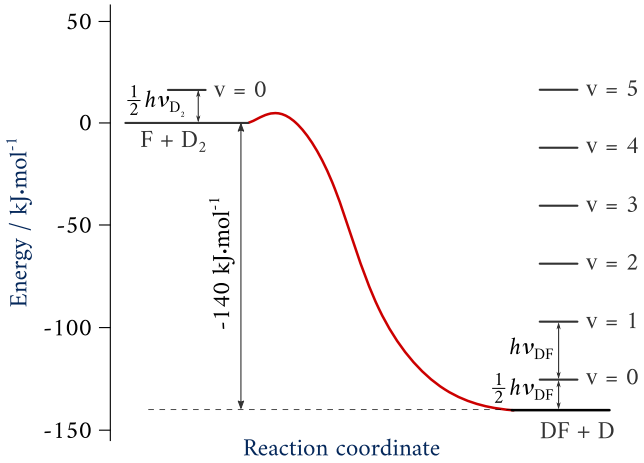


Figure 5.11.1: The potential energy diagram for the reaction $\mathbf{F(g) + D_2(g) \longrightarrow DF(g) + D(g)}$. *(CC BY-NC; Ümit Kaya via LibreTexts)*

Expanding Equation 5.11.1 to describe this assumed process, we get

$$E_{R_{(rot)}} + E_{R_{(vib)}} + E_{R_{(elec)}} + E_{R_{(trans)}} = E_{P_{(rot)}} + E_{P_{(vib)}} + E_{P_{(elec)}} + E_{P_{(trans)}} \tag{5.11.2}$$

Let's assume that $\mathbf{D_2}$ and $\mathbf{DF}$ are harmonic oscillators with $\tilde{\nu}_{D_2}$ = 2990 cm^{-1} and $\tilde{\nu}_{DF}$ = 2907 cm^{-1} .

If D_2 and DF are in their ground electronic states, then $E_{R_{(elec)}} = -D_e(D_2)$ and $E_{P_{(elec)}} = -D_e(DF)$. From experiments, we know that

$$-D_e(DF) - (-D_e(D_2)) = -140 kJ/mol$$

We also know from experiments, that the activation energy for this reaction is about 6 kJ/mol[1], so if we assume that the relative translational energy of the reactants is 7.1 kJ/mol, they will have sufficient energy to overcome the activation energy barrier.

With these data, we can write Equation 5.11.2 as

$$0 + E_{R_{(vib)}} - D_e(D_2) + 7.1\frac{kJ}{mol} = 0 + E_{P_{(vib)}} - D_e(DF) + E_{P_{(trans)}}$$

then

$$E_{R_{(vib)}} + 7.1\frac{kJ}{mol} = E_{P_{(vib)}} + (-D_e(DF) - (-D_e(D_2)) + E_{P_{(trans)}}$$

then

$$E_{R_{(vib)}} + 7.1\frac{kJ}{mol} = E_{P_{(vib)}} - 140\frac{kJ}{mol} + E_{P_{(trans)}}$$

Because $\mathbf{D_2}$ is in its ground vibrational state, $E_{R_{(vib)}} = \frac{1}{2} h\nu_{D_2} = 17.9 \frac{kJ}{mol}$

Putting this altogether,

$$17.9 \frac{kJ}{mol} + 140 \frac{kJ}{mol} + 7.1 \frac{kJ}{mol} - E_{P_{(vib)}} = E_{P_{(trans)}}$$

$$165 \frac{kJ}{mol} - E_{P_{(vib)}} = E_{P_{(trans)}} \tag{5.11.3}$$

Equation 5.11.3 tells us that the reaction will occur only if $E_{P_{(vib)}}$ is less than 165 kJ/mol because $E_{P_{(trans)}}$ must be a positive value.

If $\mathbf{DF\,(g)}$ is a harmonic oscillator, then

$$\begin{aligned} E_{P_{(vib)}} &= \left(v + \frac{1}{2}\right) h\nu_{DF} \\ &= \left(v + \frac{1}{2}\right) (34.8\, kJ/mol) < 165\, kJ/mol \end{aligned}$$

Vibrational states, v = 0, 1, 2, 3, and 4 will result in $E_{P_{(vib)}} \leq$ 165 kJ/mol. Thus $\mathbf{DF\,(g)}$ molecules in these five vibrational states will be produced by the reaction. Note that under these set of assumptions, the $\mathbf{DF}$ molecules produced in different vibrational states will have correspondingly different $E_{P_{(trans)}}$.

[1]Average of experimental E_a values listed at https://kinetics.nist.gov/kinetics/ accessed 9/22/2021

5.11: Reactions Can Produce Vibrationally Excited Molecules is shared under a CC BY-NC-SA 4.0 license and was authored, remixed, and/or curated by LibreTexts.

- **30.7: Reactions Can Produce Vibrationally Excited Molecules** is licensed CC BY-NC-SA 4.0.

5.12: Reactive Collisions Can be Studied Using Crossed Molecular Beam Machines

Crossed molecular beam experiments are chemical experiments where two beams of atoms or molecules are collided together to study the dynamics of the chemical reaction. These experiments can detect individual reactive collisions as well as determine the distribution of velocities and the scattering angle of the reaction products.[1]

Technique

In a crossed molecular beam apparatus, two collimated beams of gas-phase atoms or molecules, each dilute enough to ignore collisions within each beam, intersect in a vacuum chamber, as shown in Figure **5.12.1a**. The direction and velocity of the resulting product molecules are then measured. These data are frequently coupled with mass spectrometric data to yield information about the partitioning of energy among translational, rotational, and vibrational modes of the product molecules.[2]

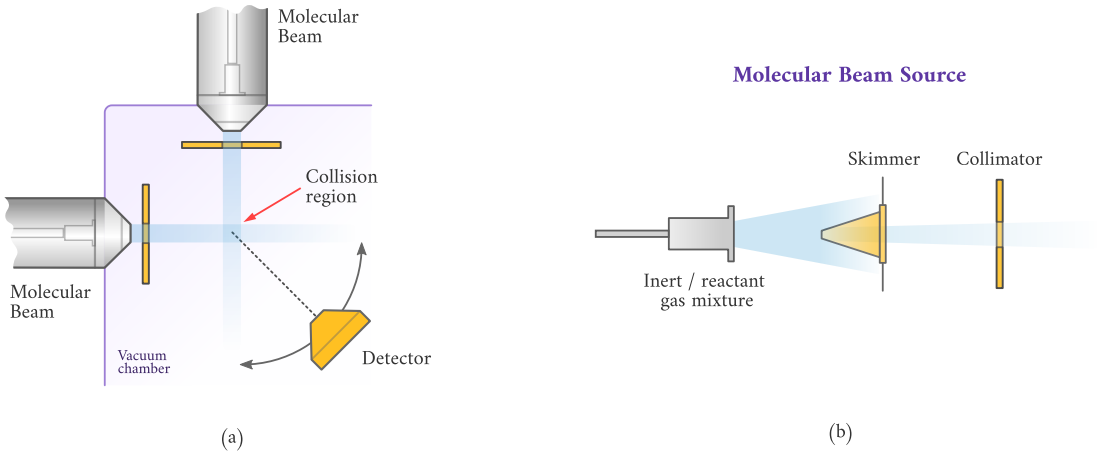


Figure **5.12.1** a) A schematic diagram of a crossed molecular beam apparatus. The two molecular beams, each containing particles of a single reactant species, intersect at the collision region. The product particles travel away from the collision region. A mass spectrometer with a moveable inlet is used to detect the product particles. b) A schematic diagram of a supersonic molecular beam source. (CC BY-NC; Ümit Kaya via LibreTexts)

History

The crossed molecular beam technique was developed by Dudley Herschbach and Yuan T. Lee, for which they were awarded the 1986 Nobel Prize in Chemistry.[3] While the technique was demonstrated in 1953 by Taylor and Datz of Oak Ridge National Laboratory,[4] Herschbach and Lee refined the apparatus and began probing gas-phase reactions in unprecedented detail.

Early crossed beam experiments investigated alkali metals such as potassium, rubidium, and cesium. When the scattered alkali metal atoms collided with a hot metal filament, they ionized, creating a small electric current. Because this detection method is nearly perfectly efficient, the technique was quite sensitive.[2] Unfortunately, this simple detection system only detects alkali metals. New techniques for detection were needed to analyze main group elements.

Detecting scattered particles through a metal filament gave a good indication of angular distribution but has no sensitivity to kinetic energy. In order to gain insight into the kinetic energy distribution, early crossed molecular beam apparatuses used a pair of slotted disks placed between the collision center and the detector. By controlling the rotation speed of the disks, only particles with a certain known velocity could pass through and be detected.[2] With information about the velocity, angular distribution, and identity of the scattered species, useful information about the dynamics of the system can be derived.

Later improvements included the use of quadrupole mass filters to select only the products of interest,[5] as well as time-of-flight mass spectrometers to allow easy measurement of kinetic energy. These improvements also allowed the detection of a vast array of compounds, marking the advent of the "universal" crossed molecular beam apparatus.

The inclusion of supersonic nozzles (figure **5.12.1*b***) to collimate the gases expanded the variety and scope of experiments, and the use of lasers to excite the beams (either before impact or at the point of reaction) further broadened the applicability of this technique.[2]

References

Wikipedia contributors. (2020, October 16). Crossed molecular beam. In *Wikipedia*, *The Free Encyclopedia*. Retrieved 01:21, September 24, 2021, from https://en.Wikipedia.org/w/index.php?title=Crossed_molecular_beam&oldid=983809904

1. Lee, Y. T. (1987). "Molecular Beam Studies of Elementary Chemical Processes". *Science*. **236** (4803): 793-8. Bibcode:1987Sci...236..793T. doi:10.1126/science.236.4803.793. PMID 17777849. S2CID 45603806

2. Herschbach, D. Nobel Lecture, Dec. 8, 1986

3. Nobel Foundation Archived July 18, 2006, at the Wayback Machine

4. Taylor, E. H.; Datz, S. (1955). "Study of Chemical Reaction Mechanisms with Molecular Beams. The Reaction of K with HBr*". *J. Chem. Phys*. **23** (9): 1711. Bibcode:1955JChPh..23.1711T. doi:10.1063/1.1742417

5. Miller, W. B.; Safron, S. A.; Herschbach, D. R. (1967). "Exchange reactions of alkali atoms with alkali halides: a collision complex mechanism". *Discuss. Faraday Soc*. **44**: 108–122. doi:10.1039/DF9674400108

5.12: Reactive Collisions Can be Studied Using Crossed Molecular Beam Machines is shared under a CC BY-SA 4.0 license and was authored, remixed, and/or curated by LibreTexts.

- **30.6: Reactive Collisions Can be Studied Using Crossed Molecular Beam Machines** is licensed CC BY-SA 4.0.

5.13: The Velocity and Angular Distribution of the Products of a Reactive Collision

Calculation of the speed distribution for DF molecules based upon the vibrational state of the molecule

This section describes how data from crossed molecular beam experiments allow us to describe the velocity and angular distribution of particles produced by the simple bi-molecular collision

$$\mathbf{F\,(g) + D_2\,(g) \longrightarrow DF\,(g) + D\,(g)} \tag{5.13.1}$$

As noted in the previous section, the internal vibrational energy of the products will affect the velocity and distribution because if $\mathbf{DF\,(g)}$ is a harmonic oscillator, then

$$E_{P_{(trans)}} + E_{P_{(vib)}} = 165\frac{kJ}{mol}$$

and

$$E_{P_{(vib)}} = \left(v + \frac{1}{2}\right)(34.8\frac{kJ}{mol})$$

Thus

$$\begin{aligned} E_{P_{(trans)}} + E_{P_{(vib)}} &= \frac{1}{2}\mu_P v_{P_r} + \left(v + \frac{1}{2}\right)\left(34.8\frac{kJ}{mol}\right) \\ &= 165\frac{kJ}{mol} \end{aligned} \tag{5.13.2}$$

The reduced mass of the products μ_P is

$$\frac{(21.01\,g/mol)(2.014\,g/mol)}{21.01\,g/mol + 2.014\,g/mol} = 1.84\,g/mol = 0.00184\,kg/mol$$

so that solving for the product velocity in Equation 5.13.2 for v_{P_r} gives

$$v_{P_r} = \sqrt{\left(\frac{2}{0.00184\,kg/mol}\right)\left(1.65 \times 10^5\,\frac{J}{mol} - \left(v + \frac{1}{2}\right)(3.48 \times 10^4)\frac{J}{mol}\right)}$$

It can be shown that the corresponding relative velocity of the $\mathbf{DF}$ molecule and the center of mass,$|\vec{v}_{DF} - \vec{v}_{cm}|$, is equal to $\frac{m_D}{M}v_{P_r}$ for this reaction, with $M = m_{D_2} + m_F$. Table 5.13.1 shows the values of v_{P_r} and $|\vec{v}_{DF} - \vec{v}_{cm}|$ for vibrational states $v = 0 - 4$.

Table 5.13.1

Vibrational state, v	relative velocity of the products, v_{P_r} in m/s	$\lvert\vec{v}_{DF} - \vec{v}_{cm}\rvert$, in m/s
0	12,700	1111
1	11,100	971
2	9270	811
3	6930	606
4	3200	280

Analysis of Crossed Molecular Beam Data

This link takes you to the 1986 Nobel Prize acceptance lecture of Yuan Tseh Lee, in which he describes the crossed molecular beam studies that his group carried out on the reaction 5.13.1. On page 3 of the lecture, you will see a center-of-mass velocity flux contour map for the reaction. This map measures the speed distribution and the angular dispersion distribution as a result of collisions between one D_2 molecule approaching from the left and one F atom approaching from the right. Moving away from the center of the graph in any direction represents an increase in speed. The dashed line circles represent the maximum speed that a molecule in

that given vibrational state can obtain. Notice that the highest vibrational state is closest to the nucleus. Thus, the map is consistent with theory, which claims that as the vibrational energy increases, the translational energy decreases.

The contour areas on the map represent a constant number of DF(g) molecules. The more closely spaced the contour lines, the greater the number of $\mathbf{DF(g)}$ molecules with that velocity in that vibrational state. An estimate of the population distribution is that roughly half the molecules are in the $v = 3$ state, roughly 25% of the molecules occupy the $v = 2$ state, and roughly 25% of the molecules occupy the $v = 4$ state. Very few molecules occupy the $v = 0$ or $v = 1$ states. The fact that there are molecules with velocities between the dashed lines shows that these **DF** molecules are in various rotational states within each vibrational state. If E_{rot} = 0 and $J = 0$, the molecular velocity distribution would be centered on each dashed line. But because these molecules do exist in various rotational states, their E_{rot} is greater than 0, and their translational energy is in between the energies of those molecules in rotational ground states. The distribution of vibrational states among the **DF** product molecules more closely resembles a normal distribution (i.e., Gaussian-like) than a Boltzmann distribution.

Example 5.13.1

Determine the populations of the five lowest vibrational states of $\mathbf{DF}(v)$ relative to $\mathbf{DF}(v = 3)$, assuming that the distribution is in thermal equilibrium at 298 K. You can assume that the **DF** molecules act as harmonic oscillators with $\tilde{\nu}_{DF}$ = 2907 cm^{-1}.

Solution

If the $\mathbf{DF(g)}$ molecules are in thermal equilibrium, the population of vibrational states will follow a Boltzmann distribution. Therefore,

$$N(v) = e^{-\frac{(v+1/2)h\nu_{DF}}{k_B T}}$$

and

$$N(v=3) = e^{-\frac{(3+1/2)h\nu_{DF}}{k_B T}}$$

so

$$\frac{N(v)}{N(v=3)} = e^{-\frac{(v-3)h\nu_{DF}}{k_B T}}$$

v	$\frac{N(v)}{N(v=3)}$
0	2.03 x 10^{18}
1	1.60 x 10^{12}
2	1.26 x 10^{6}
3	1
4	7.90 x 10^{-7}

It is clear that when the molecules are at thermal equilibrium, the population of the vibrational states decreases with an increasing v, which is not the population pattern found from the experiment.

The map also shows that a majority of $\mathbf{DF(g)}$ molecules generally head back towards the direction from which the F atom originally approached the collision. Some even head directly back from whence they came. This type of collision is called a rebound reaction. We will see in the next section that not all reactions are rebound reactions.

A different style of contour map is shown in figure **5.13.1**. In this view, the density of the dots and the intensity of their color represent the number of particles being scattered at specific angles. This map does not show the vibrational state of the DF molecules.

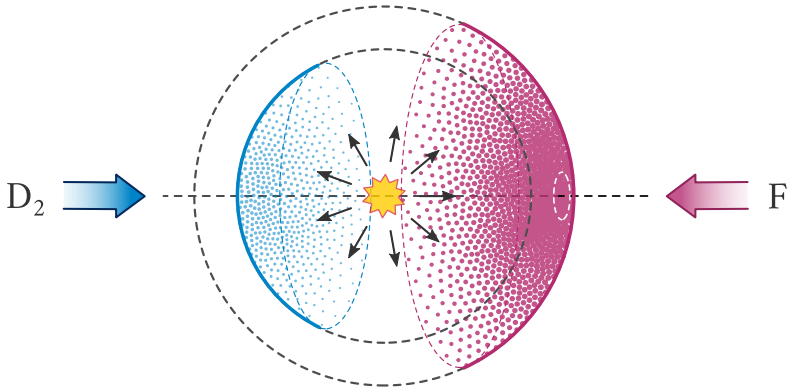


Figure **5.13.1**: A center-of-mass velocity flux contour map for the reaction $\mathbf{D_2 + F \longrightarrow DF + D}$. This map shows the angular dispersion distribution as a result of collisions between one D_2 molecule approaching from the left and one F atom approaching from the right. (CC BY-NC 4.0; Ümit Kaya via LibreTexts)

5.13: The Velocity and Angular Distribution of the Products of a Reactive Collision is shared under a CC BY-NC-SA 4.0 license and was authored, remixed, and/or curated by LibreTexts.

- **30.8: The Velocity and Angular Distribution of the Products of a Reactive Collision** is licensed CC BY-NC-SA 4.0.

5.14: Not All Gas-Phase Chemical Reactions are Rebound Reactions

Stripping Reactions

In the previous section we showed that the reaction

$$\mathrm{D_2\,(g) + F\,(g) \longrightarrow DF\,(g) + D\,(g)}$$

is a rebound reaction because the vast majority of DF molecules bounce off from the collision with $\mathrm{D_2}$ back toward the general direction from which they came. In this section we will look at **stripping reactions**, reactions in which a majority of the product molecules continue moving on after the collision in the same direction that the precursor reactant molecules were going.

In stripping reactions, the experimental hard-sphere collision cross section is generally found to be larger than the theoretical estimate. The experimental cross-section is so large that it would be possible for two particles to remain inside the collision area and yet pass by each other without colliding. It has been determined experimentally that an electron transfer between the two particles occurs before they collide. The resulting ions are then drawn toward each other because of the Coulomb potential created by the opposite charges. One such reaction involves $\mathrm{K\,(g)}$ and $\mathrm{I_2\,(g)}$. The mechanism is:

$$\mathrm{K\,(g) + I_2\,(g) \longrightarrow K^+\,(g) + I_2^-\,(g)} \qquad \textbf{(step 1)}$$

$$\mathrm{K^+\,(g) + I_2^-\,(g) \longrightarrow KI\,(g) + I\,(g)} \qquad \textbf{(step 2)}$$

After the collision, the KI molecule moves off in the same general direction as the incoming K atom.

Meta-stable Intermediates

There are other bimolecular gas-phase collision reactions in which the product molecules disperse in both forward and reverse directions after the reaction. There is no explanation for these types of post-collision scattering patterns if we insist on using a simple hard-sphere collision model. However, if the colliding particles form a single atom-molecule structure that lasts long enough for the structure to undergo many rotations before splitting apart into products, it is reasonable for the newly formed products to scatter in the forward and reverse direction.

The discovery of these various reaction types was made possible by the development and use of the crossed molecular beam instruments described in Section 30.6.

5.14: Not All Gas-Phase Chemical Reactions are Rebound Reactions is shared under a CC BY-NC-SA 4.0 license and was authored, remixed, and/or curated by LibreTexts.

- **30.9: Not All Gas-Phase Chemical Reactions are Rebound Reactions** is licensed CC BY-NC-SA 4.0.

5.15: The Potential-Energy Surface Can Be Calculated Using Quantum Mechanics

A potential energy surface (PES) describes the potential energy of a system, especially a collection of atoms, in terms of certain parameters, normally the positions of the atoms. The surface might define the energy as a function of one or more coordinates; if there is only one coordinate, the surface is called a potential energy curve or energy profile. It is helpful to use the analogy of a landscape: for a system with two degrees of freedom (e.g. two bond lengths), the value of the energy (analogy: the height of the land) is a function of two bond lengths (analogy: the coordinates of the position on the ground). The Potential Energy Surface represents the concept that each geometry (both external and internal) of the atoms of the molecules in a chemical reaction has associated with it a unique potential energy. This creates a smooth energy “landscape” and chemistry can be viewed from a topology perspective of particles evolving as they pass through potential energy "valleys" and "passes".

The PES concept finds application in fields such as chemistry and physics, especially in the theoretical sub-branches of these subjects. It can be used to theoretically explore properties of structures composed of atoms, for example, finding the minimum energy shape of a molecule or computing the rates of a chemical reaction.

5.15.1: Potential Energy Curves (2-D Potential Energy Surfaces)

The energy of a system of two atoms depends on the distance between them. At large distances the energy is zero, meaning “no interaction”. At distances of several atomic diameters, attractive forces dominate, whereas at very close approaches the force is repulsive, causing the energy to rise. The attractive and repulsive effects are balanced at the minimum point in the curve. Plots that illustrate this relationship are quite useful in defining certain properties of a chemical bond (Figure **5.15.1**).

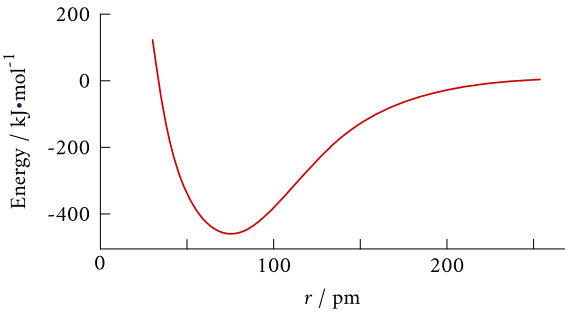


Figure **5.15.1**: A potential energy curve for the covalent bond in a H_2 molecule. The distance r is the distance between the nuclei of the two H atoms. (CC BY-NC; Ümit Kaya via LibreTexts)

The internuclear distance at which the potential energy minimum occurs defines the **bond length**. This is more correctly known as the *equilibrium* bond length because thermal motion causes the two atoms to vibrate about this distance. In general, the stronger the bond, the smaller the bond length.

Attractive forces operate between all atoms, but unless the potential energy minimum is at least of the order of *RT*, the two atoms will not be able to withstand the disruptive influence of thermal energy long enough to result in an identifiable molecule. Thus we can say that a chemical bond exists between the two atoms in H_2. The weak attraction between argon atoms does not allow Ar_2 to exist as a molecule, but it does give rise to the *van der Waals force* that holds argon atoms together in their liquid and solid forms.

5.15.2: Mathematical Definition and Computation of a Potential Energy Surface

The geometry of a set of atoms can be described by a vector, r, whose elements represent the atom positions. The vector $\boldsymbol{r}$ could be the set of the Cartesian coordinates of the atoms, or could also be a set of inter-atomic distances and angles. Given $\boldsymbol{r}$, the energy as a function of the positions, $V(\boldsymbol{r})$, is the value of $V(\boldsymbol{r})$ for all values of $\boldsymbol{r}$ of interest. Using the landscape analogy from the introduction, $V(\boldsymbol{r})$ gives the height on the "energy landscape" so that the concept of a potential energy surface arises. An example is the PES for water molecule (Figure **5.15.2**) that shows the energy minimum corresponding to optimized molecular structure for water- O-H bond lengths of 0.0958 nm and H-O-H bond angle of 104.5°

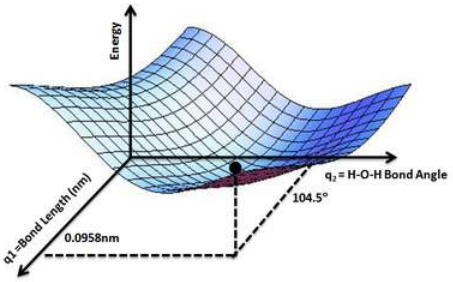


Figure 5.15.2: PES for water molecule showing the energy minimum corresponding to optimized molecular structure for water- O-H bond lengths of 0.0958nm and H-O-H bond angle of 104.5°. of Wikipedia (Credit: Aimnature).

The Dimensionality of a Potential Energy Surface

To define an atom's location in 3-dimensional space requires three coordinates (e.g., x, y,and z or r, θ and phi in Cartesian and Spherical coordinates) or *degrees of freedom*. However, a reaction and hence the corresponding PESs do not depend on the absolute position of the reaction, only the relative positions (internal degrees). Hence both translation and rotation of the entire system can be removed (each with 3 degrees of freedom, assuming non-linear geometries). So the dimensionality of a PES is

$$3N-6$$

where N is the number of atoms involves in the reaction, i.e., the number of atoms in each reactant). The PES is a hypersurface with many degrees of freedom and typically only a few are plotted at any one time for understanding. See Calculate Number of Vibrational Modes to get a more detailed picture of how this applies to calculating the number of vibrations in a molecule

To study a chemical reaction using the PES as a function of atomic positions, it is necessary to calculate the energy for **every atomic** arrangement of interest. Methods of calculating the energy of a particular atomic arrangement of atoms are well known. For very simple chemical systems or when simplifying approximations are made about inter-atomic interactions, it is sometimes possible to use an analytically derived expression for the energy as a function of the atomic positions. An example is

$$\mathrm{H} + \mathrm{H_2} \longrightarrow \mathrm{H_2} + \mathrm{H} \tag{5.15.1}$$

a system that is described by a function of the **three H–H** distances. For more complicated systems, calculation of the energy of a particular arrangement of atoms is often too computationally expensive for large-scale representations of the surface to be feasible.

5.15.3: Applications of Potential Energy Surfaces

A PES is a conceptual tool for aiding the analysis of molecular geometry and chemical reaction dynamics. Once the necessary points are evaluated on a PES, the points can be classified according to the first and second derivatives of the energy with respect to position, which respectively are the gradient and the curvature. Stationary points (or points with a zero gradient) have physical meaning: energy minima correspond to physically stable chemical species and **saddle points** correspond to transition states, the highest energy point on the reaction coordinate (which is the lowest energy pathway connecting a chemical reactant to a chemical product).

5.15.3.1: A Hypothetical Endothermic Reaction PES

Figure 5.15.3 shows an example of a PES for a hypothetical reaction system, with the corresponding 2-D energy contour map projected on the plane below. The contour map shows isolines of potential energy, using color to differentiate between high and low energies. In this figure, the highest potential energy is indicated with red, and as the color changes along the ROYGBIV scale, the potential energy decreases until violet is reached, indicating the lowest potential energy. In the PES, the z axis represents the potential energy, with the energy of the plane in the PES defined as 0 kJ. The color scheme of the PES has the same meaning as that of the 2-D contour map - red is high potential energy and violet is low potential energy.

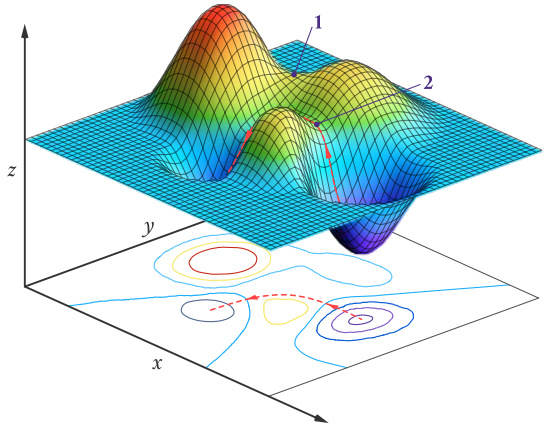


Figure 5.15.3: A 2-D contour map and corresponding Potential Energy Surface for a hypothetical endothermic reaction. See the text for a detailed explanation. (CC BY-NC; Ümit Kaya via LibreTexts)

Before the reaction, the reactants are found at (or near) the energy minimum on the right. (The deep well in the PES and the smallest, violet oval in the contour map.) As the reaction proceeds, the reactants are shown following the minimum energy pathway toward the products, as designated by the dashed red line. The point "2" designates the transition state at the saddle point, the highest energy point of the reaction process. The reaction then moves on to form the products, which sit in the potential energy well on the left. (Designated by the shallower well on the PES and by the dark blue oval on the left in the contour map.) Because the potential energy of the reactants is less than the potential energy of the products, this reaction is an endothermic reaction. The point "1" represents a second, higher energy saddle point which is the transition state for an alternative reaction that is possible for this set of chemicals.

5.15.3.2: The Exchange Reaction $H_A + H_BH_C \Rightarrow H_AH_B + H_C$

A specific application of a PES is the mapping of the reaction shown in equation 5.15.1, the exchange of hydrogen atoms in an H_2 molecule. In this map, the individual H atoms are labeled as

$$H_A + H_BH_C \rightarrow H_AH_B + H_C$$

We must take into account the collision angle between the H_A atom and the H_BH_C molecule. If we fix this collision angle at 180°, we are able to plot a PES that is dependent on the two parameters of R_{BC} and R_{AB}. The resulting PES (figure 5.15.4a) and energy contour map (figure 5.15.4b) show us that if the particles are far enough apart, the potential energy of the reaction system starts out being described by the potential energy curve for the H_BH_C molecule, and ends up being described by the potential energy curve of the H_AH_B molecule. Individually, these curves both have appearances similar to the curve shown in Figure 5.15.1. The PES and the energy contour map show the symmetrical nature of the potential energy changes that occur in this exchange process that involves products that are equivalent to the reactants.

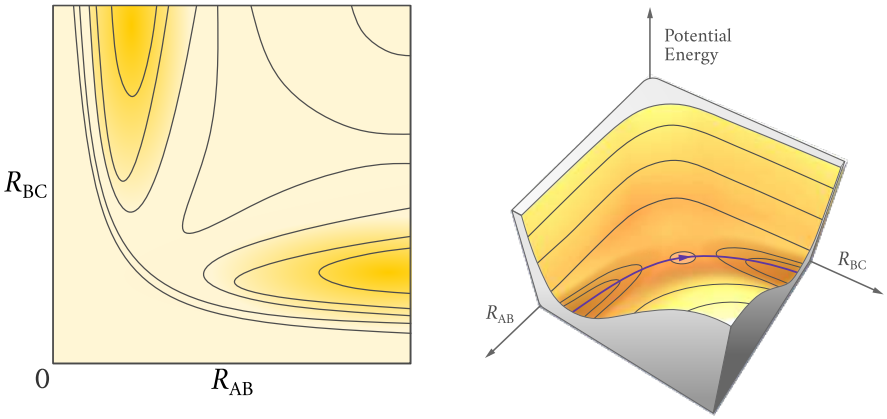


Figure **5.15.4a**: (left) The potential energy contour map for the exchange reaction $H_A + H_BH_C \rightarrow H_AH_B + H_C$. The x-axis is R_{AB}, the interatomic distance between H_A and H_B. These two atoms begin very far apart, but end up being bonded together. The y-axis is R_{BC}, the interatomic distance between H_B and H_C. These two atoms start out bonded together but end up separated and far apart. The darker the color, the lower the potential energy. (right) The 3-D potential energy surface for the exchange reaction $H_A + H_BH_C \rightarrow H_AH_B + H_C$. The darker the color, the lower the potential energy. (CC BY-NC; Ümit Kaya via LibreTexts)

As the H_A atom more closely approaches the H_BH_C molecule, the interactions between these particles begin to affect the potential energy of the system. There are many possible potential energy pathways that the reaction could follow. Figure **5.15.5** shows the energy contour map for three possible reaction pathways:

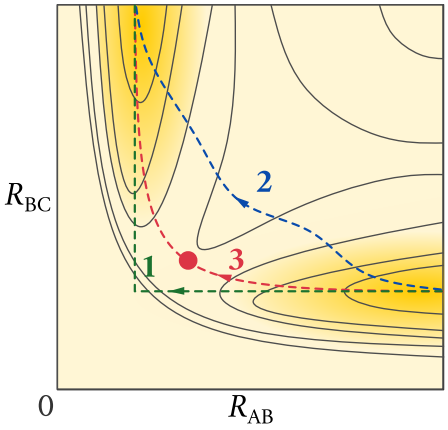


Figure **5.15.5**: An energy contour map showing three possible reaction pathways for the reaction

$$H_A + H_BH_C \rightarrow H_AH_B + H_C$$

(CC BY-NC; Ümit Kaya via LibreTexts)

In pathway 1, the H_BH_C bond length R_{BC} is held constant as the distance R_{AB} decreases. This type of interaction would lead to a continually increasing potential energy for the system as the H_A atom moves closer and closer to the H_BH_C molecule. Eventually, the new H_AH_B molecule would form, and the H_C atom would break off and would move farther and farther away.

Pathway 2 shows a second possible reaction pathway in which the H_BH_C bond length R_{BC} increases even though the H_A atom is still relatively far away. This pathway is unlikely because it requires a great deal of potential energy to stretch the H_BH_C bond before the attractive force from the H_A atom influences this bond lengthening.

As the particles travel along Pathway 3, the reactants still must pass through a potential energy maximum at the saddle point, but this local maximum is the lowest energy barrier separating reactants from products. As noted above, this saddle point is called the transition state structure (designated by the red dot in pathway 3). This is the structure that is equally poised to return to the

reactants or move forward to form products. Pathway 3 is the minimum energy pathway, and thus the one most likely to be followed during a successful reaction.

It is sometimes useful to create energy contour maps that include information about the vibrational state of reactants and products, as shown in figure **5.15.6**.

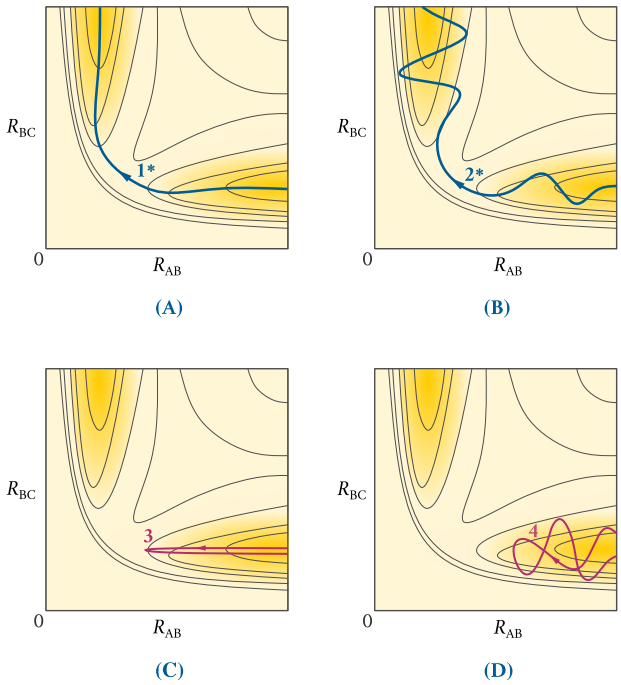


Figure **5.15.6**: Four possible collision outcomes for the exchange reaction $H_A + H_BH_C \rightarrow H_AH_B + H_C$. 6A) The minimum energy pathway which leads to a successful exchange. 6B) The successful collision of a vibrating H_BH_C molecule with an H_A atom, resulting in the formation of a vibrating H_AH_B molecule. 6C) The approach of an H_A atom to a non-vibrating, slow-moving H_BH_C molecule that has insufficient kinetic energy to escape the potential energy well, leading to an unsuccessful exchange reaction. 6D) The approach of an H_A atom to a vibrating, slow-moving H_BH_C molecule that has insufficient kinetic energy to escape the potential energy well, leading to an unsuccessful exchange reaction. (CC BY-NC; Ümit Kaya via LibreTexts)

5.15.3.3: The Exchange Reaction F + D_2 ⇒ DF + D

When modeling the potential energy for the reaction

$$\mathbf{F(g) + D_2(g) \longrightarrow DF(g) + D(g)}$$

it is useful to differentiate between the two deuterium atoms, so we can designate them as $\mathbf{D_A}$ and $\mathbf{D_B}$. Doing so allows us to determine how the potential energy of the pre-reaction system is affected by the **F** to $\mathbf{D_A}$ distance R_{D_AF} and the $\mathbf{D_A}$ to $\mathbf{D_B}$ distance $R_{D_AD_B}$ (figure **5.15.7**).

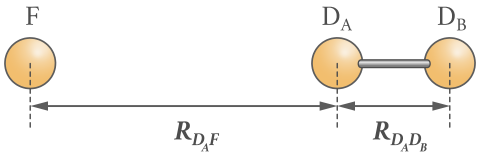


Figure **5.15.7**: Defining the distances R_{D_AF} and $R_{D_AD_B}$ (CC BY-NC; Ümit Kaya via LibreTexts)

As the **F** atom more closely approaches the $\mathbf{D_2}$ molecule, the interactions between these particles begin to affect the potential energy of the system. There are many possible potential energy pathways that the reaction could follow. Figure **5.15.8** shows the energy contour map for three possible reaction pathways:

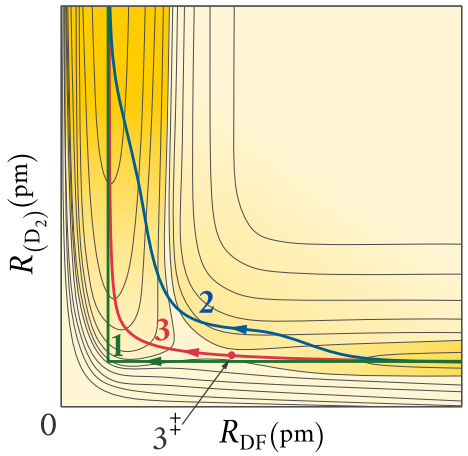


Figure 5.15.8: Three possible reaction pathways for the $\mathbf{F(g) + D_2(g) \longrightarrow DF(g) + D}$ reaction. (CC BY-NC; Ümit Kaya via LibreTexts)

In pathway 1, the $\mathbf{D_2}$ bond length $R_{D_AD_B}$ is held constant as the distance R_{D_AF} decreases. This type of interaction would lead to a continually increasing potential energy for the system as the $\mathbf{F}$ atom moves closer and closer to the $\mathbf{D_2}$ molecule. Eventually, the new $\mathbf{D_AF}$ molecule would form, and the $\mathbf{D_B}$ atom would break off and would move farther and farther away.

Pathway 2 shows a second possible reaction pathway in which the $\mathbf{D_2}$ bond length $R_{D_AD_B}$ increases even though the F atom is still relatively far away. This pathway is unlikely because it requires a great deal of potential energy to stretch the $\mathbf{D_2}$ bond before the attractive force from the F atom influences this bond lengthening.

As the particles travel along Pathway 3, the reactants still must pass through a potential energy maximum at the saddle point, but this local maximum is the lowest energy barrier separating reactants from products. As noted above, this saddle point is called the transition state structure (designated by the red dot in pathway 3, labeled as $\mathbf{3^‡}$). This is the structure that is equally poised to return to the reactants or move forward to form products. Pathway 3 is the minimum energy pathway, and thus the one most likely to be followed during a successful reaction.

If we were to plot the potential energy curve for the reaction pathway along the minimum energy pathway, we would get the familiar potential energy curve of a reaction similar to that shown in Figure 5.15.9.

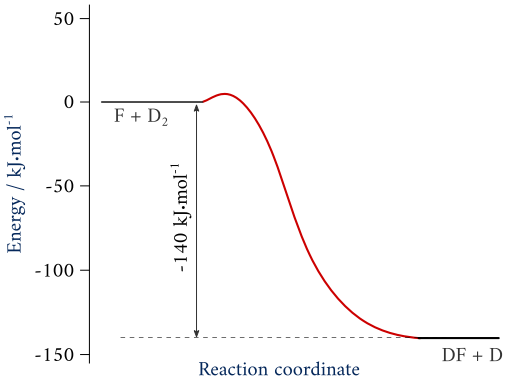


Figure 5.15.9: This graph shows the potential energy relationships for the reaction $\mathbf{F + D_2 \longrightarrow DF + D}$. The activation energy for the forward reaction is about 6 kJ/mol. The difference in potential energy between the reactants and the products is $D_e(\mathbf{D_2}) - D_e(\mathbf{DF})$. The curve's peak represents the transition state. (CC BY-NC; Ümit Kaya via LibreTexts)

Contributors and Attributions

- Wikipedia
- Stephen Lower, Professor Emeritus (Simon Fraser U.) Chem1 Virtual Textbook
- Tom Neils, Grand Rapids Community College

5.15: The Potential-Energy Surface Can Be Calculated Using Quantum Mechanics is shared under a CC BY-NC-SA 4.0 license and was authored, remixed, and/or curated by LibreTexts.

- **30.10: The Potential-Energy Surface Can Be Calculated Using Quantum Mechanics** is licensed CC BY-NC-SA 4.0.

5.16: Equilibrium Constants in Terms of Partition Functions

Consider the general gas phase chemical reaction represented by

$$\nu_A A + \nu_B B \rightleftharpoons \nu_C C + \nu_D D \tag{5.16.1}$$

where A, B, C and D are the reactants and products of the reaction, and ν_A is the stoichiometric coefficient of chemical A, ν_B is the stoichiometric coefficient of chemical B, and so on. Each of the gases involved in the reaction will eventually reach an equilibrium concentration when the forward and reverse reaction rates become equal. The distribution of reactants to products at the equilibrium point is represented by the equilibrium constant (K_c):

$$K_c = \frac{[C]^{\nu_C}[D]^{\nu_D}}{[A]^{\nu_A}[B]^{\nu_B}}$$

If the system is not at equilibrium, a shift in the number of reactants and products will occur to lower the overall energy of the system. The difference in the energy of the system at this non-equilibrated point and the energy of the system at equilibrium for any particular species is termed chemical potential. When both temperature and volume are constant for both points aforementioned, the chemical potential μ of species i is expressed by the equation

$$\mu_i = \left(\frac{\partial A}{\partial N_i}\right)_{T,V,N_{j\neq 1}} \tag{5.16.2}$$

where A is the Helmholtz energy, and N_i is the number of molecules of species i. The Helmholtz energy can be determined as a function of the total partition function, Q:

$$A = -k_B T \ln Q$$

where k_B is the Boltzmann constant and T is the temperature of the system. The total partition function is given by

$$Q = \frac{q_i(V,T)^{Ni}}{N_i!}$$

where q_i is the molecular partition function of chemical species i. Substituting the molecular partition function into the equation for Helmholtz energy yields:

$$A = -k_B T \ln\left(\frac{q_i(V,T)^{N_i}}{N_i!}\right)$$

and then further substituting this equation into the definition of chemical potential (Equation 5.16.2) yields:

$$\mu_i = \left(\frac{\partial - k_B T \ln\left(\frac{q_i(V,T)^{Ni}}{N_i!}\right)}{\partial N_i}\right)_{T,V,N_{j\neq 1}}$$

rearranging this equation the following derivative can be set-up:

$$\mu_i = -k_B T\left[\left(\frac{\partial N_i \ln\left(q_i(V,T)\right)}{\partial N_i}\right) - \left(\frac{\partial \ln\left(N_i!\right)}{\partial N_i}\right)\right]_{T,V,N_{j\neq 1}}$$

From this point Sterling's approximation

$$\ln N! = N \ln N - N$$

can be substituted into the derivative to yield:

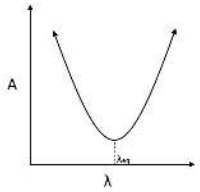
$$\mu_i = -k_B T\left[\left(\frac{\partial N_i \ln\left(q_i(V,T)\right)}{\partial N_i}\right) - \left(\frac{\partial \left(N_i \ln N_i - N_i\right)}{\partial N_i}\right)\right]_{T,V,N_{j\neq 1}}$$

From here the derivative can be rearranged and solved:

$$\begin{aligned}\mu_i = -k_B T & \left[\ln\left(q_i(V,T)\right)\frac{\partial N_i}{\partial N_i} + N_i\frac{\partial \ln\left(q_i(V,T)\right)}{\partial N_i} - \ln\left(N_i\right)\frac{\partial N_i}{\partial N_i} - N_i\frac{\partial \ln\left(N_i\right)}{\partial N_i}\right. \\ & \left. + \frac{\partial N_i}{\partial N_i}\right]_{T,V,N_{j\neq 1}} \\ = -k_B T & \left(\ln\left(q_i(V,T)\right) + 0 - \ln\left(N_i\right) - N_i\frac{1}{N_i} + 1\right) \\ = -k_B T & \left(\ln\left(q_i(V,T)\right) - \ln\left(N_i\right)\right) \\ = -k_B T & \ln\left(\frac{q_i(V,T)}{N_i}\right)\end{aligned} \tag{5.16.3}$$

A variable, λ, is then defined such that $dN_j = \nu_j d\lambda$, where j = A, B, C or D and ν_j is taken to be positive for products and negative for reactants. A change in λ therefore corresponds to a change in the concentrations of the reactants and products. Thus, at equilibrium,

$$\left(\frac{\partial A}{\partial \lambda}\right)_{T,V} = 0$$



Helmholtz Energy with respect to Equilibrium Shifts

From Classical thermodynamics, the total differential of A is:

$$dA = -SdT - pdV + \sum_j \mu_j dN_j$$

For a reaction at a fixed volume and temperature (such as in the canonical ensemble), dT and dV equal 0. Therefore,

$$\begin{aligned} dA &= \sum_j \mu_j dN_j \\ &= \sum_j \mu_j \nu_j d\lambda \\ &= d\lambda \sum_j \mu_j \nu_j \end{aligned}$$

with

$$\sum_j \mu_j \nu_j = 0$$

Substituting the expanded form of chemical potential (Equation 5.16.3):

$$\begin{aligned} -k_B T \sum_j \ln\left(\frac{q_i}{N_i}\right)\nu_j &= 0 \\ \sum_j \ln\left(\frac{q_i}{N_i}\right)\nu_j &= 0 \\ \sum_j \nu_j[\ln(q_j) - \ln(N_j)] &= 0 \end{aligned}$$

For the reaction in Equation 5.16.1:

$$\begin{aligned}&[\nu_C \ln(q_C) - \nu_C \ln(N_C)] + [\nu_D \ln(q_D) - \nu_D \ln(N_D)] \\ &- [\nu_A \ln(q_A) - \nu_A \ln(N_A)] - [\nu_B \ln(q_B) - \nu_B \ln(N_B)] = 0\end{aligned}$$

This equation simplifies to

$$\frac{(q_C)^{\nu_C}(q_D)^{\nu_D}}{(q_A)^{\nu_A}(q_B)^{\nu_B}} = \frac{(N_C)^{\nu_C}(N_D)^{\nu_D}}{(N_A)^{\nu_A}(N_B)^{\nu_B}}$$

By dividing all terms by volume, and noting the relationship $\frac{N_A}{V} = \frac{\#molecules}{volume} = \rho_A = [A]$ where ρ is referred to a number density, the following equation is obtained:

$$K_c = \frac{\rho_C^{\nu_C}\rho_D^{\nu_D}}{\rho_A^{\nu_A}\rho_B^{\nu_B}} = \frac{(q_C/V)^{\nu_C}(q_D/V)^{\nu_D}}{(q_A/V)^{\nu_A}(q_B/V)^{\nu_B}} \tag{5.16.4}$$

Hence, knowledge of the molecular partition function for all species in the reaction will ensure the calculation of the equilibrium constant.

Example 5.16.1: Reacting Diatomic Molecules

Calculate the equilibrium constant (K_c) for the reaction of $\mathbf{H_2\,(g)}$ and $\mathbf{Cl_2\,(g)}$ at 650 K.

$$\mathbf{H_2\,(g) + Cl_2\,(g) \rightleftharpoons 2\,HCl\,(g)}$$

Solution

We will use Equation 5.16.4 that uses Molecular Partition Functions to evaluate K_c.

$$K_c(T) = \frac{\left(\frac{q_{HCl}}{V}\right)^2}{\left(\frac{q_{H_2}}{V}\right)\left(\frac{q_{Cl_2}}{V}\right)} \tag{5.16.5}$$

This equation is expanded into the rotational, vibrational, translational and electronic molecular partition functions of each species.

$$K_c(T) = \frac{\left(\frac{q_{\text{trans HCl}}q_{rot\text{HCl}}q_{vib\text{HCl}}q_{elec\text{HCl}}}{V}\right)^2}{\left(\frac{q_{\text{trans}H_2}q_{\text{rot }H_2}q_{vib\,H_2}q_{elec\,H_2}}{V}\right)\left(\frac{q_{\text{trans}Cl_2}q_{\text{rot }Cl_2}q_{vib\,Cl_2}q_{elec\,Cl_2}}{V}\right)}$$

A simple problem solving strategy for finding equilibrium constants via statistical mechanics is to separate the equation into the molecular partition functions of each of the reactant and product species, solve for each one, and recombine them to arrive at a final answer (e.g., for **HCl**.

$$\frac{q_{HCl}}{V} = \underbrace{\left(\frac{2\pi m k_B T}{h^2}\right)^{3/2}}_{\text{translation}} \times \underbrace{\frac{2k_BT\mu r_e^2}{\sigma\hbar^2}}_{\text{rotation}} \times \underbrace{\frac{1}{1-\exp\left(\frac{-h\nu}{k_BT}\right)}}_{\text{vibration}} \times \underbrace{g_1 \exp\left(\frac{D_0}{k_BT}\right)}_{\text{electronic}}$$

To simplify the calculations of molecular partition functions, the characteristic temperature of rotation (Θ_r) and vibration (Θ_ν) are used.

$$\frac{q_{HCl}}{V} = \left(\frac{2\pi m k_B T}{h^2}\right)^{3/2} \times \frac{T}{\sigma\Theta_r} \times \frac{1}{1-\exp\left(\frac{-\Theta_\nu}{T}\right)} \times g_1 \exp\left(\frac{D_0}{RT}\right) \tag{5.16.6}$$

These values are constants that incorporate the physical constants found in the rotational and vibrational partition functions of the molecules. Tabulated values of Θ_r and Θ_ν for select molecules can be found here.

Species	Θ_ν (K)	Θ_r (K)	D_0 (kJ mol^{-1})
$\mathbf{Cl_2\,(g)}$	6125	0.351	239.0
$\mathbf{H_2\,(g)}$	808	87.6	431.9
$\mathbf{HCl\,(g)}$	4303	15.2	427.7

We need to evaluate Equation 5.16.6 for each species then then evaluate Equation 5.16.5 directly.

For $\mathbf{HCl}$:

$$\frac{q_{HCl}}{V} = \left(\frac{2\pi \left(2.1957 \times 10^{-24}\ \text{kg}\right) \left(1.38065 \times 10^{-23} \text{JK}^{-1}\right) (650K)}{\left(6.62607 \times 10^{-34} \text{Js}\right)^2} \right)^{3/2} \times \frac{650\ \text{K}}{(1)(15.2\ \text{K})} \times \frac{1}{1 - \exp\left(\frac{-4303\ \text{K}}{650\ \text{K}}\right)} \times (1) \exp\left(\frac{427,700 \text{Jmol}^{-1}}{\left(8.3145\ \text{J K mol}^{-1}\right)(650\ \text{K})} \right)$$

$$\frac{q_{HCl}}{V} = \left(1.4975 \times 10^{35}\ \text{m}^{-3}\right) (42.76)(1.0013)\left(2.3419 \times 10^{34}\right)$$

For $\mathbf{H_2}$:

$$\frac{q_{H_2}}{V} = \left(\frac{2\pi \left(1.2140 \times 10^{-25}\ \text{kg}\right) \left(1.38065 \times 10^{-23} \text{JK}^{-1}\right) (650\ \text{K})}{\left(6.62607 \times 10^{-34} \text{Js}\right)^2} \right)^{3/2} \times \frac{650\ \text{K}}{(2)(87.6\ \text{K})} \times \frac{1}{1 - \exp\left(\frac{-808\ \text{K}}{650\ \text{K}}\right)} \times (1) \exp\left(\frac{431,900 \text{Jmol}^{-1}}{\left(8.3145\ \text{J Kmol}^{-1}\right)(650\ \text{K})} \right)$$

$$\frac{q_{H_2}}{V} = \left(1.9468 \times 10^{33}\ \text{m}^{-3}\right) (3.71)(1.41)\left(5.0942 \times 10^{34}\right)$$

For $\mathbf{Cl_2}$:

$$\frac{q_{Cl_2}}{V} = \left(\frac{2\pi \left(4.2700 \times 10^{-24}\ \text{kg}\right) \left(1.38065 \times 10^{-23} \text{JK}^{-1}\right) (650K)}{\left(6.62607 \times 10^{-34} \text{Js}^2\right.} \right)^{3/2} \times \frac{650\ \text{K}}{(2)(0.351\ \text{K})} \times \frac{1}{1 - \exp\left(\frac{-6125\ \text{K}}{650\ \text{K}}\right)} \times (1) \exp\left(\frac{239,000 \text{Jmol}^{-1}}{\left(8.3145\ \text{J K mol}^{-1}\right)(650\ \text{K})} \right)$$

$$\frac{q_{Cl_2}}{V} = \left(5.4839 \times 10^{35}\ \text{m}^{-3}\right) (925.9)(1.00)\left(1.606 \times 10^{19}\right)$$

Combining the terms from each species, the following expression is obtained:

$$\begin{aligned} K_c &= \frac{\left(1.9468 \times 10^{33}\ \text{m}^{-3}\right)^2}{\left(1.9468 \times 10^{33}\ \text{m}^{-3}\right)\left(5.4839 \times 10^{35}\ \text{m}^{-3}\right)} \times \frac{(42.76)^2}{(3.71)(925.9)} \times \frac{(1.0013)^2}{(1.41)(1.00)} \times \frac{\left(2.3419 \times 10^{34}\right)^2}{\left(1.606 \times 10^{19}\right)\left(5.0942 \times 10^{34}\right)} \\ &= (0.003550)(0.1333)(0.711)\left(6.7037 \times 10^{14}\right) \\ &= \left(2.26 \times 10^{11}\right) \end{aligned}$$

At 650 K, the reaction between $\mathbf{H_2}\,(\mathbf{g})$ and $\mathbf{Cl_2}\,(\mathbf{g})$ proceeds spontaneously towards the products. From a statistical mechanics point of view, the product $\mathbf{HCl}\,(\mathbf{g})$ molecule has more states accessible to it than the reactant species. The spontaneity of this reaction is largely due to the electronic partition function: two very strong H—Cl bonds are formed at the expense of a very strong H—H bond and a relatively weak Cl—Cl bond.

This page titled 5.16: Equilibrium Constants in Terms of Partition Functions is shared under a CC BY-SA 4.0 license and was authored, remixed, and/or curated by Wikipedia via source content that was edited to the style and standards of the LibreTexts platform.

- **26.8: Equilibrium Constants in Terms of Partition Functions** by Wikipedia is licensed CC BY-SA 4.0. Original source: https://en.wikibooks.org/wiki/Statistical_Thermodynamics_and_Rate_Theories/Chemical_Equilibrium.

5.17: Statistical Mechnanical Transition State Theory

5.17.1: Introduction

From transition state theory the rate constant is estimated as on a per molecule basis for a reaction of the form $\mathbf{A + BC \longrightarrow Products}$ is :

$$k = \kappa \frac{k_B T}{h} K^{\ddagger}[A][BC] \tag{5.17.1}$$

or

$$k = \kappa \frac{RT}{h} K^{\ddagger}[A][BC] \tag{5.17.2}$$

on a molar basis. Where $K^{\ddagger}$ is concentration equilibrium constant between the transition state and reactants. Thus, to formulate this in terms of statistical mechanics we need a statistical expression for the equilibrium constant.

5.17.2: Accounting for the changes upon forming the transition state

It seems straight forward to substitute in the expression for the statistical mechanical equilibrium constant:

$$K_c = \frac{q_{ABC^{\ddagger}}/V}{(q_A/V)(q_{BC}/V)}. \tag{5.17.3}$$

However, the complications become clear when we expand this out to the different degrees of freedom, using the more compact notation $q^{\ddagger}$ for the transition state species partition functions and subscripts e for electronic, v for vibrational, r for rotational and t for the translational degrees of freedom:

$$K^{\ddagger} = V \frac{q_e^{\ddagger} q_v^{\ddagger} q_r^{\ddagger} q_t^{\ddagger}}{q_{Ae} q_{Av} q_{Ar} q_{At} q_{BCe} q_{BCv} q_{BCr} q_{BCt}}. \tag{5.17.4}$$

The ratio of the electronic partition functions can be separated out as the Boltzmann factor from the electronic contribution to the activation energy ΔE_o, the difference between the electronic energy of the transition state and the reactants:

$$K^{\ddagger} = V \frac{q_v^{\ddagger} q_r^{\ddagger} q_t^{\ddagger}}{q_{Av} q_{Ar} q_{At} q_{BCv} q_{BCr} q_{BCt}} exp\left(\frac{-\Delta E_o}{RT}\right). \tag{5.17.5}$$

The transition state has only 3 translational degrees of freedom, while there are 6 for the reactants.

$$q_{\text{trans}} = \left(\frac{2\pi m k T}{h^2}\right)^{3/2} V = \frac{V}{\Lambda^3} \tag{5.17.6}$$

Substituting this in and realizing that $(m_A + m_{BC})/(m_A m_{BC}) = 1/\mu$ we get:

$$K^{\ddagger} = \frac{q_r^{\ddagger} q_v^{\ddagger}}{q_{Ar} q_{Av} q_{BCr} q_{BCv}} \left(\frac{h^2}{2\pi \mu k_B T}\right)^{3/2} exp\left(\frac{-\Delta E_o}{RT}\right). \tag{5.17.7}$$

With an estimate of the geometry of the transition state the rotational and vibrational partition functions can be estimated, taking care not to count motion along the reaction coordinate as a vibration. The geometries of the reactants are known so the rotational and vibrational partition functions can be calculated.

In the unimolecular case because the transition state and the reactant have the same mass the translational partition functions for the transition state and the reactant are the same and they cancel out. Thus for this calling the reactant A we have:

$$K^{\ddagger} = \frac{q_r^{\ddagger} q_v^{\ddagger}}{q_{Ar} q_{Av}} exp\left(\frac{-\Delta E_o}{RT}\right). \tag{5.17.8}$$

If the transition state is substantially the same shape as the molecule, the rotational partitions functions may also cancel out. This would leave the vibrations that are not along the reaction coordinate.

This page titled 5.17: Statistical Mechnanical Transition State Theory is shared under a CC BY-NC-SA 4.0 license and was authored, remixed, and/or curated by Jonathan Gutow.

5.18: Chain Reactions

A large number of reactions proceed through a series of steps that can collectively be classified as a **chain reaction**. The reactions contain steps that can be classified as

- **initiation step** – a step that creates the intermediates from stable species
- **propagation step** – a step that consumes an intermediate, but creates a new one
- **termination step** – a step that consumes intermediates without creating new ones

These types of reactions are very common when the intermediates involved are radicals. An example, is the reaction

$$H_2 + Br_2 \rightarrow 2HBr$$

The observed rate law for this reaction is

$$\text{rate} = \frac{k[H_2][Br_2]^{3/2}}{[Br_2] + k'[HBr]} \tag{5.18.1}$$

A proposed mechanism is

$$Br_2 \underset{k_{-1}}{\overset{k_1}{\rightleftharpoons}} 2Br^{\cdot} \tag{5.18.2}$$

$$2Br^{\cdot} + H_2 \underset{k_{-2}}{\overset{k_2}{\rightleftharpoons}} HBr + H^{\cdot} \tag{5.18.3}$$

$$H^{\cdot} + Br_2 \xrightarrow{k_3} HBr + Br^{\cdot} \tag{5.18.4}$$

Based on this mechanism, the rate of change of concentrations for the intermediates ($H^{\cdot}$ and $Br^{\cdot}$) can be written, and the steady state approximation applied.

$$\frac{d[H^{\cdot}]}{dt} = k_2[Br^{\cdot}][H_2] - k_{-2}[HBr][H^{\cdot}] - k_3[H^{\cdot}][Br_2] = 0$$

$$\frac{d[Br^{\cdot}]}{dt} = 2k_1[Br_2] - 2k_{-1}[Br^{\cdot}]^2 - k_2[Br^{\cdot}][H_2] + k_{-2}[HBr][H^{\cdot}] + k_3[H^{\cdot}][Br_2] = 0$$

Adding these two expressions cancels the terms involving k_2, k_{-2}, and k_3. The result is

$$2k_1[Br_2] - 2k_{-1}[Br^{\cdot}]^2 = 0$$

Solving for $Br^{\cdot}$

$$Br^{\cdot} = \sqrt{\frac{k_1[Br_2]}{k_{-1}}}$$

This can be substituted into an expression for the $H^{\cdot}$ that is generated by solving the steady state expression for $d[H^{\cdot}]/dt$.

$$[H^{\cdot}] = \frac{k_2[Br^{\cdot}][H_2]}{k_{-2}[HBr] + k_3[Br_2]}$$

so

$$[H^{\cdot}] = \frac{k_2\sqrt{\frac{k_1[Br_2]}{k_{-1}}}[H_2]}{k_{-2}[HBr] + k_3[Br_2]}$$

Now, armed with expressions for $H^{\cdot}$ and $Br^{\cdot}$, we can substitute them into an expression for the rate of production of the product HBr:

$$\frac{d[HBr]}{dt} = k_2[Br^{\cdot}][H_2] + k_3[H^{\cdot}][Br_2] - k_{-2}[H^{\cdot}][HBr]$$

After substitution and simplification, the result is

$$\frac{d[HBr]}{dt} = \frac{2k_2\left(\frac{k_1}{k_{-1}}\right)^{1/2}[H_2][Br_2]^{1/2}}{1+\frac{k_{-1}}{k_3}\frac{[HBr]}{[Br_2]}}$$

Multiplying the top and bottom expressions on the right by $[Br_2]$ produces

$$\frac{d[HBr]}{dt} = \frac{2k_2\left(\frac{k_1}{k_{-1}}\right)^{1/2}[H_2][Br_2]^{3/2}}{[Br_2]+\frac{k_{-1}}{k_3}[HBr]}$$

which matches the form of the rate law found experimentally (Equation 5.18.1)! In this case,

$$k = 2k_2\sqrt{\frac{k_1}{k_{-1}}}$$

and

$$k' = \frac{k_{-2}}{k_3}$$

This page titled 5.18: Chain Reactions is shared under a CC BY-NC-SA 4.0 license and was authored, remixed, and/or curated by Jonathan Gutow.

- **12.9: Chain Reactions** by Patrick Fleming is licensed CC BY-NC-SA 4.0.

5.19: Chain Branching Explosions

5.19.1: Introduction

In addition to explosions that occur because heat generated in a reaction increases the rate of the reactions involved, it is also possible to have a radical reaction accelerate because some propagation steps increase the number of radicals. These steps are referred to as **chain branching steps**. The kinetics are similar to those in nuclear fission bombs where fission of a nucleus is initiated by collision with a neutron. Fissioning nuclei produce more than one neutron. Thus each fission event can trigger multiple new fissions, leading to rapid growth in the rate of fission events.

5.19.2: Hydrogen combustion and explosions

The seemingly simple combustion of hydrogen $2\,H_2 + O_2 \longrightarrow 2\,H_2O$serves to illustrate how this works. The reaction proceeds by a complex radical chain process. Some examples of the reactions involved are:

Initiation:

$$H_2 + \cdot O_2 \cdot \longrightarrow HO_2 \cdot + H\cdot$$

$$H_2 \longrightarrow 2\,H\cdot$$

Propagation:

$$H\cdot + \cdot O_2 \cdot \longrightarrow \cdot O \cdot + HO\cdot$$

$$H_2 + HO\cdot \longrightarrow H\cdot + H_2O$$

Branching

$$H_2 + \cdot O \cdot \longrightarrow H\cdot + HO\cdot$$

Termination

$$H\cdot + \text{wall} \longrightarrow \tfrac{1}{2}\,H_2$$

$$H\cdot + HO\cdot \longrightarrow H_2O$$

In the reactions above the fact that the ground state of O_2 has two unpaired electrons is acknowledged by indicating that it is a diradical (dots on either side). If all the radicals produced in each branching reaction start reaction chains of their own that include branching reactions the overall reaction rate accelerates leading to an explosion. Whether this occurs depends on the temperature and pressure of the sample. Two behaviors are seen: smooth reaction and explosion as shown in figure **5.19.1**.

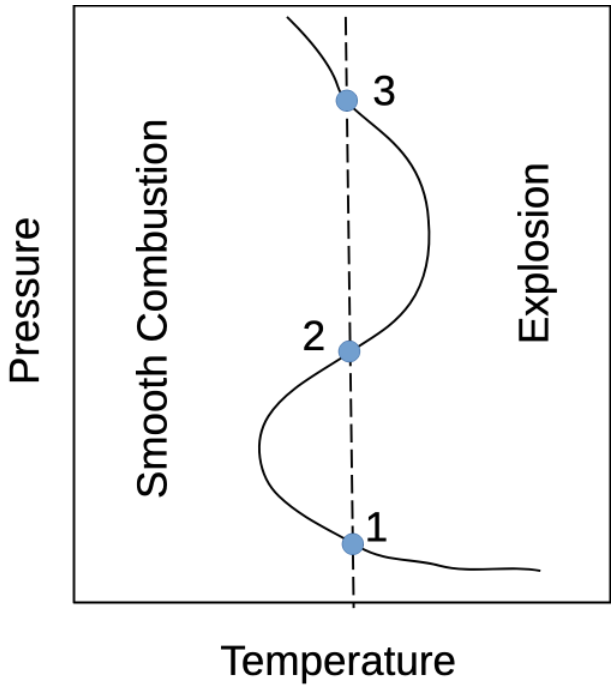


Figure 5.19.1: Cartoon of explosive behavior dependence on pressure and temperature. Smooth combustion occurs to the left of the curve and explosion to the right. The point 1, 2 and 3 indicate explosion limits 1, 2 and 3 where at the indicated temperature the reaction shifts between smooth combustion and explosive behavior.

- At low pressures radical termination on the walls dominates because a large fraction of the molecules in the sample travel to the walls before encountering each other. Higher temperatures are needed to generate enough radicals to get an explosion.
- If the temperature is low enough termination reactions (with the walls and other molecules) overwhelm the branching and only smooth combustion is observed.
- If the temperature is high enough explosive behavior is observed because radical and energy production is high enough to cause the reaction to accelerate.
- In many cases including the combustion of H_2 there is an intermediate temperature region where the reaction cycles between smooth combustion and explosion multiple times as the pressure increases as indicated by the dashed line in figure 5.19.1. The lowest pressure at which explosion is seen is referred to as the **first explosion limit**, the pressure at which the system reverts to smooth combustion is referred to as the **second explosion limit**, where it reverts back to explosive behavior is called the **third explosion limit** as shown in the figure.
  - Below the first explosion limit we are in the regime where termination steps (collisions with the walls) dominate.
  - Between the first explosion limit and the second explosion limit radicals can react and branch before they encounter the walls or species they can react with in a termination step.
  - Between the second and third explosion limits molecular density is high enough that more radicals encounter each other in termination steps or react to form long lived species that can travel to the walls and be quenched (terminated).
  - Above the third explosion limit diffusion to the walls becomes slow reducing its contribution to termination and explosive growth of radical chains takes over again.
- At some point the temperature is also high enough that the thermal energy released by the reaction is a significant accelerant of the rates and the explosion is also a thermal explosion.

5.19.3: References

1. This section is based on examples from Atkins, *Physical Chemistry*, 2nd Ed. (W. H. Freeman and Co. San Francisco, 1982) Section 27.4.

This page titled 5.19: Chain Branching Explosions is shared under a CC BY-NC-SA 4.0 license and was authored, remixed, and/or curated by Jonathan Gutow.

5.20: Kinetics of Chain Polymerization

The polymerization of alkenes occurs in a very different way than monomers that undergo condensation reactions. Whether it occurs through an anionic, cationic, or radical mechanism, polymerization of alkenes involves a chain reaction. Chain reactions are classically illustrated by radical chemistry, so we will look at a treatment of radical chain polymerization to see some of the factors that influence polymerization rates.

A typical radical polymerization starts with the thermal decomposition of a radical initiator to provide two radicals. The rate of decomposition depends only on the decomposition rate constant and the concentration of the initiator.

$$\mathrm{I} \xrightarrow{k_d} 2\,\mathrm{R}^{\cdot}$$

$$\frac{-\,d[\mathrm{I}]}{dt} = \frac{1}{2}\frac{d[\mathrm{R}^{\cdot}]}{dt} = k_d[\mathrm{I}]$$

Once the radicals have been generated, they are able to undergo radical addition to a monomer double bond. Of course, radical addition to a double bond results in a new radical where the double bond used to be. Although this is formally a radical propagation step, in polymer chemistry it is termed the initiation step, because it is the first time a monomer has undergone radical addition. This step consumes the first monomer and produces a new radical species which will become the growing radical chain. It requires a collision between the radical and a monomer, so the rate of initiation depends on those two concentrations and the chain initiation rate constant, k_i.

$$\mathrm{R}^{\cdot} + \mathrm{M} \xrightarrow{k_i} \mathrm{M}^{\cdot}$$

$$\frac{-\,d[\mathrm{M}]}{dt} = \frac{d[\mathrm{M}^{\cdot}]}{dt} = k_i[\mathrm{R}^{\cdot}][\mathrm{M}]$$

That rate law depends on a reactive intermediate. It's not a very helpful rate law, because the reactive intermediate isn't something that we have directly measured out and added to the reaction, and it might not even occur at high enough levels that we can measure its concentration as the reaction progresses. We usually look for ways to express the rate law in ways that do not include reactive intermediates. In this particular situation, the way of getting around this situation is to assume that the decomposition of the initiator is the rate determining step. Making the radicals in the first place is probably the slow part because it is heavily dependent on bond breaking, which is energy intensive. Once we have radical, it probably undergoes addition to a monomer fairly quickly, initiating chain growth. If that's true, we can assume that the chain initiation step proceeds very quickly afterward, so that the rate really depends only on the rate of the decomposition step.

$$k_i >> k_d$$

$$\frac{d[\mathrm{M}^{\cdot}]}{dt} = \frac{d[\mathrm{R}^{\cdot}]}{dt} = 2\,k_d[\mathrm{I}]$$

In practice, polymer chemists add another factor to the rate law. This factor, f, takes into account the fact that only some of the radicals from the initiator actually react with monomers to initiate growing chains. The rest decay through some other side reactions. Usually, f is assumed to be around 0.5.

$$\frac{d[\mathrm{M}^{\cdot}]}{dt} = 2\,f\,k_d[\mathrm{I}]$$

$$f = 0.3 \text{ to } 0.8$$

Once the first monomer has been initiated into a radical, it can react with another monomer to enchain it and make a new radical. This is the principal propagation step of the chain reaction. That step will keep repeating, adding more monomers into the chain. The rate constant for this step, k_{prop} or k_p, is identical no matter how many monomers have been enchained, but is distinct from k_i because of the different nature of the radical intermediates in the two different steps. For example, the radical obtained from addition to styrene looks pretty similar whether it is the first in the chain or the tenth. Each time, the rate of consumption of monomer depends on the propagation rate constant, the concentration of the monomer, and the concentration of the propagating radical. Notice that in the rate law we just write that propagating radical the same way (M dot) no matter how long the chain grows.

$$M^{\cdot} + M \xrightarrow{k_p} M\text{-}M^{\cdot}$$

$$-\frac{d[M]}{dt} = k_p [M][M^{\cdot}]$$

There is one last process, or group of processes, to complete the chain reaction cycle. In termination, two radicals combine in some way to form closed-shell products. There are a variety of ways that can happen in a radical polymerization. The simplest event conceptually is coupling, in which two radical chains come together and form a bond. That idea is shown below.

$$M^{\cdot} + M^{\cdot} \xrightarrow{k_t} M\text{-}M$$

$$-\frac{d[M^{\cdot}]}{dt} = 2\frac{d[M\text{-}M]}{dt} = 2k_t [M^{\cdot}]^2$$

Of course, that rate depends on the termination rate constant and the concentrations of both growing chains. The same would be true if the reaction terminated by conproportionation, in which one radical abstracted an alpha hydrogen from the other, forming one saturated and one unsaturated product.

Once again, these last two rates -- of propagation and of termination -- depend on concentrations of reactive intermediates, which we do not typically know. This time we will use a very standard assumption, which is that the concentration of this reactive species remains constant, being consumed as soon as it is generated. The usual way that we apply the steady state approximation is to assume zero change in concentration of the reactive intermediate. That means that the sum of all the rates for processes generating the intermediate equal the sum of all the rates consuming the intermediate. In polymer chemistry, we take a slight shortcut, and just assume that the rate of appearance of the radical in the first place equals its rate of disappearance. We already have expressions for both of those rates.

$$\text{Rate}_{term} = \text{Rate}_{init}$$

$$2k_t [M^{\cdot}]^2 = 2f k_d [I]$$

$$[M^{\cdot}] = \left(\frac{f k_d [I]}{k_t}\right)^{1/2}$$

By rearranging, we can get an expression for the reactive chain end concentration. Then we can just substitute the result into our expression for propagation rate:

$$-\frac{d[M]}{dt} = k_p [M][M^{\cdot}]$$

$$= k_p [M]\left(\frac{f k_d [I]}{k_t}\right)^{1/2}$$

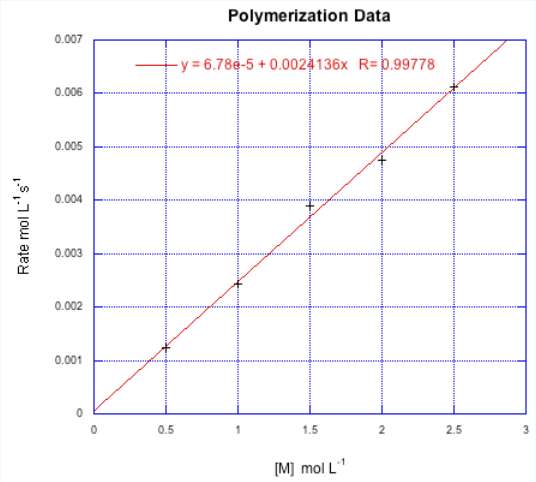
The result sums up the factors that control the growth rate for the polymer. The growth rate increases linearly with the concentration of monomer, and as the square root of the initiator concentration. The rest of the factors are just constants, so we can think of the rate law as one combined constant and those two concentration dependences. Sometimes an aggregate constant of this type is just designated k'.

Note that the propagation rate varies linearly with the concentration of growing chains, but that the termination rate varies with square of the concentration of growing chains. That difference is significant, and it underlies the strategy of living polymerization, which is to keep the concentration of growing chains low. Doing so has the adverse affect of slowing the rate of propagation, but the effect on the termination rate is much greater, making this trade-off worth it to achieve enhanced molecular weight control.

Example 5.20.1

Suppose the following data were obtained for a radical polymerization conducted at various starting concentrations of monomer. If all of the data were conducted at an initiator concentration of 0.25 mmol L^{-1}, calculate k'.

Solution



Kinetics can also be used to establish a theoretical polymer chain length. This quantity is called kinetic chain length, represented by "vee bar". In principle, it's just the ratio of the chain propagation rate to the chain initiation rate. That should tell us the number of monomers per each chain initiated. Because of our earlier assumption about the initiation rate equaling the termination rate, we can substitute the terms for those two rates and simplify the result.

$$\bar{\nu} = \frac{\text{Rate}_{\text{prop}}}{\text{Rate}_{\text{init}}}$$

but at steady state $\text{Rate}_{\text{init}} = \text{Rate}_{\text{term}}$

$$\bar{\nu} = \frac{\text{Rate}_{\text{prop}}}{\text{Rate}_{\text{term}}}$$

$$\bar{\nu} = \frac{k_p[\text{M}][\text{M}^\cdot]}{2k_t[\text{M}^\cdot]^2} = \frac{k_p[\text{M}]}{2k_t[\text{M}^\cdot]}$$

Substituting our earlier expression for the concentration of the growing radical chain ends gives a new expression.

$$\bar{\nu} = \frac{k_p[\text{M}]}{2fk_t k_d[\text{I}]^{1/2}}$$

*****

Correct expression based on earlier algebra:

$$\bar{\nu} = \frac{k_p[M]}{2(fk_t k_d[I])^{1/2}} \tag{5.20.1}$$

*****

That means that we can theoretically control the length of polymer chains, because the average length should vary linearly with the concentration of monomer and inversely with the square root of initiator concentration.

As chain reactions, cationic and anionic polymerizations have some characteristics in common with radical polymerizations. One key difference is that the initiator does not fragment into two pieces, each capable of initiating a chain; instead, one added initiator starts polymerization of one chain, without the prior decompositions step seen in radical reactions. Also, termination steps in radical reactions are dominated by radical recombinations (as well as other variations), but in anionic and cationic terminations it is more likely that the growing chain encounters an impurity and reacts with that.

Example 5.20.2

Given that for a cationic polymerization:

$$\text{Rate}_{\text{init}} = k_i\,[\text{M}][\text{I}] \text{ and } \text{Rate}_{\text{term}} = k_t[\text{M}^+]$$

Provide a steady state expression for the concentration of growing cationic chain.

Example 5.20.3

If the propagation step in a cationic polymerization is written as follows:

$M^+ + M \rightarrow M\text{-}M^+$

Provide the rate expression for cationic polymerization.

Example 5.20.4

By analogy to radical polymerization, the kinetic chain length in cationic polymerization can be expressed as the ratio of propagation rate to initiation rate. Provide an expression in terms of constants and known concentrations.

Example 5.20.5

****Units need to be fixed: k_t and k_p have units of $M^{-1}s^{-1}$ ****

In a living polymerization, chain length simplifies to $[M]_0/[I]_0$ because all initiation leads to polymerization and there are no terminations steps. Given a radical polymerization with $[M]_0$ = 4.5 M and $[I]_0$ = 1.25 mM, compare chain length in the following situations:

a. a living polymerization
b. a non-living polymerization with f = 0.5; $k_p = k_t$ = 0.003 s^{-1}; k_d = 0.0001 s^{-1}.
c. a non-living polymerization with f = 0.5; k_p = 0.003 s^{-1}; k_t = 0.3 s^{-1}; k_d = 0.0001 s^{-1}.
d. a non-living polymerization with f = 0.5; k_p = 0.003 s^{-1}; k_t = 0.003 s^{-1}; k_d = 0.1 s^{-1}.

This page titled 5.20: Kinetics of Chain Polymerization is shared under a CC BY-NC 3.0 license and was authored, remixed, and/or curated by Chris Schaller via source content that was edited to the style and standards of the LibreTexts platform.

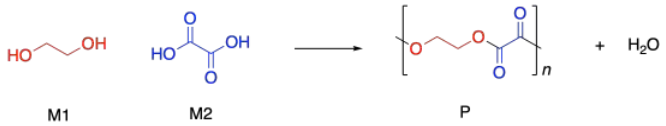
- **3.3: Kinetics of Chain Polymerization** by Chris Schaller is licensed CC BY-NC 3.0. Original source: https://employees.csbsju.edu/cschaller/Advanced/Polymers/Polycontents.htm.

5.21: Kinetics of Step-Growth Polymerization

KP2. Kinetics of Step-Growth Polymerization

It is important to understand how reactions proceed over time. This information can tell us how long it will take for a polymer to reach an optimum length. It can also provide insight into how the polymerization occurs, just as kinetics can provide insight into other reaction mechanisms.

Condensation polymers grow through a a step-growth process. The reaction generally involves substitution at a carboxyloid. For example, polyester formation often involves the substitution of an alcohol functional group at a carboxylic acid, making an ester. The drawing below illustrates that action using ethylene glycol and oxalic acid, to use common names prevalent in industry. Oxalic acid is not typically used in making polyesters, but it is drawn here as a very simple example structure.



M1 M2 P

If you know some basic kinetics, you know that we can express the rate of a reaction as the rate of change of product concentration per change in time. In this case, the product is the polymer, abbreviated P. Alternatively, we could express the rate of the reaction as the rate of change of monomer concentration per change in time. Just by looking at the equation of reaction, we expect that every time a polymer molecule is made, a monomer molecule is used up. In this case, we have a co-polymer, made of two different monomers, so that's why we could express the reaction rate as the rate of change of either monomer concentration. The negative sign in the rate suggests we are looking at the rate of disappearance of monomer; as polymer appears, monomer disappears.

$$\text{Rate} = \frac{d[P]}{dt}$$

$$= -\frac{d[M1]}{dt}$$

$$= -\frac{d[M2]}{dt}$$

If you know something about organic reaction mechanisms, you may know that the very first step in an esterification is the donation of a lone pair from an alcohol oxygen on the diol to a carbonyl carbon on the dicarboxylic acid. (It could actually be the second step, but we'll get to that later.) That first step in the mechanism is an elementary reaction. All of the other steps you would draw in a mechanism are also elementary reactions. The nice thing about elementary reactions is that we always know the rate law of each one: it's a rate constant times the concentrations of all of the species leading into that step. In this case, this first step is also the rate-determining step, so the entire reaction is governed by the rate law of that first step. It requires both monomers, so we get a simple rate law.

$$\text{Rate} = k\,[M1]\,[M2]$$

$$\text{but if } [M1] = [M2] = [M]$$

$$\text{then Rate} = k\,[M]^2$$

Note that, based on the stoichiometry (the ratio of monomers in the equation of reaction), we would probably run this polymerization with equal amounts of diol and dicarboxylic acid. Instead of worrying about M1 and M2 separately, we can call them both [M].

So, what we have here is a simple second-order rate law. This form of the rate law is called the differential rate law, because it is expressed in terms of the rate of change of one thing with the rate of change of the other. If that isn't exactly what you are interested in, and you just want to see what happens to concentrations over time, you may want to integrate this expression to obtain the integrated from of the rate law.

$$\text{Rate} = -\frac{d[M]}{dt} = k[M]^2$$

$$-\frac{d[M]}{[M]^2} = k\,dt$$

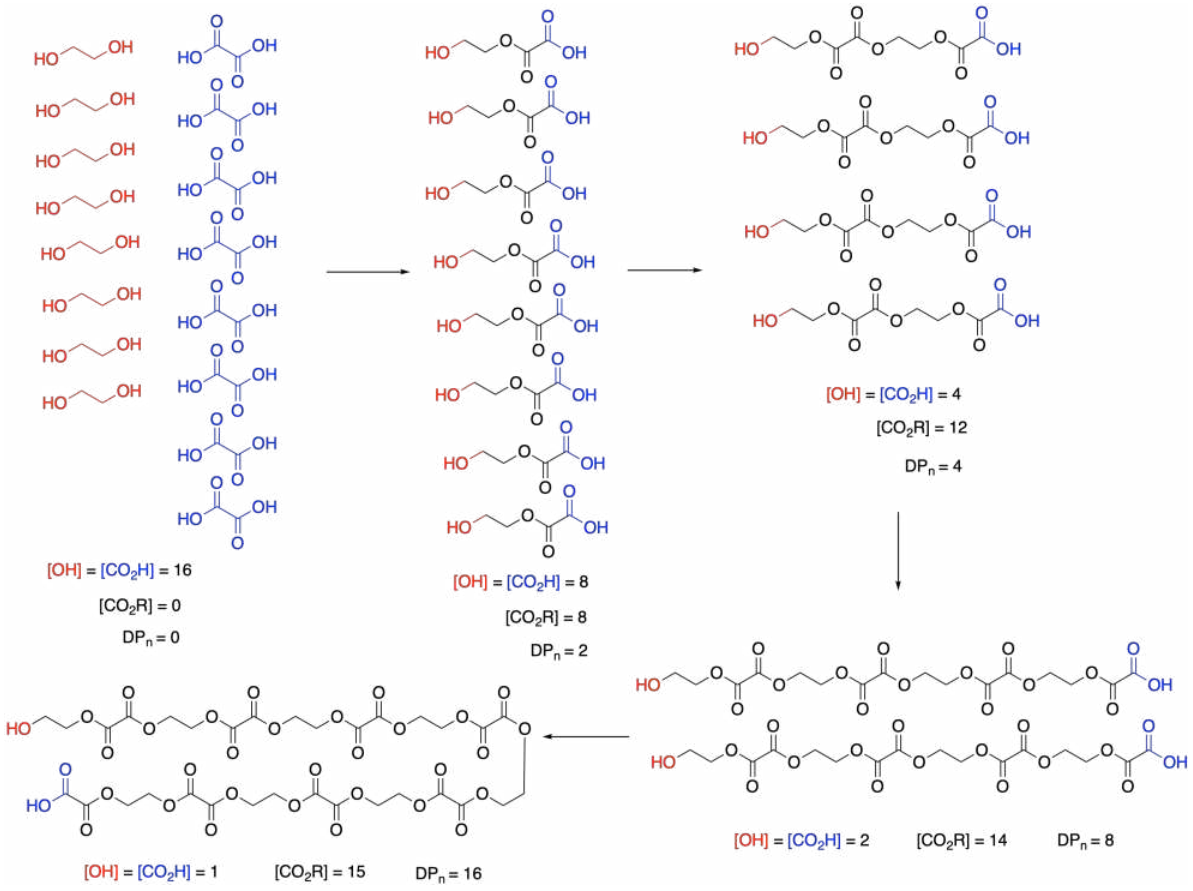
Integrating:

$$\int_{c_0}^{c_t} -\frac{d[M]}{[M]^2} = \int_{t=0}^{t} k\,dt$$

$$\frac{1}{[M]} - \frac{1}{[M]_0} = k\,t$$

If we were to measure monomer concentration periodically during the polymerization and plot its inverse over time, we would obtain a straight line. The slope of the line would be the rate constant, and the intercept would reflect the inverse of the monomer concentration with which we had started the reaction.

At this point, we need to pause and talk about what we actually mean by monomer concentration. Because of a very specific feature of condensation polymerizations, it isn't really the concentration of ethylene glycol or oxalic acid. Take a look at this drawing of this step-growth process and we will talk about why that is.



Remember that, in step-growth polymerization, the majority of molecules are probably reacting at roughly similar rates. Two monomers link together to form dimers, two dimers form tetramers, two tetramers form octamers, and so on. It won't go as perfectly as we see in this picture; there will inevitably be some stragglers that throw the averages off. But notice what this means: the monomers disappear right away. Nobody is really interested in how quickly the monomers turn into dimers. They want to know how the gowth of the polymer chain is progressing.

So, in the above expression, [M] doesn't refer to the concentrations of those two monomers at all. It refers to the concentration of the reactive functional groups in those monomers. After all, once the monomers are gone, the same esterification reaction keeps happening, and it's really the concentration of alcohol and carboxylic acid groups that matters, whether they are found on monomers, dimers, tertramers, or whatever. In these rate expressions, sometimes people will explicitly use [OH] and [CO_2H] in the rate expression, underscoring that they are really following the disappearance of those functional groups.

And notice what's happening to those functional groups. Their concentration is smoothly dropping over time. Furthermore, ester concentration, representing the new functional group in the polymer, is growing in at the same rate. [OH] and [CO_2H] drop by 8 (or in half) in the first step; [CO_2R] increases by 8, and so on. SO the rate of consumption of reactant functional groups equals the rate of appearance of product functional groups.

The other thing we are interested in here is the degree of polymerization: the number of monomers incorporated into the chain. The polymer is growing at a certain rate, but how long is it getting? Just looking at the simple scheme of polymer growth above, we see the average degree of polymerization increasing (written as *DP* or sometimes as X_n; a bar over the symbol signals that we are looking at an average). If you look carefully, you will see that the degree of polymerization is always the original monomer concentration divided by the remaining monomer concentration. That turns out to be a very important relationship.

$$\text{degree of polymerization } DP_n = \bar{X}_n = \frac{[M]_0}{[M]}$$

Note that this relationship is just the inverse of the fraction of monomer remaining (or, really, the fraction of those monomer functional groups left over).

$$\text{fraction monomer remaining} = \frac{[M]}{[M]_0}$$

The opposite quantity is the fraction of monomer converted. That describes the functional groups already converted into esters. Because we are dealing with fractions, the fraction converted is just one minus the fraction remaining. If we do a little algebra, we get a variation on that piece of information.

$$\text{fraction monomer converted } p = 1 - \frac{[M]}{[M]_0}$$

$$\text{or } 1 - p = \frac{[M]}{[M]_0}$$

$$\text{or } \frac{1}{1 - p} = \frac{[M]_0}{[M]}$$

Why did we do that last part? Because now we have arrived back at the expression for degree of polymerization. So, now we have an equivalent way of expressing degree of polymerization in terms of the fraction converted. This relationship is called the Carothers equation, in honor of Wallace Carothers, the DuPont chemist who invented nylon.

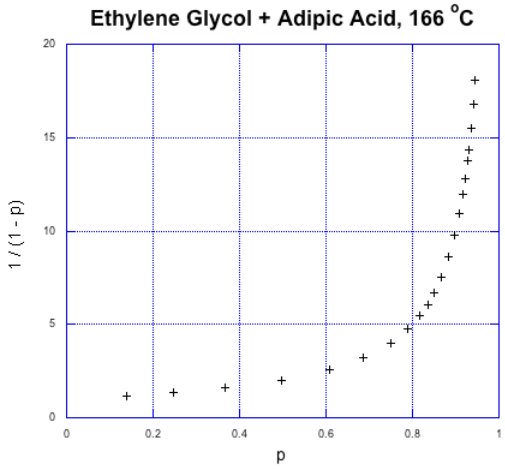
$$\text{but } \bar{X}_n = \frac{[M]_0}{[M]}$$

$$\bar{X}_n = \frac{1}{1 - p} \quad \text{(Carothers Equation)}$$

Problem KP2.1.

Predict the degree of polymerization if 75% of monomer end groups have been converted to polymer.

So, what does that relationship look like? Here's some data from Paul Flory, another DuPont chemist and Nobel laureate, obtained during the period between the World Wars when this kind of chemistry was just getting started (Flory, P. J. *J. Am. Chem. Soc.* **1937**, *59*, 466-470).



That's fraction converted on the x axis and the expression for degree of polymerization on the y axis. This is exponential growth. The degree of polymerization is starting to shoot upward dramatically. We already knew that from our introduction to step growth, but what stands out from the data is how a higher degree of polymerization, and high molecular weight, doesn't really occur until very late in the reaction. If we need high molecular weight condensation polymers, the chemistry better be pretty reliable; otherwise, if things go wrong, we'll be left with some short-chain goo instead of long-chain materials.

Now let's take these new relationships and look at them in the context of our second-order kinetics. We're starting with that same integrated rate law, but we have mulitplied everything on both sides of the equation by the starting monomer concentration. That's fair game in algebra, remember. The reason for doing that is to get a term that resembles our relationships that describe degree of polymerization.

$$\frac{[M]_0}{[M]} - \frac{[M]_0}{[M]_0} = [M]_0 k t$$

$$\frac{[M]_0}{[M]} - 1 = [M]_0 k t$$

$$\text{but} \quad p = 1 - \frac{[M]}{[M]_0}$$

$$\text{or} \quad 1 - p = \frac{[M]}{[M]_0}$$

$$\text{or} \quad \frac{1}{1 - p} = \frac{[M]_0}{[M]}$$

$$\text{so} \quad \frac{1}{1 - p} - 1 = [M]_0 k t$$

So far, we have taken the ratio we obtained in the first line and worked out its relationship to fraction converted, which we substituted in the last line. Now we bring in the Carothers equation to recall that this is really telling us how degree of polymerization changes over time. This relationship indicates the degree of polymerization should increase linearly over time.

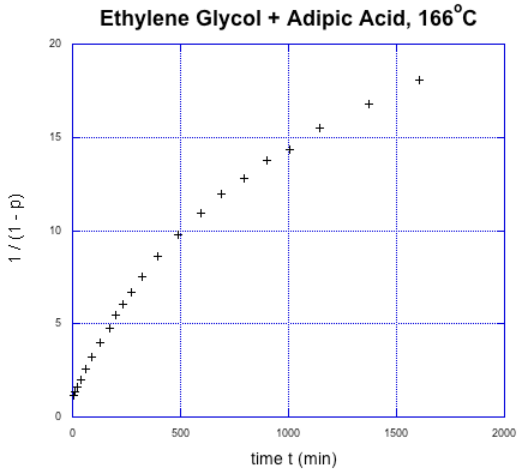
$$DP_n = X_n = \frac{[M]_0}{[M]}$$

$$\text{and} \quad \frac{[M]_0}{[M]} - 1 = [M]_0 k t$$

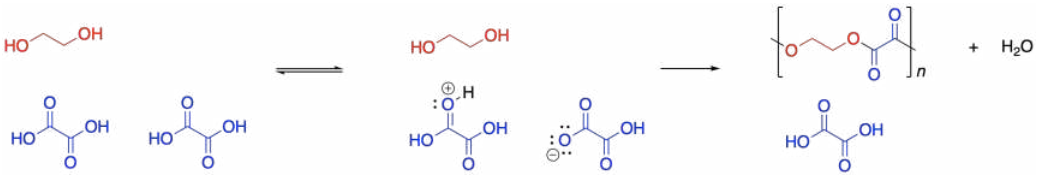
$$\text{so} \quad X_n - 1 = [M]_0 k t$$

This relationship indicates the degree of polymerization should increase linearly over time. Once again, we're going to use Flory's data to illustrate the relationship, using the fraction conversion data. He could measure that data easily, and knew how it was related

to degree of polymerization.



It was supposed to be linear. But don't worry; Flory knew what went wrong. You might know, too, if you remember a few things about substitution at carboxloids. The trouble is, we are dealing with a neutral nucleophile and a fairly unreactive electrophile. That reaction should be really slow. It isn't that slow, thoough, because it is self-catalyzed. One carboxylic acid monomer can activate another, making it a better electrophile.



That means the coupling of the alcohol with the carboxylic acid isn't the first elementary step of the reaction, but the second. Before the alcohol and carboxylic acid can come together, two carboxylic acids need to have collided already. That means we have a third order reaction. As it happens, the integrated form of a third order rate law isn't all that much more complicated, and we can do some similar algebra with it to see how the degree of polymerization would vary with time given this new information.

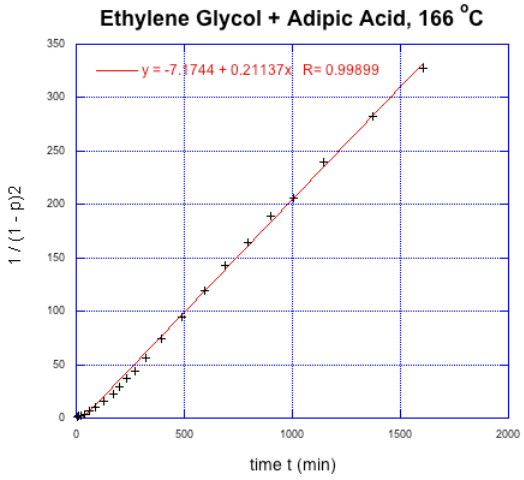
$$\frac{1}{[M]^2} - \frac{1}{[M]_0^2} = 2kt$$

$$\frac{[M]_0^2}{[M]^2} - \frac{[M]_0^2}{[M]_0^2} = 2[M]_0^2 kt$$

$$\frac{1}{(1-p)^2} - 1 = 2[M]_0^2 kt$$

We can take Flory's data again and give it this new treatment.

https://chem.libretexts.org/@go/page/547500



This time, we get a linear relationship. That correction illustrates one of the fundamental uses of kinetics, which is a tool that lets us probe how reactions happen. In this very specific case, kinetics showed that there was an extra (pre-rate determining) step in the reaction. In addition, we found that it is the square of the degree of polymerization that is increasing linearly with time.

Problem KP2.2.

Given an initial alcohol group concentration [M]0 = 17 M, determine the rate constant from Flory's data in $L^2mol^{-2}s^{-1}$.

Flory also established a statistical basis for predicting molecular weights and molecular weight distributions in polymers. For example, once we have the degree of polymerization, it is a simple step to calculate the approximate molecular weight. That's just the degree of polymerization times the molecular weight of the monomer; in other words, the number of monomers in the chain times the weight of each one. (This approach neglects any small molecules such as water that are lost during the condensation reaction.)

$M_n = DP \times M_0$

$M_n = M_0 / (1 - p)$

This is called the number average molecular weight. It's based on taking one average value for the chain length and converting that into the chain molecular weight. Of course, some chains may be much shorter (Flory actually shows, based on probability, that there will be a number of monomers left over) and as such they contribute less to the overall sample.

A second way to approach the average chain molecular weight is to assess the fraction of the total weight contributed by each chain length. The average chain molecular weight would then be given by:

$M_w = \Sigma\, \pi_x x M_0$

in which π_x is the fraction of chains of length x.

What is the fraction of chains of length x? The approach starts with considering the probability that a chain will be *x* units long. As noted above, a chain x units long has x-1 ester linkages and 2 unreacted chain ends. We know the probability of a chain end being converted to a polymer linkage is p, and in a chain x units long that will have to happen x-1 times, for a probability p^{x-1}. We also know that the probability of a functional group being left unreacted is 1-p, and that has to happen twice here, for a probability $(1-p)^2$. The probability of having a chain of length x is:

$\pi_x = x\, p^{x-1}(1-p)^2$

That means:

$M_w = \Sigma\, x\, p^{x-1}(1-p)^2\, xM_0$

$M_w = (1-p)^2 M_0\, \Sigma\, x^2\, p^{x-1}$

The series on the right is reducible to:

$\Sigma\ x^2\ p^{x-1} = (1 + p) / (1 - p)^3$

So that:

$M_w = (1\text{-}p)^2 M_0 (1 + p) / (1 - p)^3$

$M_w = M_0 (1 + p) / (1 - p)$

That provides a straightforward prediction of the weight-average molecular weight based on the fraction converted in condensation polymerization. Although M_n and M_w presented here are essentially theoretical predictions of molecular weight, these quantities can also be measured experimentally using different methods.

The ratio between these two quantities has always been used as an expression of the breadth of the molecular weight distribution, called the polydispersity index or simply the dispersity:

$D = M_w/M_n$

In the case of condensation polymerization,

$D = [M_0 (1 + p) / (1 - p)]/[M_0 / (1 - p)]$

$D = 1 + p$

Because p is always a fraction, the result is that the dispersity of a condensation polymerization is statistically expected to be less than 2.0.

Problem KP2.3.

Given 99% conversion of monomers with average molecular weight 120 g/mol, calculate M_w, M_n and D.

This page titled 5.21: Kinetics of Step-Growth Polymerization is shared under a CC BY-NC 3.0 license and was authored, remixed, and/or curated by Chris Schaller via source content that was edited to the style and standards of the LibreTexts platform.

- **3.2: Kinetics of Step-Growth Polymerization** by Chris Schaller is licensed CC BY-NC 3.0. Original source: https://employees.csbsju.edu/cschaller/Advanced/Polymers/Polycontents.htm.

5.22: Atoms and Molecules can Physisorb or Chemisorb to a Surface

In this section, we will consider both the energetics of adsorption and factors which influence the kinetics of adsorption by looking at the "potential energy diagram/curve" for the adsorption process. The potential energy curve for the adsorption process is a representation of the variation of the energy (PE or E) of the system as a function of the distance (d) of an adsorbate from a surface.

Within this simple one-dimensional (1D) model, the only variable is the distance (d) of the adsorbing molecule from the substrate surface (Figure **5.22.1**).

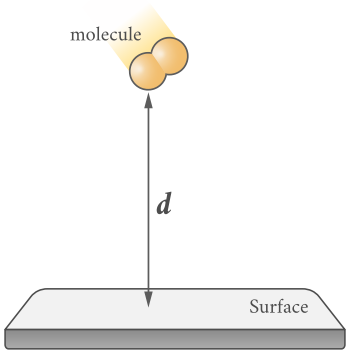


Figure **5.22.1**: A particle approaching a solid surface. (CC BY-NC; Ümit Kaya via LibreTexts)

Thus, the energy of the system is a function only of this variable i.e.

$$E = E(d)$$

It should be remembered that this is a very simplistic model which neglects many other parameters which influence the energy of the system (a single molecule approaching a clean surface), including for example

- *the angular orientation of the molecule*
- *changes in the internal bond angles and bond lengths of the molecule*
- *the position of the molecule parallel to the surface plane*

The interaction of a molecule with a given surface will also clearly be dependent upon the presence of any existing adsorbed species, whether these be surface impurities or simply pre-adsorbed molecules of the same type (in the latter case we are starting to consider the effect of surface coverage on the adsorption characteristics). Nevertheless, it is useful to first consider the interaction of an isolated molecule with a clean surface using the simple 1D model. For the purposes of this section, we will also not be overly concerned whether the "energy" being referred to should strictly be the internal energy, the enthalpy or free energy of the system. We will also make a distinction between physisorption and chemisorption. These two types of interaction with a surface are differentiated by the strength of interaction bewteen the adsorbed particle and the surface. A physisorbed particle will always be farther away from the surface than an identical particle that is chemisorbed (Figures **5.22.2** and **5.22.3**).

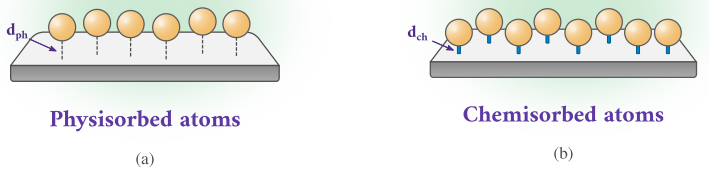


Figure **5.22.2**: a) A picture of physisorbed atoms. The atoms are, on average, a distance of d_{ph} from the surface. b) A picture of chemisorbed atoms. The atoms are, on average, a distance of d_{ch} from the surface. Note that d_{ph} is always greater than d_{ch}. (CC BY-NC; Ümit Kaya via LibreTexts)

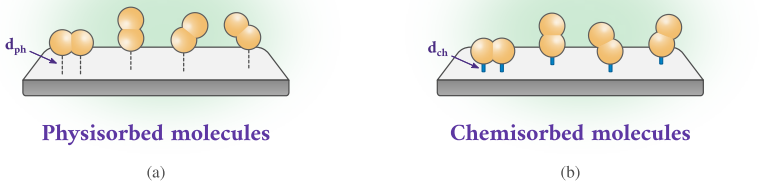


Figure **5.22.3**: a) A picture of physisorbed molecules. The molecules are, on average, a distance of d_{ph} from the surface. Note that the molecules can adsorb to the surface at various orientations. b) A picture of chemisorbed molecules. The molecules are, on average, a distance of d_{ch} from the surface. Note that the molecules can adsorb to the surface at various orientations. Also note that d_{ph} is always greater than d_{ch}. (CC BY-NC; Ümit Kaya via LibreTexts)

5.22.1: CASE I - Physisorption

In the case of pure physisorption, e.g., Ar/metals, the only attraction between the adsorbing species and the surface arises from weak, van der Waals forces. As illustrated in Figure **5.22.4** below, these forces give rise to a shallow minimum in the PE curve at a relatively large distance from the surface (typically $d > 0.3\ nm$) before the strong repulsive forces arising from electron density overlap cause a rapid increase in the total energy.

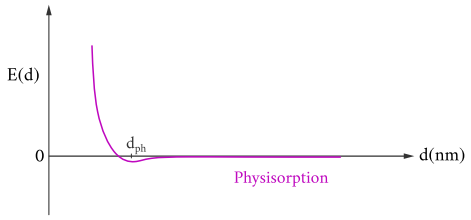


Figure **5.22.4**: A graph showing the potential energy change as a particle moves closer and closer to a surface and eventually physisorbs onto that surface. The distance d_{ph} is the equilibrium interaction distance of lowest potential energy for the physisorbed particle. (CC BY-NC; Ümit Kaya via LibreTexts)

There is no barrier to prevent the atom or molecule which is approaching the surface from entering this physisorption well, i.e. the process is not activated and the kinetics of physisorption are invariably fast.

5.22.2: CASE II - Physisorption + Molecular Chemisorption

The weak physical adsorption forces and the associated long-range attraction will be present to varying degrees in all adsorbate/substrate systems. However, in cases where chemical bond formation between the adsorbate and substrate can also occur, the PE curve is dominated by a much deeper chemisorption minimum at shorter values of *d*, as shown in Figure **5.22.5**.

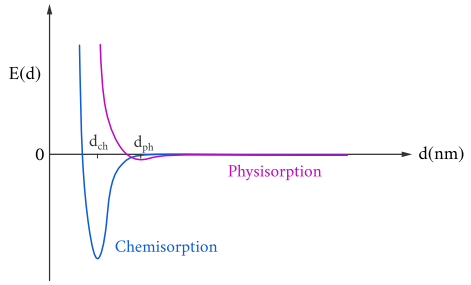


Figure **5.22.5**: A graph showing the potential energy change as a particle moves closer and closer to a surface to eventually either physisorb or chemisorb onto that surface. The distance d_{ph} is the equilibrium interaction distance of lowest potential energy for the physisorbed particle. The distance d_{ch} is the equilibrium bond distance of lowest potential energy for the chemisorbed particle. (CC BY-NC; Ümit Kaya via LibreTexts)

The graph above shows the PE curves due to physisorption and chemisorption separately. In practice, the PE curve for any real molecule capable of undergoing chemisorption is best described by a combination of the two curves, with a curve crossing at the

point at which chemisorption forces begin to dominate over those arising from physisorption alone (Figure **5.22.6**).

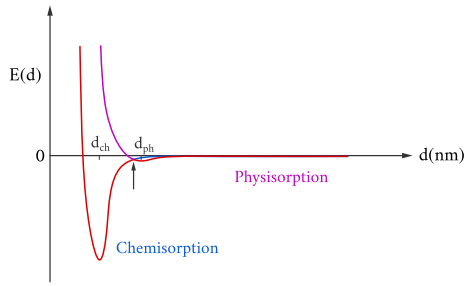


Figure **5.22.6**: The red curve is a graph showing the potential energy change as a particle moves closer and closer to a surface, eventually physisorping onto the surface, and then undergoing chemisorption onto that same surface. The distance d_{ph} is the equilibrium interaction distance of lowest potential energy for the physisorbed particle. The distance d_{ch} is the equilibrium bond distance of lowest potential energy for the chemisorbed particle. The vertical arrow points to the crossover point at which the particle approaches close enough to the surface for the forces of chemisorption to dominate. (CC BY-NC; Ümit Kaya via LibreTexts)

The minimum energy pathway obtained by combining the two PE curves is now highlighted in red. Any perturbation of the combined PE curve from the original, separate curves is most likely to be evident close to the highlighted crossing point.

For clarity, we will now consider only the overall PE curve as shown in Figure **5.22.7**:

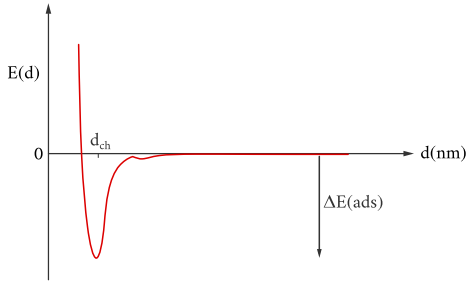


Figure **5.22.7**: A graph showing the potential energy change as a particle moves closer and closer to a surface, eventually physisorbing onto the surface, and then undergoing chemisorption onto that same surface. The distance d_{ch} is the equilibrium bond distance of lowest potential energy for the chemisorbed particle. The energy of adsorption is represented by $\Delta E(ads)$. (CC BY-NC; Ümit Kaya via LibreTexts)

The depth of the chemisorption well is a measure of the strength of binding to the surface. In fact, it is a direct representation of the energy of adsorption, whilst the location of the global minimum on the horizontal axis corresponds to the equilibrium bond distance (d_{ch}) for the adsorbed molecule on this surface.

The energy of adsorption is *negative*, and because it corresponds to the energy *change* upon adsorption, it is better represented as ΔE (ads) or ΔE_{ads} . However, you will also often find the depth of this well associated with the enthalpy of adsorption, ΔH (ads).

> *The "heat of adsorption", Q, is taken to be a positive quantity equal in magnitude to the enthalpy of adsorption ; i.e. Q = -ΔH(ads))*

In this particular case, there is clearly no barrier to be overcome in the adsorption process and there is no activation energy of adsorption (i.e. $E_a^{ads} = 0$, but do remember the previously mentioned limitations of this simple 1D model). There is of course a significant barrier to the reverse, desorption process; the red arrow in Figure **5.22.8** below represents the activation energy for desorption.

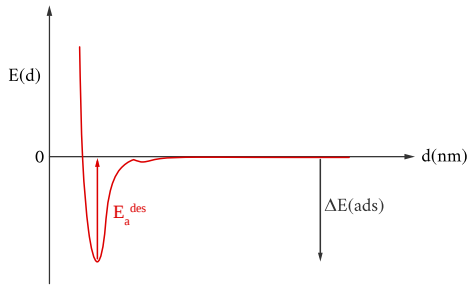


Figure 5.22.8: A graph showing both the energy of adsorption, $\Delta E(ads)$, and the activation energy of desorption, E_a^{des}. (CC BY-NC; Ümit Kaya via LibreTexts)

Clearly, in this particular case, the magnitudes of the energy of adsorption and the activation energy for desorption can also be equated i.e.

$$E_a^{des} = \Delta E(ads)$$

or

$$E_a^{des} \approx -\Delta H(ads)$$

5.22.3: CASE III - Physisorption + Dissociative Chemisorption

In this case, the main differences arise from the substantial changes in the PE curve for the chemisorption process. Again, we start off with the basic PE curve (Figure 5.22.9) for the physisorption process which represents how the molecule can weakly interact with the surface :

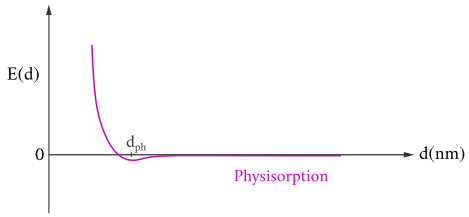


Figure 5.22.9: A graph showing the potential energy change as a particle moves closer and closer to a surface and eventually physisorbs onto that surface. The distance d_{ph} is the equilibrium interaction distance of lowest potential energy for the physisorbed particle. (CC BY-NC; Ümit Kaya via LibreTexts)

If we now consider a specific molecule such as H_2 and initially treat it as being completely **isolated** from the surface (i.e. when the distance, *d*, is very large), then a substantial amount of energy would need to be put into the system in order to cause dissociation of the molecule.

$$\mathrm{H_2 \longrightarrow H + H}$$

This amount of required energy is the bond dissociation energy $D_{(H-H)}$, which is some 435 kJ mol^{-1} or 4.5 eV.

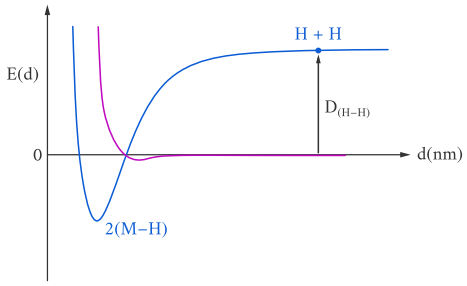


Figure 5.22.10: A graph showing the potential energy changes involved in the dissociation of an H_2 molecule. An H_2 molecule very far away from the surface has two paths by which it can end up as two separate H atoms chemisorbed onto the surface. (a) An input of 435 kJ per mole will break of the H-H bond. The separate H atoms can then eventually approach the surface and bond to it. (The red pathway) (b) The H_2 molecule can approach the surface, physisorb onto the surface, and then undergo dissociative chemisorption. (Starting on the right on the purple pathway, then switching to the red pathway at the crossover point.) (CC BY-NC; Ümit Kaya via LibreTexts)

The red dot in Figure 5.22.10 above thus represents two hydrogen atoms, equidistant (and a long distance) from the surface, and also now well separated from each other. If these atoms are then allowed to approach the surface they may ultimately both form strong chemical bonds to the substrate. This possible bonding of two H atoms to the surface (shown as 2(M-H) in the Figure) corresponds to the minimum in the red curve which represents the chemisorption PE curve for the two H atoms.

In reality, of course, such a mechanism for dissociative hydrogen chemisorption is not practical; the energy down payment associated with breaking the H-H bond is far too severe. Instead, a hydrogen molecule will initially approach the surface along the physisorption curve. If it has sufficient energy it may pass straight into the chemisorption well ("direct chemisorption") as shown below in Figure 5.22.11.

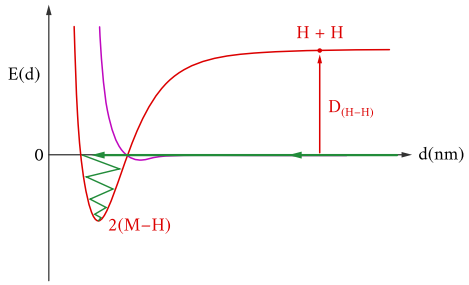


Figure 5.22.11: A graph showing the potential energy changes involved in the direct chemisorption of an H_2 molecule. The H_2 molecule approaches the surface following the green pathway, bypasses physisorption, and instead undergoes direct dissociative chemisorption. (CC BY-NC; Ümit Kaya via LibreTexts)

Alternatively, the hydrogen molecule may first undergo transient physisorption, a state from which it can then either desorb back as a molecule into the gas phase or cross over the barrier into the dissociated, chemisorptive state (as illustrated *schematically* in Figure 5.22.12).

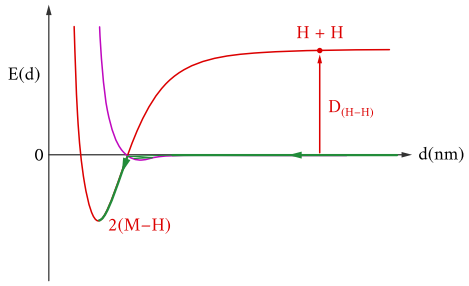


Figure 5.22.12: A graph showing the potential energy changes involved in the precursor-mediated chemisorption of an H_2 molecule. The H_2 molecule approaches the surface following the green pathway, first undergoes physisorption, and then undergoes dissociative chemisorption. (CC BY-NC; Ümit Kaya via LibreTexts)

In this latter case, the molecule can be said to have undergone "precursor-mediated" chemisorption. A picture of the process of the approach, physisorption, and dissociative chemisorption of a molecule is shown in Figure **5.22.13**. The molecule in this picture is following the general potential energy pathway described in either Figure **5.22.11** or Figure **5.22.12**.

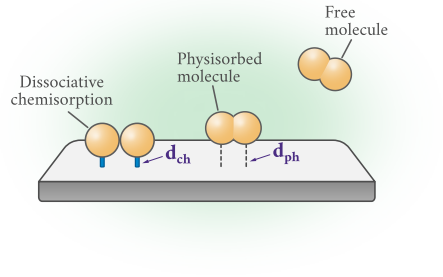


Figure **5.22.13**: The sequential process of a free molecule approaching a surface, becoming physisrobed onto the surface, and eventually undergoing dissociative chemisorption. (CC BY-NC; Ümit Kaya via LibreTexts)

The characteristics of this type of dissociative adsorption process are clearly going to be strongly influenced by the position of the crossing point of the two curves (molecular physisorption versus dissociative chemisorption) - relatively small shifts in the position of either of the two curves can significantly alter the size of any barrier to chemisorption.

In the example shown in Figure **5.22.14** below there is no direct activation barrier to dissociative adsorption - the curve crossing is below the initial "zero energy" of the system.

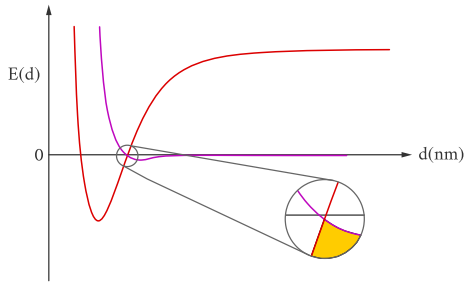


Figure **5.22.14**: The potential energy pathway for physisorption followed by dissociative adsorption in which there is no direct activation barrier. (CC BY-NC; Ümit Kaya via LibreTexts)

In the case shown in Figure **5.22.15**, there is a substantial barrier to chemisorption. Such a barrier has a major influence on the **kinetics** of adsorption.

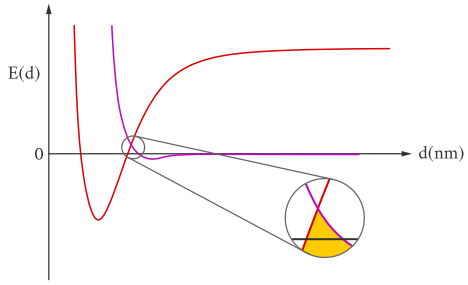


Figure **5.22.15**: The potential energy pathway for physisorption followed by dissociative adsorption in which there is an activation barrier. ((CC BY-NC; Ümit Kaya via LibreTexts)

The depth of the physisorption well for the hydrogen molecule is actually very small (in some cases negligible), but this is not the case for other molecules and does not alter the basic conclusions regarding dissociative adsorption that result from this model; namely that the process may be either activated or non-activated depending on the exact location of the curve crossing.

At this point, it is useful to return to consider the effect of such a barrier on the relationship between the activation energies for adsorption and desorption, and the energy (or enthalpy) of adsorption.

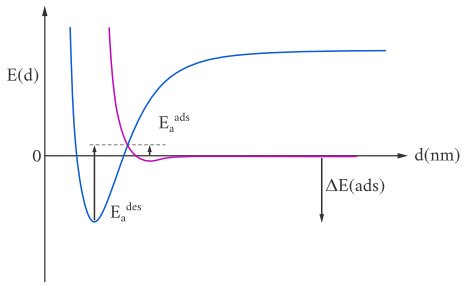


Figure **5.22.16**: A comparison of the activation energy of adsorption E_a^{ads}, the activation energy of desorption E_a^{des}, and the energy of adsorption for a molecule that undergoes physisorption, directly followed by dissociative chemisorption. (CC BY-NC; Ümit Kaya via LibreTexts)

As shown in Figure **5.22.16**,

$$E_a^{des} - E_a^{ads} = -\Delta E_{ads}$$

but, because the activation energy for adsorption is nearly always very much smaller than that for desorption, and the difference between the energy and the enthalpy of adsorption is also very small, it is still quite common to see the relationship

$$E_a^{des} \approx -\Delta H_{ads}$$

For a slightly more detailed treatment of the adsorption process, you are referred to the following examples of More Complex PE Curves & Multi-Dimensional PE Surfaces.

5.22.4: Contributors and Attributions

Roger Nix (Queen Mary, University of London)

5.22: Atoms and Molecules can Physisorb or Chemisorb to a Surface is shared under a CC BY-NC-SA 4.0 license and was authored, remixed, and/or curated by LibreTexts.

- **31.6: Atoms and Molecules can Physisorb or Chemisorb to a Surface** is licensed CC BY-NC-SA 4.0.

5.23: Isotherms are Plots of Surface Coverage as a Function of Gas Pressure at Constant Temperature

5.23.1: Introduction

Whenever a gas is in contact with a solid there will be an equilibrium established between the molecules in the gas phase and the corresponding adsorbed species (molecules or atoms) which are bound to the surface of the solid. As with all chemical equilibria, the position of equilibrium will depend upon a number of factors:

1. The relative stabilities of the adsorbed and gas phase species involved
2. The temperature of the system (both the gas and surface, although these are normally the same)
3. The pressure of the gas above the surface

In general, factors (2) and (3) exert opposite effects on the concentration of adsorbed species - that is to say that the surface coverage may be increased by raising the gas pressure but will be reduced if the surface temperature is raised.

The Langmuir isotherm was developed by Irving Langmuir in 1916 to describe the dependence of the surface coverage of an adsorbed gas on the pressure of the gas above the surface at a fixed temperature. There are many other types of isotherm (Temkin, Freundlich ...) which differ in one or more of the assumptions made in deriving the expression for the surface coverage; in particular, on how they treat the surface coverage dependence of the enthalpy of adsorption. Whilst the Langmuir isotherm is one of the simplest, it still provides a useful insight into the pressure dependence of the extent of surface adsorption.

Note: Surface Coverage & the Langmuir Isotherm

When considering adsorption isotherms it is conventional to adopt a definition of **surface coverage** (θ) which is defined as the fraction of the maximum (saturation) surface coverage N_{max} of a particular adsorbate on a given surface:

$$\theta = \frac{N}{N_{max}}, \tag{5.23.1}$$

This means the maximum θ is 1, ($\theta_{max} = 1$).

This way of defining the surface coverage differs from that usually adopted in surface science where the more common practice is to equate θ with the ratio of adsorbate species to surface substrate atoms (which leads to saturation coverages which are almost invariably less than unity).

5.23.2: The Langmuir Isotherm - Derivation from Equilibrium Considerations

We may derive the Langmuir isotherm by treating the adsorption process as we would any other equilibrium process - except in this case the equilibrium is between the gas phase molecules (M), together with vacant surface sites, and the species adsorbed on the surface. Thus, for a non-dissociative (molecular) adsorption process, we consider the adsorption to be represented by the following chemical equation :

$$S-* + M_{(g)} \rightleftharpoons S-M \tag{5.23.2}$$

where :

- $S-*$ represents a vacant surface site

5.23.2.1: Assumption 1

In writing Equation 5.23.2 we are making an inherent assumption that there are a fixed number of localized surface sites present on the surface. This is the first major assumption of the Langmuir isotherm.

We may now define an equilibrium constant (K) in terms of the concentrations of "reactants" and "products"

$$K = \frac{[S-M]}{[S-*][M]} \tag{5.23.3}$$

Caution

The units are not the same as when considering homogenous equilibria in a volume. [S-*] and [S-M] are formally concentrations in per unit area of surface (e.g. m^{-2}) rather than concentrations per unit volume.

Note that

- [S - M] is proportional to the surface coverage of adsorbed molecules, i.e. proportional to θ
- [S - *] is proportional to the number of vacant sites, i.e. proportional to $1-\theta$
- [M] is proportional to the pressure of gas, P

Hence, it is also possible to define another equilibrium constant, b , appropriate for coverage as:

$$b = \frac{\theta}{(1-\theta)P} \tag{5.23.4}$$

Rearrangement then gives the following expression for the surface coverage

$$\theta = \frac{bP}{1+bP} \tag{5.23.5}$$

which is the usual form of expressing the Langmuir Isotherm. As with all chemical reactions, the equilibrium constant, b, is both temperature-dependent and related to the Gibbs free energy and hence to the enthalpy change for the process.

5.23.2.2: Assumption 2

b is only a constant (independent of θ) if the enthalpy of adsorption is independent of coverage. This is the second major assumption of the Langmuir Isotherm.

A plot of θ vs. bP shows that as the pressure increases, θ approaches 1, meaning that nearly the entire surface is coated with a monolayer of adsorbed gas (Figure 5.23.1).

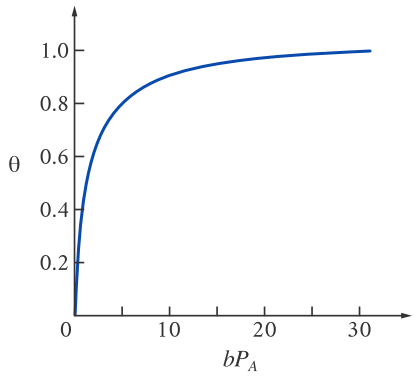


Figure 5.23.1: A plot of equation 5.23.5 which shows the nonlinear relationship between the fraction of surface coverage and the gas pressure. .(CC BY-NC; Ümit Kaya via LibreTexts)

Equation 5.23.5 can be rearranged to the form

$$\frac{1}{\theta} = 1 + \frac{1}{bP} \tag{5.23.6}$$

showing that the inverse of the fraction of occupied surface sites is a linear function of the inverse of the pressure. If we plot experimental data for the adsorption of diatomic oxygen and carbon monoxide onto a silica surface, we can see that the Langmuir adsorption isotherm describes the data well (figure 5.23.2).

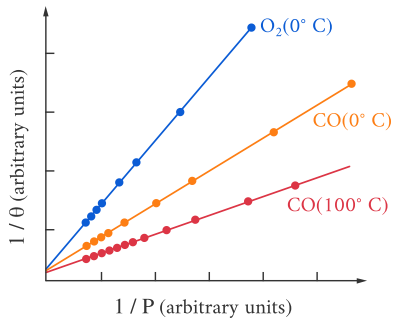


Figure 5.23.2: A plot showing the relationship of the inverse of the fraction of occupied surface sites to the inverse of the gas pressure for O_2 and CO molecules adsorbed onto a silica surface. (CC BY-NC; Ümit Kaya via LibreTexts)

5.23.3: The Langmuir Isotherm from a kinetics

The assumptions are the same as for the equilibrium argument:

- Adsorption takes place only at specific localized sites on the surface and the saturation coverage corresponds to complete occupancy of these sites.
- The rate of adsorption and desorption is independent of the surface coverage.

This is the case of a **reversible molecular adsorption**, i.e.

$$S-* + \mathrm{M_{(g)}} \underset{k_d}{\overset{k_a}{\leftrightharpoons}} \mathrm{S{-}M} \tag{5.23.7}$$

where

- $S-*$ represents a vacant surface site and
- $\mathrm{S{-}M}$ the adsorption complex.
- k_a is the rate constant for adsorption
- k_d is the rate constant for desorption

At equilibrium the rate of adsorption equals the rate of desorption $R_a = R_d$ or equivalently [S-M] is constant :

$$\frac{d[S-M]}{dt}\Big|_e = 0 = k_a[S-*]_e[M]_e - k_d[S-M]_e, \tag{5.23.8}$$

where subscript e indicates we are at equilibrium. We are interested in the concentration adsorbed to the surface, $[\text{S-M}]_e$. Solving for that yields:

$$[S-M]_e = \frac{k_a}{k_d}[S-*]_e[M]_e. \tag{5.23.9}$$

We would like to get this in a form equivalent to equation 5.23.5 in terms of θ. To do this we recognize that the maximum possible coverage is the number of binding sites per unit area on a completely clean surface, which we can represent as $[S-*]_o$. Since each S-M created removes an S-*,

$$[S-*] = [S-*]_o - [S-M].$$

Substituting this in to equation 5.23.9 and dividing through by $[\text{S-*}]_o$:

$$\frac{[S-M]_e}{[S-*]_o} = \frac{k_a}{k_d}\left(1 - \frac{[S-M]_e}{[S-*]_o}\right)[M]_e. \tag{5.23.10}$$

The ratio $\frac{[S-M]_e}{[S-*]_o}$ is θ. Thus, making the substitution and solving for θ we get:

$$\theta = \frac{k_a}{k_d}(1-\theta)[M]_e \implies \theta + \frac{k_a}{k_d}[M]_e\theta = \frac{k_a}{k_d}[M]_e \implies \theta = \frac{\frac{k_a}{k_d}[M]_e}{1+\frac{k_a}{k_d}[M]_e}. \tag{5.23.11}$$

Comparing this equation with equation 5.23.5 we recognize that $[M]_e$ is proportional to the pressure (P) and the ratio of the adsorption and desorption rates (the equilibrium constant for adsorption, K_{ads}) is proportional to b. If the gas above the solid is at low enough pressure to behave ideally you can show that $P = RT[M]_e$ and $b = (k_a/k_d)/(RT)$.

5.23.4: Energetics

We know that to a first approximation rate constants follow the Arrhenius model for their temperature dependence:

$$k = Aexp\left(\frac{-E_a}{RT}\right).$$

Thus, the ratio of k_a/k_d in equation 5.23.11 can be written as:

$$\frac{k_a}{k_d} = \frac{A_{ads}exp\left(\frac{-E_{ads}}{RT}\right)}{A_{des}exp\left(\frac{-E_{des}}{RT}\right)} = \frac{A_{ads}}{A_{des}}exp\left(\frac{E_{des}-E_{ads}}{RT}\right) = \frac{A_{ads}}{A_{des}}exp\left(\frac{-\Delta H_{ads}}{RT}\right), \tag{5.23.12}$$

where subscript 'des' refers to the desorption process and 'ads' refers to the adsorption process. Thus the equilibrium constant between adsorption and desorption will increase as the enthalpy change on adsorption gets more favorable (more negative). As you would expect the probability of sticking increases the more strongly the molecule binds to the surface.

5.23.5: Contributors and Attributions

- Roger Nix (Queen Mary, University of London)
- Jonathan Gutow (UW Oshkosh)

5.23: Isotherms are Plots of Surface Coverage as a Function of Gas Pressure at Constant Temperature is shared under a CC BY-NC-SA 4.0 license and was authored, remixed, and/or curated by LibreTexts.

- **31.7: Isotherms are Plots of Surface Coverage as a Function of Gas Pressure at Constant Temperature** is licensed CC BY-NC-SA 4.0.

5.24: Using Langmuir Isotherms to Derive Rate Laws for Surface-Catalyzed Gas-Phase Reactions

It is possible to predict how the kinetics of certain heterogeneously-catalyzed reactions might vary with the partial pressures of the reactant gases above the catalyst surface by using the Langmuir isotherm expression for equilibrium surface coverages.

5.24.1: Unimolecular Decomposition

Consider the surface decomposition of a molecule A, i.e. the process

$$A_{(g)} \rightleftharpoons A_{(ads)} \rightarrow \text{Products}$$

Let us assume that :

1. The decomposition reaction occurs uniformly across the surface sites at which molecule A may be adsorbed and is not restricted to a limited number of special sites.
2. The products are very weakly bound to the surface and, once formed, are rapidly desorbed.
3. The rate determining step (rds) is the surface decomposition step.

Under these circumstances, the molecules of A adsorbed on the surface are in equilibrium with those in the gas phase and we may predict the surface concentration of A from the Langmuir isotherm, i.e.

$$\theta = \frac{bP}{1+bP}$$

The rate of the surface decomposition (and hence of the reaction) is given by an expression of the form

$$\text{rate} = k\theta$$

This is assuming that the decomposition of $A(ads)$ occurs in a simple unimolecular elementary reaction step and that the kinetics are first order with respect to the surface concentration of this adsorbed intermediate). Substituting for the coverage, θ, gives us the required expression for the rate in terms of the pressure of gas above the surface

$$\text{rate} = \frac{kbP}{1+bP} \tag{5.24.1}$$

It is useful to consider two extremes:

5.24.1.1: Low Pressure/Binding Limit

This is the low pressure (or weak binding. i.e., small b) limit : under these conditions the steady state surface coverage, θ, of the reactant molecule is very small.

$$bP \ll 1$$

then

$$1+bP \approx 1$$

and Equation 5.24.1 can be simplified to

$$\text{rate} \approx kbP$$

Under this limiting case, the kinetics follow a first order reaction (with respect to the partial pressure of A) with an apparent first order rate constant $k' = kb$.

5.24.1.2: High Pressure/Binding Limit

This is the high pressure (or strong binding, i.e., large b) limit: under these conditions the steady state surface coverage, θ, of the reactant molecule is almost unity and

$$bP \gg 1$$

then

$$1 + bP \approx bP$$

and Equation 5.24.1 can be simplified to

$$rate \approx k$$

Under this limiting case, the kinetics follow a zero-order reaction (with respect to the partial pressure of A). The rate shows the same pressure variation as does the surface coverage, but this is hardly surprising since it is directly proportional to θ.

These two limiting cases can be identified in the general kinetics from Equation 5.24.1 in Figure 5.24.1.

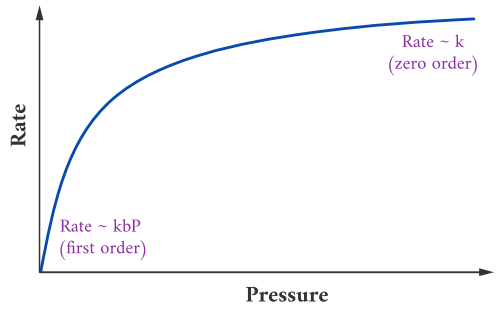


Figure 5.24.1: Plot of reaction rate versus the pressure of the reactant gas. The graph shows that at low pressures, the rate is first order with respect to the pressure of the reacting gas. At high pressures, however, the reaction approaches zero order with respect to the reacting gas.

5.24.2: Bimolecular Reaction (between molecular adsorbates)

Consider a Langmuir-Hinshelwood reaction of the following type:

$$A_{(g)} \rightleftharpoons A_{(ads)} \tag{5.24.2}$$

$$B_{(g)} \rightleftharpoons B_{(ads)} \tag{5.24.3}$$

$$A_{(ads)} + B_{(ads)} \overset{slow}{\longrightarrow} AB_{(ads)} \overset{fast}{\longrightarrow} AB_{(g)} \tag{5.24.4}$$

We will further assume, as noted in the above scheme, that the surface reaction between the two adsorbed species (left side of Equation 5.24.4 is the rate determining step.

If the two adsorbed molecules are mobile on the surface and freely intermix then the rate of the reaction will be given by the following rate expression for the **bimolecular** surface combination step

$$Rate = k\theta_A\theta_B$$

For a single molecular adsorbate the surface coverage (as given by the standard Langmuir isotherm) is

$$\theta = \frac{bP}{1 + bP}$$

Where two molecules (A & B) are competing for the same adsorption sites then the relevant expressions are (see derivation):

$$\theta_A = \frac{b_A P_A}{1 + b_A P_A + b_B P_B}$$

and

$$\theta_B = \frac{b_B P_B}{1 + b_A P_A + b_B P_B}$$

Substituting these into the rate expression gives :

$$Rate = k\theta_A\theta_B = \frac{k b_A P_A b_B P_B}{(1 + b_A P_A + b_B P_B)^2}$$

Once again, it is interesting to look at several extreme limits

5.24.2.1: Low Pressure/Binding Limit

$$b_A P_A \ll 1$$

and

$$b_B P_B \ll 1$$

In this limit that θ_A & θ_B are both very low , and

$$rate \rightarrow k b_A P_A b_B P_B = k' P_A P_B$$

i.e. *first order* in both reactants

5.24.2.2: Mixed Pressure/Binding Limit

$$b_A P_A \ll 1 \ll b_B P_B$$

In this limit $\theta_A \rightarrow 0$, $\theta_B \rightarrow 1$, and

$$Rate \rightarrow \frac{k b_A P_A}{b_B P_B} = \frac{k' P_A}{P_B}$$

i.e. *first order* in A, but *negative first order* in B

Clearly, depending upon the partial pressure and binding strength of the reactants, a given model for the reaction scheme can give rise to a variety of apparent kinetics: this highlights the dangers inherent in the reverse process - namely trying to use kinetic data to obtain information about the reaction mechanism.

Example 5.24.1: CO Oxidation Reaction

On precious metal surfaces (e.g. Pt), the CO oxidation reaction is generally believed to by a *Langmuir-Hinshelwood mechanism* of the following type :

$$CO_{(g)} \rightleftharpoons CO_{(ads)}$$

$$O_{2(g)} \rightleftharpoons 2O_{(ads)}$$

$$CO_{(ads)} + O_{(ads)} \xrightarrow{slow} CO_{2(ads)} \xrightarrow{fast} CO_{2(g)}$$

As CO_2 is comparatively weakly-bound to the surface, the desorption of this product molecule is relatively fast and in many circumstances it is the surface reaction between the two adsorbed species that is the rate determining step.

If the two adsorbed molecules are assumed to be mobile on the surface and freely intermix then the rate of the reaction will be given by the following rate expression for the bimolecular surface combination step

$$Rate = k \theta_{CO} \theta_O$$

Where two such species (one of which is molecularly adsorbed, and the other dissociatively adsorbed) are competing for the same adsorption sites then the relevant expressions are (see derivation):

$$\theta_{CO} = \frac{b_{CO} P_{CO}}{1 + \sqrt{b_O P_{O_2}} + b_{CO} P_{CO}}$$

and

$$\theta_O = \frac{\sqrt{b_O P_{O_2}}}{1 + \sqrt{b_O P_{O_2}} + b_{CO} P_{CO}}$$

Substituting these into the rate expression gives:

$$rate = k\theta_{CO}\theta_O = \frac{kb_{CO}P_{CO}\sqrt{b_OP_{O_2}}}{(1+\sqrt{b_OP_{O_2}}+b_{CO}P_{CO})^2} \tag{5.24.5}$$

Once again, it is interesting to look at certain limits. If the CO is much more strongly bound to the surface such that

$$b_{CO}P_{CO} \gg 1+\sqrt{b_OP_{O_2}}$$

then

$$1+\sqrt{b_OP_{O_2}}+b_{CO}P_{CO} \approx b_{CO}P_{CO}$$

and the Equation 5.24.5 simplifies to give

$$rate \approx \frac{k\sqrt{b_OP_{O_2}}}{b_{CO}P_{CO}} = k'\frac{P_{O_2}^{1/2}}{P_{CO}}$$

In this limit the kinetics are half-order with respect to the gas phase pressure of molecular oxygen, but negative order with respect to the CO partial pressure, i.e. CO acts as a poison (despite being a reactant) and increasing its pressure slows down the reaction. This is because the CO is so strongly bound to the surface that it blocks oxygen adsorbing, and without sufficient oxygen atoms on the surface the rate of reaction is reduced.

5.24.3: Contributors and Attributions

- Roger Nix (Queen Mary, University of London)

5.24: Using Langmuir Isotherms to Derive Rate Laws for Surface-Catalyzed Gas-Phase Reactions is shared under a CC BY-NC-SA 4.0 license and was authored, remixed, and/or curated by LibreTexts.

- **31.8: Using Langmuir Isotherms to Derive Rate Laws for Surface-Catalyzed Gas-Phase Reactions** is licensed CC BY-NC-SA 4.0.

5.25: The Structure of a Surface is Different from that of a Bulk Solid

The kinetics and thermodynamics of the chemical and physical processes that occur on the surface of a solid are greatly dependent on the structure of the surface. Few, if any surfaces are perfectly flat, and thus the cavities, protrusions, ridges, and edges of the surface must be treated differently when studying chemisorption and physisorption. Several types of spectroscopies and microscopies are available to study the atomic-scale structure of surfaces.

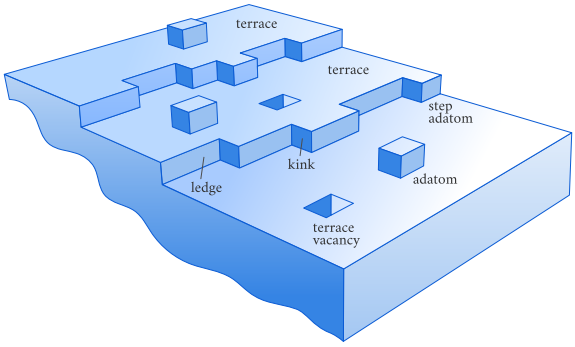


Figure 5.25.1: A schematic of a solid surface showing possible defects. The surface is composed of terraces, ledges, kinks, and steps. Terraces can contain adatoms (lone single atoms) and vacancies (missing atoms that leave cavities). (CC BY-NC; Ümit Kaya via LibreTexts)

Electron Microscopy

The two forms of electron microscopy which are commonly used to provide surface information are

- **Secondary Electron Microscopy** (SEM): which provides a direct image of the topographical nature of the surface from all the emitted secondary electrons
- **Scanning Auger Microscopy** (SAM): which provides compositional maps of a surface by forming an image from the Auger electrons emitted by a particular element.

Both techniques employ the focusing of the probe beam (a beam of high-energy electrons, typically 10 - 50 keV in energy) to obtain spatial localization.

Secondary Electron Microscopy (SEM)

As the primary electron beam is scanned across the surface, electrons of a wide range of energies will be emitted from the surface in the region where the beam is incident. These electrons will include backscattered primary electrons and Auger electrons, but the vast majority will be *secondary electrons* formed in multiple inelastic scattering processes (these are the electrons that contribute to the background and are completely ignored in Auger spectroscopy). The secondary electron current reaching the detector is recorded and the microscope image consists of a "plot" of this current, I, against probe position on the surface. The contrast in the micrograph arises from several mechanisms, but first and foremost from variations in the surface topography. Consequently, the secondary electron micrograph is virtually a direct image of the real surface structure (Figure 5.25.1).

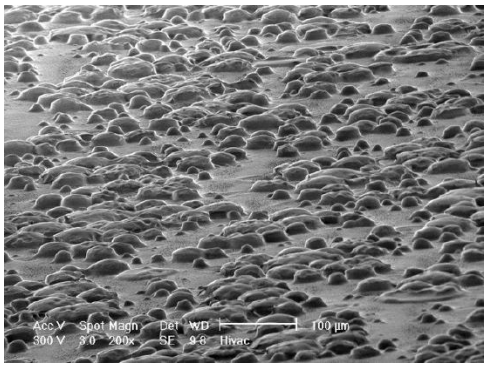


Figure 5.25.2: Low-voltage SEM micrograph (300 V) of distribution of adhesive droplets on a Post-it note. (CC BY-SA 3.0, Chivesud via Wikipedia)

The attainable resolution of the technique is limited by the minimum spot size that can be obtained with the incident electron beam, and ultimately by the scattering of this beam as it interacts with the substrate. With modern instruments, a resolution of better than 5 nm is achievable. This is more than adequate for imaging semiconductor device structures, for example, but insufficient to enable many supported metal catalysts to be studied in any detail.

Scanning Auger Microscopy (SAM)

The incident primary electrons cause the ionization of atoms within the region illuminated by the focused beam. Subsequent relaxation of the ionized atoms leads to the emission of Auger electrons characteristic of the elements present in this part of the sample surface. As with SEM , the attainable resolution is again ultimately limited by the incident beam characteristics. More significantly, however, the resolution is also limited by the need to acquire sufficient Auger signal to form a respectable image within a reasonable time period, and for this reason, the instrumental resolution achievable is rarely better than about 15-20 nm.

Low-Energy Electron Diffraction (LEED) Spectroscopy

LEED is the principal technique for the determination of surface structures. It may be used in one of two ways:

1. **Qualitatively**: where the diffraction pattern is recorded and analysis of the *spot positions* yields information on the size, symmetry, and rotational alignment of the adsorbate unit cell with respect to the substrate unit cell.
2. **Quantitatively**: where the *intensities* of the various diffracted beams are recorded as a function of the incident electron beam energy to generate so-called I-V curves which, by comparison with theoretical curves, may provide accurate information on atomic positions.

The LEED experiment uses a beam of electrons of a well-defined low energy (typically in the range 20 - 200 eV) incident normally on the sample. The sample itself must be a single crystal with a well-ordered surface structure in order to generate a back-scattered electron diffraction pattern. A typical experimental setup is shown in figure 5.25.3 below.

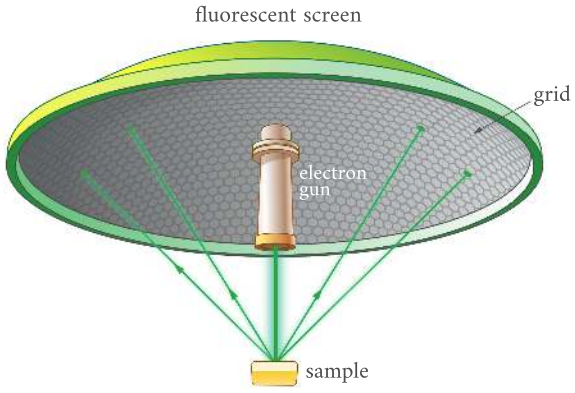


Figure 5.25.3: Schematic of a LEED experimental setup. (CC BY-NC; Ümit Kaya via LibreTexts)

Only the elastically-scattered electrons contribute to the diffraction pattern; the lower energy (secondary) electrons are removed by energy-filtering grids placed in front of the fluorescent screen that is employed to display the pattern.

Example 5.25.1

As shown by the Bragg equation, for the electrons to be diffracted, the de Broglie wavelength of the electrons has to be less than $2d$, which is twice the distance between the atomic planes. The equation used to calculate the wavelength (in nm) of backscattered electrons that are accelarated by a potential, ϕ is

$$\lambda = \left(\frac{1.504\,Vnm^2}{\phi}\right)^{1/2}$$

Calculate the minimum acceleration voltage needed to observe electron diffraction from the surface of a crystal with an interplanar spacing of 0.1250 nm.

Solution

To observe diffraction, the wavelength must be less than $2d$, so λ must be less than 0.2500 nm. Therefore,

$$0.2500\,nm = \left(\frac{1.504\,Vnm^2}{\phi}\right)^{1/2}$$

$$\phi = \frac{1.504\,Vnm^2}{(0.2500\,nm)^2}$$

$$\phi = 24.06V$$

Contributors and Attributions

- Roger Nix (Queen Mary, University of London)

5.25: The Structure of a Surface is Different from that of a Bulk Solid is shared under a CC BY-NC-SA 4.0 license and was authored, remixed, and/or curated by LibreTexts.

- **31.9: The Structure of a Surface is Different from that of a Bulk Solid** is licensed CC BY-NC-SA 4.0.

5.26: The Haber-Bosch Reaction Can Be Surface Catalyzed

The Haber-Bosch Process for Synthesis of Ammonia

An example of an industrial catalytic process is the Haber-Bosch process. Karl Bosch (1874–1940) was a German chemical engineer who was responsible for designing the process that took advantage of Fritz Haber's discoveries regarding the N_2 + H_2/NH_3 equilibrium to make ammonia synthesis via this route cost-effective. He received the Nobel Prize in Chemistry in 1931 for his work. The industrial process is called either the Haber process or the Haber-Bosch process. used to synthesize ammonia via the following reaction:

$$N_{2(g)} + 3H_{2(g)} \rightleftharpoons 2NH_{3(g)}$$

with

$$\Delta H_{rxn} = -91.8\ kJ/mol$$

Because the reaction converts 4 mol of gaseous reactants to only 2 mol of gaseous product, Le Chatelier's principle predicts that the formation of NH_3 will be favored when the pressure is increased. The reaction is exothermic, however (ΔH_{rxn} = −91.8 kJ/mol), so the equilibrium constant decreases with increasing temperature, which causes an equilibrium mixture to contain only relatively small amounts of ammonia at high temperatures (**5.26.1**). Taken together, these considerations suggest that the maximum yield of NH_3 will be obtained if the reaction is carried out at as low a temperature and as high a pressure as possible. Unfortunately, at temperatures less than approximately 300°C, where the equilibrium yield of ammonia would be relatively high, the reaction is too *slow* to be of any commercial use. The industrial process, therefore, uses a mixed oxide (Fe_2O_3/K_2O) catalyst that enables the reaction to proceed at a significant rate at temperatures of 400°C–530°C, where the formation of ammonia is less unfavorable than at higher temperatures.

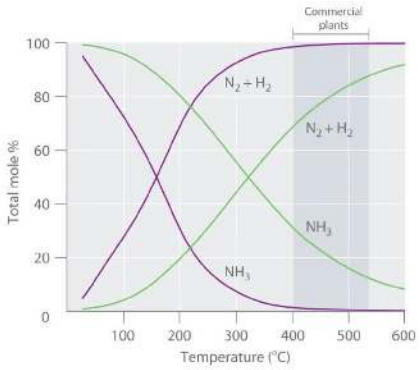


Figure **5.26.1** Effect of Temperature and Pressure on the Equilibrium Composition of Two Systems that Originally Contained a 3:1 Mixture of Hydrogen and Nitrogen: At all temperatures, the total pressure in the systems was initially either 4 atm (purple curves) or 200 atm (green curves). Note the dramatic decrease in the proportion of NH_3 at equilibrium at higher temperatures in both cases, as well as the large increase in the proportion of NH_3 at equilibrium at any temperature for the system at higher pressure (green) versus lower pressure (purple). Commercial plants that use the Haber-Bosch process to synthesize ammonia on an industrial scale operate at temperatures of 400°C–530°C (indicated by the darker gray band) and total pressures of 130–330 atm.

Because of the low value of the equilibrium constant at high temperatures (e.g., K = 0.039 at 800 K), there is no way to produce an equilibrium mixture that contains large proportions of ammonia at high temperatures. We can, however, control the temperature and the pressure while using a catalyst to convert a fraction of the N_2 and H_2 in the reaction mixture to NH_3, as is done in the Haber-Bosch process. This process also makes use of the fact that the product—ammonia—is less volatile than the reactants. Because NH_3 is a liquid at room temperature at pressures greater than 10 atm, cooling the reaction mixture causes NH_3 to condense from the vapor as liquid ammonia, which is easily separated from unreacted N_2 and H_2. The unreacted gases are recycled until the complete conversion of hydrogen and nitrogen to ammonia is eventually achieved. Figure **5.26.2** is a simplified layout of a Haber-Bosch process plant.

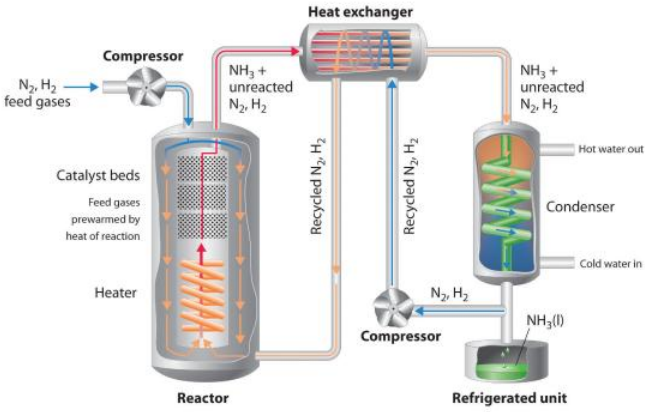


Figure **5.26.2** A Schematic Diagram of an Industrial Plant for the Production of Ammonia via the Haber-Bosch Process: A 3:1 mixture of gaseous H_2 and N_2 is compressed to 130–330 atm, heated to 400°C–530°C, and passed over an Fe_2O_3/K_2O catalyst, which results in partial conversion to gaseous NH_3. The resulting mixture of gaseous NH_3, H_2, and N_2 is passed through a heat exchanger, which uses the hot gases to prewarm recycled N_2 and H_2, and a condenser to cool the NH_3, giving a liquid that is readily separated from unreacted N_2 and H_2. (Although the normal boiling point of NH_3 is −33°C, the boiling point increases rapidly with increasing pressure, to 20°C at 8.5 atm and 126°C at 100 atm.) The unreacted N_2 and H_2 are recycled to form more NH_3.

We can write the seven reactions that are involved in the process where ad indicates that the molecule or atom is adsorbed on the catalyst

$$H_2(g) + 2S(s) \rightleftharpoons 2H(ad) \tag{5.26.1}$$

$$N_2(g) \rightleftharpoons N_2(ad) \tag{5.26.2}$$

$$N_2(ad) + 2S(s) \rightleftharpoons 2N(ad) \tag{5.26.3}$$

$$H(ad) + N(ad) \rightleftharpoons NH(ad) \tag{5.26.4}$$

$$NH(ad) + H(ad) \rightleftharpoons NH_2(ad) \tag{5.26.5}$$

$$NH_2(ad) + H(ad) \rightleftharpoons NH_3(ad) \tag{5.26.6}$$

$$NH_3(ad) \rightleftharpoons NH_3(g) \tag{5.26.7}$$

Reaction 5.26.3 is much the slowest, and therefore the rate determining step. Figure **5.26.3** summarizes the reaction scheme.

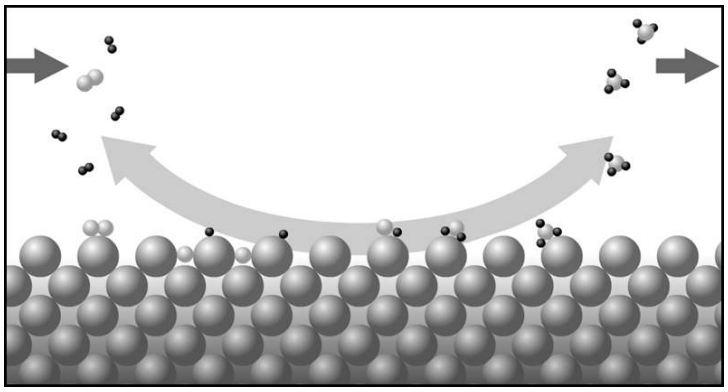


Figure **5.26.3**: A representation of the reactions Eqs. 5.26.1 to 5.26.7 with H_2 and N_2 coming in from the left and being adsorbed on the catalyst. The H_2 and N_2 then atomize on the surface of the catalyst, followed by a set of sequential reactions forming NH, NH_2 and finally NH_3 which desorbs from the catalyst as shown on the right

Gerhard Ertl worked out the energetics of the reaction shown in Figure **5.26.4** below shows the amount of energy per mole needed on the catalyst and that which would be needed in the gas phase. Ertl's Nobel Prize speech about his work on the catalytic reactions forming ammonia and other catalytic reactions can be viewed on line.

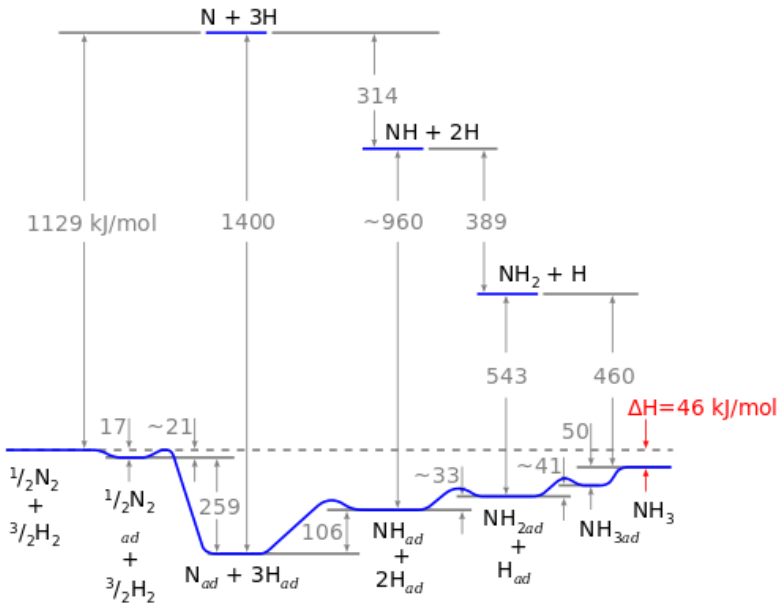


Figure 5.26.4: Ertl's group was able to measure the energy needed for each step of the Bosch-Haber process as opposed to the energy that would be needed in the gas phase.

Further studies of the Fe_2O_3/K_2O catalyst have shown that the rate of the reaction depends on the particular surface on which the reaction is occurring. Figure 5.26.5 shows the reaction rates for the synthesis of ammonia on five different surfaces of the iron.

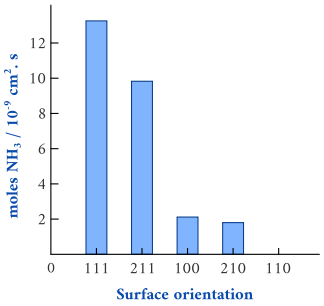


Figure 5.26.5: The rates of ammonia production for various iron catalyst surfaces. (CC BY-NC; Ümit Kaya via LibreTexts)

Contributors

- Anonymous

Modified by Joshua Halpern (Howard University), Scott Sinex, and Scott Johnson (PGCC)

Figure 5.26.3 is from the ESA, now available on the internet wayback machine

Figure 5.26.4 is from the Wikipedia Commons

5.26: The Haber-Bosch Reaction Can Be Surface Catalyzed is shared under a CC BY-NC-SA 4.0 license and was authored, remixed, and/or curated by LibreTexts.

- **31.10: The Haber-Bosch Reaction Can Be Surface Catalyzed** is licensed CC BY-NC-SA 4.0.

5.27: Photochemical Kinetics

5.27.1: Introduction

When light is absorbed by molecules it deposits energy in the molecules. This energy can be reemitted as photons in the form of phosphorescence and fluorescence, dissipated as thermal energy or provide the energy for a chemical process. The kinetics of these processes thus impact the intensity and decay rate of fluorescence (which might be used for analytical detection of species) and the kinetics of photochemical reactions. Photochemical reactions are key contributors to the maintenance of the protective stratospheric ozone layer and smog. In this section we will discuss the concept of quantum yield and some of the photochemistry of stratospheric ozone and smog.

5.27.2: Quantum yield

Quantum yield can be defined as the fraction of the absorbed photons that result in the outcome of interest, be it release of a fluorescent photon or the production of a particular chemical species. We will consider the case of fluorescence photon yield. Our kinetic model is as follows where F is the fluorofore, F* is the excited species, $h\nu_a$ is the photon of the correct energy to be absorbed, $h\nu_f$ is an emitted (fluorescent) photon, and Q is another species that can carry the energy away and thus quench the fluorescence:

$$\mathrm{F} + \mathrm{h}\nu_a \xrightarrow{k_a} \mathrm{F^*}$$

$$\mathrm{F^*} \xrightarrow{k_f} \mathrm{F} + \mathrm{h}\nu_f$$

$$\mathrm{F^*} + \mathrm{Q} \xrightarrow{k_q} \mathrm{F} + \mathrm{Q}$$

$$\mathrm{F^*} \xrightarrow{k_{rel}} \mathrm{F}.$$

The last reaction represents relaxation of the energy through additional paths to generate heat and a species that cannot fluoresce (e.g. vibrational relaxation, intersystem crossing, etc...). This mechanism yields the rate law:

$$\frac{d[F*]}{dt} = k_a[h\nu_a][F] - k_f[F^*] - k_q[Q][F^*] - k_{rel}[F^*], \tag{5.27.1}$$

where $[h\nu]$, the photon concentration is proportional to the light intensity. In the case of fluorescence detection as might be done for quantitative analysis the exciting light source is on continuously during the measurement. Thus, a steady-state should be achieved where creation and destruction of F* balance out. Setting the rate of change in [F*] to zero and solving for $[F^*]_{ss}$ yields:

$$[F^*]_{ss} = \frac{k_a[h\nu_a][F]_o}{k_a[h\nu_a] + k_f + k_q[Q] + k_{rel}}, \tag{5.27.2}$$

where $[F]_o$ is the concentration before excitation. The intensity of the fluorescence is just proportional to the rate of the emission reaction and the rate photons are absorbed is just proportional to the first photon absorption reaction rate. The quantum yield is the ratio of these:

$$\phi = \frac{k_f[F^*]_{ss}}{k_a[h\nu_a][F]} = \frac{k_f k_a}{k_a[h\nu_a]([F]_o - [F^*]_{ss})} = \frac{k_f}{k_f + k_q[Q] + k_{rel}}. \tag{5.27.3}$$

Thus if the rates of quenching and other relaxation processes were zero the quantum yield would be 1. As the concentration of quenchers increases or as the rate of other relaxation processes increases the quantum yield drops towards zero.

We can also consider how fast the fluorescence turns off (decays) after the excitation light source shuts off. Without an excitation source rate law 5.27.1 becomes:

$$\frac{d[F*]}{dt} = -k_f[F^*] - k_q[Q][F^*] - k_{rel}[F^*] = -(k_f + k_q[Q] + k_{rel})[F^*]. \tag{5.27.4}$$

This is just a first order rate law. The the time dependence of the fluorescence which is proportional to [F*] is thus:

$$[F^*] = [F^*]_o e^{-(k_f + k_q[Q] + k_{rel})t}. \tag{5.27.5}$$

Therefore, the more quencher or the faster other relaxation and the fluorescence processes are the more rapidly the fluorescence shuts off after the excitation source is removed. The inverse of the sum in parentheses in equation 5.27.5 is the fluorescence lifetime and can be monitored with fast photodetectors.

5.27.3: Atmospheric ozone

Ozone, O_3, at ground level is a pollutant. It is extremely reactive and can cause damage to lungs at low concentrations (current exposure recommendations can be found at the US EPA website). Because ozone absorbs light in the 210 to 300 nm range (UVB radiation) significant concentrations of ozone in the stratosphere help to protect organisms on the surface from exposure to these damaging UV photons. Photochemistry is integral to the formation of this "ozone layer" and processes that destroy it.

5.27.3.1: Chapman mechanism

The Chapman cycle describes the reactions involving ozone and other oxygen species that provide UVB protection:

$$O_2 + h\nu_1 \xrightarrow{k_1} 2\,O \quad \text{185 to 220 nm photons}$$

$$O + O_2 \xrightarrow{k_2} O_3^*$$

$$O_3^* \xrightarrow{k_{-2}} O + O_2$$

$$O_3^* + M \xrightarrow{k_3} O_3 + M$$

$$O_3 + h\nu_2 \xrightarrow{k_4} O_2 + O \quad \text{210 to 300 nm photons}$$

$$O_3 + O \xrightarrow{k_5} 2\,O_2$$

The second (k_2) third (k_{-2}) and fourth (k_3) reactions are often combined into a single trimolecular reaction for simplicity. This was not done here to emphasize the fact that simultaneous collisions of three gas phase species are rarely seen to contribute to reaction mechanisms. This mechanism ignores other reactions that involve these oxygen species, but provides a simple model for an initial understanding.

Consider a particular time of day. The sunlight intensity and thus the concentration of the photons involved will be constant. Additionally, molecular oxygen being about 20% of the atmosphere will have a constant concentration that is significantly larger than the ozone and other species. So, we will consider the O_2 concentration constant as well. As there are competing processes creating and destroying ozone, this will lead to steady-state concentrations of all the oxygen species in this mechanism. Without doing the steady state analysis we can still develop some conclusions about how the ozone concentration in the stratosphere will behave. The rate of the second reaction will depend on [O], which is created in the first reaction. As we go to lower altitude more of the light in the 185 to 220 nm range will have been absorbed by higher altitude oxygen molecules. This favors decreasing ozone concentration with decreasing altitude. However, at the high altitudes with lower pressure the third reaction (excited ozone falling apart) will dominate the fourth reacation where the energy is carried away before ozone can fall apart. The competition between the decrease in photoproduction of O atoms with decreasing altitude and the increase in pressure increasing the rate of collisional stabilization of ozone suggests that there will be an intermediate altitude where the ozone concentration reaches a maximum. This is what is observed as shown in the figure below.

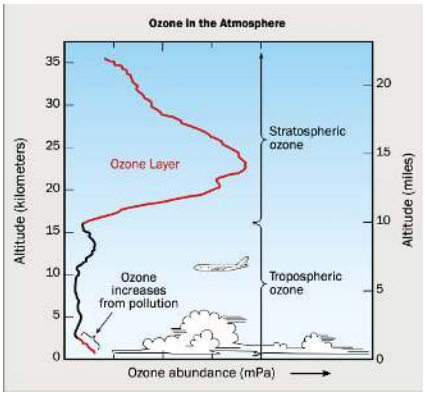


Figure **5.27.1**: Ozone partial pressure versus altitude. This shows an altitude where the concentration reaches a maximum when the production of O atoms by photodissociation is still high enough to produce ozone and the collisional stabilization is rapid enough because of the increased pressure to prevent all the energized ozone created from falling apart again. Source: *Twenty Questions and Answers About the Ozone Layer: 2014 Update*, World Meteorological Organization. https://library.wmo.int/idurl/4/54606.

5.27.3.2: Other reactions that destroy ozone

5.27.3.2.1: HO_x reactions

Below 30 km HO catalytically destroys ozone.

$$OH + O_3 \longrightarrow HO_2 + O_2$$

$$\underline{HO_2 + O_3 \longrightarrow OH + 2\,O_2}$$

$$\text{sum:}\quad 2\,O_3 \longrightarrow 3\,O_2$$

Above 40 km OH mostly reacts with free oxygen atoms and is not involved with destruction of ozone. Stratospheric OH can be produced by photodissociation of the limited amount of water vapor in the stratosphere.

5.27.3.3: NO_x reactions

NO can also catalytically destroy ozone.

$$NO + O_3 \longrightarrow NO_2 + O_2$$

$$\underline{NO_2 + O \longrightarrow NO + O_2}$$

$$\text{sum:}\quad O_3 + O \longrightarrow 2\,O_2$$

In addition NO_2 can react with OH to form HNO_3, which can then dissolve in water and be rained out.

$$NO_2 + OH + M \longrightarrow HNO_3 + M.$$

A major source of NO_x compounds are human made combustion reactions, that expose high temperature metal surfaces to atmospheric N_2 and O_2.

5.27.3.4: ClO_x reactions

Chlorine species also catalytically destroy ozone.

$$Cl + O_3 \longrightarrow ClO + O_2$$

$$\underline{ClO + O \longrightarrow Cl + O_2}$$

$$\text{sum:}\quad O_3 + O \longrightarrow 2\,O_2$$

Chlorine leaves the atmosphere through formation of the water soluble HCl which rains out:

$$Cl + RH \longrightarrow HCl + R.$$

The majority of Cl species in the atmosphere come from man made organic compounds that contain chlorine and fluorine (chlorofluorocarbons, CFCs). These molecules are stable in the troposphere so over time migrate to the stratosphere where UV light photodissociates the C-Cl bonds creating the reactive chlorine species. For example:

$$\mathrm{CClF_3 + h\nu \longrightarrow CF_3 + Cl.}$$

These CFCs were used as refrigerants and propellants due to their incredible stability near the Earth's surface. However, the decomposition in the upper atmosphere to form Cl radicals is responsible for the catalytic decomposition of ozone. The world community addressed this issue by drafting the Montreal Protocol, which focused on the emission of ozone-destroying compounds. The result of this action has been a decrease in CFC emissions and an apparent stabilization and expected future increase in stratospheric ozone. This is one example of science-guided political, industrial, and economic policies leading to positive changes for our environment.

It is noteworthy that one reason for the success of this was many commercial enterprises saw a big market for products to replace the chlorine containing CFC products that were the source of the stratospheric chlorine. Thus, they may not have fought as strongly against the regulations phasing out CFCs.

5.27.3.5: Antarctic and Artic ozone holes

Both the Antarctic and Artic exhibit seasonal (during their hemisphere's Springs) drops in stratospheric ozone concentrations. These areas over the poles of very low ozone concentration are referred to as ozone holes. How they form is a good illustration of the impact of conditions and heterogenous chemistry on the kinetics of reactions.

If you look at satellite data showing amount of ozone in a vertical column of air looking down at the planet each spring (March or September) you will observe low ozone concentrations over the Poles (especially the South Pole) compared to the surrounding atmosphere. This is shown in the montages below.

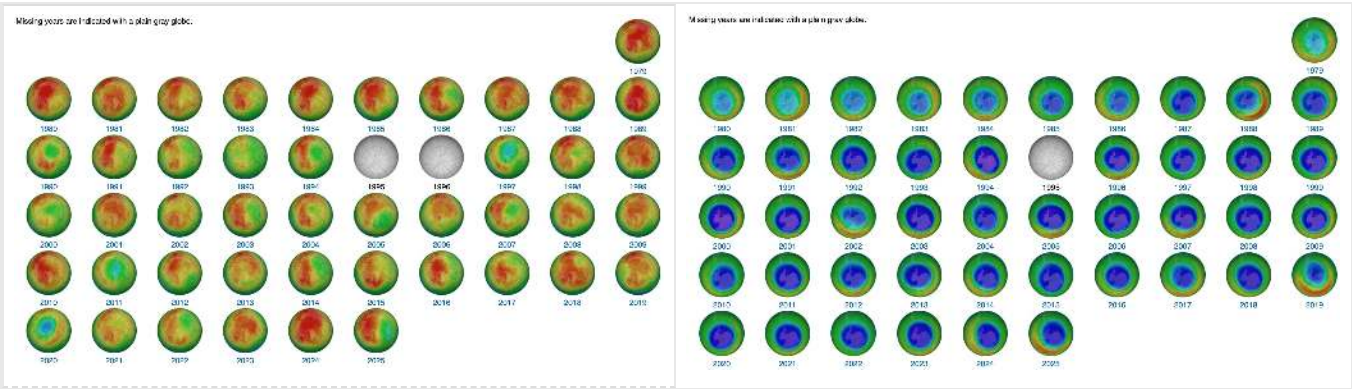


Figure **5.27.2**: Spring atmospheric column total ozone measurements. Left: Northern hemisphere in March. Right: Southern hemisphere in September. Blue is the lowest amount of ozone and red is the highest. Notice that a "hole" only forms occasionally in the Arctic (Northern hemisphere), but appears every year over the Antarctic. In the 1980s before significant amounts of chlorofluorocarbons had migrated to the stratosphere the Antarctic hole was less pronounced. More up-to-date data may be found at the NASA website from which thes images were taken: Northern hemisphere at https://ozonewatch.gsfc.nasa.gov/mon...ogy_03_NH.html and Southern hemisphere at https://ozonewatch.gsfc.nasa.gov/mon...ogy_09_SH.html.

The key to the difference between the South Pole and the North Pole is that the atmosphere around the South Pole has a stronger polar vortex (the winds that circulate clockwise around the poles when looking down at them). The stronger vortex effectively isolates the atmosphere above the South Pole from the rest of the atmosphere for a large fraction of its winter. The isolation combined with the lack of sunlight during the winter allows the atmosphere to get extremely cold. Small ice crystals form into clouds in the polar stratosphere (polar stratospheric clouds). On the surface of these ice crystals reactions occur that produce Cl_2 and HOCl from HCl and $ClONO_2$. The Cl_2 and HOCl build up during the polar winter. When the sun comes up in the spring they are photolyzed into Cl and ClO which catalyze the destruction of ozone. Because of the polar vortex the high concentrations of

these catalysts are trapped until the atmosphere warms enough for the vortex to collapse. The high concentrations of the ozone destroying species leads to a much lower steady-state ozone concentration.

If you squint at the image of the Antarctic ozone hole, you may be able to convince yourself that it has improved somewhat in recent years because of the reduced CFC emissions dictated by the Montreal Protocol. It is projected that it will be at least 2050 before it returns to behaving more like it did prior to the 1980s.

5.27.4: Photochemical smog

Smog is what we call the noxious haze that often develops in cities. The word originally referred to the combination of coal smoke and fog that was common in London, England when lots of coal was burned for heat. Here we consider what is called **photochemical smog**, which forms on sunny days when there is lots of exhaust emission from internal combustion engines.

In order for photochemical smog to form there must be adequately high concentrations of NO_x (any oxide of N), hydrocarbons, O_2 and sunlight. Thus photochemical smog is most likely to form in places like Los Angeles, California or Mexico City where the air is trapped over the city by the surrounding mountains with the prevailing wind from the west.

Photochemical smog is mainly composed of ozone and nitrogen dioxide. During the formation of ozone, nitrogen dioxide from vehicle exhaust is photolyzed by incoming solar radiation to produce nitrogen oxide and an unpaired oxygen atom. The lone oxygen atom then combines with an oxygen molecule to produce ozone. Under normal conditions, the majority of ozone molecules oxidize nitrogen oxide back into nitrogen dioxide, creating a cycle that leads to only a very slight build up of ozone near ground level. However, when volatile organic compounds (VOCs) are present in the atmosphere, the equation changes entirely. Highly reactive VOCs oxidize nitrogen oxide into nitrogen dioxide without breaking down any ozone molecules in the process. This leads to a proliferation of ozone near ground level and dense smog formation.

5.27.4.1: Reactions and composition of smog

As would be expected for a process dependent on photochemistry the composition depends on the time of day as shown in the figure below. When pollutants are produced adds additional complexity to the kinetics.

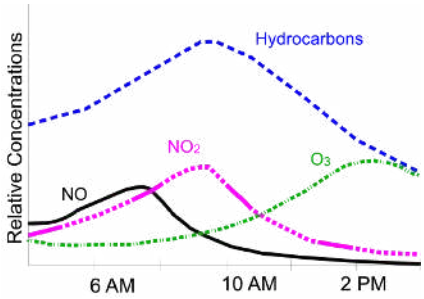


Figure **5.27.3**: Cartoon illustrating the typical time behavior of the concentration of smog components in photochemical smog. Based on figure 4.2 in G. W. vanLoon and S. J. Duffy, *Environmental Chemistry* 2 ed. (Oxford University Press, New York, 2005).

There are hundreds of chemical reactions involved in the formation of photochemical smog, but the key features can be understood in terms of only a few.

The first important reaction is the formation of NO catalyzed by hot metal surfaces in engines.

$$N_2(g) + O_2(g) \overset{\text{on hot metal}}{\longrightarrow} 2\,NO(g)$$

In figure **5.27.3** you can see the typical rise of NO concentrations because of morning rush hour traffic. Under ambient conditions the NO reacts spontaneously ($\Delta G^o_{rxn} = -69.8kJ$) to form NO_2:

$$2\,NO(g) + O_2(g) \longrightarrow 2\,NO_2(g)$$

Notice that the concentration of NO_2 rises rapidly with only a little lag from the rise in NO concentration indicating that the reaction is not only spontaneous but also quite rapid. NO_2 is brown-yellow in color and one of the main reasons smog has a color.

Simultaneous with the growth of NOx there is an increase in the concentration of hydrocarbons. In Los Angeles the hydrocarbons come from partially burned fossil fuel emissions and the plants growing in the region.

The Nitrogen Dioxide (NO_2) is the beginning of the photochemical chain. Ultraviolet (UV) radiation ($h\nu$) from the sun and decomposes the NO_2 into Nitrogen Oxide (NO) and an oxygen radical:

$$NO_2 + h\nu \rightarrow NO + O\cdot \tag{5.27.6}$$

The oxygen radical then reacts with an atmospheric oxygen molecule to create ozone, O_3:

$$O\cdot + O_2 \rightarrow O_3 \tag{5.27.7}$$

O_3 reacts readily with NO, to reverse the process, producing NO_2 and an oxygen molecule:

$$O_3 + NO \rightarrow O_2 + NO_2 \tag{5.27.8}$$

If this were all that is happening only to a temporary increase in net ozone production would be observed. To create photochemical smog on the scale observed in Los Angeles, the process must include Volatile organic compounds (VOC's).

VOC's react with hydroxide in the atmosphere to create water and a reactive VOC molecule:

$$RH + OH\cdot \rightarrow R\cdot + H_2O \tag{5.27.9}$$

The reactive VOC can then bind with an oxygen molecule to create an oxidized VOC:

$$R\cdot + O_2 \rightarrow RO_2 \tag{5.27.10}$$

The oxidized VOC can now bond with the nitrogen oxide produced in the earlier set of equations to form nitrogen dioxide and a reactive VOC molecule:

$$RO_2 + NO \rightarrow RO\text{—}\cdot + NO_2 \tag{5.27.11}$$

In the second set of equations, it is apparent that nitrogen oxide, produced in reaction 5.27.6, is oxidized in reaction 5.27.11 without the destruction of any ozone. This means that in the presence of VOCs, reaction 5.27.8 is essentially eliminated, leading to a large and rapid build up in the of the ozone typical of photochemical smog in the lower atmosphere.

So why does the NO_2 concentration drop off? Reaction 5.27.11 appears to recreate it from NO. The key is that NO and NO_2 can react with many of the VOCs to form additional compounds. These VOCs react with O_3 and NO_2 in many different ways to produce irritating molecules that contain O, N, C and H. They often contain functional groups like ketones, aldehydes and nitrate groups (-NO_2). One of the worst molecules produced is called peroxyacetyl nitrate (PAN, figure 5.27.4). PAN is a strong lachrymator, meaning that it causes tearing. PAN can also cause breathing problems for some. So once we create high O_3 concentrations with the help of sunlight we deplete the hydrocarbons and the NO_x molecules. The O_3 buildup is so high that in the evenings NO_x is used up as fast as it is produced by reactions that involve NO_2, O_3 and hydrocarbons.

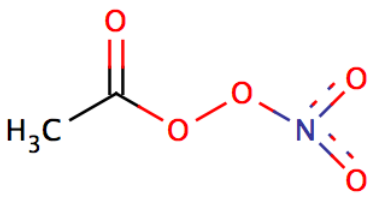


Figure 5.27.4: The Lewis structure of PAN a strong lachrymator commonly found in photochemical smog.

In summary, as shown in figure 5.27.3: In the morning, NO and VOC concentrations are high, as people fill their cars with gas and drive to work. By midmorning , VOC's begin to oxidize NO into NO_2, thus reducing their respective concentrations. At midday, NO_2 concentrations peak just before solar radiation becomes intense enough to photolyze the NO_2 bond, releasing an oxygen atom that quickly gets converted into O_3. By late afternoon, peak concentrations of photochemical smog are present.

5.27.4.2: Controlling Photochemical Smog

Every new vehicle sold in the United States must include a catalytic converter to reduce photochemical emissions. Catalytic converters force CO and incompletely combusted hydrocarbons to react with a metal catalyst, typically platinum, to produce CO_2 and H_2O. Additionally, catalytic converters reduce nitrogen oxides from exhaust gases into O_2 and N_2, eliminating the cycle of ozone formation. Many scientists have suggested that pumping gas at night could reduce photochemical ozone formation by limiting the amount of exposure VOCs have with sunlight.

5.27.5: Contributors

- Jonathan Gutow (UW Oshkosh)

5.27.6: References

1. Cooksy *Physical Chemistry: Thermodynamics* (Pearson Education, Inc. Columbus, OH, 2014) Chapter 14.

2. *Twenty Questions and Answers About the Ozone Layer: 2014 Update*, World Meteorological Organization. https://library.wmo.int/idurl/4/54606.

This page titled 5.27: Photochemical Kinetics is shared under a CC BY-NC-SA 4.0 license and was authored, remixed, and/or curated by Jonathan Gutow.

- **12.10: Catalysis** by Patrick Fleming is licensed CC BY-NC-SA 4.0.
- **7.4: Smog** is licensed CC BY-NC-SA 4.0.

Index

1: A

Absorption
- 4.14: The Dynamics of Transitions can be Modeled by Rate Equations

activation energy
- 5.11: Reactions Can Produce Vibrationally Excited Molecules
- 5.22: Atoms and Molecules can Physisorb or Chemisorb to a Surface

adsorption
- 5.22: Atoms and Molecules can Physisorb or Chemisorb to a Surface
- 5.23: Isotherms are Plots of Surface Coverage as a Function of Gas Pressure at Constant Temperature

adsorption kinetics
- 5.22: Atoms and Molecules can Physisorb or Chemisorb to a Surface

alkali metals
- 5.12: Reactive Collisions Can be Studied Using Crossed Molecular Beam Machines

ammonia synthesis
- 5.26: The Haber-Bosch Reaction Can Be Surface Catalyzed

angle of collision
- 5.7: A Reaction Cross Section Depends Upon the Impact Parameter

Angular momentum
- 3.5: The Energy Levels of a Rigid Rotor
- 4.3: Rotational Spectra of Polyatomic Molecules

angular motion
- 4.3: Rotational Spectra of Polyatomic Molecules

Anharmonicity
- 4.7: Vibrational Overtones
- 4.11: The Franck-Condon Principle

Arrhenius equation
- 5.6: The Rate of Bimolecular Gas-Phase Reaction Can Be Estimated Using Hard-Sphere Collision Theory and an Energy-Dependent Reaction Cross Section

assumption
- 5.23: Isotherms are Plots of Surface Coverage as a Function of Gas Pressure at Constant Temperature

Atomic spectroscopy
- 4.14: The Dynamics of Transitions can be Modeled by Rate Equations

attractive forces
- 5.15: The Potential-Energy Surface Can Be Calculated Using Quantum Mechanics

2: B

beating
- 3.4: The Quantum Mechanical Free Particle

Beer’s Law
- 4.15: Beer's Law

bimolecular reaction
- 5.6: The Rate of Bimolecular Gas-Phase Reaction Can Be Estimated Using Hard-Sphere Collision Theory and an Energy-Dependent Reaction Cross Section

bimolecular reactions
- 5.14: Not All Gas-Phase Chemical Reactions are Rebound Reactions

bimolecularreaction
- 5.10: A Reactive Collision Can Be Described in a Center-of-Mass Coordinate System

Boltzmann
- 2.7: The Maxwell-Boltzmann Distribution of Molecular Speeds in 3 Dimensions

Boltzmann distribution
- 5.13: The Velocity and Angular Distribution of the Products of a Reactive Collision

boltzmann_constant
- 2.10: The Equipartition Principle

3: C

catalyst
- 5.26: The Haber-Bosch Reaction Can Be Surface Catalyzed

centrifugal stretching
- 4.2: Rotational Spectroscopy of Diatomic Molecules

chain reaction
- 5.18: Chain Reactions

chemical bond
- 5.15: The Potential-Energy Surface Can Be Calculated Using Quantum Mechanics

chemical engineering
- 5.26: The Haber-Bosch Reaction Can Be Surface Catalyzed

chemical experiments
- 5.12: Reactive Collisions Can be Studied Using Crossed Molecular Beam Machines

chemical kinetics
- 4.20: Modern Applications of Laser Spectroscopy
- 5.6: The Rate of Bimolecular Gas-Phase Reaction Can Be Estimated Using Hard-Sphere Collision Theory and an Energy-Dependent Reaction Cross Section

chemical reactions
- 5.15: The Potential-Energy Surface Can Be Calculated Using Quantum Mechanics

chemicalreaction
- 5.16: Equilibrium Constants in Terms of Partition Functions

chemisorption
- 5.22: Atoms and Molecules can Physisorb or Chemisorb to a Surface
- 5.25: The Structure of a Surface is Different from that of a Bulk Solid

chemistry
- 2.10: The Equipartition Principle
- 5.7: A Reaction Cross Section Depends Upon the Impact Parameter
- 5.8: The Rate Constant for a Gas-Phase Chemical Reaction May Depend on the Orientations of the Colliding Molecules
- 5.11: Reactions Can Produce Vibrationally Excited Molecules

classical mechanics
- 3.1: Quantum Operators Represent Classical Variables

CO
- 5.24: Using Langmuir Isotherms to Derive Rate Laws for Surface-Catalyzed Gas-Phase Reactions

coherent light
- 4.16: A Two-Level System Cannot Achieve a Population Inversion
- 4.18: What is Inside a Laser?

collidingparticles
- 5.10: A Reactive Collision Can Be Described in a Center-of-Mass Coordinate System

collimated beam
- 4.16: A Two-Level System Cannot Achieve a Population Inversion

collision
- 5.3: The Frequency of Collisions with a Wall
- 5.7: A Reaction Cross Section Depends Upon the Impact Parameter
- 5.8: The Rate Constant for a Gas-Phase Chemical Reaction May Depend on the Orientations of the Colliding Molecules
- 5.14: Not All Gas-Phase Chemical Reactions are Rebound Reactions

collision cross section
- 5.2: Collisions
- 5.6: The Rate of Bimolecular Gas-Phase Reaction Can Be Estimated Using Hard-Sphere Collision Theory and an Energy-Dependent Reaction Cross Section

collision dynamics
- 5.13: The Velocity and Angular Distribution of the Products of a Reactive Collision

collision energy
- 5.2: Collisions
- 5.11: Reactions Can Produce Vibrationally Excited Molecules

collision frequency
- 5.6: The Rate of Bimolecular Gas-Phase Reaction Can Be Estimated Using Hard-Sphere Collision Theory and an Energy-Dependent Reaction Cross Section

collision model
- 5.9: The Internal Energy of the Reactants Can Affect the Cross Section of a Reaction

collisional broadening
- 4.21: Broadening Mechanisms

commutator
- 3.3: Commuting Operators Allow Infinite Precision

commute
- 3.3: Commuting Operators Allow Infinite Precision

concentration
- 5.16: Equilibrium Constants in Terms of Partition Functions

conservationofenergy
- 5.10: A Reactive Collision Can Be Described in a Center-of-Mass Coordinate System

conservationofmomentum
- 5.10: A Reactive Collision Can Be Described in a Center-of-Mass Coordinate System

continuous lasing
- 4.16: A Two-Level System Cannot Achieve a Population Inversion

ContinuousWaveLaser
- 4.19: The Helium-Neon Laser

copper vapor laser
- 4.17: Population Inversion can be Achieved in a Three-Level System

correspondence principle
- 3.1: Quantum Operators Represent Classical Variables

Coulomb potential
- 5.14: Not All Gas-Phase Chemical Reactions are Rebound Reactions

crossed molecular beam
- 5.12: Reactive Collisions Can be Studied Using Crossed Molecular Beam Machines

4: D

data analysis
- 2.11: Molar Heat Capacities

desorption process
5.22: Atoms and Molecules can Physisorb or Chemisorb to a Surface
detection techniques
5.12: Reactive Collisions Can be Studied Using Crossed Molecular Beam Machines
diatomic
4.3: Rotational Spectra of Polyatomic Molecules
diatomic molecules
3.5: The Energy Levels of a Rigid Rotor
4.6: The Harmonic Oscillator and Infrared Spectra
4.7: Vibrational Overtones
4.8: Rotations Accompany Vibrational Transitions
diatomic_molecule
4.10: Electronic Spectra Contain Electronic, Vibrational, and Rotational Information
diffusion
5.2: Collisions
diode lasers
4.18: What is Inside a Laser?
Distribution
2.7: The Maxwell-Boltzmann Distribution of Molecular Speeds in 3 Dimensions
dye lasers
4.18: What is Inside a Laser?

5: E

eigenfunctions
3.2: Eigenfunctions of Operators are Orthogonal
Einstein coefficients
4.14: The Dynamics of Transitions can be Modeled by Rate Equations
Einstein Solid Model
2.11: Molar Heat Capacities
electromagnetic radiation
4.14: The Dynamics of Transitions can be Modeled by Rate Equations
electron microscopy
5.25: The Structure of a Surface is Different from that of a Bulk Solid
electron spin
4.12: Electronically Excited Molecules can Relax by a Number of Processes
electron transfer
5.14: Not All Gas-Phase Chemical Reactions are Rebound Reactions
electronic energy
5.9: The Internal Energy of the Reactants Can Affect the Cross Section of a Reaction
electronic_excitation
4.11: The Franck-Condon Principle
electronic_transitions
4.10: Electronic Spectra Contain Electronic, Vibrational, and Rotational Information
energy
2.10: The Equipartition Principle
5.8: The Rate Constant for a Gas-Phase Chemical Reaction May Depend on the Orientations of the Colliding Molecules
energy exchanges
5.9: The Internal Energy of the Reactants Can Affect the Cross Section of a Reaction
energy levels
4.3: Rotational Spectra of Polyatomic Molecules
4.7: Vibrational Overtones
4.17: Population Inversion can be Achieved in a Three-Level System
energy of adsorption
5.22: Atoms and Molecules can Physisorb or Chemisorb to a Surface
energy probing
4.20: Modern Applications of Laser Spectroscopy
energy profile
5.15: The Potential-Energy Surface Can Be Calculated Using Quantum Mechanics
energy quantization
4.8: Rotations Accompany Vibrational Transitions
energy states
4.16: A Two-Level System Cannot Achieve a Population Inversion
energy_levels
4.10: Electronic Spectra Contain Electronic, Vibrational, and Rotational Information
enthalpy of adsorption
5.23: Isotherms are Plots of Surface Coverage as a Function of Gas Pressure at Constant Temperature
entropies
2.9: Ortho and Para Hydrogen
envelope function
3.4: The Quantum Mechanical Free Particle
equation of state
5.1: Classical Model of Ideal Gas Pressure
equilibrium
5.16: Equilibrium Constants in Terms of Partition Functions
5.26: The Haber-Bosch Reaction Can Be Surface Catalyzed
equilibrium bond length
5.15: The Potential-Energy Surface Can Be Calculated Using Quantum Mechanics
equilibrium constant
5.16: Equilibrium Constants in Terms of Partition Functions
equipartition
2.10: The Equipartition Principle
even functions
4.5: Hermite Polynomials are either Even or Odd Functions
excited state
4.12: Electronically Excited Molecules can Relax by a Number of Processes
exothermic reaction
5.26: The Haber-Bosch Reaction Can Be Surface Catalyzed
experimental cross section
5.14: Not All Gas-Phase Chemical Reactions are Rebound Reactions
experimental techniques
5.12: Reactive Collisions Can be Studied Using Crossed Molecular Beam Machines

6: F

fluorescence
4.12: Electronically Excited Molecules can Relax by a Number of Processes
Franck_Condon
4.11: The Franck-Condon Principle
free particle
3.4: The Quantum Mechanical Free Particle
frequency
5.3: The Frequency of Collisions with a Wall

7: G

gain medium
4.17: Population Inversion can be Achieved in a Three-Level System
4.18: What is Inside a Laser?
gas
2.7: The Maxwell-Boltzmann Distribution of Molecular Speeds in 3 Dimensions
5.3: The Frequency of Collisions with a Wall
gas adsorption
5.23: Isotherms are Plots of Surface Coverage as a Function of Gas Pressure at Constant Temperature
gas behavior
5.1: Classical Model of Ideal Gas Pressure
gas laws
2.6: The Gaussian Distribution of One Component of the Molecular Velocity
gas particles
5.9: The Internal Energy of the Reactants Can Affect the Cross Section of a Reaction
GasLaser
4.19: The Helium-Neon Laser
gasphase
5.24: Using Langmuir Isotherms to Derive Rate Laws for Surface-Catalyzed Gas-Phase Reactions
Gaussian
5.2: Collisions
Gaussian Wavepacket
3.4: The Quantum Mechanical Free Particle
ground state
4.12: Electronically Excited Molecules can Relax by a Number of Processes

8: H

Hamiltonian operator
3.1: Quantum Operators Represent Classical Variables
Harmonic oscillator
4.4: Harmonic Oscillator
4.5: Hermite Polynomials are either Even or Odd Functions
4.7: Vibrational Overtones
4.8: Rotations Accompany Vibrational Transitions
5.13: The Velocity and Angular Distribution of the Products of a Reactive Collision
heat capacities
2.9: Ortho and Para Hydrogen
heat capacity
2.11: Molar Heat Capacities
heat of adsorption
5.22: Atoms and Molecules can Physisorb or Chemisorb to a Surface
heat_capacity
2.10: The Equipartition Principle
HeNeLaser
4.19: The Helium-Neon Laser
Hermite polynomials
4.5: Hermite Polynomials are either Even or Odd Functions
Hermitian operators
3.2: Eigenfunctions of Operators are Orthogonal
high intensity
4.20: Modern Applications of Laser Spectroscopy
Holography
4.19: The Helium-Neon Laser
Homogeneous broadening
4.21: Broadening Mechanisms

hydrogen
2.9: Ortho and Para Hydrogen
5.26: The Haber-Bosch Reaction Can Be Surface Catalyzed

9: I

ideal gas
2.6: The Gaussian Distribution of One Component of the Molecular Velocity
5.1: Classical Model of Ideal Gas Pressure
ideal_gas
5.3: The Frequency of Collisions with a Wall
idealgases
5.10: A Reactive Collision Can Be Described in a Center-of-Mass Coordinate System
impact parameter
5.7: A Reaction Cross Section Depends Upon the Impact Parameter
industrial process
5.26: The Haber-Bosch Reaction Can Be Surface Catalyzed
Infrared Region
4.6: The Harmonic Oscillator and Infrared Spectra
infrared_absorption
4.10: Electronic Spectra Contain Electronic, Vibrational, and Rotational Information
Inhomogeneous broadening
4.21: Broadening Mechanisms
initiation step
5.18: Chain Reactions
internal energy
5.9: The Internal Energy of the Reactants Can Affect the Cross Section of a Reaction
internal vibrational energy
5.13: The Velocity and Angular Distribution of the Products of a Reactive Collision
InternalEnergy
5.10: A Reactive Collision Can Be Described in a Center-of-Mass Coordinate System
IR spectroscopy
4.6: The Harmonic Oscillator and Infrared Spectra

10: J

Jablonski diagram
4.12: Electronically Excited Molecules can Relax by a Number of Processes

11: K

kinetic energy
2.7: The Maxwell-Boltzmann Distribution of Molecular Speeds in 3 Dimensions
4.3: Rotational Spectra of Polyatomic Molecules
5.2: Collisions
5.6: The Rate of Bimolecular Gas-Phase Reaction Can Be Estimated Using Hard-Sphere Collision Theory and an Energy-Dependent Reaction Cross Section
5.7: A Reaction Cross Section Depends Upon the Impact Parameter
5.15: The Potential-Energy Surface Can Be Calculated Using Quantum Mechanics
kinetic theory
2.6: The Gaussian Distribution of One Component of the Molecular Velocity
5.1: Classical Model of Ideal Gas Pressure
kinetic_energy
2.10: The Equipartition Principle
kineticenergy
5.10: A Reactive Collision Can Be Described in a Center-of-Mass Coordinate System
kinetics
5.24: Using Langmuir Isotherms to Derive Rate Laws for Surface-Catalyzed Gas-Phase Reactions
5.25: The Structure of a Surface is Different from that of a Bulk Solid

12: L

Langmuir isotherm
5.23: Isotherms are Plots of Surface Coverage as a Function of Gas Pressure at Constant Temperature
laser
4.20: Modern Applications of Laser Spectroscopy
laser light
4.17: Population Inversion can be Achieved in a Three-Level System
laser medium
4.16: A Two-Level System Cannot Achieve a Population Inversion
LaserApplications
4.19: The Helium-Neon Laser
LaserPointers
4.19: The Helium-Neon Laser
lasers
4.12: Electronically Excited Molecules can Relax by a Number of Processes
4.18: What is Inside a Laser?
LasersInIndustry
4.19: The Helium-Neon Laser
LaserTechnology
4.19: The Helium-Neon Laser
lasing
4.16: A Two-Level System Cannot Achieve a Population Inversion
4.17: Population Inversion can be Achieved in a Three-Level System
Le Chatelier's principle
5.26: The Haber-Bosch Reaction Can Be Surface Catalyzed
learning objectives
2.11: Molar Heat Capacities
light
4.14: The Dynamics of Transitions can be Modeled by Rate Equations
LowPowerLasers
4.19: The Helium-Neon Laser

13: M

mass spectrometry
5.12: Reactive Collisions Can be Studied Using Crossed Molecular Beam Machines
maxwell
2.7: The Maxwell-Boltzmann Distribution of Molecular Speeds in 3 Dimensions
mean free path
5.2: Collisions
measurements
3.3: Commuting Operators Allow Infinite Precision
microscopies
5.25: The Structure of a Surface is Different from that of a Bulk Solid
microwave spectroscopy
4.2: Rotational Spectroscopy of Diatomic Molecules
microwave_absorption
4.10: Electronic Spectra Contain Electronic, Vibrational, and Rotational Information
model
5.8: The Rate Constant for a Gas-Phase Chemical Reaction May Depend on the Orientations of the Colliding Molecules
molecular beam experiments
5.13: The Velocity and Angular Distribution of the Products of a Reactive Collision
molecular bonding
2.11: Molar Heat Capacities
molecular bonds
4.7: Vibrational Overtones
molecular collisions
5.12: Reactive Collisions Can be Studied Using Crossed Molecular Beam Machines
molecular dynamics
2.6: The Gaussian Distribution of One Component of the Molecular Velocity
molecular geometry
5.15: The Potential-Energy Surface Can Be Calculated Using Quantum Mechanics
molecular orientation
5.7: A Reaction Cross Section Depends Upon the Impact Parameter
molecular processes
4.20: Modern Applications of Laser Spectroscopy
molecularoxygen
5.24: Using Langmuir Isotherms to Derive Rate Laws for Surface-Catalyzed Gas-Phase Reactions
molecules
2.7: The Maxwell-Boltzmann Distribution of Molecular Speeds in 3 Dimensions
4.10: Electronic Spectra Contain Electronic, Vibrational, and Rotational Information
5.3: The Frequency of Collisions with a Wall
5.8: The Rate Constant for a Gas-Phase Chemical Reaction May Depend on the Orientations of the Colliding Molecules
moment of inertia
4.3: Rotational Spectra of Polyatomic Molecules
monochromatic light
4.16: A Two-Level System Cannot Achieve a Population Inversion

14: N

negativeorder
5.24: Using Langmuir Isotherms to Derive Rate Laws for Surface-Catalyzed Gas-Phase Reactions
nitrogen
5.26: The Haber-Bosch Reaction Can Be Surface Catalyzed
nonlinear spectroscopy
4.20: Modern Applications of Laser Spectroscopy
nuclear spins
2.9: Ortho and Para Hydrogen
nuclear_kinetic_energy
4.10: Electronic Spectra Contain Electronic, Vibrational, and Rotational Information

15: O

odd functions
4.5: Hermite Polynomials are either Even or Odd Functions
optical cavity
4.18: What is Inside a Laser?

optical pumping
4.17: Population Inversion can be Achieved in a Three-Level System
OpticalTransmission
4.19: The Helium-Neon Laser
orientation
5.8: The Rate Constant for a Gas-Phase Chemical Reaction May Depend on the Orientations of the Colliding Molecules
ortho
2.9: Ortho and Para Hydrogen
orthogonality
3.2: Eigenfunctions of Operators are Orthogonal
4.5: Hermite Polynomials are either Even or Odd Functions
Orthogonality Theorem
3.2: Eigenfunctions of Operators are Orthogonal
overlap_integrals
4.11: The Franck-Condon Principle
overtones
4.7: Vibrational Overtones

16: P

para
2.9: Ortho and Para Hydrogen
particle physics
5.2: Collisions
particles
5.8: The Rate Constant for a Gas-Phase Chemical Reaction May Depend on the Orientations of the Colliding Molecules
partition function
2.9: Ortho and Para Hydrogen
periodic trends
2.11: Molar Heat Capacities
perturbation theory
3.8: Perturbation Theory Expresses the Solutions in Terms of Solved Problems
4.7: Vibrational Overtones
phosphorescence
4.12: Electronically Excited Molecules can Relax by a Number of Processes
photodissociation
4.20: Modern Applications of Laser Spectroscopy
photons
4.14: The Dynamics of Transitions can be Modeled by Rate Equations
physics
2.7: The Maxwell-Boltzmann Distribution of Molecular Speeds in 3 Dimensions
physisorption
5.22: Atoms and Molecules can Physisorb or Chemisorb to a Surface
5.25: The Structure of a Surface is Different from that of a Bulk Solid
polyatomic
4.3: Rotational Spectra of Polyatomic Molecules
polyatomic gas
5.9: The Internal Energy of the Reactants Can Affect the Cross Section of a Reaction
population inversion
4.14: The Dynamics of Transitions can be Modeled by Rate Equations
4.16: A Two-Level System Cannot Achieve a Population Inversion
4.17: Population Inversion can be Achieved in a Three-Level System
4.18: What is Inside a Laser?
potential energy
4.3: Rotational Spectra of Polyatomic Molecules
4.7: Vibrational Overtones
potential energy curve
5.11: Reactions Can Produce Vibrationally Excited Molecules
potential energy surface
5.15: The Potential-Energy Surface Can Be Calculated Using Quantum Mechanics
potential_energy_surfaces
4.11: The Franck-Condon Principle
pressure
2.6: The Gaussian Distribution of One Component of the Molecular Velocity
5.1: Classical Model of Ideal Gas Pressure
5.3: The Frequency of Collisions with a Wall
5.24: Using Langmuir Isotherms to Derive Rate Laws for Surface-Catalyzed Gas-Phase Reactions
Principle of Superposition
3.4: The Quantum Mechanical Free Particle
products
5.10: A Reactive Collision Can Be Described in a Center-of-Mass Coordinate System
5.11: Reactions Can Produce Vibrationally Excited Molecules
5.16: Equilibrium Constants in Terms of Partition Functions
propagation step
5.18: Chain Reactions
pulsed lasers
4.17: Population Inversion can be Achieved in a Three-Level System
4.20: Modern Applications of Laser Spectroscopy
Pure dephasing
4.21: Broadening Mechanisms

17: Q

Quantum Harmonic Oscillator
4.6: The Harmonic Oscillator and Infrared Spectra
quantum theory
5.15: The Potential-Energy Surface Can Be Calculated Using Quantum Mechanics
QueenMaryUniversityofLondon
5.24: Using Langmuir Isotherms to Derive Rate Laws for Surface-Catalyzed Gas-Phase Reactions

18: R

radiative decay
4.12: Electronically Excited Molecules can Relax by a Number of Processes
Raman spectroscopy
4.13: Raman Spectroscopy
random walks
5.2: Collisions
rate constant
5.6: The Rate of Bimolecular Gas-Phase Reaction Can Be Estimated Using Hard-Sphere Collision Theory and an Energy-Dependent Reaction Cross Section
reactants
5.10: A Reactive Collision Can Be Described in a Center-of-Mass Coordinate System
5.11: Reactions Can Produce Vibrationally Excited Molecules
5.16: Equilibrium Constants in Terms of Partition Functions
reaction
5.7: A Reaction Cross Section Depends Upon the Impact Parameter
5.8: The Rate Constant for a Gas-Phase Chemical Reaction May Depend on the Orientations of the Colliding Molecules
5.11: Reactions Can Produce Vibrationally Excited Molecules
reaction collision
5.9: The Internal Energy of the Reactants Can Affect the Cross Section of a Reaction
reaction dynamics
4.20: Modern Applications of Laser Spectroscopy
5.12: Reactive Collisions Can be Studied Using Crossed Molecular Beam Machines
5.15: The Potential-Energy Surface Can Be Calculated Using Quantum Mechanics
reaction kinetics
5.16: Equilibrium Constants in Terms of Partition Functions
reaction pathways
5.22: Atoms and Molecules can Physisorb or Chemisorb to a Surface
reaction rate
5.6: The Rate of Bimolecular Gas-Phase Reaction Can Be Estimated Using Hard-Sphere Collision Theory and an Energy-Dependent Reaction Cross Section
reactionkinetics
5.10: A Reactive Collision Can Be Described in a Center-of-Mass Coordinate System
reactionrate
5.24: Using Langmuir Isotherms to Derive Rate Laws for Surface-Catalyzed Gas-Phase Reactions
reactions
5.16: Equilibrium Constants in Terms of Partition Functions
rebound reaction
5.14: Not All Gas-Phase Chemical Reactions are Rebound Reactions
relative velocity
5.7: A Reaction Cross Section Depends Upon the Impact Parameter
Rigid rotor
3.5: The Energy Levels of a Rigid Rotor
4.8: Rotations Accompany Vibrational Transitions
Roger Nix
5.23: Isotherms are Plots of Surface Coverage as a Function of Gas Pressure at Constant Temperature
RogerNix
5.24: Using Langmuir Isotherms to Derive Rate Laws for Surface-Catalyzed Gas-Phase Reactions
rotational energy
5.9: The Internal Energy of the Reactants Can Affect the Cross Section of a Reaction
Rotational Spectroscopy of Diatomic Molecules
4.2: Rotational Spectroscopy of Diatomic Molecules
rotational transition
3.5: The Energy Levels of a Rigid Rotor
rotational transitions
4.8: Rotations Accompany Vibrational Transitions
rovibrational
4.9: Unequal Spacings in Vibration-Rotation Spectra
rovibrational spectra
4.8: Rotations Accompany Vibrational Transitions
rovibrational_transitions
4.10: Electronic Spectra Contain Electronic, Vibrational, and Rotational Information

ruby laser
4.17: Population Inversion can be Achieved in a Three-Level System

19: S

Schrödinger equation
4.3: Rotational Spectra of Polyatomic Molecules
Selection rules
4.6: The Harmonic Oscillator and Infrared Spectra
4.8: Rotations Accompany Vibrational Transitions
singlet state
4.12: Electronically Excited Molecules can Relax by a Number of Processes
Slater determinant wavefunction
3.9: Electron Spin, Indistinguishability and Slater Determinants
specific heat capacity
2.11: Molar Heat Capacities
spectra
4.7: Vibrational Overtones
spectral analysis
4.8: Rotations Accompany Vibrational Transitions
spectroscopic techniques
4.6: The Harmonic Oscillator and Infrared Spectra
spectroscopies
5.25: The Structure of a Surface is Different from that of a Bulk Solid
spectroscopy
4.20: Modern Applications of Laser Spectroscopy
speed distribution
5.13: The Velocity and Angular Distribution of the Products of a Reactive Collision
Spherical harmonics
3.5: The Energy Levels of a Rigid Rotor
Spontaneous emission
4.2: Rotational Spectroscopy of Diatomic Molecules
4.14: The Dynamics of Transitions can be Modeled by Rate Equations
statistical mechanics
2.6: The Gaussian Distribution of One Component of the Molecular Velocity
5.2: Collisions
5.16: Equilibrium Constants in Terms of Partition Functions
statistical thermodynamics
2.11: Molar Heat Capacities
statistical_mechanics
2.10: The Equipartition Principle
stimulated emission
4.2: Rotational Spectroscopy of Diatomic Molecules
4.14: The Dynamics of Transitions can be Modeled by Rate Equations
4.16: A Two-Level System Cannot Achieve a Population Inversion
4.17: Population Inversion can be Achieved in a Three-Level System
stripping reactions
5.14: Not All Gas-Phase Chemical Reactions are Rebound Reactions
supersonic nozzles
5.12: Reactive Collisions Can be Studied Using Crossed Molecular Beam Machines
surface coverage
5.23: Isotherms are Plots of Surface Coverage as a Function of Gas Pressure at Constant Temperature
surface interaction
5.22: Atoms and Molecules can Physisorb or Chemisorb to a Surface
surface structure
5.25: The Structure of a Surface is Different from that of a Bulk Solid
surfaceblocking
5.24: Using Langmuir Isotherms to Derive Rate Laws for Surface-Catalyzed Gas-Phase Reactions
Surfaces
5.25: The Structure of a Surface is Different from that of a Bulk Solid
symmetry
2.9: Ortho and Para Hydrogen
4.5: Hermite Polynomials are either Even or Odd Functions

20: T

temperature
2.6: The Gaussian Distribution of One Component of the Molecular Velocity
2.7: The Maxwell-Boltzmann Distribution of Molecular Speeds in 3 Dimensions
2.10: The Equipartition Principle
5.1: Classical Model of Ideal Gas Pressure
5.3: The Frequency of Collisions with a Wall
temperature dependence
5.6: The Rate of Bimolecular Gas-Phase Reaction Can Be Estimated Using Hard-Sphere Collision Theory and an Energy-Dependent Reaction Cross Section
5.23: Isotherms are Plots of Surface Coverage as a Function of Gas Pressure at Constant Temperature
termination step
5.18: Chain Reactions
theoretical estimate
5.14: Not All Gas-Phase Chemical Reactions are Rebound Reactions
thermal equilibrium
5.13: The Velocity and Angular Distribution of the Products of a Reactive Collision
thermal_equilibrium
2.10: The Equipartition Principle
thermodynamics
2.6: The Gaussian Distribution of One Component of the Molecular Velocity
2.7: The Maxwell-Boltzmann Distribution of Molecular Speeds in 3 Dimensions
2.9: Ortho and Para Hydrogen
2.10: The Equipartition Principle
5.1: Classical Model of Ideal Gas Pressure
5.2: Collisions
5.3: The Frequency of Collisions with a Wall
5.11: Reactions Can Produce Vibrationally Excited Molecules
5.16: Equilibrium Constants in Terms of Partition Functions
5.23: Isotherms are Plots of Surface Coverage as a Function of Gas Pressure at Constant Temperature
5.25: The Structure of a Surface is Different from that of a Bulk Solid
Transition dipole moment
4.8: Rotations Accompany Vibrational Transitions
transition moment integral
4.2: Rotational Spectroscopy of Diatomic Molecules
4.6: The Harmonic Oscillator and Infrared Spectra
transition_probabilities
4.11: The Franck-Condon Principle
translational energy
5.9: The Internal Energy of the Reactants Can Affect the Cross Section of a Reaction
triplet state
4.12: Electronically Excited Molecules can Relax by a Number of Processes

21: U

uncertainty
3.3: Commuting Operators Allow Infinite Precision
University of London
5.23: Isotherms are Plots of Surface Coverage as a Function of Gas Pressure at Constant Temperature

22: V

velocity
2.6: The Gaussian Distribution of One Component of the Molecular Velocity
2.7: The Maxwell-Boltzmann Distribution of Molecular Speeds in 3 Dimensions
5.3: The Frequency of Collisions with a Wall
velocity distribution
5.13: The Velocity and Angular Distribution of the Products of a Reactive Collision
vibrational energy
5.9: The Internal Energy of the Reactants Can Affect the Cross Section of a Reaction
vibrational energy levels
4.6: The Harmonic Oscillator and Infrared Spectra
vibrational frequency
2.11: Molar Heat Capacities
vibrational motion
4.7: Vibrational Overtones
vibrational state
5.13: The Velocity and Angular Distribution of the Products of a Reactive Collision
vibrational states
5.11: Reactions Can Produce Vibrationally Excited Molecules
vibrational transitions
4.8: Rotations Accompany Vibrational Transitions
vibrational_levels
4.11: The Franck-Condon Principle
vibronic_transitions
4.10: Electronic Spectra Contain Electronic, Vibrational, and Rotational Information
volume
5.1: Classical Model of Ideal Gas Pressure
5.3: The Frequency of Collisions with a Wall

23: W

wavefunction
3.3: Commuting Operators Allow Infinite Precision
wavepackets
3.4: The Quantum Mechanical Free Particle

Glossary

Sample Word 1 | Sample Definition 1

Detailed Licensing

Overview

Title: Chem 371: P-Chem 2 to Folow Combined Biophysical and P-Chem 1 (Gutow)

Webpages: 90

Applicable Restrictions: Noncommercial

All licenses found:

- CC BY-NC-SA 4.0: 73.3% (66 pages)
- Undeclared: 14.4% (13 pages)
- CC BY-SA 4.0: 4.4% (4 pages)
- CC BY 4.0: 4.4% (4 pages)
- CC BY-NC 3.0: 2.2% (2 pages)
- CC BY-NC 4.0: 1.1% (1 page)

By Page

- Chem 371: P-Chem 2 to Folow Combined Biophysical and P-Chem 1 (Gutow) - *CC BY-NC-SA 4.0*
  - Front Matter - *Undeclared*
    - TitlePage - *Undeclared*
    - InfoPage - *Undeclared*
    - Table of Contents - *Undeclared*
    - Licensing - *Undeclared*
  - 1: Thermodynamics - *CC BY-NC-SA 4.0*
    - 1.1: Review and Setting the Stage - *CC BY-NC-SA 4.0*
    - 1.2: Additional Measurable Quantities - *CC BY-NC-SA 4.0*
    - 1.3: Understanding Real Gases Using Measurable Quantities - *CC BY-NC-SA 4.0*
    - 1.4: Joule-Thompson Coefficient - *CC BY-NC-SA 4.0*
    - 1.5: Heat Engines - *CC BY-NC-SA 4.0*
    - 1.6: Multicomponent Phase Diagrams - *CC BY-NC-SA 4.0*
  - 2: Statistical Mechanics - *CC BY-NC-SA 4.0*
    - 2.1: Microcanonical and Canonical Ensembles - *CC BY-NC-SA 4.0*
    - 2.2: Statistical Thermodynamic Functions - *CC BY-NC-SA 4.0*
    - 2.3: Microconanonical (q molecular) Versus Canonical (Q) Partition Functions - *CC BY-NC-SA 4.0*
    - 2.4: From Quantum States to Partition Functions - *CC BY-NC-SA 4.0*
    - 2.5: Derivation of Ideal Gas Law - *Undeclared*
    - 2.6: The Gaussian Distribution of One Component of the Molecular Velocity - *CC BY-NC-SA 4.0*
    - 2.7: The Maxwell-Boltzmann Distribution of Molecular Speeds in 3 Dimensions - *CC BY-NC-SA 4.0*
    - 2.8: Intermolecular Interactions Correction to the Translational Partition Function - *CC BY-NC-SA 4.0*
    - 2.9: Ortho and Para Hydrogen - *CC BY-NC-SA 4.0*
    - 2.10: The Equipartition Principle - *CC BY-NC-SA 4.0*
    - 2.11: Molar Heat Capacities - *CC BY-NC-SA 4.0*
  - 3: Quantum Mechanics - *Undeclared*
    - 3.1: Quantum Operators Represent Classical Variables - *CC BY-NC-SA 4.0*
    - 3.2: Eigenfunctions of Operators are Orthogonal - *CC BY-NC-SA 4.0*
    - 3.3: Commuting Operators Allow Infinite Precision - *CC BY-NC-SA 4.0*
    - 3.4: The Quantum Mechanical Free Particle - *CC BY-NC-SA 4.0*
    - 3.5: The Energy Levels of a Rigid Rotor - *CC BY-NC-SA 4.0*
    - 3.6: The Variational Method - *CC BY-NC-SA 4.0*
    - 3.7: Linear Variational Method and the Secular Determinant - *CC BY-NC-SA 4.0*
    - 3.8: Perturbation Theory Expresses the Solutions in Terms of Solved Problems - *CC BY-NC-SA 4.0*
    - 3.9: Electron Spin, Indistinguishability and Slater Determinants - *CC BY-NC-SA 4.0*
    - 3.10: Band Structure - *CC BY-NC 4.0*
  - 4: Spectroscopy - *Undeclared*
    - 4.1: Spectroscopic Selection Rules - *CC BY-NC-SA 4.0*

- 4.2: Rotational Spectroscopy of Diatomic Molecules - *CC BY-NC-SA 4.0*
- 4.3: Rotational Spectra of Polyatomic Molecules - *CC BY-NC-SA 4.0*
- 4.4: Harmonic Oscillator - *CC BY-NC-SA 4.0*
- 4.5: Hermite Polynomials are either Even or Odd Functions - *CC BY-SA 4.0*
- 4.6: The Harmonic Oscillator and Infrared Spectra - *CC BY-NC-SA 4.0*
- 4.7: Vibrational Overtones - *CC BY 4.0*
- 4.8: Rotations Accompany Vibrational Transitions - *CC BY 4.0*
- 4.9: Unequal Spacings in Vibration-Rotation Spectra - *CC BY-NC-SA 4.0*
- 4.10: Electronic Spectra Contain Electronic, Vibrational, and Rotational Information - *CC BY-SA 4.0*
- 4.11: The Franck-Condon Principle - *CC BY-NC-SA 4.0*
- 4.12: Electronically Excited Molecules can Relax by a Number of Processes - *CC BY-NC-SA 4.0*
- 4.13: Raman Spectroscopy - *CC BY 4.0*
- 4.14: The Dynamics of Transitions can be Modeled by Rate Equations - *CC BY-NC-SA 4.0*
- 4.15: Beer's Law - *CC BY-NC-SA 4.0*
- 4.16: A Two-Level System Cannot Achieve a Population Inversion - *CC BY-NC-SA 4.0*
- 4.17: Population Inversion can be Achieved in a Three-Level System - *CC BY-NC-SA 4.0*
- 4.18: What is Inside a Laser? - *CC BY-NC-SA 4.0*
- 4.19: The Helium-Neon Laser - *CC BY 4.0*
- 4.20: Modern Applications of Laser Spectroscopy - *CC BY-NC-SA 4.0*
- 4.21: Broadening Mechanisms - *CC BY-NC-SA 4.0*

5: Moving Molecules and Chemical Kinetics - *Undeclared*

- 5.1: Classical Model of Ideal Gas Pressure - *CC BY-NC-SA 4.0*
- 5.2: Collisions - *CC BY-NC-SA 4.0*
- 5.3: The Frequency of Collisions with a Wall - *CC BY-NC-SA 4.0*
- 5.4: Transport of Matter and Energy in Perfect Gases - *CC BY-NC-SA 4.0*
- 5.5: Stokes-Einstein-Sutherland Equation - *CC BY-NC-SA 4.0*
- 5.6: The Rate of Bimolecular Gas-Phase Reaction Can Be Estimated Using Hard-Sphere Collision Theory and an Energy-Dependent Reaction Cross Section - *CC BY-NC-SA 4.0*
- 5.7: A Reaction Cross Section Depends Upon the Impact Parameter - *CC BY-NC-SA 4.0*
- 5.8: The Rate Constant for a Gas-Phase Chemical Reaction May Depend on the Orientations of the Colliding Molecules - *CC BY-NC-SA 4.0*
- 5.9: The Internal Energy of the Reactants Can Affect the Cross Section of a Reaction - *CC BY-NC-SA 4.0*
- 5.10: A Reactive Collision Can Be Described in a Center-of-Mass Coordinate System - *CC BY-NC-SA 4.0*
- 5.11: Reactions Can Produce Vibrationally Excited Molecules - *CC BY-NC-SA 4.0*
- 5.12: Reactive Collisions Can be Studied Using Crossed Molecular Beam Machines - *CC BY-SA 4.0*
- 5.13: The Velocity and Angular Distribution of the Products of a Reactive Collision - *CC BY-NC-SA 4.0*
- 5.14: Not All Gas-Phase Chemical Reactions are Rebound Reactions - *CC BY-NC-SA 4.0*
- 5.15: The Potential-Energy Surface Can Be Calculated Using Quantum Mechanics - *CC BY-NC-SA 4.0*
- 5.16: Equilibrium Constants in Terms of Partition Functions - *CC BY-SA 4.0*
- 5.17: Statistical Mechnanical Transition State Theory - *CC BY-NC-SA 4.0*
- 5.18: Chain Reactions - *CC BY-NC-SA 4.0*
- 5.19: Chain Branching Explosions - *CC BY-NC-SA 4.0*
- 5.20: Kinetics of Chain Polymerization - *CC BY-NC 3.0*
- 5.21: Kinetics of Step-Growth Polymerization - *CC BY-NC 3.0*
- 5.22: Atoms and Molecules can Physisorb or Chemisorb to a Surface - *CC BY-NC-SA 4.0*
- 5.23: Isotherms are Plots of Surface Coverage as a Function of Gas Pressure at Constant Temperature - *CC BY-NC-SA 4.0*
- 5.24: Using Langmuir Isotherms to Derive Rate Laws for Surface-Catalyzed Gas-Phase Reactions - *CC BY-NC-SA 4.0*
- 5.25: The Structure of a Surface is Different from that of a Bulk Solid - *CC BY-NC-SA 4.0*
- 5.26: The Haber-Bosch Reaction Can Be Surface Catalyzed - *CC BY-NC-SA 4.0*
- 5.27: Photochemical Kinetics - *CC BY-NC-SA 4.0*

Back Matter - *Undeclared*

- Index - *Undeclared*
- Glossary - *Undeclared*
- Detailed Licensing - *Undeclared*